TID-7695

D-1

TID-7695

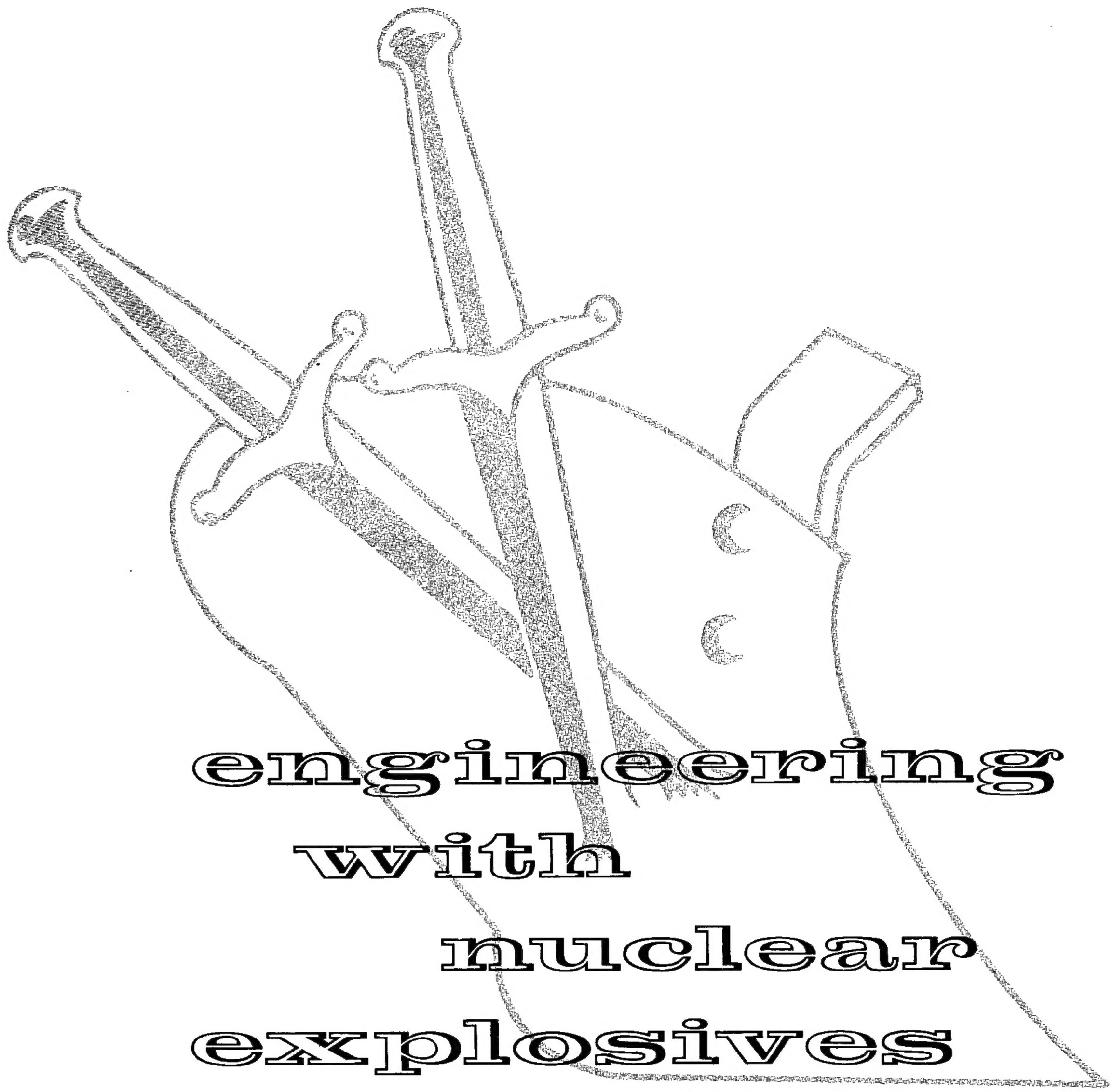

engineering with nuclear explosives

20011108 098

PROCEEDINGS OF THE THIRD PLOWSHARE SYMPOSIUM

U.S. ATOMIC ENERGY COMMISSION / Division of Technical Information

3878

Printed in USA. Price $4.50. Available from the Clearinghouse for Federal Scientific and Technical Information, National Bureau of Standards, U. S. Department of Commerce, Springfield, Va.

USAEC Division of Technical Information Extension, Oak Ridge, Tennessee

TID-7695

Nuclear Explosives
Peaceful Applications
TID 4500 (UC-35)

UNIVERSITY OF CALIFORNIA
Lawrence Radiation Laboratory
Livermore, California
and
San Francisco Operations Office
U. S. Atomic Energy Commission

Contract No. W-7405-eng-48

Proceedings of the Third Plowshare Symposium

ENGINEERING WITH NUCLEAR EXPLOSIVES

April 21, 22, 23, 1964

Sponsored by
University of California, DAVIS
Lawrence Radiation Laboratory
American Society for Engineering Education
The American Nuclear Society
United States Atomic Energy Commission

FOREWORD

The Third Plowshare Symposium was held April 21-23, 1964, in Freeborn Hall at the University of California's Davis Campus. It was sponsored by the Department of Applied Sciences, College of Engineering, Davis; the American Society for Engineering Education; the American Nuclear Society; Lawrence Radiation Laboratory, University of California; and the U. S. Atomic Energy Commission.

The theme, "Engineering with Nuclear Explosives," reflected the major objective of the Symposium; informing engineers in industry, in the military, in educational institutions, and in government agencies throughout the world of the current state-of-the-art from an engineering standpoint. The need for such an information exchange had been felt for some time by most organizations engaged in Plowshare activities. Since the last Plowshare Symposium in 1959, observation of a large number of nuclear detonations has established the reliability of predictions concerning the effects of nuclear explosions. The reliability of these predictions has a direct bearing on the use of nuclear explosions for civil and industrial purposes.

This Symposium was attended by 700 visitors and drew world-wide attention. Other nations represented at the sessions included the United Kingdom, France, Australia, Canada, Mexico, Switzerland, South Africa, Austria, and Israel.

CONTENTS

CONTENTS (continued)

CONTENTS (continued)

INTRODUCTION

Richard Hamburger

U. S. Atomic Energy Commission
Division of Peaceful Nuclear Explosives
Washington, D. C.

One of the measures of man's material progress is the amount of energy at his disposal. Early man had only his muscles to do work for him. Then domesticated animals furnished additional energy which could be used for his welfare. Mechanical inventions such as the wheel, the wedge, and the pulley added efficiency to this use of muscle power. The harnessing of water power to the wheel provided man with additional energy. Today energy from many sources are available. One family of important energy sources is explosion. For instance I drove to this meeting in a car powered by exploding gasoline. Let's look briefly at the history of explosions.

Gunpowder, the granddaddy of all explosives was probably known by the Chinese as early as 1000 AD[1], quite late in time as the history of mankind goes. By 1259 they were using gunpowder in a bamboo gun. In 1250 AD Roger Bacon, an English monk, discovered how to mix saltpeter with charcoal and sulphur to make black powder, and within a few years, the cannon was invented, followed in time by hand held firearms. Demand for these arms required a greater supply of iron and brass, which in turn simulated mining activities. In 1627, 377 years after Roger Bacon first made his black powder, a Hungarian engineer, Kaspar Weindl first used it for peaceful purposes. He placed the black powder in the cracks in the rock. His blast broke as much rock as the miners could break in many days. It is interesting to note that the value of Weindl's discovery was increased many times over by the associated activities which allowed the miner to use this discovery efficiently and to handle the extra ore that was broken. Thus rock drills replaced picks and wedges. Haulage was improved to handle the increasing volume of ore which became available. Increased efficiency allowed the mining of lower grade ores. The ability to mine lower grade ores meant that the total resources available for use were increased many times.

In 1846 nitroglycerin was discovered. By 1860 Nobel discovered how to produce nitroglycerin in quantity. In 1866 he discovered how to make dynamite. During World War I TNT came into use.

There are today many types of high and low explosives in use, from nitroglycerin to fertilizer grade ammonium nitrate. There are solid explosives, jellied explosives, and liquid explosives. Explosives come packaged in cartridges pellets, powder, and like putty so that it can be shaped.

Although most explosives are used in mining, quarrying, and construction their versatility is great. Explosives are used to start reluctant oil wells flowing. Farmers use explosives to remove tree stumps and to dig ditches. In production processes they are used for the explosive forming of metals. Small charges help rescuers find those lost at sea. The geologist and geophysicist use explosives as seismic sources to learn about the structure of the earth and to locate oil fields. One could go on for quite a while.

In 1945 the first nuclear explosive was detonated [2]. Like chemical explosives nuclear explosives will eventually have many obvious peaceful uses. When in 1627 Weindl made the first peaceful use of black powder he started a whole new technology. So when you think of peaceful uses for nuclear explosives think of them not only as larger sticks of powder, though they are also that, but as the start of a new technology, I am sure that some of the greatest benefits of nuclear

(1) One Thousand Years of Explosives by William S. Dutton, 1960

(2) The Effects of Nuclear Weapons, April 1962, p. 672

explosives will come from applications which have not yet been conceived.

It took 600 years for miners to make use of black powder. I hope the availability of information from activities like this symposium will help us find a place for nuclear explosives in industry in less time.

BIOGRAPHICAL SKETCH OF AUTHOR

Richard Hamburger has been active in Plowshare since its early days and presently is Assistant Director for Technical Operations in the AEC's Division of Peaceful Nuclear Explosives which is responsible for the Plowshare Program. Before joining the Plowshare Program, he was associated with the Inspiration Consolidated Copper Company as a geologist and mining engineer.

He attended John Hopkins University and the University of Michigan where he received his A.B. in Geology. He has done graduate work in geology at John Hopkins.

THE PLOWSHARE PROGRAM - HISTORY AND GOALS

Gerald W. Johnson

Associate Director for Plowshare
Lawrence Radiation Laboratory
Livermore, California

The applied nuclear age began a little over twenty years ago when a small group of scientists led by Enrico Fermi demonstrated the controlled release of fission energy on a minute but measureable scale under the football stands at the University of Chicago. The basic nuclear science on which this accomplishment depended was provided through fifty years of prior fundamental research which culminated in early 1939 in the key discovery of the fission process and the possibility of a chain reaction. Because soon after we were involved in a major war of survival, and one of the enemies had the potential of "getting there first," the overriding initial objective in the use of this new form of energy was properly that of building a bomb. This was, as we all know, crowned with success, and the war was promptly ended.

The military, political and social impact of this development is difficult to assess in all of its ramifications, but it was enormous. The important technical fact was that a single bomber capable of delivering about ten tons of explosive on target suddenly was able to deliver a load more than 1000 times greater--and this in the first rudimentary developmental step. The implications of this led first to an approach which is still being pursued--to develop, if possible, political controls with respect to the use of this force for warfare. The other factor that was brought out at the same time was the potential of the new source of energy for other purposes, namely power production and ship propulsion. It was the recognition of both the military and civil potentials of nuclear energy that led to the establishment of the basic policy of the United States as set forth in the Atomic Energy Act, first enacted in 1946 and periodically amended. In the declaration of the Act it is noted that "atomic energy is capable of application for peaceful as well as military purposes." In addition the stated policy of the United States is:

"a. The development, use, and control of atomic energy shall be directed so as to make the maximum contribution to the general welfare, subject at all times to the paramount objective of making the maximum contribution to the common defense and security; and

"b. The development, use, and control of atomic energy shall be directed so as to promote world peace, improve the general welfare, increase the standard of living, and strengthen free competition in private enterprise."

Following the passage of this Act in 1946, increasing attention was devoted to nuclear power development and ship propulsion. Major accomplishments were recorded in both. The ship propulsion to date has been most significant for submarines--and coupled with advances in other fields, has provided a most powerful deterrent force.

With the entry of the Soviet Union into the nuclear weapons field in 1949, and in view of their open political and military aggressiveness, it was again necessary to devote urgent attention to meeting the "paramount objectives." This threat and our resulting activities led to two important technological steps which are relevant to the present discussion. These were: (1) the achievement of the thermonuclear, or fusion, explosion, and (2) the demonstration of the clean bomb--which meant merely that the fission contribution to the explosion could be small. The significance of these two steps was that, first, fusion fuels were much cheaper and more abundant than fission fuels, and secondly, the lower fission contribution led to a reduction of the generation of those radioactivities considered to be most difficult to control.

It was recognition of these factors, coupled with the concerns raised by the Suez crisis in the Fall of 1956, which led Dr. Harold Brown to consider the possibility of using nuclear explosions to excavate an alternate sea-level canal across Israel to by-pass the Suez canal in the event it was for any reason rendered unusable.

Motivated by this possibility, Dr. Brown organized a secret meeting in February of 1957 involving the joint participation of the Los Alamos Scientific Laboratory, the Sandia Corporation laboratory, and the Lawrence Radiation Laboratory--all of which were operating under prime contracts with the Atomic Energy Commission. At that meeting a wide variety of the possible applications of nuclear explosives were discussed. Some prominence was given to the possibility of nuclear excavation for such projects as the removal of earth cover to expose ore for open pit mining, the construction of water storage basins, and the digging of canals and harbors. Rather detailed feasibility and cost analyses were included of the construction of sea-level canals across the American Isthmus. Attention was called repeatedly to the necessity for and also the probability of successful development of much cleaner explosives than the tested technology then provided. Such explosives were required in order to achieve certainty that nuclear excavation could be accomplished without the need for excessively large control of areas for a long time after the event while one waited for radioactivity to decay or disperse. The magnitude of the area and time required for control clearly would have a major impact on feasibility and cost.

Other possibilities which were described include the production of power by repeated explosions in large containers underground--a project which even at that time did not appear very attractive; increasing oil production through fracturing; and crushing ores underground to permit mining or in-situ leaching. Various scientific experiments were suggested to study the earth's structure, properties of interplanetary space, and to provide neutron sources for study of the nucleus. Discussions were devoted to isotope production and recovery with particular focus on fissionable material production.

The Suez crisis faded but the idea of Plowshare had been securely planted. Under the inspired leadership of Dr. Harold Brown and with the enthusiastic support of Professor Ernest O. Lawrence and Dr. Edward Teller, a group was formed in the Summer of 1957 at the Lawrence Radiation Laboratory to explore the whole range of potential engineering uses of nuclear explosives; and in the same year the Program was formally established by the Atomic Energy Commission. Since then the Program has received the active and enthusiastic support of the Atomic Energy Commission and the Joint Committee on Atomic Energy of the Congress. Up to that time all nuclear detonations, except for two shallowly buried military effects experiments in Nevada, had been fired either near the surface or at relatively high altitudes in the atmosphere. There was no experience with underground explosions at depths to produce craters of maximum dimensions or at greater depths to confine the explosion. The explosive technology under the pressure of military needs and with an active laboratory and test program, had made important advances.

At about this same time (1957) it had become apparent that consideration ought to be given to the possibility of testing nuclear weapons underground at the Nevada Test Site. The prime incentive for this approach was to reduce operational delays of the highly instrumented experiments, which were then conducted on towers up to 700 feet high. The fallout from these events was such that long delays were often incurred waiting for favorable meteorology to assure the deposition of the radioactivities in allowed sectors. Also, primarily because of the fallout, large organizations had to be mobilized, and the tests had to be conducted in short, highly compressed periods. This approach to development testing was costly, inefficient, and tended to be dramatic with all its adverse public reactions. For all of these reasons, following a suggestion of Dr. Edward Teller and Dr. David Griggs, the first contained experiment, RAINIER, was designed and executed in September 1957. This experiment was completely successful and demonstrated the feasibility of underground nuclear weapons testing. RAINIER was followed a year later by other detonations with yields up to 20 kilotons that tended to confirm the predictions based on the RAINIER experience. It was indicated that tests up to several hundred kilotons could be safely conducted underground at the Nevada Test Site. With the resumption of testing in 1961, the underground techniques were

perfected. Experiments are now being carried out routinely and tests up to about 200 kilotons have been sucessfully and safely fired.

The success of the RAINIER event and its analysis led to further speculations as to engineering uses of contained explosions. The general range of ideas were first reported publicly at the Atoms for Peace Conference in Geneva in the Fall of 1958 and further expanded in an article which appeared in the Scientific American of December 1958. The ideas discussed were earth-moving, water storage underground and recharging of aquifers, shattering oil shale and retorting in place, recovery of oil from the Athabasca tar sands, recovery of geothermal heat, generation of power from heat deposited in formations like salt or limestone, isotope production, and recovery of copper by in-situ leaching. Evaluations and modifications of these suggestions as well as the status of the technical background were discussed in detail during the Second Plowshare Symposium, which was open to the public, and was held in San Francisco, California, from May 13 to 15, 1959.

These were the ideas and the avenues of approach being studied when the nuclear weapons test moratorium began on November 1, 1958. In defining the United States position on the discussions at Geneva, President Eisenhower proposed that the Plowshare experiments be exempted from any agreement to suspend the testing of nuclear weapons. These experiments were to open to observation by invited representatives of other nations and the results were to be fully disclosed through the scientific press.

But such was not to be the case--the moratorium in fact precluded all nuclear tests until the resumption of nuclear weapons testing in the Fall of 1961, three years later. Thus, the advance of Plowshare was delayed for that period of time; and as a matter of fact, no nuclear experiment had been conducted for Plowshare purposes prior to the moratorium. During the moratorium period, however, detailed studies of several projects were carried out, most notably the Transisthmian canal studies, and a substantial chemical explosives cratering program was executed. The cratering program established scaling laws and provided an empirical basis for the design of nuclear experiments, as well as development of a theory. Detailed plans were developed to conduct a major excavation experiment in 1960 on the northwest coast of Alaska. That experiment was successively delayed through the moratorium period and now has been largely overtaken by events.

President Eisenhower did authorize construction of a site near Carlsbad, New Mexico, to conduct a deeply buried shot in a dry salt bed to explore the feasibility of isotope and power recovery and to conduct nuclear experiments. This event, GNOME, the first Plowshare experiment, was carried out on December 10, 1961. Also, during the following summer, on July 6, 1962, a large nuclear cratering experiment at 100 kilotons was conducted at the Nevada Test Site. A military shot early in 1962 at 400 tons in basalt provided the first nuclear cratering information in a hard dry rock. Thus, the resumption of testing permitted the extension of nuclear cratering information into the region of practical interest in one medium, and also to a new medium. The atmospheric test ban treaty has again apparently foreclosed, for the time being at least, the opportunity to proceed vigorously with the nuclear cratering program.

The resumption of underground and atmospheric testing in 1961 did provide the opportunity to make progress in the development of much cleaner nuclear explosives, a need that was recognized from the inception of the Plowshare Program to be a necessary step toward practical utilization of the explosives for excavation. After two years of work, by the end of 1963, it had become clear that this program had made a successful start--the projected fallout in excavation projects could be 100 times less than that forecast at the close of testing in 1958. Of course, had the nuclear test moratorium not intervened, this result would have been available to us much earlier. The improvement of explosives--to make them cleaner and cheaper and to assure their performance and reliability in production prototypes--is an important goal of the present program, and much of this can be accomplished under the present treaty.

At the onset of the moratorium in 1958 experience with contained nuclear explosions had been obtained only in tuff at the Nevada Test Site. Exploration and analyses of these tests provided considerable insight into the effects of nuclear explosions in this medium and did form the technical basis for suggestions of possible applications of underground explosions. Serious limitations in

making projections resulted primarily from the fact that tuff was not representative of the media of practical interest, i.e., hard, igneous rock (mining), limestone (oil shale, chemical reactions, power), and salt (power, isotope production). As mentioned previously, a shot in salt was prepared for during the moratorium and finally executed on December 10, 1961. Another test was prepared for during the moratorium as part of the program to study detection of nuclear explosions. Such a test would influence the development of provisions of the then discussed comprehensive test ban. This test, of great interest also to Plowshare, was designed to be conducted in granite and preparations were made for its execution. This experiment was conducted soon after the resumption of testing in February of 1962. In addition to these events, a large nuclear weapons test program was undertaken in the alluvium (a lightly cemented sand and gravel) at the test site, and underground explosions up to about 200 kilotons have been successfully contained.

As a consequence of these events, we now have available phenomenological data on explosions in tuff, alluvium, granite, and salt. The only major natural media yet to explore are a decomposing material like dolomite or limestone, and perhaps one of the hydrocarbon-bearing media. From the interpretation of the results from these explosions some of the early suggestions as to possible applications appear more favorable and others less.

It might be of interest to you to know that by the end of this fiscal year (July 1, 1964) the American Congress will have appropriated a total of about $45,000,000 for this program. At the present time the budget is running at about $12,000,000 annually. In addition to the AEC program, the Corps of Engineers initiated a program to study the engineering aspects of excavation and are operating at about $1,000,000 annually, exploring such questions as modeling with high explosives, slope stability and participating in general engineering projects.

BIOGRAPHICAL SKETCH OF AUTHOR

Gerald W. Johnson is Associate Director for Plowshare at the Lawrence Radiation Laboratory, Livermore. He received his B.S. in Physics with the highest honors in 1937, his M.S. in 1939 from Washington State College, and his PhD. from the University of California, Berkeley, in 1947.

Dr. Johnson has served as Assistant Professor of Physics at Washington State College; Associate Physicist at Brookhaven National Laboratory; Special Assistant to the Director of Research, Atomic Energy Commission, and as a Physicist at the Lawrence Radiation Laboratory.

At the Lawrence Radiation Laboratory, his general areas of responsibility were field testing of nuclear weapons and devices, and more recently are exploration of scientific and industrial uses of nuclear explosives. He has held positions as Test Division Leader and Associate Director for Weapons Tests. He has been associated with the Laboratory since July 1953, except for a period from July 1961 to September 1963 when he served as Chairman of the Military Liaison Committee to the Atomic Energy in Washington, D.C. In September 1963 he resumed his work at the Lawrence Radiation Laboratory on Plowshare.

CHARACTERISTICS OF NUCLEAR EXPLOSIVES

W. J. Frank

Lawrence Radiation Laboratory, University of California
Livermore, California

ABSTRACT

The characteristics of nuclear explosives of particular interest to mining and public works construction are cost, diameter, and radioactivity produced. The relationship between these properties is discussed in general terms within the limits of classification. A few specific data points are given.

Nuclear explosives were developed for military purposes; you would expect most of the technical details to be classified, and they are. However, if nuclear explosives are going to be used in mining and public works construction, a few technical facts will have to be made available. The most important facts are the size (the diameter, in particular), the cost, and the radioactivity produced.

A nuclear explosive produces its energy by two processes: the fission of uranium and plutonium, and the fusion of two isotopes of hydrogen--deuterium and tritium. The tritium is contributed by the splitting of the lighter isotope of lithium (Li^6). While most of the radioactive by-products of a nuclear explosion come from fission, neutrons from the thermonuclear reactions can induce activity in the materials of the assembly and the surrounding medium.

The traditional unit for measuring nuclear explosive energy is the kiloton. It is equivalent to one trillion (10^{12}) calories or 1.2 million kilowatt hours. For comparison: one of the largest electrical generating plants in the Bay Area produces a kiloton of energy every 20 minutes, while every 10 minutes the sun deposits on the order of a kiloton of energy on this Campus (the University of California, Davis). A pound of uranium has about 8 kilotons of potential fission energy; a pound of thermonuclear fuel has about three times that amount in potential fusion energy.

The adjective 'uncontrolled' has often been applied to the energy from nuclear explosives. Actually, this energy is as controllable as that from any explosive, as controllable as the gasoline and air mixture used to run your car engine. You can meter out the amount of energy to be released; you can designate the location of release; you can determine the time of release. The only point of uncontrollability is in the fact that you can't change your mind and turn off the energy release halfway through the explosion.

Nuclear explosives can be designed to optimize some single property. If you want an especially large external source of neutrons to use in measuring cross sections, we can enhance that property. If you want a very high internal neutron flux to produce special isotopes by neutron absorption, we can achieve that goal. If a small diameter is very important to you (as it often is in military applications), we can design for that. If your most important requirement is low cost, we can give priority to that feature. Often there are trade-offs between properties in these special designs.

Several examples of trade-offs in early industrial applications suggest themselves. For excavation, the design must reach a compromise between diameter (emplacement cost), explosive cost, and radioactivity produced (safety cost). For deeply buried applications, the emphasis will be on small diameter over explosive cost and radioactivity produced. For certain mining applications, you may wish to minimize tritium production to avoid ground water contamination or ventilation problems on re-entry. In this case, a design with a high percent of fission yield may be acceptable since the fission products will be trapped in the melted rock and, if necessary, personnel can be shielded from the radiation.

For excavation explosives, the cased diameter required for the emplacement hole would

range from 36 inches for 100 kilotons to 48 inches for 1 megaton, while the produced radioactivity would be on the order of a few kilotons of equivalent fission yield. (I use the words 'produced radioactivity' or 'equivalent fission yield' to refer to the total gamma ray dosage produced.) To simplify production and design, the excavation explosives would have quantized yields; a typical sequence of yields might be 100 kt, 200 kt, 500 kt, 1 Mt, and so on. Since crater dimensions are determined both by yield and burial depth, the effect of the fixed yields can be compensated for by changes in burial depth.

For mining and deeply buried applications, the explosive diameter could be as small as 1 foot for 10 kilotons, or 2 feet for 1 megaton.

The cost of special nuclear materials runs like this: the AEC sells U-235 and buys reactor plutonium for about $5,000/lb. Each potential kiloton of yield costs about $600. Thermonuclear fuel, fortunately, is a good deal cheaper. The Oak Ridge isotope book lists Li^6D at about $2500/lb. Its cost is only around $100 for each potential kiloton of yield. It is perhaps fortunate that most of the 'bad' properties of nuclear explosives (namely, high cost and radioactivity) are associated with just one item--fissile material. We can thus concentrate our research on reducing or eliminating this material from our designs, and hold out the hope that both these problems will dwindle and may in time disappear.

Plowshare nuclear explosives are expensive for a number of reasons. The nuclear materials (Pu, U, LiD) are expensive; they are difficult to handle and require special techniques. The production runs for Plowshare projects will involve only small numbers of explosives; further, they involve precision tooling and gauging, and 100% inspection on all parts. Finally, there are the problems introduced by security.

Let's compare nuclear explosives on a cost per pound basis with some other items made in small production runs. A Rolls Royce costs about $4/lb, as opposed to the mass produced car at $1/lb. Precision measuring instruments are $10-15/lb, while machine tools like lathes and jig grinders are $3-6/lb. The rather rare powered sailplane costs $19/lb, as compared with a Piper Super Cub at $8/lb. Reactors and reactor parts have many production problems in common with nuclear explosives. Their costs range from several hundred dollars per pound for complete reactor cores to $40/lb for replacement core elements. Nuclear explosives now range near the top of this spectrum. As the Plowshare program progresses from the 20 devices for Carryall to the 300 needed for a trans-Isthmus canal, perhaps production economies will allow us to move from Rolls Royce prices to Chevrolet prices.

I doubt that you will ever be able to buy nuclear explosives at your neighborhood hardware store. It seems unlikely that the government will allow such overwhelming packages of energy to circulate freely. In 1958 the AEC established the principle of providing a nuclear explosive service. The user provides the site and the cased hole. The AEC provides the explosive. Since the AEC has recently released a new policy statement on projected charges for nuclear explosives, I would like to close this paper with that statement.

AEC POLICY STATEMENT

As a part of its Plowshare Program to investigate and develop peaceful uses for nuclear explosives, the AEC has encouraged industry and other groups to participate in the program by anayzing the possible uses of nuclear explosives in their specific fields. To allow such investigations the Commission, in 1958, released, within the limits permitted by the national defense and security, a schedule of cost estimates for nuclear explosives and related services, including safety studies.

Since that time, improvements have been made both in the design of nuclear explosives and in their emplacement, as well as in the technology of the explosion and its effects. One of the most significant technological advances has been in the development of thermonuclear explosives with very low fission yields. Also, costs of safety studies, which were included in the 1958 charges, can be accurately estimated only for each individual situation. These developments indicate that the charge for nuclear explosives ultimately developed for peaceful uses will cost less than predicted in 1958.

Consequently, the Commission has revised its estimates and now projects a charge of $350,000 for a nuclear explosive with 10-kiloton yield and $600,000 for a nuclear explosive of 2-megaton yield. Interpolations may be made for other yields based on a straight line drawn between these two charges on semi-logarithmic paper, as shown on

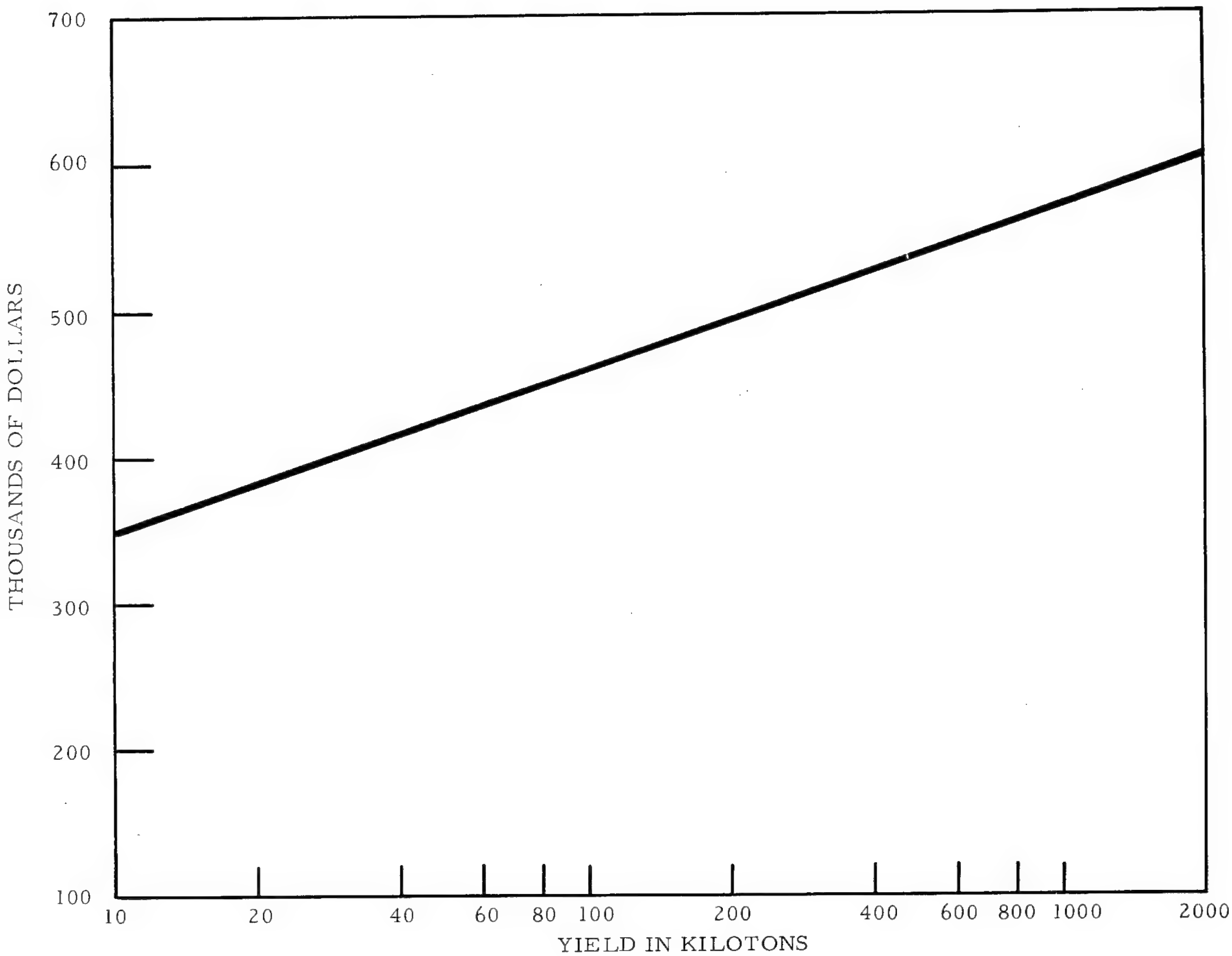

Fig. 1. Projected charges for thermonuclear explosives.

Figure 1. These charges cover nuclear materials, fabrication and assembly, and arming and firing services. Significant related services which are not covered by these projected charges are safety studies, site preparation including construction of holes, transportation and emplacement of the devices, and support. For such of these related services as are supplied by the AEC, the user would be expected to pay full cost in accordance with the present AEC policy. These costs depend significantly on the number of explosives detonated at one time.

These projected charges are released only for use in feasibility studies and evaluations and are based on a projection to a time when explosives will be produced in quantity for routine commercial utilization. Nevertheless, the Commission believes that these projected charges are sufficiently representative of the future situation to warrant their use in feasibility studies. At the present time, the Commission is not authorized to supply nuclear explosives and related services on a commercial basis, although the Commission may engage in research and development arrangements, including demonstrations of a particular peaceful application for nuclear explosives.

The Commission believes that more research and development is needed before any routine commercial applications are practical. Therefore, the Commission will continue to work with other groups in studying the contribution their

proposals for projects could make to the research and development program. It is expected that technical and economic information can be derived from such projects to help develop and demonstrate peaceful uses for nuclear explosives. In such projects it can be expected that the Commission will negotiate the charge to be made for the nuclear explosives and related services based upon a number of factors, including the nature of the contribution by the other party, the economic value of the project to the other party, and the value of information to be received by the Commission. Although the projected charges discussed above might be used as a basis for discussion of costs to be assumed by the AEC in such projects, it should be recognized that the costs to be assumed by the AEC as finally negotiated might be significantly different from the projected charges.

BIOGRAPHICAL SKETCH OF AUTHOR

W.J. Frank was born and raised in Kansas City, Missouri; he served in the Army for three years during World War II. He received his B.S. in Physics from the University of Illinois at Urbana in 1948, and his Ph.D. in Physics from the University of California at Berkeley in 1953. Since that time, he has been with the Lawrence Radiation Laboratory at Livermore.

HEAVY ISOTOPE PRODUCTION BY NUCLEAR DEVICES

D. W. Dorn

Lawrence Radiation Laboratory, University of California
Livermore, California

ABSTRACT

Since the 1952 thermonuclear detonation, "Mike," there has been interest in use of nuclear explosives to achieve very high neutron exposures, greatly in excess of those available from reactors. Fields which could benefit from these grossly increased fluxes are: nucleogenesis, nuclear structure of the very heavy elements, fission processes, stability trends in the heavy nuclei, and chemistry of new elements. Counting Mike, there have been four successful experiments in this field. A figure of merit for these shots is the ratio of the amount of elements produced with mass number equal to 246 to that of mass number 245. This ratio, R, depends sensitively on the thermal flux achieved.

Shot	Sponsoring Laboratory	Date	$R \equiv \frac{A=246}{A=245}$	Implied thermal flux (moles n/cm^2)
Mike	LASL	11/52	0.38	2.0
Anacostia	LRL	11/62	0.48	2.5
Kennebec	LRL	6/63	0.69	4.7
Anchovy	LASL	11/63	0.4	2.0

Since Mike, all experiments have used devices of low yield which can be readily contained underground. Conceptual designs now exist which should be able to give considerably higher neutron exposures.

In November 1962 an event took place which was to have a profound effect on political alignments of the world. This event was the detonation of "Mike," the first large thermonuclear device. The political implications of this experiment overshadowed what, to many of us, has come to be a major advance in the development of scientific tools. By this I mean the experimentally verified, extremely high thermal neutron flux observed in Mike. Subsequent to this observation, the Atomic Energy Commission established a study program to investigate this particular characteristic of nuclear devices. Under the program, Los Alamos Scientific Laboratory and Lawrence Radiation Laboratory, Livermore, have studied the mechanisms of high fluxes, capture systematics, general stability characteristics, and more specifically, nuclear design to accomplish this massive neutron irradiation.

Utilization of these grossly increased fluxes can be expected to significantly advance understanding in many fields. For instance, in cosmology, the study of nucleogenesis has always been difficult because of the lack of controlled experimental techniques of investigation. With the advent of these high-flux "machines" it will now be possible to simulate the supernova R process (neutron capture on a rapid time scale) and to study relative abundances of highly neutron-rich nuclides. This will cast light on naturally occurring processes and will assist in interpreting naturally occurring mass ratios. Also, in the study of nuclear structure, branching ratios for the various modes of decay (alpha, beta, and spontaneous fission) give important information on the influence of single-particle structure on energy levels of these complex nuclei. Johansson[1] and Zamick[2] have had some success in attributing nuclear properties, in the region of uranium and beyond, to specific shell model configurations. In addition, Perlman[3] has suggested that the short time scale involved in these capture processes may "freeze in" high spin states. That is, successive capture of neutrons may synthesize metastable states of high angular momentum.

Another use of this high flux is the synthesis of samples of spontaneously fissioning odd-A (non-zero spin) nuclei. Observation of the angular

correlation of fission products will give information on shapes of nuclei at or near scission (the moment of actual fission), and will contribute to our knowledge of the fission processes. Understanding stability trends of these superheavy nuclei has also proven to be an extremely difficult problem. Foreman and Seaborg[4] observed a correlation of the drop in spontaneous fission lifetimes with the minor shell of 152 neutrons (Fig. 1). Other investigators[1, 5-12] have considered this and other problems of these nuclei. Werner and Wheeler,[12] for example, have treated general stability characteristics of superheavy nuclei (Fig. 2). Conclusions reached in that work way be modified by composition-dependent terms as pointed out by Brandt, et al.[13] Difficulties in extrapolations like these are demonstrated by Fig. 3 which shows the unphysical precipitous drop[14] of the spontaneous fission lifetimes of uranium isotopes with increasing A. Investigation of stability trends using nuclear devices can be expected to differentiate between the presently existing theories and to stimulate new ideas. Mass formulas have been developed by many people,[15-18] but here again, the range of validity should probably be restricted to near the known nuclei. Extension of the data will contribute significantly to our knowledge and understanding of the mass surface. Finally, the chemistry of these new elements is extremely

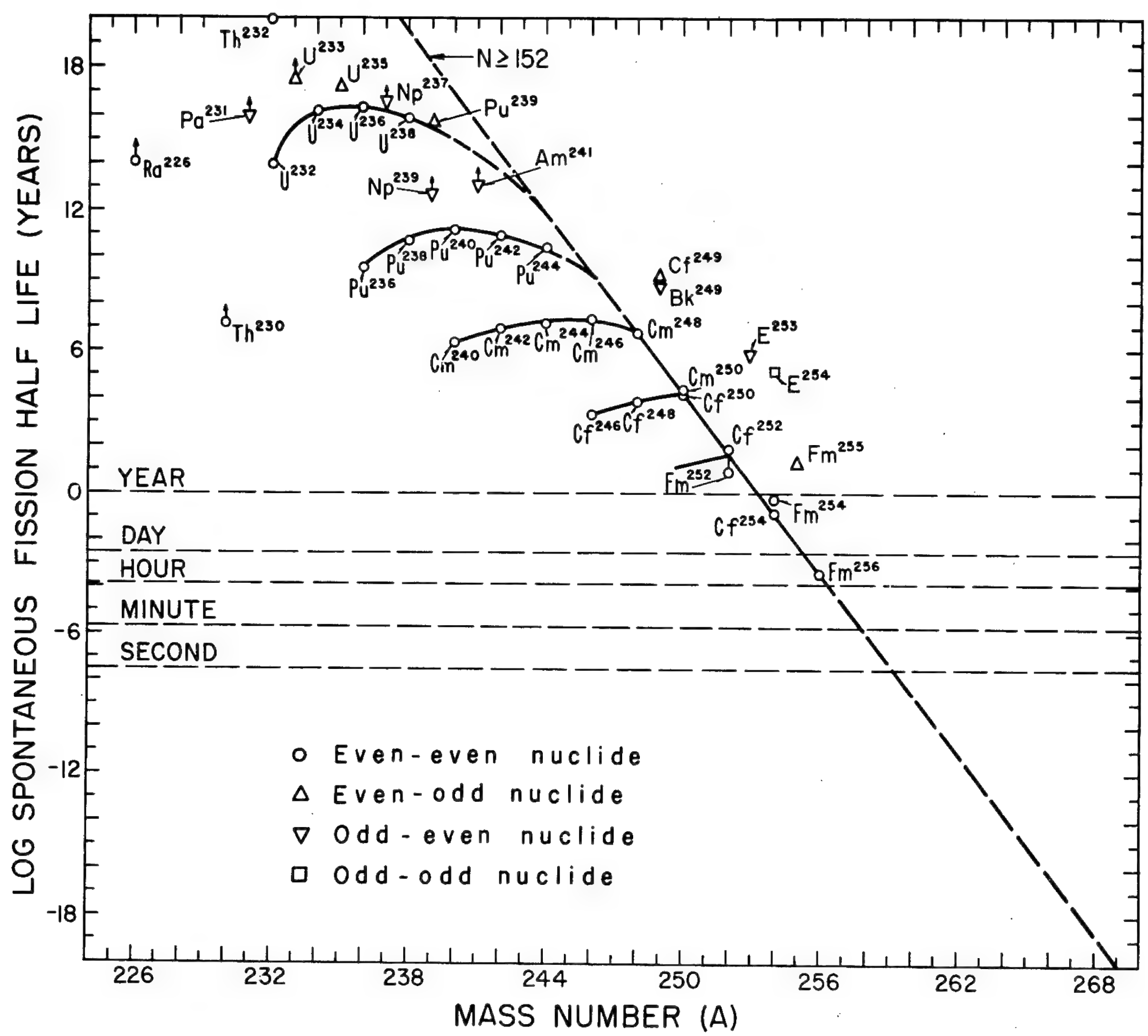

Fig. 1. Spontaneous fission half-lives as a function of mass number (from Foreman and Seaborg[4]).

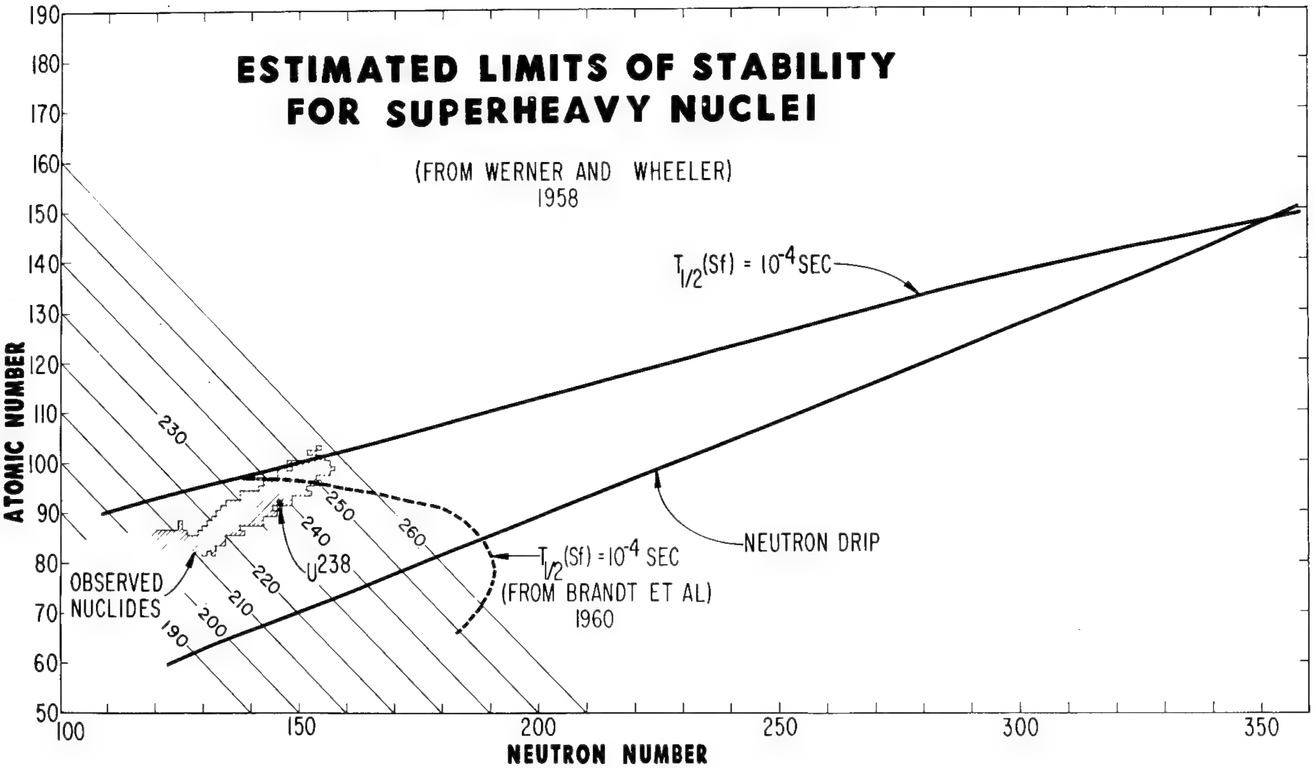

Fig. 2. Estimated limits of nuclear stability for superheavy nuclei (from Werner and Wheeler[12] and from Brandt et al.[13]).

interesting. Lawrencium is thought to be the last member of the actinide series; therefore, it is important to verify the predicted different chemical properties of elements 104 and beyond.

Comparing the relative neutron flux in Mike and in, for example, the HFIR (high flux isotope reactor at Oak Ridge), shows that, on a consistent model, Mike calculates to have given about 2 moles of neutrons per square cm (Fig. 4), while a full year irradiation in the HFIR gives about 0.15 mole per square cm. In addition, if a typical capture path for a reactor passes through a nuclide with either a high destruction cross section or a short spontaneous fission half-life, further irradiation of the sample may prove fruitless. An example of this is the high losses occurring in reactors at californium 254. This set of problems is exchanged for an unknown but presumably different set when we use a nuclear device (the new problems include mainly the question of the systematics of capture and destruction cross sections, and decay rates for increasing mass number of the same element). Figure 5 contrasts the capture paths followed in a reactor with those in a nuclear device.

There have been four successful experiments in the Atomic Energy Commission's heavy element program. In evaluating these, a useful figure of merit is furnished by the ratio of the total amount of elements produced with mass number equal to 246 to that of mass number 245. Since these mass numbers consist mainly of plutonium and americium isotopes, their radiochemical detection is straightforward, and a high degree of confidence can be placed in the ratio. To obtain the thermal flux implied by this ratio, we can either calculate explicity, as in Ref. 13, or make an approximate analytic calculation as follows:

$$R \equiv \frac{N^{246}}{N^{245}} = \frac{2\ 1 - e^{-2\sigma\phi} - 4\sigma\phi e^{-\sigma\phi}}{1 + e^{-2\sigma\phi} - 2e^{-\sigma\phi}}$$

where $\sigma = 0.4b$; $\sigma_{244} = \sigma_{246} = \sigma$; $\sigma_{245} = 2\sigma$;

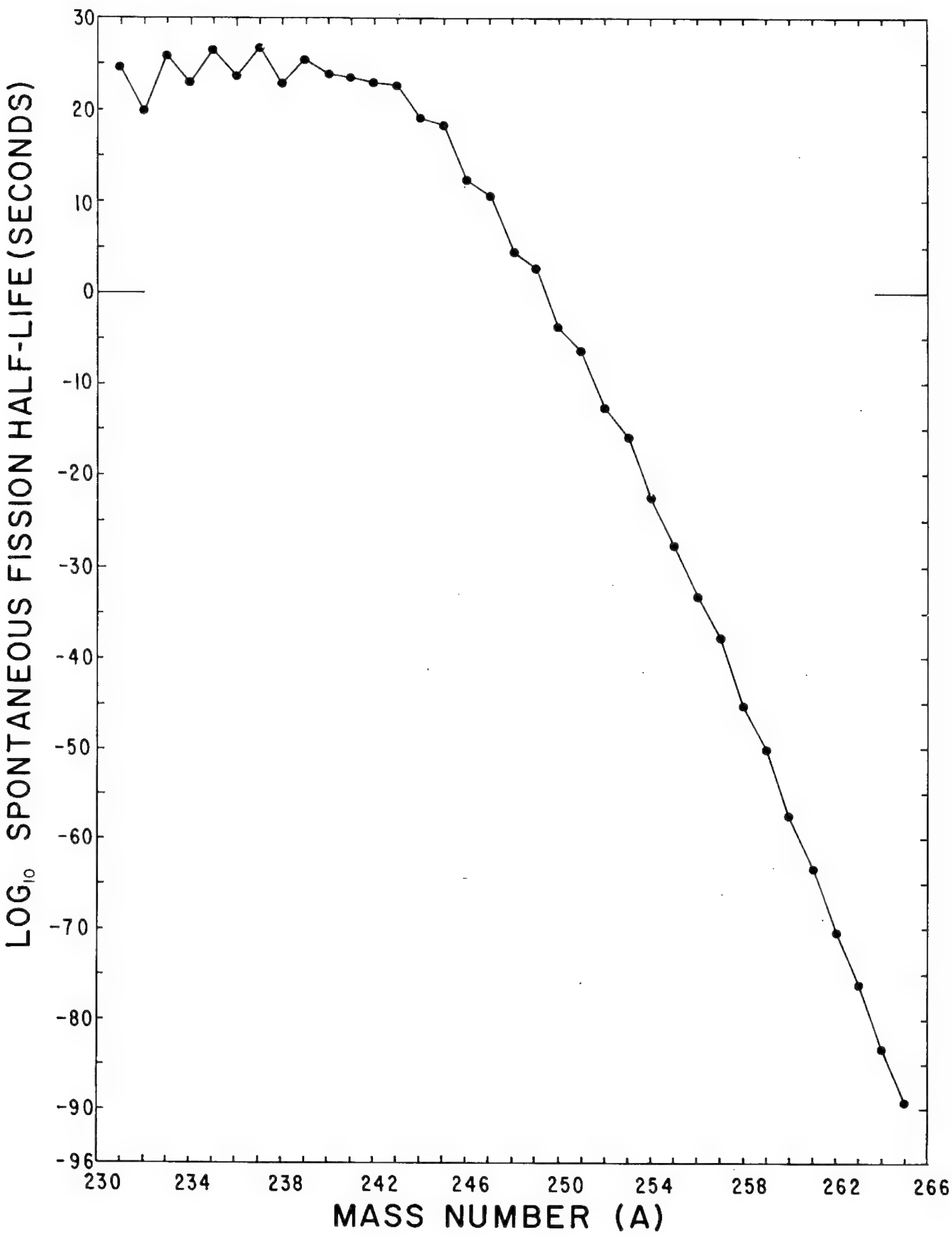

Fig. 3. Spontaneous fission half-lives for isotopes of uranium (from Dorn[14]).

$\sigma_{n,2n} = \sigma_f = 0$; $N^{244} = s/\sigma\phi\,(1 - e^{-\sigma\phi t})$; ϕ is thermal (10 keV) flux. Figure 6 gives results of the approximate calculation. As can be seen from Table I, a significant improvement in thermal flux has been achieved. Concurrently with this, a factor of about 1000 decrease in yield has also taken place. Effects of this reduction in yield are most dramatically shown by a comparison of Fig. 7 which shows the "Mike" experiment results at the Bikini atoll and Fig. 8 which is an overview of a typical test area at the Nevada Test Site. Figure 9 shows a comparison of the element yields of one of the experiments with the Mike results.

As in any other development program, many problems remain. The extreme conditions existing in thermonuclear devices make it difficult to predict, with any degree of confidence, actual configurations and conditions. In addition, in a

typical underground experiment at the Nevada Test Site, the reclaimed fraction of the device is of the order of 10^{-10}. The fact that this fraction is so minute requires extremely sophisticated radiochemical techniques for the isolation and detection of new nuclides. Past experiments have served mainly to define relevant physical parameters; further experiments involving designs presently being studied both at Los Alamos Scientific Laboratory and Lawrence Radiation Laboratory should be able to give considerably higher neutron exposures.

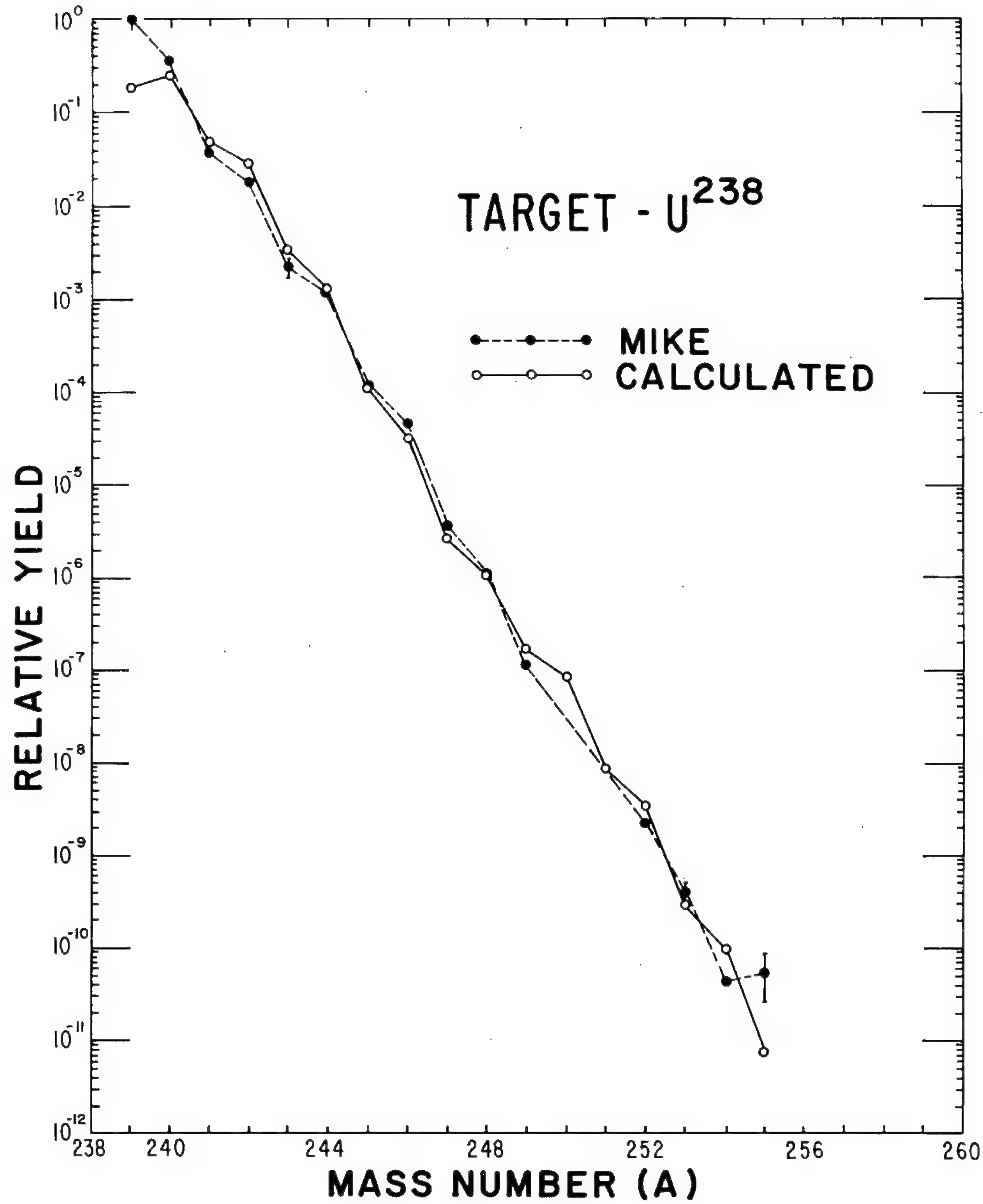

Fig. 4. Comparison of Mike heavy-element yields with the theoretical yields obtained assuming two flux regions (99.99% of the target at 2 moles-n/cm^2 thermal flux and 0.01% at 8 moles-n/cm^2) and spontaneous fission half-lives as predicted by Dorn[5] with the condition that $T_{1/2}$ (spontaneous fission) $\geq T^2_{1/2}$ (β^- decay).

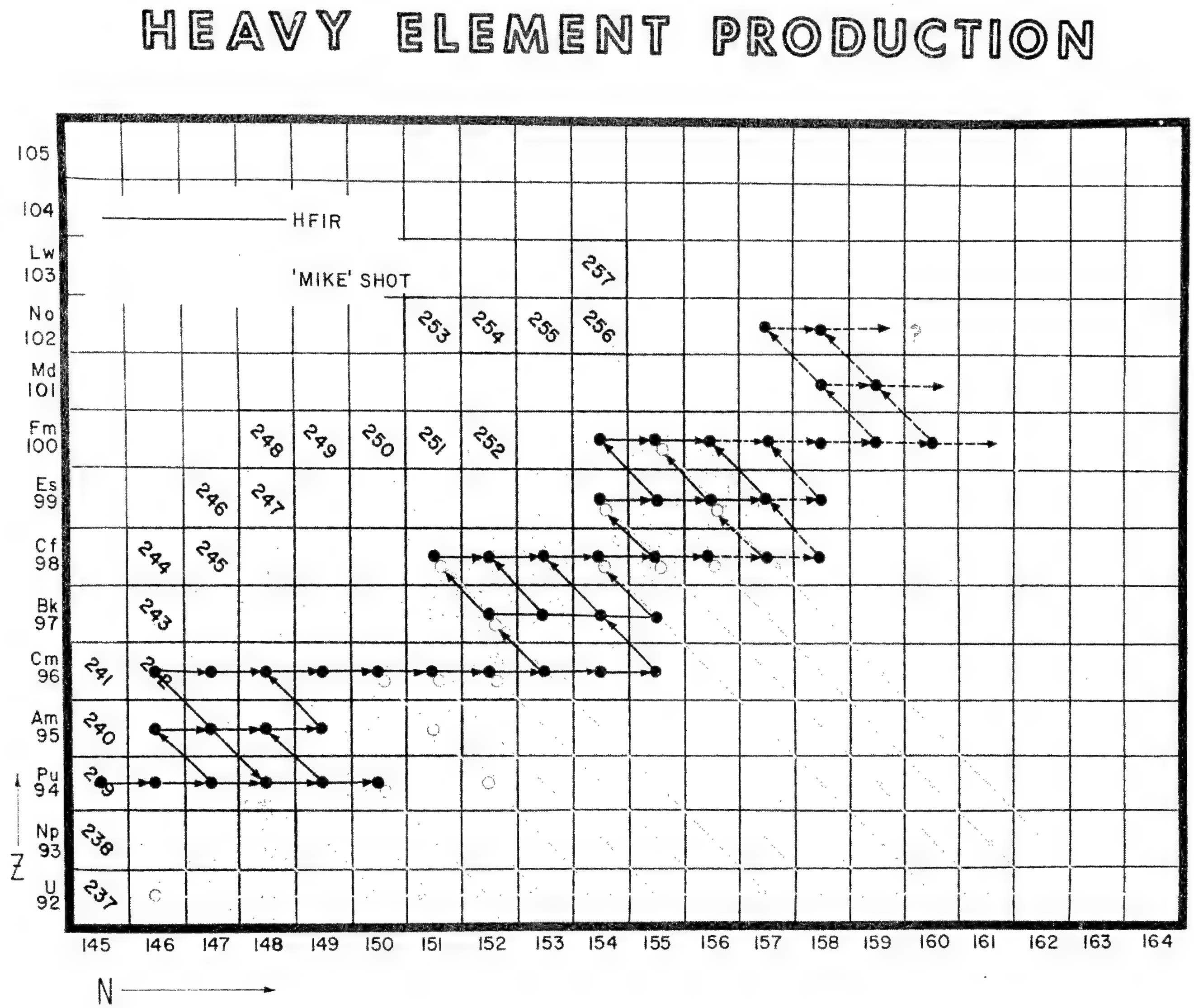

Fig. 5. Comparison of capture paths followed in a reactor with those followed in a nuclear device.

Table I. Heavy-elements program experimental data.

Shot	Sponsoring Laboratory	Date	$R \equiv \frac{A=246}{A=245}$	Implied thermal flux (moles n/cm^2)
Mike	LASL	11/52	0.38	2.0
Anacostia	LRL	11/62	0.48	2.5
Kennebec	LRL	6/63	0.69	4.7
Anchovy	LASL	11/63	0.4	2.0

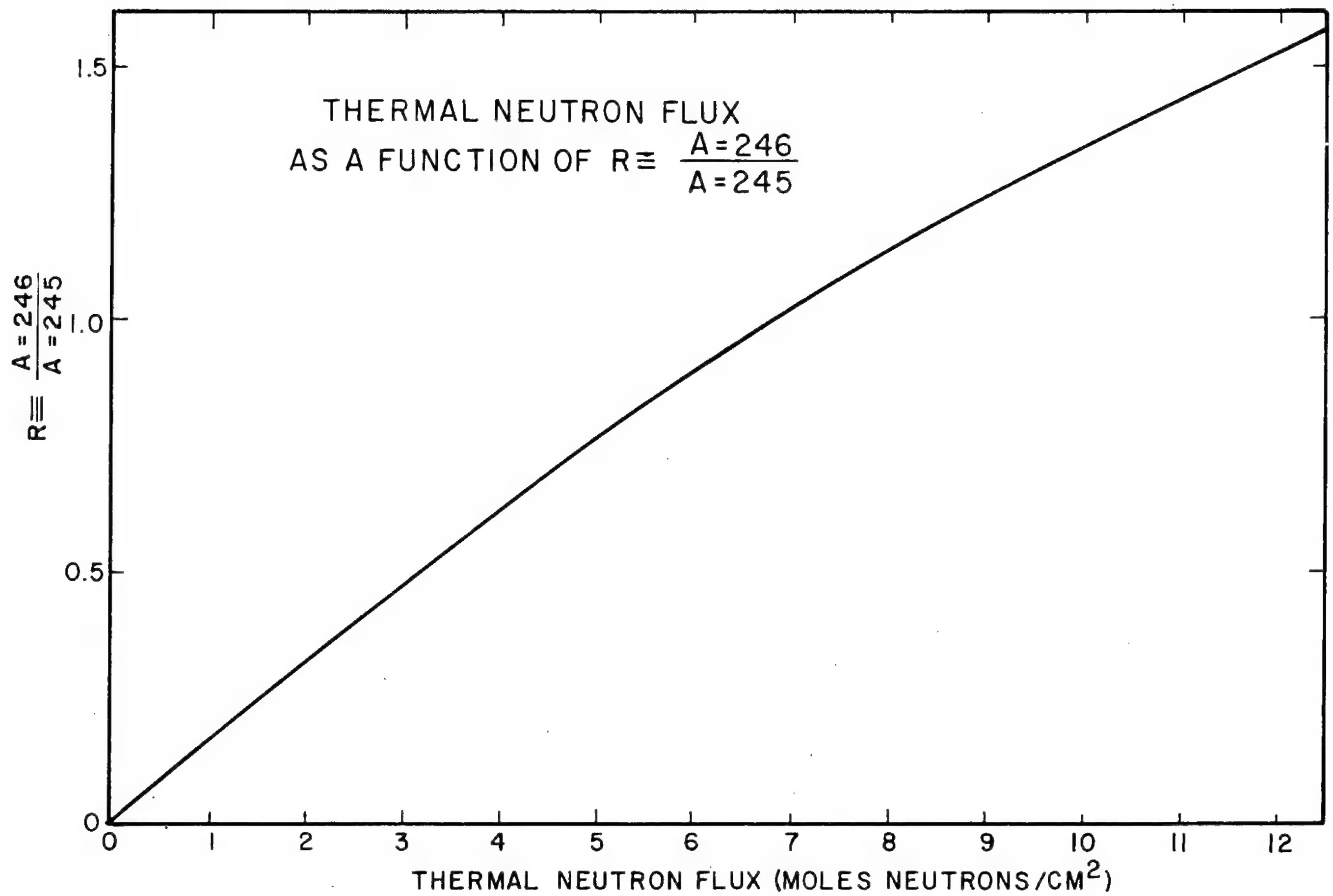

Fig. 6. Thermal neutron flux (10 keV) as implied by the ratio of the amount of mass number 246 to that of 245.

REFERENCES

1. S. A. E. Johansson, Nuclear Phys. 12, p. 449, 1959.
2. Zamick and C. Y. Wong, private communication.
3. I. Perlman, private communication.
4. B. Foreman and G. T. Seaborg, J. Inorg. and Nuclear Chem. 7, 305, 1958.
5. D. W. Dorn, Phys. Rev. 121, p. 1740, 1961.
6. W. J. Whitehouse and W. Galbraith, Nature 169, p. 494, 1952.
7. G. T. Seaborg, Phys. Rev. 85, p. 157, 1952.
8. J. R. Huzenga, Phys. Rev. 94, p. 158, 1954.
9. W. J. Swiatecki, Phys. Rev. 100, p. 937, 1955.
10. A. Ghiorso, Proceedings of the International Conference on the Peaceful Uses of Atomic Energy, Geneva, 1955 (United Nations, New York, 1956), Vol. 7, Paper P/7.8.
11. E. K. Hyde, University of California, Lawrence Radiation Laboratory Report UCRL-9036, 1960 (unpublished).
12. F. G. Werner and J. A. Wheeler, Phys. Rev. 109, p. 126, 1958.
13. R. Brandt, F. G. Werner, M. Wakano, R. Fuller, J. A. Wheeler, Proc. of International Conference of Nuclidic Masses, Hamilton, Ontario, University of Toronto Press, p. 94, 1960.
14. D. W. Dorn, Phys. Rev. 126, p. 693, 1962.
15. H. B. Levy, University of California, Lawrence Radiation Laboratory Report UCRL-4588, 1955 (unpublished).

16. A. G. W. Cameron, Atomic Energy of Canada Limited, Chalk River Report CRP-690, 1957 (unpublished).
17. F. S. Mozer, Phys. Rev. 116, p. 970, 1959.
18. P. A. Seegar, Nucl. Phys. 25, p. 1, 1961.

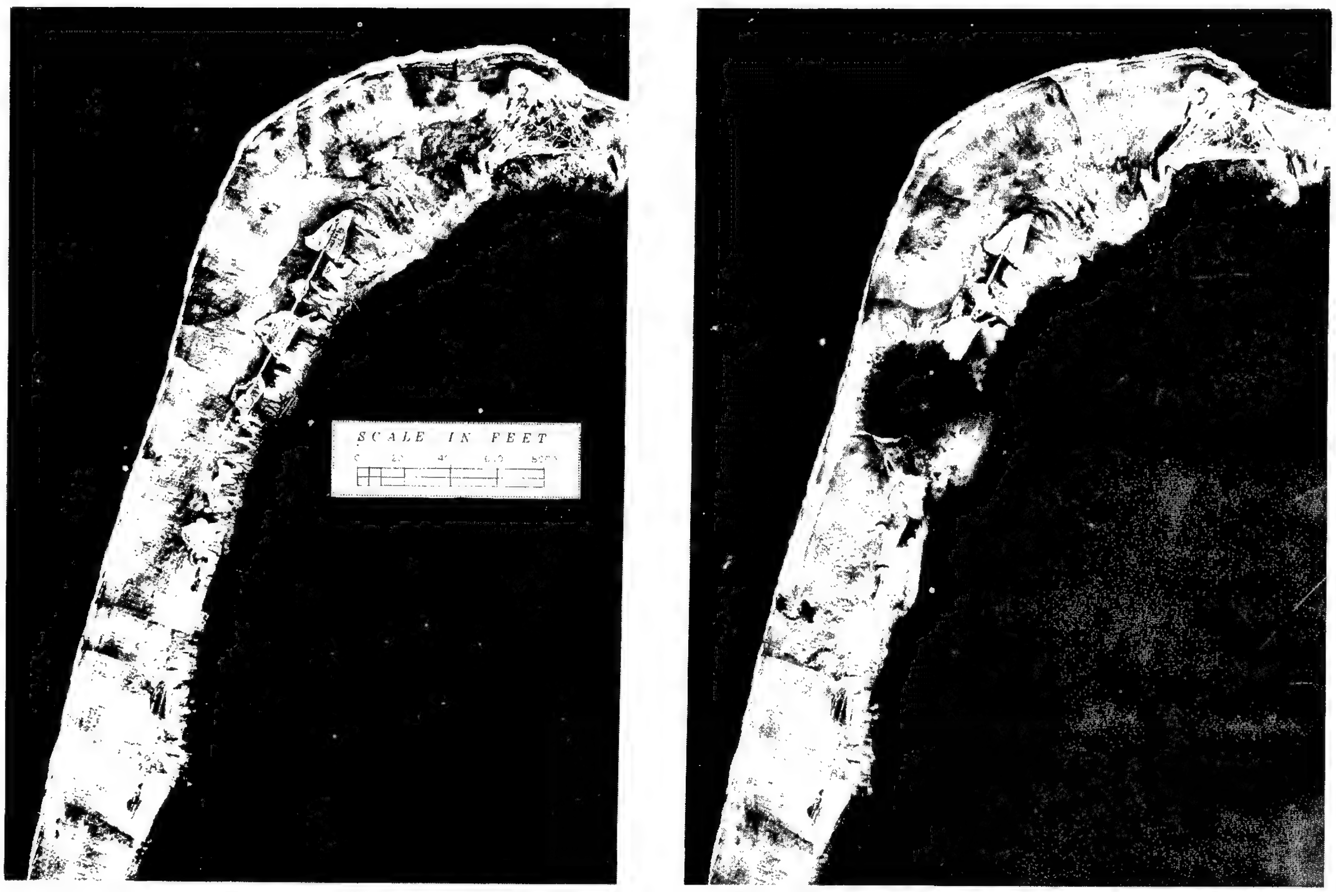

a

b

Fig. 7. Site of the 1952 thermonuclear experiment, Mike.

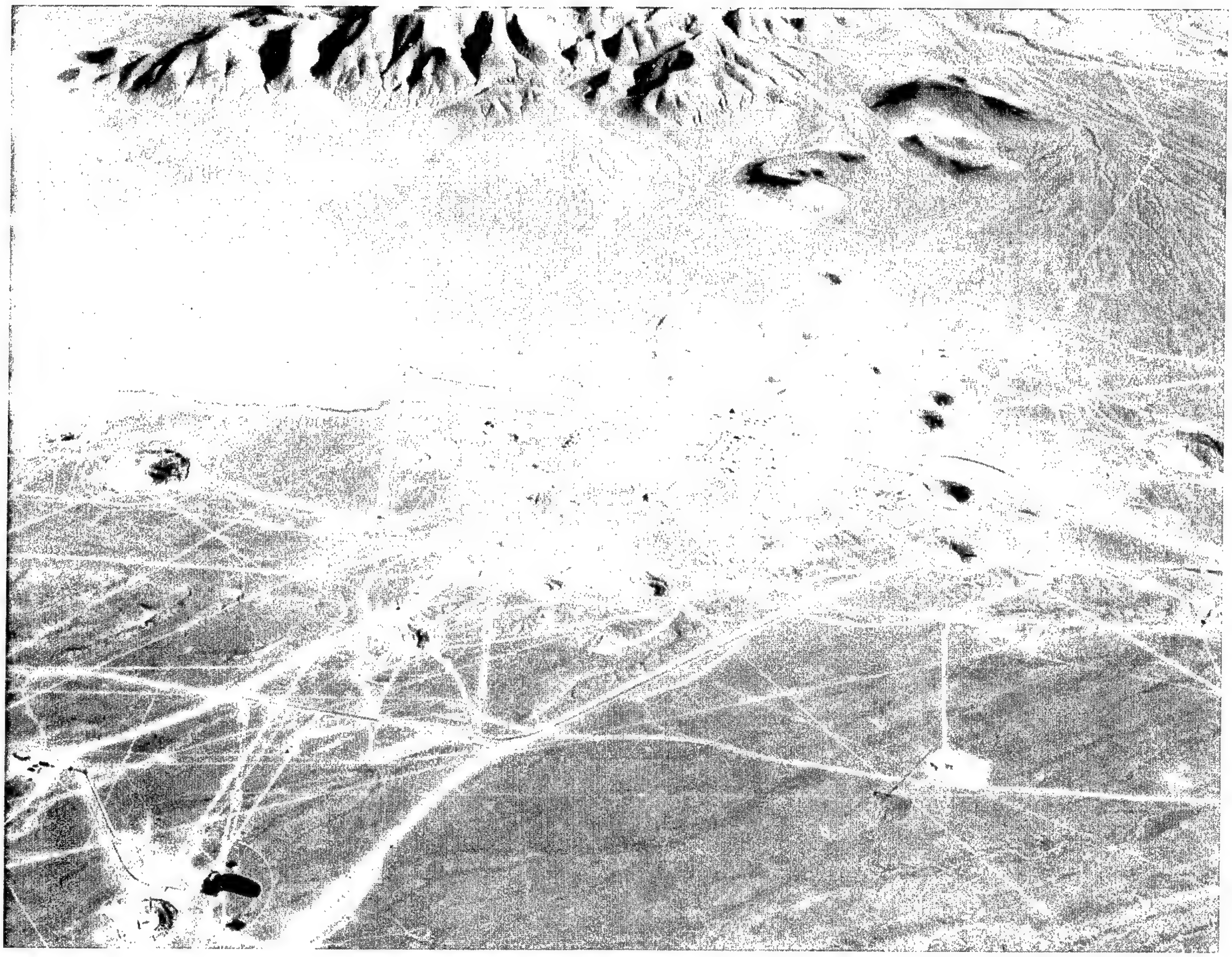

Fig. 8. Test area 9 at the Atomic Energy Commission's Nevada Test Site.

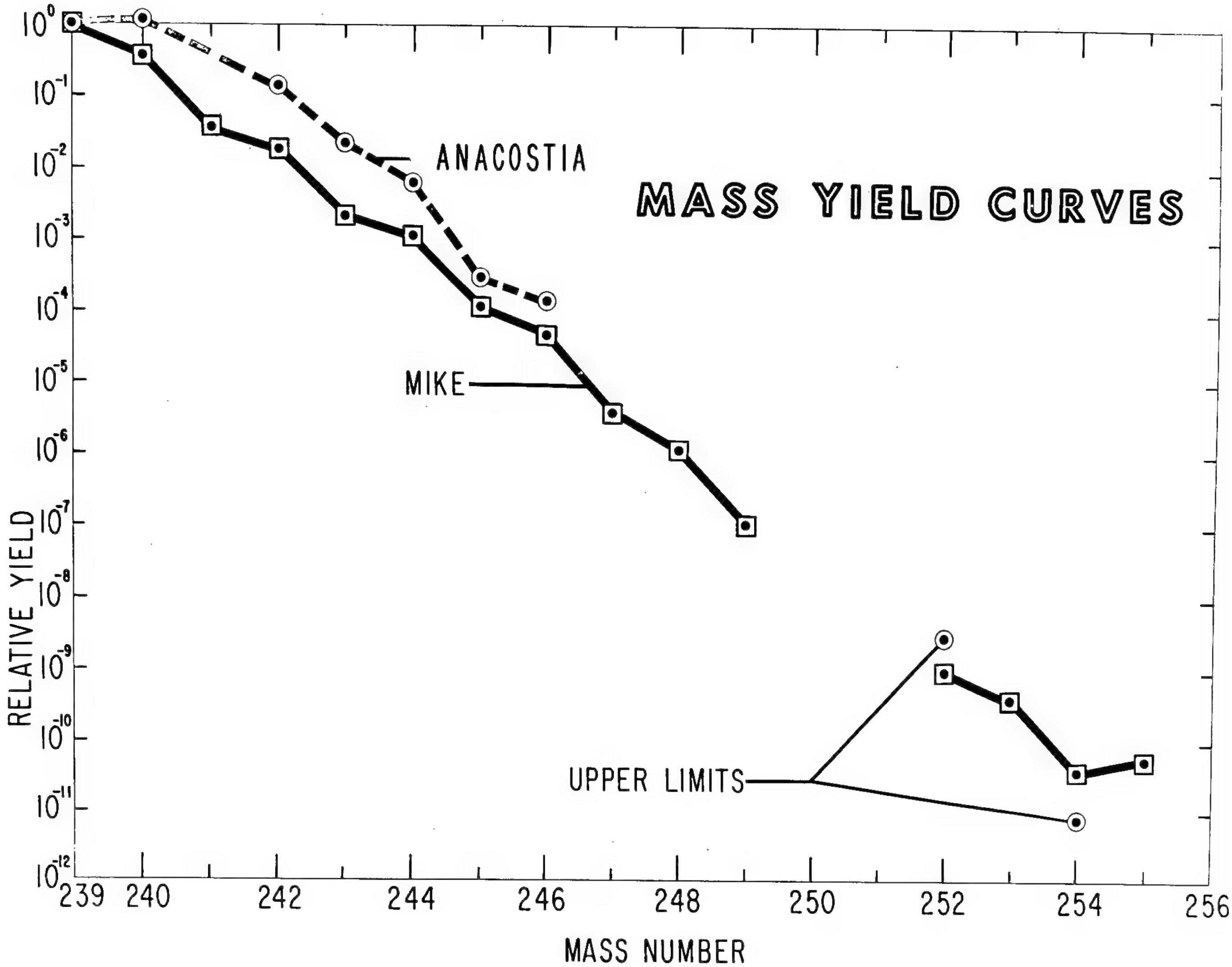

Fig. 9. Comparison of the element yields of the Anacostia experiment with Mike experiment.

BIOGRAPHICAL SKETCH OF AUTHOR

David William Dorn was born in 1930 in Detroit, Michigan. His undergraduate work was done at Purdue University from which he was granted the B. Sc. degree (physics) in 1952. He subsequently served with the United Nation's Forces in Korea until 1955. After release from the Navy, he returned to Purdue and completed his work for the PhD in 1959. Since graduation, he has been with the Lawrence Radiation Laboratory, Livermore.

APPLICATIONS OF NUCLEAR EXPLOSIVES TO MEASUREMENTS OF NEUTRON INTERACTIONS BY FOIL ACTIVATION: THE "WHEEL" METHOD

G. A. Cowan

Los Alamos Scientific Laboratory, University of California
Los Alamos, New Mexico

ABSTRACT

Neutrons from nuclear explosions which are resolved in energy by time of flight can be observed directly by measurement of a current output from a suitable detector, or indirectly by delayed counting of activation products in a foil detector. The foil technique requires rapid transport of detector material past a collimating slit and has been dubbed the "wheel" method. This method is particularly advantageous where subsequent radiochemistry is necessary for further discrimination of a complex neutron interaction, as in measurement of individual fission product yields as a function of neutron energy. Another advantage is that the necessary field equipment is relatively simple. Its chief disadvantage is that, for statistics equivalent to the direct method, channel acceptance widths must be an order of magnitude larger and achievable neutron energy resolution is correspondingly poorer. In addition, there are many neutron interactions of interest which can be observed directly, but which produce no useful activation product.

In the "wheel" method, the collimating slit width, speed of the wheel, and distance from the source ordinarily define the energy resolution since the pulse width at neutron energies of 100 eV and higher is not a limiting factor. At 300 meters from the source, a detector velocity of 3×10^4 cm/sec, and a collimating slit width of 0.1 cm, the energy resolution available is $(3.1 \times 10^{-2}\ E_{eV}^{1/2})$%; e.g., 0.3% at 100 eV. The resolution available from a direct recording method, at a pulse width of 2×10^{-7} sec and a corresponding channel width, is an order of magnitude better. Below 10 eV, due to pulse broadening of the neutrons by moderation, the two methods have comparable resolution.

The "wheel" method has been used in three experiments to measure the symmetry of fission in U^{235} at individual resonances and in one experiment to measure resonance capture cross sections of a variety of elements. Some representative results are discussed.

The very large fluxes of energy-resolved neutrons which are available from nuclear explosions provide an opportunity to use a form of data recording which is impractical for neutron time-of-flight measurements in the laboratory. I am referring to data obtained by foil activation techniques in which the neutron interaction produces a radioactive nucleus. This radioactive product is subsequently recovered and counted in the laboratory. When this technique can be used, it has certain advantages to recommend it:

1. Fast detector and data recording equipment are minimized.
2. Subsequent radiochemistry can discriminate between complex neutron interactions, as in the measurement of individual fission product yields or the simultaneous measurement of (n, 2n), (n, p), and (n, α) cross sections.
3. Counting of multiple samples can provide redundant data with a consequent increase in confidence level.

However, the activation technique will frequently not be the method of choice because it demands large amounts of laboratory work compared to direct electronic data recording and usually requires larger channel acceptance widths for comparable statistics. In addition, there are many neutron interactions of interest which can

*This work performed under the auspices of the U. S. Atomic Energy Commission.

be observed directly, but which produce no useful activation product.

We will consider a nuclear explosion which produces a pulse of neutrons of assorted energies which is 10^{-7} second FWHM. The time required for a neutron of energy E_n to reach the target over a flight path of length D is $t = D/V_nE^{1/2}$. Then $dt/dE = - D/2V_nE^{3/2}$. The detector material is transported past a collimating slit of width w at a speed V_{wh}. Neutrons of a given energy will interact with the detector at a distance S from the starting point (the position of the detector when the explosion went off) given by $S = V_{wh} t = V_{wh} D/V_nE^{1/2}$. Then $dS/dE = - V_{wh} D/2V_nE^{3/2}$. At 300 meters from the source, with a detector velocity of 3×10^4 cm/sec and a collimating slit width of 0.1 cm, the energy resolution available is $(3.1 \times 10^{-2}E^{1/2})\%$; e.g., 0.3% at 100 eV. These conditions define a channel acceptance width of 3.3 μsec. This is about ten times wider than the over-all pulse width which is intrinsically available from the initial pulse width plus moderation time at 100 eV. The moderation time increases inversely with the square root of neutron energy but is comparable to the channel width only below 1 eV. Thus, over most of the epithermal region, the resolution is determined by the channel width and is, for the conditions given here, 10 nanoseconds per meter.

A 10-kt explosion can provide about 10^{11} neutrons/cm^2-eV at 100-eV energy at 300 meters distance. If the detector is 1% black for a given neutron reaction, and the slit-width corresponds to 0.3 eV at 100 eV, then the number of neutron interactions in a channel width is 3×10^8/cm^2, a number adequate to provide 1% or better statistics in reasonable counting times unless the product has a very long half-life or is produced only a very small fraction of the time.

My own experiments with these time-of-flight energy-resolved neutrons were conducted in the following way: moderated neutrons from the nuclear explosion were collimated and fell on a wheel which rotated rapidly past the collimating slit. In the Gnome experiment the wheel velocity and slit width defined a channel acceptance width of 34 μsec.

Exposed U^{235} metal foil attached to the wheel was autoradiographed and resonance fission bands showed as discrete bands defined by the collimator. These bands were cut out and analyzed for fission products representative of both asymmetric and symmetric modes of fission, typically Mo^{99} and Ag^{111}. The data from the Gnome experiment indicated increases in yields of symmetric fission products as compared to thermal fission at four levels in the neutron energy region 8.8 to 40 eV. Thirteen levels showed a decrease in symmetry. The relative frequency of symmetric fission varies by nearly a factor of two from level to level. It has not yet been demonstrated that this effect is spin dependent.

The "wheel" technique was also used by Lawrence Radiation Laboratory experimentalists in the Gnome event to measure the neutron capture excitation functions of U^{238}, Th^{232}, Au^{197}, and Hf^{180}. Each of the neutron capture products from these target isotopes is a beta-emitter of reasonable half-life and can be measured either by radiochemical analysis or by direct foil counting. Both methods were used in this experiment. Since the objective was to measure capture cross sections, it was necessary to know the neutron flux as a function of energy. The system designed to measure this flux consisted of a He^3 scintillation counter with photomultiplier outputs displayed on oscilloscopes and recorded on film. These film records were lost when sufficient radioactive debris vented to fog the emulsions.

Although no absolute cross sections were obtained from the experiment, the data demonstrated good resolution of the well-known resonances in U^{238} in the 20 to 100 eV region. The absence of neutrons at energies below 10 eV indicates closure of the pipe, premature closure of a B^{10} neutron shutter across the collimating slit, or a high moderator temperature. It is one of the limitations of this method that fluxes of neutrons below 10 eV will fall off sharply due to the difficulty of keeping moderator material in the vicinity of a kiloton nuclear explosion sufficiently cold. Where neutrons are required in the few eV region, it may be necessary to use devices of fractional kiloton yield and to utilize a shorter flight path.

In the next wheel experiment, planned for this spring, we expect to characterize several resonances in plutonium fission by their symmetry. Some work at the MTR reactor in Idaho indicates that the effect from level to level will be an order of magnitude greater than in U^{235}. It may be possible to conclude that the effect on symmetry is spin-dependent or is the consequence of changes in multiple channels available for fission

at each resonance. If the effect is demonstrated to be spin-dependent, it will be a useful means for characterization of the spins of a large number of levels in fissile elements.

BIOGRAPHICAL SKETCH OF AUTHOR

George Arthur Cowan is a native of Worcester, Massachusetts. His educational and professional background is as follows: Worcester Polytechnic Institute, B.S. Chem., 1941; Carnegie Institute of Technology, D. Sc., Chem., 1950; Research Asst., Palmer Lab., Princeton Univ: cyclotron, 1941-42; Research Asst., Metallurgical Lab., Univ. of Chicago, 1942-1945 (stationed Mallinckrodt, St. Louis, 1942; M.I.T., 1942; Oak Ridge, 1944 (Research Asst., Pupin Lab., Columbia Univ., 1945; Research Asst., Los Alamos Sci. Lab., 1945-1946 (stationed Operation Crossroads, Bikini, 1946); Teaching Asst., Instructor (graduate student) Carnegie Inst. of Technology, 1946-1949; Staff Member, Los Alamos Sci. Lab., 1949-Present (Group Leader, Radiochemistry Group, 1955-Present; Assoc. Division Leader, Test Division, 1957-Present)

APPLICATIONS OF NUCLEAR EXPLOSIONS IN CROSS-SECTION MEASUREMENTS

B. C. Diven

Los Alamos Scientific Laboratory, University of California
Los Alamos, New Mexico

ABSTRACT

The use of underground nuclear explosions as pulsed neutron sources for neutron measurements is discussed. Comparisons are made with laboratory neutron sources and the types of measurements especially suited to the explosion source are described. Before the explosion source can be exploited properly, many questions must be answered concerning production and use of beams from these sources. An outline is presented for a program of studies of detectors and neutron beam characteristics. This program will develop some of the techniques necessary to use nuclear detonations in measurements which cannot be carried out in the laboratory.

INTRODUCTION

Except in selected energy ranges, monoenergetic neutron sources are not available. Consequently, many cross-section measurements must be made with continuous spectra of neutrons. In order to obtain a cross section as a function of neutron energy, a method must be devised to sort out the neutrons so that effects may be studied one energy at a time. The pulsed-beam time-of-flight method has been used for several decades as a solution to this problem. Neutrons are produced in bursts. The source may be a reactor, in which case the beam may be mechanically chopped by a high-speed rotor. The source may be an accelerator which can be arranged to produce neutrons in bursts of any desired duration and repetition rate. The neutron detector is located at a distance from the source and the neutrons from one burst arrive at the detector at different times, depending upon their velocities. The arrival time therefore measures the energy of the neutron. An example of a cross-section measurement is the measurement of a fission cross section. A thin layer of fissionable material is deposited on a metal backing. A detector of fission fragments, such as a solid state detector, is placed near the fissionable layer. The detector responds promptly with a pulse for each fission fragment which strikes it. The time between production of the neutron burst and the detector pulse is measured and the event is recorded in the appropriate time channel of a multichannel time analyzer. Each time channel corresponds to a different neutron energy. The number of events recorded in a channel is proportional to the number of neutrons of that energy which struck the fissionable material and to the fission cross section. An additional detector which makes use of a known cross section is used to monitor the number of neutrons corresponding to each time channel.

A nuclear explosion produces an intense burst of neutrons in a fraction of a microsecond. It is possible to use these neutrons in time-of-flight experiments which are analogous to the laboratory experiments that we have just described. The differences in techniques in the two cases result primarily from the very intense pulse produced by the explosion relative to the intensities produced by accelerators. Cross-section measurements with explosion sources generally involve such a large number of events in a short time that our detectors cannot analyze each nuclear event separately, but must produce a signal which is proportional to the rate at which these events are taking place. We can use the example of a fission cross-section measurement again. Let's assume we place our sample of fissionable material a few hundred meters from an underground nuclear explosion. We provide a flight path in vacuum for a narrow beam of neutrons which traverse the sample. Our solid state detector is placed out-

side of the beam but near the sample where it can catch fission fragments. A few microseconds after the explosion, the fastest neutrons begin to arrive. Fission events are produced in the sample. Each fragment which strikes the detector produces a small amount of charge (a few $\mu\mu$ Coulombs), but the rates are so high (10^4 per microsecond) that a current is produced at the output of the detector whose amplitude is proportional to the product of neutron flux and fission cross section. A record of this current as a function of time allows the calculation of the cross section as a function of neutron energy.

Now let's compare laboratory sources and explosion sources. Explosion sources provide us with neutrons having energies from a few tens of electron volts to 14 million electron volts (MeV). Two types of accelerators are needed to cover the same range. Above 100 thousand electron volts (keV) the Van de Graaff accelerator is the most useful. Monoenergetic neutrons can be produced and the entire range can be covered with an energy resolution better than 1%. On the other hand, the source strength is low if the neutron energy spread is kept low. The total number of neutrons produced per year by a Van de Graaff machine is less than 10^{16}. The explosion source can produce a few moles of neutrons per pulse since we get about 10^{24} neutrons for each 4 kilotons of yield. The energy resolution which can be achieved with the explosion source depends upon flight path, and with underground explosions is 1/2 to 5% at 14 MeV compared to 1/10 to 1% with the Van de Graaff. At the lower energies below 1 MeV, the explosion source has better resolution than the Van de Graaff even at a short flight path such as 100 meters.

At energies below 100 keV, the best laboratory machines for producing neutrons are electron linear accelerators operating at 20 to 50 MeV and proton accelerators operating at a few hundred MeV. These machines produce continuous spectra and are more easily compared to the explosion source because time of flight techniques are used with both. The accelerators can produce something like 10^{21} neutrons per year, compared to 10^{24} per pulse for the explosion. The pulse duration is similar for each. If a neutron moderator is used to intensify the low-energy neutrons, the pulse duration is determined by the moderator. When unmoderated sources are used, 1/10-microsecond resolution is commonly used with accelerators and can also be achieved with explosion sources. Energy resolution depends upon the pulse duration and the flight path. The usual figure of merit is the time resolution divided by the flight path. The longest flight paths on accelerators are about 300 meters. This would be an average path for an explosion source. The resolution for both systems is similar, although the explosion source has enough intensity to make longer flight paths possible. The intensity of the neutron emission from the source is very different in our two examples. All 10^{24} neutrons are emitted from the explosion source in less than 10^{-7} second to produce a source strength of 10^{31} neutrons per second. The accelerator produces 10^{12} neutrons per burst, which amounts to less than 10^{20} per second. The repetition rate of 10 to 1000 pulses per second from the accelerator compares to a few per year for the explosion source.

RELATIVE USEFULNESS OF LABORATORY AND EXPLOSION SOURCES

Advantages of the Explosion Source

Now that we have listed the main characteristics of our source, let's compare it to other methods of cross-section measurements. First, we'll look at the advantages of the bomb source. We will list these advantages as:

1. good resolution
2. high average rate of production of neutrons
3. high instantaneous flux.

If we are talking about 0.1 nsec/m resolution, the explosion doesn't have any overwhelming advantage. For example, the time-of-flight setup at Columbia University's Nevis cyclotron has about this resolution for their total cross-section measurements in the energy region from a few eV to 100 keV. It is worth noting, however, that the Columbia group is working on total cross sections rather than partial cross sections for which intensity is often a serious problem. In the MeV region we can have about 2-1/2% energy resolusion at 14 MeV. This is not as good as can be obtained with a thin target on a Van de Graaff, but it is as good or better than most cross-section measurements because of intensity problems when measuring partial cross sections. Let's con-

clude, then, that we have no great advantage over existing accelerators so far as energy resolution is concerned.

Our next advantage is high average rate of production of neutrons. The number of neutrons produced in a few bomb shots is much higher than the number produced in a year by any accelerator. The advantage is only two or three orders of magnitude over the best electron linacs. It is even possible that a proton accelerator which was designed specifically for use as a pulsed neutron source might begin to approach the bomb source in average production rate. However, no such machine now exists and we should expect that measurement of some of the partial cross sections which require hopelessly long running time on accelerators will be done with bomb sources.

The first two "advantages" are important, but not overwhelming. The third is the most important. The neutron production rate at a few moles in 0.1 microsecond exceeds 10^{31} neutrons/second. We need not consider any competition from accelerators in instantaneous flux. Ultimately, then, we must expect the most spectacular nuclear explosion experiments to be those which exploit the high flux from this source. One type of measurement which can be made only with explosion sources is measurement of cross sections of highly radioactive samples in which the background produced in a detector by the source greatly exceeds the desired effect produced by the laboratory neutron beam. In this case the intense flux is crucial. An example of a measurement of this type would be the capture cross sections of Pa^{233} or of some of the fission products. Another would be the neutron-induced fission cross section of Cm^{244} or Cf^{252}.

To summarize the discussion of advantages, we can expect bombs to help produce good resolution measurements of cross sections requiring large integrated fluxes and especially cross sections of very radioactive materials.

Disadvantages

Now, to be honest, we must list some of the disadvantages of using explosion sources for cross-section measurements. We will grade them from unimportant to sometimes crucial disadvantages:

1. field work away from home
2. one-shot affairs with no chance of correcting mistakes as an experiment progresses
3. large numbers of experiments and experimenters to produce conflicts in measurements
4. no possibility to record individual events and hence no pulse-height analyses or coincidence criteria.

First, let's dispose of No. 1. A reasonable program of measurements on three or four shots per year would take one away from the Laboratory for about as much time as we spend at meetings like this. Let's guess about a week in the field per shot. Even though this may be a little optimistic, it is not a major factor in any program and it is similar to the way many groups make measurements on accelerators away from their home laboratories.

Now consider No. 2. It is true that these experiments are one-shot affairs. However, they are only a little more extreme than a session on an accelerator. Remember that we would plan to space our shots as uniformly as possible and that one can repeat his experiments about as often as accelerator people do on the elaborate time-of-flight setups. These experimenters must not have any major errors in setup when they go on the machine for a 2-week run. For both the explosion and the accelerator experiments, a lot of very careful testing in the laboratory is in order before the final "run" is made. It is true, however, that minor faults can be corrected in the laboratory experiments during a run and that one must be more careful in prerun testing of equipment on the bomb shots.

Our third disadvantage is more real. The effort involved in producing a good collimated beam is large enough that there will always be a tendency to get as many simultaneous experiments as possible on each shot. The result is a formidable problem in being sure that every one "gets the word." Fortunately, our test divisions have been working under these conditions for many years and seem to be very proficient at minimizing confusion.

All of the preceding "disadvantages" were really nuisances—not serious disadvantages. The fourth is a genuine disadvantage. At the very high fluxes we use, it is hopeless to make use of much of the information concerning the reactions which are taking place in our detectors. We cannot

measure the energy released in individual events in order to bias out certain backgrounds. Neither can we make use of coincidence requirements to select the type of events we want. While our high beam intensities override certain types of background (sample-associated), we have fewer means of discrimination against other kinds of background (beam-associated). Furthermore, some types of experiments become impossible. An example would be the detection of (n, 2n) reactions by observation of pairs of neutrons.

NECESSARY DEVELOPMENTS TO PRECEDE A NUCLEAR MEASUREMENT PROGRAM

Detector Development

The detectors which will be used in cross-section measurements must be capable of operating at very high output currents. Individual events will not be recorded. We will require a large number of events in one resolving time which can be as small as 10^{-7} second. Furthermore, the nature of the neutron spectrum requires a very large dynamic range for the detectors because the amplitude of the detector signal will vary not only in proportion to the cross section being studied, but also in proportion to the rate of arrival of neutrons. In extreme cases we may require that a detector be linear over a factor of 10^4 in output current. Such a range may extend from 1 milliampere to 10 amperes. It is also important that the detector operate properly at a low signal level even though the signal may have been a hundred times larges a few microseconds earlier. In other words, a large pulse in the detector must not be followed by even a 1% "tail" that lasts as long as a few microseconds. Rather little is known about detectors when operated under these conditions. It does seem likely that some type of solid state detector will be satisfactory for many applications. We are able to duplicate some of the conditions in the laboratory by subjecting the detectors to intense pulses of charged particles from a Van de Graaff. With these methods we have been able to rule out some types of detectors as candidates for field use, but there remain some which seem likely to be satisfactory if used with caution. We plan to develop solid state detectors for protons, alpha particles, fission fragments, and gamma rays.

Neutron Beam Characteristics

One standard problem in all pulsed-beam time-of-flight systems with continuous spectra is the problem of beam purity. All neutrons are emitted from the source in a short period of time. They have a continuum of energies which become sorted out over the long flight path so that the time of arrival of a neutron at a detector is a measure of its energy. If the source were a point source and no scattering material existed, the arrival time would be an ideal measure of velocity, the uncertainty in velocity being only the Δt during which neutrons were emitted. Actually, our source (the same as an accelerator source) is surrounded by a great mass of shielding material. The neutrons can bounce around the room which contains the source and finally scatter down the evacuated flight path. The extra distance covered while scattering about the room produces a longer flight path and hence an error in the measure of the energy of these neutrons. A similar, but smaller effect, is produced by neutrons which scatter from bomb materials to produce an error in flight path. Scattering from the walls of the collimater produces a small error in flight path, but if the neutrons are inelastically scattered part way down the path a large change in energy is produced which destroys the relationship between energy and time for these neutrons. This beam purity problem is a familiar one for experts in the accelerator time-of-flight business. The very long flight paths available with explosion experiments and excellent shielding along this path are favorable circumstances for the design of a collimator. We have every reason to believe that we can produce a beam of neutrons of about 1 square centimeter which will have very little contamination of "wrong energy" neutrons. Of course it remains necessary that we demonstrate this fact and also that we have a measure of this contamination in order to handle properly the subtraction of backgrounds.

Some of the techniques for investigating beam purity have been well worked out in the resonance region (up to 10 keV) which has been covered with continuous sources. The sort of distortions which are produced by scattering in the vicinity of the source produce a low-energy "tail" on a resonance and are best studied by observing the distortion and broadening of a very sharp isolated

resonance. The effect of scattering far from the source is studied by blacking out the beam at certain resonances with a scattering sample which is thick (that is, transmits no neutrons at resonance), but is fairly transparent at most energies. The rate of detection of neutrons at resonance where no correct energy neutrons can reach the detector gives a measure of the fraction of the beam which consists of "bad" neutrons. In the MeV region, collimators are studied in the laboratory with monoenergetic sources, using the time of flight to measure contamination of the beam. Since we cannot obtain a monoenergetic source from a nuclear explosion, we will be forced to develop some new techniques. While some time may be required, I have no doubt that the necessary measurements of beam purity can be made at all energies. Most of our first experiments will have to be concerned with investigations of detector response and of beam quality.

Data Storage

Those programs which use accelerators for pulsed sources generally have data storage and processing as a major part of the job. Typically, a week or two on an accelerator produces enough data to bury the experimenter for months. The problem may be at least as severe for the explosion source work because several orders of magnitude more neutrons are produced and a much larger energy range can be covered at once. At this point we derive some advantage from the fact that we don't have to handle individual events. We receive from the detector an analog signal whose amplitude is associated with the quantity we wish to measure. It is not necessary to sort and store each of the millions of events which occur. This fact reduces the complexity of the data collecting equipment, but the storage and processing remain formidable.

A well-developed data storage procedure for bomb tests uses oscilloscope recordings. A photograph of an oscilloscope trace is actually a rather efficient method of storage. With care it is possible to record both vertical and horizontal positions of an oscilloscope spot to one part in a thousand. This allows one million bits of information to be stored on the photograph. One makes the necessary compromise between the number of horizontal (time) points he wants to record and the precision (number of vertical points) in signal amplitude and applies several traces to one oscilloscope by use of multiple sweeps and multiple beams. It is clear that a lot of useful data can be recorded with oscilloscopes, but probably a better method for the future will involve magnetic storage of some sort. Magnetic tapes are improving in frequency response so that in a few years it will probably be possible to record on tape or drums at the desired rate. In the meantime, oscilloscopes will allow us to record the necessary information to perform our preliminary experiments.

LASL PROGRAM

Several groups at Los Alamos are involved in preparations for cross-section measurements with explosion sources. In general, they are directed toward understanding the behavior of various types of detectors and to measurement of the quality of the beam emerging from the collimating system. Some prototype experiments are planned. These will consist of measurements of well-known cross sections in an effort to make a proof test of an experimental system. A realistic time scale for development of the necessary methods of measurement is about a year, with three or four shots involved. In that time, not all problems will be solved and probably not all of the desirable detectors will be developed, but we should know enough by then to start getting some very interesting results. Any little tidbits of new information we might glean in a shorter time will be appreciated, but we don't expect very much in a short time. Naturally, there won't be a magic date after which all our problems are solved. On the contrary, the methods must undergo continuous development so that after we learn to do some measurements reliably, our program will consist of some measurements of cross sections by methods already understood while at the same time we will be working on new methods for other kinds of measurements which we don't yet know how to do.

SUMMARY

In summary, nuclear detonations supply a very intense burst of neutrons which in many ways should prove to be superior to conventional accelerators for neutron cross-section work. The most

attractive applications will consist of measurements on highly radioactive samples. Another category will be certain partial cross sections which require a large number of neutrons. Energy resolution will be as good or better than can be obtained in the laboratory. If a vigorous program is undertaken now with a dozen staff members working on three or four shots, we probably can start getting new cross-section data in a year's time. The data can be the sort that are needed for weapon and reactor development as well as for basic nuclear physics, and which are not likely to be obtainable in any other way in the foreseeable future.

BIOGRAPHICAL SKETCH OF AUTHOR

B.C. Diven was born in Chico, California. He received the A.B. (Physics) from the University of California, Berkeley, in 1941, and the M.S. and Ph.D. from the University of Illinois in 1950. He has been a staff member, Physics Division, Los Alamos Scientific Laboratory 1943-1946; 1950 to present.

PROPOSAL OF EXPERIMENTS ON ELECTROMAGNETIC RADIATION FROM A DISTANT NUCLEAR EXPLOSION

Wilson K. Talley and Edward Teller

Department of Applied Sciences, University of California
Davis – Livermore

ABSTRACT

A nuclear explosion is particularly suited to checking whether or not light velocity is independent of frequency. This question is of some interest when the radiation beam passes close to the sun. Such a check would put to the test a postulate of general relativity which has never been explicitly verified. This and other experiments could be made more interesting by emitting a greater fraction of the energy in the radar spectrum. A method of accomplishing such experiments will be discussed.

THE CONSTANCY OF LIGHT VELOCITY

In an extremely brief time a nuclear explosion emits electromagnetic radiation ranging from γ rays down. If such a device is detonated in free space, the theory of relativity predicts that, save for those wavelengths long enough to be affected by the few free electrons between source and observers, there will be no dispersion of the signal. The constancy of light velocity has been verified before, but a nuclear explosion is particularly suited for such an experiment: the rise time of the pulse is of the order of 10^{-8} second and if the separation between bomb and observer is several hundred times that from earth to the moon, the ratio of emission pulse to transit time is of the order of 10^{-10}. Those frequencies for which free space at the orbit of the earth appears to be an absolute vacuum spans a ratio of 10^{12} or 10^{13}. Hence, one should be able to verify the constancy of light to 1 part in 10^{10} over a major portion of the frequency spectrum.

There is a natural phenomenon that might allow similar accuracy. This is the supernova, which may have a characteristic rise time in the order of hours and a transit time of 10^7 years: a ratio of emission to transit time of 10^{-10}. Although the spectrum observed on earth ranges only from red to violet, space satellites could examine energies up to x-rays. Also, in some part of the spectrum the emission rise time could well be of the order of seconds, and more distant supernovae might be observed: a ratio of 10^{-14} or better might be possible. Unfortunately for the experimenter, the supernova is a rare occurrence, a typical galaxy may produce only one such event in a thousand years. Since the time sequence of emission in various wavelengths is not known, supernovae at different distances would have to be compared. To increase the observed frequency of such events, many galaxies must be watched from satellite stations. This introduces uncertainties as to where in a galaxy the explosion occurs, through what material the light passes, and the precise length of the transit time. Further, the intrinsic mechanism of the supernova is not well understood: there might well be more than one characteristic sequence of events giving rise to a variety of emission curves. In any case the investigation of supernova explosions in the whole electromagnetic spectrum is a most exciting task for the astronomer.

THE EFFECT OF FREE ELECTRONS

A second and concurrent experiment would easily yield information as to the density of free electrons in space. The group velocity of electromagnetic radiation in space is known to depend on

the free electron density as

$$v = c\left[1 - (\omega_p/\omega)^2\right]^{1/2}$$

where the plasma frequency is

$$\omega_p = \left(\frac{4\pi n_e e^2}{m_2}\right)^{1/2}$$

(n_e = density of electrons per cc, m_e = mass of electrons). For frequencies far less than ω_p, this may be approximated by

$$v = c\left[1 - \frac{1}{2}\left(\frac{\omega p}{\omega}\right)^2\right]$$

$$= 2.998(10^{10}) - 1.343(10^{-3})\lambda^2 n$$

$$= 2.998(10^{10}) - 1.206(10^{18})\ n/f^2.$$

Hence, observing the delay for different radar frequencies can determine the intervening electron density integrated over the path of the ray.

Consider a bomb in an orbit about the sun which is similar to the earth's orbit. When the bomb is almost directly opposite the earth, it is detonated. The radiation, observed by a series of satellites (see Fig. 1) will give the integrated electron density about the sun, for

$$\text{transit time} = 2\int_0^{\left(r_e^{\,2}-b^2\right)^{1/2}} \frac{dx}{v}$$

$$= \frac{2}{e}\int_0^{\left(r_e^{\,2}-b^2\right)^{1/2}} \frac{dx}{\left(1 - f_p^{\,2}/f^2\right)^{1/2}}$$

$$= \frac{2b}{c}\int_0 \frac{\sec^2\theta\, d\theta}{\left[1 - \frac{8.97(10^3)n}{f^2}\right]^{1/2}}.$$

Unless the dependence of n on position is known, this definite integral cannot be calculated. However, the observed delays at the various frequencies will give information about the electron density near the sun. If the experiment is performed during both quiet and active solar years, the changes in electron density can be measured.

The electromagnetic waves that can be used for such an experiment are limited by the attenuation which they experience in transit. (A further consideration is that the wave can be no longer than the characteristic length of the sphere of emission, say 100 cm.) As the wavelength approaches that corresponding to the plasma frequency, a greater fraction of the energy resides in the polarization of the electrons — if then the relaxation time of the electrons is less than one cycle, this energy can be lost in electron collisions. At the plasma frequency, the wave ceases to propagate; at frequencies somewhat greater than the plasma frequency, the wave is rapidly absorbed. At shorter wavelengths, the high conductivity of the plasma makes the j^2/σ losses negligible.

LIGHT VELOCITY IN A GRAVITATIONAL FIELD

In contrast to the many independent experimental verifications of special relativity, general relativity has been confirmed in only four fundamentally independent experiments. One basic postulate of the general theory is that, no matter how a light ray is bent by a gravitational field, the velocity is independent of frequency. It is proposed to test this prediction.

The bending of a beam of light as it grazes the sun may be explained by an analogy with physical optics; in a high-potential gravitational field light behaves as though it has a lower effective velocity. The correction term introduced in Einstein's theory is

$$V \approx c(1 - \phi/c^2)$$

where the gravitational potential ϕ = GM/r.

At the orbit of the earth, $\phi/c^2 = 0.992(10^{-8})$, and at the sun's surface, $0.212(10^{-5})$. If some other frequency-dependent correction term exists, it almost certainly is less than this observable correction.

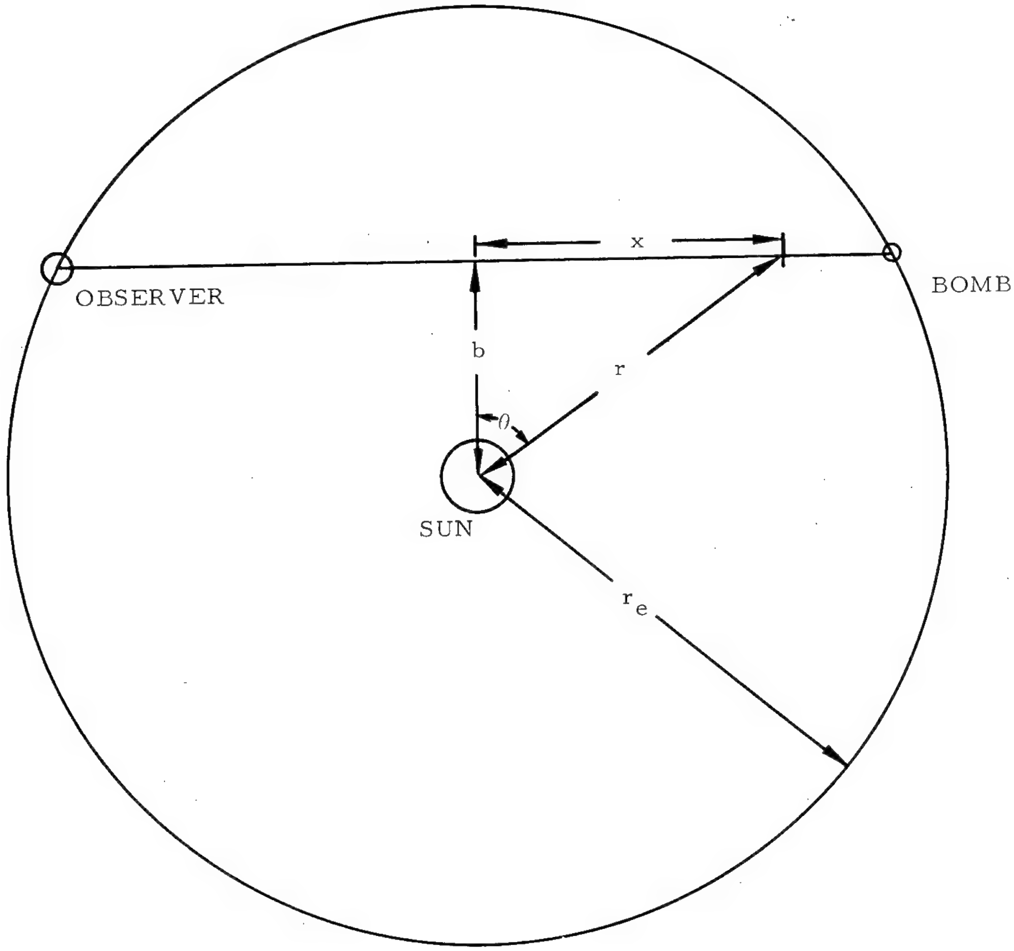

Fig. 1. Geometrical arrangement of nuclear device, observer, and the sun.

One can send signals past the sun and examine the various frequencies for unpredicted differences in delays. Consider the situation illustrated in Fig. 1: Since we have

$$V = c(1 - \phi/c^2) = c(1 - GM/rc^2)$$

the transit time is

$$\text{transit time} = \tau = \int_0^{t_{max}} dt$$

$$= 2 \int_0^{\left(r_e^2 - b^2\right)^{1/2}} \frac{dx}{V}$$

$$= \frac{2}{c} \int_b^{r_e} \frac{r^2 dr}{(r^2 - b^2)^{1/2} \left(r - \frac{GM}{c^2}\right)}$$

$$= \frac{2}{c} \left\{ (r^2 - b^2)^{1/2} + a \ln \left[r + (r^2 - b^2)^{1/2} \right] - \frac{a^2}{(b^2 - a^2)^{1/2}} \left[\arcsin \left(\frac{a\, r_e - b^2}{b(r_e - a)} \right) + \frac{\pi}{2} \right] \right\}$$

where

$$a \equiv GM/c^2$$

then

$$\tau = \frac{2}{c}\left\{\left(r_e^2 - b^2\right)^{1/2}\right.$$

$$+ a \ln\left[\frac{r_e + \left(r_e^2 - b^2\right)^{1/2}}{b}\right]$$

$$\left. - \frac{a^2}{\left(b^2 - a^2\right)^{1/2}}\left[\arcsin\left(\frac{a\,r_e - b^2}{b(r_e - a)}\right) + \frac{\pi}{2}\right]\right\}.$$

Let $b = r_{sol} = 0.696(10^{11})$cm, grazing incidence and $r_e = 1.49(10^{13})$cm,

then

$\tau = 0.994(10^3) + 5.96(10^{-5})$ sec. The ratio of dispersion delay to transit time is then 6×10^{-8}.

The competing natural process, that of the supernova, is of the same order; e.g., assume that a supernova occurs in a galaxy at a point 7×10^{21} cm (about 7000 light years) from the center and that within the sphere of this radius the mass is that of 10^{11} suns, 10^{44} grams. For this example

$$\phi \approx 10^{15}$$

and

$$\phi/c^2 \approx 10^{-6}.$$

The transit delay is then

$$\tau = \int_0^R \frac{dr}{c\left[1 - \frac{GM}{c^2(r + r_g)}\right]}$$

$$\approx \frac{R}{c} + \frac{r_g}{c}\frac{\phi}{c^2}\ln R/r_g$$

where

$$R/c = 10^7 \text{ years},\ r_g/c = 7 \times 10^3 \text{ years}.$$

$$\tau = 10^7 + 5 \times 10^{-2} \text{ years},$$

hence this ratio of delay to transmit time is 5×10^{-9}. This ratio may be bettered for some actual supernovae, but lack of knowledge of the gravitational field at the position of the supernova reduces the value of this observation: the controlled experiment with nuclear devices offers the same nominal accuracy, but with fewer experimental uncertainties.

If a dependence of light velocity on frequency exists in a gravitational field, then electromagnetic waves from stellar radiation sources would suffer different deflection at different wavelengths when the ray grazes the sun. The accuracy of such an observation could not rival the accuracy of 10^{-10} which can be attained in a nuclear explosion. Such an accuracy might be approached in the narrow spectrum of visible light. In the much broader regions of infrared and the even wider range of short-wave radiation extending to γ rays, accurate deflection measurements cannot be performed.

To conclude this section, it would be most surprising if the results of the experiment conflict with the predictions of the general theory. It is not the purpose of the proposed experiment to disprove the theory, but, in testing it, to add another experimental verification of this elegant structure of theoretical physics.

GENERATION OF A RADAR PULSE

For the experiments outlined, it would be useful to divert the largest possible portion of the bomb's radiation into the radar region; normally, the major part of the energy is carried by γ the and x rays. In an explosion an electric field is built up around the explosive due to the Compton-recoil of electrons on the surface of the bomb which are hit by the early γ rays from the incipient explosion. But the potential in this field is limited to the energy of the γ rays, that is to a few million volts.

The field can be enhanced if foil is distributed around the explosive. Then a few million volts can be built up on the average between neighboring foils, due to emission of Compton electrons by one foil and stopping of these electrons by the next foil. Much more intensive fields can be produced in this way.

There exists a serious problem concerning the reduction of the electric field due to the dipoles induced in the foil. One way to solve this problem would be to orient the foil in a direction

perpendicular to the field. Due to the short time scale of the following events the foil will not lose its orientation. But it may not be easy to orient the foil.

A much simpler procedure would be to limit the concentration of the foil. This will, however, increase the mean free path of the electrons traveling between foils. As a consequence a lesser field strength will be attained. The foil concentration should be adjusted to maximize the field.

It might be best to use dielectric material, for instance, mica foil. Unfortunately the bombardment of these foils by x rays and γ rays will render them conducting. One may provide shielding in the early stages against x rays. Conductivity due to γ rays may be decreased if a material is used in which photoelectrons are readily trapped. This question needs careful investigation.

In any case the distribution of foil can give a strong, though somewhat uncertain, enhancement of the field. If foil is distributed on one side of the explosive, a strong dipole can be generated. Emission with a maximum in the region of a hundred megacycles can be accomplished in this manner. It may be possible to shift the maximum intensity to higher frequencies by use of somewhat elaborate arrangements which utilize the specific mechanisms by which the electric fields near the explosive can be made to disappear in a very short time.

BIOGRAPHICAL SKETCHES OF AUTHORS

Edward Teller, nuclear physicist, is a native of Hungary who in 1941 became a citizen of the United States.

Until 1939, he was absorbed by the pursuits of the theoretical physicist, attempting to understand the behavior of molecules, atoms and nuclei. But the discovery of the fission process and the menace of Nazi Germany drew him to work on atomic explosives.

Unlike many of the nuclear physicists who helped develop the world's first atomic bomb, Dr. Teller continued to work on nuclear weapons after Hiroshima and the end of World War II. He did this in the firm belief that there were many unexplored applications of nuclear energy and because he felt that the United States would need advanced nuclear weapons to successfully oppose future dangers.

After World War II, Dr. Teller made significant contributions to developments of atomic weapons and to the design of the world's first hydrogen bomb. He was a member of the General Advisory Committee of the Atomic Energy Commission from 1956 to 1958, helped establish the Nation's second nuclear weapons laboratory at Livermore, California, and served as director of the Livermore Laboratory from 1958 to 1960.

Dr. Teller's current research is concerned chiefly with the peaceful applications of nuclear energy. He has returned to academic life as Professor-at-Large of Physics at the University of California and as Chairman of the newly formed Department of Applied Science at Davis and Livermore.

Born in Budapest in 1908, Dr. Teller received his university education in Germany, receiving his Ph.D. from the University of Leipzig in 1930. After research and teaching in Gottingen, Copenhagen, and London in the early 1930's, he came to this country and was professor of Physics at George Washington University, Washington, D. C., from 1935 to 1941. His wartime assignments took him from Columbia University, to the University of Chicago until 1952 and since then at the University of California. He is the co-author of The Structure Of Matter (1948), Our Nuclear Future (1958) and The Legacy of Hiroshima (1962).

Wilson K. Talley received the A.B. (Physics) from the University of California, Berkeley, in 1956. His Masters in Physics was awarded by the University of Chicago in 1957, and he received his Ph.D. in Nuclear Engineering from the University of California, Berkeley, in 1964.

His professional background is as follows: 1956 – Dynamics Engineer, Convair, Pomona, Calif. 1957-58 – Jr. Physicist, Shell Development Corp., Emeryville, Calif. 1959 – Physicist, Lawrence Radiation Laboratory, Berkeley. 1960 – Research Physicist, Institute of Engineering Research, University of California, Berkeley. 1960-63 – Teaching Assistant, Teaching Associate, Teaching Fellow, University of California, Department of Nuclear Engineering, Berkeley. 1963 – Assistant Professor, Department of Applied Science, College of Engineering, University of California, Davis–Livermore.

CALCULATION OF THE SHOCK WAVE FROM AN UNDERGROUND NUCLEAR EXPLOSION IN GRANITE

Theodore R. Butkovich

Lawrence Radiation Laboratory, University of California
Livermore, California

ABSTRACT

The capability of calculating the close-in effects of the shock wave from an underground nuclear explosion has been demonstrated. Agreement was obtained between calculation and measurements using a spherically symmetric, hydrodynamic, elastic-plastic code called SOC for the Hardhat event, a 5-kiloton nuclear detonation in granite. This capability is dependent upon having a more or less complete description of the elastic and dynamic properties of the materials involved. When this information is available, agreement within the limits of uncertainty of the measurements can be calculated for peak pressures, peak particle velocities, shock wave time of arrival, and pressure pulse shapes.

INTRODUCTION

The capability of predicting the phenomena from underground nuclear explosions on the surrounding media is becoming increasingly important. These predictions are useful in a number of ways. Certain engineering criteria regarding such things as stemming and placement of surface installations can be established. Possible damage to existing underground structures from shock effects can be determined. Shock wave propagation is also important in crater formation from buried charges.

In any underground nuclear explosion, the shock front that propagates from the shot point carries with it energy from the explosion, and distributes this energy by doing work on the surrounding material. In the process, the material undergoes changes in both its physical and mechanical states. If enough energy is deposited in the material, it will vaporize or melt thus changing its physical state, or cause it to crush or crack.

During the past few years, special computer codes have been developed for predicting the close-in phenomena of underground nuclear explosions using the laws of physics, and the knowledge of the properties of the materials in which the detonations occur. As a consequence, a better understanding of experimental observations and measurements has evolved.

A spherically symmetric, Lagrangian, hydrodynamic-elastic-plastic code called UNEC (Underground Nuclear Explosion Code) (Nuckolls, 1959), was used in earlier calculations. Presently, a new code called SOC (Seidl, 1964) is being used in making these calculations. SOC is similar to UNEC in that it makes a rather direct use of an experimentally determined shock Hugoniot, but differs in that it uses different equations for calculating elastic-plastic behavior and internal energy. SOC also allows for strain-rate effects such as occur during pressure buildup and decay at the wave front.

Calculations, using the SOC code, were made for the Hardhat event, a 5-kiloton nuclear explosion. The device was detonated at the bottom of a 950-foot-deep, vertical hole in granite at the Nevada Test Site. The Hardhat event was chosen for these calculations, because of the rather large number of different close-in measurements that were made in a range extending from the hydrodynamic to the elastic regions.

MEASUREMENTS

For the Hardhat event, a variety of close-in measurements were made on a horizontal radius from the detonation point. An access shaft and tunnel had been provided, and holes were drilled from the tunnel for instrumentation (Figure 1).

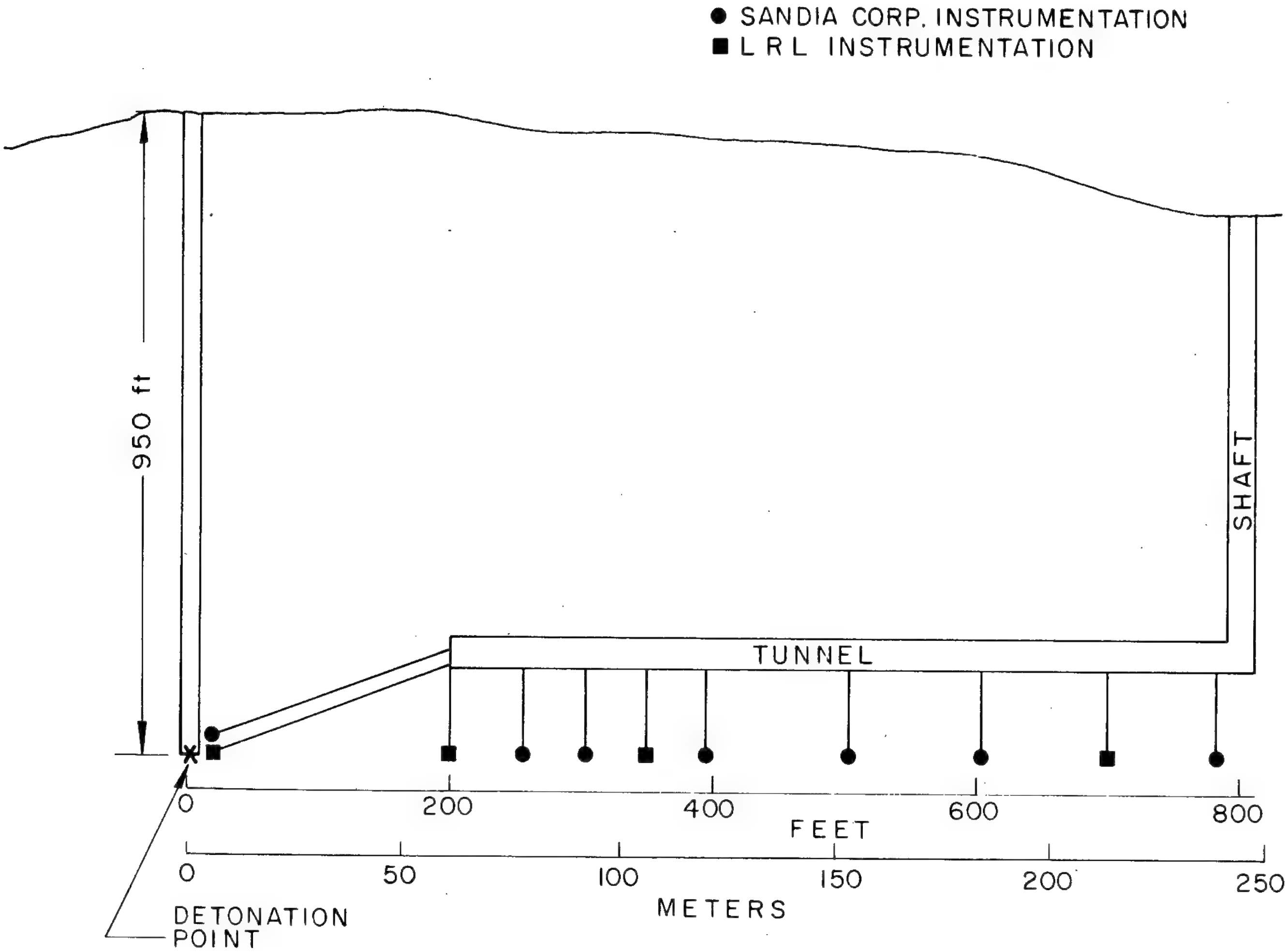

Fig. 1. Layout of instrumentation of Hardhat event.

In the hydrodynamic region, times of arrival of the shock wave were measured with special transducers in the range from 7.35 to 24.1 meters (24 to 79 ft) (Chabai and Bass, 1963). Peak pressure measurements were made in two locations, one of 460 kilobars at 5.51 meters (18.1 ft) (Chabai and Bass, 1963), and another of 664 kilobars at 4.85 meters (15.9 ft) (Lombard, 1963).

In the elastic region, there was an array of accelerometers, velocity and displacement gauges, and stress and strain measurement instruments distributed in the range from 78 to 460 meters (265 to 1500 ft) (Perret, 1963, and Swift, 1962). From this, some measurements are of particular interest here. The time of arrival as determined by the accelerometers are shown in Figure 2. The average velocity of the shock wave was 5526 meters/second (18,130 ft/sec.). With this shock velocity U_s and the peak velocity measurements U_p, peak pressures were determined from the Hugoniot relationship.

$$P = U_p U_s \rho_0$$

where ρ_0 is the initial density of the material. Pressure history measurements were made in two locations (Heusinkveld et al., 1962) with peak radial stresses of 4.0 kilobars at 61 meters (200 ft) and 1.2 kilobars at 106.7 meters (350 ft).

THE SOC CODE

Before any meaningful calculation can be attempted, a more or less complete description of the materials involved has to be obtained. The

Hugoniot equation of state, the shock energy to vaporize and melt, plastic yield conditions, dynamic strength properties, and elastic properties are all input to a SOC code calculation. Some of these parameters can be determined by rather well developed techniques, but others are not easily determinable and must be estimated on the basis of other related measurements.

Except in the vaporized region, the equation of state of the material is made up from experimental data. When the material is vaporized, the equation of state is expressed as a theoretical pressure-energy-density relationship normalized to the Hugoniot, and extending to the Thomas-Fermi-Dirac region at high energies. In the liquid and plastic states, the material is represented by the Hugoniot curve relating pressure and specific volume at the shock front. At the shock front discontinuity, a nonlinear Richtmyer-von Neumann artifical viscosity (q) is used. The wave front is determined from a maximum in q, which lies at the center of the discontinuity and travels with the wave front velocity. During the unloading, the Hugoniot can be corrected to approximate the unloading isentrope, by using an appropriate Gruneisen Γ. When shock pressures are great enough to vaporize the material on unloading, a transition to the gas equation of state, is made irreversibly.

In spherical symmetry, there are two principal stresses, (σ_r) normal and (σ_T) tangent to the wave front. That is, a distinction is made between these and the fluid-like pressure (P), where

$$P = \frac{\sigma_r + 2\sigma_T}{3}.$$

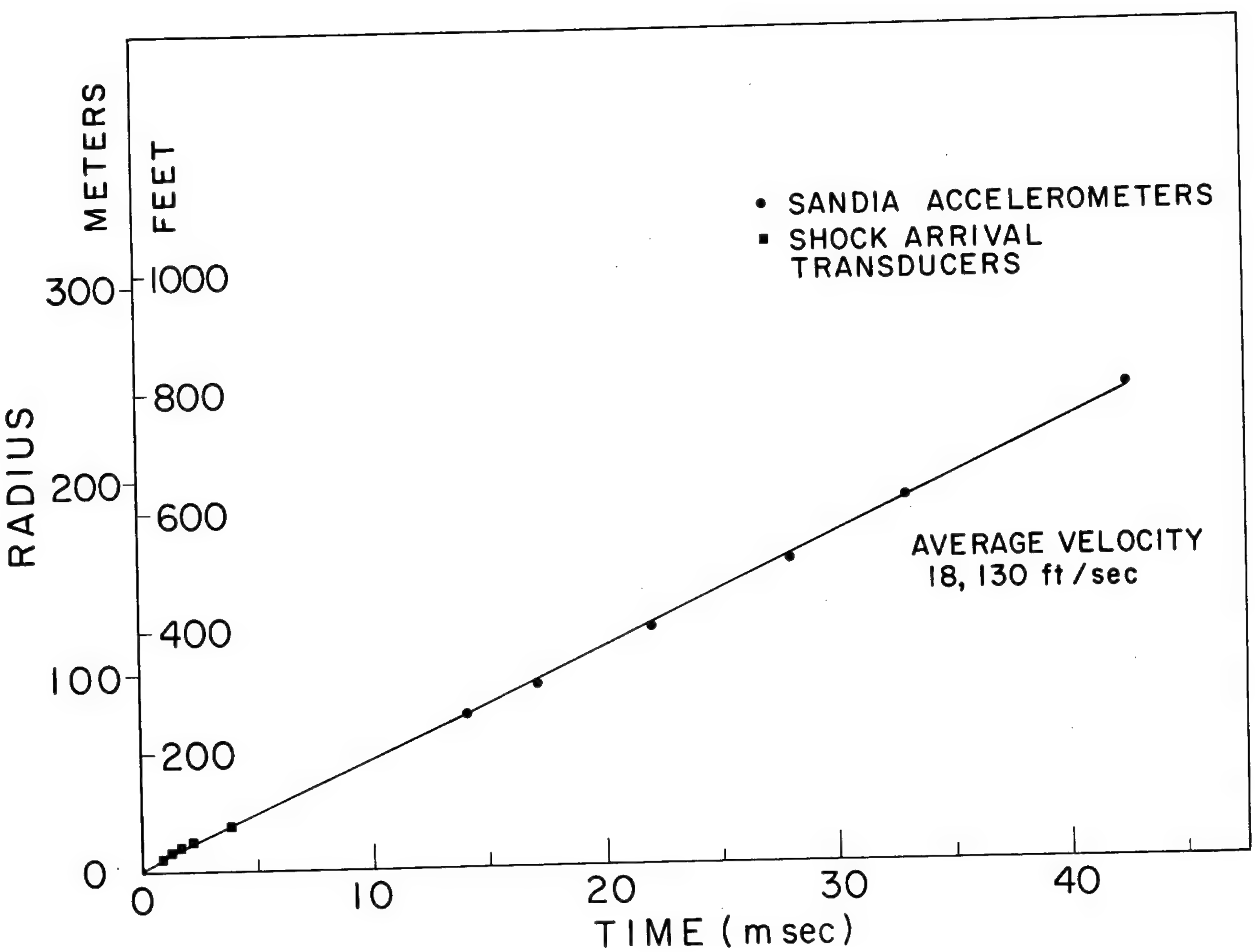

Fig. 2. Time of arrival data.

In the liquid state, the material is isotropic and the shear is zero. However,

$$\sigma_r = P + \frac{4}{3}K, \text{ and } \sigma_T = P - \frac{2}{3}K$$

where K, the so-called stress deviator is expressed by

$$K = \frac{\sigma_T - \sigma_r}{2} .$$

K is calculated differently if the material is crushed.

The plastic yield conditions are expressed in terms of K (Seidl, 1964), where K is equal to or less than the yield stress. For many materials, the yield stress is a function of the strain rate. When knowledge of this behavior is available, different yield conditions can be imposed according to whether the strain rates are high, as occurs at the shock front, or the pressure is slowly rising, or falling off on unloading.

The elastic region of the pressure-density curve is required to agree with sonic velocities in the material. In an isotropic elastic medium, the two characteristic sonic velocities, longitudinal (V_ℓ) and shear (v_S), are related by

$$v_\ell^2 \rho_0 = k + \frac{4}{3}G$$

and

$$v_s^2 \rho_0 = G,$$

where G is the shear modulus. ρ_0, v_ℓ, and v_S are taken from in-situ measurements. The bulk modulus (k) can also be obtained from hydrostatic measurements. Stephens (1963) has shown that excellent agreement occurs between hydrostatic and dynamic measurements in the elastic region for eight different rock types.

Dynamic strength properties of the rock are less easily determinable. The bulk tensile strength of most rock masses are zero, or at most very small, because of the highly fractured state in which they are usually found. Dynamic compressive strength of rocks are not as easily obtained, and in most cases must be estimated, perhaps, something like twice or three times static measurements. In the case where the material has open cracks, the compressive stress that can be supported without crushing the material is always less than when cracks are closed and also depend on the strain rate. If the material does crush, then it is assumed that a type of Coulomb friction exists, somewhat like the resistance to shear for loose sand.

At the start of a calculation, the material is divided into two or more regions, a central gas region into which the energy from the explosion is put as internal energy of the gas, and the regions outside in which the material is initially plastic-elastic. The regions are divided into equal thickness zones to the outside. This is the ground surface in a vertical calculation, or extends somewhat beyond the region of interest in the horizontal case. After the shock wave has passed and the energy from the explosion distributed, the material state of each zone may have changed by expanding the vaporized region or melting it, depending on whether the internal energy to vaporize or melt was exceeded. Crushed or cracked regions form if the peak stresses that developed in each region exceed the crushing or tensile strength, respectively.

THE CALCULATIONS

For the Hardhat event, predictions were made based on a 5-kiloton nuclear explosion, 950 feet below the surface in granite (Seidl, 1962) using the best available data at that time. These predictions were useful in determining instrument placement, and for range and time settings of the measuring equipment. Since then, more data on the properties of granite have become available, and with the measurements to compare with results, adjustments of some of the input parameters for granite used in the original calculation were made to cause better agreement.

In determining the dynamic equation of state of a material, measurements are made in the laboratory by subjecting representative samples of the material to strong shocks generated by high explosives. Lombard (1961) has compiled data of shock velocity (U_S) and particle velocity (U_P) on a number of rock types, amongst which is granite. From these measurements the so-called Rankine-Hugoniot conditions can be obtained:

$$P - P_0 = \rho_0 U_s U_p,$$

$$\rho/\rho_0 - 1 = \frac{U_p}{U_s - U_p},$$

$$E - E_0 = \frac{P - P_0}{2} (1/\rho_0 - 1/\rho)$$

where P is pressure, E specific internal energy, and ρ the instantaneous density. The subscripts refer to initial values. Figure 3 is a plot of the data for granite. The scatter at the lower pressures is due to several causes. An elastic precursor of about 40 kilobars has been measured for granite (Grine, 1960). This means that a two-wave structure exists to about 320 kilobars; above which the shock velocity is greater than the dilatational sonic velocity. A number of polymorphic transitions of the mineral constituents of granite

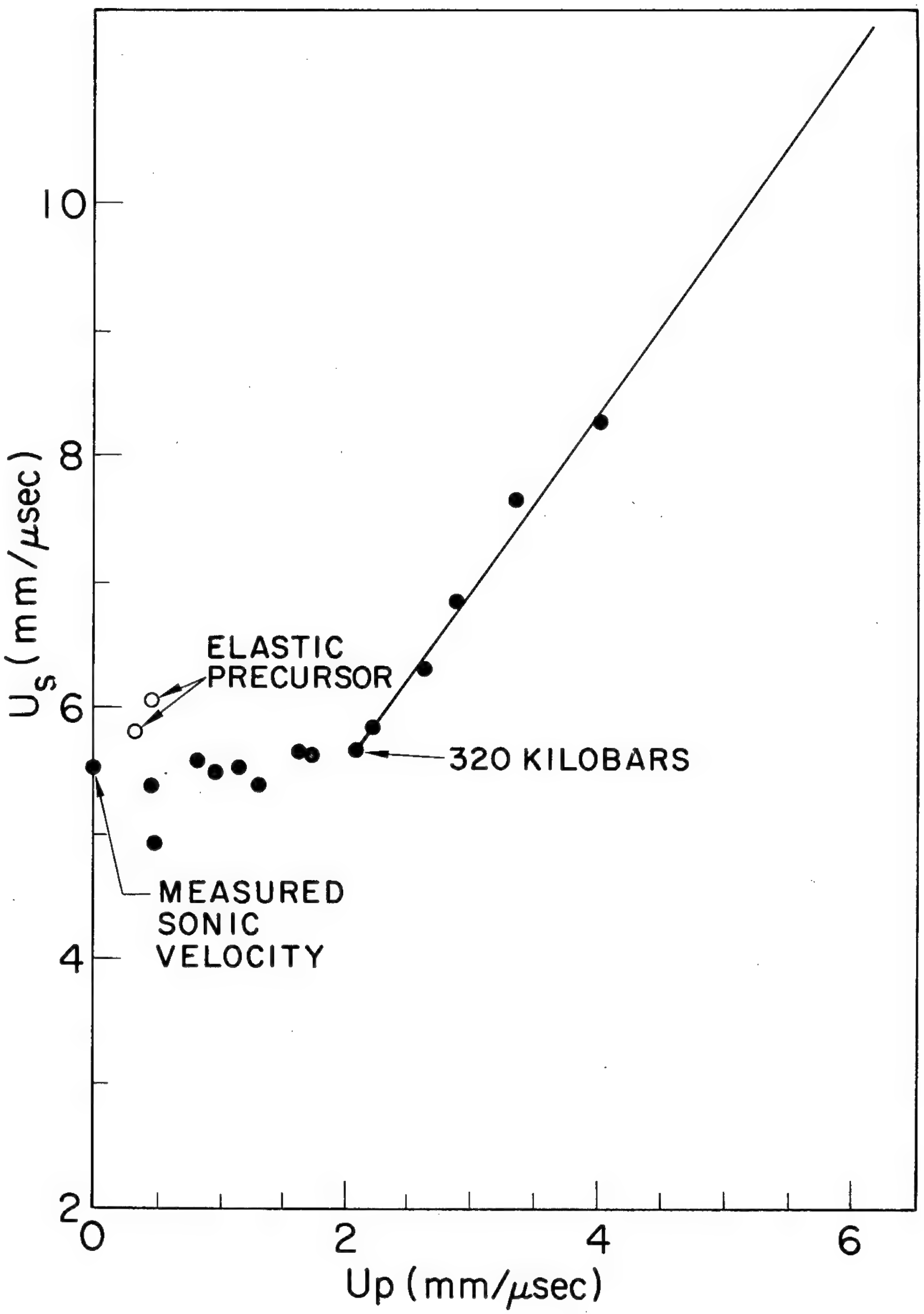

Fig. 3. Hugoniot measurements for granite.

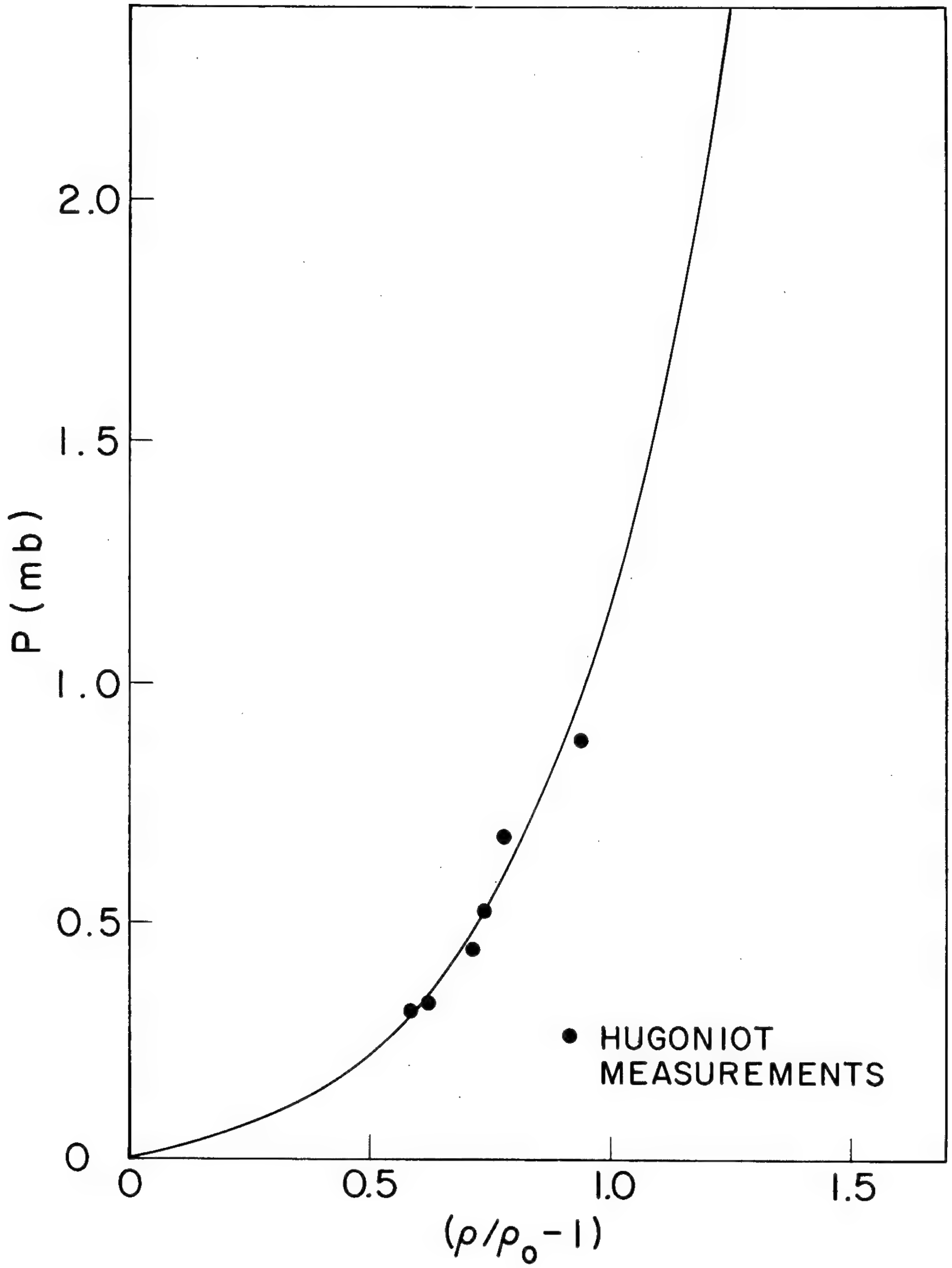

Fig. 4. Shock Hugoniot for granite.

below 320 kilobars further complicate the interpretation of the measurements.

In the elastic region, the equation of state of granite is defined by the bulk modulus and the shear modulus. Figure 4 is a plot of the granite Hugoniot, which is put into the SOC code as a linearly interpolated P vs μ table, where $\mu = \rho/\rho_0 - 1$. In-situ seismic measurements of the dilatational and shear velocities in granite are 5440 meters/sec (17,850 ft/sec) and 3050 meters/sec (10,000 ft/sec), respectively (United Electrodynamics, 1962). The average measured wave front velocity of 5526 meters/sec (18,310 ft/sec) is in good agreement with the in-situ seismic velocities. Derived from the seismic measurements, the bulk modulus and shear modulus used in the calcula-

tions were 0.361 and 0.315 megabar, respectively. This corresponds to a wave front velocity of 5380 meters/sec (17,646 ft/sec) in the elastic region. Since the wave front velocity is greater at pressures above about 320 kilobars, the average velocity is somewhat higher, so as to give good agreement with the shock wave time of arrival measurements.

The dynamic properties of granite were estimated and adjusted to obtain good agreement between measurement and calculation. To do this a number of parameter studies were carried out by varying specific input values to the code.

The dynamic yield stress for high strain rates or fast-rising pressure pulses was made to be consistent with the measured 40-kilobar elastic precursor. However, the yield stress for a slowly rising pressure pulse was varied from 10 to 1 kilobars. Figure 5 shows the results for calculations using 10, 5, and 2.5 kilobars. Reducing the

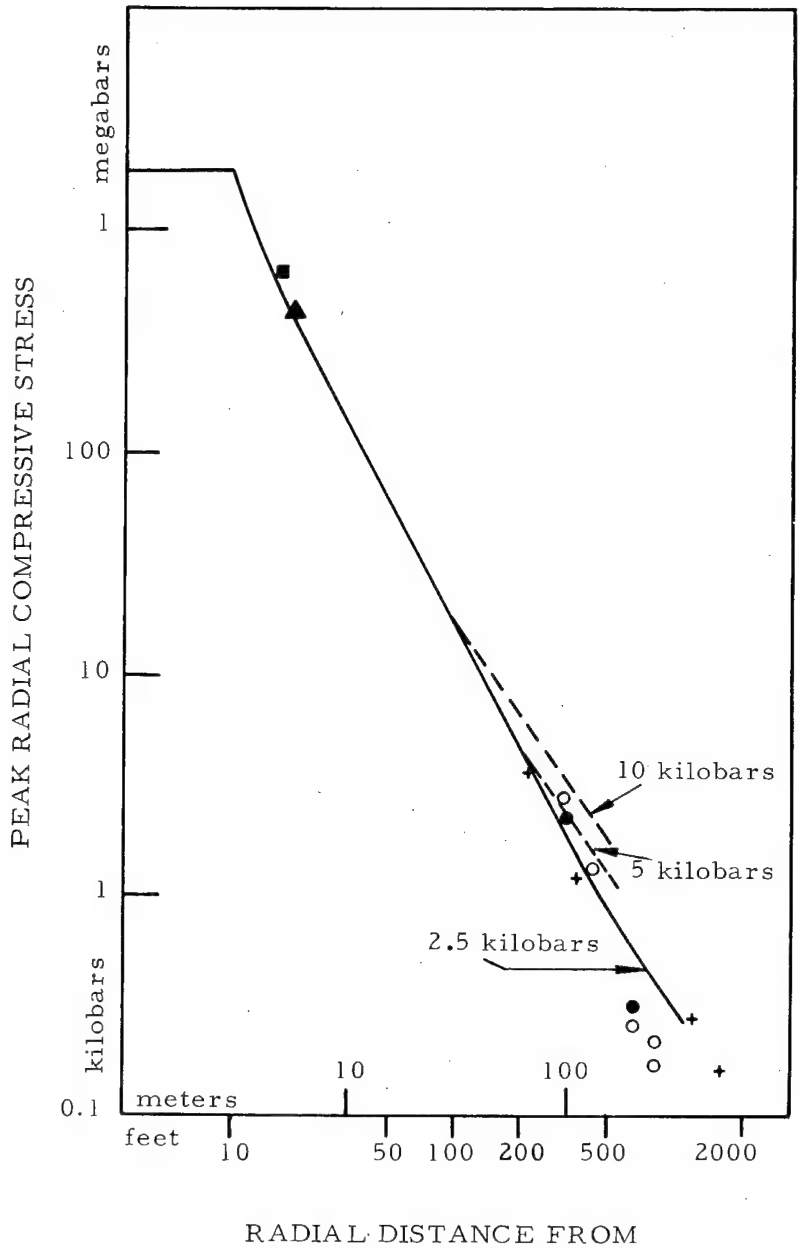

Fig. 5. Results of calculations of yield stress for a slowly rising pressure pulse.

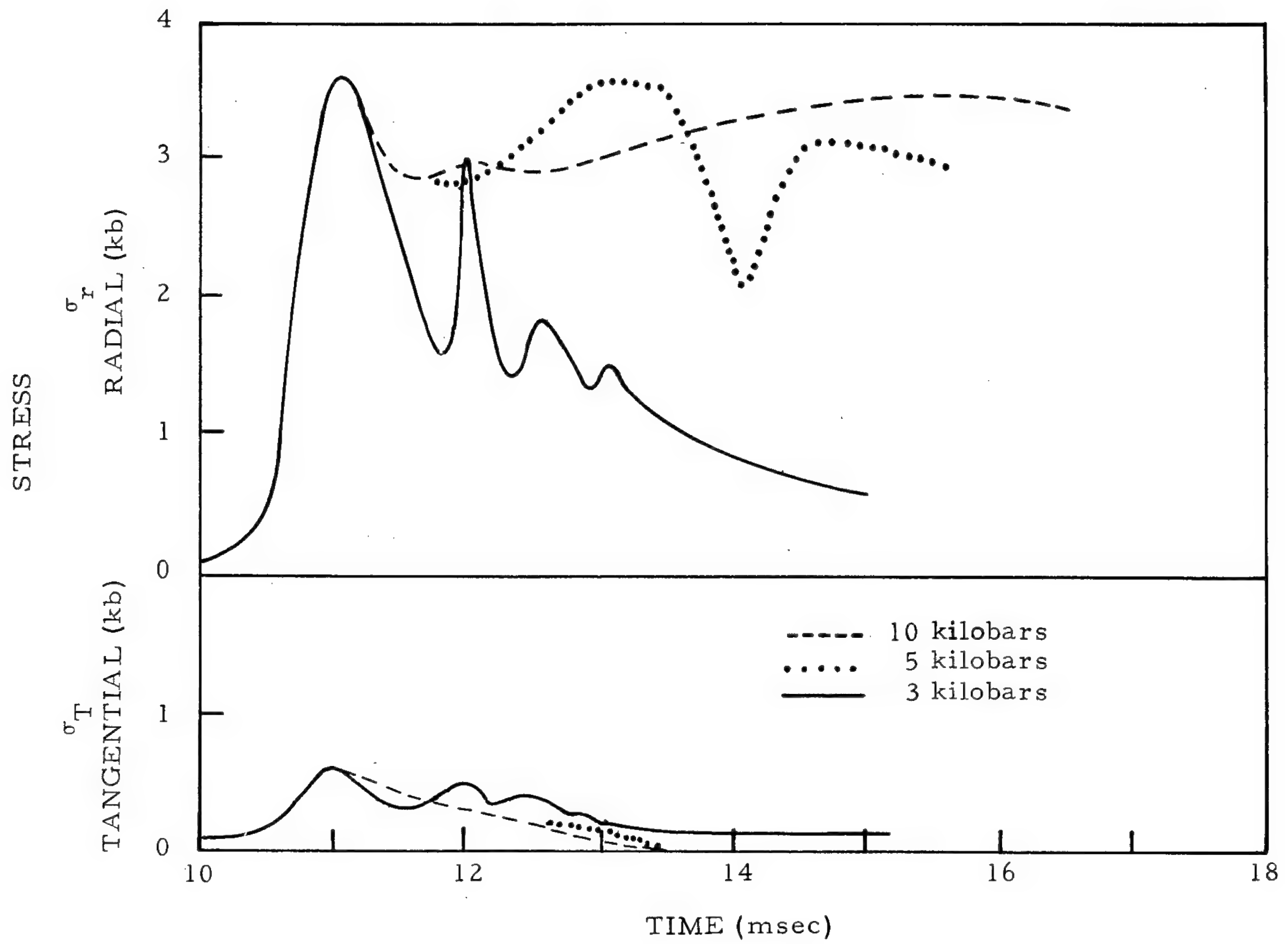

Fig. 6. Results of parameter study varying the compressive strength for the unconfined case.

yield stress further to 1 kilobar caused no further change within the limits of the calculation. These results suggest that when the material deforms plastically at a lower yield stress, more energy is deposited in the plastic state leaving less energy available for the farther out regions; hence, the peak pressures drop off more rapidly.

Birch (1942) reports static measurements of compressive strength for granite of 10 kilobars for confined tests and 1.5 kilobars for unconfined tests. The dynamic compressive strengths were assumed to be twice the values from static tests; 20 kilobars for the case when the material is confined with no open cracks and high strain rates, and 3 kilobars for the unconfined case with open cracks or for slowly rising pressure pulses. A parameter study varying the compressive strength for the unconfined case was made to determine the effect on stress pulse shape. Figure 6 shows the results of this study where the calculated radial and tangential stress pulses are plotted for the zone nearest 61.8 meters (203 ft) from the detonation center, where stress history measurements were made. For the compressive strength of 10 and 5 kilobars, the material cracks when the tangential stress goes to zero. The material remains elastic-plastic and the radial stress remains high. For a compressive strength of 3 kilobars, the material crushes when the peak stress exceeds this value, and the radial stress pulse shape very nearly approximates the measured pulse shape. The higher values of compressive strength make the material more rigid than it is in reality. It is of interest to note that the Hardhat tunnel collapsed completely out to a radius of 137 meters (450 ft) (Lombard and Cauthen, 1964). The peak

radial stress at this point is 1.2 kilobars. Total tunnel collapse should occur somewhat beyond the limit of crushing, as the failure was primarily due to spall.

The bulk tensile strength used in all these calculations was zero; however, a calculation was made assuming the tensile strength equal to the over-burden of 77 bars. No appreciable differences were noted in the stress pulse shapes.

The Γ Gruneisen was set equal to 1.0, knowing that it was greater than zero and less than two. Since the calculation was concerned primarily with material behavior near the stock front, a small error in the unloading isentrope would have little effect there. Vaporization occurred behind the shock front when the internal energy exceeded 0.584×10^{12} ergs per original cc. Melting occurred when the internal energy was greater than 0.093×10^{12} ergs per original cc. These values are equivalent to a shock vaporization pressure of 2.14 megabars and a shock melting pressure of 456 kilobars, if the Gruneisen Γ was zero, and the Hugoniot becomes the unloading isentrope. With Γ being set equal to one, these pressures are slightly higher.

The calculation was made in two steps. First, a fine-zoned case was run to more precisely determine the fall-off of peak pressure with distance in the region above 100 kilobars, and the limit of vaporization. The 5 kilotons were distributed uniformly as internal energy of a sphere of iron gas, with an average density and volume equal to that of the device canister. The second case used coarser zoning to cover the region below 100 kilobars, where the pressure was falling off less rapidly. It assumed that the initial density of the gas was approximately equal to the total mass of material vaporized, divided by the volume of the vaporized region. In both cases, the average initial bulk density of granite was 2.67 g/cm^3.

The peak shock pressure as a function of distance from the detonation center is shown in Figure 7, along with limits of vaporization, melting, crushing and cracking. Peak pressure falls off as $r^{-1.94}$ in the region below approximately 1 megabar for a 5-kiloton detonation in granite.

Pressure-history measurements (Heusinkveld et al, 1962) at 61.8 meters (203 ft) and 109.7 meters (360 ft) are plotted in Figure 8. Superimposed on these plots are the calculated pressure histories for the nearest zone position. From this, the curves are displaced 0.03 msec in time at most. The oscillatory shape at the calculated curves is due to the mathematical method the code uses. The true pulse shape should be more like the envelope formed by the peaks. The large discrepancy in arrival time between the calculated and observed pressure pulse at 360 ft is attributed to an error in instrument position determination, since this is the only one of many measurements that does not fall on the shock time of arrival curve.

The peak particle velocity vs radius is plotted in Figure 9. The measurements shown were obtained by integration of the acceleration-time data, and by direct observation of velocity gauge signals. Sandia data seem to indicate the velocity to be falling off faster than that calculated. However, measurements by Swift (1962) at 457 meters (1500 ft) seem to agree better with the calculation.

DISCUSSION OF RESULTS

The agreement between calculation and measurements for the Hardhat event has demonstrated the capability for predicting with considerable accuracy the close-in effects of the shock wave from an underground nuclear explosion. The differences that are noted are due to uncertainties in the measurements of the phenomena, in measurements of the material parameters, and the fact that a spherical model was assumed.

Measurements of material properties upon which the input parameters are based are made on selected samples or in areas that are similar to the detonation region, but are not necessarily representative. Often there are large variations in the structural geology for a given type of material within one area. The properties of the materials upon which the calculation is based must exhibit an average behavior of the medium.

The code uses a spherical model, whereas in reality the geometry of the device room in an underground nuclear explosion is rarely spherical. Also, the detonation is not truly a point source, and a small displacement of the detonation center can mean a rather large discrepancy in peak pressure within the first few meters.

The device yield itself is based on measurements, and each measurement has an uncertainty. The uncertainty can be due to a number of sources. such as time and position resolution or instrument design and calibration. Some measurements are obviously in error and are discarded because of disagreement with other reliable values.

In the Plowshare group, a major effort is being made to better understand the phenomenology of underground nuclear detonations by code development, obtaining better input parameters to these codes, and improved measurement techniques.

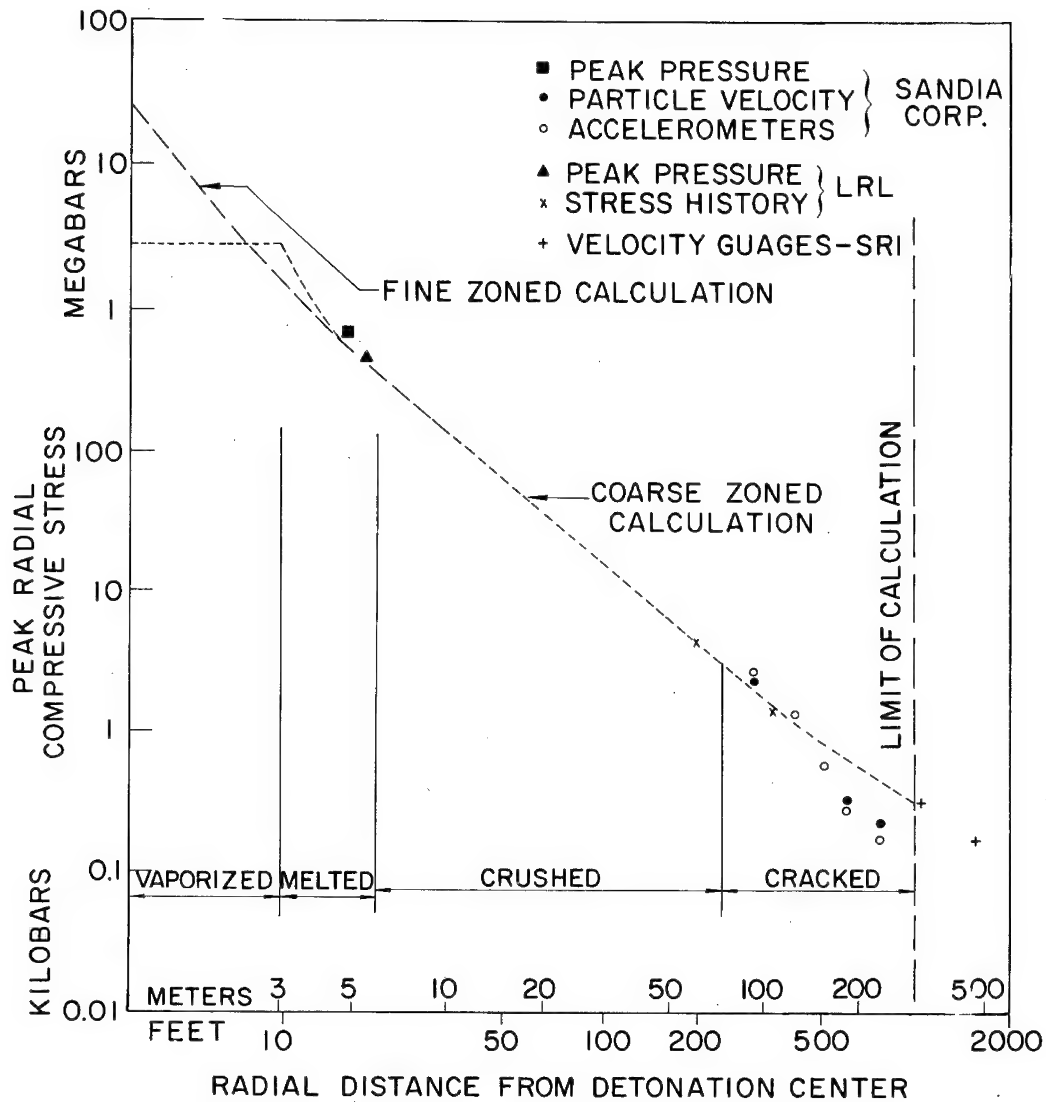

Fig. 7. Hardhat event, peak radial stress vs radius.

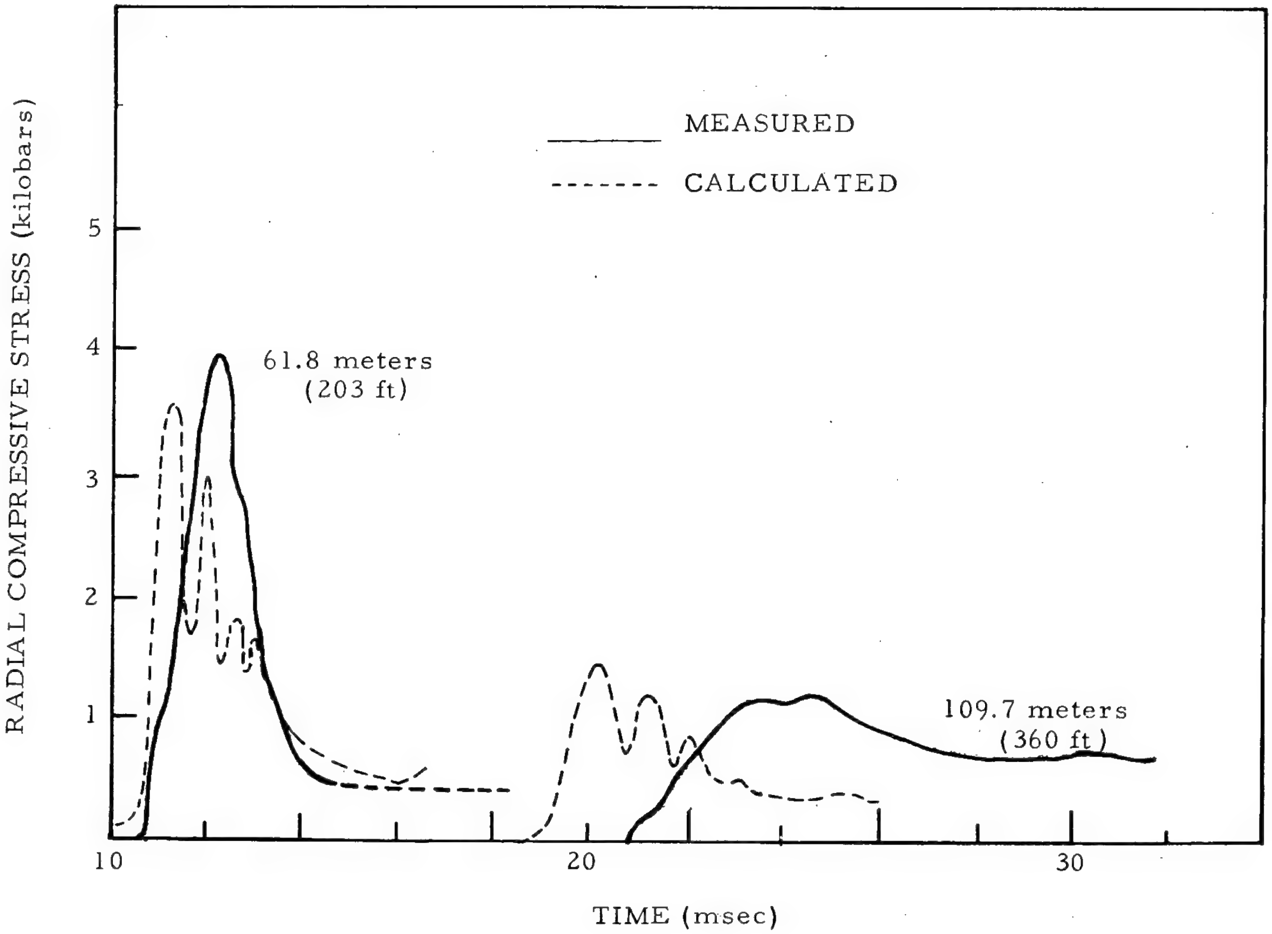

Fig. 8. Pressure history measurements.

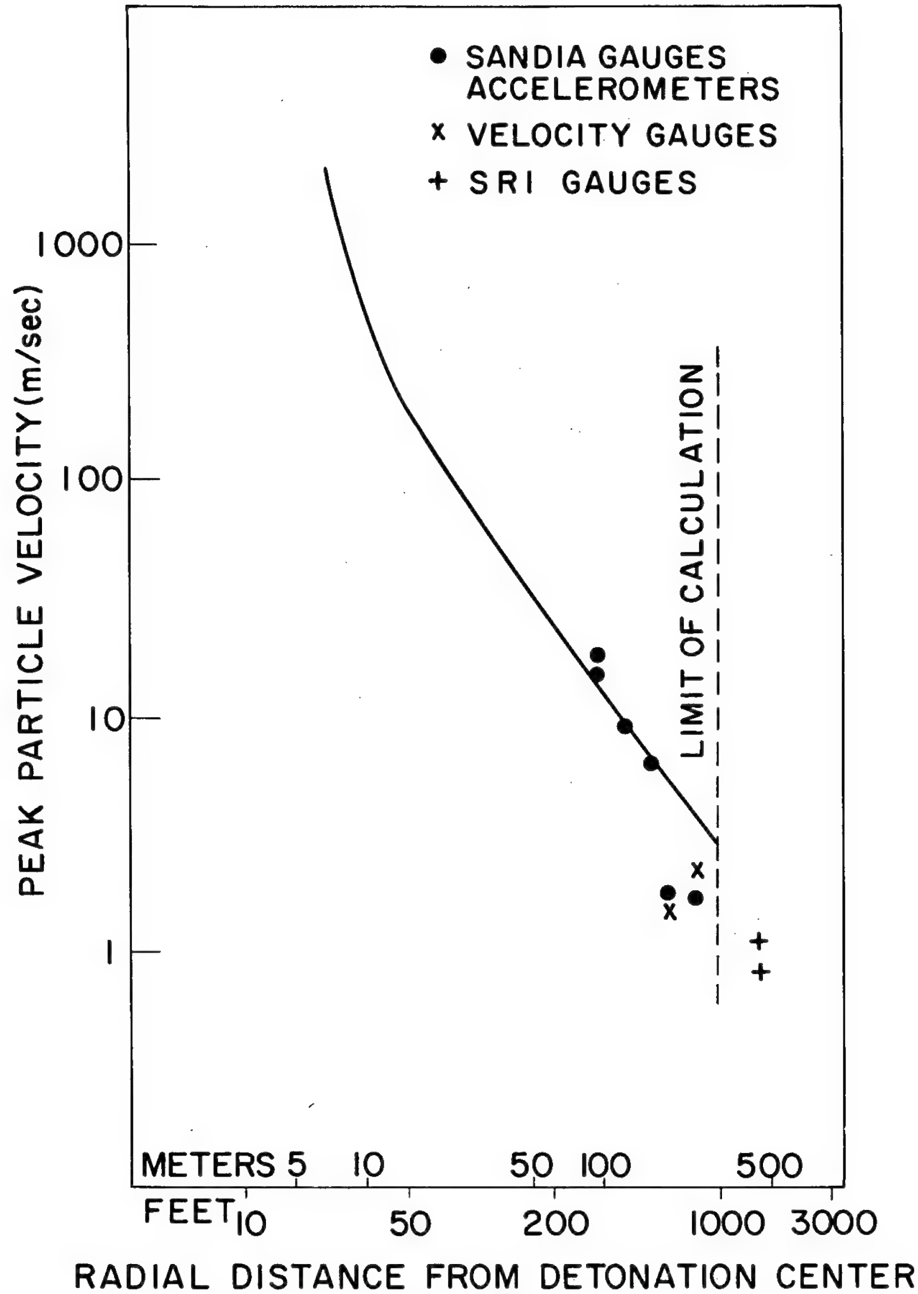

Fig. 9. Peak particle velocity vs radius.

BIBLIOGRAPHY

1. Birch, F., Handbook of Physical Constants, Geological Society of America, Special Papers 36, 1942.
2. Chabai, A. J. and Bass, R. C., Sandia Corp. Research Report, SC-4741, 1963.
3. Grine, D. R., Equation of State of Granite and Salt, Stanford Research Institute, Final Report, Project PGD-3244, 1961.
4. Heusinkveld, M., Holzer, F., Marks, R., and Harris, D., Stress History Measurements with Piezoelectric Crystals, Hardhat Preliminary Report, Project 26.21, K Div., LRL, 1962.
5. Lombard, D. B., The Hugoniot Equation cf State of Rocks, Lawrence Radiation Laboratory, Livermore, Rept. UCRL-5675, 1959.
6. Lombard, D. B., and Cauthen, L., Shock and Seismic Effects of Underground Explosions, to be published, 1964.
7. Perret, W. R., Free-Field Ground Motion Studies in Granite, Sandia Corp., POR-1803, 1961.
8. Seidl, F. G. P., Publication describing SOC code, to be published, 1964.
9. Seidl, F. G. P., Machine Calculation (Viz., SOC) of the Fall-off with Distance of the Peak Pressure and Peak Particle Velocity Produced by a 5 kt Nuclear Explosion, 950 feet Below the Surface of a Semi-Infinite Granite Medium, UCRL Internal Memorandum UOPKA 62-6, 1962.
10. Swift, L. M., Measurement of Close-in Earth Motion, Preliminary Report Hardhat Event, VUP-2101, 1962.
11. United Electrodynamics, Compression and Shear Wave Velocities, Preliminary Report VUP-2500, 1962.

BIOGRAPHICAL SKETCH OF AUTHOR

Theodore R. Butkovich was born in Chicago, Illinois. He served in the U.S. Army for three years during World War II. He received his B.S. and M.S. degrees in Physics from Depaul University in Chicago. From 1952 to 1959 he was employed as a physicist by the U.S. Army Corps of Engineers, doing research on snow and ice. Since 1959, he has been with the Lawrence Radiation Laboratory in Livermore as a physicist with the Plowshare Division.

CRATERING EXPERIENCE WITH CHEMICAL AND NUCLEAR EXPLOSIVES*

Milo D. Nordyke

Lawrence Radiation Laboratory, University of California
Livermore, California

ABSTRACT

Over the past 13 years, a considerable body of data on explosive cratering has been developed which is applicable to nuclear excavation projects. These data were obtained from more than ten cratering programs using chemical explosives (TNT or nitromethane) and seven nuclear cratering detonations. The types of media studied have ranged from marine muck to hard, dry basalt, although most effort has been devoted to craters in NTS desert alluvium and basalt. These data have led to the development of depth-of-burst curves that relate crater dimensions to the depth of burst and the yield of the explosive. Comparison of these depth-of-burst curves with similar data by Russian investigators reveals some marked discrepancies.

Considerable effort has also been devoted to the study with chemical explosives of the use of linear explosives and rows of point charges. On the basis of these studies it has been generally concluded that the use of a row of point charges spaced a distance apart equal to about one single crater radius will result in (1) a smooth-sided ditch with a width and depth approximately equal to a single crater diameter and depth, (2) lips on the sides of the ditch which are about twice the single crater lip height, and (3) a lip on the end which is one-fourth or less than the lip height on the sides of the ditch. All row charge data to date are in desert alluvium. Plans are being actively pursued to conduct a row charge experiment in basalt with five 20-ton chemical-explosive charges (nitromethane) in the near future.

INTRODUCTION

Over the past 13 years a considerable body of data on explosive cratering has been developed for application to nuclear excavation projects. These data were obtained from some ten cratering programs using chemical explosives (TNT or nitromethane) and seven nuclear cratering detonations. The types of media studied have ranged from marine muck to hard, dry basalt, although most effort has been devoted to craters in NTS desert alluvium and basalt. Considerable effort has also been devoted to the study with chemical explosives of the use of linear explosives and rows of point charges. This paper is intended to be a summary of these data and a statement of the understanding which has been developed from them.

To better understand cratering data, it is best to establish a set of definitions for craters. Figure 1 shows the cross section of a typical crater in rock. For reference purposes, a detailed and precise set of crater dimensions and terminology are given in Appendix A. For the purposes of this paper, however, the simplified version shown in Fig. 1 will suffice. The apparent crater is defined as that surface which is visible when one stands on the edge of the crater as measured from the original ground surface. The true crater is defined as the boundary between the broken and crushed fallback material and the rock which has been relatively undisturbed by the cratering action. In general, a lip is formed around the crater. The lip is composed of uplifted and deformed rock or soil with the upper portion of the lip consisting primarily of material which has been ejected and thrown out of the crater. For the purposes of nuclear excavation, our primary interest has been in apparent crater dimensions, although it is obvious that the true crater plays an extremely strong role in determining the character and usefulness of the crater.

*Work performed under the auspices of the U. S. Atomic Energy Commission.

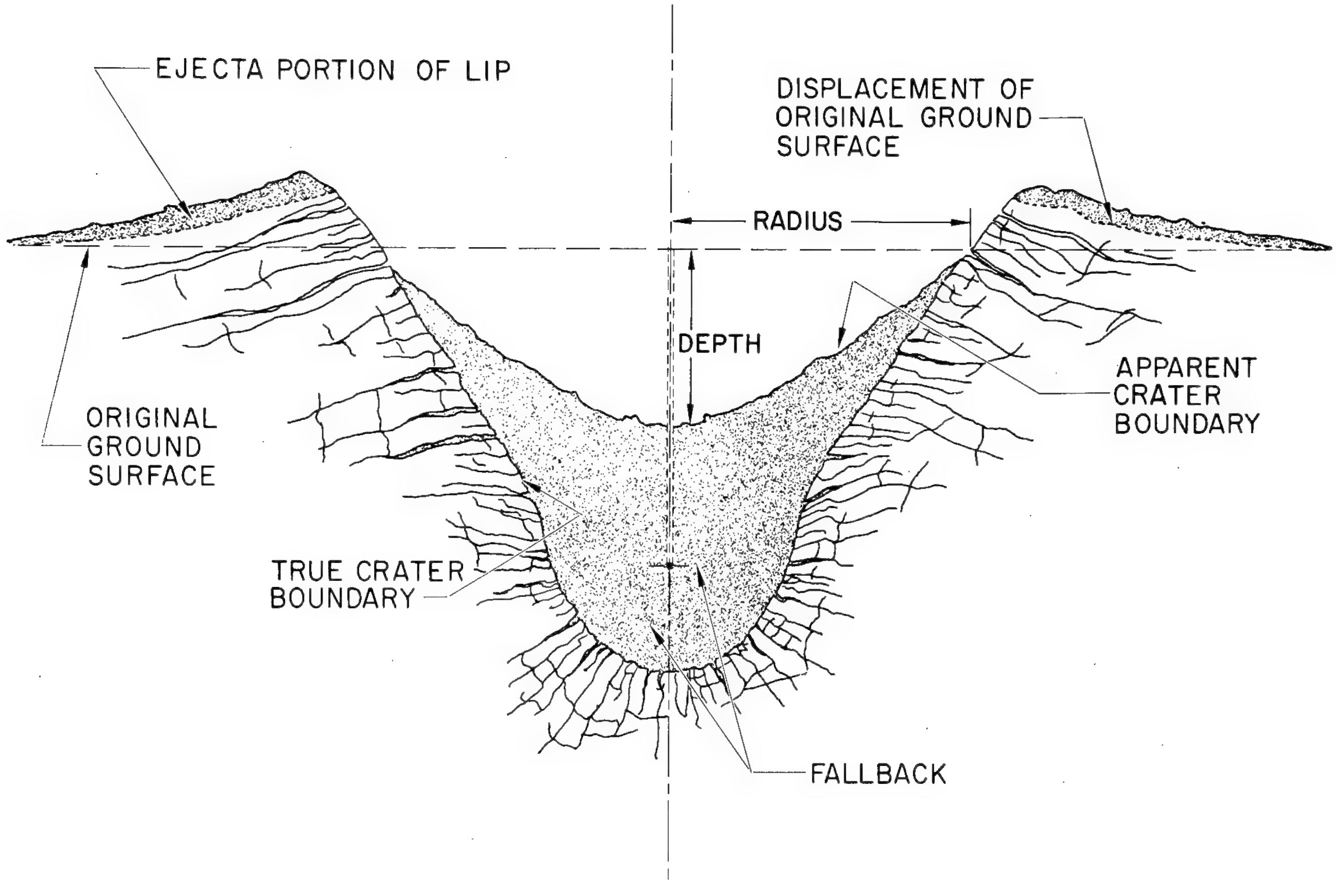

Fig. 1. Cross section of a typical crater in rock.

Figure 2 shows a schematic depth-of-burst curve in which the crater depth or diameter has been plotted as a function of the depth of burial. For surface burial a rather small crater is obtained. As depth of burial is increased, crater dimensions also increase until a maximum is reached. This maximum point is generally termed optimum depth of burial. Increasing the depth of burial beyond optimum results in reducing crater dimensions until ultimately a point is reached where the effects of the explosion are contained in the ground. As will be seen later, the point of containment is somewhat difficult to define and is extremely variable from one medium to another.

Some method must be used to correlate results from cratering explosions with different yields or charge weights. Dimensional analysis suggests the basic scaling law in which dimensions are proportional to $W^{1/3}$, where W is the weight of the explosive in pounds, kilograms, or kilotons. Distances or times associated with explosions of different charge weights can be put on the same scale for comparison purposes by dividing them by $W^{1/3}$. Quantities, such as pressures and velocities, are constant. Thus, at the same scaled distance and same scaled time we should have the same actual pressure in the shock wave and the same actual particle velocities. However, the analysis that leads to $W^{1/3}$ ignores the action of several factors such as gravity and the strength or internal frictional forces of the medium. While the extent of these forces is difficult to evaluate quantitatively, one can show that their effect would be to lower the exponent and lead toward $W^{1/4}$ scaling.[1] Empirical analysis of high-explosive cratering data in alluvium has shown that $W^{1/3.4}$ type of scaling best correlates all of the high-explosive data.[2] Insufficient data are available in any other media to calculate what scaling exponent should be used. In

the absence of these data, $W^{1/3.4}$ scaling has been used in this paper for the scaling of all data.

It should be noted that the forces which lead toward $W^{1/4}$ scaling are most important for apparent crater dimensions and do not as strongly influence true crater dimensions. It is generally recommended that $W^{1/3}$ scaling be used for all effects, except when discussing apparent crater phenomena.

It is characteristic of explosion crater data that very large scatter is encountered. This makes interpretation of data very difficult and requires a large amount of data for a high degree of confidence to be developed. In addition, the amount of scatter appears to be a function of the yield of the explosion and the characteristics of the medium. In desert alluvium, where the medium breaks into rather small particles ranging from gravel size down to fine dust, charge sizes of 200 pounds are fairly adequate for obtaining basic cratering curves. The scatter of the data observed is approximately 10 to 15%. In a hard rock medium, however, such as basalt, which breaks into particles ranging from 6 inches up to 6 feet, 1000-pound charges result in craters which have a very high amount of scatter. As a result of cratering work in basalt, it has been concluded that any charge weight smaller than 40,000 pounds will not give significant data in basalt.

Since Plowshare is interested in the utilization of craters for useful purposes such as canals and railroad and highway cuts, we are interested not only in the effects of point charges but also the effects of rows of charges detonated simultaneously. The first portion of this paper will consist of a summary of the point-charge cratering data in the various media followed by a discussion of the results from row-charge cratering work.

POINT CHARGE CRATERING DATA

Alluvium

Chemical-Explosive Data

Over the past 13 years a large amount of data has been obtained on the cratering characteristics of the sand-gravel mixture known as NTS desert

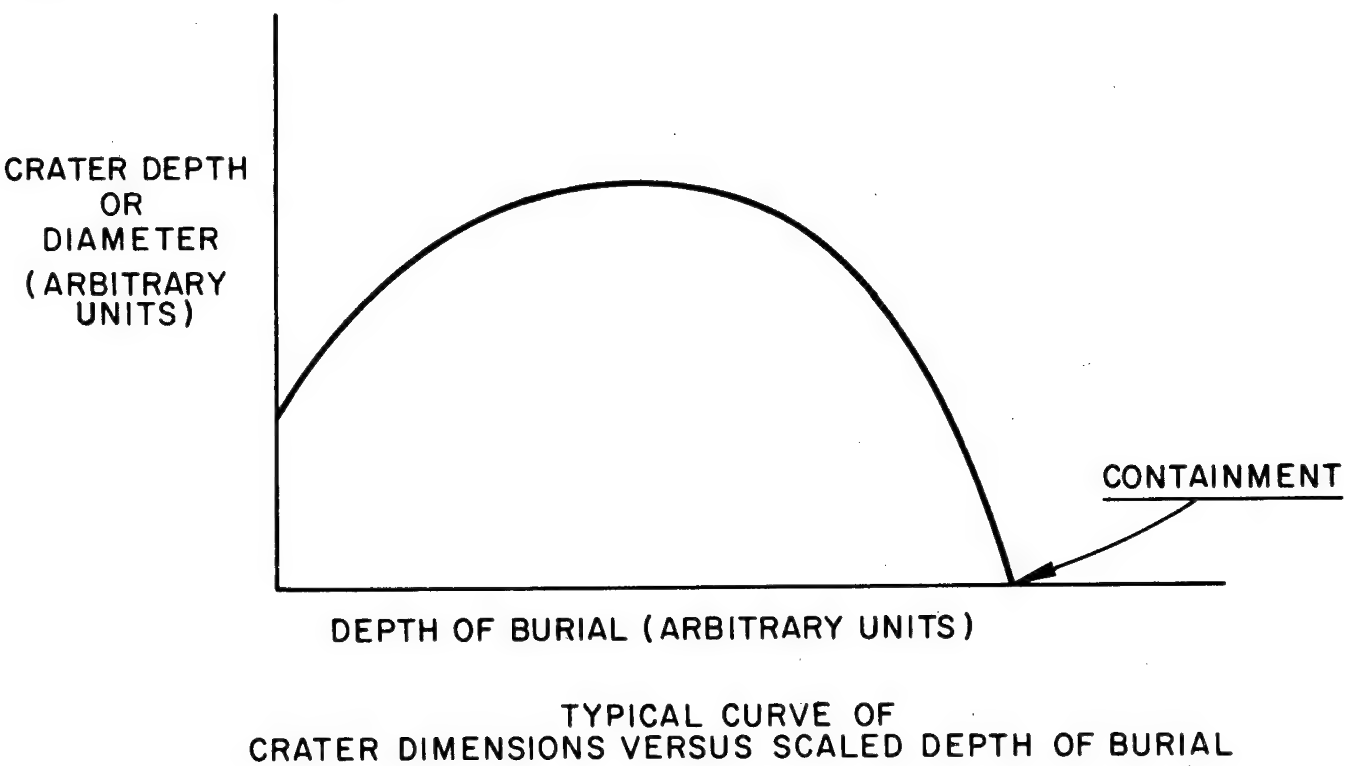

Fig. 2. Schematic depth-of-burst curve.

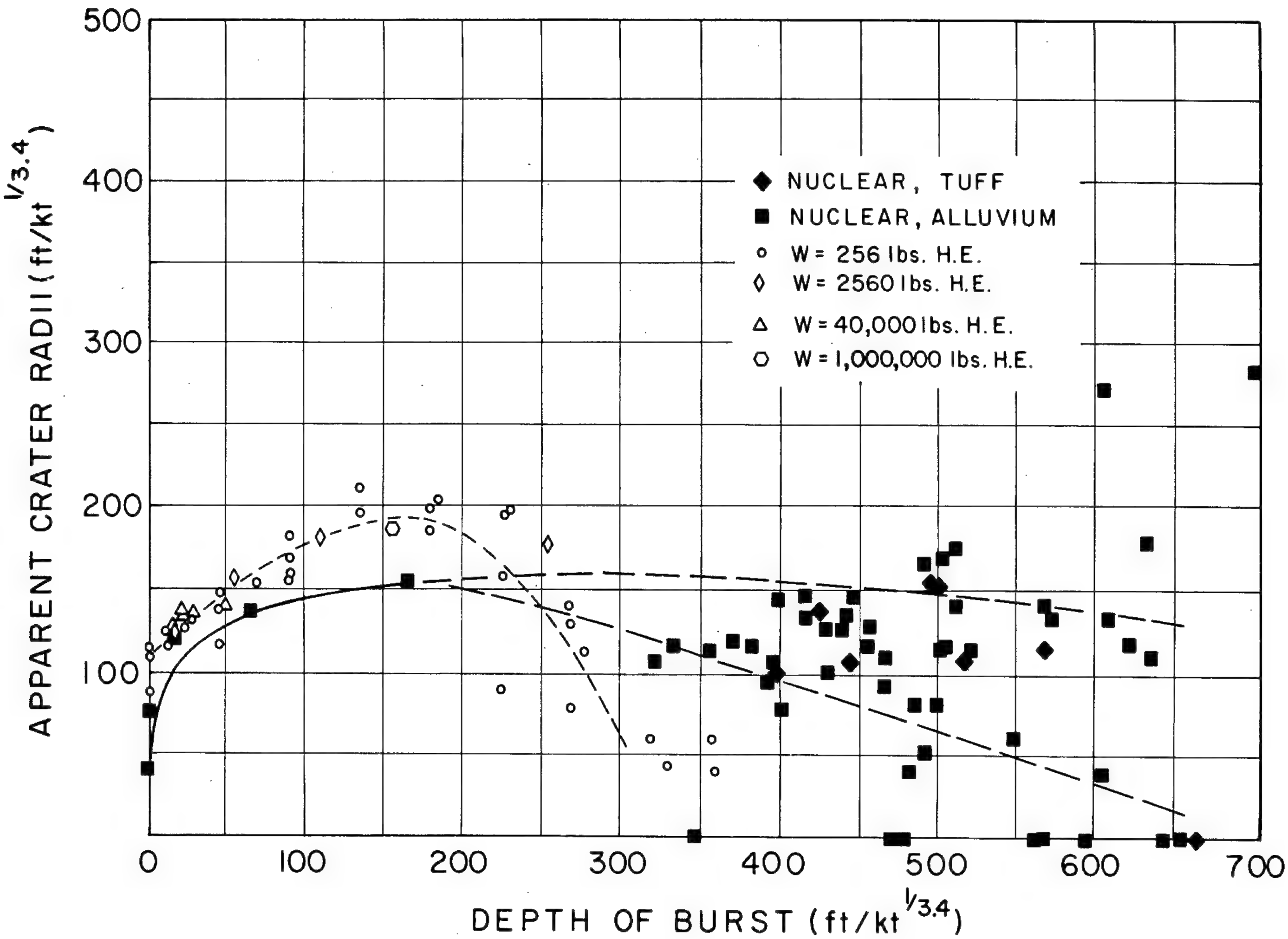

Fig. 3. Plot of high explosive (H.E.) and nuclear explosive apparent crater radius data vs depth of burst; NTS desert alluvium, $W^{1/3.4}$ scaling.

alluvium. This has resulted from a number of cratering programs from 1950 to 1955 sponsored by the Department of Defense in connection with determining the effects of nuclear weapons,[3,4] as well as a number of cratering programs sponsored by the Plowshare Program from 1959 to 1963.[5-7] The charge weights varied from 256 to approximately 1,000,000 pounds. These chemical-explosive cratering data are shown in Figs. 3 and 4. The dashed curves shown in Figs. 3 and 4 are least-square fits to the 256-pound data. The 40,000-pound data were used to calculate the proper scaling exponent, which has been used in the plotting of these data.

Of particular significance in the chemical-explosive cratering data is the point represented by the Scooter explosion which was a 1,000,000-pound cratering detonation at almost optimum depth of burial.[7] The purpose of the Scooter event was to confirm what kind of scaling should be used in the yield range of approximately 1 kiloton. As can be seen, scaling the Scooter data point by $W^{1/3.4}$ scaling results in a very good agreement with the rest of the high-explosive cratering data in alluvium.

Figure 5 shows the two curves for depth and radius of craters in desert alluvium from chemical explosives from Figs. 3 and 4, together with two curves for prediction of crater dimensions from current Russian cratering work. The first of these, labeled "Pokrovskii Theory," is a prediction of crater dimensions according to the equations[8]:

$$W = \frac{\rho Z^{3.5}}{1.8 \times 10^6} \left[1 + \left(\frac{R}{Z}\right)^2\right]^2$$

$$D = \frac{2R - Z}{3}$$

where

- W = charge weight in lb
- Z = depth of burst, ft
- R = apparent crater radius, ft
- D = apparent crater depth, ft
- ρ = medium density, g/cm^3.

These equations are based on a theoretical approach to cratering by G. I. Pokrovskii, one of the leading Russian experts in the subject of explosive cratering.

The second set of curves, labeled "Sadowski and Pokrovskii," are the semiempirical curves for craters

$$W = \frac{k_b Z^{3.5}}{250} \left[0.4 + 0.6 \left(\frac{R}{Z}\right)^3\right]$$

$$D = \frac{2R - Z}{3}$$

which are recommended in the current Russian Blasters Handbook[9] and are credited to S. A. Sadowski and G. I. Pokrovskii. This latter curve is recommended for explosions where the depth of burst is at a depth greater than 75 feet.

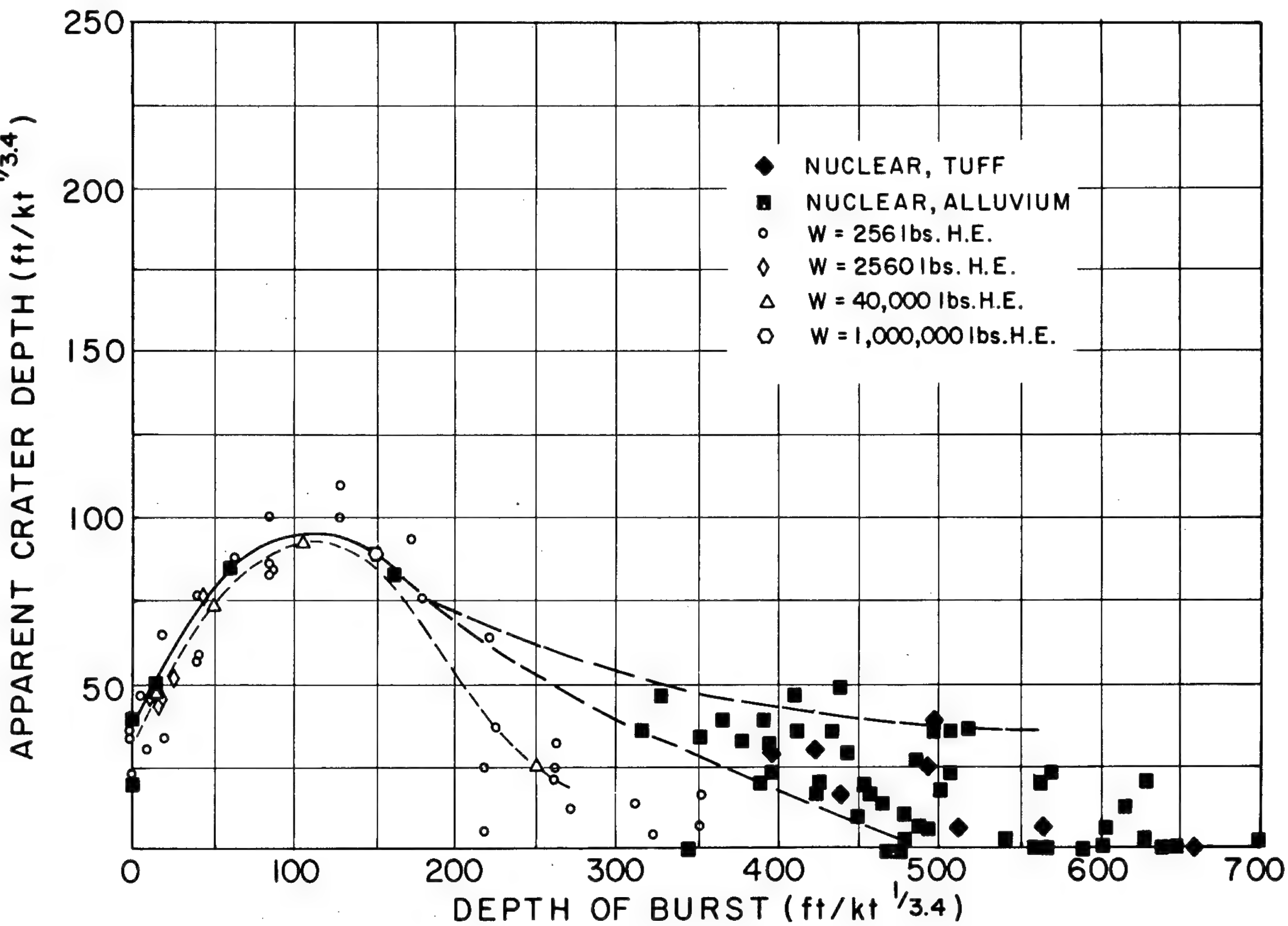

Fig. 4. Plot of high explosive (H. E.) and nuclear explosive apparent crater depth data vs depth of burst; NTS desert alluvium, $W^{1/3.4}$ scaling.

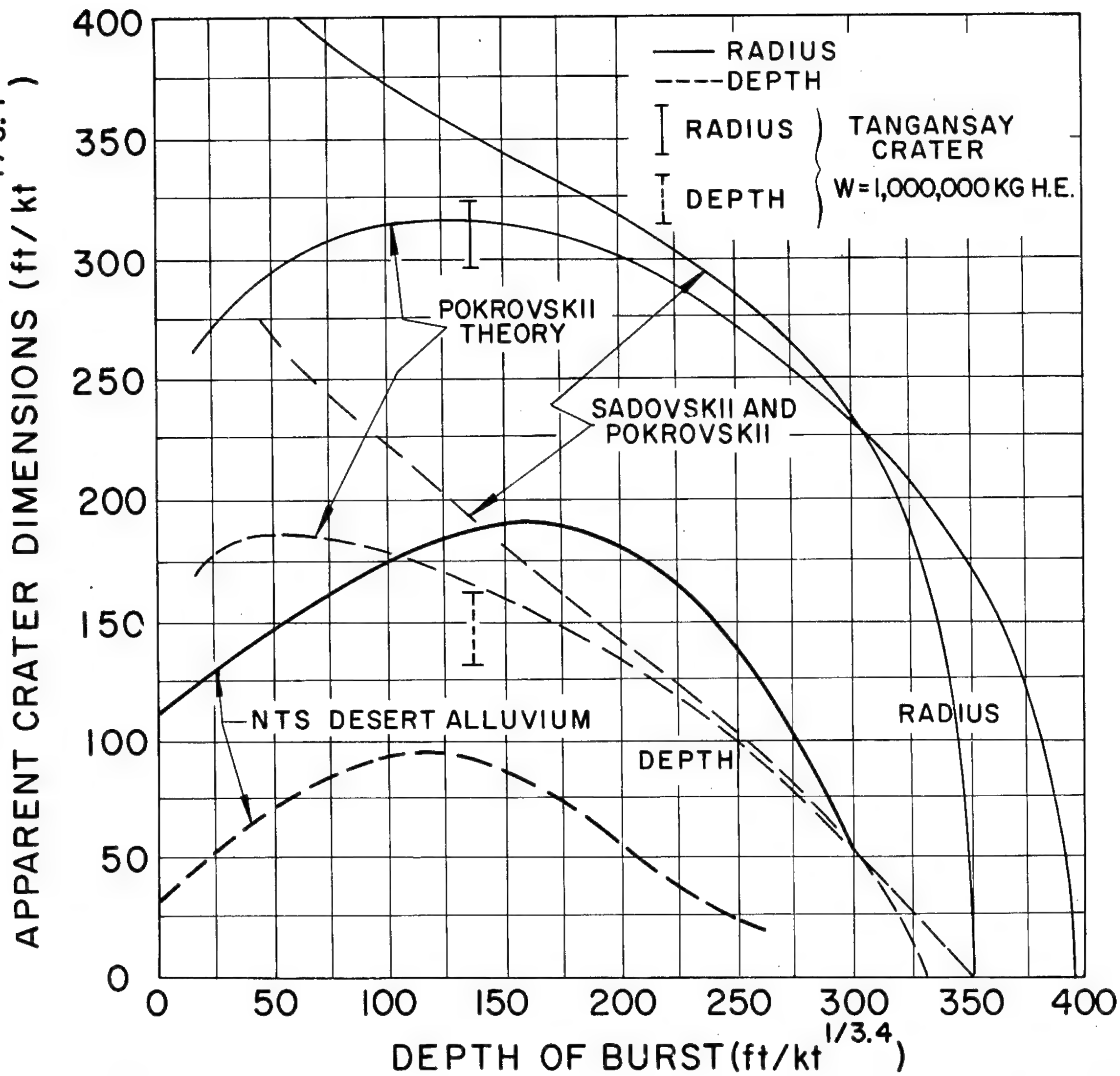

Fig. 5. Comparison of NTS desert alluvium apparent crater dimensions curves and Russian crater dimensions curves.

As can be seen, these two Russian curves compare quite favorably with each other, but are significantly higher than our curves for desert alluvium, both with respect to depth and radius. The medium considered here for the Pokrovskii curves is characterized by a density of 1.6, which is the only parameter used in these equations. For the Sadowski and Pokrovskii curves, the constant k_b is estimated to be equal to 1.5 for a sand-gravel mixture.

Also shown in Fig. 5 is the data point reported for the 1,000,000-kilogram chemical-explosive crater at Tangansay in the Province of Kazakstan,[10] which was detonated in 1957. The purpose of this crater was essentially the same as the purposes of the Scooter crater, to determine the correct scaling exponent to be used at large yields.[11] The agreement between the experimental Tangansay crater and the Russian curves is remarkably good. The medium mentioned in the reports available indicates it to be a clay-loam medium. There does not appear to be any reasonable explanation for the wide divergence of the cratering curves except the possibility of the

type of explosive used. Reports available indicate the explosive used in the Tangansay crater was ammonium nitrate. United States experience has not indicated that this explosive is as much better than TNT as this crater would require.

Nuclear Explosive Data

Table I shows a summary of most of the pertinent nuclear cratering data that have been obtained since 1951. Not shown is a large amount of data obtained from explosions at much larger depths of burst which will be discussed in a later section. The nuclear data points for desert alluvium have been plotted on Figs. 3 and 4. These nuclear cratering data include the Jangle S and Jangle U cratering explosions at very shallow depths of burial which were fired in 1951. Also shown is the Teapot ESS explosion at a moderate depth of burial which was fired in 1955 and the slightly buried Johnnie Boy shot detonated in 1962. All of these detonations were fired as part of nuclear weapons effects tests.

Another data point of extremely great significance is that representing the Sedan detonation. Sedan was detonated on 6 July 1962 at a depth of 635 feet in the desert alluvium of Area 10 at NTS very near the site of the Jangle U and Teapot ESS craters. The yield of the explosion was approximately 100 kilotons. The crater resulting from this explosion had a radius of about 600 feet and a depth of 320 feet. Figure 6 shows a view of Area 10 with the Sedan crater in the foreground, the Jangle U and Teapot ESS craters in the right background, and the Scooter crater in the left background. The scale of the Sedan crater may be judged from the construction equipment on the lip of the crater in the foreground of the picture. Figure 7 is a closer view of the crater showing the true crater outcropping around the perimeter of the crater. Figure 8 shows a still closer view of the crater taken from one side of the lip showing the outcropping of the up-turned true crater surface with the talus slopes of fallback material below extending to the bottom of the crater. In the bottom of the crater three men can be identified. The Sedan crater was very symmetrical with the radius varying by less than a few percent around its circumference. As can be seen in Fig. 4, the Depth of the Sedan crater is slightly larger than one would predict on the basis of the chemical-explosive data and the use of $W^{1/3.4}$

Table I. Summary of nuclear cratering data from the Nevada Test Site.

			Dimensions of Apparent Crater				
Shot name	Medium	Yield (kt)	Depth of burst (ft)	Radius (ft)	Depth (ft)	Volume (yd^3)	Lip height (ft)
Jangle S	Alluvium	1.2 ± 0.1	-3.5*	45	21	1.65×10^3	-
Johnnie Boy	Alluvium	0.5 ± 0.2	1.75	61	30	5.3×10^3	10
Jangle U	Alluvium	1.2 ± 0.1	17	130	53	3.7×10^4	8
Teapot ESS	Alluvium	1.2 ± 0.1	67	146	90	9.6×10^4	20
Sedan	Alluvium	100 ± 15	635	604	320	6.6×10^6	15 - 100
Danny Boy	Basalt	0.42 ± 0.08	110	107	62	3.6×10^4	15 - 30
Neptune**	Tuff	0.115 ± 0.015	100	100	35	2.2×10^4	-

*Detonated 3.5 ft Above Surface

**Neptune was Detonated 100 ft Beneath a 30° Slope

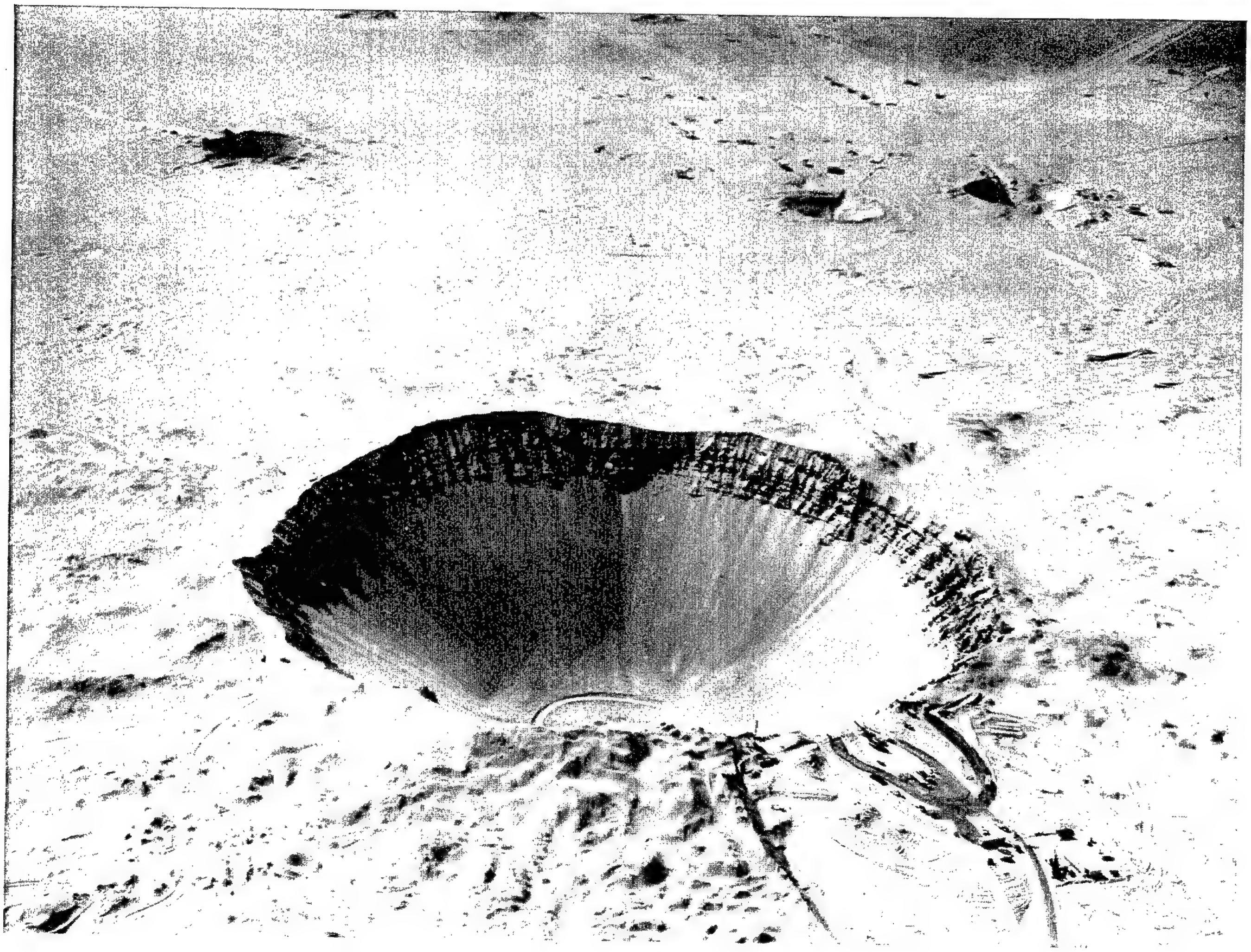

Fig. 6. Aerial view of Area 10, NTS showing the 100-kt Sedan crater in the foreground and three earlier kiloton-range craters.

scaling. The crater radius in Fig. 3, however, is significantly smaller than one would expect on the same basis.

A great deal of serendipitious data have been obtained from the nuclear weapons tests conducted in Areas 3, 9, and 10 of the Nevada Test Site over the past several years. When a large nuclear explosion is detonated at a depth of burial much deeper than optimum, a large underground cavity is formed which ultimately collapses, resulting in a large subsidence crater at the surface of the ground. Figure 9 shows a schematic cross section of such a crater as reconstructed from post-shot drill-hole information. Figure 10 is a photograph of a typical subsidence crater a few seconds after it has collapsed. The data points for a large number of these subsidence craters whose scaled depths of burial vary from 300 to 700 feet/$kt^{1/3.4}$ have been plotted on Figs. 3 and 4. In some cases the detonation point was located in weakly cemented tuff, whereas in others it was located in alluvium. In all cases the major portion of the collapse chimney region was in alluvium. The nature of the medium surrounding the detonation point has been indicated on the graphs.

These subsidence cratering data for large-yield explosions have had a significant effect on our predictions of the size craters expected at large depths of burial in desert alluvium. Shown on Figs. 3 and 4 as solid lines are the nuclear crater curves that would be expected for large nuclear explosions in desert alluvium. It should

be noted that subsidence craters are only expected in a medium such as desert alluvium where no bulking during collapse is observed. In a rock-type medium where bulking does occur, the volume of the underground cavity would not be transmitted to the surface as it is in alluvium but would be distributed throughout the chimney region in the form of voids between the broken rock. In most rock media the collapse region would, in fact, not even reach to the surface of the ground.

Basalt

Chemical-Explosive Data

The cratering data available for hard rock are extremely sparse. The only data of any significance at all on apparent crater dimensions that was available prior to 1960 was from a cratering program sponsored by the Panama Canal Company as part of the 1947 Isthmian Canal Studies.[12] This program consisted of about 20 cratering detonations with the charge weights ranging from 8 to 200 pounds. Because of the small charge weight and the fact that the charges were cylindrical in shape, these data are not considered to be relevant to the problem of nuclear excavation.

To obtain cratering data for hard rock that would be useful to the Plowshare Program, Project Buckboard was undertaken in the Summer of 1960. This program, sponsored by Plowshare and executed in the field by Sandia Corporation, was a direct result of the 1960 Isthmian Canal Studies by the Atomic Energy Commission and

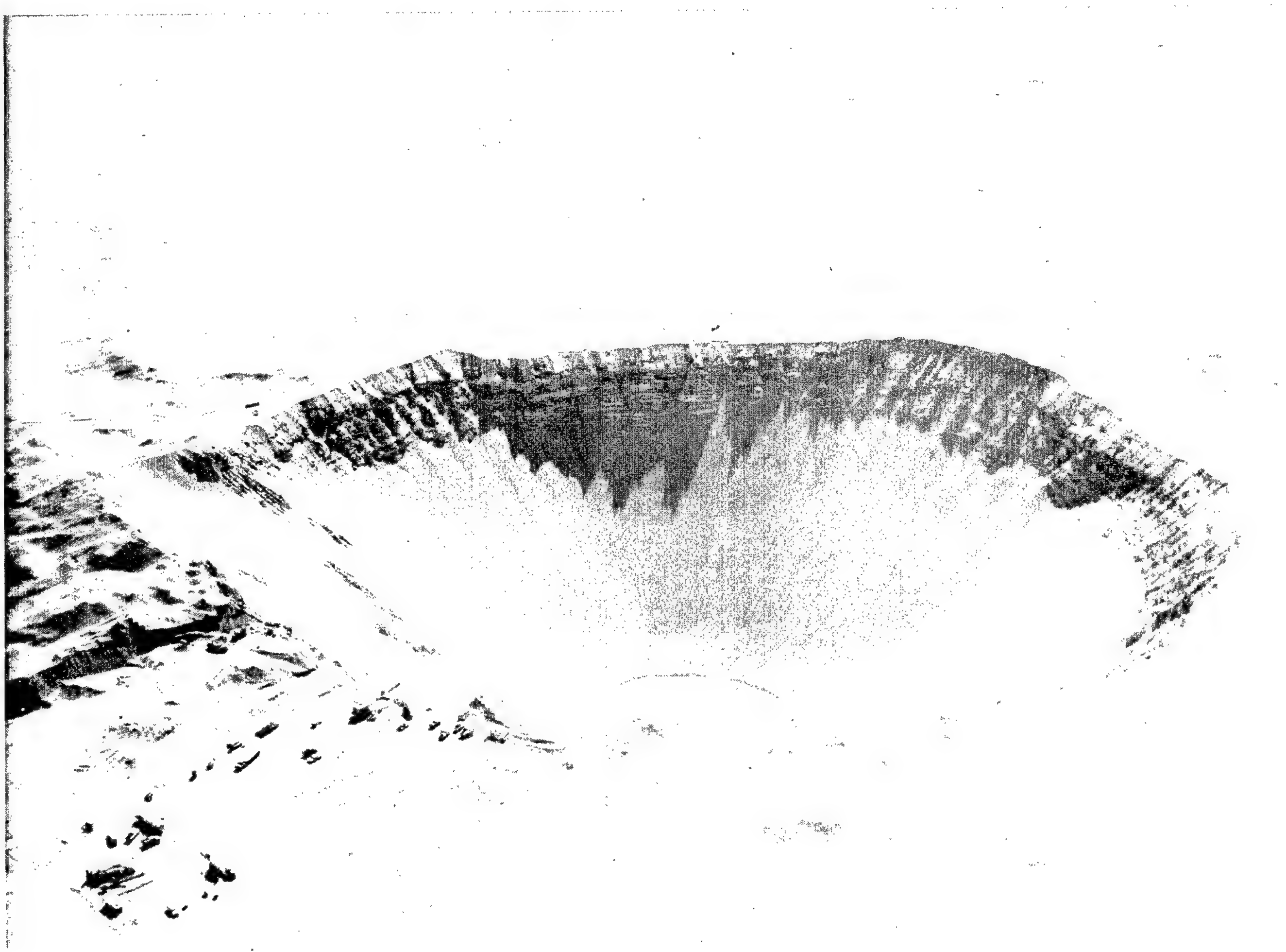

Fig. 7. Aerial view of Sedan crater showing construction equipment on edge of crater.

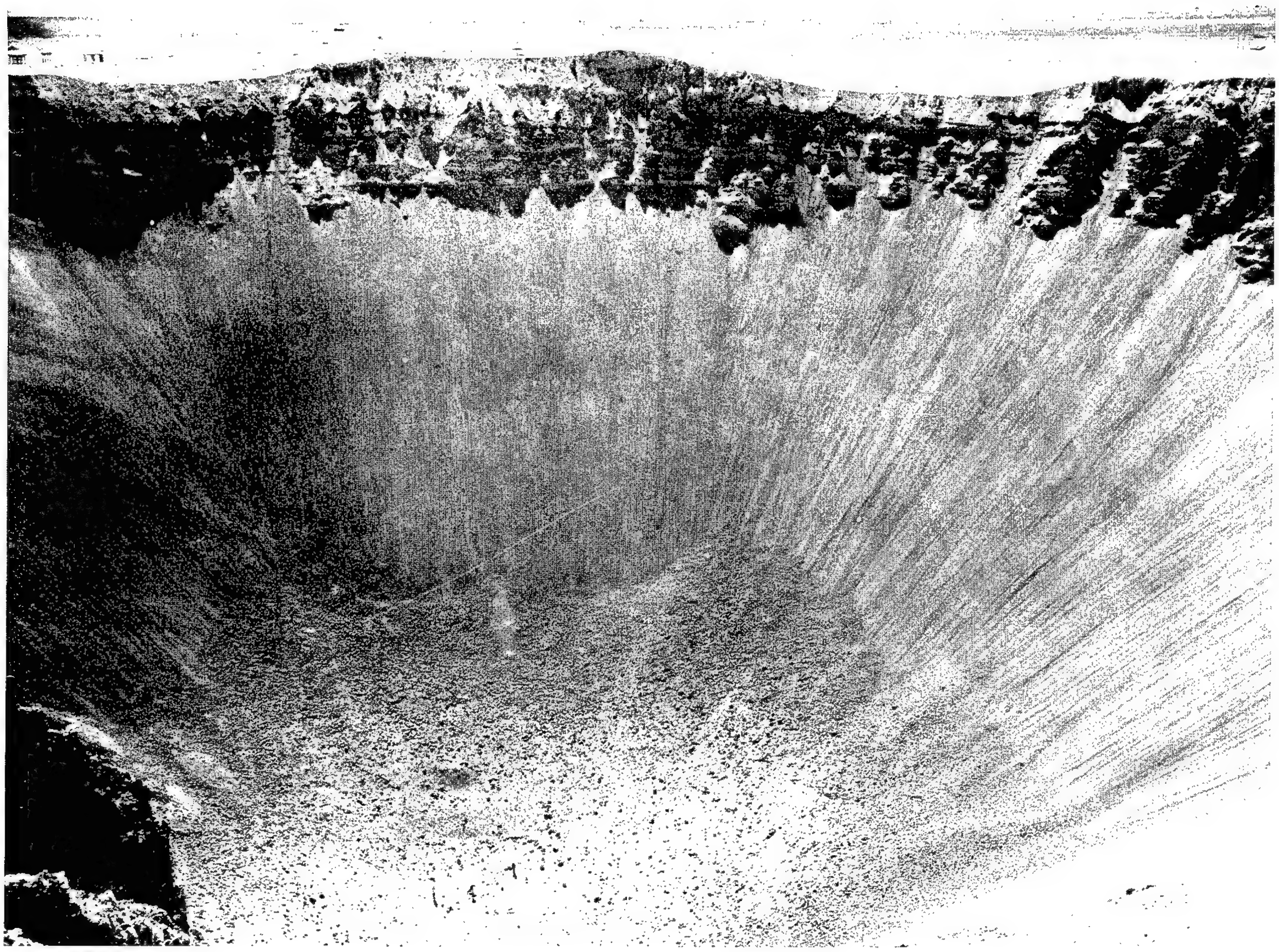

Fig. 8. View of Sedan crater taken from the lip and showing the outcropping true crater at the top of the apparent crater, and the talus slopes below. Note the three men in the bottom of the crater.

the Panama Canal Company and consisted of ten 1000-pound and three 40,000-pound detonations in basalt.[13] The site was a basalt-topped mesa in the Forty-Mile Canyon area on the west side of the Nevada Test Site. Scaled depth of burial for the 1000-pound shots varied from about 45 feet/$kt^{1/3.4}$ to 230 feet/$kt^{1/3.4}$. The three 40,000-pound shots were at scaled depths of burial of 85, 142, and 185 feet/$kt^{1/3.4}$. These data are shown in Figs. 11 and 12. The scatter of the data for the 1000-pound shots would appear to be at least ±25% and visual observation of the craters leads to the conclusion that 1000-pound charges in a hard rock such as basalt do not result in meaningful apparent crater data. The apparent craters for the 40,000-pound charges, however, would appear to be much more relevant. It should be mentioned that the crater resulting from the intermediate shot at 142 feet/$kt^{1/3.4}$ was half in cinders and half in solid basalt. The effect of this on crater dimensions was somewhat difficult to estimate, but the unusually large dimensions of this crater relative to the other craters made this data point appear to be somewhat anomalous.

In an effort to obtain more and better data in basalt, a cratering program was undertaken in the Spring of 1964 by the U. S. Corps of Engineers Nuclear Cratering Group at Livermore. This program consisted of four 40,000-pound shots using the liquid high-explosive called nitrometh-

ane. These data are also plotted on Figs. 11 and 12. This cratering program was conducted at the same site as Buckboard and was called Pre-Schooner.

Also shown on Figs. 11 and 12 is a curve fit by eye to the 40,000-pound data. The 1000-pound crater data, where the particle size of the fallback was much larger in proportion to the crater than for the 40,000-pound craters, and the data point for the anomalous Buckboard crater at 142 feet/$kt^{1/3.4}$ were given essentially no weight. Comparison of the 1000-pound crater data and the 40,000-pound crater data does not allow derivation of an empirical scaling exponent for basalt, but it does indicate that a scaling such as $W^{1/3.4}$ is adequate and that $W^{1/3}$ would not correlate the data properly.

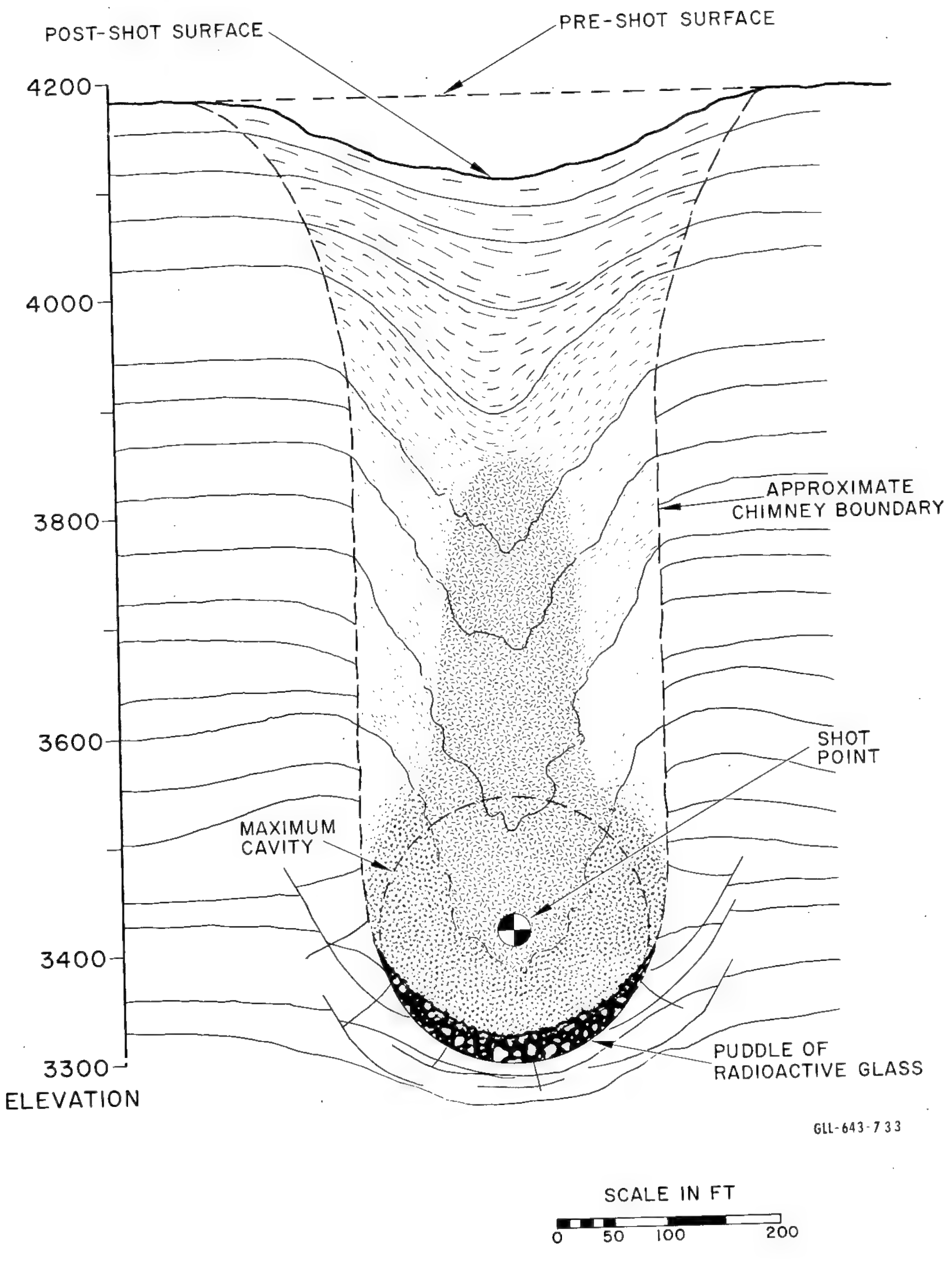

Fig. 9. Schematic cross section of a typical subsidence crater in alluvium.

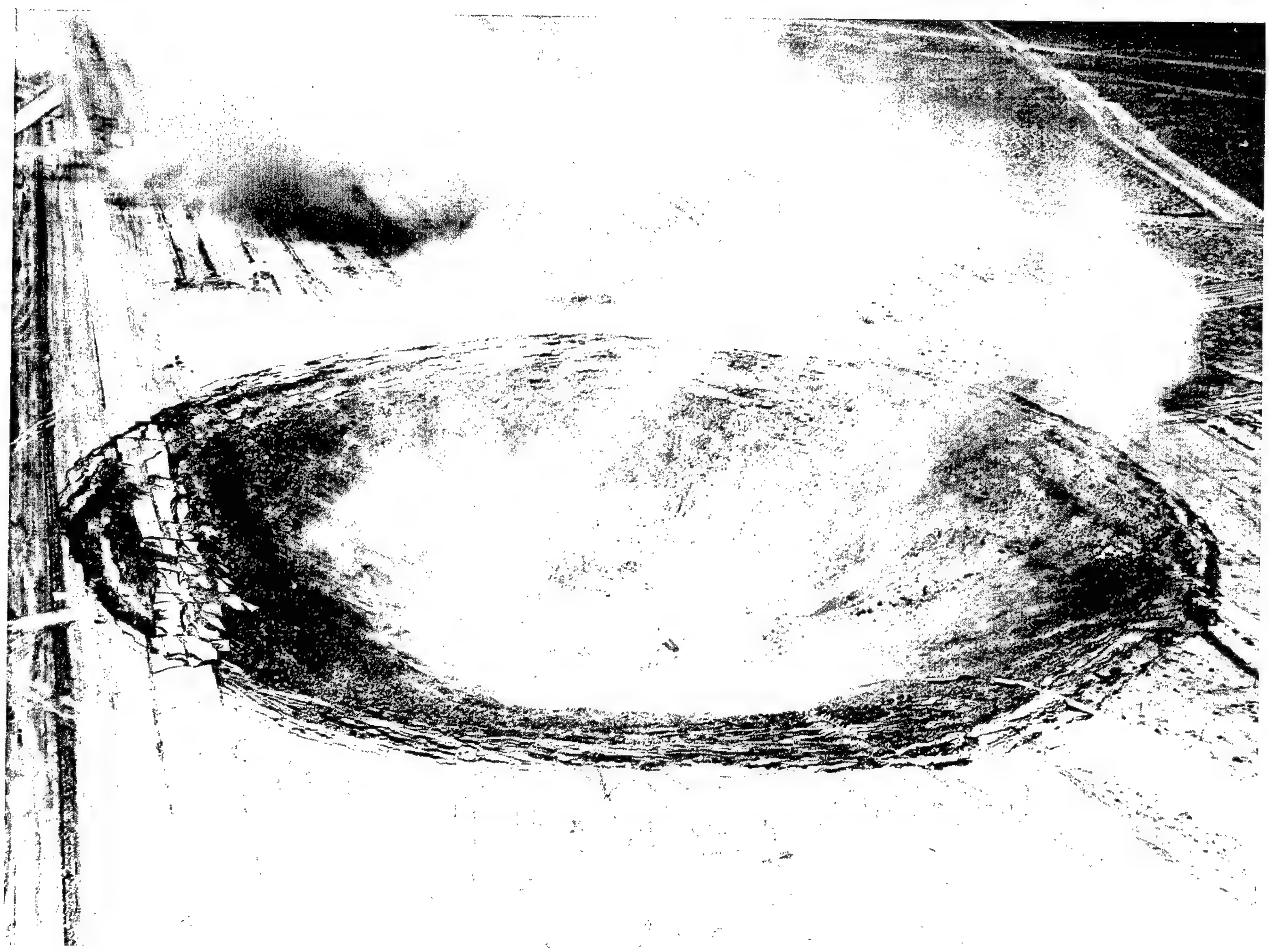

Fig. 10. Aerial view of a typical subsidence crater taken several seconds after collapse.

Nuclear Explosive Data

The data points from the one nuclear cratering event in hard rock, called "Danny Boy",[14] are shown on Figs. 11 and 12. This was a 0.42-kt nuclear explosion buried at a depth of 110 feet in the same basalt as was used for the Buckboard and Pre-Schooner chemical-explosive cratering programs. The crater dimensions are shown in Table I. Figure 13 is an aerial view of the Forty-Mile Canyon area showing the Danny Boy crater in the center. The roads going off to the horizon were used for fallout collection on the Danny Boy event. Figure 14 is a closer aerial view of the Danny Boy crater showing the size of the fallback debris in relation to the trucks on the lip of the crater. Although it is not apparent from this picture, the Danny Boy crater is very symmetrical. The lip varies in height from 15 to 25 feet. The data point for the depth of the Danny Boy crater on Fig. 12 appears to agree fairly well with the curve predicted on the basis of the high-explosive data. The point for the radius on Fig. 11 appears to be approximately 10 to 15% below the curve. This effect on the depth being approximately equal to the high-explosive data and the radius about 10 to 20% low, corresponds to what has been observed for desert alluvium.

Other Media

There have been numerous cratering programs in the past in a variety of media. Unfor-

tunately, many of these data are not applicable either because of failure to measure apparent crater dimensions, concentration of the data at too shallow a depth of burst for our purposes, unusual charge shapes, or the use of too small a charge weight to give significant data. The only programs whose results have been found to be at all useful to Plowshare are the cratering studies conducted by the Panama Canal Company referred to above.[15-18] Perhaps the best summary of what cratering data do exist in other media is given in the compendium recently published by the Waterways Experiment Station.[19]

The only other nuclear cratering data in a medium other than alluvium or basalt has come from the Neptune event.[20] Neptune was a 0.110-kt nuclear cratering explosion detonated about 100 feet under the sloping side of the Rainier mesa. The medium surrounding the detonation point was tuff. The results of this explosion are summarized in Table I.

LINEAR AND ROW CHARGE DATA

Alluvium

A number of cratering programs have been carried out in alluvium to study the cratering characteristics of linear and row charges. The first program along this line, called "Project Toboggan," was sponsored by Plowshare and conducted by Sandia Corporation.[21] It consisted of about 92 detonations using line charges in the Yucca Dry Lake area at the Nevada Test Site. Sponsored by the Plowshare Program, a great deal of row-cratering work on a continuing basis has been carried out by Sandia Corporation at its field testing site near Albuquerque, New Mexico,[22] using charge weights ranging from 8 to 64 pounds.

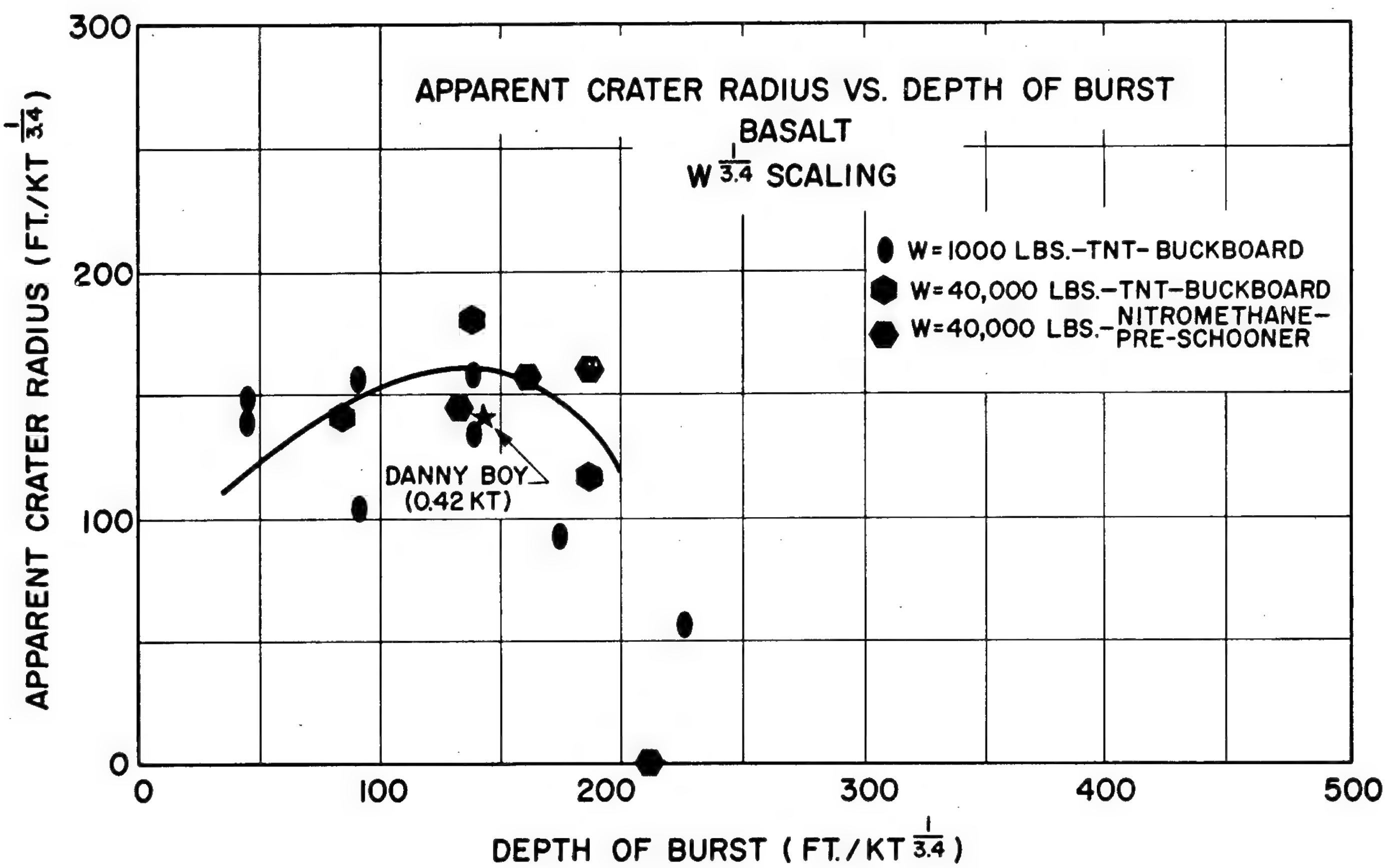

Fig. 11. Plot of high explosive (H.E.) and nuclear explosive apparent crater radium data vs depth of burst; basalt, $W^{1/3.4}$ scaling.

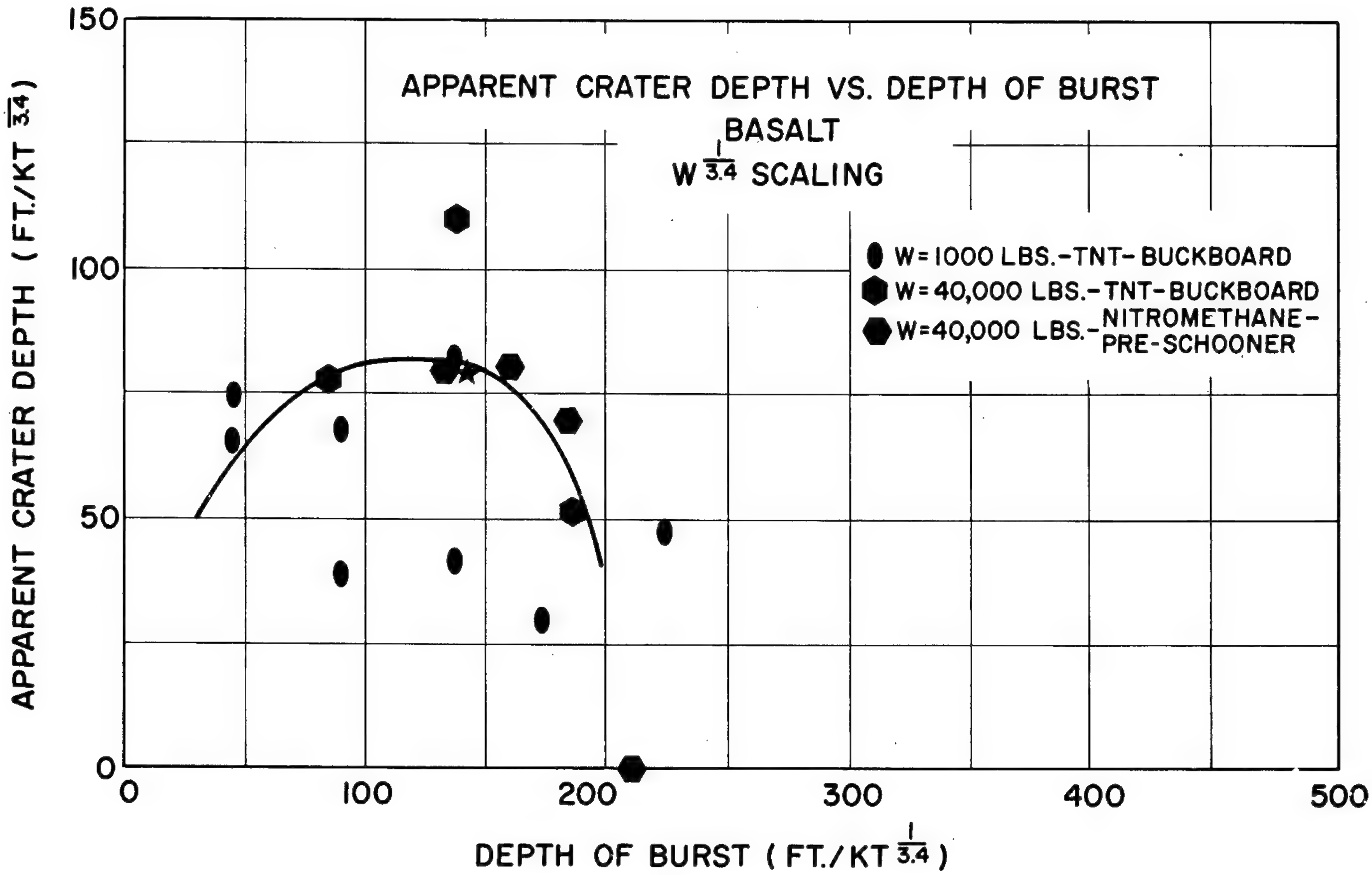

Fig. 12. Plot of high explosive (H.E.) and nuclear explosive apparent crater depth data vs depth of burst; basalt, $W^{1/3.4}$ scaling.

In an effort to obtain row-cratering data in the same desert alluvium in which the large amount of single-crater data discussed above is available, Project Rowboat was sponsored by Plowshare in 1960 in Area 10 at NTS. This program consisted of eight detonations, each utilizing four 256-pound charges in a row detonated simultaneously. This program was extended in 1963 by the U. S. Corps of Engineers Nuclear Cratering Group in the Pre-Buggy Program.[23] This program consisted of a number of cratering shots utilizing 1000-pound charges of nitromethane. Each detonation consisted of five charges in a row, again detonated simultaneously. In an extension of this program in July 1963 conducted by LRL, termed Pre-Buggy II, these cratering data were extended to two unique geometries: One consisted of two craters connected end-on in an attempt to explore the problem of connecting two craters. The other unusual geometry involved 13 charges using the same depth of burst, but three different spacings. The Pre-Buggy area is shown in Fig. 15. The two connecting craters are shown in the Pre-Buggy II area and are labeled CC'. The 13 charges with three different spacings are labeled Row H.

The purpose of these row cratering experiments has been to determine (1) what is the effect on crater dimensions of variation in the spacing between charges; (2) what is the effect of spacing on the irregularity or cusping in the crater; and (3) what is the shape of the lip relative to the lip obtained with point charges, both on the sides of the crater and on the ends of the crater. The conclusion from the existing row-charge data can be summarized as follows: (1) use of a spacing equal to approximately a single crater radius results in a smooth-sided crater with apparent dimensions of about 10 to 20% larger than expected on the basis of single-charge data; (2) use of spacing of about 1.25 times a single crater radius results in a ditch with dimensions approximately equal to those expected from single charges; (3) using a

spacing of 1.5 times a single crater radius results in a crater which is somewhat smaller than a single crater radius and quite irregular in cross section. These three spacings were used for the Row H and the effect of the various spacings can be seen in Fig. 15 as well as in Fig. 16, which is an aerial view of the Row H, Pre-Buggy II.

The other significant conclusion from the above cratering programs is that when four or five or more charges in a row are fired simultaneously under conditions that result in a uniform ditch, the lips on the sides of the crater are considerably higher than would be expected from single crater lips, being approximately 50 to 100% higher, whereas the lip on the end of the crater is virtually nonexistent. This effect is well illustrated in Fig. 17, an end view of one of the Pre-Buggy craters showing the high lip on the sides of the crater and the absence of lip on the end of the crater in the foreground. This effect, of course, is extremely significant when one is discussing the concept of making a long channel where it is necessary to connect a number of ditches.

It is interesting to compare the above criteria on spacing with that recommended by a number of Russian handbooks on the subject of cratering.[8,9] Although most of their interest has been in craters with depth of burial at optimum or 20 to 30% less than optimum, the recommended spacing they give is equal to the radius of the crater plus the depth of burst of the crater divided by two. For the region of optimum, this is essentially the same criteria as outlined above.

It must be pointed out that the above conclusions with respect to row charges are based upon cratering programs in alluvium or alluvial type

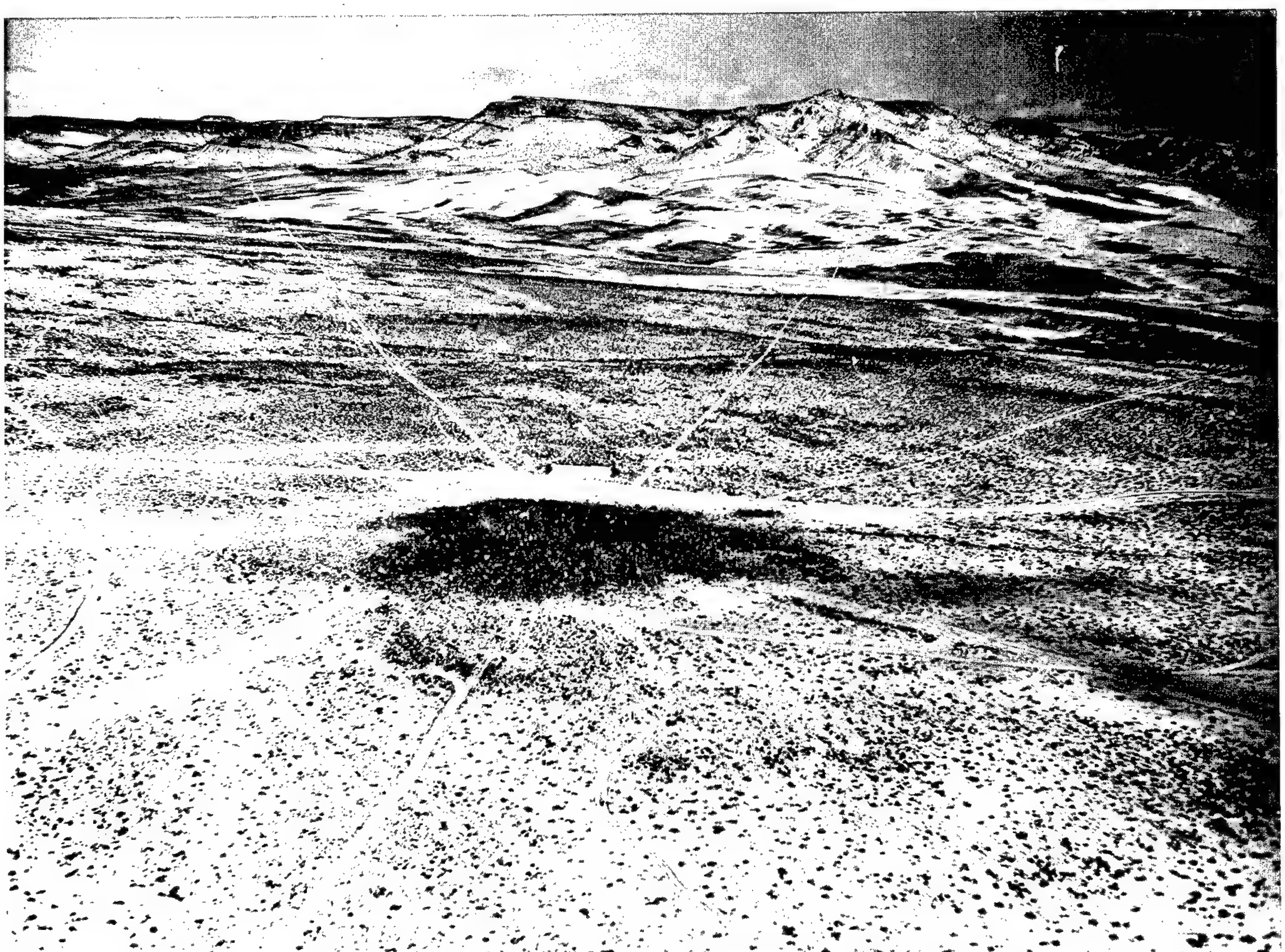

Fig. 13. Aerial view of Buckboard Mesa, NTS, showing Danny Boy crater.

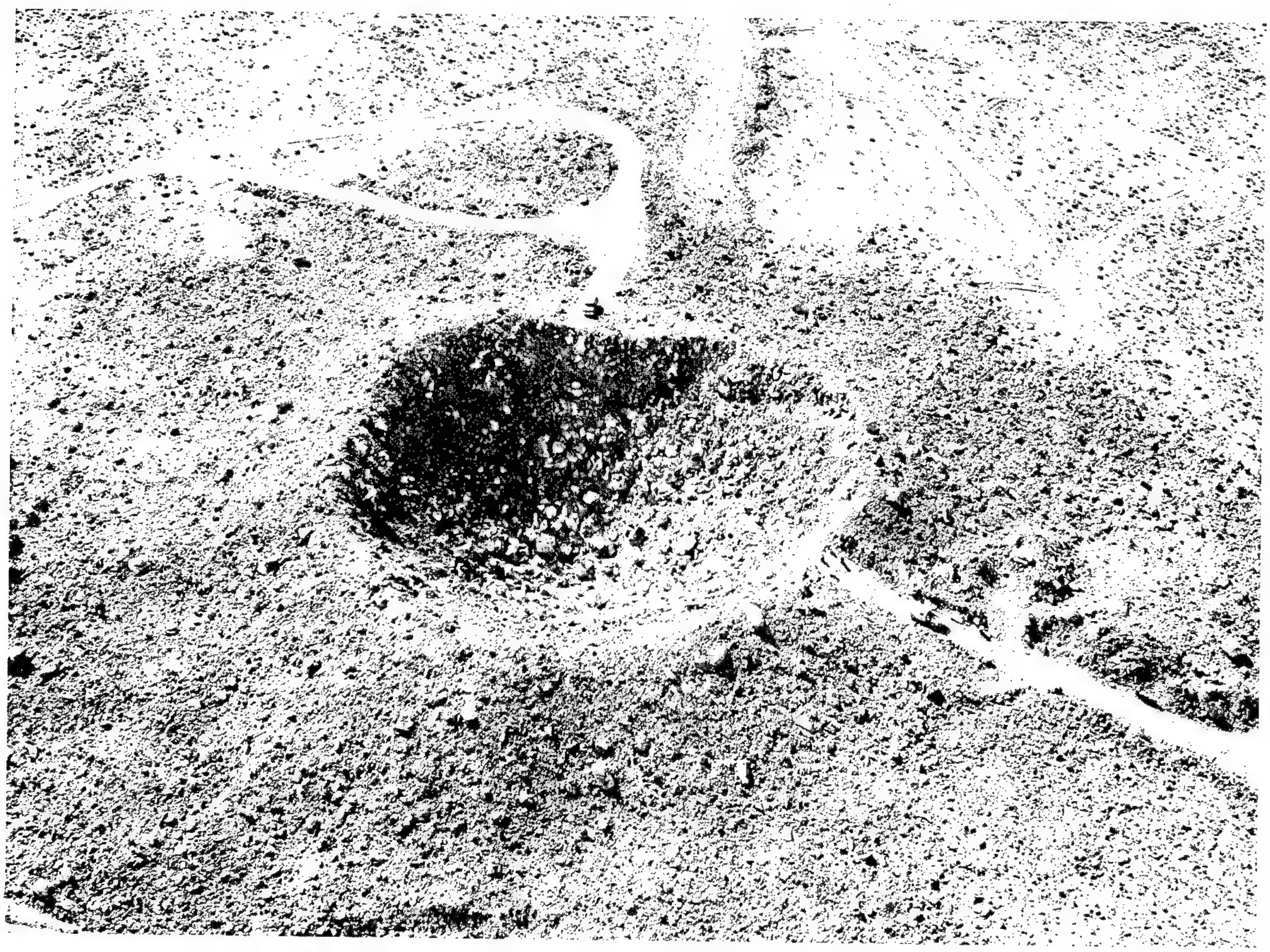

Fig. 14. Aerial view of Danny Boy crater showing particle size of fallback in relation to vehicles on lip.

materials. At present there are no data on row charges in anything like a hard rock. Since most nuclear excavation applications will be in hard rock, it is regarded as extremely important to extend these conclusions to that medium. Plans are currently under way for the execution of a row-charge cratering experiment in the basalt at Buckboard Mesa. As currently planned, this project will consist of five nitromethane spheres, each containing 40,000 pounds of nitromethane. The planned depth of burial corresponds to a scaled depth of burial of 185 feet/kt$^{1/3.4}$.

CONCLUSIONS

As outlined above, a large quantity of cratering data has been obtained over the past 13 years in a number of media. One medium in particular, NTS desert alluvium, has been exhaustively explored with both high-explosive point charges, nuclear point charges, and high-explosive row charges. One other medium, basalt, has been explored moderately well with large-yield charges and cratering curves have been determined. These two media, in general, are expected to bracket the types of media to be encountered in nature and so the range of crater dimensions to be expected for nuclear excavation projects will, in all probability, fall between these two. A large amount of row-charge data has been obtained in alluvium. A number of significant conclusions relevant to nuclear excavation have been drawn and plans are being actively pursued to either confirm or deny these assumptions in media other than desert alluvium.

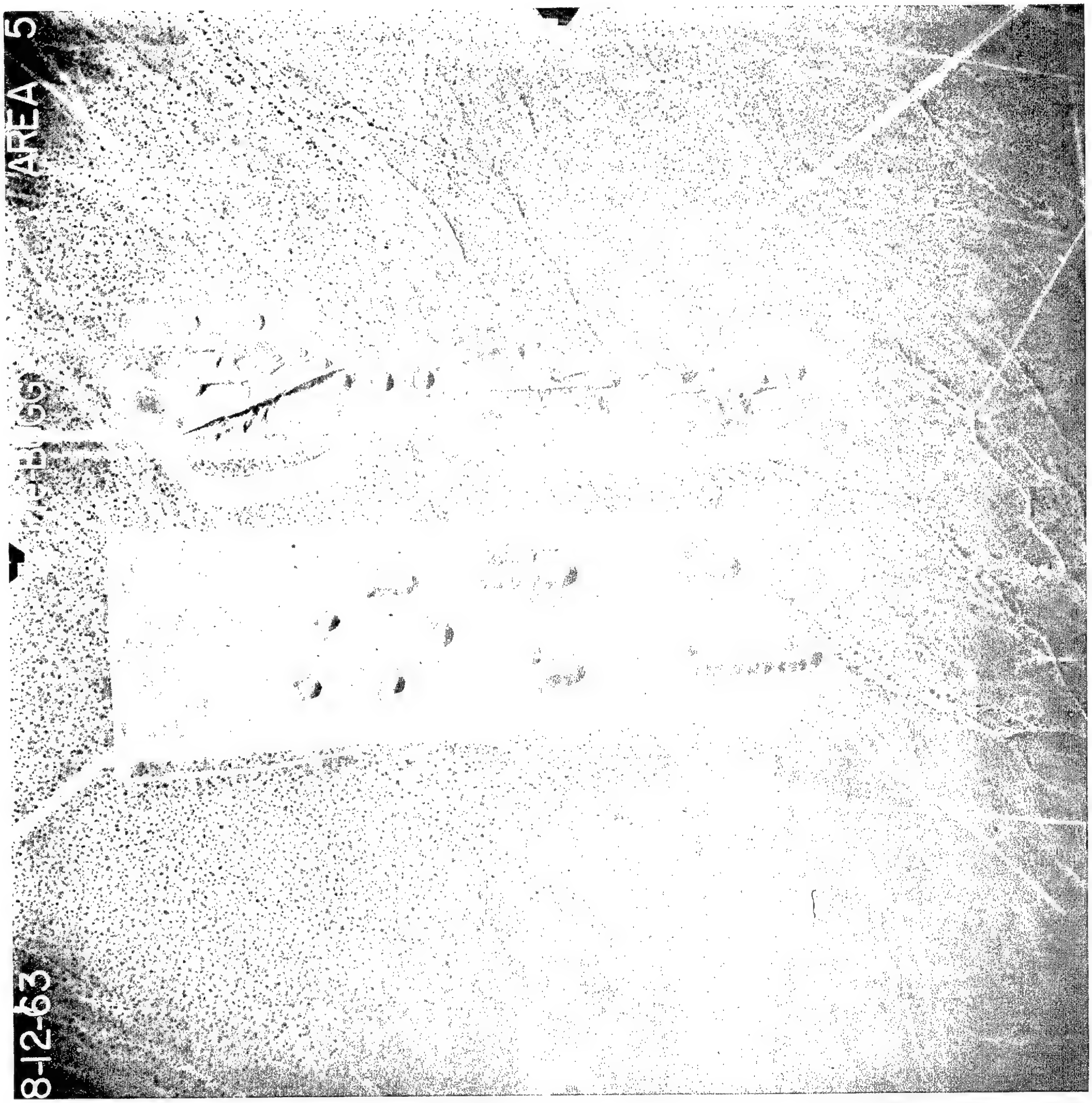

Fig. 15. Vertical aerial view of Pre-Buggy crater in Area 5, NTS.

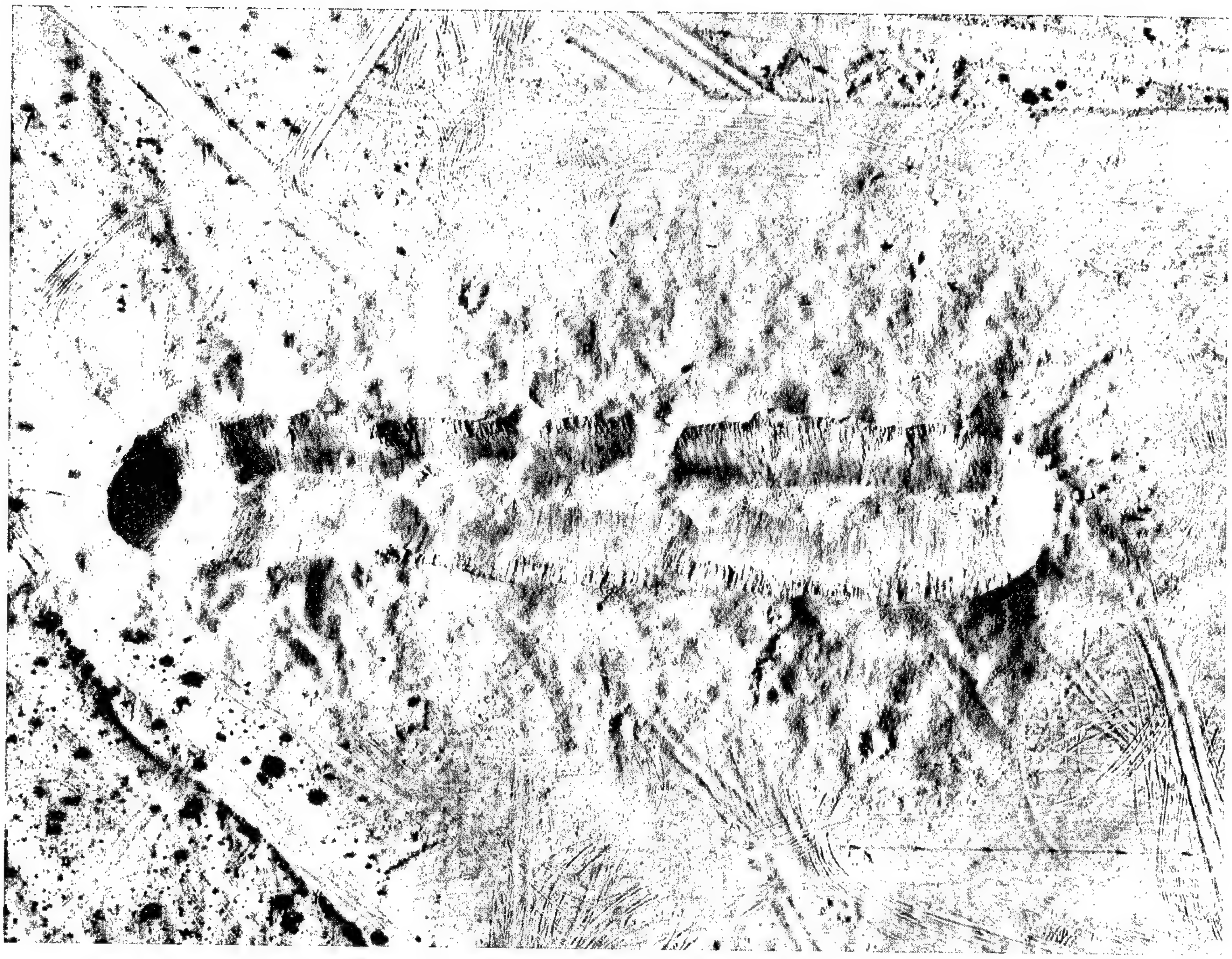

Fig. 16. Vertical aerial view of Pre-Buggy crater H, showing effect of change of spacing from one radius spacing on the left to one and one-half spacing on the right.

Fig. 17. End view of Pre-Buggy crater showing high side lip and absence of lip on the end.

REFERENCES

1. Sedov, L. I., "Similarity and Dimensional Methods in Mechanics," Academic Press, New York, p. 251 ff., 1959.
2. Nordyke, M. D., "An Analysis of Cratering Data from Desert Alluvium," Journal of Geophysical Research 67, No. 4, p. 1965, 1961.
3. Sachs, D. C. and Swift, L. M., "Small Explosion Tests, Project Mole, Final Report," Stanford Research Institute, AFSWP-291, 1955.
4. Lewis, J. G., "Crater Measurements, Operation Teapot," Engineering Research and Development Laboratory, WT-1105, 1958.
5. Murphey, B. F., "High Explosive Crater Studies: Desert Alluvium," Sandia Corporation, SC-4614(RR), 1961.
6. Vortman, L. J., et al., "Project Stagecoach, Final Report," Sandia Corporation, SC-4596(RR), 1960.
7. Perret, W. R., et al., "Project Scooter, Final Report," Sandia Corporation, SC-4602(RR), 1963.
8. Pokrovskii, G. I. and Fedorov, I. S., "Effect of Shock and Explosion on Deformable Media," Gos. Izd., 1957.
9. Dokuchaev, M. M., et al., "Handbook on Drill Blasting Operation in Construction," Gos Izd., 1962.
10. Kogen, S. D., et al., "The Difference in the Period of Seismic Waves Excited During Underground Explosion and Earthquakes," Proceedings of the Academy of Sciences of the U.S.S.R., 219, No. 6, pp. 1283-1286, 1959.
11. Lavrentiev, M. A., private communication, 1964.
12. "Crater Tests in Basalt," Panama Canal Company, Isthmian Canal Studies Memo 284-P, 1948.
13. Vortman, L. J., et al., "Project Buckboard, Final Report," Sandia Corporation, SC-4675(RR), 1962.
14. Nordyke, M. D. and Wray, W. R., "A Nuclear Cratering Detonation in Basalt," Journal of Geophysical Research 69, No. 4, pp. 675-690.
15. "Crater Tests in Gatun Sandstone," Panama Canal Company, Isthmian Canal Studies Memo 285-P, 1948.
16. "Crater Tests in Residual Clay," Panama Canal Company, Isthmian Canal Studies Memo 287-P, 1948.
17. "Crater Tests in Marine Muck," Panama Canal Company, Isthmian Canal Studies Memo 286-P, 1948.
18. "Crater Tests in Cucaracha and Culebra Formations," Panama Canal Company, Isthmian Canal Studies Memo 283-P, 1948.
19. "Compendium of Crater Data," Waterways Experiment Station, Technical Report No. 2-547, 1960.
20. Shelton, A. V., Nordyke, M. D. and Goeckermann, R. H., "The Neptune Event," Lawrence Radiation Laboratory, UCRL-1105, 1958.
21. Carlson, R. H., "High Explosive Ditching from Linear Charges," Sandia Corporation, SC-4483(RR), 1961.
22. Vortman, L. J. and Schofield, L. M., "The Effect of Row Charge Spacing and Depth on Crater Dimensions," Sandia Corporation, SC-4730(RR), 1963.
23. Graves, E., Wray, W. and Pierce, R., "Scope of Chemical Explosive Cratering Experiment, Pre-Buggy, Preliminary Report," U.S. Army Corps of Engineers Nuclear Cratering Group, PNE-300, 1963.

APPENDIX A

Recommended Crater Terminology

A serious lack of consistency of terminology has characterized numerous articles published in recent years reporting research in the cratering field. The need for a uniform system of terminology to provide a common basis of expression has thus become increasingly apparent.

The system here proposed was developed as a result of conferences held at the Lawrence Radiation Laboratory in Livermore, California, and at the Atomic Energy Commission Nevada Test Site during November and December 1963 by representatives of several organizations currently engaged in research in the nuclear cratering field.[1,2,3] The purpose of the conferences was to consider the problem of formulation of a unified system of crater terminology.

An effort has been made to formulate both notation and terminology which will have practical use in the study and representation of nuclear and high-explosive craters, and which will provide a basis for an orderly expansion of terminology as becomes necessary in the future.

---

[1] Plowshare Division, Lawrence Radiation Laboratory, Livermore, California.

[2] U. S. Army Engineer Waterways Experiment Station, Vicksburg, Mississippi

[3] U. S. Army Engineers, Nuclear Cratering Group, Livermore, California.

RECOMMENDED CRATER NOMENCLATURE

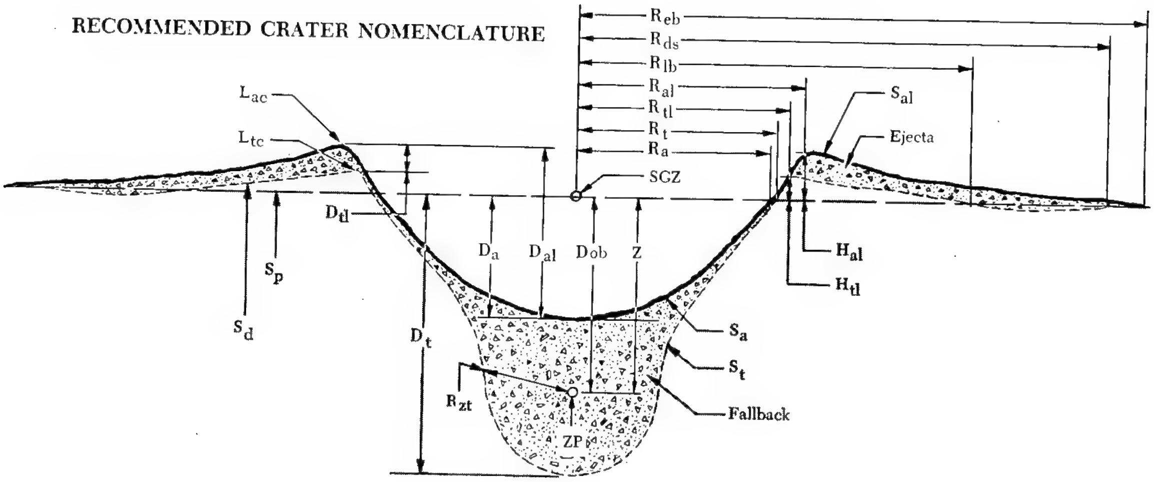

D_a . . . Maximum depth of apparent crater below preshot ground surface measured normal to the preshot ground surface.*

D_{al} . . . Depth of apparent crater below average apparent crater lip crest elevation.

Dob . . Normal depth of burst (measured normal to preshot ground surface).

D_t . . . Maximum depth of true crater below preshot ground surface.

D_{tl} . . . Depth of true crater lip crest below apparent crater lip crest.

Ejecta . Material above and or beyond the true crater and includes: (1) foldback; (2) breccia—ballastic trajectory; (3) dust—aerosol transport; etc.

Fallback . Material fallen inside the true crater and includes: (1) slide blocks; (2) breccia and stratified fallback—ballastic trajectory; (3) dust—aerosol transport; (4) talus; etc.

H_{al} . . . Apparent crater lip crest height above preshot ground surface.

H_{tl} . . . True crater lip crest height above preshot ground surface.

L_{ac} . . . Apparent crater lip crest.

L_{tc} . . . True crater lip crest.

R_a . . . Radius of apparent crater measured on the preshot ground surface.

Note: The radius measurements pertain only to single charge craters and represent average dimensions. If crater shape deviates substantially from circular, the direction of measurement must be specified. An average radius value can also be determined by dividing the plan area by π and taking the square root.

R_{al} . . . Radius of apparent lip crest to center.

R_{ds} . . . Outer radius of displaced surface.

R_{eb} . . . Radius of outer boundary of continuous ejecta.

R_{lb} . . . Outer radius of true lip boundary.

R_t . . . Radius of true crater measured on the preshot ground surface.

R_{tl} . . . Radius of true lip crest to center.

R_{zt} . . . Distance between the zero point and the true crater surface measured in any specified direction. When measured in a direction below the zero point is equivalent to lower cavity radius.

S_a . . . Apparent crater surface, e.g. rock-air or rubble-air interface.

S_{al} . . . Apparent lip surface.

SGZ . . Surface ground zero.

S_d . . . Displaced ground surface.

S_p . . . Preshot ground surface.

S_t . . . . True crater surface, e.g. rock-air or rock rubble interface.

V_a . . . Volume of apparent crater below preshot ground surface.

V_{al} . . . Volume of apparent crater below apparent lip crest.

V_t . . . Volume of true crater below preshot ground surface.

V_{tl} . . . Volume of true crater below true crater lip crest.

Z . . . . Vertical depth of burst (equivalent to dob when crater is formed on a horizontal surface).

ZP . . . Zero Point—effective center of explosion energy.

Note: The following definitions apply to linear craters only. Linear crater refers to the excavation formed by overlapping crater effects resulting from a row of charges. All above terms applicable to single craters apply also to linear craters with the exception of the radius terms which are replaced by the width terms below.

W_a . . . Width of apparent linear crater measured on the preshot ground surface.

W_{al} . . Width of apparent lip crest measured across linear crater.

W_{ds} . . Width of displaced surface measured across linear crater.

W_{eb} . . Width of outer boundary of continuous ejecta measured across linear crater.

W_{lb} . . Width of true crater outer lip boundary measured across linear crater.

W_t . . . Width of true linear crater measured on the preshot ground surface.

W_{tl} . . . Width of true linear crater lip crest measured across crater.

*All distances, unless specified otherwise, are measured parallel or perpendicular to preshot ground surface.

BIOGRAPHICAL SKETCH OF AUTHOR

Milo D. Nordyke received his B.A. in Physics from the State University of Iowa, Iowa City, Iowa, in 1951, and his M.A. in Physics from the University of California, Berkeley, California, in 1959.

In 1951 he joined the staff of the National Bureau of Standards Laboratory (which later became the Naval Ordnance Laboratory), where he was engaged in experimental research for proximity fuse development. In 1955 he transferred to the Lawrence Radiation Laboratory, Livermore, where he participated in nuclear explosives design. In 1959 he became a member of the Laboratory's Plowshare Division as a physicist with special interest in nuclear excavation. He is presently the coordinator of the Field Programs Group in the Plowshare Division.

CALCULATION OF EXPLOSION-PRODUCED CRATERS

J. B. Knox
R. W. Terhune

Lawrence Radiation Laboratory, University of California
Livermore, California

ABSTRACT

This study develops a simple, two-dimensional model of cratering physics for high-explosive sources in alluvium during the gas acceleration phase of excavation. The model requires knowledge of the earth's free-surface topography and motion at the time the surface gas acceleration begins (t_G), and the cavity pressure and volume. At t_G, the overburden material, that material between the cavity and the earth's free surface, is assumed to be a homogeneous, incompressible, viscous fluid. At this time the cavity is approximated by two hemispheres: (a) the radius of the lower hemisphere is calculated by a one-dimensional, hydrodynamic, plastic-elastic model (SOC), and (b) the radius of the upper hemisphere is calculated from mass conservation of the overburden material. In the model the upper hemispheric surface is subdivided into elemental surface areas, and mass zones are defined which subtend these elemental surface areas. By applying Newton's second law with a simple frictional force (calibrated on the Scooter event) to each mass element, and by assuming that the cavity gas behaves adiabatically, the cavity evolution, mound development, and the formation of the lip through up-thrust are numerically simulated.

With the development of a calibrated, numerical simulation model of excavation processes during the surface gas acceleration phase, the capability of the model to estimate the apparent crater radii and depths for 1/2-kt, high-explosive (H.E.) sources at various emplacement depths is explored. Assuming a reasonable angle of repose for alluvium, 45°, crater radii for scaled depths of burst from about 10 to 65 m are predicted. These estimated apparent crater radii compare very favorably with the observed crater radii (Nordyke, 1961) for H.E. in alluvium. Further, the crater depths, for certain types of craters, are also reasonably predicted.

INTRODUCTION

In this study, a physical-numerical model is used to investigate processes important for cratering with high-explosive sources in desert alluvium. High explosives do not vaporize much of the rock (or soil) surrounding the initial cavity containing the explosive. Thus a relatively simple, and in some cases a well-known, equation of state exists for the high-explosive cavity gas for an appropriate range of pressures. However, nuclear explosives are known to vaporize a great deal of surrounding rock or soil during the early part of the cavity life history (Nuckolls, 1959, Rawson, 1962). This vaporized material is believed to condense late in the life history of the cavity (Knox and Terhune, 1963), and prior to vent of the cavity gas to the atmosphere, such that the latent heat of condensation plays an important role in nuclear excavation. So far, no numerical-physical model of the response of a geologic environment to a nuclear explosive includes this effect of condensation on the hydrodynamics at late times. Thus, the calculation of the cavity pressure at late times including the effect of condensation is one of the current unsolved problems in the calculation of craters formed by nuclear explosives. By restricting this initial study to craters formed by high explosives, this cavity pressure problem is deferred. Further, by restricting this study to the calculation of events in desert alluvium, the need of estimating the amount, position, and kinematics of material fractured and prepared for additional acceleration by the cavity gas pressure is temporarily avoided. This study, then, develops a theoretical model (for H. E. sources) of the cavity life history, the mound

development, and the formation of the lip (by up-thrust) up to the time of vent of the cavity gas to the atmosphere. Assuming a 45° angle of repose for alluvium, and by normalizing the calculation with a simple frictional force to the Scooter event, it is possible with this model to estimate radii of explosion-produced craters with reasonable accuracy.

The gas acceleration phase of excavation with high explosives is formulated as a simple two-dimensional, initial-value problem requiring knowledge of the earth's free-surface topography and motion at the time the surface gas acceleration phase begins, t_G, and knowledge of the cavity pressure and volume. At t_G, the model assumes that the overburden material between the cavity and the free surface is a homogeneous, incompressible, viscous fluid. The initial subsurface cavity is approximated in the model by two hemispheres. The radius of the lower hemisphere is calculated by asymptotic behavior of a one-dimensional, hydrodynamic, plastic-elastic model of the response of a geologic environment to a high explosive. The radius of the upper hemisphere is calculated from conservation of mass in the overburden material, and the homogeneous, incompressibility assumption. At t_G, the upper hemisphere of the cavity surface is subdivided into elemental surface areas, and mass zones of overburden material are formed which subtend these elemental surface areas. By applying Newton's second law of motion with a simple frictional force to each mass element, and by assuming the cavity gas behaves adiabatically, the evolution of the cavity, the mound, and the up-thrust formation of the lip are numerically simulated.

With the development of a calibrated, numerical-physical model of excavation processes during the gas acceleration phase, it is natural to explore the capability of the model to calculate apparent crater radii for other depths of burial of the 1/2-kiloton high explosive. To do this, the cavity volume and pressure at t_G have been calculated for each selected depth of burial. Further, the position and velocity of the earth's free surface at t_G has been calculated semiempirically. The development of the cavity, mound, and the earth's free surface during the gas acceleration phase has been numerically simulated for several depths of burial of the 1/2-kiloton H. E. source. Assuming a reasonable angle of repose for alluvium of 45°, the apparent crater radii are predicted and are compared with the observed crater radii (Nordyke, 1961) for H. E. in alluvium.

With an interest during the last several years of the Plowshare Program in the mechanisms of cavity formation and cratering, there has developed considerable literature relevant to the subject of this paper. An initial calculational model of the mechanisms of cavity formation and the shock propagation into the surrounding environment has been developed (Nuckolls, 1959; Maenchen and Nuckolls, 1961). This work resulted in the development of the underground nuclear effects code (UNEC)—a one-dimensional, Lagrangian, hydrodynamic, plastic-elastic code—which subsequently has been extended (Seidl, 1964, unpublished). This latter work has led to the development of the SOC code; a one-dimensional, Lagrangian, hydrodynamic, plastic-elastic code capable of predicting the response of a layered geological environment to explosive sources, including effects of cracking and internal friction. Other physical differences between SOC and UNEC models have been reported (Butkovitch, 1964). The SOC model serves as a tool for calculating the initial conditions of the calculational model of the gas acceleration phase of excavation developed in this present paper. Because of this role of SOC, it has been important to verify the code. In this regard, the calculation of the shock propagation in granite by SOC and its comparison with physical measurements on the Hardhat event has been investigated recently (Butkovich, 1964).

Some of the concepts and discussion of processes important for cratering have previously been reported (Nordyke, 1961). Models of the gas acceleration phase of excavation have been recently developed (Knox and Terhune, 1963). This present study is an extension of the latter work.

DESCRIPTION OF OBSERVED SURFACE MOTION - SCOOTER

It is pertinent to describe the features of ground-surface motion for the Scooter event, a 1/2-kiloton high-explosive buried at the optimum depth for cratering. The Scooter event, as far as United States Cratering experiments are concerned, is the first large-scale, high-explosive experiment in which the cratering mechanisms of spall and gas acceleration are clearly separable in time on surface-motion measurements.

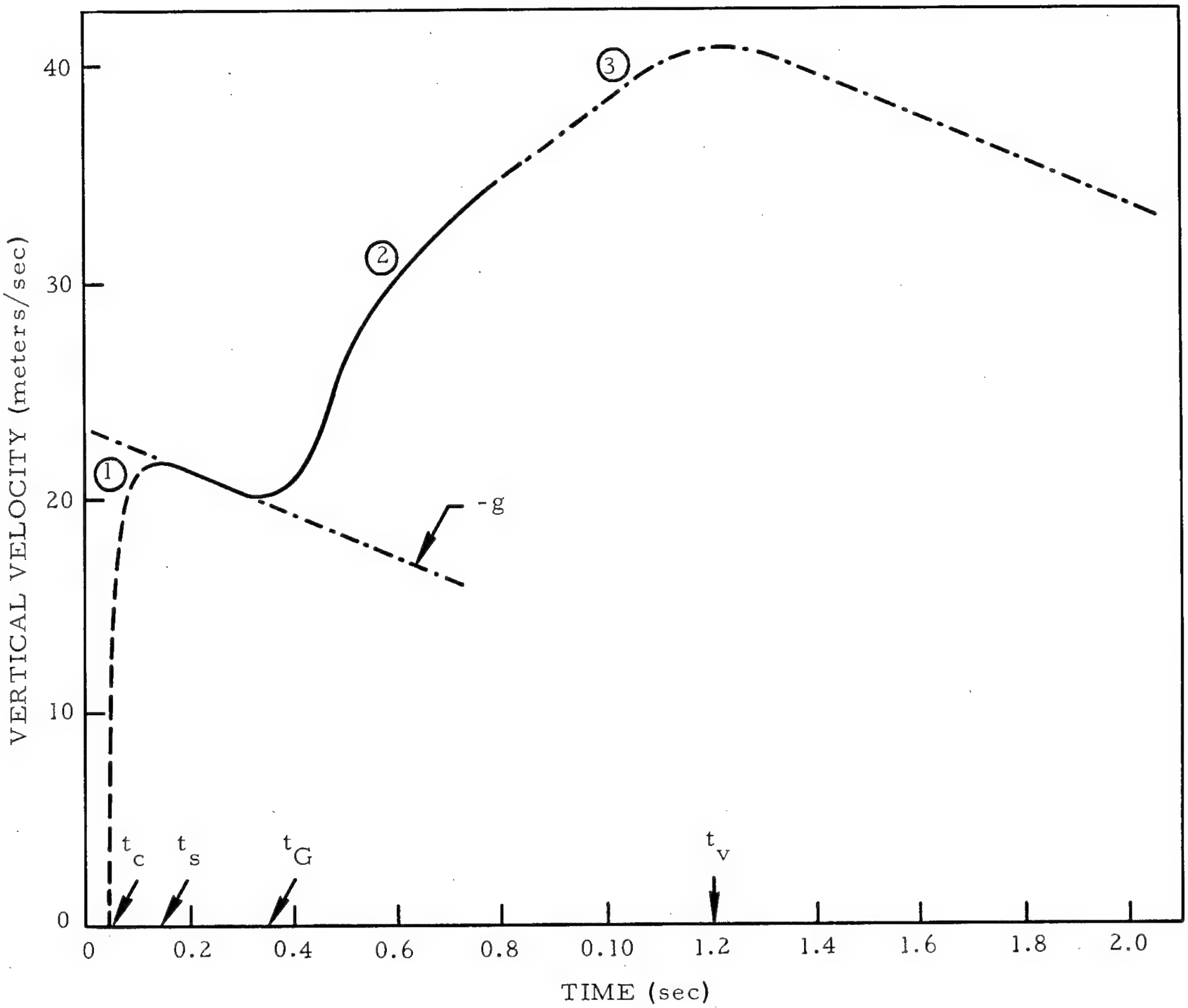

Fig. 1. The observed vertical velocity of the earth's free surface, Scooter ground zero.

In the Scooter event, targets were placed on the ground surface and photographed by high-speed cameras. The target-position data (Feigenbaum, S. A., and P. L. Wegkamp, 1961) is independently smoothed six times by the running mean smoothing operator (Holloway, 1958) in order to suppress inherent errors in the observed position coordinates. This successive smoothing operation filters noise from the position coordinate records and thereby focuses on the significant scale of free surface motion. After this successive smoothing, the two position coordinates are differentiated in order to compute the velocity and acceleration components of each target (Knox and Terhune, 1963).

Figure 1 shows the vertical velocity as a function of time for the Scooter ground-zero target. The salient features of this ground motion are: (a) a maximum spall velocity of 21.3 meters/second, occurring at about 0.12 second; (b) the first period of free fall lasting about 0.23 second; (c) a second period of acceleration—associated with cavity-pressure induced changes of momentum of the mound material—of the order of 3 to 4 g; and (d) a terminal period of free fall.

The general features of the ground surface motion shown in Fig. 1 are characteristic of the entire mound. The validity of this method of analyzing visual target information to obtain velocities and accelerations has been previously

explored (Knox and Terhune, 1963). The velocity and acceleration components so obtained have been compared with those derived from unsmoothed displacement data on Scooter (Vortman, 1963, private communication).

Several times of special interest are shown in Fig. 1; these times are defined as follows:

1. t_c – the time of peak spall acceleration of the earth's free surface over ground zero.
2. t_s – the time of peak spall velocity.
3. t_G – the time of the beginning of the surface gas acceleration phase of surface motion.
4. t_v – the time of first significant venting of the cavity gas to the atmosphere.

Relevant to Fig. 1: segment 1 is derived from unsmoothed displacement information (Vortman, 1963, private communication); segment 2 is the vertical velocity as determined from smoothed target information; and segment 3 is extrapolated and schematic.

CHRONOLOGY OF EXPLOSION - PRODUCED CRATERS

Before describing the model of the gas acceleration phase of excavation, it is profitable to present a brief résumé of the chronology of explosion-produced craters. The purpose of such a résumé is to link conceptually the time history of the earth's free-surface motion to the cavity history, events in the media, and to the operative catering processes. Table I contains this résumé.

Some of the significant features of this résumé will be discussed in the course of this paper. However, the résumé is presented at this time for inspection and orientation purposes, without reference or justification. This résumé, although greatly influenced by the subsequent analysis of Scooter, is considered to be applicable to the chronology of nuclear-explosion-produced craters.

MODEL OF GAS ACCELERATION PHASE OF CRATER FORMATION

Consider a high-explosive source emplaced at a depth D below the initially horizontal ground surface. The interval of time during which the model is applicable has already been defined in Section III as $t_G \leq t \leq t_v$. To construct a simple, physical model of the gas acceleration phase of crater formation, it is assumed that:

1. The processes are axially symmetric with respect to the center line shown in Fig. 2.
2. The material above the expanding cavity is a homogeneous, incompressible, viscous fluid.
3. The radius of the cavity in the lower hemisphere is independent of time.
4. The cavity gas at any given time during the gas acceleration phase is isobaric and isothermal.
5. The pressure and volume changes in the cavity are adiabatic with a value of gamma of 1.03 (Higgins, 1964, private communication).

The following quantities are defined and shown in Fig. 2:

1. r is the radial coordinate measured from the center of the explosive, WP.
2. ∇r is the unit radial vector.
3. D is the depth of burial.
4. θ is the colatitude of an arbitrary point on the cavity surface.
5. λ is the longitude of an arbitrary point on the cavity surface.
6. ϕ denotes axis of symmetry.
7. ∇R is the unit radial vector in polar coordinates.
8. R is the radial polar coordinate on the undisturbed, horizontal earth's surface.
9. $w(R, \theta)\nabla r$ is the radial velocity of the earth's surface.
10. r_G is the radial distance from the WP (or charge center) to the ground surface.
11. $\bar{r}$ is the radial distance from the working point to the center of mass of the mass element in the model.
12. p_a is the atmospheric pressure applied to the mound surface, and p_c is the cavity pressure.
13. δS_G is the element of mound surface subtended by the element of cavity surface δS_c, where $\delta S_c = r^2 \sin\theta\, \delta\theta\, \delta\lambda$.
14. The subscript i refers to the ith mass zone in the two-dimensional model (where $0 \leq i \leq \ell$, and i = 0 is the axis of symmetry).
15. $r_{c,0}$ is the radius of the lower hemisphere of the cavity at the time t_G and is set equal to the cavity radius calculated by

SOC at the time the rarefaction wave returns to the top of the expanding cavity.

16. r_c is the radius of the upper hemisphere of the cavity. (The manner in which r_c is derived at the time t_G is discussed in Section V.)

The governing equations for the model applicable to the ith mass element at the time t^n are as follows. The radial equation of motion for the center of gravity of the ith mass element is

$$\dot{\bar{w}}_i^n = p_c^n \frac{\delta S_{ci}^n}{\delta M_i} - p_a \frac{\delta S_{Gi}^n}{\delta M_i} - g \cos \theta_i - K\bar{w}_i^n \quad (1)$$

where

$\bar{w}_i^n$ and $\dot{\bar{w}}_i^n$ are the radial velocity and acceleration of the ith center of gravity, respectively, at $t^n = n\Delta t$;

K is the frictional coefficient;

Table I. Resume of the chronology of explosion-produced craters.

Time	$t < t_c$	$t_c < t < t_s$	$t_s < t < t_G$	$t_G < t < t_v$	$t > t_v$
Cavity	Period of rapid spherical cavity growth	Slow spherical cavity growth	Asymmetrical cavity growth begins during this time interval	Upper hemisphere of cavity expands asymmetrically while the cavity pressure induces motion in the overburden	Cavity gas vents
Media	Compressional wave moves spherically outwards	Period of spall acceleration of free surface. Maximum spall velocity occurs at t_s	Rarefaction wave returns to cavity and a wave of recompaction is assumed to move upwards through medium	Wave of recompaction reaches the earth's free surface at t_G. During this time interval cavity pressure induces momentum changes in the mound (and at the free surface)	Collapse of mount material may begin
Earth's free surface	At rest	The rarefaction and shear waves are excited at the free surface for $t > t_c$	First period of free fall	Period of surface gas acceleration (magnitude is interpreted to depend on type of explosive and noncondensable gas production)	Terminal period of free fall
Operative cratering process	Cavity volume is being formed by compaction and work done on the environment	Cavity volume is being formed by compaction and work done on the environment. Spall develops	Spall—disassembled overburden "coasts" upwards in -g acceleration field	Gas acceleration (e.g., cavity-pressure-induced momentum changes in the mound of overburden and at free surface)	Mound collapse. fallback
Remarks	Calculated by SOC[a]	SOC calculation may become approximate, in the medium, due to 2-dimensional effects from shear waves. H. E. cavity volume and pressure calculations appear reasonable	SOC computation is stopped when the rarefaction returns to the top of the expanding cavity in order to provide calculation of cavity pressure and volume	Overburden material is approximated by a homogeneous, incompressible viscous fluid	Base surge and main clouds begin their formation and ejecta are visible

[a]Chronology applies to those crater formations in which $t_s < t_G$, which implies separable periods of spall and gas acceleration. The Scooter event, whose surface motion is illustrated in Fig. 1, appears to satisfy this criteria ($t_s < t_G$).

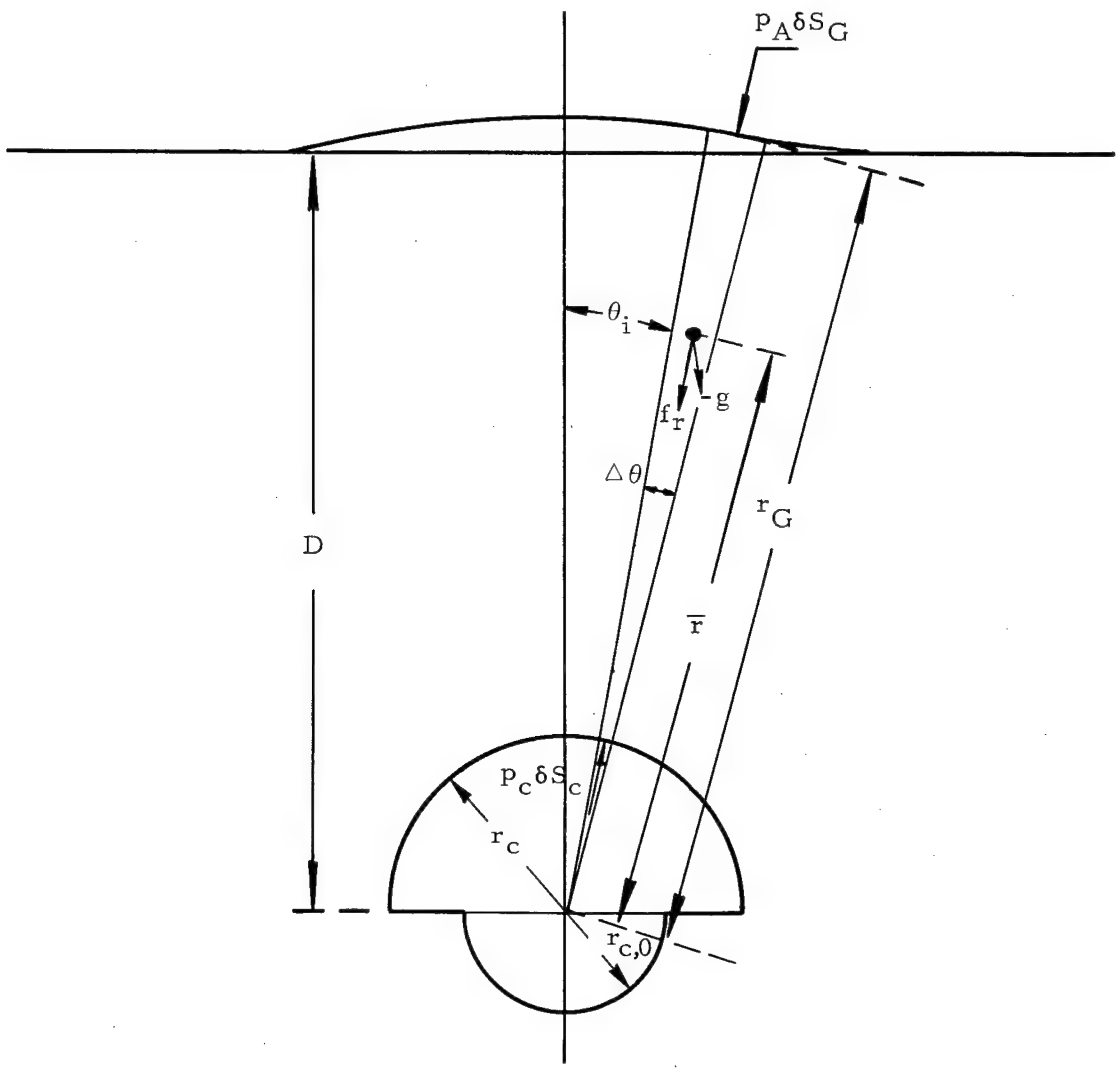

Fig. 2 Geometrical definitions for model of gas acceleration phase $(t_G \le t \le t_v)$ of crater formation.

$$\frac{\delta S_{ci}^{\,n}}{\delta M_i} = \frac{3}{\rho} \frac{\left(r_c^{\,2}\right)^n}{\left(r_G^{\,3} - r_c^{\,3}\right)^0};$$

$$\frac{\delta S_{Gi}^{\,n}}{\delta M_i} = \frac{3}{\rho} \frac{\left(r_G^{\,2}\right)^n}{\left(r_G^{\,3} - r_c^{\,3}\right)^0}.$$

The component of acceleration normal to ∇r is ignored in comparison to $\dot{\bar{w}}_i^n$.

From the homogeneous, incompressibility assumption,

$$\left(\bar{r}^2 \bar{w}\right)_i^n = \left(r_G^{\,2} w_G\right)_i^n = \left(r_c^{\,2} w_c\right)_i^n. \qquad (2)$$

And from the assumption that pressure-volume changes in the cavity are adiabatic,

$$\left(p_c V^\gamma\right)^n = \text{const} \qquad (3)$$

where

V^n is the cavity volume at t^n.

Equations (1) through (3) provide a basis for calculating: (a) the cavity surface as a function

of time, (b) the mound history, and (c) the lip formation, assuming that:

(i) The ith center of mass moves independently from the neighboring mass centers, except for coupling by way of the cavity pressure.

(ii) The ith center of mass remains at rest once $\overline{w}_i^n \leq 0$. This is a reasonable assumption for the relevant time interval $(t_G \leq t \leq t_v)$.

The computational scheme used for the numerical integration of this model is discussed in Appendix A.

The governing equations of the model, (1) to (3), contain a simple frictional concept, one in which the frictional force is proportional to the radial velocity of the center of mass. The principal objection to such a prescription of friction is that it is an oversimplification.

Related physical problems from fluid dynamics and the atmospheric sciences suggest several possible forms of the frictional force which may be important for the mound dynamics. For instance, in the center of the mound the usual Newtonian frictional stress may be operative (Holmboe, 1944). Secondly, near the side of the moving mound material it is conceivable that a boundary layer might develop between slowly moving environmental material and the moving mound material. From the atmospheric sciences in the study of analytical solutions to the bouyant motion of a warm bubble in the atmosphere (Priestley, 1959), a simple frictional force proportional to the vertical velocity is used in the vertical momentum equation, modeling the dilution of specific momentum by entrainment. Relevant to the same atmospheric problem, models have been explored in which the frictional force is proportional to the square of the vertical velocity (J. S. Malkus and R. T. Williams, 1963; J. Levine, 1959). Since the applicability and the relative importance of these above frictional effects on the mound dynamics is not known at this time, the simplest possible frictional force, $-K\overline{w}$, is hypothesized.

INITIAL CONDITIONS

The initial information (at $t = t_G$) required for the numerical integration of the model of the gas acceleration phase of excavation (PUSH II) are: (a) $r_{c,0}$, r_c, and the cavity pressure p_c, and (b) the mound configuration, and the radial free surface velocity, w^o_{Gi}.

Cavity Conditions at t_G

The radius of the lower cavity hemisphere is that cavity radius calculated by SOC at the time the rarefaction intersects the top of the expanding cavity (t_r).

At t_G, the volume of the upper cavity hemisphere equals $[(2/3)\pi r^3_{c,0}]$ plus the change in mound volume up to the time t_G.

At t_G, the cavity pressure is

$$p_c(t_G)\left(\frac{2}{3}\pi r^3_{c,0} + \frac{2}{3}\pi r^3_c\right)^\gamma = p_c(t_r)\left(\frac{4}{3}\pi r^3_{c,0}\right)^\gamma$$

where, $\gamma = 1.03$ (for H. E. and $p_c(t_r)$ is calculated by SOC.

Mound Conditions at t_G (for $t_G > t_s$)

To prescribe the initial mound configuration and $(w_G)^0_i$, the peak radial spall velocity $(\hat{w}_s)$ is calculated as a function of explosive yield and distance to the center of the explosive in a given medium, for all $i(0 \leq i \leq \ell)$ (Knox and Terhune, 1963). The free-surface velocity at t_s has the horizontal and vertical components $U_i(t_s)$ and $V_i(t_s)$, respectively, that are computed by means of wave equation from measured (or assumed) values of $\hat{w}_s$, θ_i, and the ratio of the compressional wave velocity to the shear velocity in the medium. (See Appendix B.)

Consider the coordinate system shown in Fig. 3, in which the origin x and y is at the intersection of the line of symmetry and undisturbed ground level. The Cartesian position coordinates of the free-surface element of the ith zone at time t_G are computed as follows:

$$x^0_i = (r_G)^0_i \sin \theta_i \qquad (4)$$

$$(r_G)^0_i = \left[y^0_i + D\right]/\cos \theta_i \qquad (5a)$$

$$y^0_i = y_i(t_s) + V_i(t_s)\Delta t - \frac{1}{2}g(\Delta t)^2. \qquad (5b)$$

where g is the acceleration of gravity, $\Delta t = t_G - t_s$

$t_G - t_s$

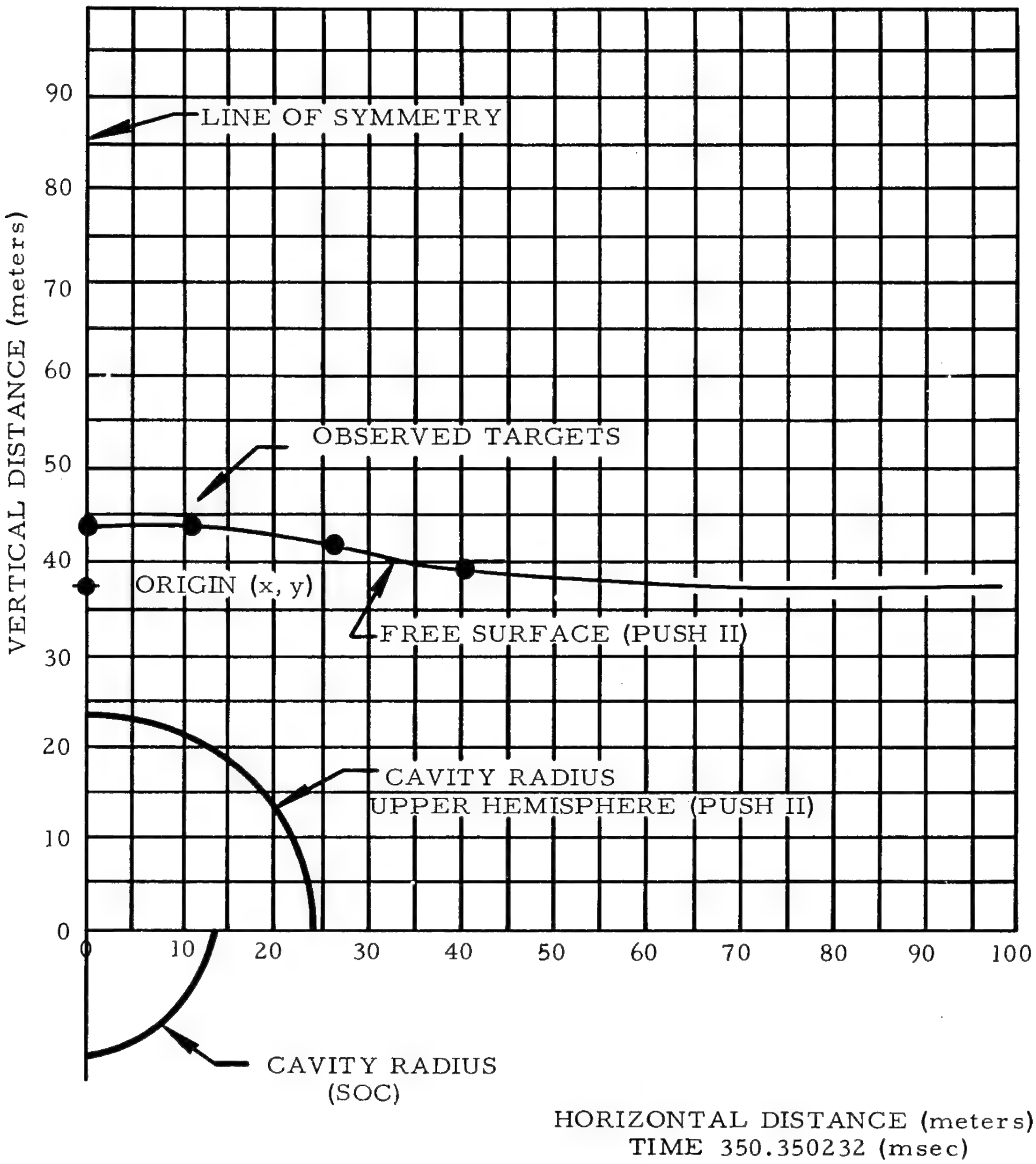

Fig. 3. The initial mound and cavity conditions used in the gas acceleration phase model of the Scooter event.

$$y_i(t_s) = \frac{1}{2} V_i(t_s)(t_s - t_c) \qquad (6)$$

and

D is the depth of burial.

The initial (t_G) radial free-surface velocity is approximated by

$$(w_G)_i^0 = V_i^0 / \cos \theta_i. \qquad (7)$$

In the general case, t_G and t_s must be computed. However, for this initial study of 0.5-kt H. E. events in alluvium, it is assumed that: (a) $(t_s - t_c) = 0.1$ second (observed on Scooter); and (b) $t_G = t_r + h/c_p$, where h is the vertical

thickness of the overburden material along the axis of symmetry at t_r, and c_p is the speed of propagation of the recompaction wave, normalized to the Scooter event ($c_p = 22.914\ p_c(t_r)/h$), (as previously mentioned, $p_c(t_r)$ is calculated by SOC). From the above assumptions

$$h = \hat{w}_s (t_r - t_c) - D - r_{c,0}. \tag{8}$$

Figure 3 shows the mound configuration calculated at t_G using the above method for $t_G \geq t_s$, and it compares the calculated mound shape to the observed positions of four visual targets (at t_G) on Scooter. This figure also shows the radius of the lower cavity radius (13.8 m), and the radius of the upper cavity radius (~22.0 m) used in the model for the Scooter event. The maximum error in the mound configuration is estimated from the target positions to be 1.0 m. In regard to the lower cavity hemisphere radius, the observed cavity radius on Scooter (Rawson, 1963, private communication) is 13.1 m, whereas the value of $r_{c,0}$ calculated by SOC (at t_r) is 13.8 m.

NORMALIZATION OF THE MODEL TO THE SCOOTER EVENT

The numerical simulation model of the gas acceleration phase of excavation now requires normalization against experiment in order to evaluate the coefficient of friction [K in Eq. (1)]. The cavity and mound conditions (Fig. 3) constitute the initial conditions for the normalization calculations of the Scooter event. The values of other physical parameters of the model are: gamma = 1.03, p_a = 0.85 bar, and $p_c(t_r)$ = 108 bars. The results of several normalization computations indicate that the coefficient of friction, K, is 0.9. This value of K is considered to give the best fit of the observed ground-zero target motion by the model for the several computations shown in Fig. 4. The radial velocity of four visual targets on the Scooter event are, in Figs. 5a, b, c, and d, compared to the corresponding vertical velocity of the mound calculated by the model with K = 0.9.

HISTORY OF THE CAVITY, MOUND, AND LIP (t_G TO t_v)

Scooter, at Optimal Depth of Burial

Figure 6 shows the development of the cavity and mound and the formation of the lip as calculated by the normalized model during the gas acceleration phase of excavation. During the interval from t_G = 0.350 to 0.600 sec, the upper hemisphere of the cavity expands asymmetrically, such that there is a suggestion of the formation of a subsurface cusp on the cavity surface, and the top of the cavity is at the undisturbed ground level at 0.600 sec. At the observed time of vent, the model indicates that the overburden material, separating the cavity from the atmosphere, is as thin as 4 m on the line of symmetry, and the cavity pressure at this time is 7.24 bars. This calculation with the model may be allowed to extend beyond t_v, recognizing that the shell of overburden is disrupted during the actual venting. Figure 7 shows such an extended calculation for Scooter at 3.45 sec, at which time the side of the mound is nearly vertical and the true crater prior to collapse is defined. By constructing a reasonable angle of repose for alluvium, through the point of maximum curvature on the deformed earth's free surface, an estimate of the apparent crater radius can be geometrically constructed as well as a rough estimate of lip height. In this manner, the model gives an apparent crater radius of 45 m and a lip height of ~4.5 m, which compares well with the observed values of 46.5 m and 2.7 m, respectively (Perret, Chabai, Reed, and Vortman, 1963). It is probably clear that the above simple criteria of collapse can not lead to a very precise estimate of lip height.

One-half-kt H. E., Shallow Depth of Burial

An example of the history of the cavity, mound, and lip formation is given in Fig. 8 for 0.5-kt H. E. with the charge center at a depth of 7.62 m. The time of the beginning of the surface gas acceleration phase of excavation is calculated to be about 4 msec, and the cavity pressure at this time is estimated (through a SOC calculation)

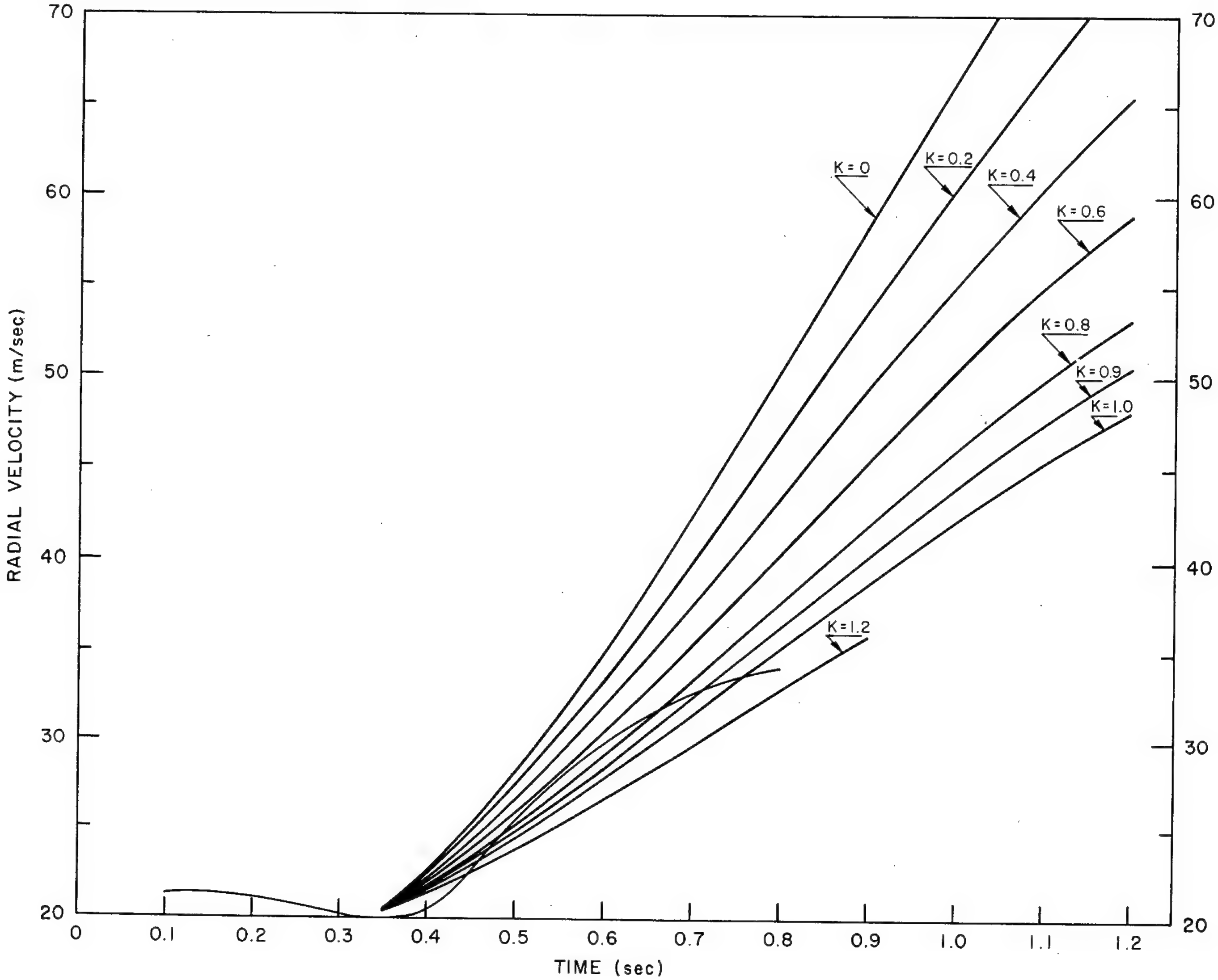

Fig. 4. Ground-zero surface motion calculated by the model for Scooter as a function of the frictional coefficient K.

to be 2500 bars. The calculated sequence of events shown in this figure indicates that the cavity pressure and spall imparts a very large momentum to the overburden material surrounding the upper cavity hemisphere. By the end of this sequence, friction has degraded the momentum to such an extent that the lip material has all but stopped its outward movement. It is clear that the material to the left of line AB is unsupported from beneath and, hence, should collapse near the edge of the true crater. The intersection of line AB with undisturbed ground level gives an estimate of 29 m for the radius of the apparent crater. It is reasonable in this case that there would be little fallback in the center of this shallow crater, so that the depth of burial of 7.62 m plus the lower cavity radius of 7.0 m (from SOC) yields an excellent estimate of crater depth.

One-half-kt H. E., Deep Burial

An example of the history of the cavity, mound, and lip formation is given in Fig. 9 for 0.5-kt H. E., with the charge center at a depth of 53.4 m. In this example, the surface gas acceleration phase of excavation begins at 1.06 sec.

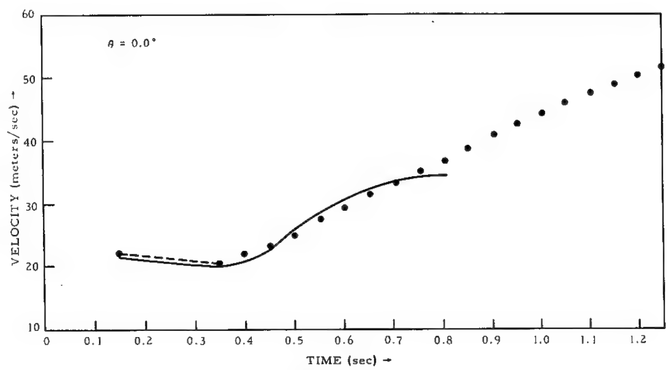

Fig. 5a

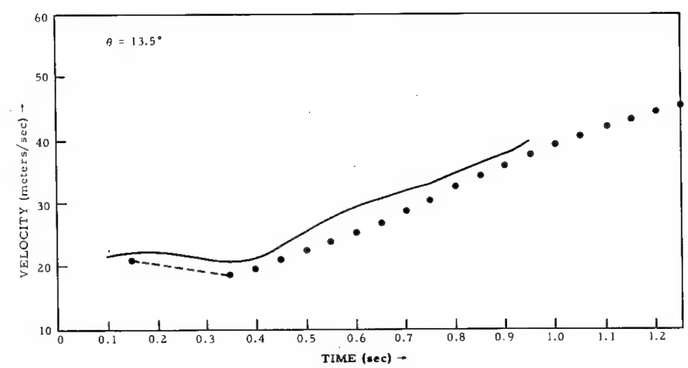

Fig. 5b

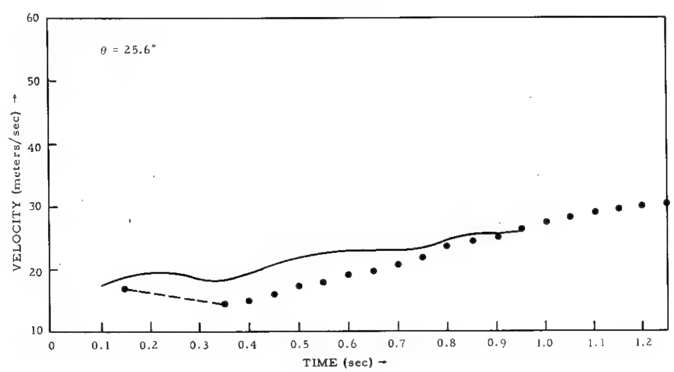

Fig. 5c

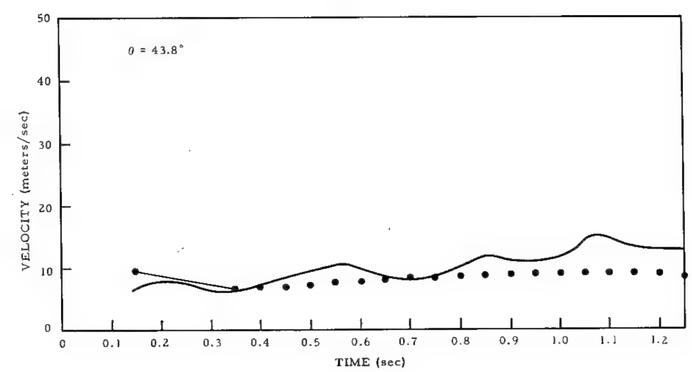

Fig. 5d

Fig. 5. Comparison of observed vertical velocity of targets, Scooter event, to calculational vertical velocities in the normalized normal. (a) target $\theta = 0°$, (b) target $= 13.5°$, (c) target $\theta = 26°$, and (d) target $\theta = 43.5°$.

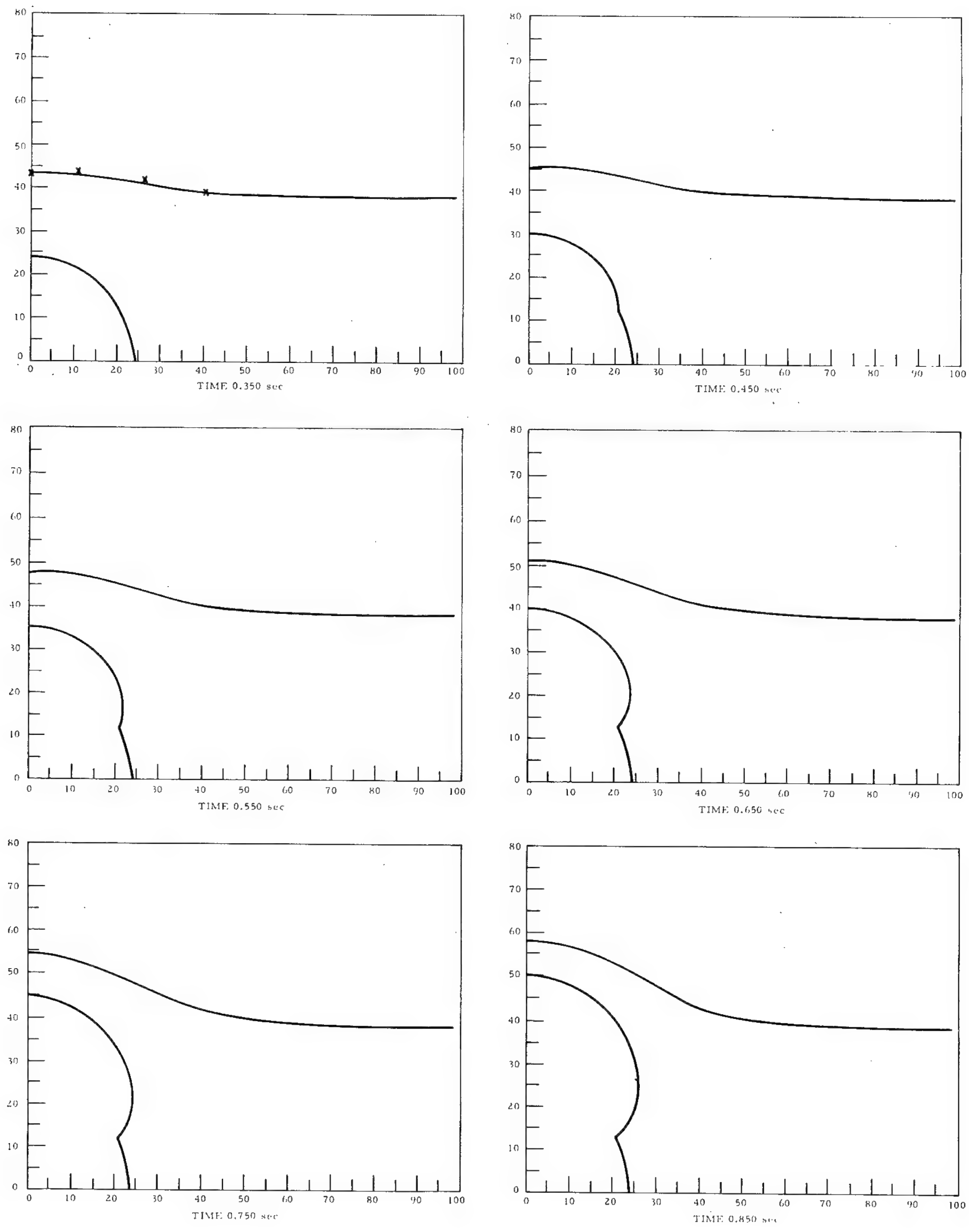

Fig. 6a. Calculated history of the cavity, mound, and lip—Scooter event.

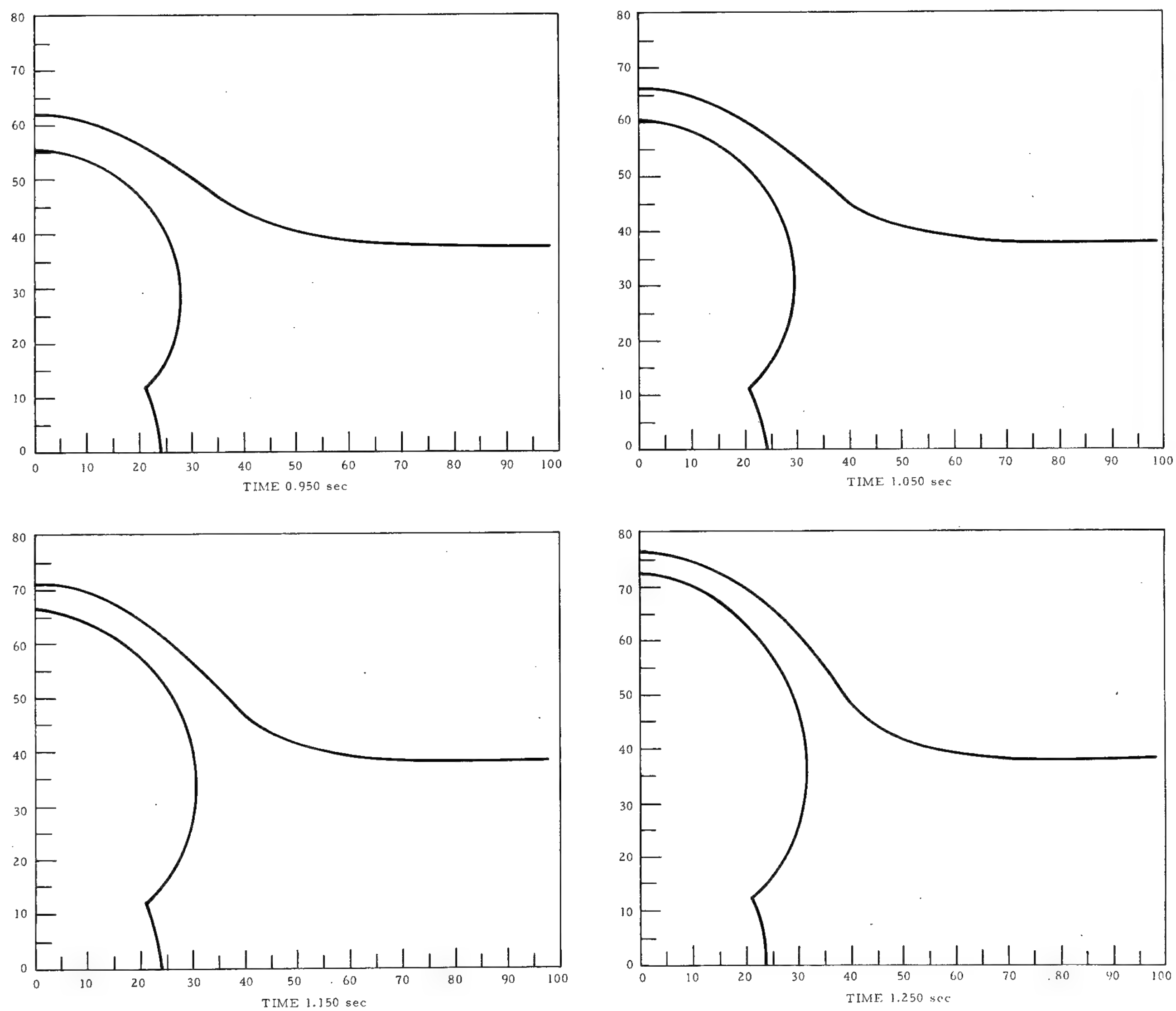

Fig. 6b. Calculated history of the cavity, mound, and lip—Scooter event.

For deep burial, it is evident that the overburden pressure is sufficient, over most of the upper cavity surface, so that little outward motion occurs after t_G. Rather, during the gas acceleration phase, a narrow chimney of cavity gas pushes, at first, almost vertically, and only expands radially as it approaches the undisturbed ground level. Inspection of Fig. 9 suggests that the apparent crater radii in this case may lie between: (a) the point of maximum curvature on the earth's free surface, and (b) the most remote element of the earth's free surface moving at the beginning of the gas acceleration phase.

DISCUSSION

It is pertinent to describe the predictive possibilities of the proposed model of the gas acceleration phase of excavation (PUSH II). To do this, PUSH II calculations have been performed for a 0.5-kt H. E. source emplaced at depth of N x 7.62 m, where $1 \leq N \leq 7$. Estimates of the apparent crater radius R_c have been prepared as follows: (a) for N = 1, R_c is approximated as discussed in Section VIIa, (b) for $2 \leq N \leq 5$, R_c is well approximated by the projection of the point of maximum curvature on the earth's free

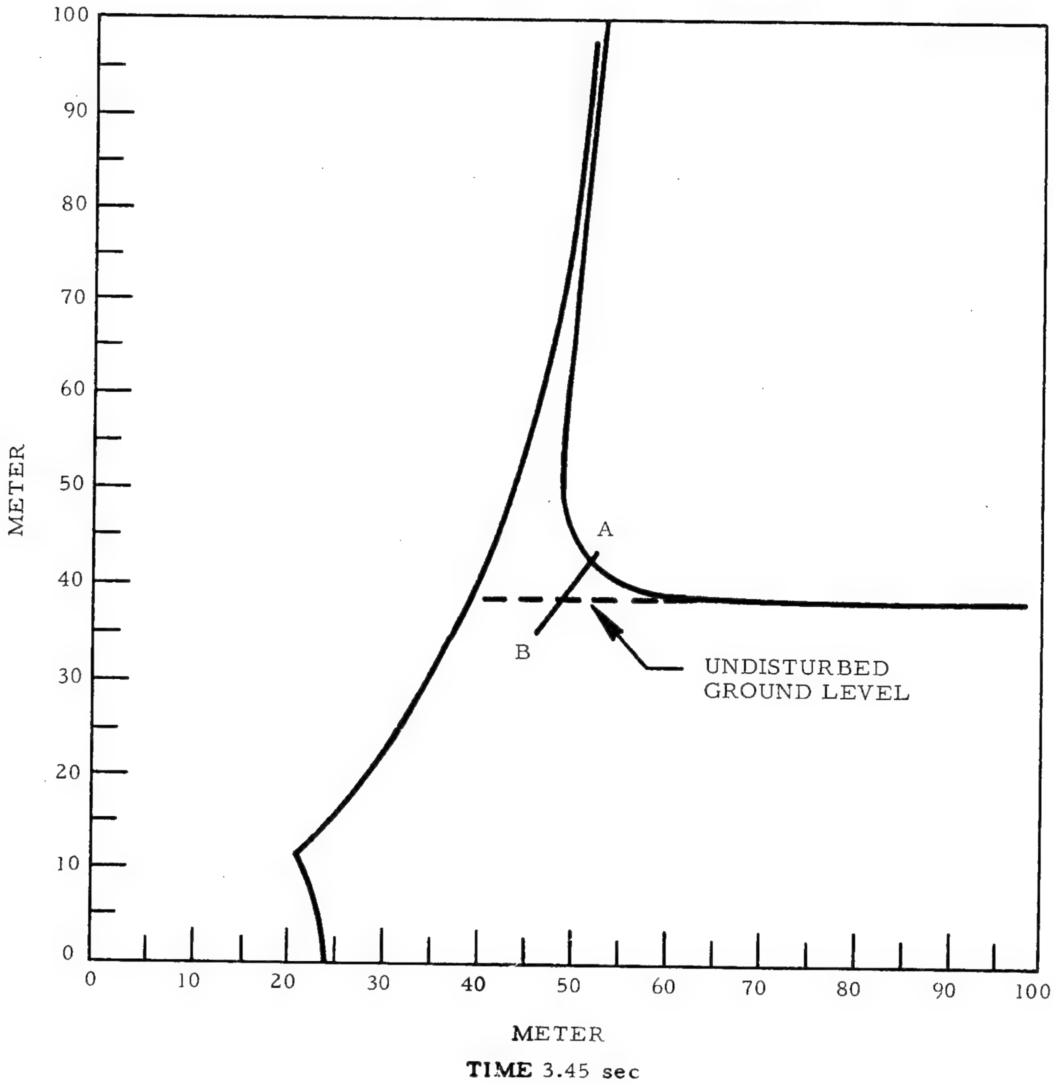

Fig. 7. Calculated true crater for the Scooter event at 3.45 seconds, prior to collapse.

surface (at t_G plus a few seconds) along the surface of stable repose to undisturbed ground level (curve I in Fig. 10), and (c) for $N > 5$, it is very likely that a quantitative collapse model is required before R_c can be estimated well. The above estimates of R_c are shown in Fig. 10. This figure also shows, for purposes of comparison, the experimentally determined apparent crater dimensions (Nordyke, 1961) for H. E. sources in alluvium normalized to 1-kiloton yield. It is evident that the R_c estimates prepared from PUSH II are in reasonable agreement with experiment for scaled depths of burial less than or equal to 50 m.

The estimates of apparent crater depth for shallow excavation, prepared in a manner discussed in Section VIIa, are shown in Fig. 10. A comparison of these results with the observed apparent crater depths suggests that for shallow depths of burial, the PUSH II initial conditions give a very reasonable estimate of apparent crater depth.

To date, the authors have not developed a calculational model of the apparent crater configuration after collapse. The purpose of such a model would be to estimate the final apparent crater configuration from PUSH II mound conditions at t_G plus several seconds. Such a collapse

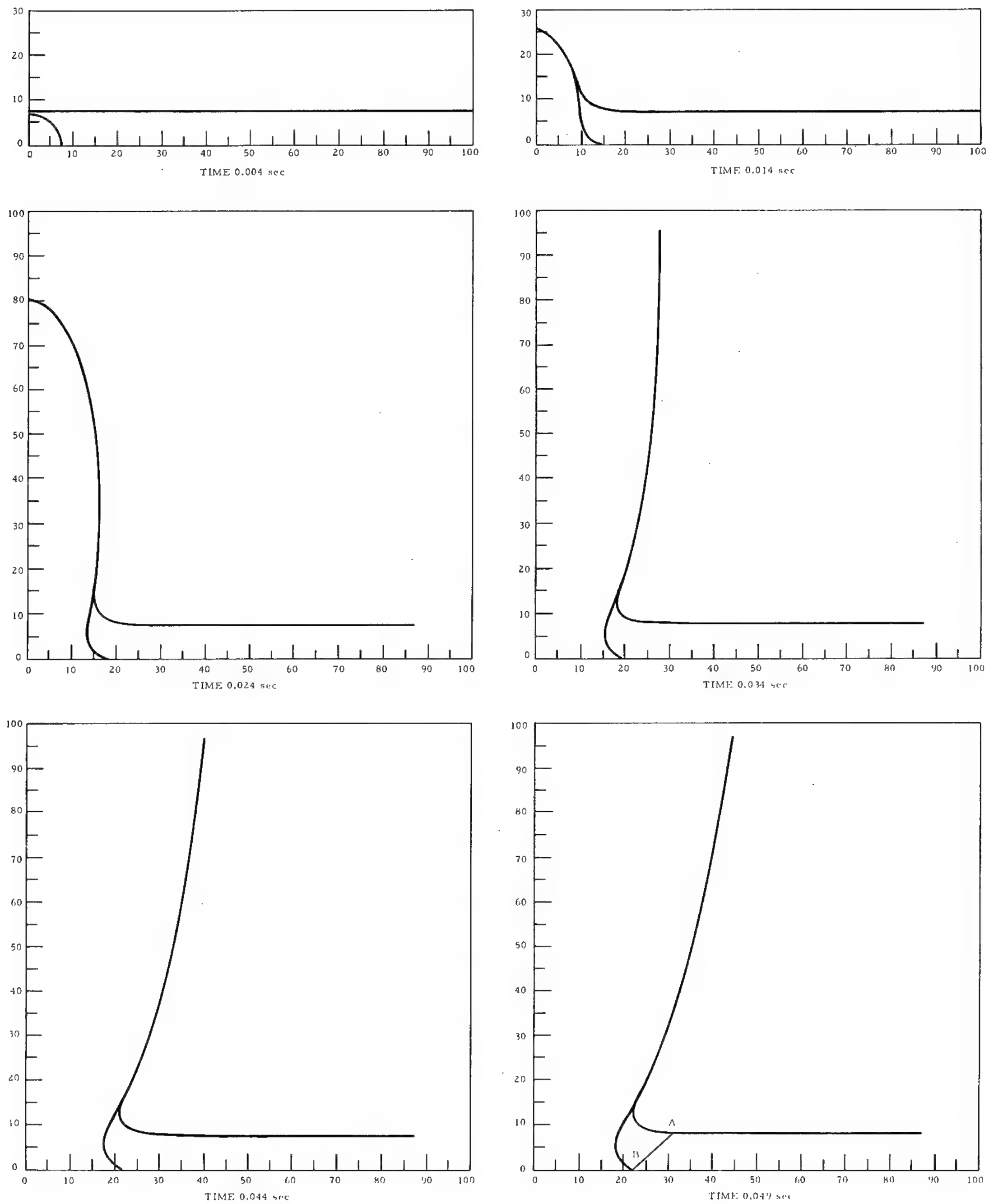

Fig. 8. Calculated history of cavity, mound, and lip—shallow burial.

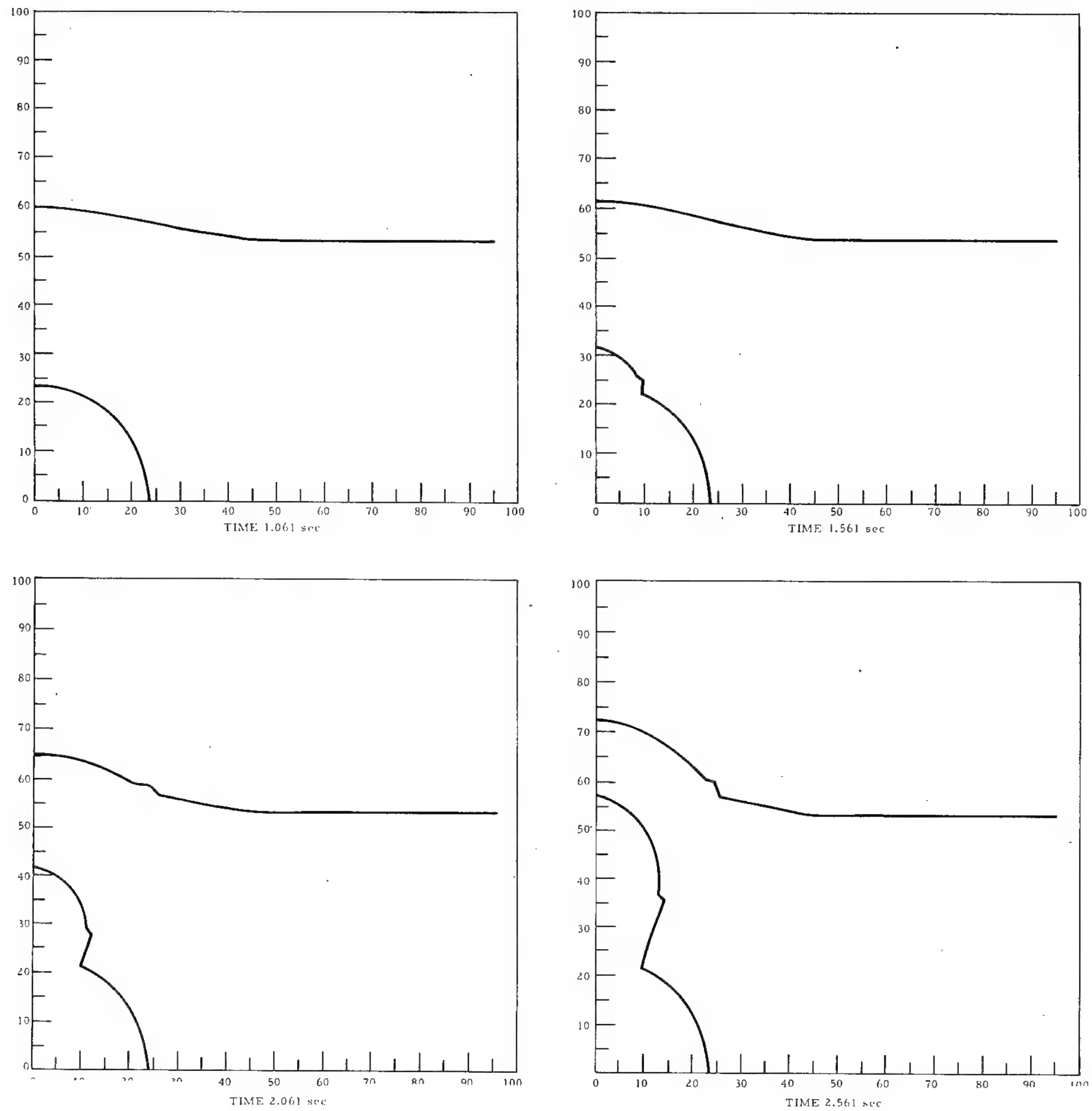

Fig. 9a. Calculated history of cavity, mound, and lip—deep burial.

model is probably required before more refined estimates of apparent crater radius and depth become available.

CONCLUDING REMARKS

This study has developed a simple, two-dimensional, numerical-physical model of cratering physics during the gas acceleration phase of excavation for high-explosive sources in alluvium. Further, the estimates of the apparent crater radius and depth (for certain types of craters) obtained from the model compare favorably to the observed apparent crater dimensions. The application of this model to deeper burial leads to an upward-moving chimney of gas which at late times radially accelerates the surface material. This radial change in material motion required by the theory with deep burial suggests that extrapolation of experimental crater dimension data to large scaled depths of burial (greater than about 65 meters) is probably unreliable.

REFERENCES

1. Butkovich, T. R., "Calculation of the Shock Wave from an Underground Nuclear Explosion in Granite," Plowshare Symposium, April 1964.
2. Feigenbaum, S. A. and P. L. Wegkamp, Final Report, "Photographic Earth Motion Study Scooter Event," Edgerton, Germeshausen, and Grier, Inc., Report No. L-510, 1961.
3. Holloway, J. L., "Smoothing and Filtering of Time Series and Space Fields," Advances in Geophysics, 4, pp. 351-388, 1958.
4. Holmboe, J., et al., (1964), "Dynamic Meteorology," John Wiley Co., New York, N. Y., p. 378.
5. Knox, J. B. and R. W. Terhune, "Cratering Physics Concepts Derived from an Analysis of Ground Surface Motion," Lawrence Radiation Laboratory, Livermore, Rept. UCID-4664, 1963.

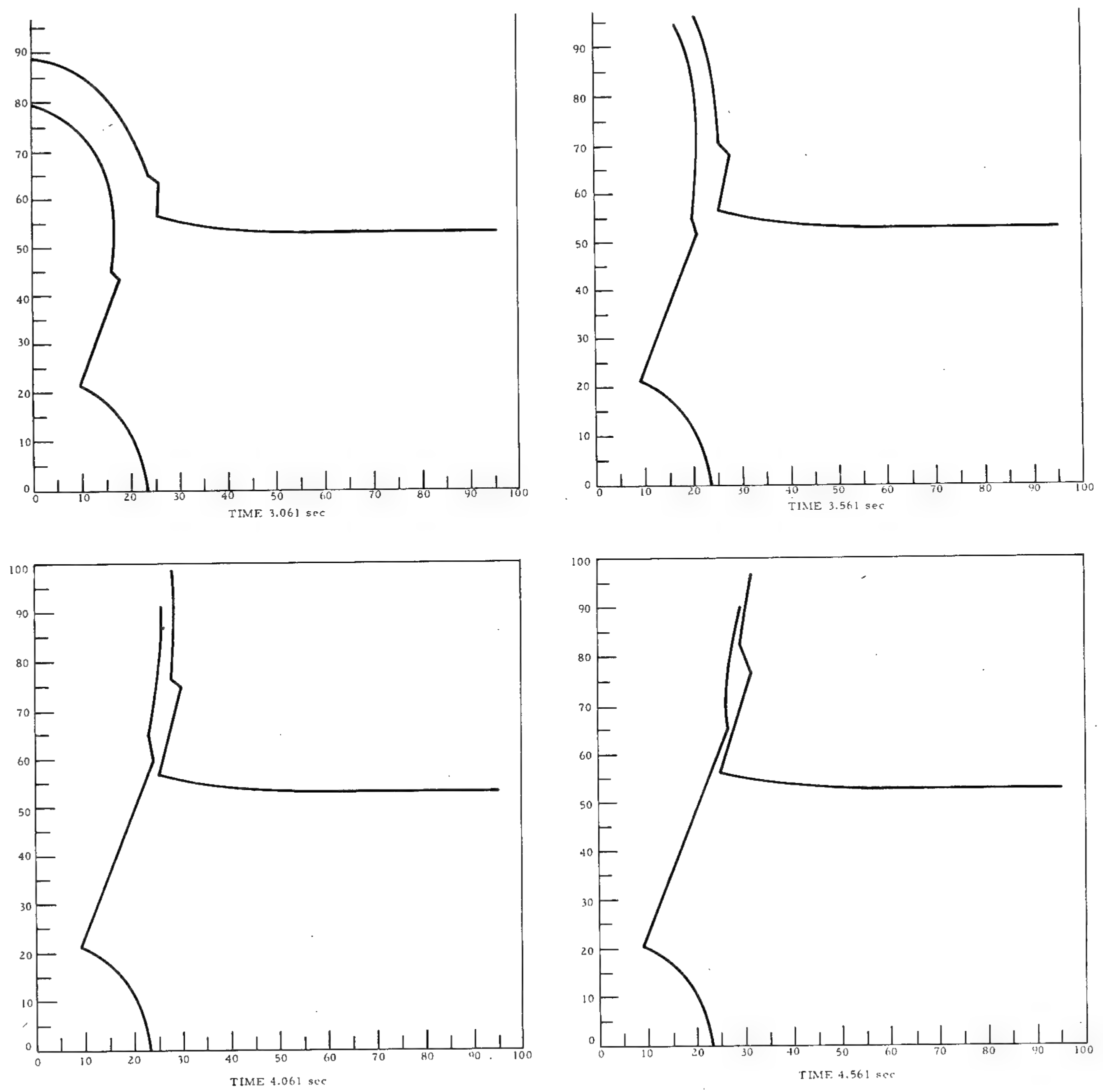

Fig. 9b. Calculated history of cavity, mound, and lip—deep burial.

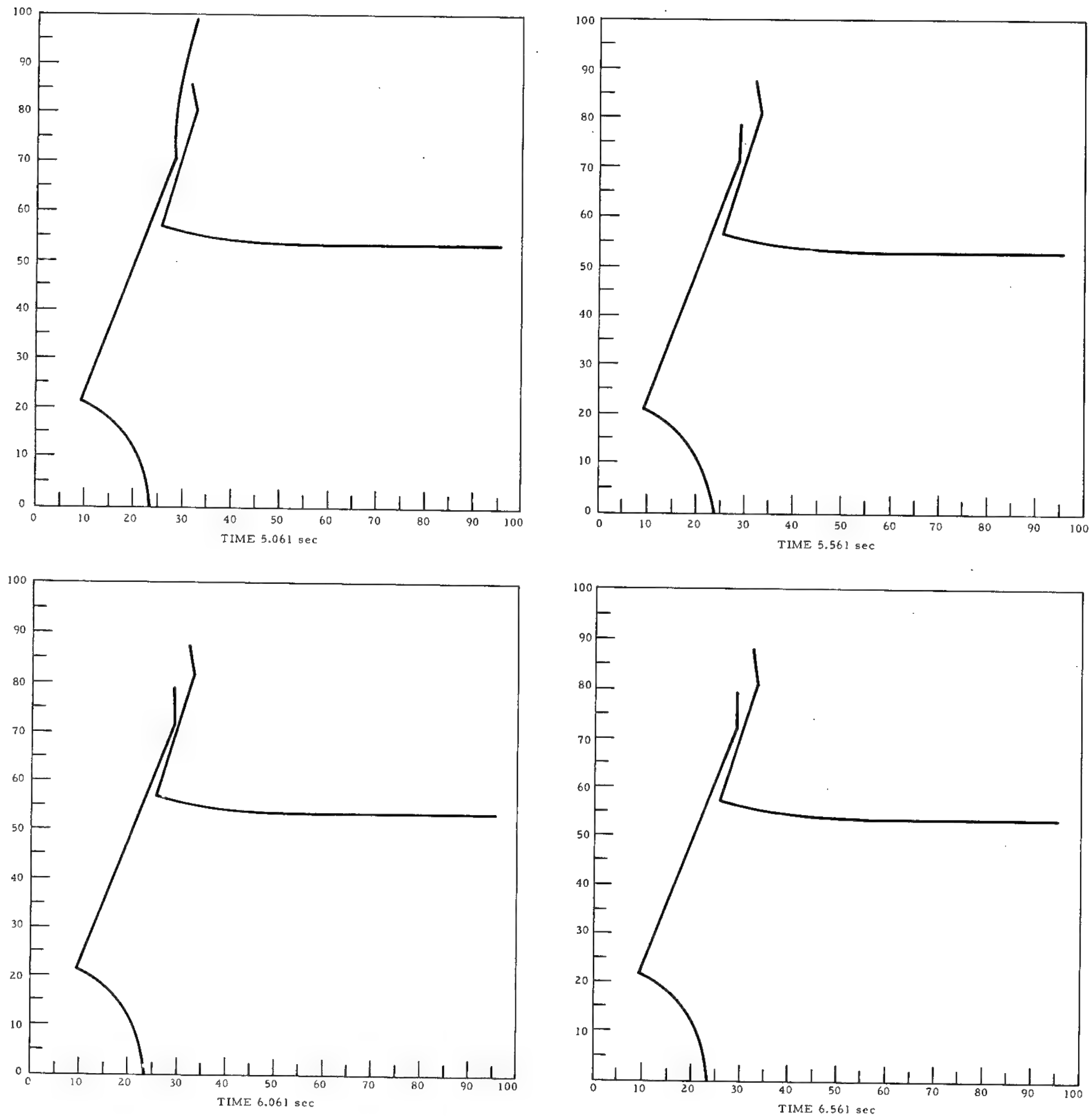

Fig. 9c. Calculated history of cavity, mound, and lip—deep burial.

6. Levine, J., "Spherical Vortex Theory of Bubble-like Motion in Cumulus Clouds," J. Meteor., 10, pp. 653-662, 1959.
7. Maenchen, G. and J. H. Nuckolls, "Calculation of Underground Explosions," Lawrence Radiation Laboratory, Livermore, Rept. UCRL-6438, Part II, p. J1-6, 1961.
8. Malkus, J. S. and R. T. Williams, "On the Interaction Between Severe Storms and Large Cumulus Clouds," Meteor. Monographs, 5, Wo. 27, pp. 59-64, 1963.
9. Nordyke, M. D., "On Cratering. A Brief History, Analysis, and Theory of Cratering," Lawrence Radiation Laboratory, Livermore, Rept. UCRL-6578, 1961.
10. Nuckolls, J. H., "A Computer Calculation of Rainier (the First 100 Milliseconds)," Lawrence Radiation Laboratory, Livermore, Rept. UCRL-5675, pp. 120-134, 1959.
11. Perret, W. R., A. J. Chabai, J. W. Reed, L. J. Vortman: "Project Scooter." Final Report, Sandia Laboratory, Albuquerque, New Mex., p. 168, October 1963.

12. Priestley, C. H. B., "Turbulent Transfer in the Lower Atmosphere," The University of Chicago Press., p. 130, 1959.

13. Rawson, D. E., "Review and Summary of Some Project Gnome Results," Lawrence Radiation Laboratory, Livermore, Rept. UCRL-7166, p. 17, 1962.

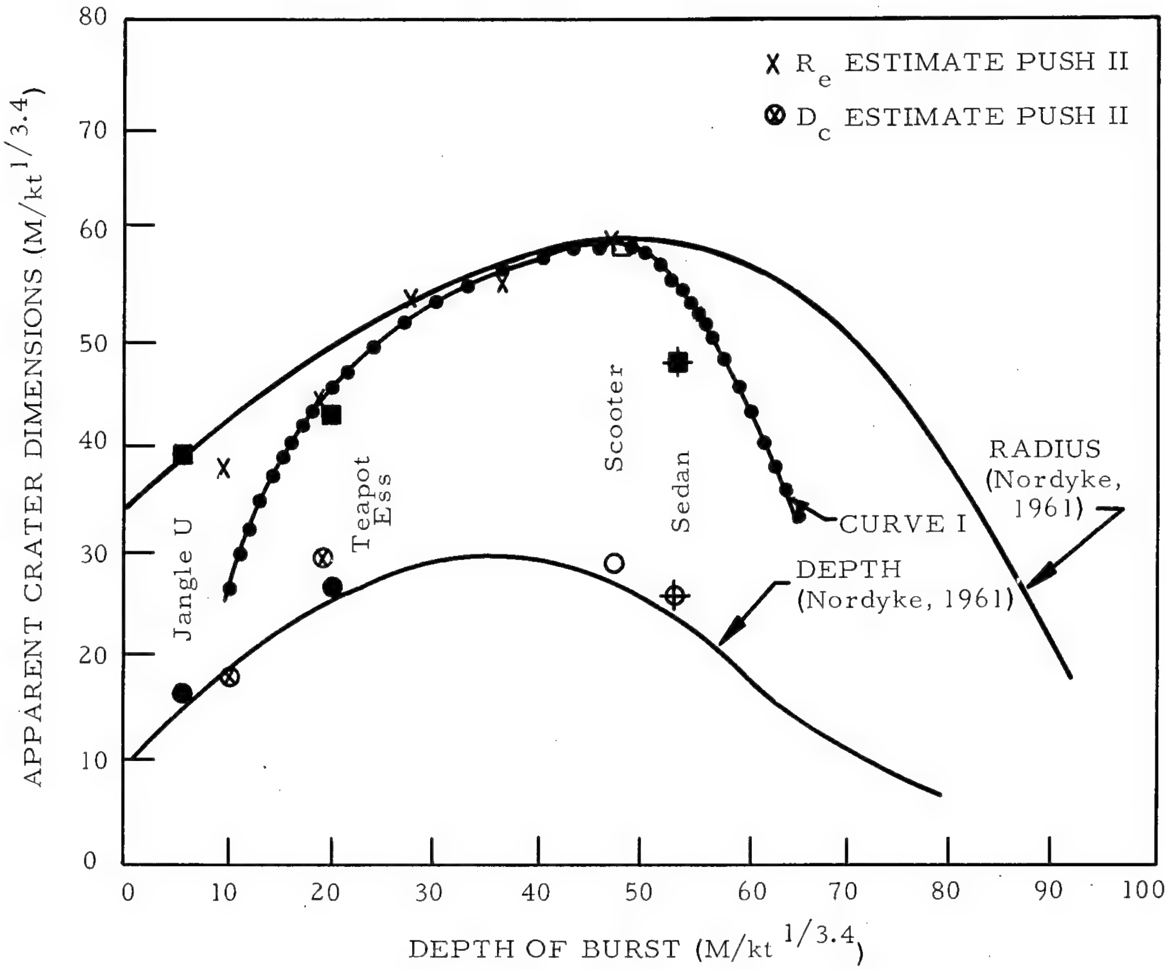

Fig. 10. PUSH II estimates of apparent crater radius and depth compared to experimental results (H. E. sources in alluvium).

APPENDIX A

Computational Scheme

Given the following quantities at t_G:

$$w_{Gi}^{n},\ r_{Gi}^{n},\ p_{c}^{n},\ r_{ci}^{n},\ r_{c,0}$$

where,

$n = 1 \rightarrow t = t_G$

$n = n + 1 \rightarrow t = t + \Delta t$

$i \rightarrow$ ith mass element

$0 \geq i \geq \ell \rightarrow 0^0 \geq \theta_i \geq 90$

the calculation scheme is as follows:

1. $\bar{r}_i^{n} = \frac{3}{4}\left[\left(r_{Gi}^{n}\right)^4 - \left(r_{ci}^{n}\right)^4\right] \Big/ \left[\left(r_{Gi}^{n}\right)^3 - \left(r_{ci}^{n}\right)^3\right]$ $\quad i = 0, \ell$

2. $cm_i = \left(r_{Gi}^{n}\right)^3 - \left(r_{ci}^{n}\right)^3$ $\quad i = 0, \ell$

3. $cm2_i = \left(\bar{r}_i^{n}\right)^3 - \left(r_{ci}^{n}\right)^3$ $\quad i = 0, \ell$

4. $\bar{w}_i^{n} = w_{Gi}^{n}\left(r_{Gi}^{n}\right)^2 \Big/ \left(\bar{r}_i^{n}\right)^2$ $\quad i = 0, \ell$

5. $w_{ci}^{n} = w_{Gi}^{n}\left(r_{Gi}^{n}\right)^2 \Big/ \left(r_{ci}^{n}\right)^2$ $\quad i = 0, \ell$

6. $\dot{\bar{w}}_i^{n} = \frac{3p_c^{n}\left(r_{ci}^{n}\right)^2}{\rho\, cm_i} - \frac{3p_a\left(r_{Gi}^{n}\right)^2}{\rho\, cm_i} - g \cos\theta_i - K\bar{w}_i^{n}$ $\quad i = 0, \ell$

7. From derivatives of steps 4, 5, 6

   $\ddot{\bar{w}}_i^{n},\ \dddot{\bar{w}}_i^{n},\ \dot{w}_{Gi}^{n},\ \dot{w}_{ci}^{n}$ $\quad i = 0, \ell$

8. $\bar{r}_i^{n+1} = \bar{r}_i^{n} + \bar{w}_i^{n}\Delta t + \dot{\bar{w}}_i^{n}\frac{(\Delta t)^2}{2} + \ddot{\bar{w}}\frac{(\Delta t)^3}{6} + \dddot{\bar{w}}\frac{(\Delta t)^4}{24}$

9. $n = n + 1 \qquad t = t + \Delta t$

10. $r_{Gi}^{\,n} = \left[\left(\overline{r}_i^{\,n}\right)^3 - cm2_i\right]^{1/3}$ $\qquad i = 0, \ell$

11. $r_{Gi}^{\,n} = \left[cm_i + \left(r_{ci}^{\,n}\right)^3\right]^{1/3}$ $\qquad i = 0, \ell$

12. $v_c^{\,n} = \frac{2}{3}\pi\left[r_{c,0}^{\,3} + \sum_{i=1}^{\ell}\left(r_{ci}^{\,n}\right)^3 \cos\left(\theta - \frac{\Delta\theta}{2}\right) - \cos\left(\theta + \frac{\Delta\theta}{2}\right)\right]$

13. $p_c^{\,n} = p_{c,0}\left(v_{c,0}/v_c^{\,n}\right)^{\gamma}$

14. $\dot{\overline{w}}_i^{\,n}$ step 6 $\qquad i = 0, \ell$

15. $\overline{w}_i^{\,n} = \overline{w}_i^{\,n-1} + \left(\dot{\overline{w}}_i^{\,n} + \dot{\overline{w}}^{\,n-1}\right)\frac{\Delta t}{2}$ $\qquad i = 0, \ell$

16. $w_{ci}^{\,n}$, $w_{Gi}^{\,n}$ step 4, 5

17. Return to step 7.

APPENDIX B

Free-Surface Velocity at Time t_s

Consider a Cartesian coordinate system, origin at ground zero, with coordinate axes (x, y) shown in Fig. B-1. In this appendix, the following notations and definitions are used:

v_0 is the radial particle velocity associated with the compressional wave at the free surface

U_i is the x-component of the free-surface velocity

V_i is the y-component of the free-surface velocity

$\frac{\alpha}{\beta}$ is the ratio of the compressional velocity to the shear velocity

θ_p is the angle of incidence of compressional wave

θ_s is the angle of reflection of shear wave

$\hat{w}_s$ is the peak radial spall velocity

W is yield of the explosive

D is depth of burial

a_0 is an empirical constant

m is an empirical constant.

For an initial horizontal free surface, v_0 is approximated by:

$$v_0 = \frac{1}{2} w_s = \left(\frac{1}{2} \frac{a_0 W^{m/3}}{r^m}\right).$$

The x, y components of the surface velocity at t_s are:

$$U_i = v_0\left[\left(1 + \frac{A_2}{A_1}\right)\sin\theta_p - \frac{B_2}{A_1}\left(\frac{\alpha}{\beta}\cos\theta_s\right)\right]$$

$$V_i = v_0\left[\left(1 - \frac{A_2}{A_1}\right)\cos\theta_p - \frac{B_2}{A_1}\left(\frac{\alpha}{\beta}\sin\theta_s\right)\right]$$

where, $\left(\frac{A_2}{A_1}\right)$ and $\left(\frac{B_2}{A_1}\right)$ are found by simultaneous solution of

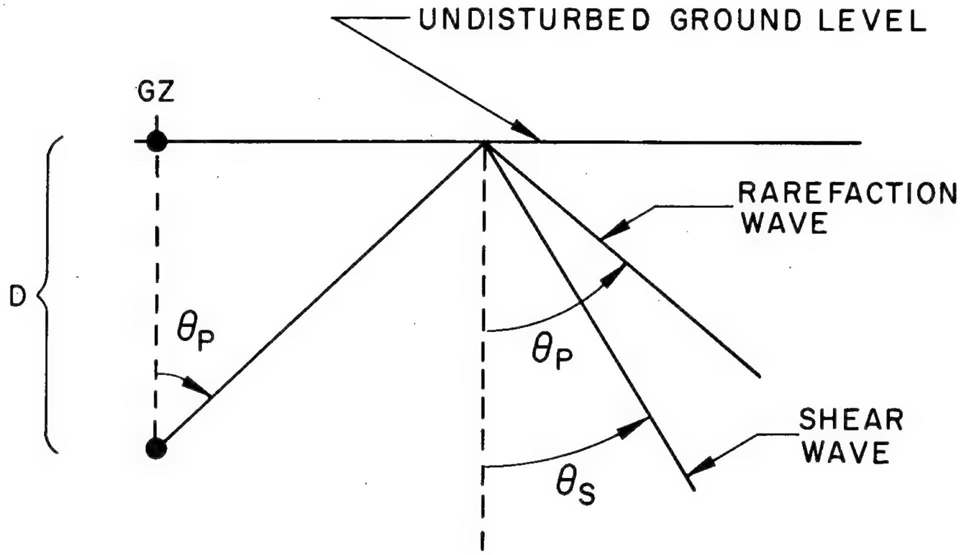

Fig. B-1. Geometrical definitions for prescription of free-surface velocity at t_s.

$$2\left(1 - \frac{A_2}{A_1}\right)\cot\theta_p + \frac{B_2}{A_1}\left(\cot^2\theta_s - 1\right) = 0$$

$$\left(1 - \frac{A_2}{A_1}\right)\left[2\cot^2\theta_p + \frac{(\alpha/\beta)^2 - 2}{\sin^2\theta_p}\right] + 2\frac{B_2}{A_1}\cot\theta_s = 0.$$

The angles θ_p and θ_s are related by:

$$\sin\theta_s = \frac{\beta}{\alpha}\sin\theta_p.$$

Constants for the calculation of U_i, V_i in alluvium are as follows:

a_0 = 36.58 m/sec,

m = 2.142,

$\left(\frac{\alpha}{\beta}\right)$ = 1.591

BIOGRAPHICAL SKETCHES OF AUTHORS

Joseph B. Knox was born in Pittsburgh, Pennsylvania. From 1942 to 1946, he served as a meteorologist with the U.S. Army Air Force in the Mediterranean Theater of Operation. He received his B.A. (1949), M.A. (1950), and Ph.D. (1955) degrees from the University of California at Los Angeles.

From 1955 to 1958, Dr. Knox served as Instructor and Assistant Professor in the Department of Meteorology at UCLA. At the same time, he was engaged as a consultant to the Rand Corporation in connection with the prediction of radioactive fallout. Since 1958, he has been associated with the Lawrence Radiation Laboratory with primary interests in dynamical wind prediction, numerical analysis, fallout prediction, meteorological and hydrological safety problems connected with the engineering applications of nuclear explosives, and cratering physics. Since October 1963, he has served as Group Leader for the Plowshare Theoretical and Computations Group.

Robert Terhune is a native of Seattle, Washington. He received the B.S. in Physics from San Diego State College in 1961. He was employed as a physicist by General Dynamics, San Diego, California, from 1961 to 1963. Since 1963 he has been employed as a physicist at the Lawrence Radiation Laboratory, Livermore.

ENGINEERING PROPERTIES OF EXPLOSION - PRODUCED CRATERS

W. C. Sherman, Jr.
W. E. Strohm, Jr.

U. S. Army Engineer Waterways Experiment Station
Vicksburg, Mississippi

ABSTRACT

The study of the engineering properties of nuclear-explosion-produced craters has thus far been limited primarily to the Sedan crater in desert alluvium and the Danny Boy crater in basalt. Extensive preshot and postshot field and laboratory investigations have been made to evaluate the preshot engineering properties of the media and the changes which occur in these properties as a result of the explosions. In addition to changes in basic engineering properties, such as density and shear strength, large-scale effects such as strata distortion, displacements, and fracturing in the cratered media have been investigated. Results of the studies of the Sedan and Danny Boy craters are presented. The nature and characteristics of the fallback materials and disturbed materials beyond the crater are presented. Various engineering problems associated with the use of explosion-produced craters are outlined and the limitations imposed on the use of cratering for excavations because of the scarcity of empirical data are discussed.

INTRODUCTION

The tremendous energy unleashed by nuclear explosions provides an answer to man's continuous quest for more practical and economical means of accomplishing large-scale earthmoving projects. Since nuclear excavations can be made for as little as 1/10 to 1/20 the cost of conventional excavations, the benefit to large excavation and earthmoving projects is obvious. In nuclear excavations, very large and very deep excavations are dealt with for the reason that excavation costs per unit volume are inversely proportional to the yield of the device. No precedents exist to permit a forecast of all the problems resulting from the practically instantaneous removal of huge quantities of material from great depths below the ground surface; consequently, it is essential to examine very closely the effects of, and engineering problems attendant to, the initial experiments involving the use of nuclear explosions in moving earth.

For over a year, the U. S. Army Engineer Waterways Experiment Station (WES) has been conducting an investigation of the engineering properties of nuclear craters, the objective being to develop procedures for evaluating the stability of slopes and the strength of foundation materials adjacent to nuclear excavations for use in future engineering projects. In addition, a theoretical study is being made of the cratering mechanisms affecting the engineering properties of crater media. This paper outlines available information on the engineering properties of materials adjacent to nuclear craters and how these properties affect the engineering utilization of these excavations and adjacent materials.

INVESTIGATIONAL PROGRAMS

General Plan

Because of the infinitely varied soil, rock, and geologic conditions which may be encountered in nature, it would be impossible to evaluate all the possible changes in engineering properties of material that might occur as a result of an explosion-produced crater. Thus far, the investigations have been limited to relatively homogeneous deposits. The basic approach to the problem is twofold: First is the empirical approach in which extensive preshot and postshot investigations are

samples. Geophysical logs similar to those made in the preshot borings were also made in the postshot borings and the results were compared.

The results of the postshot field mapping indicated that the surface of the ejecta along the crater lip varied from 35 to 95 ft above the preshot ground surface. The upward displacement of the preshot ground surface varied from 2 to 17 ft. Mapping and examination of the trenches indicated that the ejecta consisted primarily of foldback materials. Foldback materials consist of relatively undisturbed strata found in inverted order along the edge of the crater. In the northeast quadrant, where the ejecta thickness was greatest and a large slide had occurred shortly after detonation, ejecta consisted of slide blocks, relatively undisturbed masses of material which are believed to have been moved laterally from an initial position within the cratered area by the blast. The ejecta investigated retained its original structure and stratification, and results of field density tests in this material indicated that the densities did not differ significantly from the natural soil densities.

The fallback materials in the crater consisted of loose, silty, sandy gravel with cobbles and boulders, and the measured field densities near the surface were as low as 70 lb per cu ft, which is near the minimum density on the basis of laboratory tests conducted. Measurements of the slope angle of the fallback material indicated that the slope had an average angle of repose of 35; which agrees with the angle of internal friction determined in the laboratory on these materials in their loosest state.

A comparison was made of the preshot and postshot densities of the material below the preshot ground surface based on the results of the geophysical Densilogs and also on the arithmetic average of densities of the undisturbed samples. No evidence of a decrease in density which might account for the observed upward displacement of the preshot ground surface was noted. On the contrary, the results indicated that, on the basis of the Densilogs, the average dry density increased after detonation about 11 to 12 lb per cu ft at a distance of 600 to 600 ft from ground zero and increased about 3 to 6 lb per cu ft at a distance of 800 ft from ground zero. Although undisturbed samples were not obtained from the preshot boring made 600 ft from ground zero, it is probable that the preshot dry densities were equal to those of samples from borings at 800 ft from ground zero; on this basis, the weighted average dry density at a distance of about 600 to 660 ft was at the most only several pounds per square foot greater than the preshot density. Comparison of preshot and postshot undisturbed sample densities at 800 ft from ground zero also indicated little or no increase in density, which is not in accord with the increase indicated by the Densilogs. It is considered that the undisturbed sample densities are more reliable than the Densilog densities, since Densilog results are affected by the degree of saturation of the material forming the walls of the borings, and there probably were differences in this respect between preshot borings and postshot borings. This is possible since postshot borings were filled with drilling mud for a longer time prior to logging than were the preshot borings.

The crater slopes above the upper limits of the fallback materials include exposed portions of the true crater surface and ejecta. The slopes in these materials are extremely ragged, reflecting distortions caused by the explosive forces of the detonation and subsequent slumping of the crater walls into the crater. The average slope of the surface of these upper materials is about 38°, although in many instances some of the strata are found standing at much steeper slopes for limited vertical distances. The angle of internal friction, ϕ', of the in-situ soils adjacent to the upper slopes was found in laboratory tests to range between 40 and 48°, with an average value in the order of 43°. Ignoring any effects of cementation which may be present, the factor of safety of these upper slopes with respect to sliding is given by the expression:

$$\text{Factor of Safety, FS} = \frac{\text{tangent } \phi'}{\text{tangent of slope angle}}$$

$$= \frac{\tan 43°}{\tan 38°} = 1.2.$$

This factor of safety indicates relatively stable slopes, although environmental effects such as weathering by wind and rain will have considerable influence on the final slopes. Latent disturbance beyond the crater walls which was not disclosed by the subsurface explorations may also affect the stability of the slopes. Available data indicate that the upper slopes of the crater walls receded as much as 12 ft in a 3-1/2-month period. This degradation will continue, probably at a decreasing rate as the slopes tend to flatten with time.

made of cratered media to evaluate fully the changes resulting from a nuclear detonation. At the present time WES has completed an investigation of the Sedan crater and has partially completed an investigation of the Danny Boy crater; the results of these investigations will be described subsequently. An important phase of this work is to delineate and define those properties of a deposit which are of interest from an engineering standpoint. Of particular importance are those properties which affect the behavior and stability of large, jointed rock masses as nuclear detonation would be most advantageous in excavating rock. Current knowledge on this subject is very meager, and, consequently, the study of the stability of natural and cut slopes in rock is a necessary supplement to the field investigations of nuclear craters in rock. The second approach, which may be termed the "theoretical approach," involves the development of a suitable theory or theories for predicting the changes that would occur in media of various types and conditions using data from models and field tests.

Theoretical Studies

A theoretical study of cratering mechanisms affecting the engineering properties of crater media is being conducted for WES by Dr. A. B. Vesic of the Georgia Institute of Technology.[1] A preliminary theory has been developed which enables rational analysis of camouflets, subsidence craters, and the deep craters that are of primary interest from an engineering standpoint. In this theory, it is assumed that the material adjacent to the cavity behaves as a rigid-plastic solid, whose strength can be defined by a Mohr's envelope. The theory indicates that the efficiency of nuclear charges as compared with conventional explosive charges of the same energy yield depends on the properties of the crater media, as well as on the depth of burst and the level of the yield. Further extensions of the theory are now being made to include such effects as soil dilatancy, compression in the plastic zones, strain hardening, etc. An analysis of all major cratering investigations in the light of the new theory is being conducted in connection with these problems. Theoretical and experimental studies are also being conducted to gain information on excess pore water stresses which might develop in the media adjacent to the crater, as well as on volume and structural changes such as fracturing and remolding of various types of soils.

Sedan Event

The Sedan 100-kt subsurface shot on 6 July 1962 at the Nevada Test Site formed a crater approximately 320 ft deep and approximately 1200 ft in diameter. Geologic and soils investigations were made prior to the shot to determine the properties of the subsurface soils and to provide a basis for estimating the changes in these properties resulting from the detonation. The locations of preshot and postshot borings are shown in Fig. 1. The subsurface soils at the Sedan site are made up of a series of alluvial beds, which consist primarily of silty to sandy gravel (generally well graded) to a depth of 1200 ft. All of the materials exhibited some degree of cementation and, although the degree varied widely, the strength of the cementation was relatively weak in most cases. The ground-water table at the site was about 1600 ft below ground surface and, consequently, had no bearing on either the cratering mechanism or the stability of the resultant slopes.

The preshot field investigation included two undisturbed borings, U-1 and U-2, to depths of 200 and 430 ft at distances of 800 and 400 ft, respectively, from ground zero to obtain 6-in.-diameter undisturbed samples, and two split-spoon borings to depths of 200 and 300 ft at distances of 1100 and 600 ft, respectively, from ground zero. The borings were made along a line bearing N 45° W from ground zero. Because of the presence of large gravel sizes, penetration data from the split-spoon borings were of little value. Drilling mud had to be used in all borings and considerable difficulty was encountered in obtaining the undisturbed samples because of the gravel. Various geophysical logs were made of each of the four borings. Of the various logs (Densilog, Electrolog, Focus Log, Gamma-ray/neutron, and Minilog/caliper), only the Densilog provided useful information. Only about one month was available for the preshot field work, and all desired work was not accomplished; however, it is believed that the initial subsurface conditions were reasonably well defined.

Laboratory testing of the preshot undisturbed samples consisted of natural density and relative density determinations; triaxial compression shear strength tests; and classification tests, in-

cluding determinations of grain size, specific gravity, and chemical constituents. Testing of the undisturbed samples was extremely difficult because of the gravelly nature of the material. In general, the preshot investigations indicated that the materials were relatively uniform in character to the depths investigated (about 430 ft), except that the upper 110 ft contained somewhat more silt and less gravel than the underlying soils. In the upper 110 ft the natural density increased with depth from about 93 lb per cu ft at a depth of 32 ft to about 113 lb per cu ft at a depth of about 110 ft; otherwise, no important differences in soil properties were noted. Below a depth of about 110 ft, the foundation soils were found to be at an average density of about 113 lb per cu ft, close to the maximum possible density. The angle of internal friction at natural density for all materials average about 43°.

The postshot profile of the Sedan crater is also shown in Fig. 1. Important features are the original preshot ground surface, the displaced preshot ground surface, the postshot ground surface, the apparent crater surface, the true crater surface (which has not been completely delineated), fallback materials, and ejecta, which consist of material thrown out of the crater.

Postshot explorations included borings and geological mapping of the exposed surfaces of the ejecta in a trench extending radially from the crater lip crest on the same line as the preshot borings. The two deep postshot borings, SA-2A and SA-3A, shown in Fig. 1 (preshot borings also are shown) were made to obtain undisturbed samples for testing and comparison with the initial results. Four 48-in.-diameter Caldweld-type borings were also used in investigating the ejecta materials. The walls of the exposed true crater and ejecta were mapped and strata were classified and correlated with strata in the walls of the trench and of the 48-in.-diameter borings. A second trench excavation along the crater lip was made by Lawrence Radiation Laboratory (LRL) in connection with providing access to the bottom of the crater, and the walls of this excavation were also mapped to determine the character of the ejecta deposits. Laboratory tests similar to the preshot tests were performed on postshot undisturbed

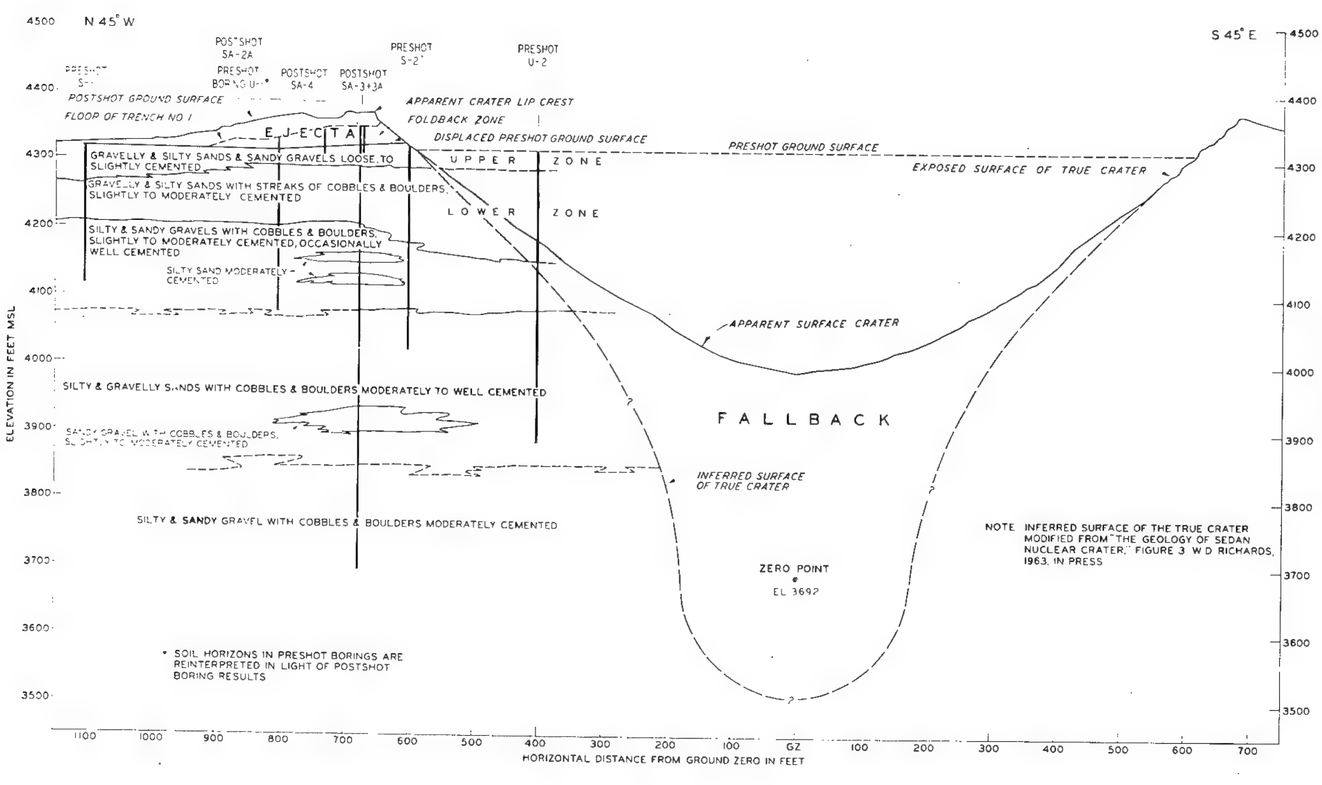

Fig. 1. Generalized soil conditions at Sedan crater.

Danny Boy Event

The Danny Boy event took place in a basalt mesa at the Nevada Test Site. The materials at the site consist of a thin mantle of residual soils overlying vesicular basalt containing layers of volcanic ash to variable depths, below which hard, dense basalt is found at least within the vicinity of the true crater (see Fig. 2). The Danny Boy crater is approximately 220 ft in diameter and 60 ft in depth. A profile through the crater is shown in Fig. 2, together with the logs of three of the postshot borings. Only limited preshot field investigations were made at this site. Angled borings, made under the direction of LRL after the shot, have indicated the approximate location of the true crater. A single trench excavation by WES indicated that the uplift of the original ground surface at the crater periphery is about 9 ft. Maximum lip height is about 28 ft above true ground surface. There is no reliable evidence of any foldover at the crater lip. Postshot field investigations, which are still in progress, include careful inspection of oriented NX cores, water pressure tests at intervals of depth in the drill holes to establish the degree of joint opening, and use of the borehole camera. Three borings have been drilled beyond the crater edge and two borings in the crater.

A second boring, located in the center of the crater, was carried to a depth of 124.5 ft below el 5410 ft msl, the bottom of the crater. Considerable core loss occurred and many cavities were encountered in this boring, and it was not possible to inspect the bore walls with a TV camera or to obtain photographs with the borehole camera because of intruding rock fragments. The log of this boring is not shown in Fig. 2 because the data are not considered sufficiently complete to provide a reliable indication of the character of the underlying material. It is planned to ream the hole to a diameter which will permit inspection using the TV and borehole cameras.

In general, the presence of caliche filling in the natural rock joints made it relatively simple to distinguish between the natural joints and blast-induced fractures. A preliminary study has been made of the jointing and fracture data from the cores obtained from postshot borings. These analyses, as indicated in Fig. 2, indicate that the zone of abundant blast-induced fractures is concentrated in the dense basalt. Relatively few blast-induced fractures were noted in the vesicular basalt. Although not conclusive, the results of the pressure tests tend to confirm the results of the preliminary conclusion regarding the zone of abundant blast-induced fractures.

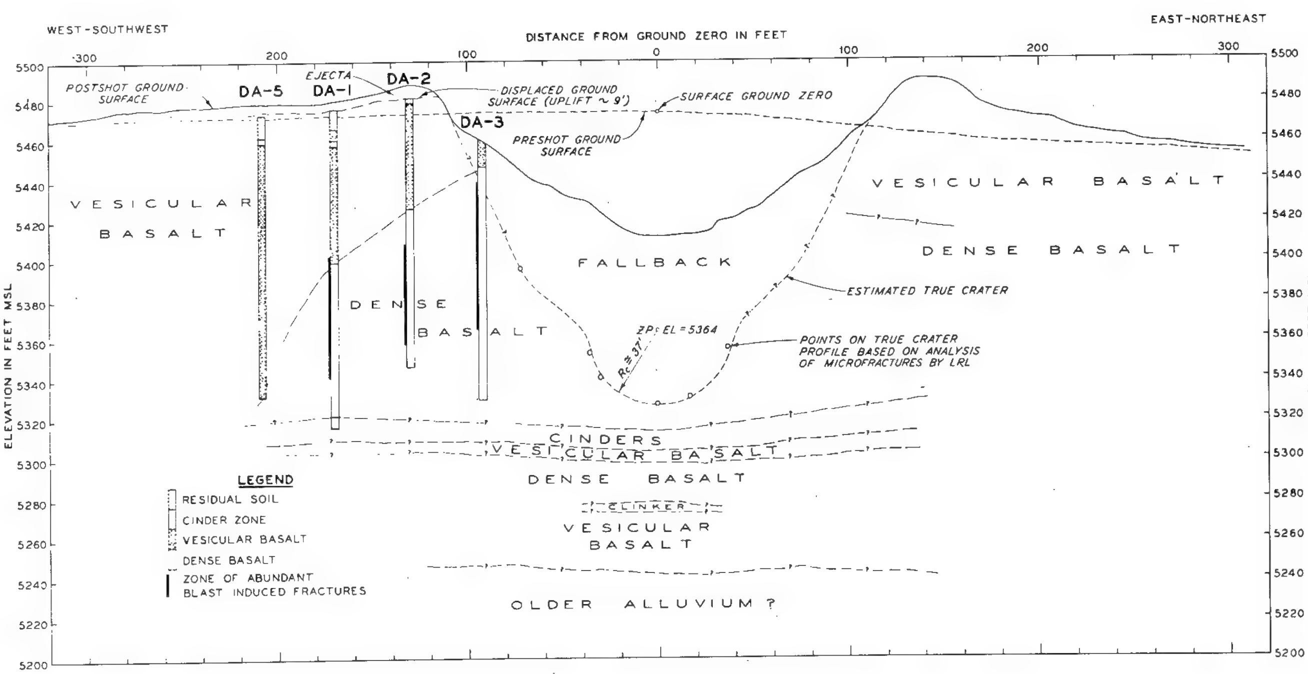

Fig. 2. Foundation conditions at Danny Boy crater.

The use of the borehole camera permits a very detailed examination of the rock mass with depth. The considerable amount and variety of data obtained complicate the analysis, and steps are being taken to utilize an electronic computer for this purpose. Data on rock type, dip and strike of fractures and joints, type of joints and fractures (blast-induced and natural), joint opening, and types of joint filling are being put on computer cards, and the programs being developed will be used to correlate the data in greater detail. This information, it is hoped, will provide significant information on character and magnitude of blast-induced joints and fractures. Subsequently, the data will be used as a basis in determining the overall strength of the rock mass forming the crater slopes. A limited program of laboratory tests is being performed on the core materials.

At the Danny Boy site, the groundwater level is well below the level of detonation. The slopes of the fallback materials in the lower part of the crater do not exceed their angle of repose, which is estimated to be about 35°. The slopes of the true crater walls above the fallback materials range from 50 to 60°. No quantitative assessment has yet been made regarding the degree of stability of these slopes.

ENGINEERING PROBLEMS ASSOCIATED WITH EXPLOSION-PRODUCED CRATERS

Stability of Crater Slopes

The question of the stability of crater slopes is probably the most important of the engineering problems associated with the use of nuclear explosives for excavation purposes. As in any permanent excavation of importance, a properly designed slope having an adequate factor of safety with respect to sliding is essential. If the slopes are too steep, extensive slides can seriously destroy the usefulness of an excavation, result in loss of life and property, or result in costly and difficult maintenance. Present knowledge on the stability of crater slopes is somewhat meager. However, data from the Sedan and Danny Boy investigations, together with theoretical studies and experiences with conventional excavations, permit some insight into this problem. A brief discussion of the immediate and long-term stability of slopes and excavations created by nuclear explosives is presented below.

Immediate stability. During the throwout period following a subsurface nuclear explosion, the soils just outside the crater walls are subject to dynamic forces which allow the crater walls to stand at steeper angles than they would normally stand under static loading. When the dynamic forces are dissipated, the crater walls must necessarily readjust to an equilibrium condition under static loading conditions. As described by Whitman,[2] failures and readjustments which occur shortly after the throwout periods are functions of the immediate stability of the crater slopes. Evidence from model tests on sands and also observations of the Sedan crater indicate that such readjustments or slope failures occur shortly after the throwout periods.

In addition to gravity forces, another factor which can generate failures under static conditions is the surcharge load imposed by the ejecta materials. The ejecta materials may provide a significant increase in loading in some cases. In referring to crater slopes, what is meant is the slopes which are formed after these very early slope failures have occurred. WES experience indicates that, in the case of immediate stability, slopes of dry sands will be in the order of 30 to 40°, depending on the density of the sand. Slopes of materials consisting of large rock fragments may be as steep as 45°. If sand deposits are below the groundwater table before detonation, the resultant seepage forces in the sands after throwout will reduce the stable slope angle to about one-half, or 15 to 20°. Very little is known concerning the results of cratering in sands and gravels below the water table; however, it is probable that seepage forces which depend on the height of the original water table above the bottom of the crater would be an important factor. In the case of fine-grained cohesive soils such as clays, the strength is dependent on the undrained shear strength of the clay material, the height of the slope, and the depth of the clay beneath the bottom of the excavation. Nuclear explosives may result in extensive remolding with consequent decrease in shear strength of some clays. Deep-seated rotational slides may occur in deep deposits of soft clays shortly after the throwout period. The creation of conditions leading to instability of nuclear excavations in such deposits because of steep, unsafe initial slopes cannot be overemphasized, since large mass movements will later take place with possibly serious consequences.

Another problem related to immediate stability occurs with explosions in soft, sensitive clays and fine, loose sands. Since soft, sensitive clays show almost no strength in the remolded state, they will tend to flow as a viscous liquid as the slide occurs. A small initial slide may therefore have catastrophic consequences, as the liquefied clay will flow and will thus not provide any support for the exposed clay face, with the result that the whole of an otherwise stable slope may fail and a series of retrogressive slips may take place under undrained conditions. Saturated fine, loose sands, also subject to liquefaction as a result of shock, may also tend to flow as a liquid. No records of experiences with buried nuclear explosives in such soils are available; however, the consequences can be deduced from experiences with conventional excavations in such materials.

Slopes in intact rock are dependent on the joint pattern, and the creation of fractures and extension of the joint openings which occur as a direct result of the blast. The strength of individual specimens of rock apparently has very little relation to the stability. Under certain conditions, the release of in-situ stresses or tectonic stresses may also play an important role in the stability of rock slopes. According to Terzaghi,[3] a massive rock with a random joint pattern has an angle of internal friction of about 70°. Consequently, rock slopes in nuclear craters may be stable at this angle; although if the rock is greatly fragmented, this angle may be as low as 45°.

Again, according to Terzaghi,[3] the angle of internal friction of stratified rock may range between 30 and 90°, depending on the inclination of the bedding planes. No information is available on cratering in stratified materials in which the bedding planes are not parallel to ground surface. However, it is clear that in such cases stable slopes might be realized on one side of a canal or harbor while unstable slopes would be present on the other side.

The dynamic forces exerted on groundwater present in a rock deposit have a considerable effect in altering the strength of the deposit. Studies in Europe with conventional blasting techniques indicate that dynamic forces on the pore water and the water in the joints play an important part in blasting efficiency. Consequently, the loosening and shattering effect of a nuclear explosive would probably be much more extensive in a saturated or moist rock deposit than in a dry rock.

Long-term stability. Below the bottom of an excavation formed by a buried nuclear explosion, vertical stresses above any point are relieved by the weight of material removed. This relief of the vertical stresses permits vertical expansion; and if sufficient time elapses, the water content of the material increases because of the soil expansion. If the expansion is appreciable, as in the case of a cohesive soil, the loss of cohesive shear strength results. This is the basic reason why, when long-term stability is required, slopes should be designed flatter than those required to meet short-term stability consideration. For instance, it is quite feasible to construct practically vertical excavation slopes in clays and shales (to a limited height, of course), which may be stable for a relatively short time. However, these materials will eventually slough and fail until a stable slope is reached. Other very important factors affecting long-term stability are changes taking place after excavation, such as changes in groundwater level, buildup of hydrostatic water pressures in the bedding layers, and other stress changes resulting from construction of buildings, etc., along the top of the slopes. Under these conditions may be included saturation and slumping of the relatively loose fallback materials. The reduction in long-term stability as a result of weathering may also be a factor in tropical climates.

Long-term stability conditions are particularly difficult to assess in cohesive-type soils, especially in the case of shale-type rocks. At the present time, there is no dependable basis for designing safe slopes in shales utilizing results of laboratory shear tests. The shattering and alteration of such materials caused by a nuclear explosion introduce other factors which cannot be evaluated at present; however, it can be said with considerable certainty that strength would be reduced. The greatest differences between stable short-term and stable long-term slopes are found in clay and shale deposits, and much additional research is needed to evaluate their long-term shear strength.

The problems which the Corps of Engineers and others have had with designing safe slopes in shales are well known. Considerable attention was focused on this problem as a result of the tremendous Culebra and Cucaracha failures along the Panama Canal. A very good description of these slides is presented by Binger and Thompson.[4] An interesting outcome of these investigations was a

field slope chart which has been used as a guide in selecting safe design slopes for the Cucaracha shales. Since that time, the Missouri River Division has developed modifications of the field slope charts for use in designing excavation slopes involving the shale formations along the Missouri River.[5] This approach, while not the whole answer by any means, is invaluable where sufficient empirical data are available to permit construction of such charts. Local experiences with specific soil and geologic conditions provide an invaluable guide in selecting the proper slope. At the present time, the U. S. Bureau of Mines, in conjunction with some of the large mining concerns, is doing extensive research to develop criteria for the safe design of excavation slopes for deep, open-pit mines in the western part of the United States.

One of the important problems which must be faced is how to obtain, by nuclear detonation, excavations of the desired cross section in various types of materials. Let it be assumed that the necessary procedures and information to design a safe slope for a specific site are available; what can be done if this safe slope is appreciably flatter than that which would be produced by a single buried nuclear explosive? It is possible that the use of two or more simultaneous detonations in various cross-section arrays, and perhaps of different yields, may be necessary to produce the desired flatter slopes. No work has been done along this line as yet; however, further studies will be necessary to establish techniques for producing excavated craters in which safe excavation slopes are to be realized

Summary on Slope Stability

In summary, nuclear explosions in rock and granular media will generally provide slopes which are stable, although consideration should be given to the effect of geological discontinuities and water pressures. At the present time, there is some pessimism about the use of nuclear explosives in single-row charges for excavations in cohesive soils, including some of the shales, inasmuch as the long-term stability considerations require slopes which are much flatter than those which can be produced economically by nuclear detonations. Considerably more research is needed in the field of evaluating the long-term shear strengths of such types of soils. In assessing the problem of slope stability, it is recommended that normal precautions be taken, based on available theory and experience. The recent investigations of rock slopes by Terzaghi and others also offer valuable guides in this respect. It should be emphasized that design of safe slopes, even with excavation by conventional techniques, is quite difficult and complex under certain circumstances; and this difficulty and complexity may be compounded many times by introducing excavation by nuclear explosives. Further studies are needed to establish methods for using nuclear explosives in producing excavations having the desired slopes for long-term stability. It is hoped that current and future quantitative measurements of the engineering properties of large nuclear craters in different environments will provide useful information in this respect.

Fallback materials. The area between the lower portion of the apparent and true craters is filled with materials designated as fallback. Investigation of craters in desert alluvium and jointed basalt indicates that these materials are generally in a loose condition, at least near the surface, although evidence of some stratification has been observed in addition to the presence of slump blocks from the crater walls. Some compaction of the materials may have resulted from the manner in which they were deposited; however, in general, the materials at the peripheral limits lie at the angle of repose. From the standpoint of slope stability, these materials can be considered as stable; however, they may be affected by erosion and, in the case of fine, cohesionless materials, possible liquefaction under certain conditions. No information is yet available on the character of fallback materials produced by detonations in clay.

Erosion due to backwash. The initial slopes of craters formed under water or adjacent to bodies of water may be affected by backwashing and attendant filling of the craters. The amount of material washed into the crater depends principally on the types of materials involved. High-explosive tests at the WES indicated that considerable material was backwashed into the craters in sand, while relatively little was moved into the craters created in stronger cohesive soils. Much of the

filling was undoubtedly due to backwash erosion, which probably would play an important part in the immediate slope failure process.

Foundation Characteristics of the Crater Lip Area

In the engineering utilization of explosion-produced craters, it is quite probable that the areas along the lip of the crater may also be used for structures such as buildings, wharfs, highways, railroads, etc. Consequently, the foundation characteristics of these materials are of great importance. In the immediate vicinity of the crater, the lip is covered by ejecta. For detonations in desert alluvium, the ejecta consist principally of foldback materials covered by a thin veneer of dust and breccia. No evidence of foldback was noted on the rock material at the Danny Boy crater. The irregular topography of the ejecta along the crater lip indicates that considerable grading and leveling would be required for construction in this area. Fortunately, however, on the basis of studies at the Sedan crater, the foldback materials apparently retain their original stratification and density and offer foundation conditions almost as favorable as the original surface strata.

Utilization of Ejecta

Buried explosions in rock produce ejecta consisting of an assortment of broken rock sizes. Indirect evidence at the Danny Boy crater indicates that the sizes of the rock material are related to the sizes of the rock units defined by the joint system. This leads to the possibility of using such explosions for the manufacture of aggregate and for production of large rock sizes for use as riprap and other protection. Manufacture of aggregate by a single explosion can be classified in two types of work: (a) for the rapid manufacture of aggregate when time is an important factor, and (b) when time is not too critical and a conventional recrushing plant can be installed and utilized. The aggregate manufactured can be classified as (a) that immediately available by utilization of a rock-raker, (b) that immediately available for secondary crushing, and (c) that material that would require secondary blasting prior to crushing. The larger sizes could, of course, be used directly for riprap and other protection. Studies are in progress at the Danny Boy crater, to evaluate the particle-size distribution, quantities that are available for instant usage by the rock-rake method, and the quantity that can be utilized without a secondary shooting for recrushing. Various testing of the cores has been made to determine, as far as possible, the characteristics of the crushed rock and these qualities in respect to its use for a concrete aggregate.

NEEDED FUTURE INVESTIGATIONS

The problem of designing safe excavation slopes of relatively deep excavations constructed by routine methods is difficult and complex and is one which has attracted the attention of many organizations, in particular the mining industry in connection with the stability of deep open-pit mine slopes in rock. Methods are needed to permit evaluation of the engineering properties of such deposits for obtaining quantitative data on which to base the stability of the slopes. In evaluating the engineering properties of nuclear craters, the additional problem arises of evaluating the effects of the explosion on the in-situ properties. The stability of large masses of material, such as would be involved in a slide of an excavation 400 or 500 ft deep, is a subject of much current research. Geophysical tools of various types play an important role in evaluating the overall properties of such media. Considerable effort is required to evaluate pertinent engineering properties and an understanding of the various phenomena involved in the stability of deep excavation slopes is far from clear. Of particular importance is the need for quantitative characterization of the behavior of fissured and fractured rock masses. In addition to the problem of evaluating these properties of deposits under static conditions, it is necessary to evaluate the effects of nuclear explosions on the engineering properties of various media. Deep nuclear explosions have thus far been conducted only in a relatively homogeneous desert alluvium and in a basalt. To extend the knowledge to other media, it is essential that a wide variety of foundation media be investigated before nuclear explosives can be used for excavations with confidence. Some of the types of formations in which information is de-

sired are saturated, fine-grained media and stratified media such as sandstones, shales, etc. The problem of nuclear explosions on nonlevel surfaces also remains to be solved.

BIBLIOGRAPHY

1. Vesić, A. B., and Barksdale, R. D., "Theoretical Studies of Cratering Mechanisms Affecting the Stability of Cratered Slopes," prepared for U. S. Army Engineer Waterways Experiment Station by the Georgia Institute of Technology, September 1963.
2. Whitman, R. V., "Soil Mechanics Considerations Pertinent to Predicting the Immediate and Eventual Size of Explosion Craters," Sandia Corp. Report SC-4405(RR), 1959.
3. Terzaghi, K., "Stability of Steep Slopes on Hard Unweathered Rock," Geotechnique, December 1962.
4. Binger, W. V. and Thompson, T. F., "Excavation Slopes" taken from "Panama Canal - The Sea Level Project: A Symposium," Transactions of ASCE, 114, 1949.
5. Knight, D. K., "Oahe Dam: Geology, Embankment, and Cut Slopes," Journal of the Soil Mechanics and Foundation Division, ASCE, 89, No. SM-2, March 1963.

BIOGRAPHICAL SKETCHES OF AUTHORS

Walter C. Sherman, Jr., is a native of Chicago, Illinois. He received his B.S. in Civil Engineering from Purdue University in 1946, and his M.S. in Civil Engineering from Harvard University in 1947. He has been employed at U.S. Army Engineer Waterways Experiment Station, Vicksburg, Mississippi, as a soils engineer since 1947, except for a brief tour as design engineer on air base construction in Spain in 1955. He is currently Chief of the Engineering Studies Section, Soils Division.

William E. Strohm, Jr., is a native of Santa Fe, New Mexico. He received his B.S. in Civil Engineering from New Mexico State University in 1952. He served as an officer with the U.S. Army Corps of Engineers from 1952 to 1954, and attended the University of Texas as graduate student in soil mechanics from 1954 to 1956. Since 1956, he has been employed at the U.S. Army Engineer Waterways Experiment Station as project engineer on soil mechanics research projects.

CONTAINED NUCLEAR DETONATIONS IN FOUR MEDIA -- GEOLOGICAL FACTORS IN CAVITY AND CHIMNEY FORMATION

Charles R. Boardman
David D. Rabb
Richard D. McArthur

Lawrence Radiation Laboratory, University of California
Livermore, California

ABSTRACT

Underground nuclear tests in tuff, alluvium, rock salt, and granite have yielded data essential to the evaluation of the effects of contained nuclear detonations. The data indicate that for these mediums the cavity radius is predictable within ±20% without regard to the physical or chemical properties of the rock in the immediate shot environment. Properties of the chimney of broken rock resulting from collapse of the cavity, on the other hand, are found to be related to the physical properties of the rock and to preshot structural weaknesses within the rock.

INTRODUCTION

Recent underground nuclear tests conducted by the U. S. Atomic Energy Commission have yielded data on the effects of contained nuclear explosions in four rock mediums: tuff, alluvium, rock salt, and granite. This report presents and compares data obtained primarily through exploratory mining and drilling into the postshot environment of 35 such events.

With one exception, these events were either weapons development or military effects tests. Only five were explored in detail for the purpose of defining the postshot environment, the remainder being typically explored with two or three postshot drill holes. As a result, the data are not as complete as would be desirable. However, comparison of the available data does provide a measure of the sensitivity of explosion-produced effects to the properties and structures of the containing rock medium.

The phenomena considered in this report are: (1) the cavity created by the expansion of the explosion-produced gases, (2) the chimney of broken rock resulting from collapse of the cavity, and (3) the zone of fractured rock immediately beyond the chimney.

CAVITIES

The size and shape of cavities produced by contained nuclear explosions have been inferred primarily from drilling data obtained in the region below the shot point. Measurements above the shot point were impossible, since in all cases the original cavity produced by the explosion collapsed within seconds to hours after detonation of the device.

The lower cavity boundary is characterized by a melt-rock interface such as that shown in Figure 1. Measurements of the distance from the shot point to various points on this interface indicate that the cavity is roughly spherical prior to collapse. Departures from spherical symmetry have been observed, however. In several cases, cavity radii measured laterally are about 10% greater than those measured directly below the shot point. Since most radii have been measured below the shot point, this is the measurement chosen for the present study.

It was shown by Nuckolls (1959) that the radius of the Rainier cavity could be explained by having the cavity expand until the pressure of the gas within it is balanced by the weight of the overlying rock. The equation for scaling cavity radii,

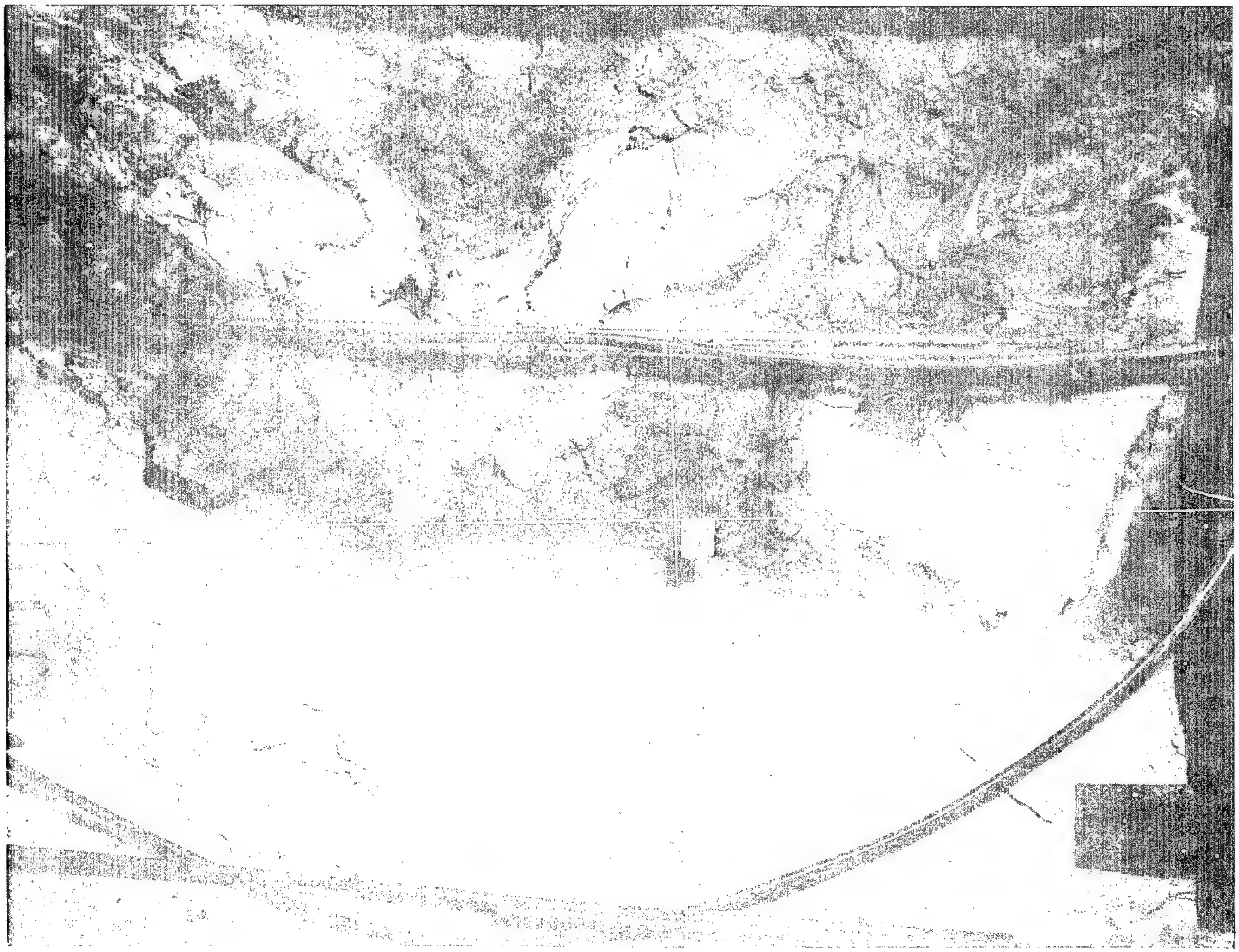

Fig. 1. The edge of Rainier cavity 19.8 meters below ground zero.

based on this assumption and derived in Appendix I, is

$$R = C \frac{W^{1/3}}{(\rho h)^{1/4}}$$

where

R = cavity radius in meters

C = a constant to be empirically derived

W = yield in kilotons (a kiloton is defined as the prompt release of 10^{12} calories or 4.2×10^{19} ergs)

ρ = average of overburden density in grams per cubic centimeter

h = depth of burial in meters.

By applying this equation to the 35 events studied, with the exception of one very low yield event, the constant C is found to vary within ±20%. With the data limited to a single medium (with more than two data points) the minimum variation of C is ±7%. The experimentally determined values are shown in Table I. The unclassified data used in this study are given in Appendix II.

As shown in Appendix I, the ratio of specific heats (γ) of the gases produced by vaporization of the rock is assumed to be 4/3 for all rock mediums considered. Part of the variation in the constant C can therefore be accounted for by the actual difference in γ associated with nuclear explosions in the four rock types. This variation is illustrated by the divergence of the least-squares fit for data

points obtained for events in tuff and alluvium in Figure 2. (Only the unclassified data points are shown in this figure.)

The chemical composition of Nevada Test Site tuff, granite, and alluvium are similar except for water (see Table II) and carbonate content. It is probable therefore that the difference in the ratio of specific heats of the gases produced by vaporization of these rocks is due to differences in water and carbonate content. An increase in those constituents of the rock which form gas at low temperature, such as water, results in an increase in the quantity of gases produced by the explosion, and in turn an increase in cavity pressure. Therefore, all other parameters being equal, it is reasonable to expect that cavities produced by a nuclear explosion in tuff should be larger than those produced in alluvium or granite. It should be noted that the difference in the constant C for tuff and alluvium is much greater than that for alluvium and granite, while the difference in percentage water content in all three cases is large. Therefore, it appears that the effect of increased water content is not linear when comparing one rock type with another.

Typical physical and elastic properties of alluvium, granite, rock salt, and tuff are shown in Table II. Comparison of these properties with the experimental values obtained for C indicates that the exception of water content there is essentially no correlation between cavity size and the properties of the containing rock medium as presented. For example, alluvium has a greater porosity and consequently more space available for compaction than tuff; yet a larger cavity radius is attained in tuff for a given yield and overburden pressure. Also, the average C for granite is only slightly smaller than that for alluvium (indicating similar cavity radii for a given yield and overburden pressure) whereas the porosities of these two rocks differ greatly.

Based on these considerations it is apparent that the physical properties of the rock in which a nuclear explosion occurs have little effect, if any, on the size of the cavity produced. The limiting parameters are the device yield, the gas-producing constituents of the rock such as water, the depth at which the device is detonated, and the average density of the overburden.

CHIMNEY SIZE

Upon collapse of the cavity, a roughly cylindrical chimney of broken rock is formed with a radius approximately equal to that of the cavity. When collapse does not extend to the earth's surface, the top of the chimney appears to be dome-shaped as shown in Figures 3 and 4. Surface subsidence craters indicate that the top flares outward when chimney growth is interrupted by the earth's surface as shown in Figure 5.

Since the radii of the chimney (cylinder) and cavity (sphere) are about the same, the following relationship makes possible an approximation of chimney height in rock masses which break homogeneously throughout and which undergo little or no compaction upon collapse of the cavity.

$$\frac{4}{3}\pi R^3 = k\pi R^2 H,$$

or

$$H = KR$$

Table I. Experimental values of C.

	No. events	Range of C	Average C
Alluvium	15	54.8-74.9	65.9
Tuff	10	72.6-81.9	78.1
Tuff/alluvium	7	58.4-76.1	67.8
Granite	2	59.1-62.1	60.6
Rock salt	1	--	63.6

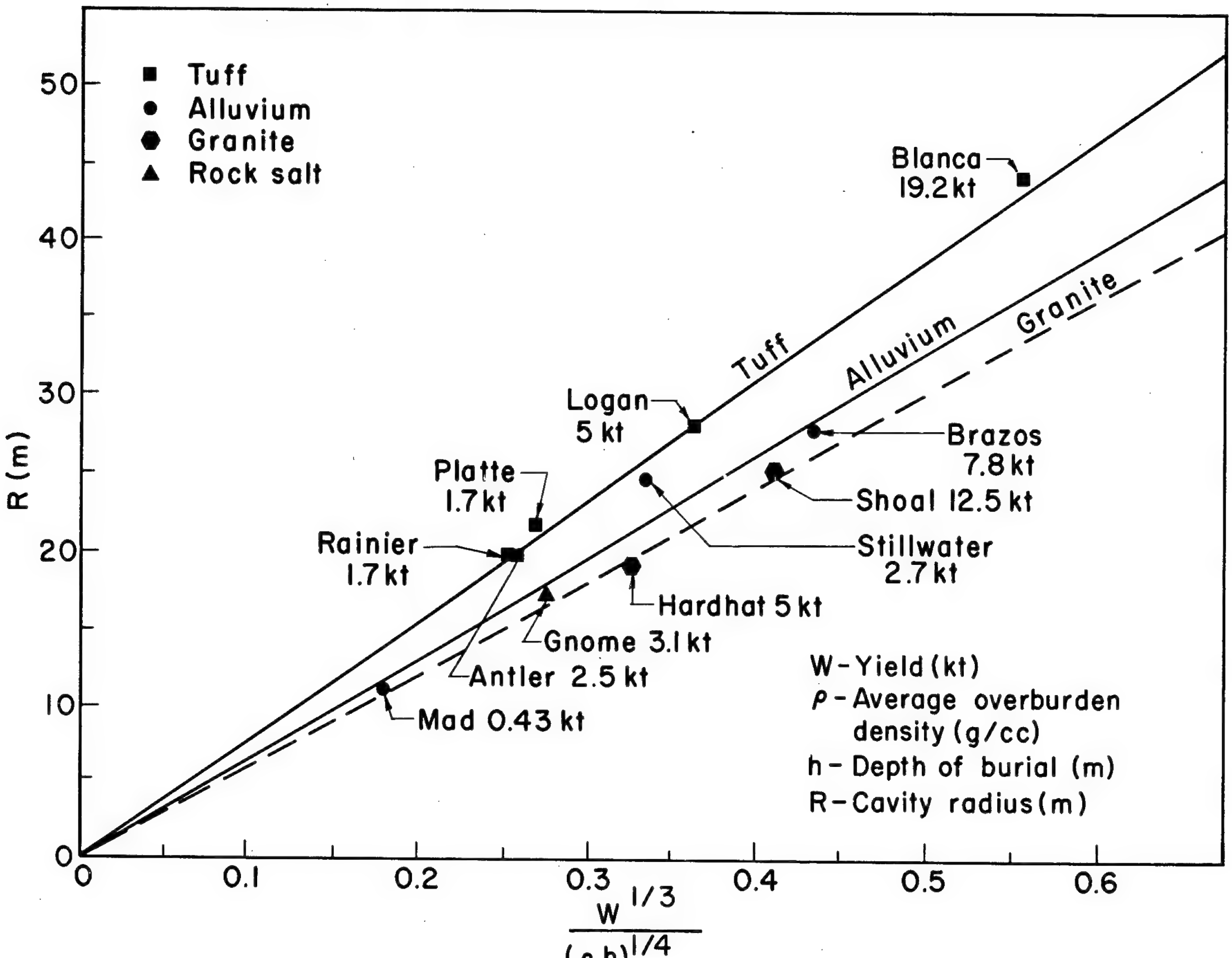

Fig. 2. Cavity radius, R, as a function of yield and overburden pressure.

where

R = cavity/chimney radius in meters

H = chimney height in meters

K = 4/3k.

In order to compensate for the departure from cylindrical symmetry at the top and bottom of a chimney, H is taken as the chimney height above shot point. This in effect substitutes the volume of the chimney rock below the shot point for the volume of rock not included in the chimney but within an imaginary cylinder around the apex. Since the shape of the dome is not well defined, such a substitution is warranted for approximations of chimney volume.

Using the preceding equation, K was found to be 4.5 and 4.2, respectively, for the Hardhat and Shoal events in granite. Using chimney heights and cavity radii from eight events (only five of which are unclassified and can be shown in Figure 6), the least-squares determination of the K for tuff is 5.3. Because of the inhomogeneity of tuff beds at the Nevada Test Site (some are almost like sand, others are competent), the variation in K values for tuff is about +30 and -40%. The more competent beds tend to terminate chimney development, whereas less competent beds break into blocks which pack tightly upon collapse, producing less bulking and consequently higher chimneys.

Most chimneys associated with detonations in alluvium extend to the surface (see Appendix II). Their apices, represented by surface subsidence craters (Figure 7), are not accurate indicators of

the total height that might have been attained had the surface not halted collapse. In addition, subsidence crater volumes in several cases closely approach the calculated cavity volumes, implying that the weakly consolidated alluvium underwent little or no volume change (bulking) when the collapse of the cavity and the formation of the chimney occurred. Therefore, a plot of cavity radius versus chimney height for this rock type would be without meaning.

The Gnome event, a nuclear detonation in a stratified, flat-lying evaporite deposite in New Mexico, resulted in a standing open "chimney" (Figure 8) which extended only 27.1 meters above the original shot point (Rawson et al., 1964). The collapse of the rock-salt beds was limited to about 10 meters from the roof of the cavity and was influenced by separations at bedding planes and clay seams. The existing cavity is unstable and frequent rock falls have been observed 1-1/2 years following the explosion

Table II. Some typical properties of four rock types.

	Alluvium	Granite	Rock salt	Tuff
Physical Properties				
Bulk density, natural state (g/cm^3)	1.6-1.8[a]	2.67[a]	2.2[b]	1.85[c]
Bulk density, dry (g/cm^3)	1.5[a]	2.67[a]	2.18[b]	1.6[c]
Grain density (g/cm^3)	2.5[a]	2.69[a]	2.25[b]	2.35[c]
Porosity	40%	0.9%	3%[b]	32%
Total water content (by wt)	13%[a]	0.9%[a]	1%	20%
Elastic Properties				
Compressional velocity (km/sec)	1.79[d]	5.52[e]	4.08[b]	2.26[f]
Shear velocity (km/sec)	1.12[d]	3.38[e]	2.15[b]	1.08[f]
Poisson's ratio	0.33	0.31	0.31[b]	0.34
Young's modulus (x 10^{11} $dynes/cm^2$)	0.53	7.93	2.41	0.68
Shear modulus (x 10^{11} $dynes/cm^2$)	0.20	3.03	0.97	0.25
Bulk modulus (x 10^{11} $dynes/cm^2$)	0.52	7.65	2.14	0.72

[a]Skrove, J. W., Lawrence Radiation Laboratory, Livermore, private communication.

[b]U. S. G. S., 1962.

[c]Diment et al., 1959.

[d]Warner, S. E., Lawrence Radiation Laboratory, Livermore, private communication.

[e]Guido, R. S., Lawrence Radiation Laboratory, Livermore, private communication.

[f]Young, 1961.

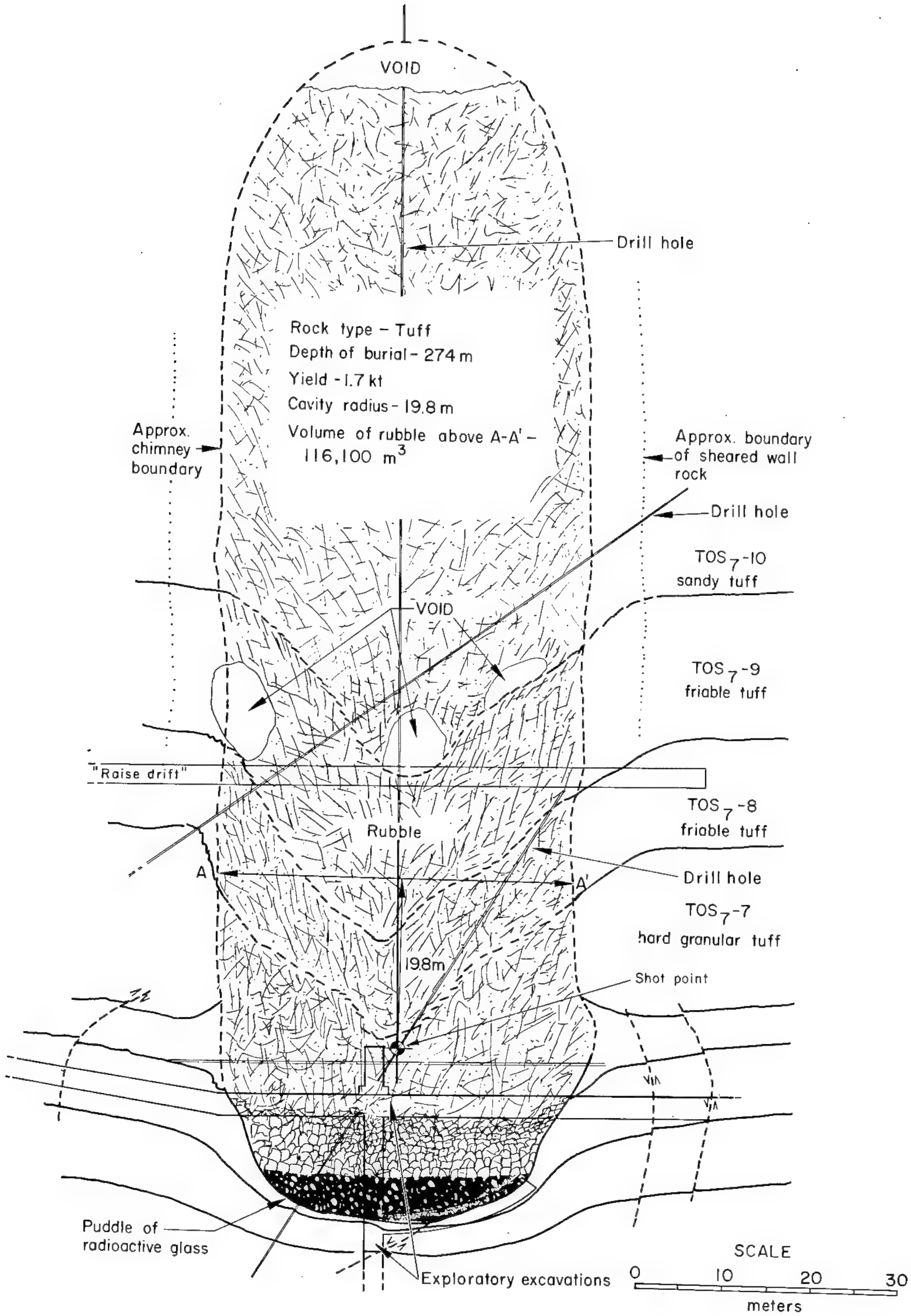

Fig. 3. Rainier schematic cross section (Wadman and Richards, 1961; Thompson and Misz, 1959).

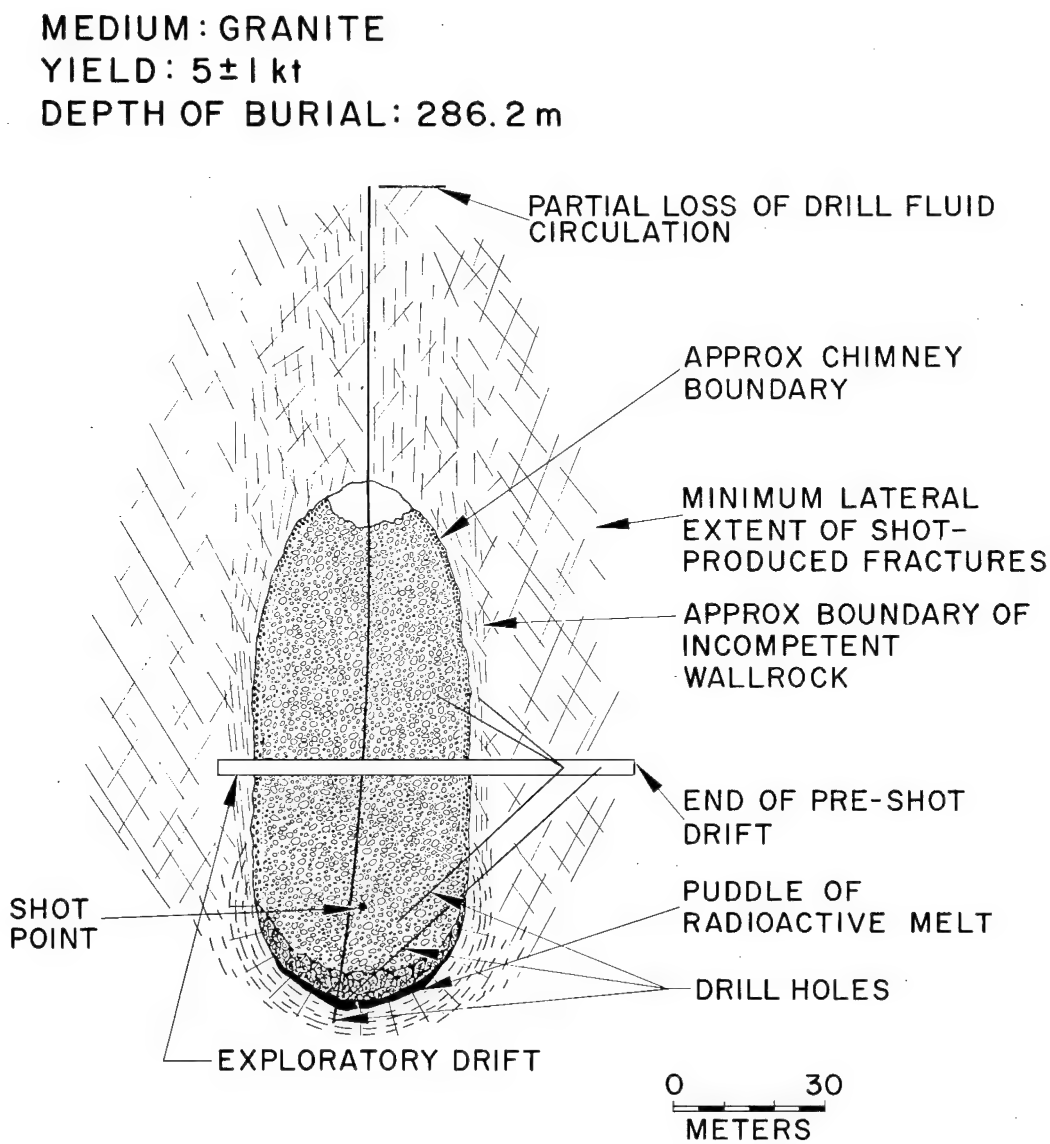

Fig. 4. Hardhat schematic cross section (McArthur, 1963).

PREDICTION OF CAVITY COLLAPSE

The question arises as to whether or not cavity collapse will occur in a given geological environment. The only event in which significant collapse did not occur was Gnome. The strength of the Gnome rock salt is less than that of unfractured granite, but greater than that of tuff. Since collapse occurred in the granite, it would seem that the mechanism of collapse is not greatly dependent on the strength of the rock as determined on unfractured isotropic samples. The strength of large rock masses, however, is limited by the frequency and orientation of the contained weaknesses such as faults, joints, and bedding planes. The rock above the Hardhat and Shoal shot points was characterized by interconnecting natural fractures, whereas the only pre-existing planes of weakness above the Gnome shot point were unconnected horizontal bedding planes. Had the granite not been so fractured and jointed or had the yield been significantly smaller (producing a cavity with a smaller cross-sectional area), the Hardhat cavity possibly would not have collapsed. Since the Hardhat cavity did stand for about 11 hours after detonation, it has been suggested that

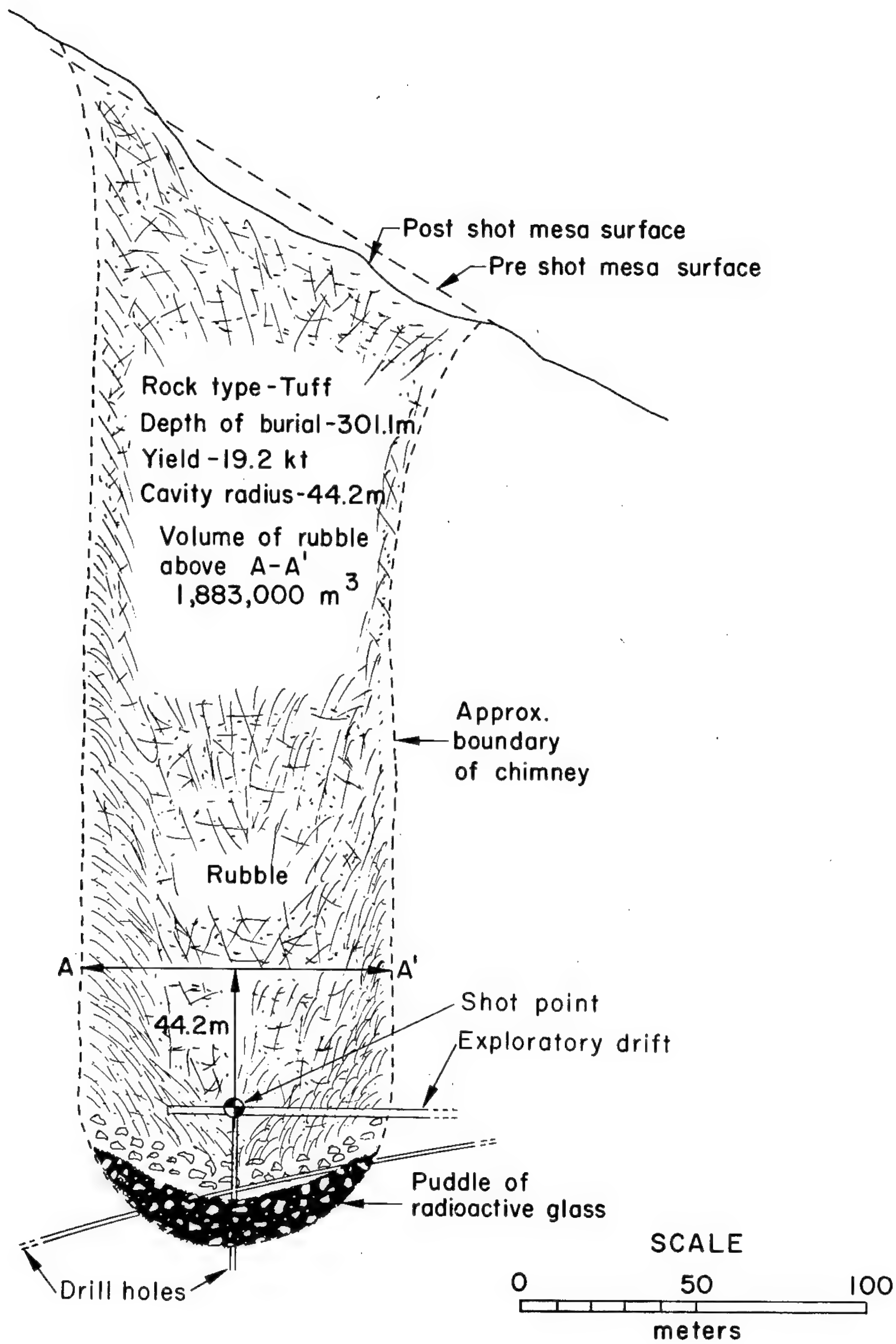

Fig. 5. Blanca schematic cross section.

the change in thermal stresses as the cavity slowly cooled also influenced collapse. It appears, therefore, that the properties of the rock as well as natural geologic structures are important factors in cavity collapse.

DISTRIBUTION OF INTERSTITIAL VOID IN CHIMNEY

The void space of the initial cavity, translated into the chimney as interstitial void, is irregularly

distributed in tuff and alluvium. This is evidenced by numerous cavities of varying dimensions encountered in postshot drilling and mining. Also, exploratory mining in tuff near shotpoint level indicates that this region is generally well compacted; i. e., the void space between particles is reduced by deformation of the particles. The ratio of cavity volume to chimney volume varies from 0.18 to 0.35 for tuff and up to 0.14 for alluvium. The interstitial void of the Hardhat granite chimney appears to be more evenly distributed. The cavity/chimney volume ratio for this event is 0.28.

RUBBLE PARTICLE SIZE

In tuff, rubble particles range in size from minute grains to large boulders 10 to 15 meters in diameter. Estimates of particle size distributions determined from geologic maps of drifts penetrating the Logan and Blanca chimneys (Richards, W. D., Lawrence Radiation Laboratory, Livermore, unpublished work) and the Rainier chimney (Wadman and Richards, 1961), all in tuff, are shown in Table III. In addition to the concentration of smaller particles near the chimney edge indicated by this table, the Logan and Blanca chimneys have a similar concentration in the center of the chimney. Typical chimney rock in a tuff environment is shown in Figure 9.

Visual estimates of granite particle sizes 3 meters inside Hardhat chimney, at a level 27 meters above the shot point (McArthur, 1963) are given below:

Particle diameter (m)	Percentage of total
> 0.3	10
0.15-0.3	40
< 0.15	50

Maximum observed particle dimension is approximately 1 meter in this region (see Figure 10). Farther inside the chimney, at the same elevation, the maximum particle diameter increases to about 1.3 meters. More information on the Hardhat chimney will be available when the postshot work now in progress is finished.

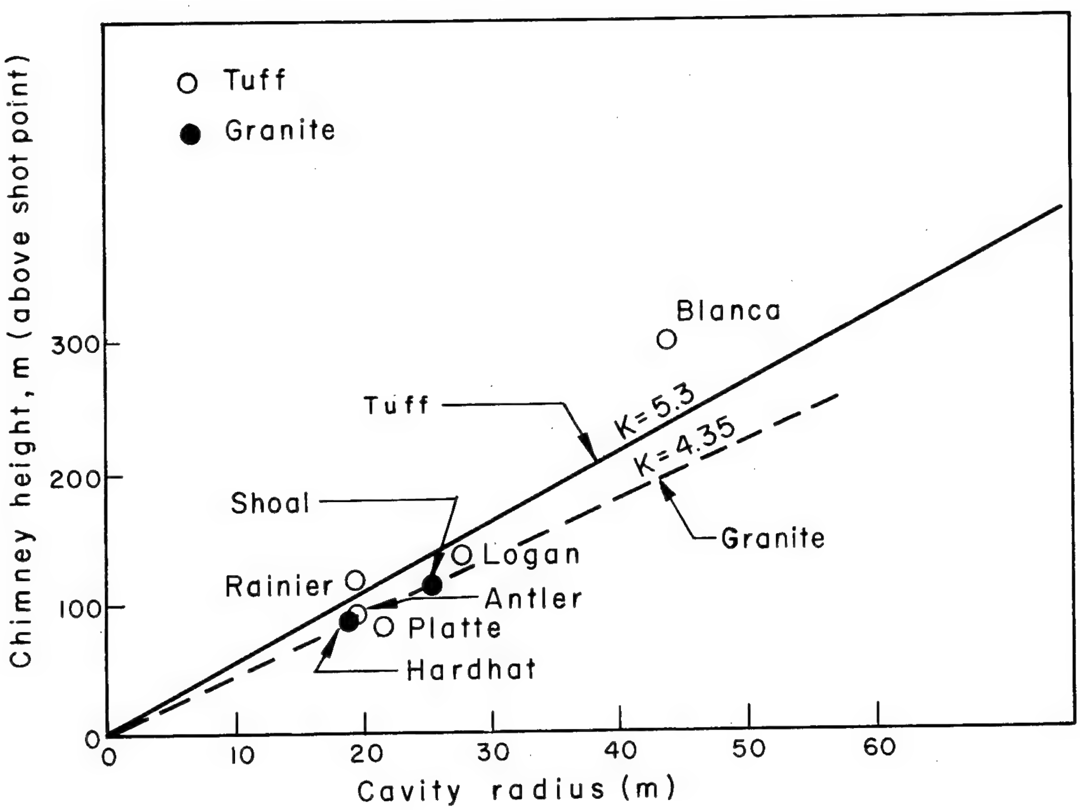

Fig. 6. Chimney height, H, as a function of cavity radius.

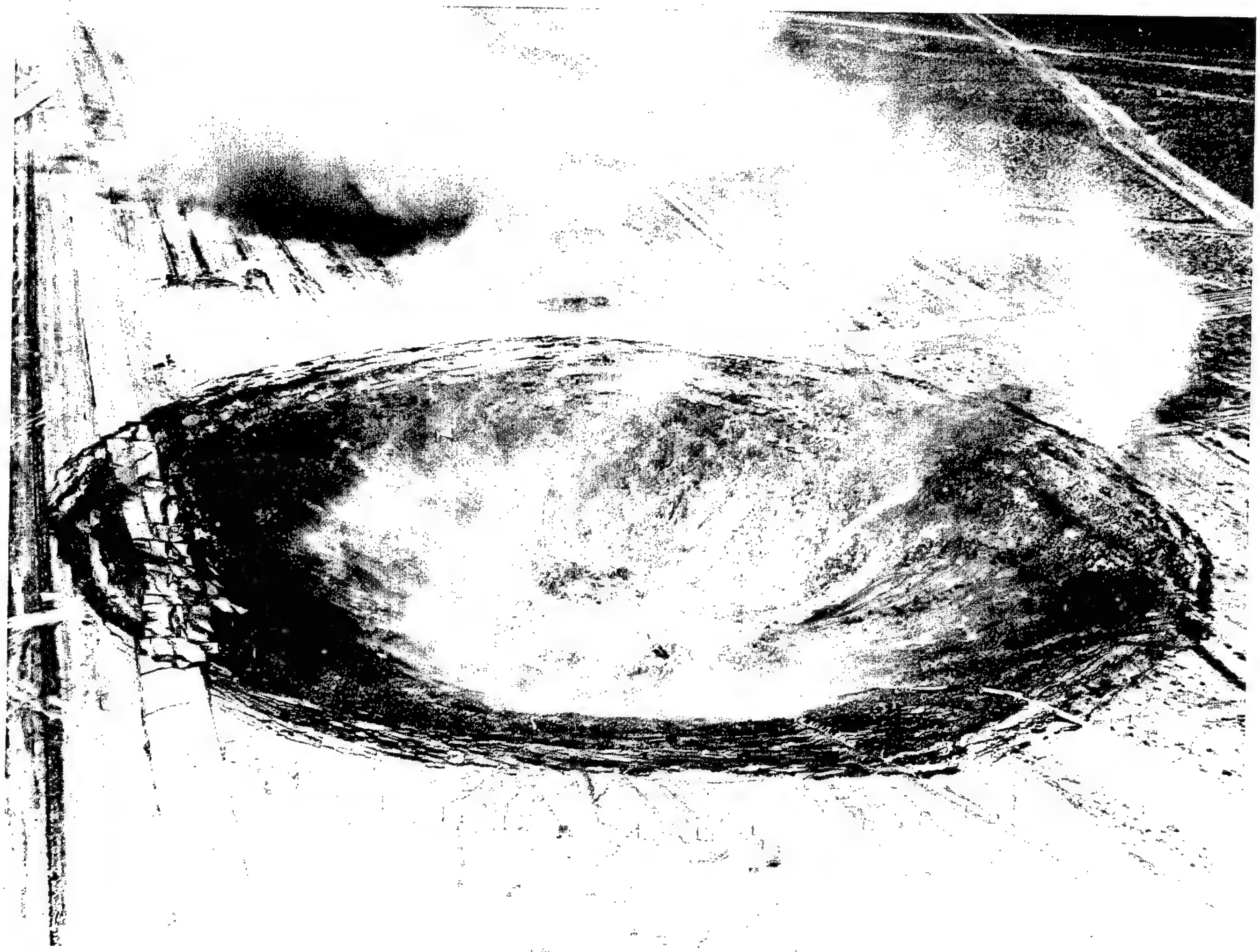

Fig. 7. Subsidence crater in alluvium.

Table III. Estimated particle size distribution, tuff chimneys.

Event	Drift location	Percent of particles under 0.6 m diam	Maximum observed diam (m)	Percent of particles under 0.6 m diam in outer 0.3R
Rainier	7.3 m below shot point	13	4.6	64
Logan	Shot-point level	20	7.6	54
Blanca	Shot-point level	17	12.2	65

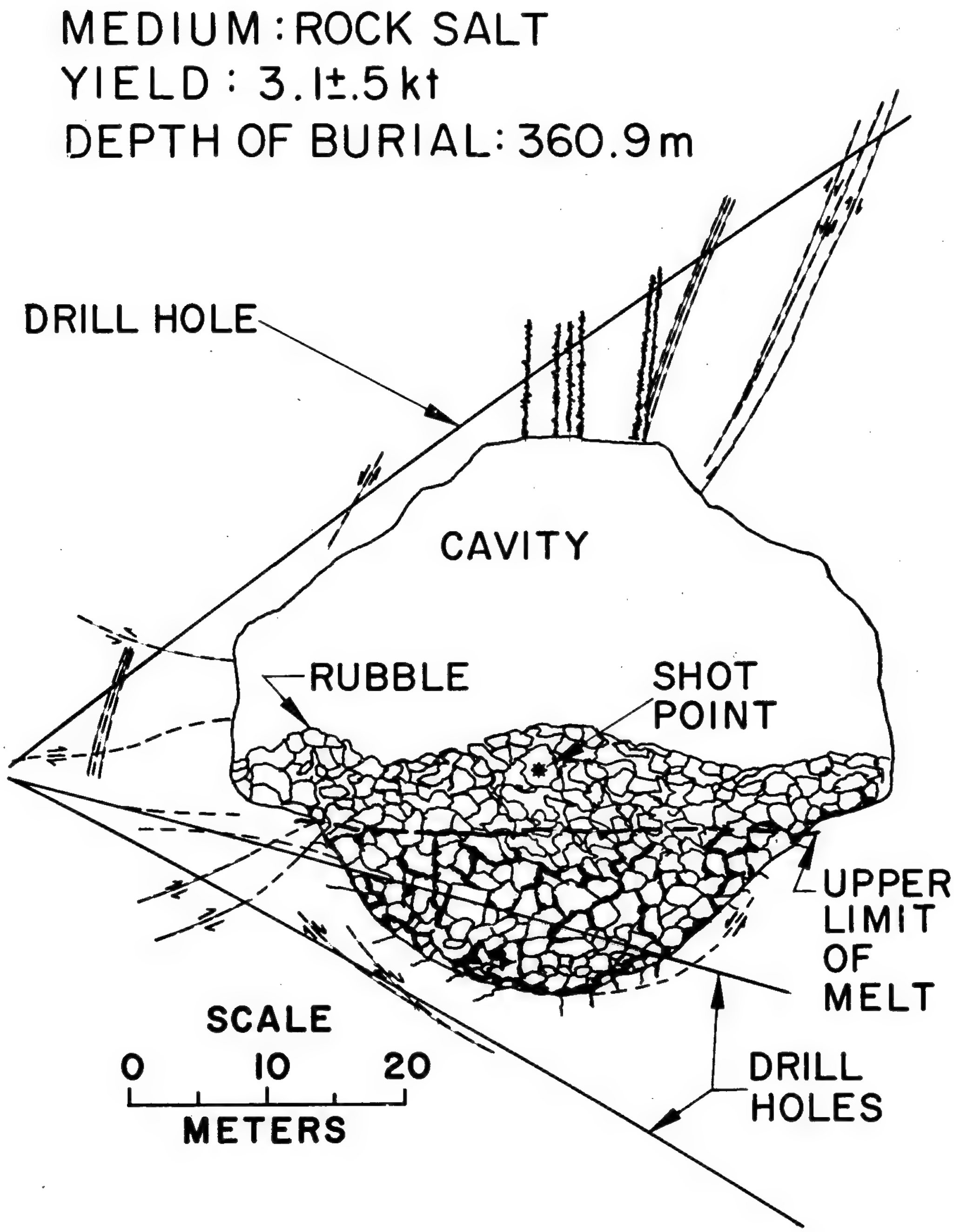

Fig. 8. Gnome cavity profile.

Roughly 50% of the rubble on the floor of the Gnome rock salt cavity near shot-point level is less than 0.6 meter in diameter. The remaining 50% is composed primarily of roof slabs ranging up to 6 meters in the maximum dimension (Rawson et al., 1964).

The preceding data indicate the influence of interconnecting fractures and joints on the maximum block size. These structures were essentially nonexistent in the Gnome shot environment and very infrequent in the tuff. The Hardhat granite, on the other hand, had three major and two

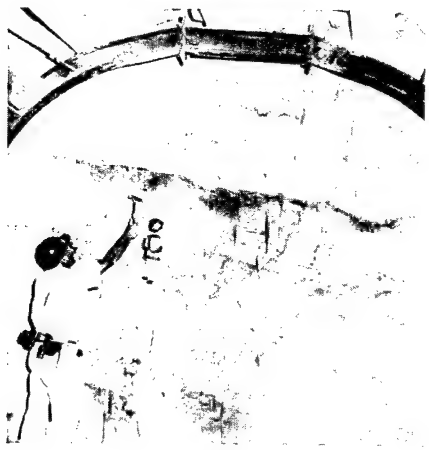

(a)

(b)

(c)

Fig. 9. Rainier Tuff; (a) Typical preshot condition. (b) Chimney edge in 'raise' drift. (c) Draw point near center of chimney in 'raise' drift.

minor sets of closely spaced intersecting fractures and joints, and consequently, smaller particles in the collapsed chimney rubble.

DISPLACEMENT OF COLLAPSED ROCK UNITS

The configuration of collapsed rock units in a tuff shot environment is illustrated in the schematic cross section of Rainier (Figure 3). Note the continuity of the beds through the collapsed area. Vertical displacements determined from this figure and a similar cross section of Logan are given in Table IV.

These data indicate that in tuff, downward displacements of approximately one cavity radius can be expected for distances of from 0 to 1.5R directly above the shot point. Displacements of about one-half cavity radius are observed from 0 to 1.5R above a point midway between the shot point and the chimney edge. The erratic manner in which displacements diminish upward is mainly due to differential movement between blocks.

FRACTURES

Existing data on fractures in tuff and alluvium have been obtained chiefly from drill-hole cores and are likely to be misleading because of the difficulty in differentiating shot-produced fractures. Rock salt, however, lends itself well to the analysis of fractures that connect with the explosion-produced cavity, since radiation damage caused by migration of gaseous fission products along fracture planes produces a distinctive coloration. Also, since preshot fractures were not present in the Gnome shot environment, all slickensided fractures could definitely be distinguished as shot phenomena. Using these characteristics as the differentiating criteria, the maximum observed fracture limits for the Gnome event were 65.5 meters laterally and 22.9 meters vertically below the shot point (Rawson et al., 1964).

Postshot fractures mapped in Rainier Exploratory Drift No. 1 have a maximum horizontal extent of about 54.9 meters from a vertical line passing through the shot point in one direction and 38.1 meters in the opposite direction (Wadman and Richards, 1961). Exposures in the Rainier shaft indicate a minimum extent of 27.7 meters below the shot point. Postshot fractures not related to spall off tunnel walls in the Hardhat granite extend at least 54.9 meters horizontally from

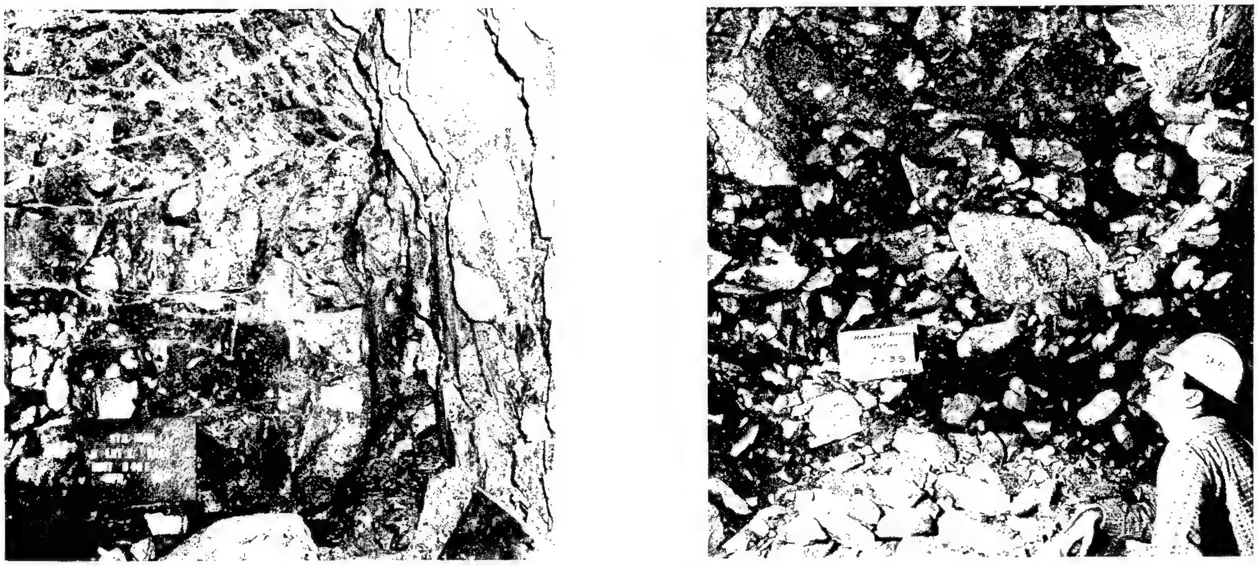

(a) (b)

Fig. 10. Hardhat granite shown (a) in typical preshot condition, and (b) broken in shot-produced chimney, 27 meters above shot point and 3 meters inside chimney.

Table IV. Vertical displacements of broken rock in collapsed rock units of Logan and Rainier.

Event		Postshot vertical distance above shot point (m)	Downward displacement (m)
Logan	(R = 28 m)	17.4	25.9
	(H = 134 m)	37.5	27.4
		53.0	19.2
		65.5	15.2
		85.3	19.2
		100.6	12.5
		112.8	10.4
Rainier	(R = 19.8 m)	1.5	21.3
	(H = 117.7 m)	31.7	20.4

a vertical line through the shot point and have good permeability up to 48.8 meters laterally from this line. Based on these limited data, it appears that fractures can be expected to extend about two to three cavity radii laterally and less than one and a half cavity radii below the shot point.

The extent of fractures (probable partings along pre-existing planes of weakness) above the shot point is shown for three events in Table V. The maximum vertical extent of the zone of increased permeability above the shot point may be estimated for a given yield and geologic environment by multiplying the predicted cavity radius by the appropriate scaling factor shown in this table.

SUMMARY

The size of cavities created by contained underground nuclear explosions is governed primarily by:

1. The yield of the nuclear device.
2. The bulk density of the rock above the charge location and the depth of burial of the charge (device), which together define the pressure resisting cavity growth.
3. The amount of gas-producing materials which condense at low temperatures in the immediate shot environment.

The physical and chemical properties of the four rock mediums in which contained nuclear explosions have been conducted appear to have relatively little effect on cavity size. Experience has shown that cavity size can be predicted to within ±20% independent of rock type and to within about ±7% for a given rock type. Since the physical properties of the four mediums tested (tuff, granite, rock salt, and alluvium) show such a considerable variation and still permit ±20% predictability, it is reasonable to expect that the same predictive capability exists for most other rock types as well. A detailed study of the effects of substances which produce gas at low temperatures, especially water, on cavity growth may significantly refine the predictability of cavity radii.

While a predictive capability for chimney formation has not yet been developed, it is evident that important limiting parameters, in addition to cavity size, are the nature and orientation of natural structural weaknesses and the strength of the unfractured rock.

When a chimney forms, its radius is about the same as that of the initial cavity, but its height varies considerably, depending upon the rock's bulking characteristics and the strength of the overlying rock mass. Rubble particle size is influenced greatly by pre-existing interconnecting fractures and joints in the rock. Concentrations of smaller particles have been noted near the chimney edge.

Based on the limited data available in tuff, rock salt, and granite, the maximum extent of the zone of fractured rock outside the chimney may be roughly approximated as 1.5R below the shot point, 2 to 3R laterally, and about 6 to 8R above the shot point, where R is the cavity radius.

Table V. Extent of fractures above shot point, based on drilling fluid circulation losses.

Event	R_{cav} (m)	Rock type	Max observed extent of fractures (F_{max}) above shot point (m)	Scaling factor (F_{max}/R_{cav})
Gnome[a]	17.4	Rock salt	106.7	6.1
Hardhat[b]	19.2	Granite	147.2	7.7
Rainier[c]	19.8	Tuff	117.7	5.9

[a] Rawson et al., 1963.

[b] McArthur, 1963.

[c] Thompson and Misz, 1959.

APPENDIX I
Derivation of Radii Scaling

A brief derivation of radii scaling for cavities produced by contained nuclear explosions which assumes an adiabatic expansion of gases to the overburden pressure.

For an adiabatically expanding gas from state 1 to state 2:

$$P_1 V_1^{\gamma} = P_2 V_2^{\gamma}$$

where P is the cavity pressure, V the volume, and γ the ratio of specific heats of the vaporized rock.

The final cavity pressure in a nuclear explosion is assumed to be balanced by the weight of the rock above (the overburden). Thus

$$P = \rho g h$$

where ρ is the average density to the surface, h is the depth of burial, and g is the acceleration constant. To compare two explosions at different overburden pressures (P_1 and P_2) we substitute $\rho_1 g h_1$ and $\rho_2 g h_2$ in the first equation for P_1 and P_2 and solve for V_1 or V_2.

$$\frac{V_1}{V_2} = \left[\frac{\rho_2 h_2}{\rho_1 h_1}\right]^{1/\gamma}$$

or

$$\frac{R_1}{R_2} = \left[\frac{\rho_2 h_2}{\rho_1 h_1}\right]^{1/3\gamma}$$

where

$$V = \frac{4}{3}\pi R^3$$

and R is the cavity radius.

Now to allow for differences in yield from cube-root scaling:

$$R \propto W^{1/3}$$

where W is the yield in kilotons, and hence

$$R = C \frac{W^{1/3}}{(\rho h)^{1/3\gamma}}$$

where C is a constant. Assume the normal value of 4/3 for γ, from the polytropic gas model. (Values of for polyatomic gases given in Handbook of Chemistry and Physics differ slightly from 1.33.) Then

$$R = C \frac{W^{1/3}}{(\rho h)^{1/4}} .$$

APPENDIX II

Data from Thirteen Underground Detonations[a]

Medium	Event	Yield, W (kt)	Depth of Burial, h (m)	Overburden Density, (g/cc)	Cavity Radius, R (m)	Chimney Height, H (m)	C[b]	K[c]
Tuff	Rainer	1.7	274	1.9	19.8	117.7	79.0	5.9
	Logan	$5.0^{+0.2}_{-0.4}$	283.5	1.8	28	134.1	77.9	4.8
	Blanca	19.2 ± 1.5	301.1	1.8	44.2	301.1[d]	80.1	6.8
	Antler	2.46 ± 0.25	402	1.9	19.8	90.5	76.7	4.6
	Platte	1.7 ± 0.15	191.4	2.2	21.6	81.6	81.9	3.8
Alluvium	Mad	0.43 ± 0.04	181.1	1.8	11.3	Unknown	63.4	--
	Stillwater	2.7 ± 0.3	181.1	1.8	24.7	181.1[d]	74.9	--[d]
	Brazos	7.8 ± 1.0	256.3	1.8	27.7	256.3[d]	64.7	--[d]
Tuff/Alluvium	Cimarron	11.2 ± 2	304.8	1.8	32.6	304.8[d]	70.5	--[d]
	Hoosic	3.1 ± 0.3	187.1	1.8	25.9	187.1[d]	76.1	--[d]
Granite	Hardhat	5.0 ± 1.0[e]	286.2	2.7	19.2	85.6	59.1	4.5
	Shoal	12.5 ± 2.0[e]	367.4	2.7	25.6[f]	108.5[g]	62.1	4.2
Rock Salt	Gnome	3.1 ± 0.5	360.9	2.3	17.4	Minor collapse	63.6	--

[a] Data for all events except Shoal: Richards, W. D., Lawrence Radiation Laboratory, Livermore; unpublished work.

[b] $C = R\frac{(\rho h)^{1/4}}{W^{1/3}}$.

[c] K = H/R.

[d] Chimney growth interrupted by earth's surface.

[e] Private communication, A. J. Chabai, Sandia Corporation, Albuquerque, New Mexico.

[f] Determined on basis of temperature profile.

[g] Determined from television monitoring of postshot drill hole by Sandia Corporation.

ACKNOWLEDGEMENTS

The helpful suggestions of G. C. Werth, G. H. Higgins, G. T. Pelsor, and D. E. Rawson are gratefully acknowledged. The work was done under the auspices of the U. S. Atomic Energy Commission.

REFERENCES

1. Diment, W. H., et al., "USGS Investigations in the U12e.05 and U12b.01 Tunnels, Nevada Test Site," TEM-997, TEM-998, 1959.
2. McArthur, Richard D., "Geologic and Engineering Effects, the Hardhat Event (Preliminary)," GNI-63, February 1963.
3. Nuckolls, John H., "A Computer Calculation of Rainier," Lawrence Radiation Laboratory, Livermore, Rept. UCRL-5675, May 1959.
4. Rawson, Donald E., Charles R. Boardman, and Nanette Jaffe, "The Environment Created by a Nuclear Detonation in Salt," PNE-107F, (to be published), 1964.
5. Thompson, Thomas L., and John O. Misz, "Geologic Studies of Underground Nuclear Explosions-Rainier and Neptune," Lawrence Radiation Laboratory, Livermore, Rept. UCRL-5757, October 28, 1959.
6. U. S. Geological Survey, "Project Gnome Hydrologic and Geologic Studies," PNE-130F, 1962.
7. Wadman, Ross E., and William D. Richards, "Postshot Geologic Studies of Excavation Below Rainier Ground Zero," Lawrence Radiation Laboratory, Livermore, Rept. UCRL-6986, July 1961.
8. Young, D. D., Jr., "In Situ Measurements of Elastic Properties," Lawrence Radiation Laboratory, Livermore, Rept. UCRL-6477, 1961.

BIOGRAPHICAL SKETCHES OF AUTHORS

Charles R. Boardman was born in Lawton, Oaklahoma. After three years of Army service he attended the University of California in Berkeley, receiving the AB degree in Geology in 1959.

He is employed as a geologist in the Lawrence Radiation Laboratory Plowshare Division. His current assignment involves the determination of environmental changes in rock masses resulting from contained underground nuclear explosions.

David D. Rabb was born in Denver, Colorado, and received his B.S. from the University of Agrizona in 1937, and his M.S. in Metallurgy in 1939. He was assistant metallurgist, Inspiration Consolidated Copper Company from 1939 to 1941. He served in the U.S. Army from 1941 to 1945. He specialized in metallurgical research on titanium, uranium and base metals and in metallurgical plant design at Battelle Memorial Institute, Columbus, Ohio, from 1946 to 1952. Recalled to active duty in 1952, he served as a Lieutenant Colonel, Ordnance Corps, U.S. Army. After assignments as contract inspector, cryogenic engineer and Special Weapons Officer, he was released from active duty in 1957 and joined a nuclear weapon division at Lawrence Radiation Laboratory.

His current assignment is administrator for the Plowshare Division and consultant for metallurgical programmatic studies and engineering work particularly associated with underground nuclear test operations.

Richard D. McArthur was born in Zanesville, Ohio. He received the B.S. in Geology from the University of Ohio in 1950. From 1950 to 1954 he was employed as an exploration geologist by Armco Steel and Lone Star Steel. His primary activities were concerned with mineral exploration and development. From 1954 to 1959 he was employed by Superior Oil Company as an exploration geologist. Since 1959 he has been with the Lawrence Radiation Laboratory as a geologist. He has been primarily concerned with the postshot exploration and investigation of Plowshare Program experiments. In addition, he is engaged in a program of miniature high-explosive studies where laboratory studies of contained explosions are made using charges on the order of one gram.

DISTRIBUTION IN GROUNDWATER OF RADIONUCLIDES FROM UNDERGROUND NUCLEAR EXPLOSIONS*

Frank W. Stead

U. S. Geological Survey
Denver, Colorado

ABSTRACT

Radionuclides released from underground nuclear explosions in the Plowshare Program will be initially distributed in the medium by direct explosive action; long-lived and biologically significant radionuclides may later enter into and move with groundwater flow. Where adequate precautions have been taken, as at the Nevada Test Site and at other sites such as Plowshare Project Gnome, no significant post-explosion movement of radionuclides can as yet be demonstrated; however, radioactive waste disposal operations clearly indicate that; radionuclides can be transported considerable distances by groundwater flow. A single, universally applicable prediction of the character and extent of possible radionuclide contamination of groundwater is precluded by the complex interrelationship and variability of the environmental factors; thus, each proposed site of a Plowshare nuclear explosive application must be carefully evaluated, to determine if unique geologic and hydrologic conditions are present which might permit relatively rapid and prolonged migration of radionuclides.

INTRODUCTION

The radionuclides released from large underground nuclear explosions are distributed initially by direct explosive action in the immediate vicinity of the explosion. At some later time, these nuclides may be transported by groundwater in possibly hazardous concentrations and to sufficient distances to raise problems of water management. Our ability to forecast when, where, and how these radionuclides may move is a necessary prelude to large-scale peaceful applications of nuclear explosions in the Plowshare Program.

It seems appropriate to follow the approach of Darwin who wrote "I must begin with a good body of facts and not from a principle (in which I always suspect a fallacy)." Reviewed separately are some facts on (1) the amount and nature of the radionuclides from large fusion-fission nuclear explosions, (2) the initial distribution of the biologically significant nuclides, and (3) the transport of these nuclides by groundwater.

*Publication authorized by the Director, U. S. Geological Survey. Prepared in cooperation with the U. S. Atomic Energy Commission.

RADIONUCLIDES

Only the long-lived radionuclides, those in excess of a 5-year half-life, are important in considering the postexplosion distribution and transport in groundwater. In general, groundwater moves slowly, requiring years rather than months or days to move a distance of 1 mile. Thus, short-lived nuclides moving in groundwater would undergo radioactive decay to relatively insignificant amounts within short travel distances.

The biologically significant, as well as long-lived, radionuclides are few in number, and for this discussion will be limited primarily to (1) H^3 (tritium), a residual product from fusion reactions, (2) Co^{60}, a neutron activation product, and (3) Sr^{90}, a fission product. Tritium with a 12-year half-life is not as dangerous in the biological sense as other radionuclides, as it emits only weak beta-radiation. The recommended maximum permissible concentration (MPC) in drinking water for occupational workers continuously exposed (168-hour week) is 3×10^{-8} Curie H^3/cc in contrast to 1×10^{-12} Curie Sr^{90}/cc, or a factor of 10^4 higher MPC for tritium.[1] The MPC (168-hour week) for Co^{60} in water is 5×10^{-10} Curie/cc, midway

between the MPC's for H^3 and Sr^{90}. Although Cs^{137} with a 30-year half-life is produced in fission reactions in amounts (Curies) equal to Sr^{90}, the MPC of Cs^{137} is two orders of magnitude higher than Sr^{90}; Cs^{137} tends to be more firmly held in the solid by exchange mechanisms than is Sr^{90}, and is thus considered less important than Sr^{90}.

Basic physical data on the reaction products from pure fission and pure fusion explosions[2] are summarized in Table I. To recast these data in terms that will illustrate the reaction products formed in a hypothetical underground explosion in the Plowshare Program, I have made three assumptions: (1) The explosion is a 1-megaton fusion device triggered by a 10-kiloton fission device, (2) the explosion will be fully contained underground in the sense that the fireball and the direct neutron flux will not reach the atmosphere, and (3) the explosive device will be surrounded by borated materials which capture neutrons without producing radioactivity, thereby reducing the neutron flux and the resultant induced activities by one order of magnitude. The environment in which the explosion occurs is assumed to be average crustal materials with a porosity of 20% and saturated with water. Calculations based on these assumptions are shown in Table II.

The fission and fusion reaction products postulated in Table II for an underground explosion are proportionately the same as those for atmospheric explosions quoted in Table I. The induced activities for an underground explosion[3] differ considerably from those for an atmospheric explosion, reflecting the chemical composition of the medium around the explosion — that is, rock as opposed to air.

Several conclusions may be drawn from the data in Table II.

1. Activities induced in average crustal material by the neutron flux from the explosion are relatively short-lived, these activities consist primarily of Al^{28} (2.3-min half-life), Mn^{56} (2.6-

Table I. Reaction products of 1-megaton-equivalent (10^{15} calories) atmospheric explosions. Modified from Table I, Leipunsky, 1959.

	Pure fission explosion	Pure fusion explosion
Number of fissions	1.45×10^{26}	
Number of fusion reactions[a]		1.45×10^{27}
Number of neutrons released	2.2×10^{26}	1.45×10^{27}
Amount of Sr^{90} (fission)	1.47×10^5 Curies	
Amount of C_s^{137} (fission)	1.57×10^5 Curies	
Amount of C^{14} (activation)[b]	2.34×10^4 Curies	1.49×10^5 Curies
Amount of H^3 (residual)[c]		6.67×10^6 Curies

[a] At 180-MeV energy release for ten single H^2-H^3 reactions, equivalent to the prompt energy release of one single fission.

[b] For $N^{14}(n,p)C^{14}$ reaction, assuming for fission air burst that one-seventh as much C^{14} is formed per unit energy as for fusion air burst.

[c] Assuming 1 atom H^3 per 180-MeV energy released.

Table II. Reaction products for an underground explosion, consisting of 1-megaton fusion and 10-kiloton fission.

Source	Fission products (Curies)	Induced products (Curies)[a]	Fusion products (Curies)
Fission (10 kt)	3.0×10^{9}[b]	10^5	
Sr^{90}	1.5×10^3		
Cs^{137}	1.6×10^3		
Co^{60}		Small	
C^{14}[c]		Small	
Fusion (1 Mt)		10^8	
H^3			6.7×10^6
Co^{60}		10^4	
C^{14}[c]		15	

[a] Induced gamma-ray activities at 1 hour after detonation, based on average chemical composition of earth's crust.

[b] Fission-product gamma-ray activities at 1 hour after detonation, decaying at $T^{-1.2}$.

[c] Following Leipunsky[2] in Table 1, C^{14} from fission and fusion reactions shown separately.

hr half-life), Na^{24} (15-hr half-life), Fe^{59} (45-day half-life), Fe^{55} (2.7-yr half-life), and Co^{60} (5.2-yr half-life). The total activities decrease very rapidly; four orders of magnitude in the first week. At the end of 1 year, the induced activities, except for roughly 10^4 Curies of Co^{60}, are insignificant compared to the longer-lived Sr^{90} (28-yr half-life) and H^3 (12-yr half-life).

2. Although the activation product C^{14} is long-lived (5600-yr half-life), the total amount produced — 15 Curies from the fusion neutron flux and a negligible amount from the fission flux — can be considered insignificant when distributed in the large volume of material around an underground explosion.

3. Fission-product activities do not decrease as rapidly as the induced activities, but drop by three orders of magnitude in the first week and by five orders of magnitude in the first year. At the end of 1 year, Sr^{90} and Cs^{137}, both with about 30-year half-lives, are the principal remaining fission products of recognized biological importance. Sr^{90} is assumed to be the more significant nuclide, and Cs^{137} is not considered further in the following calculations.

4. Tritium at 6.7×10^6 Curies is the predominant long-lived nuclide (12-yr half-life) from the fusion reaction; Sr^{90} at 1.5×10^3 Curies is the predominant long-lived nuclide (28-yr half-life) from fission; and Co^{60} at 10^4 Curies is the predominant nuclide (5.2-yr half-life) from neutron activation.

For a nominal 1-megaton explosion in average crustal material, the relative activities of the total fission products, the induced activities, H^3, Co^{60}, and Sr^{90} with increasing time after the explosion are shown in Figure 1. At the end of 1 year, the amounts of H^3, Co^{60}, and Sr^{90} are relatively unchanged, whereas the other nuclides either have been sharply reduced by decay or are present in

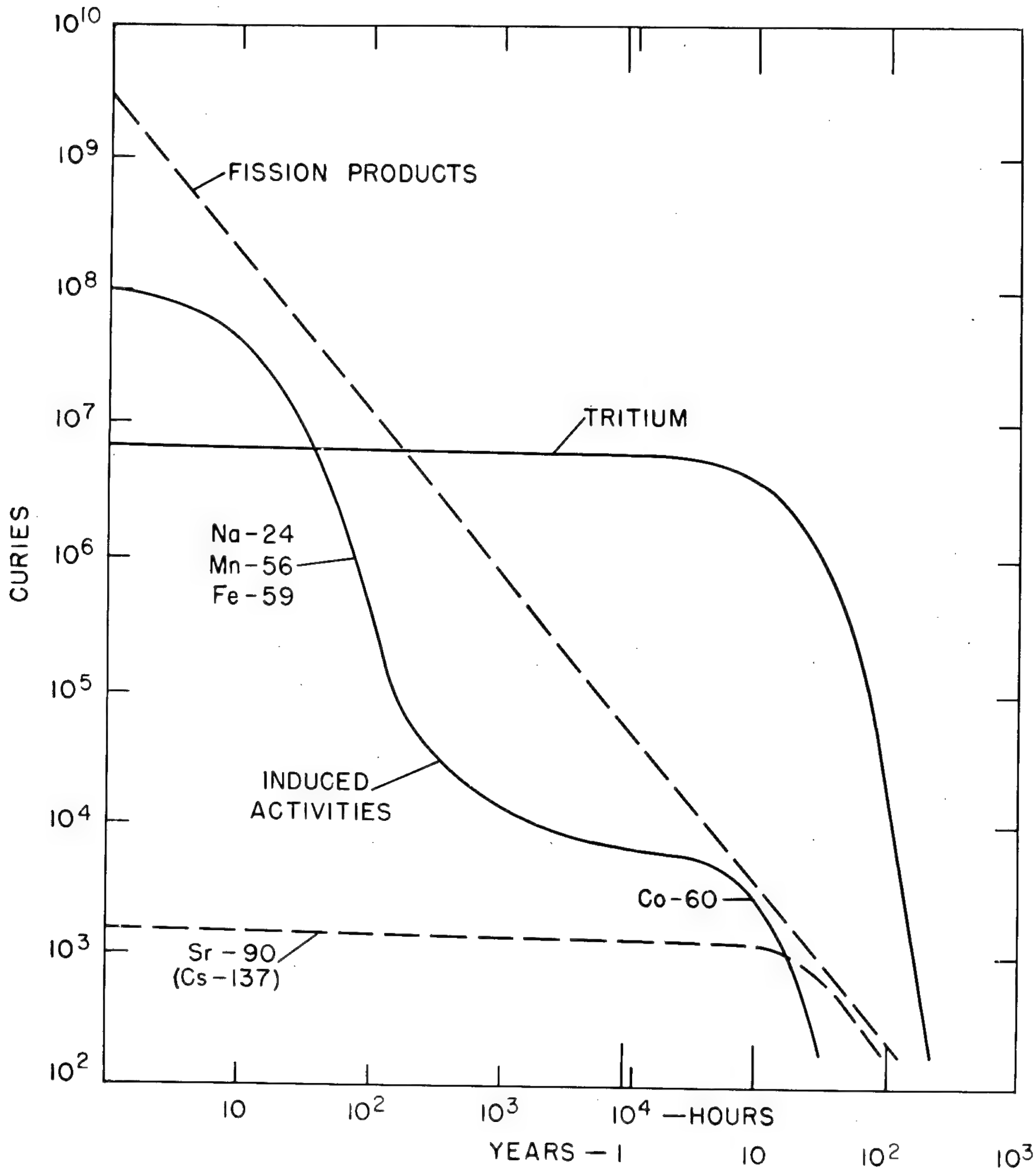

Fig. 1. Radionuclides from nominal one megaton fusion-fission explosion in average crustal material.

less than significant amounts. Tritium after 1 year is the most abundant remaining nuclide by two orders of magnitude. After 10 years, H^3 is still the most abundant nuclide and is now three orders of magnitude greater than Co^{60} and Sr^{90}. After 100 years, H^3, decreasing more rapidly than Sr^{90}, is only two orders of magnitude more abundant than Sr^{90}. In terms of curies of activity, in the period from 1 to 100 years, H^3 is by far the most abundant nuclide from a nominal 1-megaton fusion-fission explosion.

INITIAL DISTRIBUTION OF RADIONUCLIDES

The initial distribution of H^3, Co^{60}, and Sr^{90} can now be calculated on the basis of the effects

expected[4] around a nonventing underground explosion, consisting of 1-megaton fusion energy release and 10 kilotons of fission release. For comparative purposes, the nuclide distribution is calculated for two dissimilar rock types: A dolomite, a carbonate rock with low porosity and low water content; and tuff, a volcanic rock with high porosity and high water content.

In an average dolomite, it is assumed: (1) That the radius of the cavity space created by the explosion is 310 feet (95 m), (2) that the radius of crushed zone surrounding the cavity is 650 feet (200 m), (3) that the grain density of dolomite is 2.8, and its porosity (water saturated) is 0.05 (5%), and (4) that radionuclides are distributed only in the crushed zone by direct explosive action, and that the post-explosion collapse of the crushed zone into the cavity does not perturb the initial nuclide distribution.

On these assumptions, the mass of solids in the crushed zone will be 7.66×10^{13} grams, the mass of water in the pore space will be 1.4×10^{12} grams (or ml), and the total mass will be 7.8×10^{13} grams.

Assuming that Sr^{90} is all soluble and uniformly distributed throughout the dolomite in the crushed zone, its initial concentration in the total mass of the crushed zone would be 1500 Curies in 7.8×10^{13} grams, or 1.9×10^{-11} Curie/gram. The assumption of uniform distribution is reasonable in that Sr^{90} has a precursor, Kr^{90} (33-second half-life), which is a noble gas and could be injected from the early-stage cavity with its high-pressure gases into the openings created in the crushed zone around the cavity. Further, data from postexplosion studies indicate that the volatile and gaseous nuclides are distributed in and beyond the crushed zone,[5] in contrast to the refractory nuclides which are predominantly held in the thin melted shell on the cavity wall.

When equilibrium is reached in the exchange of Sr^{90} between the dolomite matrix and the contained pore water,[6] the amount of Sr^{90} in the water is expressed by the equation

$$K_d = \frac{\text{activity-solid}}{\text{activity-water}} \times \frac{\text{volume-water}}{\text{weight-solid}}$$

where K_d, the distribution coefficient for dolomite,[7] is 10. The Sr^{90} activity in the water is then 2.8 Curies; and the Sr^{90} concentration in the water, 2.8 Curies in 1.4×10^{12} ml, is then 2×10^{-12} Curie/ml.

The MPC (168-hr week) for Sr^{90} in water is 1×10^{-12} Curie/ml, so that the initial Sr^{90} concentration in the contained pore water in this hypothetical example would be about the same as the MPC. For pure dolomite with less clay minerals and other impurities than the "average" dolomite selected, and with large amounts of Ca and Mg ions in the pore water, the K_d for Sr^{90} would be lower, possibly by as much as two orders of magnitude; the Sr^{90} concentration in the water would be correspondingly increased.[8] Conversely, many dolomites and limestones are less pure than the "average," and would have a higher K_d for Sr^{90}.

The only long-lived activity of possible importance induced in average crustal materials is Co^{60} (5.2-yr half-life) at 10^4 Curies. The cobalt content of carbonate rocks (0.2 to 2.0 parts per million) is at least one order of magnitude less than the average (23 ppm) for the earth's crust.[9] Thus, about 10^3 Curies of Co^{60} would be distributed throughout the crushed zone, and its initial concentration would be 1.3×10^{-11} Curie/g. Co^{60} is analogous to Sr^{90} in exchange behavior, and after reaching exchange equilibrium between the dolomite and the pore water, its concentration in water would be 1.33×10^{-12} Curie/ml. The MPC (168-hr week) for Co^{60} in water is 5×10^{-10} Curie/ml, so the concentration is roughly two orders of magnitude less than the MPC.

In a nonventing underground explosion, it is assumed that essentially all tritium would rapidly form tritiated water, either by oxidation or by exchange, and that tritium exchange between tritiated water and the rock matrix would be negligible. The tritium concentration in the pore water, therefore, would be 6.7×10^6 Curies H^3 in 1.4×10^{12} ml, or 4.8×10^{-6} Curie/ml.

The MPC (168-hr week) for H^3 in water is 3×10^{-8} Curie/ml, so the H^3 concentration in the water (about 1100 acre-feet, or 1.4×10^6 m^3) in the crushed zone is two orders of magnitude higher than the MPC. After allowance is made for radioactive decay, this tritium concentration in the water could be further reduced in significant degree only by dilution and mixing with ground water outside the crushed zone, not by exchange mechanisms.[10]

Variations in the chemical composition of the dolomite would not affect the H^3 concentration in the pore water; variations in the water content of the rock would, of course, directly affect the H^3

concentration, as illustrated by a hypothetical explosion in water-saturated tuff or alluvium.

The distribution of radionuclides in volcanic tuff and alluvium, such as at the Nevada Test Site, can be similarly calculated, where the cavity radius would be 370 feet (approximately 110 m), the crushed zone radius 780 feet (250 m), the grain density 2.4, the porosity (water saturated) 0.3 or 30% and the K_d for Sr^{90} and Co^{60} at 100; then the concentration of these nuclides in water in the crushed zone would be: Sr^{90} at 1.8×10^{-13} Curie/ml, Co^{60} at 1.2×10^{-12} Curie/ml, and H^3 at 4.5×10^{-7} Curie/ml. The Sr^{90} concentration is one order of magnitude less than the MPC (168-hour week) of 1×10^{-12} Curie/ml. The Co^{60} concentration, based on 10^4 Curies, since the Co content in the volcanic tuff and associated alluvium is about the same as in average crustal materials, is two orders of magnitude less than the MPC of 5×10^{-10} Curie/ml. The tritium concentration, which would not be appreciably decreased by any exchange reactions of tritiated water with the tuff medium, is still above the MPC of 3×10^{-8} Curie/ml by an order of magnitude, and is now contained in 13,000 acre-feet (or about $15 \times 10^6 m^3$) of water.

The distribution of radionuclides, where the underground explosion is at the depth of burst for maximum throwout crater dimensions, can be calculated from data showing that, on the average, 10% of the total reaction products will escape to the atmosphere.[11] Such escape to the atmosphere serves only to reduce the amount of reaction products available for initial distribution in the rock matrix and associated pore water.

In the early gas-phase venting associated with cratering, proportionately more of the radionuclides which behave as volatile substances, such as H^3, Kr^{85}, Sr^{85}, Kr^{90}, Sr^{90}, I^{131}, Cs^{137}, and Ba^{140} are vented than are the nuclides such as Zr^{95}, Ce^{144}, and the rare-earth nuclides, which behave in the manner of refractory materials.[12] Except for the long-lived H^3 and Sr^{90}, and again excluding Cs^{137}, the "volatile" nuclides are short-lived and do not affect this appraisal of possible long-term contamination of groundwater, although these short-lived nuclides do contribute to atmospheric contamination and the related problems of random, localized radioactive fallout.[13]

Both Sr^{90} and H^3 act as volatiles in the early gas-phase venting associated with cratering; Sr^{90} because of the gaseous nuclide precursor, and H^3 because it is combined in water vapor. It is known that Sr^{90} is enriched in the early stage of venting by a factor of about 5, which, compounded with a 10% release, would reduce the ground concentration by somewhat less than one order of magnitude. During the early stage of venting, H^3, although its behavior is not well documented, is probably more volatile than Sr^{90}, so that its ground concentration would be reduced by at least one order of magnitude. If 99% of the H^3 became combined in water vapor, a noncondensing gas when associated with the high temperature and pressure of an underground explosion, and were vented to the atmosphere (and this is a possibility), the H^3 concentration in groundwater would be reduced by two orders of magnitude.

TRANSPORT OF RADIONUCLIDES

All data from underground nuclear explosions fail to demonstrate anything but trivial transport of radionuclides by groundwater, following the initial explosion-produced distribution. This lack of positive data, however, is expectable. At the Nevada Test Site, the depth of burst for all but a few of the underground explosions has been above the regional water table or water-saturated zone, in which nuclide transport by groundwater flow might occur and then be detected. At other sites, such as Project Gnome near Carlsbad, New Mexico, and Project Shoal near Fallon, Nevada, the geologic and hydrologic environments have been carefully evaluated and selected, prior to the nuclear explosions, to minimize the possibility of widespread initial distribution of nuclides and their later transport by groundwater.

Data bearing on the groundwater transport of radionuclides can be drawn from (1) experience in the disposal of radioactive wastes to the ground, (2) the behavior of naturally occurring radionuclides in groundwater, (3) the observed groundwater flow patterns around underground nuclear explosions, one above and the other below the water table, and (4) field and laboratory studies of the groundwater flow patterns and the exchange capacities for specific environments and sites.

Ground disposal of radioactive wastes from reactor operations has been practiced for many years at AEC installations such as Hanford, Oak Ridge, Savannah River, and the National Reactor Testing Station.[14] The total release of long-lived radionuclides to the ground has been as great as the activities which might be released from many

applications of large megaton-range nuclear explosives in the Plowshare Program. As in all cases, the ground disposal of nuclides has been carefully monitored and accompanied by detailed studies of the geology, hydrology, and soil chemistry and useful data on groundwater transport of nuclides have been developed.

At Hanford, about 2.5×10^6 Curies of mixed fission products, contained in 4.5×10^9 gallons of water, have been discharged to sub-surface cribs and trenches dug in glacio-fluviatile soil. The water table is from 200 to 350 feet below these disposal sites, and movement of the radionuclides is much retarded by sorption of the nuclides on the soil particles as the waste-containing water percolated downward to the water table. When radionuclides with greater than a 3-year half-life are detected in concentrations exceeding 10% of the MPC (168-hr week) in the groundwater beneath a particular disposal site, the use of that site is discontinued. The measured rates of groundwater flow in the glacio-fluviatile sediments are from 170 to as much as 440 feet/day, with the maximum velocities being four to five times greater than the average velocities. Although 33,000 Curies for Sr^{90} have been discharged to the ground, in no case has Sr^{90} been detected (at greater than 6×10^{-14} Curie/ml) in groundwater at distances of more than a thousand feet from the point of entrance into the groundwater system.

In contrast to the behavior of Sr^{90}, Ru^{106} in the Hanford wastes is in a complex chemical form that does not exchange readily with the sediments, and has been observed to move about 8 miles in less than 1 year at rates approaching 160 feet/day. Based on comparison between the rates of movement of nitrates and Ru^{106} in the groundwater, the rate of movement of Ru^{106} may be about 80% of the rate of groundwater flow, indicating that very little retardation of Ru^{106} movement is caused by ion-exchange reactions with the medium.[15] Around an underground nuclear explosion, however, it is extremely unlikely that high ionic concentrations of nitrate or acids similar to waste disposal solutions would be generated; thus, the normally high K_d for Ru^{106} in simple chemical form would govern its behavior, with the rate of movement of Ru^{106} then being a small fraction of the average rate of flow of groundwater.

At Chalk River, Canada, following the NRX reactor accident in December 1952, about 1×10^6 gallons of water containing 1000 Curies of Sr^{90} were pumped into a trench dug in glacial sands, where the water table was a few feet below the surface and where the rate of groundwater flow was 0.5 feet/day; scanty data suggest that the bulk of the Sr^{90} has moved less than 100 feet in 9 years. Two experimental disposals were later made and carefully studied; one in 1954 containing 60 Curies of Sr^{90} in 1500 gallons of high nitrate content, and another in 1955 containing 300 Curies of Sr^{90} in 11,000 gallons of high-acid waste solution. Both these disposals were made directly into groundwater, where the rate of flow was 1.5 feet/day and the distribution coefficient, K_d, for Sr^{90} was about 20. By 1960, after the high initial ionic concentration of the nitrate and acid solutions had been neutralized by reaction with the sediments, the rate of advance of Sr^{90} was about 15 feet/year, or about 1/40th the velocity of the groundwater flow.[14]

Experience gained from waste disposal operations shows that (1) the maximum velocity for some fraction of the total groundwater flow, based on measurements such as at Hanford, are several-fold greater than the average velocity calculated from the regional hydraulic gradient and a few pumping tests of wells; (2) without fairly extensive subsurface information, the location and direction of such high-velocity groundwater tongues are impossible to predict; (3) the rate of movement of Sr^{90} in most environments tends to be a small fraction of the average rate of movement of groundwater; and (4) some short-lived nuclides, such as Ru^{106} with a 1-year half-life and not particularly significant in the biologic sense, may move considerable distances at rates approaching the average flow of groundwater, where the groundwater solution contains abnormally high concentrations of competing or complexing ions.

Extensive data on uranium and radium in rocks and in the associated groundwater have been accumulated during the postwar search for uranium ores.[16] Radium is analogous to strontium in its chemical behavior and has a one order of magnitude lower MPC than does Sr^{90}. Where the Ra^{226} content in both rock and groundwater is known, the distribution coefficient, K_d, for Ra can be calculated. For the volcanic tuff at the Nevada Test Site, the environmental K_d for Ra is 6700, and the K_d for Sr in the same environment is about 4000. For groundwater drawn from limestone aquifers in Nebraska and Iowa, the average K_d for Ra is 10, in good agreement with the K_d for

Sr^{90} determined for the Culebra dolomite at the Project Gnome site.[7] A large uranium orebody in sandstone in Wyoming is below the water table and contains about 5000 Curies of radium; groundwater in the orebody, rather high in sulphate, contains more than 2000 $\mu\mu$Curie/liter with a calculated K_d for Ra of 540. Dewatering wells near the edge of the orebody show about 10$\mu\mu$Curie/liter. A production well for drinking water, also very high in sulphate, yields groundwater containing 0.8 $\mu\mu$ Curie/liter with a calculated K_d for Ra of 600; this well is less than 1 mile from the edge of the orebody but, as measured down the regional groundwater gradient, is about 3 miles from the orebody. These data suggest that, where the K_d for Ra can readily be calculated, the behavior of Ra can be used as an index to the behavior of Sr^{90} introduced in that particular environment.

Marichal[17] has pointed out an interesting relationship around the Marcoule Production Center of the French Atomic Energy Commission; namely, that the distribution and fixation of polluting radionuclides are closely linked to the distribution of K^{40} in the environment. As K^{40} in many rocks reflects both the distribution and abundance of clay minerals, the components of a rock which retard or fix the movement of radionuclides in water, the K^{40} distribution as indicated by gamma-ray logs of drill holes, other radioactivity measurements, and general knowledge of the rock type might provide a crude index of where any radionuclides moving into the environment might be concentrated.

Data bearing on the modification of the regional groundwater flow pattern by an underground nuclear explosion are extremely few and do not suggest any sharply defined changes, except immediately over the cavity where postshot collapse forms a vertical column with possibly greater transmissibility for groundwater. Following the postshot exploration of the Rainier event at the Nevada Test Site, an attempt was made to introduce water into the crushed rock a few feet below the bottom of the cavity and into the rubble filling the lower hemisphere of the cavity. The crushed rock under the cavity did not accept any detectable amount of water, indicating that the very low permeability of the volcanic tuff was not increased by the effects of the explosion; the rubble, composed of rock fallen under gravity from the chimney zone created by cavity collapse, accepted water at the rate of 50 gallons per day per square foot.

An underground explosion of intermediate yield, detonated below the water table in Yucca Valley at the Nevada Test Site, produced a cavity which in collapsing formed a subsidence crater at the ground surface; the volume of subsidence is about equal to the volume of explosion-produced cavity, indicating that the volume or density of the collapsed rock is not significantly changed. The column of volcanic rock and alluvium, in dropping into the cavity, carried with it the water table and saturated zone, as shown by postshot measurements of the water table in an exploratory drill hole. The slow rate at which this depression in the water table is being filled will require several years to restore the original position of the water table. During this period of filling, the radionuclides from the explosion distributed in the crushed zone around the cavity and in the rubble collapsed into the cavity cannot be transported by any significant outward flow of groundwater.

Field and laboratory studies of the regional groundwater system, the chemical composition of the groundwater, and the exchange capacities of the rocks at specific sites have provided data needed to evaluate the possible movement of radionuclides from an underground nuclear explosion; such studies have been undertaken for Project Gnome[7] and for Project Chariot[18] in the Plowshare Program. The first step in evaluation of the public safety of a proposed project, in terms of possibly hazardous concentrations of radionuclides being transported by groundwater, is determination of the velocity and direction of the regional groundwater flow; the second step is determination of chemical composition of the groundwater and of the physical and chemical properties of the rock matrix; the third is determination of the specific K_d's for the radionuclides expected from the particular nuclear explosion, using representative samples of the rock and the native groundwater from the site.

The average velocity and direction of flow at a site can usually be defined either from existing hydrologic data or from a few supplemental observation wells; however, marked variations from the average flow do occur and are impossible to delimit without a wealth of subsurface data. Such variations in flow are caused by the heterogeneous nature of rocks and create considerable longitudinal and lateral dispersion of any radionuclide

concentration moving in the groundwater, with the result that some fraction of the nuclide concentration may be far in advance of the average flow.[19] In waste disposal operations, it is somewhat standard practice to increase the average regional flow rate by a safety factor of 10 to accommodate these unpredictable variations from the average rate.

Obtaining chemical analyses of representative groundwater samples presents no problems other than the obvious limitation imposed by the number and spacing of water or exploratory wells in the site vicinity. Variations in groundwater chemical composition directly affect the K_d's for the various nuclides; where the groundwater is suspected to move through several rock types, or where multiple aquifers are present, rather extensive subsurface data will be required.

The distribution coefficient, K_d, is defined as the ratio of the concentration of a particular radionuclide on the solid to the concentration of that nuclide in the adjacent liquid, at equilibrium. Because of the unique nature of the K_d, each combination of radionuclide, rock matrix, and groundwater composition will yield a different K_d; no present theory permits extrapolating laboratory values of K_d for relatively simple and pure combinations to the heterogeneous field conditions. The present best approach, therefore, is to determine a "working" K_d for a nuclide such as Sr^{90}, using representative samples of the rocks and associated — or closely simulated — groundwater, or, alternatively, observing the nuclide movement under imposed flow conditions between observation wells.

As pointed out by Ionue and Kaufman,[20] and Higgins,[6] given accurate data on (1) the average flow rate of groundwater, with some measure of variations from the average, (2) the porosity and permeability of the medium, (3) the chemical composition of water, and (4) the effective K_d's for the significant nuclides for the combinations of rock matrix and groundwater within the site area, the groundwater transport of radionuclides can be predicted, at least to a first-order approximation.

For the hypothetical 1-megaton fission-fusion explosion in dolomite, the transport of the radionuclides, Sr^{90} and H^3, by groundwater can be calculated, assuming that the groundwater flow rate in the dolomite is 10 feet per day, that the value of the K_d remains constant, and that the flow is completely laminar. The average flow rate of a single nuclide such as Sr^{90} is related to the flow rate of the groundwater by the equation:

$$\text{flow (ion)} = \frac{\text{flow (water)}}{1 + K_d \rho}$$

where K_d is the distribution coefficient for that ion, and ρ is the ratio of the mass of the solid to the volume of the water per unit volume of the rock. Using a K_d of 10 for Sr^{90}, the flow rate of Sr^{90} is then 0.2 feet per day, or the movement of Sr^{90} is retarded by ion exchange between the solid and the water to one-fifieth of the flow rate of the groundwater, which is consistent with the observed behavior of Sr^{90} under natural conditions in waste disposal operations.[21] H^3, however, does not enter appreciably into ion exchange reactions, although as tritiated water it does exchange with chemically bound water in the rock matrix and thus will be slightly retarded in respect to the groundwater flow rate, by a few percent in a clean sand to possibly 50% in a rock high in clay minerals.[22]

The foregoing calculation of the groundwater transport of Sr^{90} is a satisfactory first approximation, but may require several modifications, some of which tend to be order of magnitude in our present state of knowledge. First, hydrodynamic dispersion will spread the radionuclide-carrying water both logitudinally and laterally, thereby diluting the initial concentration by possibly one or more orders of magnitude; conversely, dispersion will cause some small fraction to move severalfold more rapidly than the average flow rate of the water, creating difficult problems of locating and monitoring such excursions. Secondly, in a dolomite, the groundwater flow may be largely along fractures rather than through the rock as a whole. Although the K_d for the dolomite may remain constant, the distribution of the ion, Sr^{90}, between the solid and the liquid phase varies according to the effective volume/mass (V/M) ratio. The effective mass of the dolomite matrix for exchange reaction — that along the fracture — might be a small fraction of the total mass; the concentration of Sr^{90} in the water would increase proportionately, possibly by an order of magnitude.[7]

SUMMARY

The initial explosion-produced distribution of the biologically significant radionuclides around large underground nuclear explosions is at, or a

few orders of magnitude greater than, the MPC (168-hour week) for these nuclides in drinking water, after the nuclides reach equilibrium between the rock matrix and the associated groundwater. No radical modifications of either the flow pattern or the chemical composition of the groundwater, at moderate distances such as from 5 to 10 cavity radii from the point of explosion, have as yet been demonstrated or seem likely to occur. Closer to the point of explosion, where the cavity may collapse either completely to form a subsidence surface crater or partially to form a chimney above the cavity, the present, although scanty, data indicate that groundwater will flow inward toward the cavity for a considerable period of time, possibly years, rather than through and away from the rubble-filled cavity and surrounding crushed zone.

After the restoration of the groundwater flow to preexplosion conditions, the radionuclides will be transported by groundwater down the regional hydraulic gradient and away from their initial explosion-produced distribution. Given a reasonable amount of data on the geologic and hydrologic setting of a site area, the average rates and concentrations of radionuclide transport by groundwater can be calculated, with validity within one or two orders of magnitude. Considering the rather high residual uncertainities in such calculations, where such approximations suggest any possibility of hazardous concentrations of nuclides within an arbitrarily defined travel distance, additional subsurface data together with adequate monitoring of the groundwater flow will be required to delimit and manage such possibly contaminated groundwater.

The nuclide, Sr^{90}, characterizing the long-lived fission products, will be significantly retarded in its groundwater transport in essentially all geologic environments; the rate of movement of Sr^{90} will rarely be more than a few percent of the average rate of groundwater flow., and in many environments will a small fraction of a percent. The nuclide, Co^{60}, characterizing long-lived induced activities, will also be significantly retarded in its groundwater transport, more so than Sr^{90}. The nuclide, H^3, residual from fusion reactions, is not significantly retarded in its groundwater transport; tritium may well be the most important of all the long-lived nuclides in evaluating possibly hazardous radionuclide concentrations in groundwater.

From a nominal 1-megaton fission-triggered fusion explosion contained underground, H^3 is by far the most abundant nuclide in the period from 1 to 100 years after the explosion. As tritiated water is transported by groundwater flow away from its initial explosion-produced distribution, dilution primarily by hydrodynamic dispersion must be relied upon to reduce the tritium concentration in the water. Hydrodynamic dispersion varies widely, from little in a hemogeneous porous medium to considerable in highly heterogeneous medium, and is difficult to predict within several orders of magnitude.

The groundwater transport of radionuclides, following the initial explosion-produced distribution, may not create any unmanageable problems in the postexplosion movement and concentration of nuclides in water supplies. It will be necessary to understand and fully document the particular geologic and hydrologic environment around each proposed application of a nuclear explosive in order to permit prediction of where and under what conditions possibly hazardous radionuclide concentrations in groundwater could occur.

REFERENCES AND NOTES

1. "Maximum Permissible Body Burdens and Maximum Permissible Concentrations of Radionuclides in Air and Water for Occupational Exposure," Nat. Bur. Std. U. S., Handbook No. 69, 1959; also, K. Z. Morgan, Science 139, p. 3555, 1963. The quoted values for the MPC (maximum permissible concentration) for radionuclides in drinking water are those recommended for occupational workers continuously exposed (168-hour week) within a controlled area; for the general population outside of a controlled area, the recommended MPC is reduced" . . . to levels not exceeding one-tenth of the maximum permissible concentrations allowed in air, water, and foodstuffs for continuous occupational exposure . . averaged over periods up to 1 year."

2. O. I. Leipunsky, "Radiation Hazards from Clean Hydrogen Bomb and Fission Atomic Bomb Explosions," At. Energy (U. S. S. R.) 3, p. 530, 1957; English translation in U. S. Congressional Hearings on Fallout from Nuclear Weapons Tests, pp. 2423-2447, May 5-8, 1959.
3. R. E. Batzel, "Radioactivity Associated with Underground Nuclear Explosions," Univ. Calif. Rept. UCRL-5623, 1959.
4. C. R. Boardman, D. D. Rabb, and R. D. McArthur, "Characteristic Effects of Contained Nuclear Explosions for Evaluation of Mining Applications," Univ. Calif. Rept. UCRL-7350, 1963.
5. Alfred Clebsch, Jr. and F. B. Barker, "Analyses of Ground Water from Rainier Mesa, Nevada Test Site, Nye County, Nevada, "U. S. Geol. Survey Rept. TEI-763, 1960, available from Off. Tech. Serv., Dept. Comm.
6. G. H. Higgins, "Evaluation of Ground Water Concentration Hazard from Underground Nuclear Explosions," Univ. Calif. Rept. UCRL-5538, 1959.
7. "Final Report — Hydrologic and Geologic Studies for Project Gnome (U. S. Geological Survey)," U. S. Atomic Energy Commission Plowshare Program Rept. PNE-130F, 1962, available from Off. Tech. Serv., Dept. Comm.
8. Y. Ionue and W. J. Kaufman, "Studies of Injection Disposal," 2nd Conference on Ground Disposal of Radioactive Wastes, Off. Tech. Serv., Dept. Comm., TID-7628.
9. B. Mason, Principles of Geochemistry (Wiley, New York), 1952.
10. F. W. Stead, "Tritium Distribution in Ground Water Around Large Underground Fusion Explosions," Science 142, p. 3596, 1963.
11. A. V. Shelton, "Radioactivity and Earth Motion," Univ. Calif. Rept. UCRL-5675, 1959.
12. R. H. Goeckerman, "Disposition of Radioactivity, " Univ. Calif. Rept. UCRL-5675, 1959; E. C. Freiling, "Fractionation in Surface Bursts," in Fallout from Nuclear Weapons Tests — Proceedings of a Conference, Off. Tech. Serv., Dept. Comm., TID-7632, 1962.
13. E. A. Martell, "Possible Contribution of Underground Nuclear Explosions to Recent Fallout over the United States," in U. S. Congressional Hearings on Radiation Standards, Including Fallout, June 4-7, 1962.
14. "Ground Disposal of Radioactive Wastes — 1959 Conference Proc.", TID-7621; also, "Second Ground Disposal of Radioactive Wastes Conference — 1962," TID-7628; both reports available from Off. Tech. Serv., Dept. Comm.
15. D. W. Pearce et al., "Radioactive Waste Disposal to Ground at Hanford," in Disposal of Radioactive Wastes — Proc. of Sci. Conf., Intern. Atomic Energy Auth., Monaco, 1960.
16. R. C. Scott and F. B. Barker, "Data on Uranium and Radium in Ground Water in the United States, 1954 to 1957," U. S. Geol. Survey Prof. Paper 426, 1962.
17. M. Marichal, "Control of the Surrounding Radioactive Pollution," Bull, Inform. Sci. Tech. (Paris), No. 72-73, 1963.
18. A. M. Piper, "Potential Effects of Project Chariot on Local Water Supplies," U. S. Geol. Survey open-file report TEI-810, 1962.
19. B. L. Schmalz and W. S. Keys, "Retention and Migration of Radioactive isotopes in the Lithosphere at the National Reactor Testing Station, Idaho," in Intern. Conf. on Retention and Migration of Radioactive Isotopes in Soil, Paris, France, 1962.
20. Y. Ionue and W. J. Kaufman, "Prediction of Movement of Radionuclides through Porous Media," Health Phys. 9, pp. 705-715, 1963.
21. V. Spitsin, V. C. Balukova, and T. V. Ermanov, "Studies of Sorption and Migration of Radioactive Elements in Soils," in Treatment and Storage of High-Level Radioactive Wastes — Proc. of Symposium, Intern. Atomic Energy Auth., Vienna, 1963.
22. P. J. Parsons, "Movement of Tritium from Chalk River Liquid Disposal Area.," Atomic Energy Canada Ltd., Chalk River Rept. CRER-1146, 1963.

BIBLIOGRAPHY

1. Higgins, G. H., "Calculation of Radiation Fields from Fallout," Lawrence Radiation Laboratory, Rept. UCID-4539, January 1963.
2. Knox, J. B., "Prediction of Wind and Fallout," Lawrence Radiation Laboratory, Livermore, Rept. UCID-4662, 1964.
3. Nordyke, M. D. and W. R. Wray, "Cratering and Radioactivity Results from a Nuclear Cratering Detonation in Basalt," Lawrence Radiation Laboratory, Livermore, Rept. UCRL-6999, Rev. II, October 1963.
4. U. S. Army Engineer Nuclear Cratering Group, Corps of Engineers, Livermore, California, "Engineering Manual on the Use of Nuclear Explosions for Large-Scale Excavation," Revised Draft, June 1963.

BIOGRAPHICAL SKETCH OF AUTHOR

Frank W. Stead is a native of New York City. He received his B.S. in Physics from the City College of New York in 1935, M.A. in Geology from Columbia University in 1937, and Ph. D. in Geology from Columbia University in 1941. His professional experience is as follows: 1937-40 Instructor in Geology, City College of New York. 1941 Instructor at Lehigh University and Assistant at Columbia University. 1942-present U.S. Geological Survey. 1945-54 Chief, Technological Planning and Development Unit. 1954-59 Chief, Uranium Research and Resources Group. 1960-62 Chief, Special Projects Branch (Nevada Test Site and related studies). 1962-Research Geologist – occurrence of uranium and thorium; radioactivity measurements; occurrence of minor elements. Currently investigating potential applications of nuclear explosives to the management and development of water resources.

FALLOUT CALCULATIONS AND MEASUREMENT*

M. M. Williamson, Captain,
U. S. Army Corps of Engineers

Lawrence Radiation Laboratory, University of California
Livermore, California

ABSTRACT

The first portion of the paper is a general discussion of fallout and the definition of various terms peculiar to any discussion of fallout problems. Sources of radioactivity and types of radiological hazards as they pertain to nuclear excavation are also discussed.

The remainder of the paper is devoted to outlining the steps which might be taken in the preshot planning and postshot evaluation of fallout problems as applied to a nuclear excavation project. The preshot planning phase includes a discussion of the data necessary for fallout prediction, fallout prediction techniques, and interpretation of the fallout prediction in terms of on-site and off-site radiological safety.

The postshot phase includes a discussion of some of the data which must be collected after firing, how these data may be collected, and how the data are used for fallout pattern construction and other calculations necessary to evaluate radiological hazards. Also included is the interpretation of the fallout pattern to determine re-entry times, actual on-site and off-site radiological hazards, and the fraction of the total activity vented as prompt fallout.

INTRODUCTION

Safety is an important consideration in any construction project. There are a few special safety problems which are inherent to large-scale construction projects involving nuclear explosives. One of the most important of these problems is the problem of radiological safety.

When a nuclear cratering explosive is fired, a large amount of earth is thrown upward along with a certain amount of vaporized material and radioactive debris from the thermonuclear explosive. As the violent motion caused by the explosion subsides, the material begins to fall back to earth, but the solid particles are already being contaminated by condensation of the vaporized fission products and other radioactive materials upon them. Most of the contaminated material falls to earth within a few hours and is referred to as local fallout. Some of the gaseous fission products and extremely small particles, however, may take weeks or months to fall back to earth and are referred to as tropospheric fallout. This paper is concerned only with local fallout.

A nuclear excavation project must be accomplished in such a manner that the radioactivity produced by the explosion does not reach the human populace in amounts great enough to cause harmful effects. This means that during the planning phase of the project one must determine what amounts and kinds of radioactivities will be produced and how these activities will be distributed following the explosion. The estimated exposures must then be compared with health standards to determine what areas, if any, may require control and monitoring.

RADIATION DOSES

Two types of radiation dose must be considered, the external dose and the internal dose. The external dose from whole-body irradiation by gamma-emitting radionuclides can be estimated in terms of the amount of fission products and

*Work performed under the auspices of the U. S. Atomic Energy Commission.

gamma-emitting induced radionuclides which escape from the crater, and the distribution of this escaped activity.

The internal dose comes from radionuclides which may be assimilated or ingested and concentrated and/or retained by vital body organs, with possible resultant harmful effects. The internal dose is a much more complex problem to evaluate than the external dose. Alpha, beta, and gamma radiation contribute to the internal dose. It is necessary, therefore, to consider a great many specific fission product radionuclides and induced radionuclides. In addition, it is necessary to estimate the amount of each radionuclide produced, its depositional and airborne distribution, human uptake and retention of each radionuclide, the organ or organs affected, etc.

SOURCES OF RADIOACTIVE FALLOUT

In a nuclear excavation explosion there are three sources of radio-activity:

1. fission product activity from the nuclear explosive,
2. activity from induced radionuclides produced by neutrons from the thermonuclear processes interacting with device materials and with soil and rock surrounding the device, and
3. activity from radionuclides actually produced in the thermonuclear processes.

For any given nuclear excavation explosion, the amount of fission product activity produced is determined from the fission yield of the device. The amount of radioactivity from radionuclides induced in the device materials and from the thermonuclear processes can be determined from previous performances of the device. Soil-induced activities can be estimated from a soils analysis of the material surrounding the device and estimates of the numbers and energies of the neutrons escaping the device and reaching these materials. Much of the soil-induced activity can be eliminated by using neutron-absorbing materials in and around the device to reduce the number of neutrons available for soil activation.

FALLOUT PREDICTION

The radioactivity generated by a deeply buried nuclear cratering explosion is distributed in three ways:

1. A large fraction of the activity produced is trapped by particles of debris and ejecta which fall back into the crater or on the lip and end up buried in the rubble.
2. A much smaller fraction of the activity produced escapes from the crater, is injected into the dust cloud in the form of particulates, and is deposited as local fallout.
3. A smaller fraction of the activity produced escapes from the crater, is injected into the dust cloud in the form of gas or solids carried by minute dust particles, and may be carried for great distances and contribute to tropospheric fallout.

Radiological safety, and hence fallout predictions and calculations, is primarily associated with local fallout.

The amount of local fallout which escapes the crater has been shown to be mainly dependent on the ratio of depth of burst (DOB) to depth of apparent crater (DOC), and the type of material in which the detonation takes place. Figure 1 shows the dependence on this ratio. The Danny Boy and Sedan events are plotted in Fig. 1, Danny Boy illustrating a cratering explosion in dry basalt and Sedan illustrating a cratering explosion in alluvium with a moisture content of 10 to 20%. The curve shows that the escaped activity decreases sharply as the ratio of DOB/DOC increases, a characteristic that is very important for nuclear cratering applications. A ratio of DOB/DOC of about 2.0 is optimum, giving a crater with near optimum dimensions with a low radio-activity escape. A lesser ratio of DOB/DOC results in greater crater dimensions but also greater activity escape, while a greater ratio results in less activity release but also a smaller crater. The steep slope of the curve shows that increasing the DOB/DOC ratio slightly, decreases the escaped radioactivity two or threefold. Using the expected DOB/DOC ratio and the curve of Fig. 1, one can estimate the fraction of the radioactivity produced by a nuclear cratering explosion which will escape the crater as local fallout.

The escaped radioactivity is distributed downwind from the nuclear cratering detonation as the particles of the dust cloud settle to earth. The distribution depends on the dimensions of the dust cloud, the winds acting on the dust cloud and the particle size and activity distribution in the cloud.

After the explosion projects the earth particles, vaporized material, and explosive debris into a roughly cylindrical cloud, a downward and

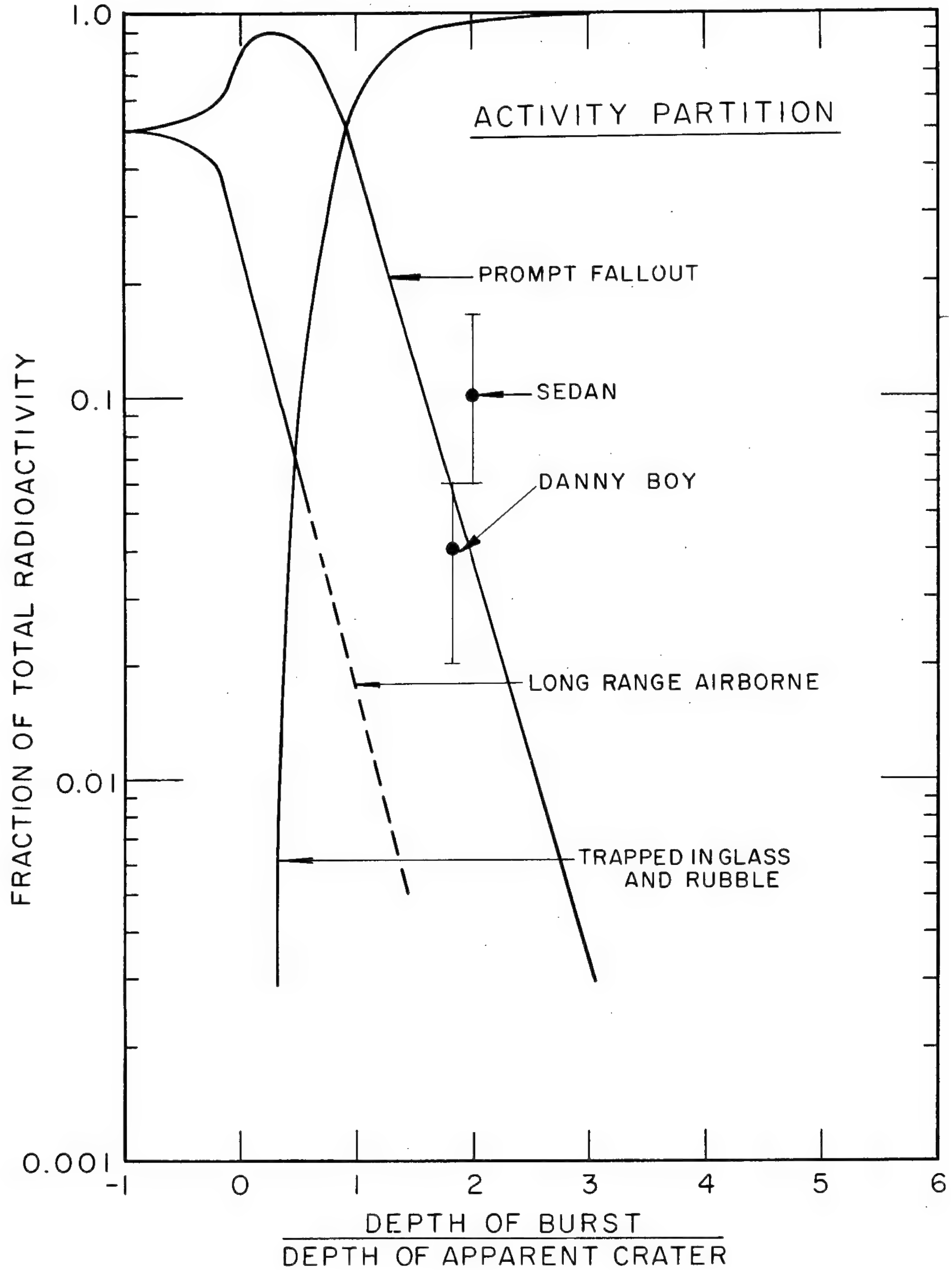

Fig. 1. Radioactivity escape from a nuclear cratering detonation as a function of depth of burst/depth of apparent crater ratio.

outward flow of the mass of the cloud under the action of gravity leads to the formation of a base surge. The base surge rolls out to distances greater than the main cloud diameter but it remains at a lower height. The main cloud, which contains the hot gases from the explosion, continues to rise and expand, possibly oscillating about an equilibrium point, until equilibrium is reached with the atmosphere.

The phenomenon of cloud formation is extremely complex. It is affected by meteorological conditions, depth of burst, total yield, and type of material being excavated. In a dry non-gas-generating material such as basalt, the main cloud is either not present or is invisible. In a gas-generating medium, such as alluvium with 10% or more moisture content, the main cloud becomes a well-developed cloud, separate from the base surge, rising to heights greater than the height of the base surge. Experience is lacking in the prediction of cloud dimensions from nuclear explosions, but much work is being done with high explosives to gain a better understanding of the basic phenomena involved. One method that has been used to obtain cloud dimensions is based on the application of the theory of cloud dynamics to scale the cloud dimensions from previous detonations fired under similar emplacement and meteorological conditions.

Several fallout prediction procedures have been developed by various agencies. Three systems are presently in use in the Plowshare Division of the Lawrence Radiation Laboratory: a system developed by A. V. Shelton of LRL, a system developed by J. B. Knox of LRL, and a system developed by the U. S. Weather Bureau. The first two systems have both been programmed for computers as the hand calculations are very detailed.

The Knox fallout prediction model uses the following factors to predict dose rates in the surface pattern.

1. Cloud dimensions at the time of cloud stabilization.
2. Particle size distribution in the cloud and activity distribution as a function of particle size.
3. Fall velocity of the particles in still air as a function of particle size and height in the atmosphere.
4. Time and space prediction of the mean layer wind appropriate for the layers through which the particles fall.
5. The wind shear tangential and normal to the mean layer wind.
6. The effect of horizontal eddy diffusion on the growth of the horizontal radius of disks of radioactive particles as the disks fall earthwards.

The Weather Bureau system is a means of scaling the fallout pattern from a previous detonation to the detonation in question. The system uses two basic equations:

$$\text{Dose Rate}' = \text{Dose Rate}\left(\frac{\overline{V}}{\overline{V}'}\right)^2\left(\frac{S}{S'}\right)\left(\frac{F'}{F}\right)\left(\frac{W'}{W}\right)\left(\frac{h}{h'}\right)^2$$

and

$$X' = X\left(\frac{\overline{V}'}{\overline{V}}\right)\left(\frac{h'}{h}\right)$$

where

$\overline{V}$ = mean windspeed
S = wind shear
F = escape fraction
W = fission yield
h = main cloud height
X = distance from ground zero

and where primed quantities refer to the detonation in question and unprimed quantities refer to the previously fired explosion. The wind shear and mean wind speed are taken for the top 60 to 70% of the cloud.

The Shelton fallout prediction system utilizes an empirically determined table of cloud-fraction fall rates. This system is outlined in more detail here, not because it is any better than many other systems, but rather because the author is more familiar with this system and has considerable experience in its use.

The cloud is divided into ten disks of equal height and the mean wind speed, direction of the mean wind vector in the layer, and wind shear within the layer are determined from a hodograph of the predicted zero-time wind conditions. A downwind range is then chosen for investigation and the average time of arrival of fallout from each layer at that range is determined by dividing

the range to the midpoint of the layer by the mean wind speed in each layer. The average fall rate of a particle in any layer falling to the earth at the chosen range can then be determined by dividing the height to the midpoint of the layer by the average time of arrival of fallout. Particles in the near and far edges of the cloud fall at different rates and the difference in these rates is the fall-rate interval for a given layer. The average fall rate is used to obtain a value from the cloud model of the fraction of the cloud falling per 0.05 knot fall-rate interval. This value is then multiplied by the fall-rate interval to obtain a value of the fraction of the cloud falling at that range for each layer. This cloud fraction is then divided by the cross-sectional area of the cloud to determine the fraction of the cloud falling per unit area from cloud layer at the chosen range. The cloud has been acted on by the wind shear, however, so the disks tend to spread as the cloud moves downwind so that as each disk is projected on the ground not only has its center been displaced from the adjacent disks, it has also been spread so that it is no longer circular. An area correction is applied to account for the spreading of each disk and an overlap correction is applied to account for displacement of the disk from the other disks within the cloud. After these corrections have been applied, there results a final value of the fraction falling per unit area from each cloud layer at the chosen range. These calculations are then repeated for several ranges. A pattern can now be constructed by drawing radial lines from ground zero in the direction of the effective wind in each layer and striking arcs at the ranges investigated. The values of the fraction falling per unit area at a given range from a given cloud layer can now be plotted at the intersection of that range arc and the radial drawn in the direction of the effective wind in that layer.

This array of values can be used in many ways. A pattern can be drawn by connecting, in a logical manner, those points of equal value, using logarithmic interpolation between known values. The resultant contours of fraction of the cloud falling per unit area can be used to predict isotopic concentrations of specific nuclides of interest in respect to the internal dose, assuming there is no isotopic fractionation between the nuclide produced and those in the cloud, and that the radioactivity in uniformly distributed throughout the cloud. Then the isotopic concentration at a given time at a given contour is merely the amount of the nuclide produced, corrected appropriately for decay of the nuclide (in atoms, curies, etc.), multiplied by the value of the contour (i.e., the cloud fraction falling per unit area).

A pattern of dose or dose rate from gamma radiation can also be constructed from the array of values. Fission products uniformly contaminating an infinite plane surface at a rate of 1 kt/mile^2 cause a certain dose rate and infinite dose (author recommends 3400 R/hr at H + 1 hr and 10,500 R from H + 1 hr to infinity as calculated by G. H. Higgins, UCID-4539). The amount of fission products in the cloud can be calculated as the product of the fission yield and the escape fraction. Then the product of the amount of fission products in the cloud, the value of the fraction of the cloud falling per unit area, and the appropriate conversion factor give the value of infinite dose or dose rate at a specified point. Again logarithmic interpolation is used between known points to determine the location of the isodose rate or isodose contours. Use of appropriate decay factors enables construction of patterns of dose rate at any given time or dose in any given time interval. An example of a predicted fallout pattern is shown in Fig. 2.

If there are significant amounts of gamma-emitting induced activities produced, they can be included in the fallout pattern by converting them into equivalent fission yields, i.e., the equivalent yield of fission products which would cause the same infinite dose or dose rate as the radioactivity from the induced nuclide. This is done by calculating the amount of the nuclide produced and applying appropriate factors to account for the total and average gamma energies emitted by the nuclide. A complete discussion and description of these calculations can be found in UCID-4539 (Ref. 1).

The calculations just described were for infinite plane surface dose and dose rate. However, the roughness of the terrain will provide a certain amount of shielding from gamma radiation. Often a correction of the predictions is made to account for this terrain shielding (author recommends a valud of 0.8 as proposed by Higgins, UCID-4539). An additional correction is sometimes applied to infinite dose calculations to account for the fact that man spends some of his time inside a building or away from home, which decreases the dose absorbed to about one-half the infinite dose.

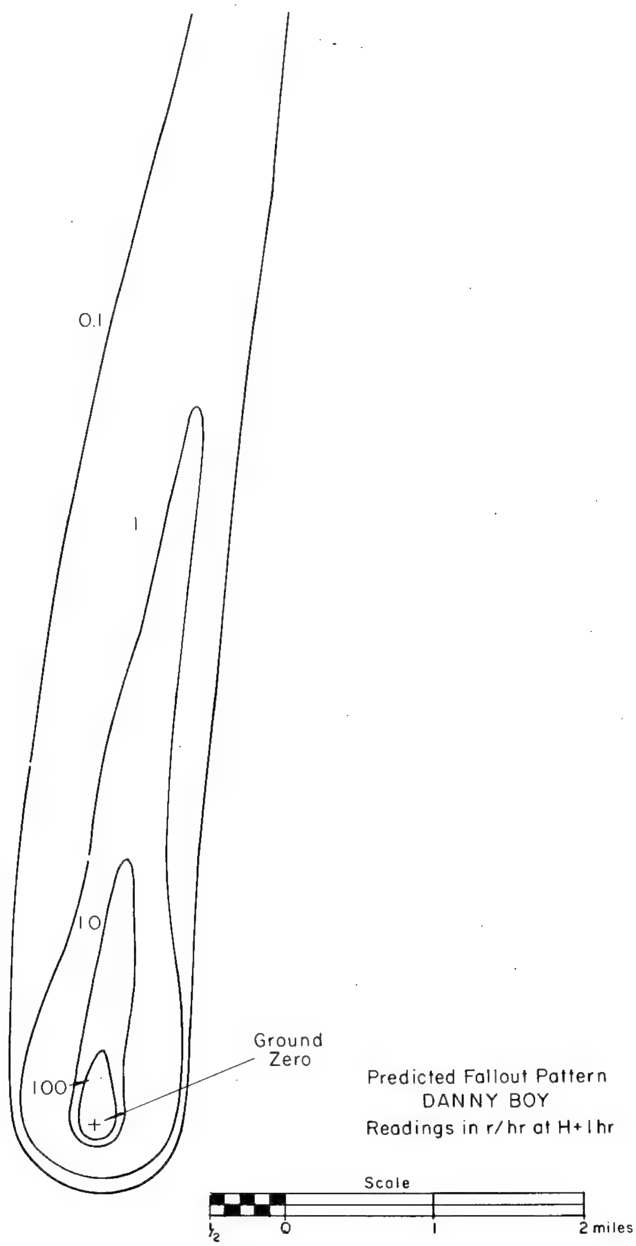

Fig. 2. Predicted fallout pattern.

PREDICTED FALLOUT PATTERN INTERPRETATION

These fallout patterns can be used to determine those areas in which the radiation dose might be expected to exceed health standards and thus require temporary evacuation of the inhabitants. By applying appropriate decay factors to the pattern it is possible to determine the time when the evacuees may return.

FALLOUT PREDICTION LIMITATIONS

The limitations of fallout prediction must be understood, as well as the capabilities. Scientific knowledge is still needed to better develop this field, especially as applied specifically to nuclear excavation. There has been relatively little experience to date in the nuclear cratering field. One cannot expect to exactly duplicate the weather conditions used in the prediction without undue delay in detonation schedules. The behavior of the nuclear cloud is extremely ccmplex and not well understood at this time and more nuclear experience is needed. Very close-in prediction of fallout is not good with present prediction systems. Fractionation, or enrichment of specific nuclides during the venting process or later is neither well understood nor is it usually accounted for in present prediction systems.

DATA COLLECTION

In order to develop data for comparison with predictive capabilities, nuclear excavation operations are designed to include a number of technical programs to document fallout. The data sought generally will include:

1. fallout samples for radiochemical analysis to determine decay rates and relative amounts of induced activities, and
2. survey readings to determine the intensity of radiation and the areal extent of the fallout pattern.

In a nuclear cratering explosion, some 70 to 90% of the local fallout is deposited within a very few miles of ground zero. This area must be well surveyed so that the most accurate pattern possible can be constructed. This is essential to a complete integration of the fallout pattern and hence determination of the escape fraction. This close-in pattern is also used to determine when it is safe to reenter the immediate area of the excavation and when it is safe for construction crews to reenter and carry on construction activities.

The downwind area of the fallout pattern is not as critical for calculational aspects, but must be well documented since this is the area in which any radiological hazard to the public would occur. It is therefore necessary to have accurate infor-

mation of this portion of the pattern to determine when the populace can be allowed to return safely to those areas which may have required evacuation.

There are several ways of obtaining the necessary data to properly determine the actual fallout pattern:

1. Remote area monitoring systems using hard-wire telemetry.
2. Aerial monitoring using monitoring equipment in aircraft.
3. Ground monitoring using hand-held monitoring equipment.

The third method is, at present, the most accurate, although it requires more personnel and considerably more time.

Remote area monitoring can be used to determine the initial intensities in those areas where initial radiation might be expected to be too high to permit ground monitoring or where continuous monitoring is desired. Care must be taken to shield these instruments against contamination by the deposited material which would give rise to false readings. Advantages of this system are the possibility of obtaining continuous readings over a given period and obtaining very early and high radiation intensities.

Aerial monitoring is difficult to use since the information gathered is very hard to assess. First, it is difficult to determine the exact aircraft position at the time any given reading was taken. Second, it is difficult to convert the reading in counts per minute to a radiation intensity on the ground since air temperature and pressure have a large attenuation effect on the radiation reaching the instrument. At present there is no well-established conversion factor to change these aerial readings to ground intensities.

Remote area monitoring and aerial monitoring are, however, useful methods for determining initial fallout intensities and fallout pattern shape to a fair approximation, thus giving a very early comparison with the fallout prediction so that additional measures may be taken should they be necessary, to ensure public safety.

FALLOUT PATTERN CONSTRUCTION

The fallout pattern is best constructed using ground survey readings of gross gamma radiation intensities in roentgens per hour. Conversion of these readings to a common time gives an array of data points which can be connected, in a logical manner, to obtain the isodose rate contours of the fallout pattern. Actual fallout patterns are shown for Danny Boy, a 430-ton cratering explosion in dry basalt (Figs. 3, 4, 5) and Sedan, a 100-kt cratering explosion in alluvium in which less than 30% of the yield came from fission (Figs. 6, 7).

Conversion of the readings to a common time is done by use of the equation

$$\text{Dose rate at time } t = (\text{dose rate at } H + 1)\ t^{-x}.$$

The exponent, x, can be determined from radiochemical analysis of the samples taken. When fission product activity is the dominant factor in the fallout, the decay rate will be on the order of $t^{-1.2}$ or $t^{-1.3}$. The presence of significant amounts of induced activity can lead to decay schemes that are markedly different from the usual fission product decay behavior.

The dose rate pattern can be used to construct a pattern of dose in any given time interval. Radiation dose is merely the integration of the dose rate over a given time period

$$\text{Dose}_{t_1 \rightarrow t_2} = \int_{t_1}^{t_2} \text{dose rate at unit time } t^{-x}\, dt$$

where t^{-x} is the established decay rate. Generally, t is expressed in hours, and then dose rate at unit time would be the dose rate 1 hour after the explosion. The actual infinite dose fallout pattern for Sedan is shown in Fig. 8.

The dose-rate pattern can also be used to determine isotopic concentrations by using a calculation similar to those previously described to convert isodose rate contours into fractions of the cloud falling per unit area, and thence into atoms or curies per unit area, of the isotope of interest. It must be borne in mind that these calculations assume no fractionation and that the radioactivity is uniformly distributed in the cloud. If the fractionation of any particular nuclide is known, it may be directly applied to the above calculations.

ACTUAL FALLOUT PATTERN INTERPRETATION

The actual fallout patterns can be compared with the predictions to determine the accuracy of the prediction system and to ascertain whether or

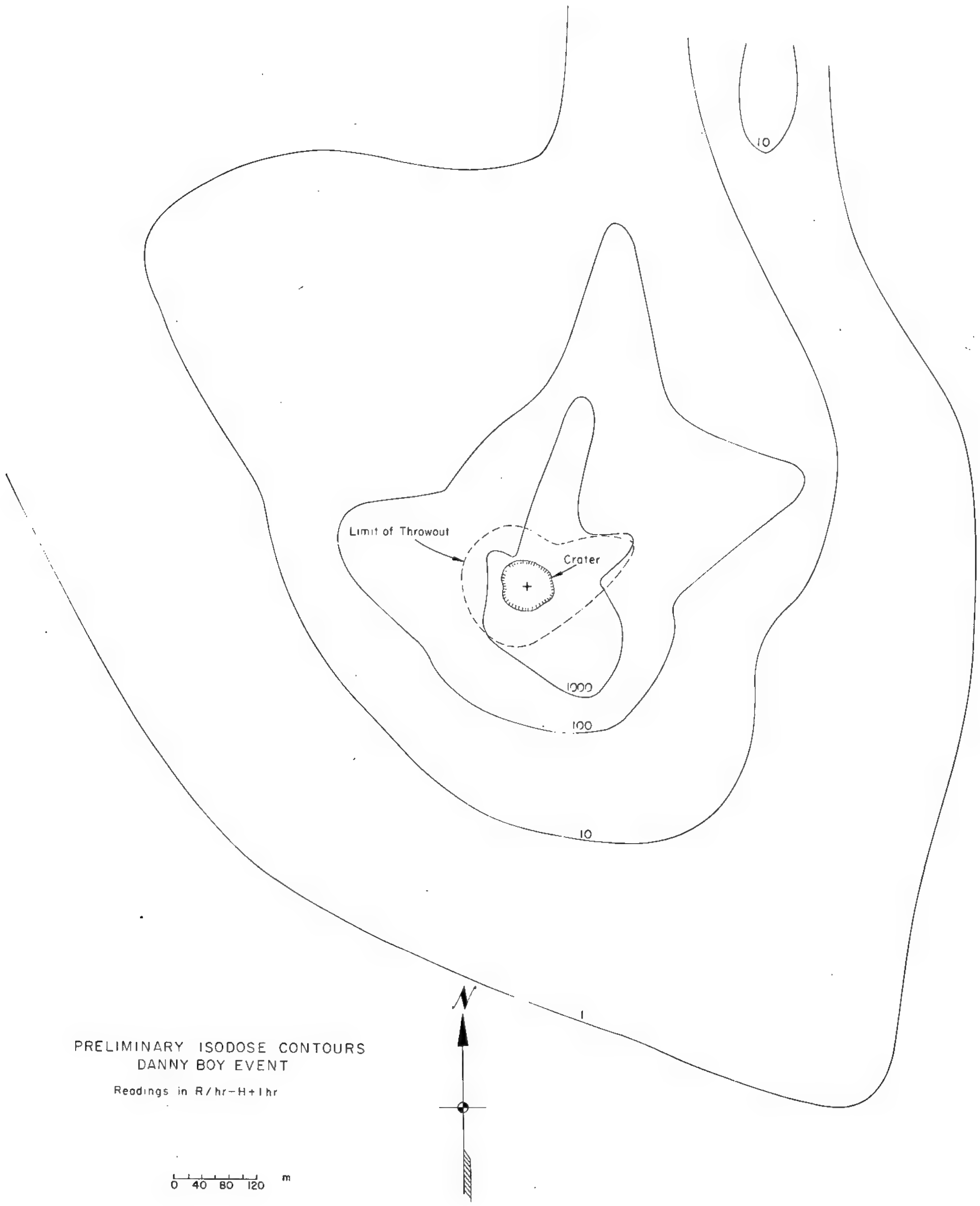

Fig. 3. Danny Boy close-in fallout pattern.

not the predicted reentry times for evacuees still hold. Gross differences should long before have demanded immediate remedial action from comparison of preliminary patterns. Here, however, the patterns must be carefully studied to determine those minor differences which may or may not be significant over a long time period.

The close-in fallout pattern is principally used to evaluate crater reentry times for construction crews. Fallout prediction systems are of little use in this area and experience to date makes scaling to other detonations only a reasonable guess of in-crater intensities. Work is being done in this area but at present it is felt that a complete evaluation would be required using postshot data and continuing ground monitoring to accurately determine crater reentry times.

Another important use of the fallout pattern is the determination of the escape fraction which in turn is used in future predictions. In this paper,

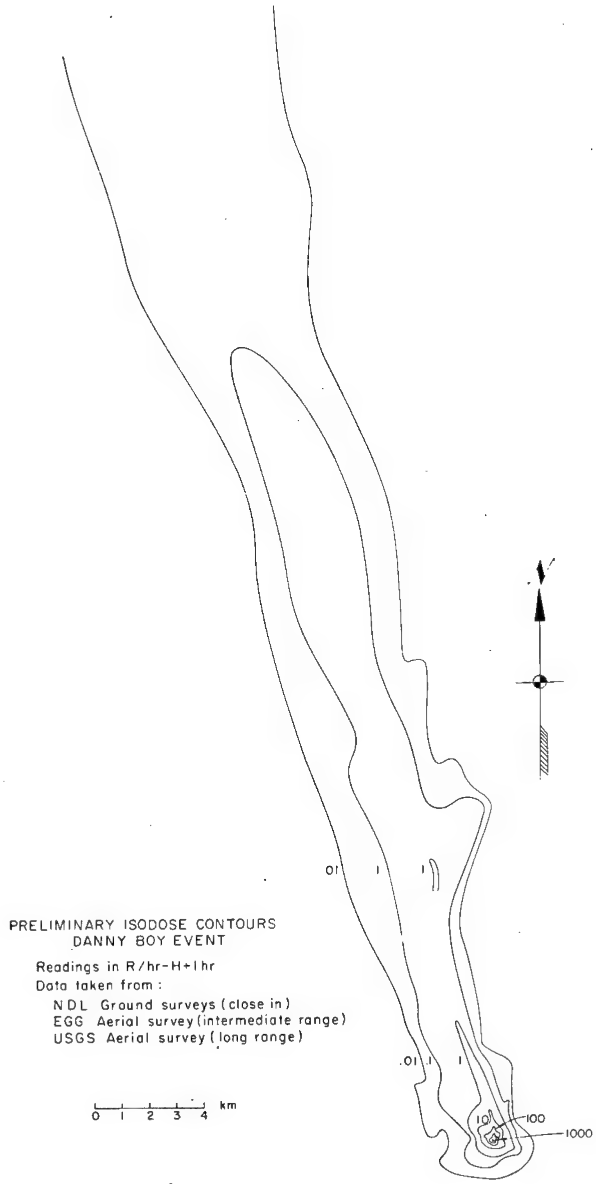

Fig. 4. Danny Boy intermediate range fallout pattern.

the escape fraction is arbitrarily defined as the fraction of the total fission product gamma activity produced which falls as local fallout outside the area of the crater and the ejecta or direct throwout. This determination is made by an integration of the fallout pattern of isodose rate contours. The total activity in the fallout pattern equals

$$\int_{A_1}^{A_2} I \, dA$$

where A_1 and A_2 are the areas enclosed by the highest and lowest intensity contours, respectively.

This integral can perhaps best be evaluated by plotting the data points on log-log paper, determining the equations of the curves connecting the data points, or of an average straight line fit, and then inserting these equations into the above integral. This method allows simple extrapolation to obtain the intensity vs area curve in close to the throwout and out beyond the last measured contour. Because the exponent in the I vs A curve for the long-range portion of the pattern is always less than -1.0, IA rapidly decreases for the smallest values of I and very small error can be introduced in the integral in extrapolating A to infinity.

The total activity thus calculated in units of R-mile^2/hr, can be converted to an equivalent fission yield using the density conversion constant 3400 (R-mile^2/hr-kt) and including a correction for terrain shielding as previously recommended. This calculation results in the equivalent fission yield found in the fallout pattern, and when divided by the actual fission yield of the device, gives the fission escape fraction.

When gamma activity other than fission product activity is present in significant amounts it must be accounted for in these calculations either by reducing the contour intensities to that fraction which is due to the contribution of the fission products alone, or the other activities must be converted to equivalent fission yields which are then added to the fission yield of the device.

ADDITIONAL PROBLEMS

Additional problems which are receiving attention, but about which experience is lacking, are the redistribution of fallout by wind and water, effects of large and small terrain features on cloud movement and fallout deposition and the effect of precipitation on the radioactive dust cloud.

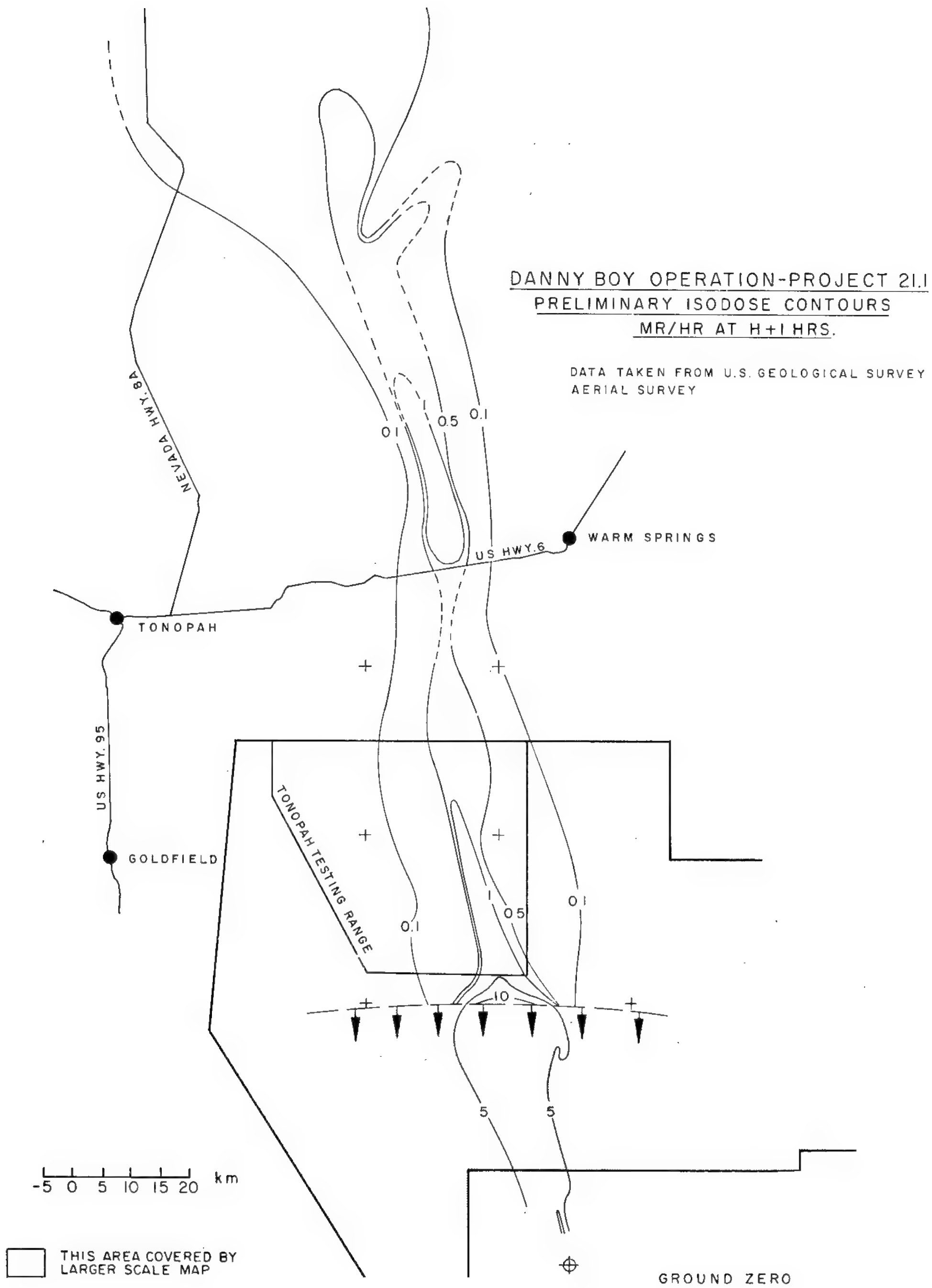

Fig. 5. Danny Boy long range fallout pattern.

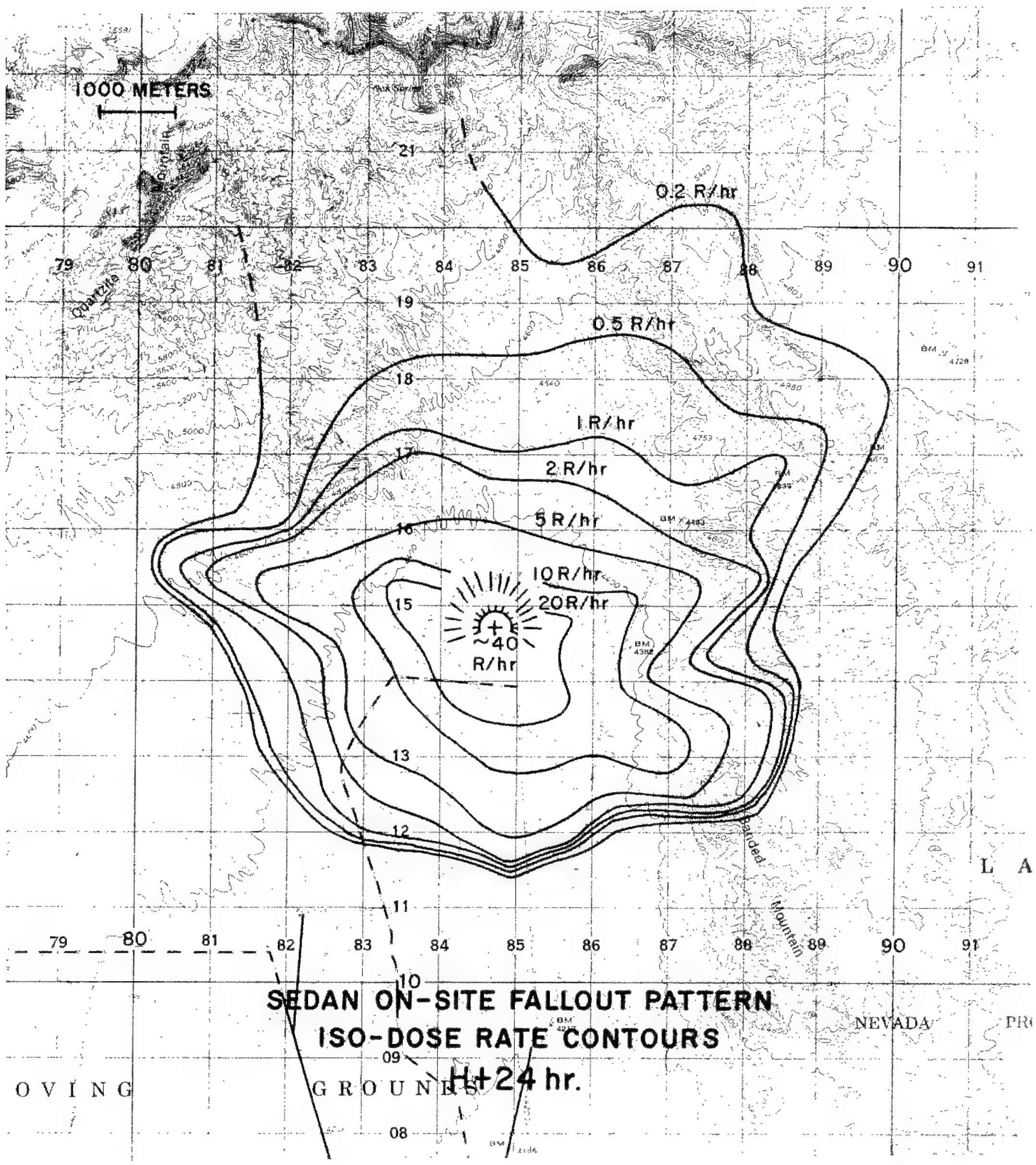

Fig. 6. Sedan close-in fallout pattern.

SUMMARY

The problem of radiological safety must be evaluated in terms of the external dose and the internal dose. Fallout prediction, while having its limitations, is sufficiently accurate to safeguard the public from the radioactivity released in a nuclear excavation explosion. Complete documentation of the fallout from a nuclear excavation explosion is necessary to ensure public safety. The principles outlined here apply, in general, to any nuclear explosion which releases radioactivity to the atmosphere.

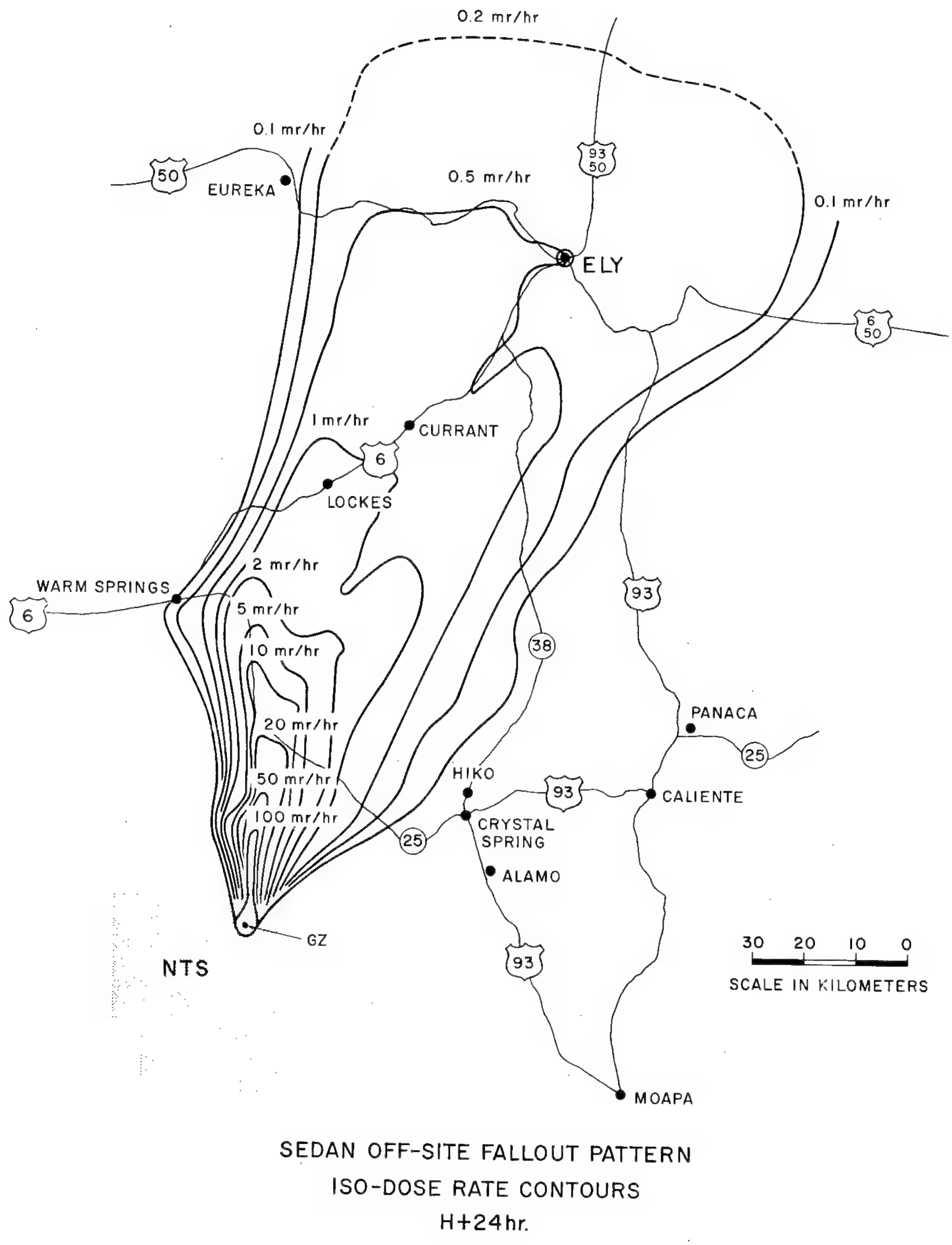

Fig. 7. Sedan long range fallout pattern.

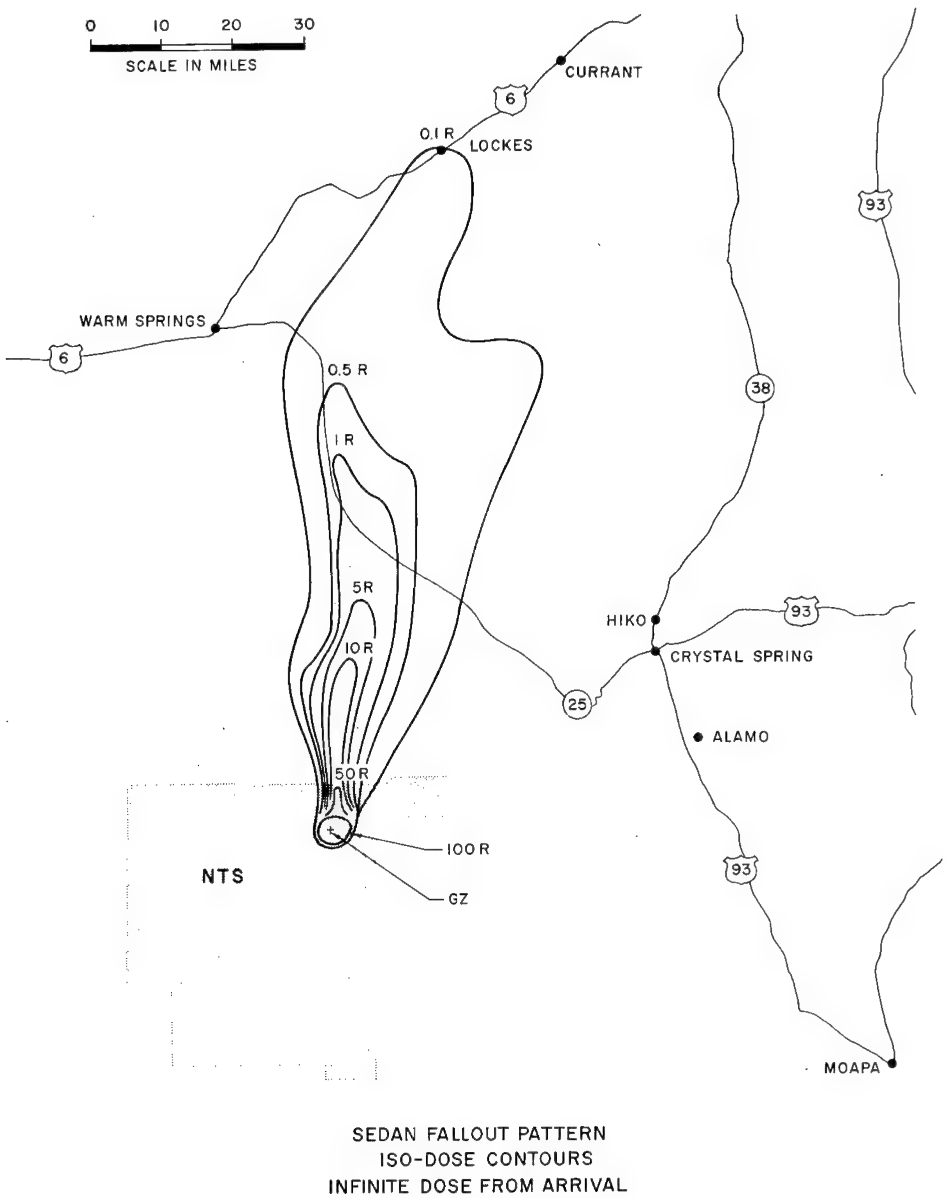

Fig. 8. Sedan integrated dose pattern.

BIOGRAPHICAL SKETCH OF AUTHOR

Captain Williamson is a native of Montana. He graduated from the United States Military Academy in 1956. He spent two years with an Army Engineer construction battalion in Orelans, France, and one year with an Army Engineer terrain intelligence detachment in France.

He spent two years at Iowa State University studying civil engineering and nuclear engineering. Since 1962 he has been working as a research associate in the Lawrence Radiation Laboratory Plowshare Division.

CHARACTERISTICS OF RADIOACTIVITY PRODUCED BY NUCLEAR EXPLOSIVES

John A. Miskel

Lawrence Radiation Laboratory, University of California
Livermore, California

ABSTRACT

The amounts and kinds of radioactivities produced by detonation of a nuclear explosive are dependent upon the specific design of the explosive. The two design extremes are a pure fission device, which will produce about 1.4 X 10^{23} fissions, and therefore about 2.8 X 10^{23} fission products, per kiloton of energy released, and a pure thermonuclear device which would produce no fission products, but would produce approximately 10^{23} atoms of tritium per kiloton. In both cases, interaction of escaping neutrons with the materials of the device itself, and with the surrounding media, could lead to further radioactivities.

The behavior and ultimate fate of the activities produced by the explosion depend on the composition of the medium in which the detonation occurs, the nature of the detonation, and the chemical species involved.

Some typical cases are described.

The production of energy by nuclear reactions results in the production of radioactive nuclei. Therefore, in considering the possible utilization of nuclear explosives for peaceful purposes it is necessary to be able to predict the expected activities, their amounts, and dispositions.

These activities may arise from two sources: (1) They may be a direct result of the energy producing nuclear reaction, or (2) they may be the result of the interaction of a product of that nuclear reaction with some other material. The obvious example of the first source is the fission products which arise in the fission process; the activation of the environmental materials by neutron capture is an example of the second source.

The total radioactivity resulting from an explosion depends, of course, on the detailed design of the device and on the specific environment in which it is detonated. The device can range from one where energy is derived solely from fission to, ideally, one whose energy is derived solely from thermonuclear reactions.

In the fission process, two fragments are produced with a total kinetic energy of about 170 MeV. After losing their internal excitation energy, these fragments undergo on the average about 3 beta decays before reaching stability. The six beta decays per fission release an additional energy of about 21 MeV divided between gamma rays (about 5 MeV), beta particles (about 6 MeV), and neutrinos (about 10 MeV). In addition, about 2.5 neutrons with an average kinetic energy of 2 MeV are emitted per fission. If one considers only the prompt energy from fission, about 180 MeV per fission, there are 1.46 x 10^{23} fissions per kiloton.

A kiloton of fission therefore produces 2.9 x 10^{23} fission fragments; these fission products are distributed in mass according to the well-known fission yield curve shown in Figure 1. Although the fission yield curves differ somewhat in detail for different fissioning nuclei, the general shape is the same for neutron-induced fission of U^{235}, U^{238}, and Pu^{239}. In the fission process the directly formed fragments are generally neutron rich. Therefore, they beta decay in order to become more stable. Since each beta decay process increases the nuclear charge by one unit, the chemical species changes with each decay. The physical-chemical behavior of the radioactivity

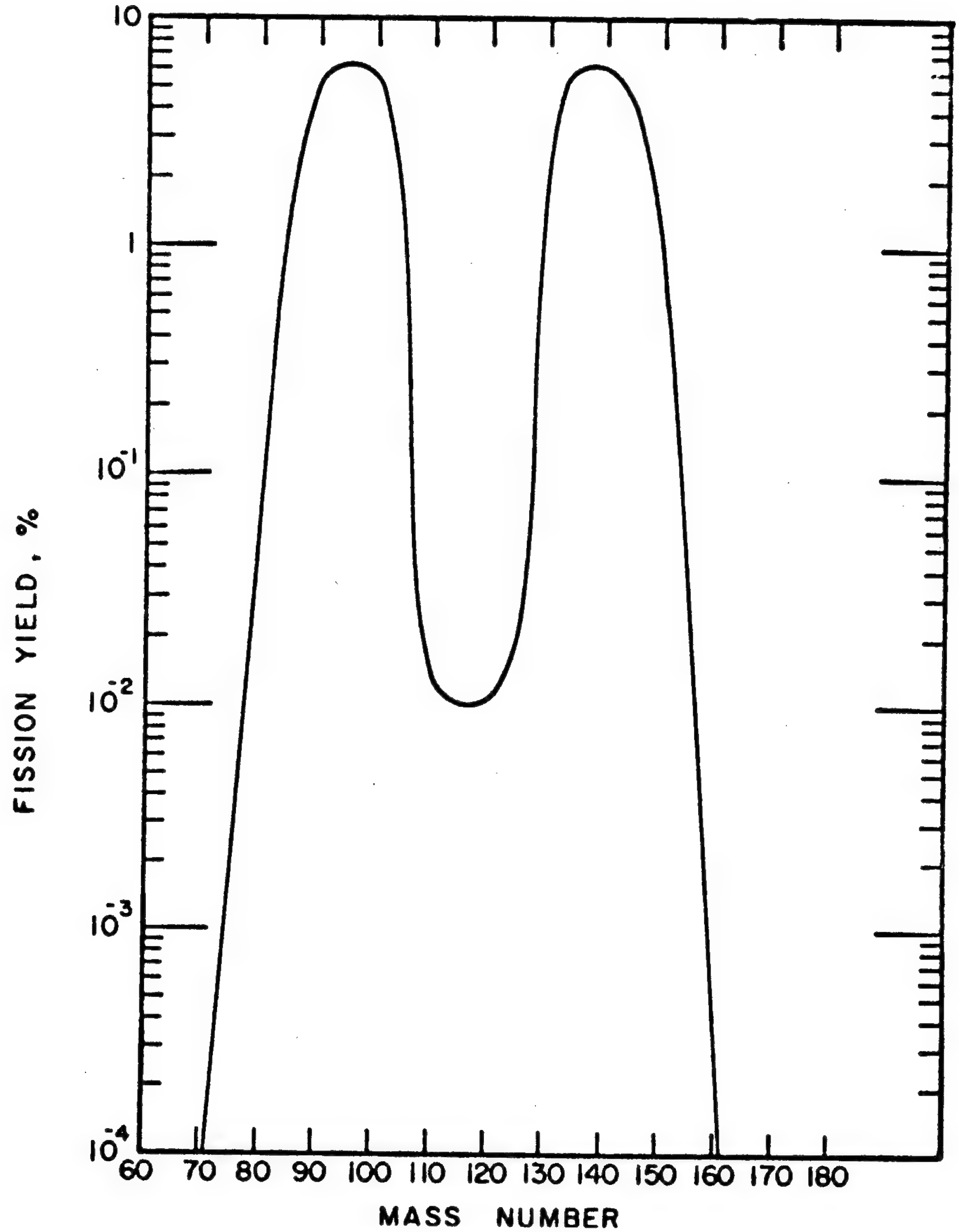

Fig. 1 Yield-mass curve for thermal fission of U^{235}.

resulting from fission is therefore strongly dependent on the time scale.

The excess neutrons produced in the fission process (about 1×10^{23} neutrons per kiloton) ultimately interact with matter, either the structural materials of the device or the materials of the immediate environment, and may result in the production of other radioactive species. In general these activities are produced by neutron capture (n, reactions) and decay directly to a stable isotope. Their chemical behavior is not, therefore, time dependent insofar as their radioactivities are concerned.

The fusion process, the energy source in thermonuclear devices, results in approximately ten times as many neutrons per kiloton as does

the fission process. These neutrons undergo reactions similar to those of the neutrons resulting from the fission process although the higher initial energy of these neutrons increases the possibility for (n, 2n) and (n, p) reactions. In addition to the neutrons, tritium is produced in relatively large amounts, on the order of 7×10^3 to 5×10^4 curies per kiloton of fusion.

Since the behavior of the fission products is dependent on their chemical nature, the percentage contribution of various elements to the total fission activity for several times is given in Table I. The various elements have been grouped into volatile, refractory, and intermediate.

In a cratering experiment the expected fate of the various activities can then be roughly pre-

Table I. Percent contribution of elements to total activity produced in fission.

	Element	1 sec	10 sec	30 sec	1 min	5 min	10 min	1 h	1 day
Volatile	Kr	3.6	3.8	5.0	5.8	4.3	2.5	4.2	-
	Xe	4.6	2.6	3.8	4.6	9.0	5.0	3.5	14
	Br	2.5	3.3	5.0	6.0	2.2	-	1.0	-
	I	3.4	4.0	6.0	7.0	3.5	3.5	7.0	16
	Te	1.9	2.7	2.5	2.0	3.5	9.0	14	3.9
	Se	1.3	1.5	1.0	-	-	-	-	-
	Total	17.3	17.9	23.3	25.4	22.5	20.0	29.7	33.9
Intermediate	Sn	1.3	1.1	-	-	-	-	-	-
	Sb	-	1.0	2.3	3.7	5.0	2.3	2.0	-
	Cs	9.5	7.0	7.0	7.0	8.0	8.0	8.0	-
	Rb	7.0	8.0	8.0	8.0	11.0	7.0	4.8	-
	Mo	-	3.0	6.0	6.0	5.0	7.0	3.0	4.2
	Tc	-	1.2	4.0	8.0	5.0	9.0	7.0	-
	Total	17.8	21.3	27.3	32.7	34.0	33.3	24.8	4.2
Refractory	Ba	11	7.0	2.6	2.4	8.0	9.0	8.0	1.1
	Sr	11	6.0	4.0	5.0	11	4.0	3.7	6.5
	Y	15	11	9.0	8.0	4.6	7.0	5.0	13
	Zr	12	12	7.0	3.5	-	-	-	8.6
	La	7.0	9.0	8.0	4.0	2.8	9.0	10	1.6
	Nb	5.0	10	12	11	8.0	5.0	6.0	18
	Ce	2.5	4.7	3.0	1.0	2.5	5.0	4.4	6.6
	Pr	-	1.7	3.7	5.0	4.6	3.7	5.0	2.9
	Nd	-	-	-	-	-	-	1.0	-
	Total	63.5	61.4	49.3	39.9	41.5	42.7	43.1	58.3

dicted by consideration of the time at which the debris is vented. The absolute amount of any species that emerges into the atmosphere will depend, of course, on the depth of burial and nature of the medium.

Some typical decay chains, which lead to isotopes of interest from a health and safety standpoint are:

$$Br^{89} \xrightarrow{4.4\ sec} \underset{(4.59\%)}{Kr^{89}} \xrightarrow{3.2\ min} Rb^{89} \xrightarrow{40\ sec} \underset{(4.79\%)}{Sr^{89}} \xrightarrow{54\ days} Y^{89}$$

$$Br^{90} \xrightarrow{1.6\ sec} \underset{(5.0\%)}{Kr^{90}} \xrightarrow{33\ sec} Rb^{90} \xrightarrow{2.7\ min} \underset{(5.77\%)}{Sr^{90}} \xrightarrow{28\ yr} \underset{(5.77\%)}{Y^{90}} \xrightarrow{64\ h} Zr^{90}$$

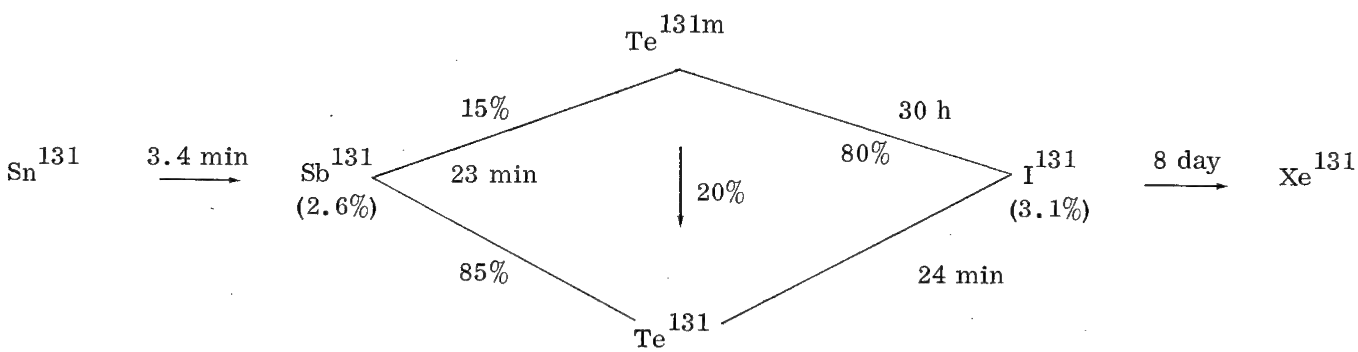

(The percentages in parentheses are the cumulative fission yield to that point in the decay chain.)

Thus, in a detonation that ruptured the surface to produce a crater in a matter of a few seconds, one would expect the Sr^{89} and Sr^{90} to behave in a manner of their volatile precursors and be enriched in the vented debris. Iodine^{131}, with its precursors, would behave in a manner more characteristic of the intermediate groups than of the volatiles.

The effect of the medium in which the detonation occurs on the fate of the activities is tied to the chemical stability of the compounds that might form. In the extremely high temperature existing during the explosive phase, one expects almost all species to exist as unassociated ions. During the early cooling phases, if the debris is exposed to the atmosphere, the stable oxides probably form, or perhaps the nitrides. If the cooling occurs while the debris is still contained, the system may be in a reducing atmosphere leading to the formation of elements and hydrides rather than of oxides and nitrides. The subsequent radioactive decay, if it occurs after venting, may result again in an oxide, or, if the density of inert debris is sufficiently high and the chemical affinity large enough, reactions with the media may occur resulting in silicates, aluminates, etc., depending on what is available. Another possibility is that an atom, after being formed by the decay of its parent, will collide with some inert material and stick to the surface. The real behavior is therefore quite difficult to predict with any degree of precision with the available data.

The behavior of the activities resulting from neutron capture reactions can be predicted in somewhat the same fashion as the fission products, but no consideration of the decay chains is necessary in general.

If we consider a device designed for a Plowshare application with a total energy of 1 megaton and assume it to be 1% fission and 99% fusion, then we can make some estimates of the various activities produced, and can speculate as to their ultimate fates.

The fission involved would be 10 kilotons, with the associated 2.9×10^{24} fission products and about 10^{24} neutrons. The fusion would produce about 10^7 curies of tritium and 1.4×10^{27} neutrons.

As a first approximation, we can assume that the device is surrounded by a nonactivating neutron absorber, such as boron, which reduces the emergent neutron flux by a factor of 100. The total number of neutrons out is then about 1.4×10^{25}.

The activation products resulting from the neutrons depend on the medium; Plateau Basalt, the composition of which is given in Table II, has

Table II. Composition of Plateau Basalt.

Oxide	SiO_2	TiO_2	Al_2O_3	Fe_2O_3	FeO	MnO	MgO
wt%	48.8	2.19	13.98	3.59	9.78	0.17	6.70
Oxide	CaO	Na_2O	K_2O	H_2O	P_2O_5		
wt%	9.38	2.59	0.69	1.80	0.33		

Table III. Percentage of neutrons captured by various elements in Basalt.

Element	Si	Ti	Al	Fe	Mn	Mg	Ca	Na	K	H	P
% neutron capture	12	14.8	2.8	43.4	2.5	9.7	6.7	4.1	1.3	2.8	0.08

Table IV. Neutron activation products in basalt.

	Nuclide	Half-life	Radiations	Curies at t_O
Activation Products	Si^{31}	2.62 h	β^-, 1.47 MeV γ, 1.26 MEV (~0.1%)	7×10^7
	Fe^{55}	2.7 yr	γ 0.006 MeV	7.5×10^5
	Fe^{59}	45 day	β^-, 0.27, 0.46 MeV γ, 1.1, 1.28 MeV	3.8×10^4
	Mn^{56}	2.58 h	β^-, 2.8, 1.0, 0.6 MeV γ, 0.85, 1.81, 2.13 MeV	8.4×10^8
	Ca^{45}	165 day	β^-, 0.255 MeV no γ	4.3×10^4
	Na^{24}	15 h	β^-, 1.4 MeV γ, k, 37, 2.76 MeV	1.9×10^8
	K^{42}	12.4 h	β^-, 3.55 MeV, 1.99 MeV γ 1.53 MeV (~20%)	2.8×10^6
	P^{32}	14.3 day	β^-, 1 7 MeV no γ	1.8×10^5
Fission Products	Sr^{90}	28 yr	β^-, 0.45 MeV no γ	1.8×10^3
	Mo^{99}	66 h	β^-, 1.2, 0.41 γ, 0.140, 0.75	6.7×10^6
	I^{131}	8 day	β^-, 0.61 MeV γ, 0.36 MeV	1.28×10^6
	Nd^{147}	11 day	β^-, 0.81 MeV γ, 0.09 MeV	7.5×10^5

been used to calculate the activities to be expected from the detonation of a device such as we have assumed.

The fraction of the escaping neutrons reacting with any element in the surrounding medium can be calculated on the assumption that the neutrons are essentially thermalized before reacting and then using the known thermal neutron capture cross sections. In Table III are given the percentages of the neutrons captured by the various elements in basalt, calculated in this way and assuming that oxygen does not contribute. In a medium with low water content, such as basalt, it might be better to use a somewhat higher value than thermal for the average neutron energy, at the time of capture. However, the relative cross sections, and therefore the fractions of neutrons captured, do not change drastically in most cases.

In basalt, several of the principal constituents lead to stable or quite short-lived isotopes. Thus, titanium, which accounts for 14 to 15% of the neutrons, which leads to a 6-minute activity; aluminum, accounts for 6%, a 2.3-minute activity; and magnesium accounts for 1% and has a 10-minute activity.

The predominant activities, with half-lives greater than a few minutes, produced by neutron capture in basalt are listed in Table IV. The total activities are based on 1.4×10^{25} neutrons being captured in the medium.

For comparison, the numbers of curies of several fission products produced by this device are also indicated in Table IV.

In addition to the isotopes listed in Table III, several of the light elements may undergo (n, α) or (n, p) reactions to produce activities. This is particularly true for the thermonuclear neutrons; considerable Na^{24} may be produced by Al^{27} (n, a), some Na^{22} by Na^{23} (n, 2n), and some scandium isotopes from titanium. The steels and other construction materials may produce other species such as Co^{60}, Co^{57}, Co^{58}, and Mn^{54}.

The amounts of activities tabulated above are the totals produced by the device. In a cratering-type application, only fractions of the amounts produced would be vented into the atmosphere. The specific fractions will depend on the chemical behavior of the substance involved. Using the crude classifications of Table I, it would appear (for a venting time of a few seconds) that even if one assumed all of the "volatiles" and half of the "intermediates" were in the atmosphere, and remained there after the fall-back of the major part of the total mass vented occurred, this would be less than one-third the total fission product activity produced. It would be expected that, after radioactive decay, the less volatile nuclides formed would be scavenged by the particulate matter as it falls out.

The induced activities from basalt, except for the sodium, potassium, and phosphorus, are "refractory."

The distribution of activities has two immediate consequences. One is related to the reentry problem where, in order to do further construction or to utilize the results of the explosion it is necessary for people to return to the active area. The second is related to the problem of introducing the activities into the biosphere.

The first problem is concerned primarily with the level of γ radiation, whereas all types of radiations are of interest for the second problem. A considerable amount of experience exists on prediction of downwind deposition and of radiation fields from clouds of known composition. There is a more limited experience in determining cloud composition from partially contained detonations.

Studies are under way at Livermore to investigate the system more thoroughly. In any forthcoming Plowshare experiments, a large number of measurements will be made in order to document the distribution of a representative variety of radioactive species. In addition, laboratory experiments on thermodynamic properties of the various elements are being conducted to enable better predictions of the high-temperature reactions and condensations phenomena to be made.

BIOGRAPHICAL SKETCH OF AUTHOR

John A. Miskel received his B.S. in Chemistry, from the University of California, Berkeley, in June 1943, and his Ph.D. in Chemistry and Physics, from Washington University, St. Louis, Missouri, in 1949 (Gladys Hermanns scholar; AEC Fellow). His professional experience is as follows: 1943-1946 Los Alamos Scientific Laboratory: Neutron excitation functions, heavy element chemistry, fission process studies. 1949-1955 Brookhaven National Laboratory: High-energy nuclear reactions, atomic effects of nuclear decay, nuclear decay schemes. 1955-Lawrence Radiation Laboratory, Livermore: Radiochemical diagnostics, nuclear spectroscopy, investigations of the fission process, excitation functions, studies of debris from nuclear devices. 1961 OEEC Sr. Visiting Research Fellow, Nobel Institute of Physics.

HAZARDS TO MAN FROM RADIOACTIVITY

John W. Gofman

Lawrence Radiation Laboratory, University of California
Livermore, California

ABSTRACT

Potential biological hazards, directly to man or indirectly via biospheric members involved in man's food chains, represent a major consideration in engineering applications of nuclear explosives. Indeed it is possible that the biological problems presented are more difficult of solution than will be many of the technical engineering problems. Production of a variety of radioactivities is an inevitable concomitant of the utilization of nuclear explosives. To some extent there is an element of choice based upon nuclear explosive design as to which chemical elements are represented among the radioactivities produced. Development work may enable reduction in production of certain radioactivities, but it is unlikely that order-of-magnitude reductions can be achieved easily. Therefore, it is a matter of great moment to have realistic guidelines concerning potential biological hazards so that the engineering problem can be evaluated. It is the purpose of this discussion to consider the basis for whatever guidelines currently exist, the uncertainties involved, and the kinds of information that are required if such guidelines are to be made more definitive.

INTRODUCTION

This Symposium is dedicated to the subject of Plowshare. It is appropriate, therefore, that our considerations be addressed to those potential hazards of radioactivity to man truly pertinent for immediate or long-range Plowshare objectives.

The technological, engineering problems requiring solution, for projects such as nuclear excavation, appear clearly manageable. Concern over potential biological hazards associated with such projects represents a more formidable hurdle. One may justifiably inquire, "Do we not have definitive radiation standards to guide us in assessing potential biological hazards and can we not live within those standards?" It is our purpose now to evaluate these pertinent questions as realistically as possible.

If this discussion of the question of radiation standards and their reliability leaves more questions than it provides answers, the conclusion is part of a broad dilemma facing society today. This dilemma arises from the fact that technological advances in the physical and engineering sciences have made a variety of projects feasible, while the biological and medical knowledge requisite to assess "biological cost" is far from adequate. However, the field of nuclear energy is not unique in this regard, for in a variety of other ways we now can and do make willful changes in man's environment without any real evaluation of the short or long range effects upon <u>man.</u>

The radiation guides, or standards, pertinent for Plowshare are painfully uncertain. Why and how they are uncertain must now be considered in detail.

"BIOLOGICAL COST" VERSUS "BENEFIT" CONCEPT

It has become fashionable in recent years to state that we must weigh the hazards to man from ionizing radiation against the benefits to be anticipated from exposure to such radiation. This highly reasonable approach makes good sense so long as we deal in the abstract. It falters badly when we look for the masses to be placed in the balance pans. Undoubtedly a major step forward will have been taken if <u>concrete</u> evaluations of <u>benefit</u> were given serious attention. Otherwise, no real comparison of hazard with benefit is

possible even when the potential hazard is truly known.

Categories of Hazards

The potential hazards of radiation to man may be subdivided into three major types:

(a) Those arising from high radiation doses delivered at a rapid rate.

(b) Those arising from high radiation doses delivered at a slow rate.

(c) Those arising either from low doses of radiation delivered rapidly or from low doses delivered over a very long period of time (years).

We can immediately dismiss consideration of (a) and (b) from this discussion since Plowshare projects involving such exposures on a planned basis will simply not be considered. The evidence is quite firm, and known to everyone, that high doses of radiation delivered rapidly can be lethal to humans. While the evidence is not so clear-cut for high total doses delivered over a protracted period, no serious consideration of Plowshare programs involving such radiation is contemplated.

Plowshare programs are concerned with the possibilities that involve, or may involve, delivery, rapidly or slowly, of low total doses of ionizing radiation to a small segment of the human population. Boldly, but frankly, stated, we have no direct, valid information on the subject of injury to be anticipated in humans either for the generation receiving such radiation or for their descendants. There may be a net biological cost; there may be almost none or none. Dicta, in this area, are commonplace, such as "Any radiation above natural background levels is harmful." Valid evidence to back such authoritative statements does not exist--but, on the other hand, valid evidence contradicting such dicta is also lacking.

It is of interest to point out here that man has, in all likelihood, always lived under conditions exposing him naturally to several sources of ionizing radiation and that considerable variation exists in the intensity of such sources over the globe. It can be asked immediately whether or not valuable answers might come via comparisons of populations residing in areas of high versus low background radiation levels. For example, on the Colorado plateau humans experience approximately 1-1/2 times the background levels as do those residing in sea level communities. Further, in regions such as Kerala in India background radiation levels are more than 15 times as high (due to thorium-bearing sands) as they are in other regions of India. Comparisons between regions of high and low natural backgrounds are highly desirable, but are, at best, extremely difficult to execute in a meaningful fashion. Clearly, there is no gross evidence that residence (even over several generations) upon the Colorado plateau is more hazardous than is residence in San Francisco or New York City. But such gross evidence is not adequate for a significant evaluation of the low-dose radiation hazard question.

Since leukemia and bone cancer are known as possible sequelae of high-dose irradiation in man, comparisons have been made of the leukemia and bone cancer incidence rate between San Francisco and Denver. The results indicate that San Francisco (with 2/3 of the natural background radiation level of Denver) has approximately 1-1/2 times the incidence rate of such diseases compared with Denver. Crudely, and in all likelihood falsely, such results could be used to argue that low-dose radiation might actually be protective against leukemia and bone cancer. The real point deserving emphasis here is that the comparison should not have been made at all, for it lacks all the elements of a well-controlled study. If every pertinent feature of the population samples in the two areas were identical, and if every environmental factor (aside from radiation level) were identical, and if medical diagnosis and disease reporting were identical in the two areas, then a valid comparison might be made. All of the "if" provisos remain unevaluated and hence the answers obtained must remain suspect and unsatisfactory. In the Kerala, India area the problem of appropriate reference control population samples may prove even more difficult, although studies of the area are underway by the Indian government.

Inappropriate comparisons should be condemned as a potential source of information no matter what the results may be. It is regrettable that proponents of one or the other side of the radiation hazard question have, in the past, been willing to make opportunistic use of invalid information.

Other Inappropriate Comparisons

There are pitfalls of other kinds inherent in poorly conceived assessment of the low-dose radiation hazard question. It is particularly crucial that those interested in possible Plowshare projects appreciate such pitfalls. For, if a "favorable" result attends a particular invalid approach ("favorable" being equated with minimal radiation hazard), the mirage created should and will soon disappear under critical review of the evidence. On the other hand, credence lent to an "unfavorable" result of an invalid approach can, until criticized, inhibit valuable contributions Plowshare programs may make to man's welfare. Examples of both types of invalid approach are the following:

The "Favorable" Result of an Invalid Approach

Population samples can be identified where all the members have received fairly large doses of total body irradiation, e.g. 100-300 rods, including subjects having received radiation therapy, the Rongelapese, and others. Let us exclude immediate radiation effects and consider the long-term effects (of consequence for Plowshare) such as leukemia or cancer induction. The statement can be made that the failure to discover excessive cancer or leukemia in certain of these population samples "proves" that even fairly large radiation doses are without long-time adverse effects. Suppose, however, that other evidence leads to an expectation of excessive leukemia at a rate of one case per 10,000 exposed subjects per year. If the total population sample under observation is 500 persons, then an incidence rate of 1 per 10,000 per year leads to an expectation of an excess of 0.05 cases per year in this small population sample (500 subjects). Patently, there exists no way to observe such an excess incidence rate in a population sample of 500 persons. Thus, the apparently "favorable" absence of excessive leukemia under such circumstances is no answer at all.

The "Unfavorable" Result of an Invalid Approach

This phenomenon has arisen where only part of the evidence is considered. As an illustration, the evidence currently available indicates that leukemia incidence has been steadily rising for some three decades (even after correction for improvement in the medical reporting of disease). Where one fallaciously to compare such incidence post-atom bomb tests with that before large-scale nuclear energy release, the conclusion could be drawn that atom bomb testing and fallout had produced the increase in leukemia incidence rate. However, examination of all the evidence would have indicated precisely the same trend qualitatively and quantitatively in the pre-atom bomb period. Thus, such evidence is, again, no evidence with respect to the radiation hazard question.

SPECIFIC TYPES OF RADIATION HAZARD OF CONCERN TO PLOWSHARE PROGRAMS

As mentioned previously, two potential types of radiation exposure are of immediate concern for Plowshare; (a) low doses of radiation delivered rapidly and (b) low doses of radiation delivered in small increments over a protracted period. In either such case the acute radiation syndrome is irrelevant. Of real concern are two types of so-called delayed effects. First is the possibility of transmission of radiation effects to offspring, from one or both exposed parents. Such heritable effects are classed as genetic, and, in the main, are currently considered to arise only from radiation delivered either to the testis of the male or the ovary of the female. All other possible radiation effects are grouped under the term "somatic" effects, meaning those produced directly in the individuals actually receiving the radiation. Foremost among the somatic effects are two, radiation-induced aging and the induction of malignant disease (including disorders such as leukemia).

Indeed it may well be that both these somatic effects are part of a single one. What is known of radiation-induced aging seems not to represent any specific effect but rather an acceleration of several phenomena that occur spontaneously without added radiation but which occur at a lower rate. Aging is presently defined by many as a change characterized by an increased statistical risk of occurrence of a variety of major causes of death due to so-called degenerative diseases. Since malignancy is one such cause of death it is appropriate to consider it within the aging framework. The phenomenon of "life shortening" often

referred to as a late effect of radiation is also an expression of the aging parameter as here defined. Some have equated a particular quantity of absorbed ionizing radiation energy with a loss of some number of days, weeks, or months of life span. This really has meaning only in so far as there occurs an increased statistical risk of occurrence of one of the degenerative diseases.

One popular concept holds that somatic and genetic effects of radiation are really expressions of a single phenomenon occurring in different groups of cells. The phenomenon suspected is alteration of the molecular architecture or composition of the information-bearing nucleic acids of cell nuclei. Where such alterations occur in reproductive cells (either of the ova line or the sperm line), we can experience genetic effects. Where the alterations occur in body cells other than reproductive cells, we can experience somatic effects. There exist alternative explanations to this unifying one, and only additional evidence can resolve the question of mechanism of effect.

Current concepts are that irradiation effects upon a particular set of cells requires actual delivery of energy to those cells, either by direct hit effects or by secondary products of the irradiation, such as free radicals or excited molecules. One special concern, still compatible with effect at the site of irradiation, is over the impact of transmutation of elements within biological macromolecules. Biological integrity is almost certainly determined by highly specific chemical structure within a variety of macromolecules, some, of molecular weights in the multi-million range. A transmutation of a C^{14} atom into an N^{14} atom through β-decay leaves a new macromolecule, wholly aside from absorption of decay energy. The extent of information loss or alteration resulting from the carbon being replaced by nitrogen is part of a complex, highly intriguing problem, probably not characterized by a single solution.

Indirect effects due to irradiation at a distance from the cells can occur. One mechanism for such effects is the result of existence of endocrine loops in highly organized species such as mammals. Thus secretions of the adrenal gland do affect the pituitary gland; the converse is also true. For our present purposes the problem is large and complex even excluding the additional possible complexities due to this or other potential types of indirect effect.

THE GENETIC EFFECT

Potential genetic damage via irradiation of reproductive cells (sperm line or ova line) must receive prime consideration by Plowshare scientists. The genetic effect may prove to represent the major limiting biological factor in peaceful applications of nuclear energy. It has been recommended by authoritative bodies that the totality of man-made radiation burden to the reproductive tissues of man should not exceed the equivalent, per generation, of that delivered from natural background sources for population-wide exposures. This amounts to an exposure of the order of 0.1 rad per year to the reproductive tissues, a guideline very restrictive in comparison with occupational guides. Further, this type of recommendation implies that whenever part of this total dose has been compromised, as by weapons testing, reactor installations, or by other projects, the remainder allowable for possible Plowshare activities is correspondingly reduced during that generation. So restrictive are the implications of these recommendations and so readily does codification make revision difficult, it is pertinent here to consider carefully the validity of our criteria with respect to the genetic effects of irradiation.

Some Major Unsolved Problems Concerning Genetic Effects

Linearity Concept

For many years there existed a dogma, even without any data on man or mammals, that gonadal irradiation produced mutations in proportion to the total dose of radiation, irrespective of the rate at which the radiation is delivered. Further, such dogma generally held that one could think of concepts such as a "doubling dose" for mutations in reproductive cells. The implication inherent in this concept is that the numerous gene loci capable of undergoing mutation are of equivalent sensitivity to radiation. Important researches of the Russells and their co-workers at Oak Ridge have had major unsettling effects upon such assertions in genetics and have major implications

for criteria concerning "acceptable" doses to reproductive tissues.

Among the crucial contributions of the Russells to this problem area are the following:

(1) Mutation frequency per unit dose of radiation is much higher for the mammal (mouse) than for drosophila (fruit fly), which has previously represented the basis for extrapolations to man.

(2) There does exist a major effect of dose rate on mutation frequency, an effect differing markedly between the two sexes. For the male mouse dose rates of 90 r/min. produce in spermatogonial cells (those cells of real consequence for long-term risk) three to four times the mutation frequency produced by the same total dose delivered at 0. 009 r/min. Further reduction in dose rate, to 0. 001 r/min, did not apparently further reduce the mutation frequency in the male mouse. For the female mouse the oogonia of the ovary are even more affected by dose rate than are the spermatogonia in the male. In the female, major alterations in mutation frequency occurred between dose rates of 0. 009 r/min. and 0. 001 r/min., with the possibility open of still lower frequencies at lower dose rates.

(3) Both in the male and female mouse there exists a great difference in susceptibility of different gene loci to mutation from radiation, factors of the order of 30 fold difference in sensitivity having already been determined.

(4) If the initial post-irradiation period is excluded, there is no evidence that mutation frequency (as expressed in offspring) decreases with time past the irradiation period. This suggests that spermatogonia bearing mutated genes are not preferentially weakened. The implication is, of course, that if a particular frequency of mutations has been induced in the spermatogonia, that frequency may be fixed during the reproductive life of the particular animal.

For man, there are several critical questions raised which thwart us in the effort to assign a value to the genetic hazard of radiation. Among these questions are the following:

(1) Is the average mutation frequency per unit radiation dose in man more like that in the mouse than in the fruit fly (a fifteen fold difference in sensitivity existing between the later two) - or is it grossly different from both?

(2) Is the range of variability in sensitivity of individual gene loci greater in humans or less than in the mouse, where the Russells have already observed a 30-fold range in sensitivity?

(3) Do mutations of greater severity in effect upon the individual have a greater or lesser radiation sensitivity than those of lesser severity?

(4) Do human males differ from females in mutation frequency per unit does of radiation and do the two sexes differ (as in the case of the mouse in response to dose rate?

(5) Is it true for man, as it appears to be for the mouse, that spermatogonia with mutations tend to survive and divide uninfluenced by the mutated genes they bear? If this is true, one avenue of "repair" of genetic damage becomes unavailable - namely, loss of potentially defective spermatogonia from the reproductive process.

There is another area, as yet unsolved, of great pertinence to the human genetic problem. Most geneticists agree that a high proportion of mutations are deleterious in the "homozygous" state (where the particular mutant gene is provided to the offspring from both parents). Some of these genes in the "heterozygous" state (where only one parent provides a mutated gene) may confer a disadvantage to the individual. In some known cases, for the human, the heterozygous state, for particular genes, under certain environmental conditions, confers a distinct advantage to the individual. Thus, for example, the gene for "sickling" trait, an abnormality leading the individual to produce a biochemical variant of the hemoglobin molecule, differing from normal hemoglobin by one amino acid in the protein chain, can provide an advantage in the heterozygous state. In areas where malaria is endemic, such heterozygous individuals have a greater chance of surviving, as a result of increased resistance to malaria than do individuals who produce only normal hemoglobin. There is a severe price exacted for such protection against malaria in that individuals homozygous for the sickling trait succumb to a fatal disease known as sickle-cell anemia. This price exacted of a small number

of individuals provides increased survival probability for a much larger number of persons.

This effect is known as the "heterotic" effect and is, of course, highly dependent upon environmental circumstances. Its existence makes us skeptical of pronouncements that mutations, in their net effect, are always bad, in either the homozygous or the heterozygous state. Currently we are so naive in this area that we are ill able to appraise the extent, for a particular environment, to which the heterozygous state we have for so many recessive genes may facilitate our ability to cope successfully in our struggle for survival. Furthermore, in an era like the current one, time scales of alteration of man's effective environment are being shortened at a rate never before envisioned. Which aspects of our inheritance will be advantageous or disadvantageous under these rapidly changing environmental circumstances (shrinking of the globe, population migrations, introduction of new materials) can hardly be delineated. Indeed the pace of environment alteration currently being practiced by the human race, a pace which no one seems able to regulate on rational grounds, may well make such issues as low dose radiation hazard trivial by comparison with others. This, however, by no means should be misconstrued as any effort to minimize the low dose radiation hazard problem.

SOMATIC EFFECT

If the state of our knowledge concerning effects transmissible to future generations is unsatisfactory, the corresponding state of knowledge concerning somatic effects is hardly better - and is possibly much worse.

It was mentioned above that one view of the mechanism of effect of radiation upon the generation receiving the radiation is that of mutation of cells other than reproductive cells. Various types of cells in the adult, exclusive of reproductive cells, retain the capacity of division and can undergo mutations transmissible to the descendants of those cells. Cancer and other degenerative diseases have been ascribed to such mutations in somatic cells, although the supporting evidence for this is highly controversial.

At the time when it was believed that no dose-rate effect existed for genetic mutation in reproductive cells, it was glibly stated by some that no such dose rate effect would be anticipated for corresponding somatic mutations. The corollary of such an assumption was that sequelae of somatic mutation would occur in proportion to the total dose of radiation, irrespective of dose rate. But a dose-rate effect has been established for the genetic effect and it has been established for at least certain somatic mutations in the mouse. How the dose-rate effect varies with cell type, with species, with phase of cell cycle -- all these remain unanswered questions. And whether or not somatic mutations have any causal role in acceleration of aging (including cancer induction) is simply speculative at this time.

Cancer induction in humans or in experimental animals still represents a phenomenon only very poorly understood. Fragments of enormously valuable information are available, but no consistent picture has emerged. In this area alone some major questions still unanswered are the following:

(a) Both for spontaneous and inducible malignancies in mammalian species there exist inherited differences in susceptibility. In certain mouse strains specific cancer-producing hydrocarbons (such as 7, 12 - dimethylbenzanthracene) produce regularly a very high frequency of cancer of the breast (total body irradiation also being capable of inducing breast cancer). Why the breast is so inordinately susceptible to this effect in particular mouse strains is not clear. It is clear, however, that heredity is of great importance in conferring susceptibility, for the same dose of the same hydrocarbon does not exert this cancer-producing effect in other mouse strains. Furthermore, Huggins has shown the inheritance of susceptibility is a dominant trait (only one parent needs to provide the gene for "susceptibility" to render the offspring susceptible). Crossing of pure resistant strains of mouse with susceptible strains produces susceptible offspring, whether the father or mother is from the resistant strain. Extrapolation of such knowledge to other cancers, to other cancer-producing agents, to other species is currently impossible.

(b) All the studies of dose-rate dependency for malignancy induced by a particular total radiation dose are equivocal in the low dose ranges, which are those of greatest interest. Even if

somatic mutation is a basis for cancer production, it is not clear how many events per cell are required - an issue with major implications for the quantitation of risk versus dose and of the effect of dose rate. Further, sensitivity per somatic gene locus is unknown.

(c) Essentially all of the good evidence for humans as well as for experimental animals indicates that induction of leukemia or cancer occurs when doses exceed approximately 1/4 or 1/5 of that required for lethal effects upon a high proportion (50%) of subjects acutely. Much evidence concerning such high doses indicates that chemical or tissue architecture is either temporarily or permanently disrupted. For example, in the blood-forming system, the lymphocytes, closely involved in the immunity problem, do show major effects from such high doses of radiation, but these effects cannot be safely extrapolated to low doses. The evidence concerning cancer production indicates that tissue state, immune responses, and possibly virus activation may be at the root of malignancy induction. If these should be dominant influences, then unless the radiation dose is of sufficient intensity as to produce tissue architectural alterations, alterations in immune responses, or some combination thereof, there may possibly exist no relation between low total doses of radiation and malignancy induction or even between high total dose, adequately protracted in delivery, and malignancy induction.

These difficult questions, whether acceleration of degenerative effects in general, or cancer production in particular represent cellular responses, tissue architectural responses, or alterations in immunity mechanisms are not settled for the mouse or any other species. And even if we were willing to extrapolate to man from other species, the data for extrapolation are lacking.

PROCEDURE FOR PLOWSHARE PROGRAMS IN THE ABSENCE OF DEFINITIVE INFORMATION CONCERNING RADIATION EFFECTS IN MAN

(1) Above all, it is important <u>not</u> to misinterpret the absence of definitive information concerning low-dose radiation effects upon man as being equivalent to <u>absence of effect</u>.

(2) Since no evidence has yet been produced indicating a more drastic effect per unit dose at low total doses or at low dose rates than at high total doses or high dose rates, the conservative approach of linear extrapolation will provide a reasonable upper limit upon the hazard potential. It is almost certain that codified regulations will be based upon such extrapolations until and unless definitive information replaces extrapolation.

(3) It can be expected, in the absence of definitive information that regulations may from time to time as fears rise and fall concerning the margin of safety required when dealing with the uncertainties inherent in an extrapolated estimate of hazard. Rather than to chafe under such shifting regulations, Plowshare technologists should best devote their creative energies toward any reasonable breakthroughs that minimize access of radiation and radionuclides to the biosphere. Such countermeasures should be considered for every step of the pathway to man and should start with the nuclear explosive.

(4) Biology should be encouraged and assisted to endeavor to close the gap between biological understanding of man and his environment and the explosively-growing technological capability of altering that environment. The biological and medical progress required to assess accurately the impact of Plowshare programs upon man is not parochial or drudgerous. Rather it represents the kind of progress required to cope with man's health and welfare, irrespective of nuclear explosives, in the world of today and tomorrow.

REFERENCES

An excellent recent symposium was dedicated to questions such as those considered here. The reader will find, therefore, that many of the issues are discussed in detail in those references.

The Present Status of the Radiation Hazard:

1. "Somatic Hazards of Radiation" Brues, A. M. Proceedings of the American Philosophical Society, 107, pp. 1-4, 1963.
2. "The Late Effects of Radiation" Curtis, H. J. Ibid, 107, pp. 5-10, 1963.
3. "Genetic Hazards of Radiation" Russell, W. L. Ibid, 107, pp. 11-17, 1963.
4. "Exposure Rates and Protective Measures Against Radiation" Warren, S. Ibid, 107, pp. 18-20, 1963.

BIOGRAPHICAL SKETCH OF AUTHOR

John W. Gofman is Director, Bio-Medical Research Division, Associate Director, Lawrence Radiation Laboratory, Livermore. He received his A.B. in Chemistry from Oberlin College in 1939, his Ph. D. in Chemistry from the University of California in 1943, and his M.D. from the University of California in 1946.

He served as Group Leader of the University of California Plutonium Project from 1942 to 1944, and was an intern at the University of California Hospital from 1946 to 1947.

Dr. Gofman's areas of research have been radiochemistry, macromolecules, lipoproteins, arterisoclerosis, trace element determination, and x-ray spectroscopy.

AIR BLAST FROM CRATERING EXPLOSIONS

Jack W. Reed

Sandia Laboratory
Albuquerque, New Mexico

ABSTRACT

Shock wave overpressure versus distance relations and scaling laws for spherical explosions in air are reviewed. For cratering bursts a modified source wave is proposed, with a strong wave shot upward and a reduced wave emitted horizontally along the ground. Some energy originally directed upward is diffracted into horizontal propagation so that at large distances there appears to be less relative amplitude attenuation than is observed close-in.

Amplitude attenuation increases with scaled depth of burst, varies with certain material characteristics around a burst, and appears to decrease with increased yield. Results from Sedan, a 100-kiloton explosion near optimum depth for cratering in desert alluvium, showed that blast pressure amplitudes were about 20 percent as large as would have been expected from the same yield but burst in free air.

Atmospheric temperatures and winds may cause refractive focusing of blast waves and greatly extend the normal range of light damages to windows, plaster, etc. Surface temperature inversions may enhance blast pressures for 20 to 30 miles, jet-stream winds may focus waves out to 100 miles and ozonosphere conditions at 100-to 150,000-feet altitudes may cause light damage several hundred miles from megatonclass cratering explosions.

Relations between small overpressures and nuisance damages which they may cause are not clear, but some large windows have been reported broken with as little as 0.03-psi overpressures. The noise may be audible or even startling with 0.002-psi overpressure, and depends on shape of the pressure-time trace and wave frequency.

INTRODUCTION

One of the several possible hazards from large nuclear excavation projects is air blast which may, on occasion, propagate great distances with damaging intensity. At tens or hundreds of miles range these damage levels are not severe enough for military use.

Relatively weak blast waves can alarm people, however; they can break windows, crack plaster, and create considerable nuisance—without actually destroying any buildings or killing any people.

If a hemispheric shock wave were assumed from a 10-megaton cratering burst, some very large windows might be broken as much as 80 miles away. For comparison, the same yield, but air burst, would give the same effects at 300 miles.

*This work was supported by the U. S. Atomic Energy Commission.

Blast propagation through the atmosphere is not so uniform, however, because our atmosphere's stratifications of temperatures and winds make it serve as a distorting lens for sound and blast radiations. In result, some areas get much less and some areas may get much more blast intensity than the hemispheric wave assumption would indicate.

We have worked on this problem at Sandia Corporation since 1951, both at the Nevada Test Site and on Pacific tests, to assure public and employee safety both on and off the test sites. We have made many measurements, derived many explanations for the results, and published a large number of reports about long-range blast propagation from yields ranging from 1 pound of high explosive to several megatons and burst at levels ranging from deep underground nearly to outer space. A list of selected unclassified references is attached to this paper.

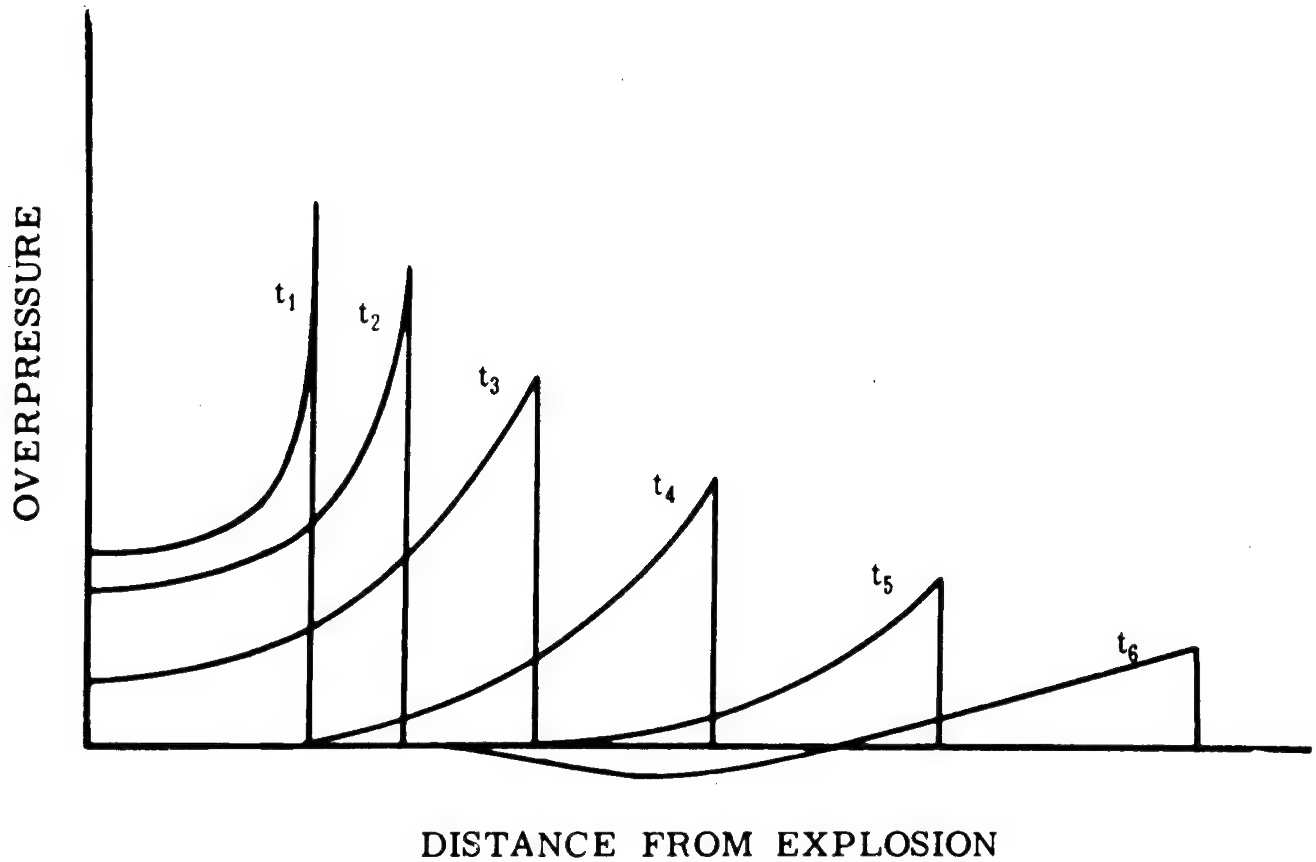

Fig. 1. Variation of overpressure with distance at successive times (from The Effects of Nuclear Weapons).

We do not have all the answers with accuracies ordinarily expected by the engineering profession. Like weather forecasts, our predictions are still subject to considerable error. This factor must be considered in the safe application of blast predictions. We are, however, usually able to say that a factor of two error range will encompass the results—when the inputs to our prediction calculations are less than an order of magnitude outside the range of our experience.

BASIC AIR BLAST AND SCALING LAWS

Blast calculations begin with an assumed spherical explosive source at uniform high temperature and pressure. Laws of hydrodynamics and radiation processes allow calculation of shock wave behavior which agrees well with experience out to distances where blast overpressure is down to a few psi. Figure 1, taken from The Effects of Nuclear Weapons, shows the early shock wave pressure-distance profiles as they change with time. The general pressure-time curve shape with a sharp pressure rise, a gradual decay to a rounded negative phase, and a slow recovery to ambient pressure is often carried to very large distances. At long range, when complex atmospheric refraction processes are at work, however, the wave is usually heard as a rumble from several cycles of nearly sinusoidal pressure oscillation. Wavelengths generally increase and sound frequency decreases as source yield or distance is increased.

Theoretical calculations for the overpressure versus distance relation have been made for certain standard conditions, and scaling laws have been derived for extrapolation to other uniform burst conditions. One reference standard, called IBM Problem M, has been satisfactorily used for many years. It provides calculated tabulations of

several shock parameters from a 1-kiloton nuclear burst, in the free atmosphere removed from any reflectors, at 1000-millibars air pressure (near sea level), and 300°K air temperature (27°C or 82°F). The overpressure-distance curve from this calculation is shown in Fig. 2.

This IBM Problem M curve is scaled to other yields and atmospheric pressures by the equations given in the figure. These show that a constant overpressure–ambient–pressure ratio (shock strength) is maintained when distance is changed in proportion to the cube root of the new yield and inversely proportional to the cube root of the burst altitude ambient air pressure. For 1-megaton, 1000-kt, free-air burst at sea level, the curve is shifted to 10 times larger ranges since $(1000)^{1/3} = 10$. For a 1-kiloton burst near 50,000-feet elevation where air pressure is about 100 mb, the standard curve is shifted to $(1000/100)^{1/3} = 2.15$ times greater ranges and then overpressures are decreased by 100/1000, conserving shock strength and moving the whole curve down on the figure as shown. A standard curve for other yields or altitudes may be similarly constructed.

Since it is not of major importance to blast prediction, it is not shown on Fig. 2, but there is a third scaling equation, necessary in maintaining energy flux similarity, which shows that arrival times and pulse duration, t, are changed according to

$$t = t_M \left(\frac{W p_M}{W_M p}\right)^{1/3} \left(\frac{C_M}{C}\right)$$

where C is ambient sound speed. Sound speed is proportional to the square root of absolute air temperature.

For a burst in a real atmosphere where temperatures and sound speeds change with altitude and where winds, which convect blast or sound waves, may vary in both speed and direction with altitude, predictions must be considerably modified, but the scaled overpressure-distance curve gives a convenient starting point. For bursts near or under the ground surface, the distant pressure wave can be similarly scaled, but overpressures

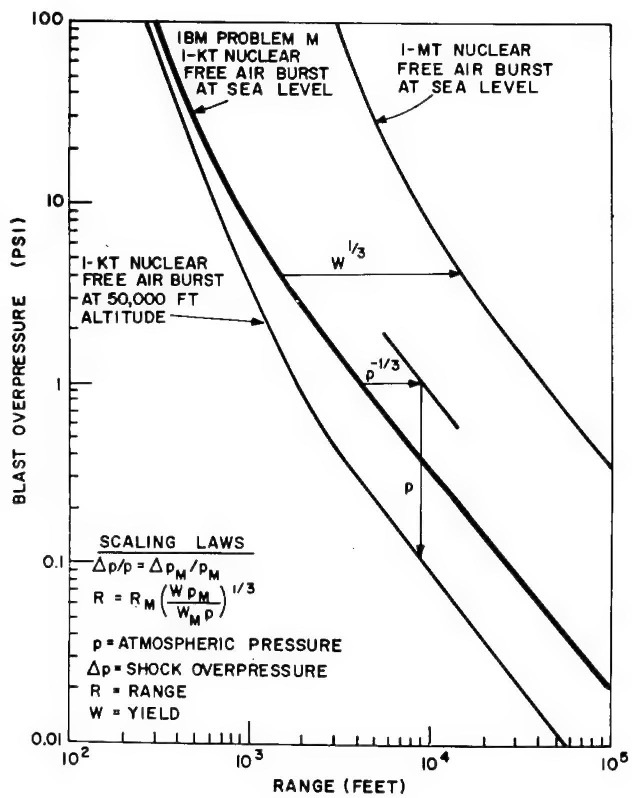

Fig. 2. Standard explosive overpressure-distance curves.

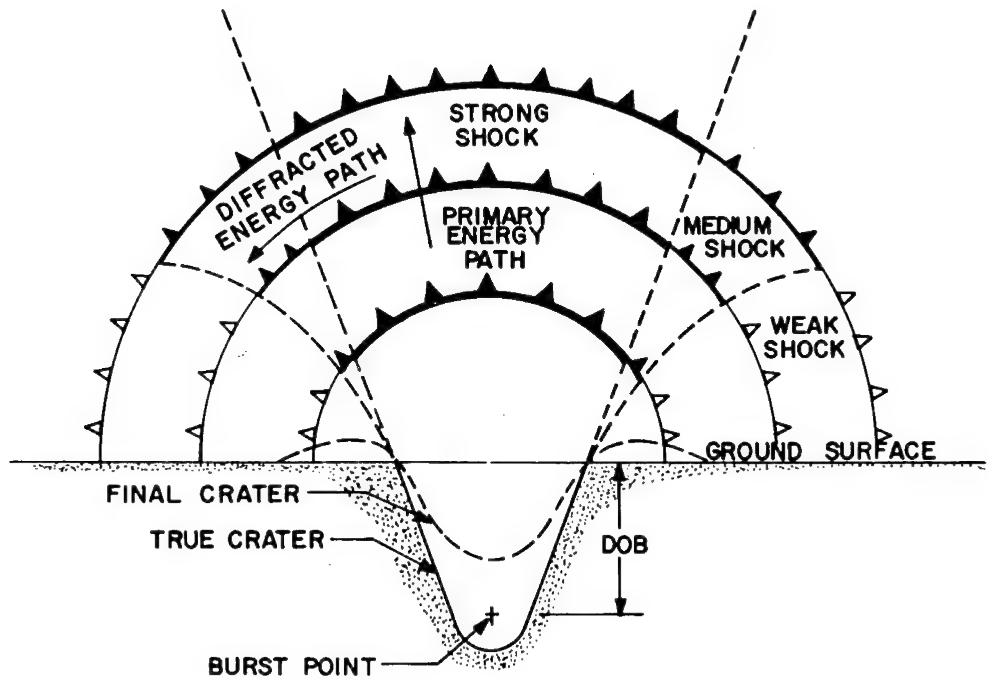

Fig. 3. Air blast source model for cratering explosions.

must be considerably attenuated because much of the initial blast energy is lost in forming the crater.

AIR BLAST FORMATION IN CRATERING BURSTS

Observations from a number of cratering experiments have led us to derive a model for the air blast wave source as shown in Fig. 3. A very strong shock is blown upward through a conical volume and comparatively little energy is carried horizontally outward along the ground surface. Consequently, blast pressures measured close in and on the ground are much smaller than would be observed the same distance from a surface burst (hemispherical geometry). As the strong wave carries upward, some energy is diffracted down into the shadowed region so that the apparent attenuation decreases with increased distance. This may be restated in supplementary form that the transmission factor, defined as the ratio of overpressure to that expected at the same range from the same yield but free-air-burst, increases with distance or range. That this is true is shown in Fig. 4, with curves found by measurements made on a number of Plowshare high-explosives experiments. Beyond a few miles, however, the equalizing effects of diffraction appear to have mostly been completed. At longer ranges pertinent to off-site predictions, there is considerable scatter among the data points, but it appears that a single averaged transmission factor may be used for each burst. This transmissivity decreases with increased scaled burst depth; it appears to increase somewhat with increased yield; it is smaller for nuclear explosives than for the same yields of H. E.; and it depends on the material surrounding the explosives. These various factors have not been adequately defined as yet, but observations of future cratering blasts are planned to refine current estimates. Also, the basic assumed source model in Fig. 3 has not been verified by direct measurement, but the necessary measurements above and around surface zeroes are being planned.

A collection of transmission-factor data points from several experiments is shown in Fig. 5, for various scaled depths-of-burst (dob). It is to be noted that transmissivities vary by a factor of two around the average for nearly every shot. These points were mostly obtained around 100 miles or more from burst points in several directions. Scatter was caused by atmospheric changes in space and time between conditions along the crater shot blast ray path and the path of the air

burst calibration shot rays. For extrapolation to larger yields, the Sedan data show air blast amplitudes average around 20 percent as large as expected from 100-kt free airbursts. This is for near optimum cratering burst depth in desert alluvium with a significant moisture content. The Danny Boy data, for dry, hard basalt rock, average about 10 percent transmissivity. We have yet to establish how this difference should be apportioned between effects of the yield difference and the moisture difference.

We have not yet derived a blast prediction technique for row charges, or ditch diggers. This can be complicated by firing intervals (if not simultaneous) and existing scaling procedures may not be applicable. At best, the source wave may be approximated by a wave from one shot with the total yield. At worst, for off-site problems, blast pressure amplitudes may be added directly and acoustically so that peak overpressures expected from n devices in a ditching program would be n-times the amplitude expected from a single device. There is some evidence, collected close in from small-scale H. E. tests, that this latter pessimistic situation may occur in directions perpendicular to the charge row.

ATMOSPHERIC REFRACTION EFFECTS

It may have seemed curious that meteorologists have gotten so involved in explosives blast physics and acoustic phenomena. Therefore, an attempt will be made here to show how the atmosphere affects long-range propagation to the extent that multimegaton bursts have been heard as only a dull rumble at 30- to 40-miles range, while an irate mother claimed her sleeping child was knocked from his bed, 7 miles from a 100-lb H. E. blast. There are dozens of other comparisons to show that refractive sound lens effects caused by our layered atmosphere may more than overcome minor explosion source effects such as decimal points that distinguish kilotons from megatons or containment factors which distinguish atmospheric blasts from underground bursts.

The mechanism of atmospheric refraction may be appreciated with help of the diagrams in Fig. 6. A typical atmospheric sound velocity versus altitude structure is shown in the left portion, developed by adding to the sound speed in air, and dependent on air temperature, the directed wind component — in some direction of interest. A vertical plane shock-wave front, shown at times of 0,

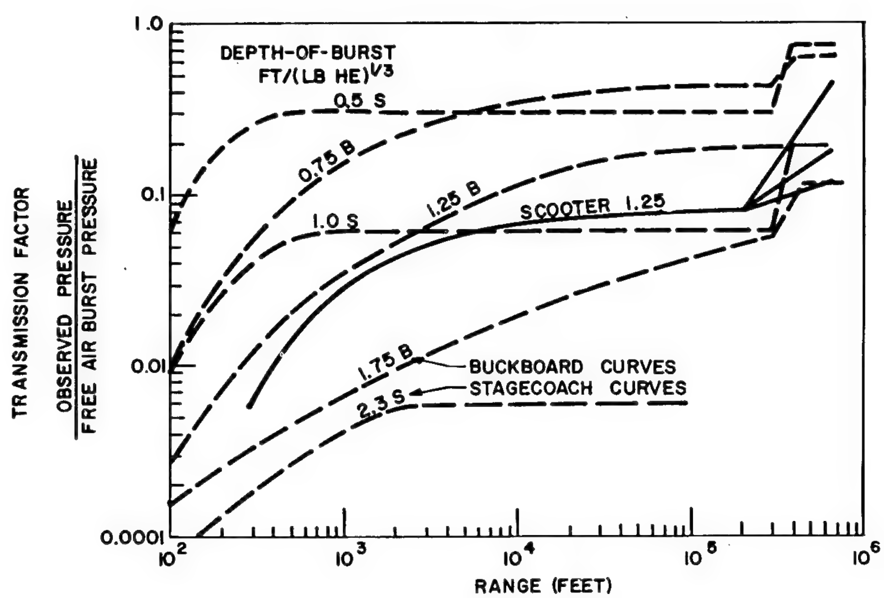

Fig. 4. Air blast transmission factor increase with distance.

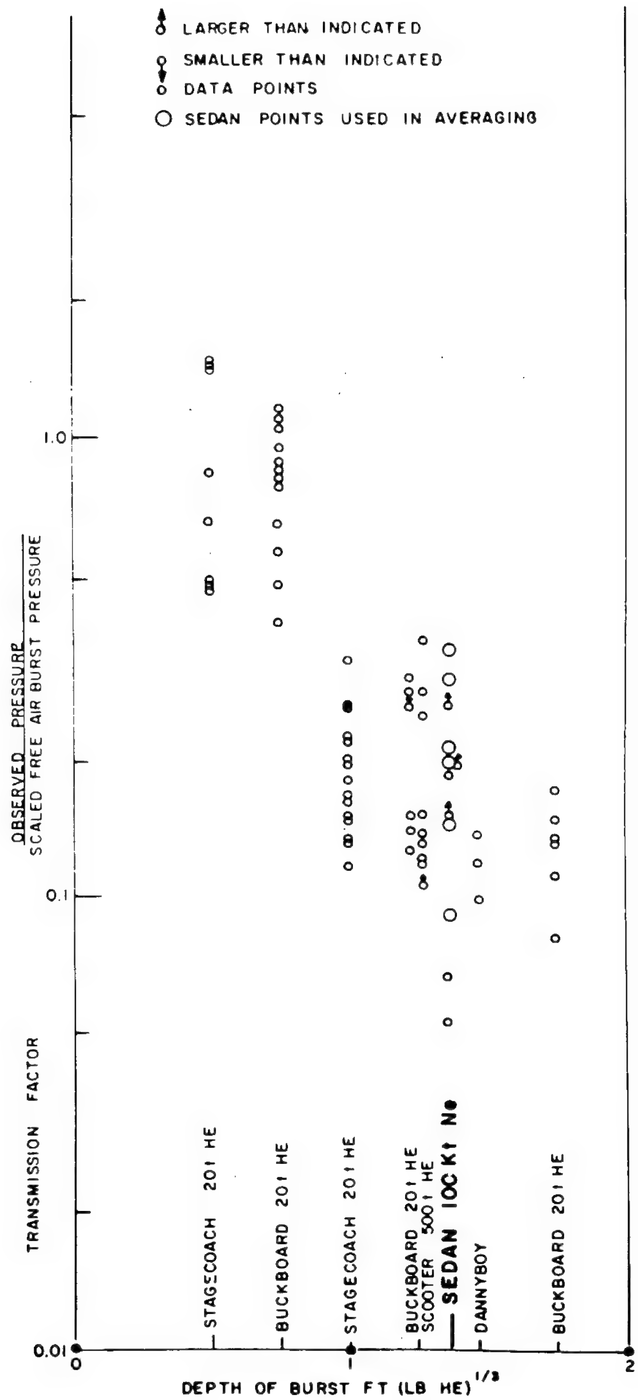

Fig. 5. Air blast transmissivity versus scaled burst depth.

1, and 2 units, becomes increasingly distorted as it moves to the right with wave points at different altitudes moving with different sound velocities. Sound or shock rays, perpendiculars to the front, are bent upward where sound velocity decreases with altitude and are turned toward earth in layers where sound velocity increases with altitude. These ray paths may be calculated by application of Snell's law of refraction. When applied to a point-source wave, rays which initially diverge radially may have their vertical direction reversed when they enter a layer in the atmosphere where directed sound velocity is greater than at the ground or burst level. Some typical calculated ray path patterns demonstrating this are shown in Fig. 7. Where sound velocity decreases, then increases with altitude, the wave front is turned over and returned to ground some distance away. At this large range it may be focused or converged in varying degrees. At shorter ranges, in the zone of silence, only relatively weak sound waves reach ground by diffraction as the stronger wave passes far overhead.

There are three important atmospheric layers where this ducting or sound channeling may take place. Under some weather conditions, particularly on clear, calm nights, temperatures may increase with altitude in a shallow surface layer which may range from a few hundred feet to a few thousand feet thick. This inversion layer restricts spherical wave expansion for the lower emission angle parts of the initial blast wave so that something like cylindrical expansion and energy divergence occurs. Out to a few tens of miles range this condition may cause blast amplitudes two to three times as great as standard homogeneous atmosphere spherical propagation. Beyond these ranges, terrain and atmosphere irregularities cause leakage and losses so that distant effects are not serious.

Upper winds may be quite strong, particularly in jet streams where even 200-mph speeds are occasionally observed. This tube of high-speed flow generally blows from southwest through northwest directions in temperate latitudes, and is strongest in winter and at altitudes between 25,000 and 40,000 feet. These winds may cause high sound velocities and sound ducting downwind over as much as a whole direction quadrant. Waves ducted by jet streams usually strike at ranges from 30 to even 100 miles from the source and may be considerably focused. As much as 15 times amplification over standard blast pressures have been observed in narrow rings 40 miles from test explosions at Nevada Test Site.

In the high atmosphere between 100,000 and 180,000 feet, air temperatures are nearly as warm as at the ground. When wind vectors are added to sound speeds at these levels in the ozonosphere, or mesosphere as it is sometimes called, sound ducting is calculated to give a noisy band at 75 to 150 miles distance as shown in Fig. 8. Here again, considerable focusing may be affected, but observed blast amplitudes "only" reach six to ten times standard values and the average amplification factor is about two or three. This propagation is seasonally directed, generally toward the east in winter and toward west in summer, downwind from ozonosphere circulations. Upwind,

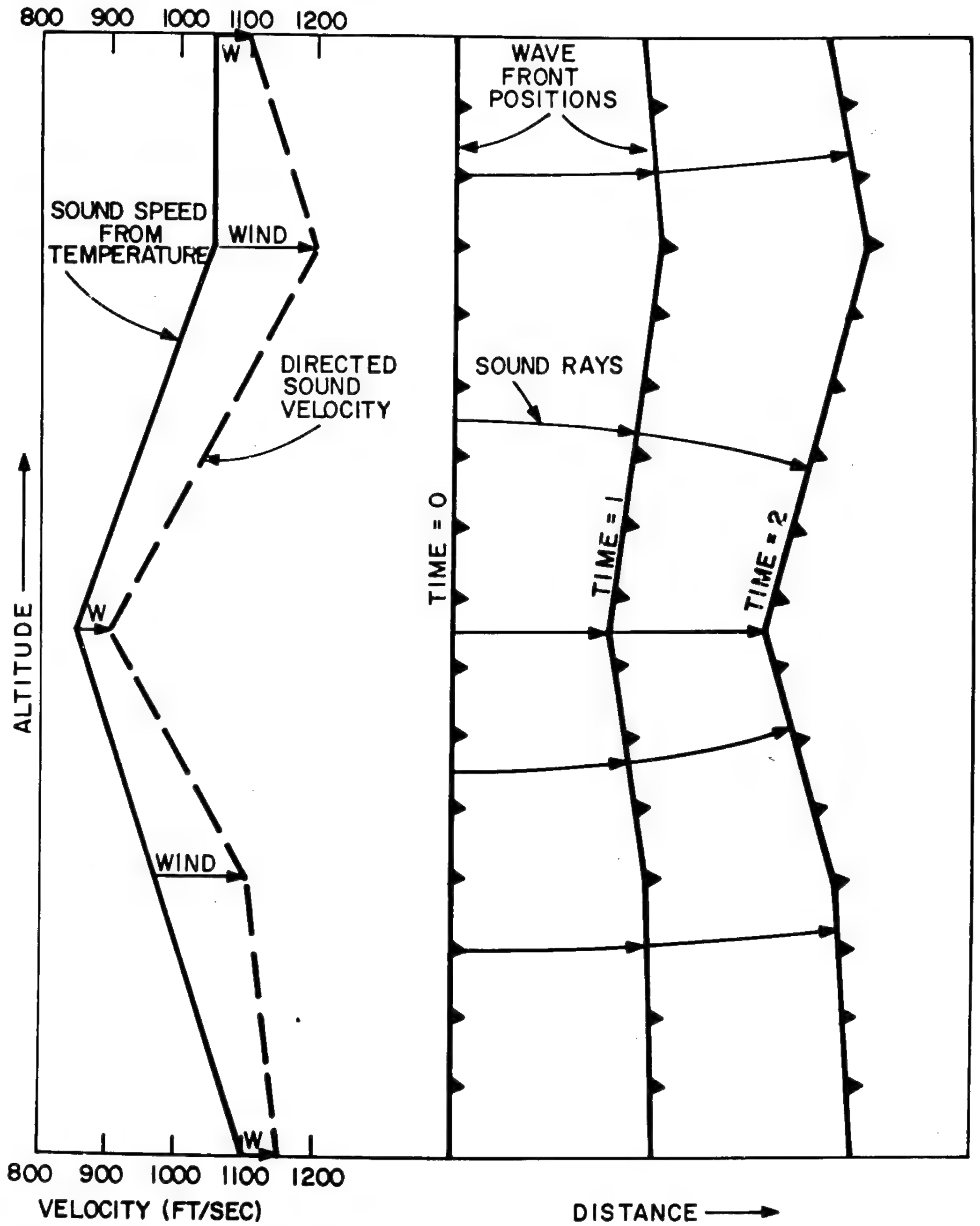

Fig. 6. Shock wave distortion by layered atmospheric temperature and wind structure.

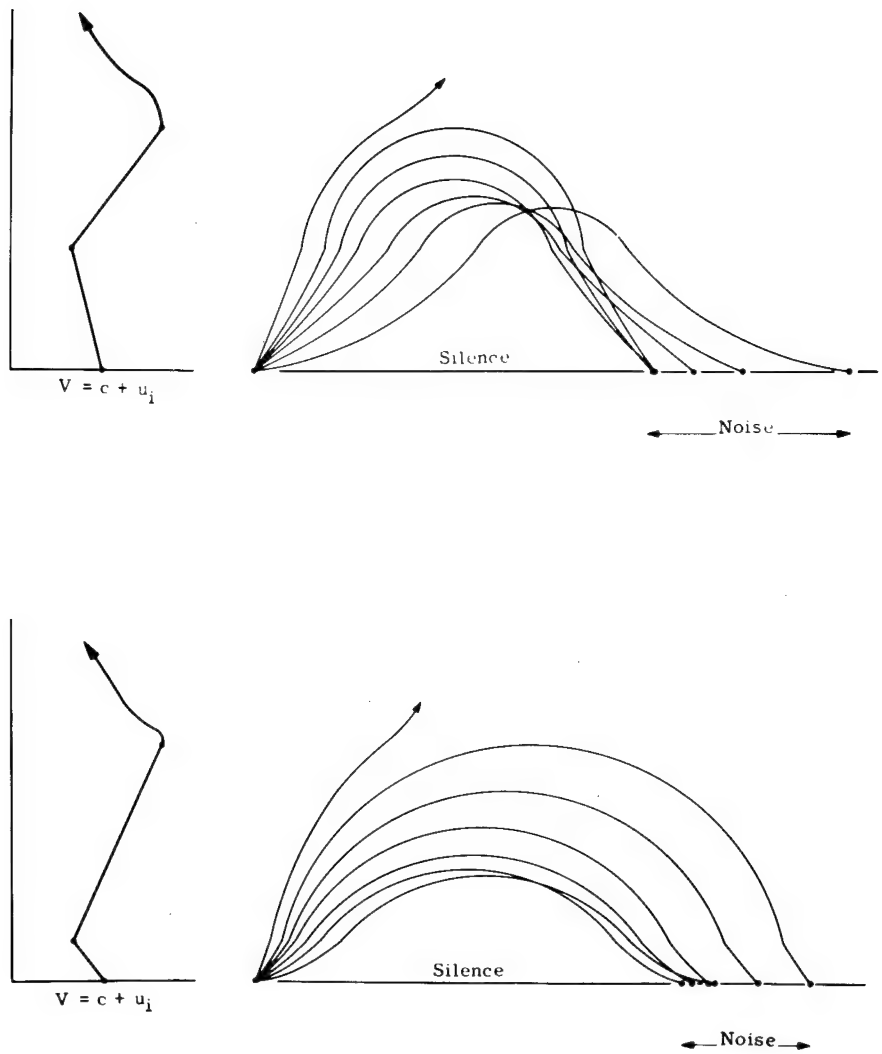

Fig. 7. Typical calculated sound ray paths.

waves are usually refracted away from the ground and only small pressure oscillations are recorded, caused again by diffraction down into the shadowed zone. Stations on a circle of 135 miles radius from Nevada tests usually record 40 times greater amplitudes downwind than upwind. This is about the same difference as is expected from comparing standard blasts from 1 kiloton with blasts from 10 megatons.

All of these ducted waves, on striking ground, are almost perfectly reflected and may repeat their cyclic path through the atmosphere to greater distances. Thus, waves from multimegaton bursts may be recorded after the second time around the world. However, in ground reflections and in air propagation, higher frequency components in the wave front are absorbed or attenuated so that at large distances the apparent loudness is much reduced and damages from thunderous claps are less likely. Instead, more gradual compressions are found, but they may still force large windows out or crack plaster walls.

DAMAGING OVERPRESSURE LEVELS

Experience in Nevada has shown that 2-mb (0.03 psi) overpressures begin to break large store windows. Smaller windows take larger overpressures so that near 40 mb (0.6 psi) most small casement windows are smashed, but even then many survive. A statistical effect must be assumed in damage estimation for small overpressures. The

probability of one window breaking at 10 mb may be quite small. Even in a test structure with several windows exposed, none may break and this pressure assumed safe. But when this blast is applied to a city with thousands of similar windows, mounted with varying degrees of stresses, many will be broken and public furor may be devastating to a project.

We are currently engaged in a study of damages claimed in San Antonio, Texas, from the explosion of November 13, 1963, at Medina Base. With thousands of claims, a reasonably accurate census of the millions of windows and a typical blast prediction, we hope that a statistical relation between small blast overpressures and percents or fractions of percents damage probabilities can be derived.

Sonic boom experimenters have found that windows may be broken by less than 1 mb overpressures, but from shorter ranges and faster pressure rises than are generally encountered in nuclear tests. Plaster damage is known to occur when blast overpressures are too small to break windows. Since this type of cracking is usually present in any house and occurs with house settling, door slams, etc., it is usually not worth making a claim for unless it coincides with the more obviously caused damage of broken windows.

EXAMPLE: 10-MEGATON CRATERING EXPLOSION

A prediction for overpressure-distance curves for a 10-megaton sea-level burst at optimum cratering depth is shown in Fig. 9. The standard curve was scaled from the curve for 1-kiloton in Fig. 2, multiplying ranges by $(10,000)^{1/3}$, and then attenuating overpressures to 20 percent of standard values in accord with the results of Sedan shown in Fig. 5. This curve would only be appropriately used in an atmosphere with everywhere constant temperature and no wind. Upwind, or wherever sound rays are not calculated to land, overpressures would be about what are shown by the lower curve, labelled "diffracted." In such upwind areas, windows would not likely be broken beyond 25 miles. Shot under a temperature inversion, or low-level wind shears which would cause sound velocity to increase with height, the "inversion" curve shows extensive damage could extend 40 miles, but an inexperienced guess would drop this curve to the 2-mb level near 100-miles range, as terrain irregularities took their increasing toll of the available blast energy.

Of much more serious concern, the "focused" curve shows how jet-stream winds could cause extensive blast damages out beyond 150 miles. The

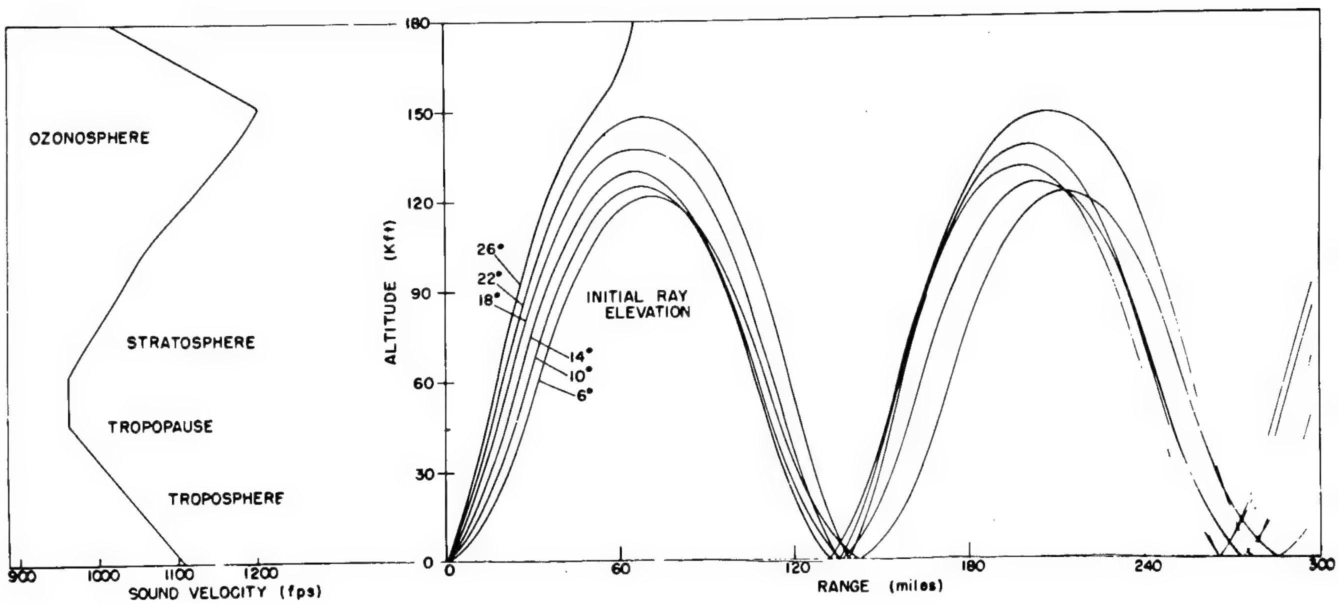

Fig. 8. Sound ray paths through the ozonosphere from RAYPAC (Ray Path Analogue Computer).

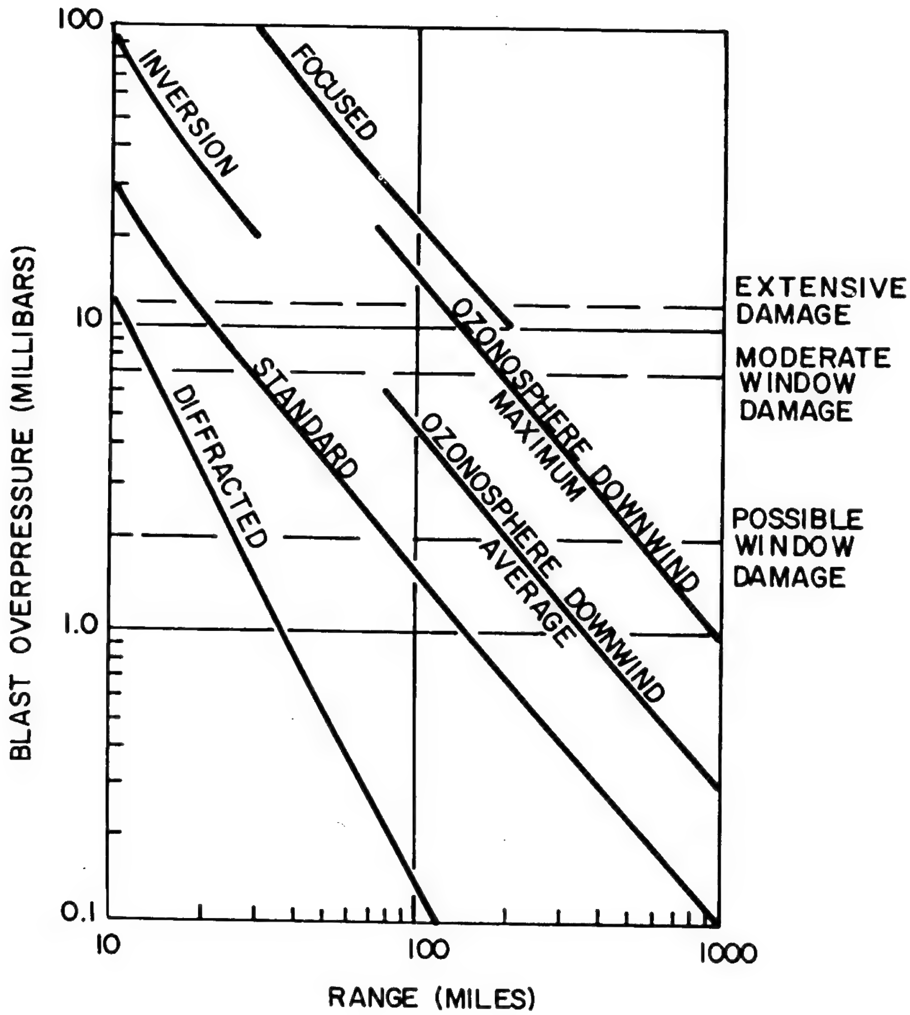

Fig. 9. Blast predictions for 10-megaton cratering explosion.

moral, as it has been learned in Nevada, is to wait for better weather. Ozonosphere ducting, on the average, would carry 2-mb waves, to break some large windows, to about 200 miles downwind. This would be in the second noise ring after a reflection by ground near 100 miles. On occasion, and not yet seriously predictable, some windows might be broken out to 500-miles downwind range. It appears that major excavation projects of this type should be conducted, if possible, during a season when high-altitude winds are blowing away from any populated areas.

BIBLIOGRAPHY

1. Cox, E. F., H. J. Plagge, and J. W. Reed, Meteorology Directs Where Blast Will Strike, Bulletin of the American Meteorological Society, 35, pp. 95-103, March 1954.
2. Cox, E. F., Sound Propagation in Air, Handbuck der Physik, XLVIII, pp. 455-578, Springer-Verlag, Berlin, 1958.
3. Vortman, L. J., et al., Project Stagecoach: 20-Ton HE Cratering Experiments in Desert Alluvium Chapter 9, Final Report SC-4596 (RR), Sandia Corporation, May 1962, OTS $4.00.
4. Vortman, L. J., et al., Project Buckboard: 20-Ton and 1/2-Ton High Explosive Cratering Experiments in Basalt Rock, Chapter 9, Final Report SC-4675 (RR), Sandia Corporation, August 1962, OTS $4.00.
5. Perret, W. R., et al., Project Scooter, Chapter 6, Final Report SC-4602 (RR), Sandia Corporation, October 1963.
6. Reed, J. W., and Church, H. W., Sedan Long Range Blast Propagation, Final Report PNE-202F, Sandia Corporation, June 1963, OTS $0.75.

BIOGRAPHICAL SKETCH OF AUTHOR

Jack W. Reed attended USAF Meteorological School at Chanute Field, Illinois, and served as weather officer during World War II and the Korean conflict. He received his B.S. degree in mathematics from the University of New Mexico in 1948. He joined Sandia Corporation in 1948. Since 1951 he has worked with or in Sandia's Research Organization studying atmospheric propagation of blast and fallout from nuclear explosions. Mr. Reed is Chief, Blast Prediction Unit, AEC Nevada Test Site.

SEISMIC WAVE PROPAGATION

W. V. Mickey

U. S. Coast and Geodetic Survey
Washington, D. C.

ABSTRACT

The Coast and Geodetic Survey has recorded and analyzed over 6000 seismic data channels from seismograph recordings at distance ranges of less than 0.5 to over 350 km, in conjunction with the current nuclear detonation program starting in September 1961.

Prediction functions for transitory earth motion in terms of displacement, velocity, and acceleration have been developed for yield ranges of less than .05 to 200 kt.

Vibration perceptibility thresholds from biophysical sources are reviewed with particular application to seismology.

Calculations of percentage of total source energy conversion to seismic energy is evaluated over the yield range of 0.43 to 200 kt for several different media. The relative seismic energy for contained and cratering nuclear detonations are presented.

Seismic propagation characteristics for several events are studied.

INTRODUCTION

From September 15, 1961, to the present the Coast and Geodetic Survey has recorded over 6000 seismic data channels from more than 70 nuclear events at distance ranges of less than 0.5 km to over 350 km. The Washington Post on January 24, 1964, reported the 104th nuclear detonation since the resumption of testing. Only two events of the contiguous United States series were outside of the Nevada Test Site. One was in New Mexico and one was near Fallon, Nevada.

Prior to the resumption of the current test series, the Coast Survey had started seismic monitoring nuclear detonations during the Crossroads tests in the Pacific in 1946.

Table I is a list of the declassified nuclear detonations for the test series which started September 15, 1961.

INSTRUMENTS

The strong-motion seismographs consisted of a camera, dynamic elements, timing devices, and remote control circuitry. Torosional or compound pendulums comprised the dynamic elements with their motion, relative to the earth, recorded on photographic paper through a system of optical levers.

The Benioff seismograph system was comprised of variable reluctance seismometers operated with free periods of 1 sec and damping 0.62 critical, recording on 35-mm film through a 5-cps galvanometer with WWV programmed time control.

The geophone system consisted of a coil moving in the field of a permanent magnet generating sufficient voltage to deflect a sensitive galvanometer. Electronic amplification and selective filtering were used. Three type geophones were used with natural frequencies of 1, 2, and 8.5 cps with damping 0.65 critical. Recording was on photographic paper and magnetic tape.

PERCEPTION THRESHOLD

Richter (1958) reported that "the lower limit of acceleration perceptible to persons has been set by observations and experiments near 1 gal (0.001 g or 1 cm/sec^2)." He reports further that "Human beings begin to notice shaking when the acceleration approaches 1 gal (1 cm/sec^2). Some

Table I. From Vela Uniform Periodic Information Digest Insert, Vol II, No. 11, November 1, 1963

The following Table reviews the latest declassified test information (NTS):

Event	Time (z)		Yield kt	Medium	Depth ft
ANTLER	17:00:00.120	15 Sep 61	2.4	TUFF	1350
FISHER	23:04:59.632	3 Dec 61	13.5	ALLUVIUM	1202
GNOME*!	19:00:00.004	10 Dec 61	3.1	SALT	1184
MAD	18:00:00.163	13 Dec 61	0.43	ALLUVIUM	603
STOAT	16:30:00.135	9 Jan 62	4.5	ALLUVIUM	1005
AGOUT I	18:00:00.133	18 Jan 62	5.9	ALLUVIUM	835
STILLWATER	18:00:00.164	8 Feb 62	2.8	ALLUVIUM	625
ARMADILLO	16:30:00.125	9 Feb 62	6.6	ALLUVIUM	796
HARDHAT	18:00:00.100	15 Feb 62	4.5	GRANITE	950
CHINCHILLA I	16:00:00.132	19 Feb 62	1.8	ALLUVIUM	504
CIMARRON	18:00:00.160	23 Feb 62	11	ALLUVIUM	1000
DANNY BOY	18:15:00.118	5 Mar 62	0.43	BASALT	110
BRAZOS	18:00:00.120	8 Mar 62	7.8	ALLUVIUM	850
HOOSIC	18:00:00.163	28 Mar 62	3	TUFF	518
DORMOUSE II	18:00:00.131	5 Apr 62	9.7	ALLUVIUM	856
PLATTE	18:00:00.125	14 Apr 62	1.6	TUFF	628
AARDVARK	19:00:00.103	12 May 62	40	TUFF	1434
HAYMAKER	18:00:00.123	27 Jun 62	56	ALLUVIUM	1351
SEDAN!	17:00:00.147	6 Jul 62	100	ALLUVIUM	635
BILBY	17:00:00.130	13 Sep 63	200±	TUFF	2413
SHOAL	17:00:00.100	26 Oct 63	12.5	GRANITE	1200

*Carlsbad, New Mexico

! GNOME and SEDAN are part of the AEC Plowshare Program to develop peaceful uses of nuclear explosives.

Note: BILBY and SHOAL were not included in the original Table.

persons are nauseated when no shaking is noticed by anyone."

Earthquake intensity scales have been established which refer to the degree of shaking of a specified place. The Modified Mercalli Scale of 1931 defines intensity I as, "Not felt. Marginal and long-period effects of large earthquakes." Intensity II is "Felt by persons at rest, on upper floors, or favorably placed." At some place between these two definitions the threshold of perceptibility can be placed. Two notable attempts have empirically related the intensity scale to

acceleration. The equation reported by Richter placed the intensity at 1-1/2 to represent perceptibility with a resultant acceleration of 1 cm/sec^2 (1 gal or 0.001 g). Hershberger (1956) arrived at an acceleration of 0.55 cm/sec^2 (0.55 gal or 5.6×10^{-4} g).

Neumann (1960) related the Intensity Scale to vibrational velocities with the 1-1/2 intensity at 0.21 cm/sec. This would differ from the earlier concepts since at frequencies less than 1.6 cps the threshold would be less than 1 cm/sec^2, and for frequencies greater than 1.6 cps the threshold would be more than 1 cm/sec^2.

Biophysicists have studied the effects of vibration on man in simulated environments in order to design protective devices. Goldman and von Gierke (1961) reported on three stages as thresholds of perception, of unpleasantness, and of tolerance. They inferred that the first level was determined more reliably than the last two. Figure 1 was taken from their report with notes added. The shaded area is about one standard deviation on either side of the mean. Data were averaged from seven sources. At frequencies of 1.5 to about 4 cps, the threshold is more nearly proportional to jerk or time rate of change of acceleration, while from 4 to about 30 cps the response is between particle velocity and displacement. The dashed line from 1.5 to 4 cps represents jerk at 0.054 g/sec and the line from 4 to 30 is velocity at 0.087 cm/sec.

Also included on the graph is the threshold of detectibility at the finger tips to tangential vibration. From 4.5 to about 20 cps this is proportional to a displacement of 0.0012 cm. From 30 to 200 cps the threshold response approaches jerk and beyond 200 cps, it approaches the second integral of the harmonic displacement function. The original figure indicated a threshold of 10 g at 1000 cps.

The low point of the threshold curve is at 0.0025 g at 5 cps. The g threshold is larger than that reported by Richter by a factor of 2.5, and the particle velocity threshold is less than that reported by Neumann by a factor of 2.4. Based upon the graph in Goldman and von Gierke (1961), the threshold and tolerance limits are separated by about 2 orders of magnitude at 3 cps. The range between threshold of feeling to minor injury at 1 minute or less exposure is about 3 orders of magnitude.

Figure 2 is a revised version of one appearing in the Vibration Handbook cited above. It shows the approximate threshold of perception in peak-to-peak displacements of subjects in standing or supine positions with repetitive vertical impact pulses similar to vibration from pile drivers, heavy tools, heavy traffic, etc. This would be the response to irregular, random vibration. Also shown on the figure are the perception thresholds of 0.054 g/sec, 0.0025 g, 0.087 cm/sec, and 0.0012 cm. The spectrum of most interest to the seismologist is normally less than 10 cps.

DAMAGE CRITERIA

The Bureau of Mines (Duvall and Fogelson, 1962) reviewed some 40 papers on residential structure damage from blasting, but only 3 had actually observed damage at measured vibration levels. A statistical evaluation related constant particle velocities over a wide frequency range (about 2 to 600 cps) to damage. They concluded that particle velocities of 13.7 cm/sec (5.4 in./sec) produced only minor damage, and that major damage was observed at 19.3 cm/sec (7.6 in./sec). A criterion of 5.08 cm/sec (2 in./sec) was recommended and compared to the following criteria:

Langefors, Kihlstrom and Westerbert (1958)
- 5.85 cm/sec (2.8 in./sec) no noticeable damage
- 10.80 cm/sec (4.3 in./sec) fine cracks and fall of plaster
- 22.90 cm/sec (9.1 in./sec) serious cracking

Crandell (1949)
- Energy ratio 3 (8.4 cm/sec, 3.3 in./sec) safe
- Energy ratio 3 to 6 caution
- Energy ratio above 6 (11.9 cm/sec, 4.67 in./sec) danger

Edwards and Northwood (1960)
- Below 5.08 cm/sec (2 in./sec) safe
- Between 5.08 and 10.16 cm/sec caution
- Above 10.16 cm/sec (4 in./sec) damage

The Bureau of Mines recommended a designation of only two zones, a safe zone and a damage zone, rather than the three suggested by the other investigators, since the limits of more than two zones could not be determined with statistical reliability. The number of observations used in the Bureau of Mines analyses were:

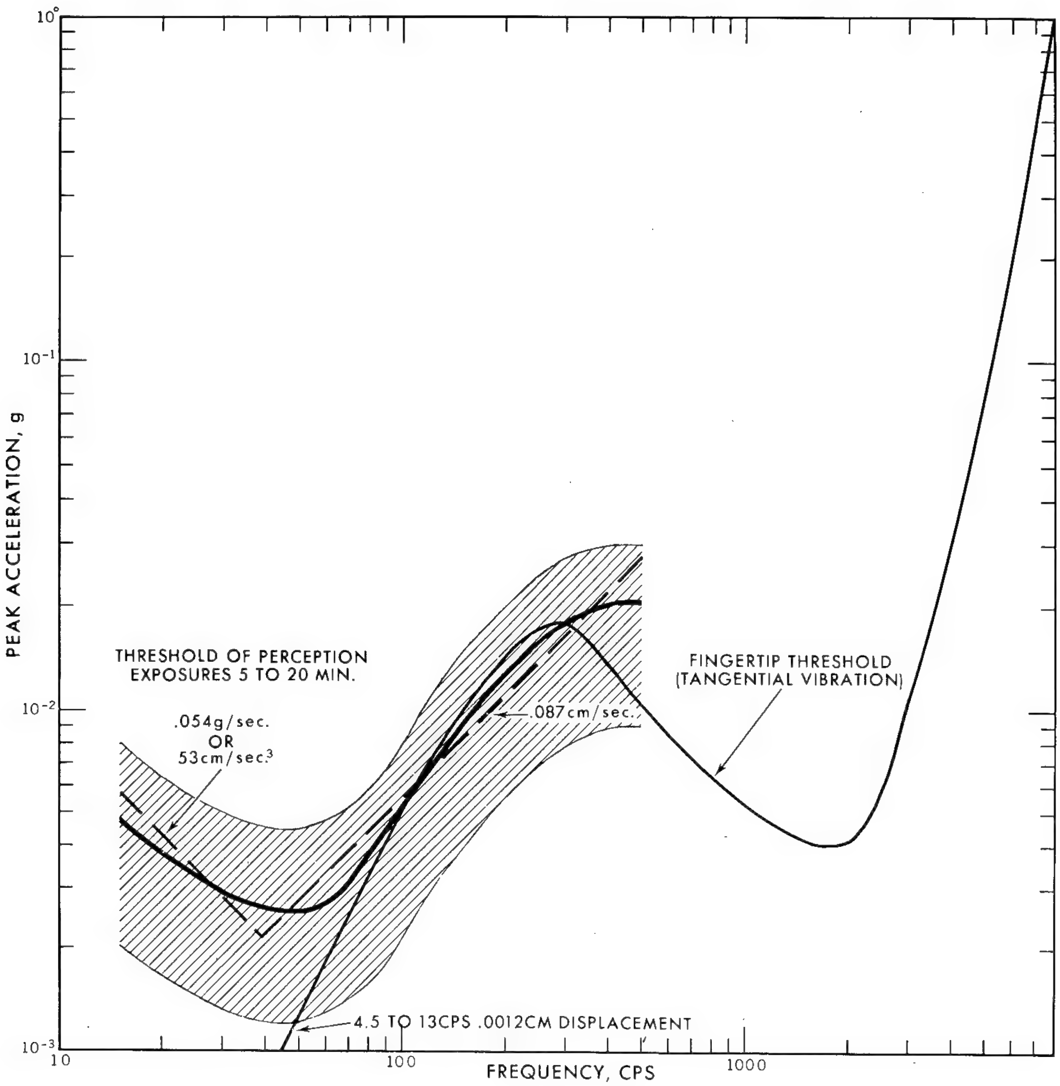

Fig. 1. Threshold of perception with data averaged from seven sources. Shaded area abouc one standard deviation on either side of the mean. (From Goldman and von Gierke, 1961).

Investigator	Number of observations: Major damage	Minor damage
Edwards and Northwood	13	6
Bureau of Mines	34	26
Langefors, et al.	16	32
	63	64

If the upper limit of the safe zone is accepted as 5.08 cm/sec and the threshold perception is 0.21 cm/sec, the upper limit is only 24 times greater than the perception threshold. The number of observations used to arrive at the 5.08 cm/sec (2 in./sec) is an indication that more information is needed to properly define the potential damage zone. The threshold for minor damage for residential structures could be near 8 cm/sec as deduced from the data. Figure 6 of the Bureau

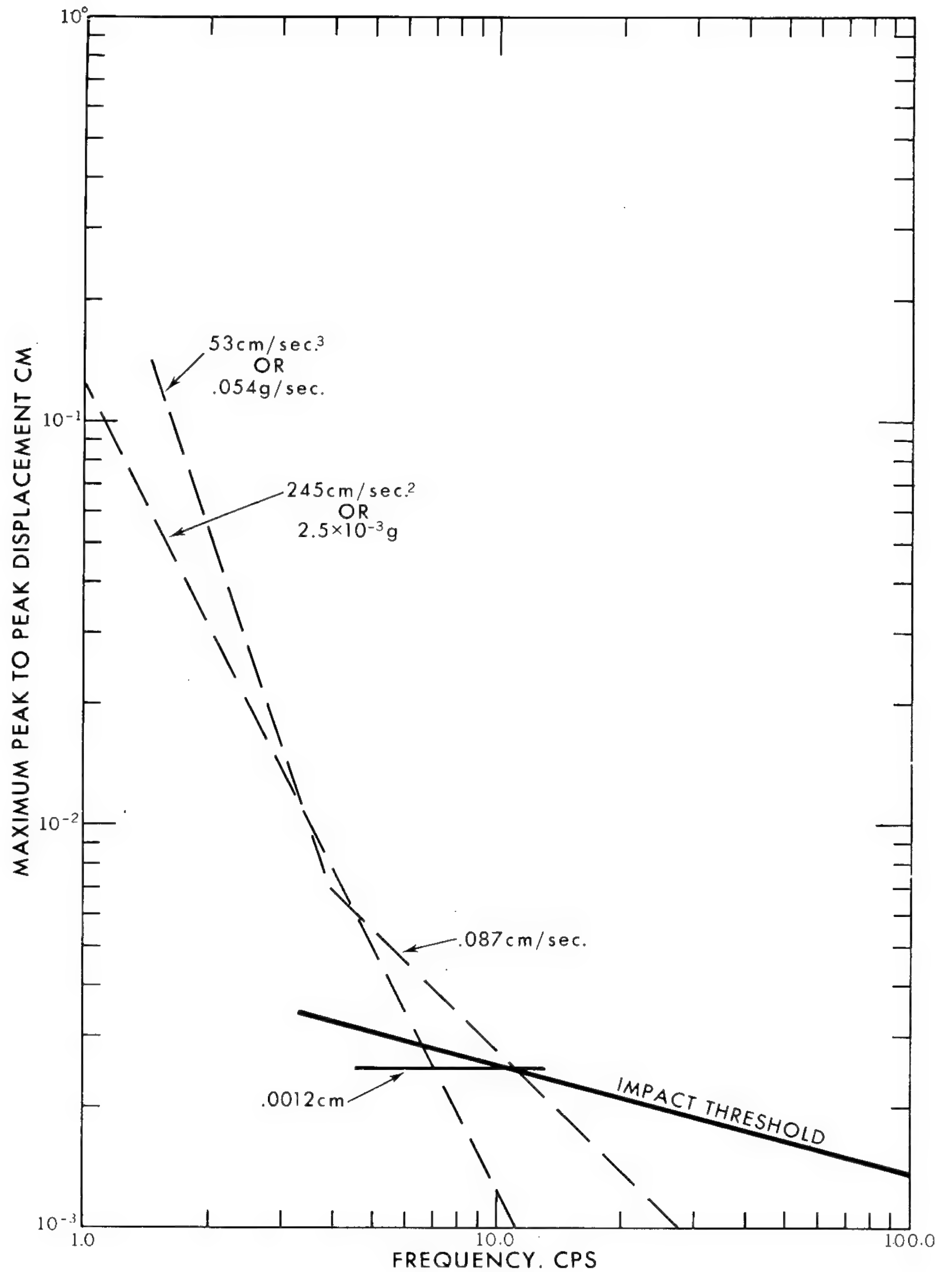

Fig. 2. Threshold of perception of peak-to-peak displacement from repetitive vertical impact pulse sources shown as heavy line. Shown as dashed lines are the perception thresholds of Fig. 1, 0.054 g/sec, 0.0025 g, 0.087 cm/sec, and 0.0012 cm.

of Mines report shows minor damage at 13.7 cm/sec (5.4 in./sec) and major damage at 19.3 (7.6 in./sec).

PREDICTED EARTH MOTION FROM EXPLOSIONS

The Coast Survey has developed prediction equations for transitory peak earth particle motion in terms of displacement, velocity, and acceleration.

The following equations have been derived from the data collected since September 1961:
U. S. Coast and Geodetic Survey Strong-Motion Seismographs

$$a = k_a W^{0.54} R^{-1.4} \qquad 0.4 \text{ to } 21.3 \text{ km}$$

k_a for alluvium = 0.0041

k_a for tuff = 0.0103

k_a for granite = 0.0246

$$d = k_d W^{0.8} R^{-1.2} \qquad 0.4 \text{ to } 21.3 \text{ km}$$

k_d for alluvium = 0.0027

k_d for tuff = 0.00675

k_d for granite = 0.0163

Portable Benioff Seismometers

$$d = k_d W^{0.8} R^{-1.2} \qquad 18 \text{ to } 350 \text{ km}$$

k_d for alluvium = 0.000165

k_d for tuff = 0.000412

k_d for granite = 0.00099

Moving Coil Geophones

$$v = k_v W^{0.67} R^{-1.5} \qquad 18 \text{ to } 350 \text{ km}$$

k_v for alluvium = 0.0144

k_v for tuff = 0.036

k_v for granite = 0.0862

Wood-Anderson seismometers at distances of 100 to 200 km from Nevada Test Site recorded motions compatible with the equation for the portable Benioff system.

It is apparent that the prediction equations for the strong-motion displacement meters are not applicable to the distance range of the Benioffs. This is probably an indication that a simple power function does not apply for all distance ranges.

The Bureau of Mines report (Thoenen and Windes, 1942) developed an equation based on average overburden for displacement with the following charge size and range limit.

Charge (lb)	Distance range (ft)
1,000-15,000	500-6,000
100-1,000	100-6,000
10-100	100-1,000

$$A = \frac{C^{2/3}}{100} \left(0.07\epsilon^{-0.00143d} + 0.001\right)$$

where

A = maximum resultant amplitude, in.
d = distance, ft
C = explosive charge, lb.

For outcrops, divide amplitude by 10. For deep or abnormal overburden, multiply by 3.

At a distance of 6000 ft for a 2-ton charge, the normal overburden would result in an amplitude of 0.0117 cm (0.0046 in.), or for deep shots 0.0351 cm (0.0138 in.). Using the Coast Survey formula the displacement would be 0.033 cm (0.013 in.).

Willis and Wilson (1960) computed a displacement formula from yields of about 1 ton to 19 kt and found that the following formulas were applicable:

$$A = W R^{-3/2}\, 10^{-3.42} \qquad 1 \text{ to } 200 \text{ km}$$

$$A = W R^{-1/2}\, 10^{-(5.12+0.031R)} \qquad 100 \text{ to } 1000 \text{ km}$$

where

A = observed maximum vertical ground displacement in cm
W = charge size in tons
R = distance in km

Using the first equation for a 1.7-kt detonation such as Rainier at 200 km, the first equation gives a displacement of 2.3×10^{-4} cm (9.1×10^{-5}

in.). The Coast Survey equation for tuff gives 2.75×10^{-4} cm.

A recent publication by the Bureau of Mines (Duvall, et al., 1963) reported prediction equations for particle velocities from charges of 200 to 3000 lb at distances of 150 to 300 ft. The equation (changed to the metric system) for vertical components of motion was:

$$v = 0.017 W^{0.73} R^{-1.74} \qquad \text{(limestone)}$$

where

v = particle velocity in cm/sec
W = yield in tons
R = distance in km.

From a detonation of 5 kt at a distance of 1 km, the predicted velocity would be 53.1 cm/sec (21 in./sec). The Coast Survey equation for the same conditions would be 11.2 cm/sec (4.4 in./sec) for tuff and 27.5 cm/sec for granite.

Dimensional analysis for a point-source energy release relates displacement, velocity, and acceleration as follows:

$$\frac{d}{\left(W^{1/3}\right)} = k_d\left(\frac{R}{W^{1/3}}\right)^{-n_d}$$

$$v = k_v\left(\frac{R}{W^{1/3}}\right)^{-n_v}$$

$$AW^{1/3} = k_a\left(\frac{R}{W^{1/3}}\right)^{-n_a}$$

where

d, v, and a = transitory earth particle displacements, velocities, and acceleration
k_d, k_v, and k_a = constants for each parameter
n_d, n_v, and n_a = constants for each parameter.

Based upon a scaled-range concept, the Coast Survey and Bureau of Mines particle velocities would scale:

$$v = k_v\left(\frac{R}{W^{0.447}}\right)^{-1.5}$$

$$v = k_v\left(\frac{R}{W^{0.421}}\right)^{-1.74}$$

The data scatter prevented a predicted motion relative to vertical, radial, or transverse components for the Coast Survey data.

Stanford Research Institute (Swift 1963) derived particle motion equations from the Gnome experiment which satisfied cube-root scaling:

$$d_{cm} = 0.00229 W_{ton}^{0.81} R_{km}^{-1.43}$$

or

$$\frac{d}{\left(W^{1/3}\right)} = 0.00229\left(\frac{R}{W^{1/3}}\right)^{-1.43}$$

$$v_{cm/sec} = 0.422 W^{0.55} R^{-1.65}$$

or

$$v = 0.422\left(\frac{R}{W^{1/3}}\right)^{-1.65}$$

$$a_g = 0.206\, W^{1/3} R^{-2}$$

or

$$a\left(W^{1/3}\right) = 0.206\left(\frac{R}{W^{1/3}}\right)^{-2}$$

Displacement measurements were from 805 to 3219 meters, velocities from 805 to 9450 meters, and accelerations 805 to 9450 meters.

Figures 3, 4, and 5 are plots of the peak displacements, velocities and accelerations for the 200-kt Bilby event. The SRI equations would predict earth motions of 1.67 cm, 7.79 cm/sec, and 0.118 g at a distance of 10 km. The measured values are close to the predictions.

Figure 6 is a graph of the particle velocity equations from the Bureau of Mines, SRI, and the Coast Survey for a megaton detonation. It is interesting to note that the predicted 8 cm/sec distance varies from 13 to 27.5 km.

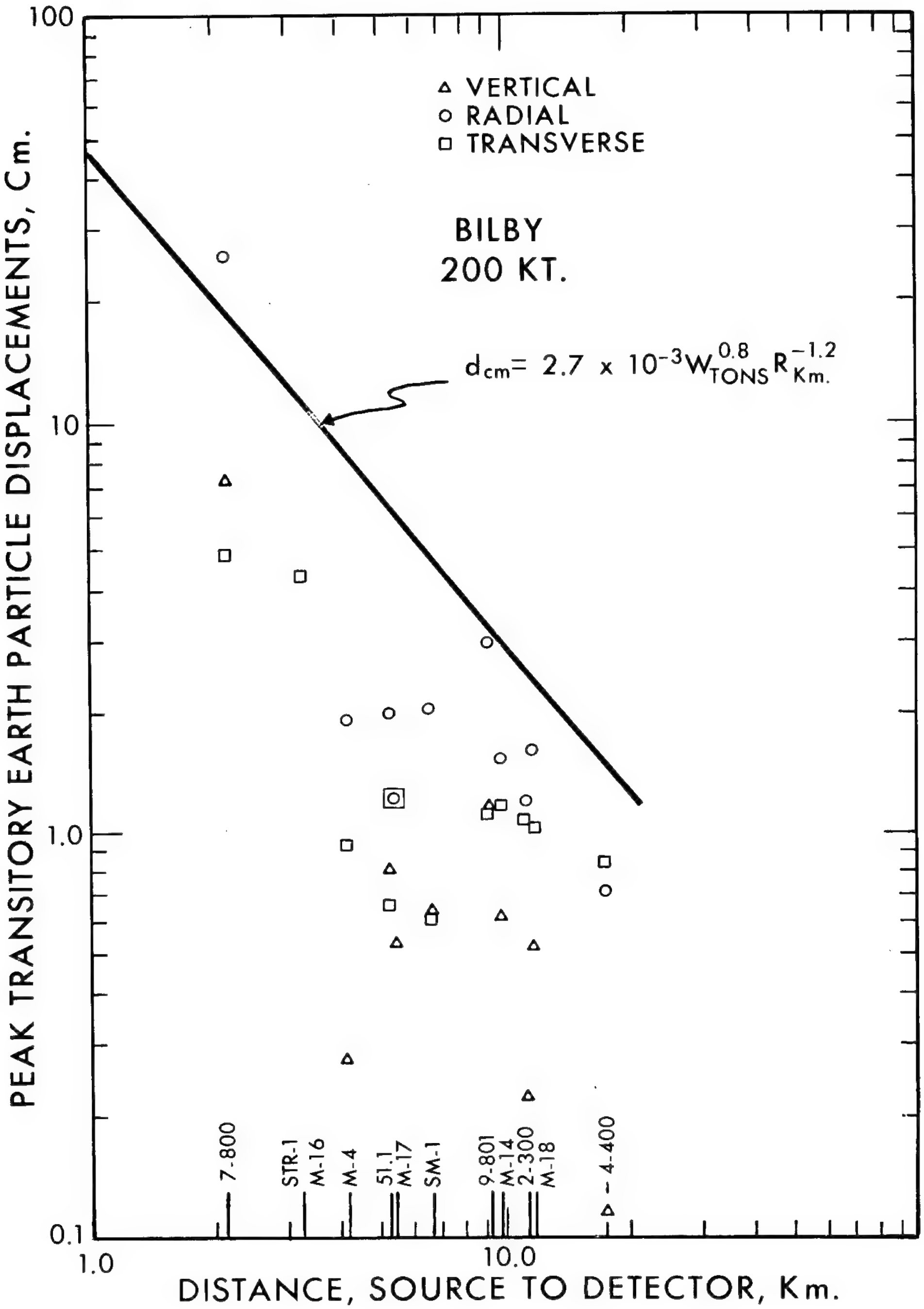

Fig. 3. Peak transitory earth-particle displacement versus distance for event Bilby. The solid line is the prediction function.

The Bureau of Mines equations were derived with information in the ton range, SRI in the 3-kt range and for the Coast Survey up tc 200 kt. At most, the earth motion should not scale greater than unity and from the Bilby data the amplitudes would be only a factor of five greater for a 1-megaton detonation.

Over 120 stations have been occupied since 1961. Stations on deep alluvium consistently gave larger amplitudes than those on competent rock by as much as one order of magnitude. The prediction functions for the strong-motion measurements were based on the alluvial station locations, since the largest majority of experiments were in

desert alluvium; therefore, motions recorded on rock would be lower than the predictions.

While the velocity measurements were usually made off-site, the foundation material was normally rock. In some cases it was impossible to get a station on competent material at the required ranges and azimuths. In these cases the recorded motions seldom exceed the predictions by a factor of two.

In view of Plowshare applications, it is interesting to postulate the minor damage zones for various size detonations. Assuming

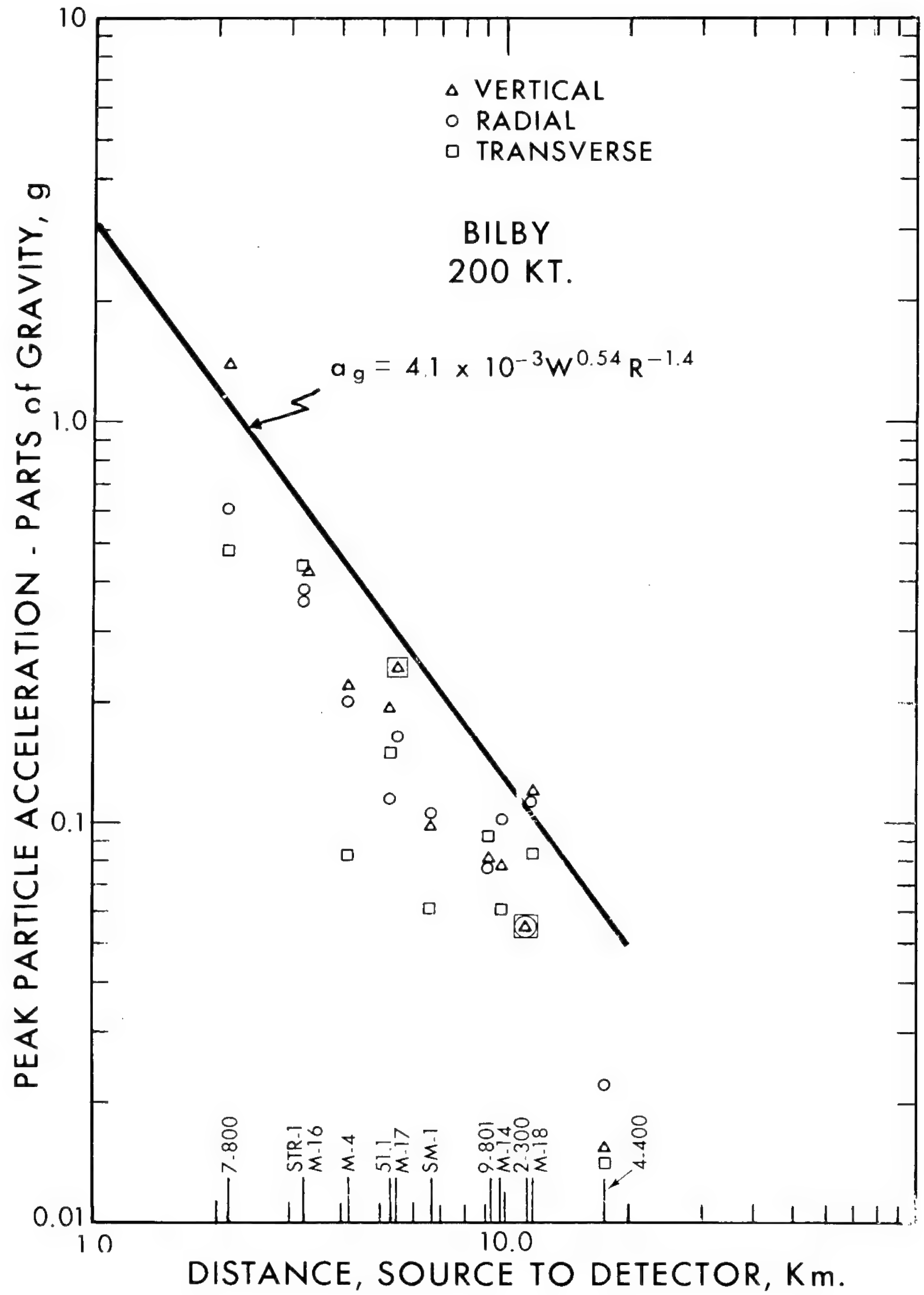

Fig. 4. Peak transitory earth-particle accelerations versus distance for event Bilby. The solid line is the prediction function.

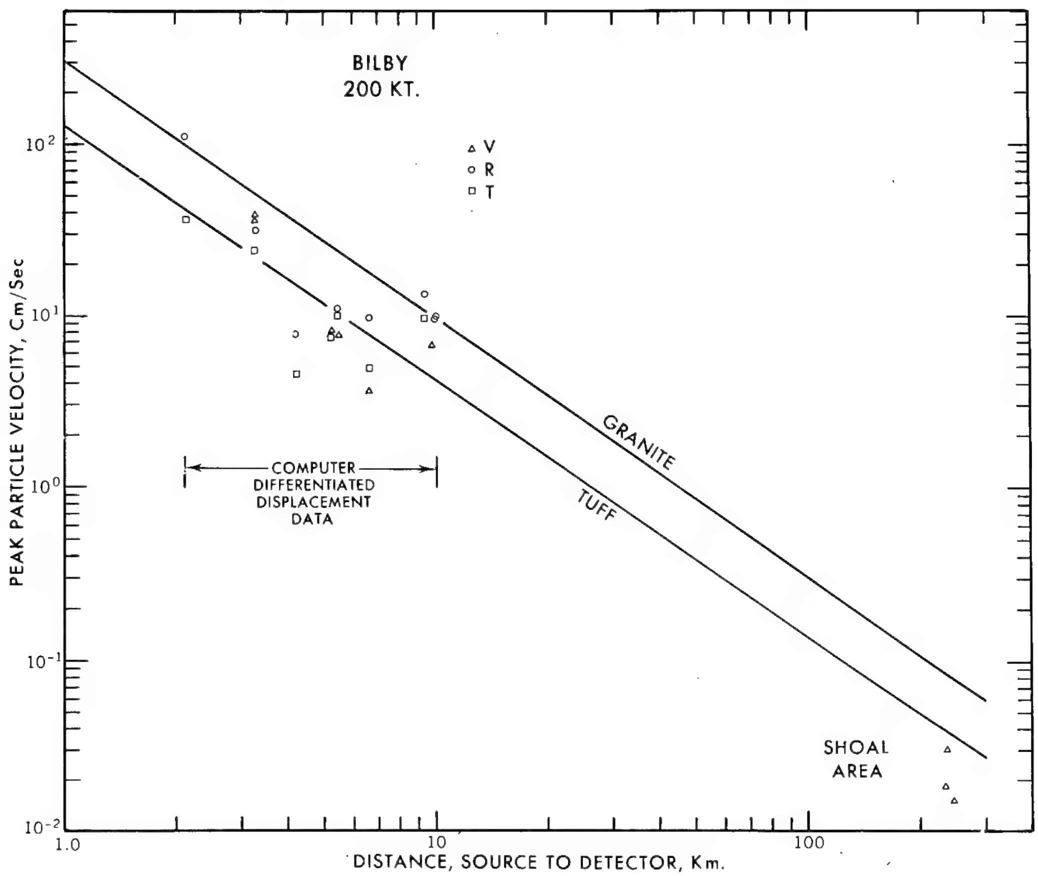

Fig. 5. Peak earth-particle velocities versus distance from Bilby. Digitized displacement data were differentiated to arrive at particle velocity. Shoal area points were measured particle velocities.

that a particle velocity of 8 cm/sec defines the lower limit of the minor damage zone, the following distances and detonation yields are evident from the equation.

Yield kt	Shot Medium Distance km (mile) Tuff	Granite
100	4.7 (2.91)	8.4 (5.21)
200	6.4 (3.97)	11.4 (7.07)
500	9.6 (5.95)	17.1 (10.60)
1000 (1 Mt)	13.1 (8.12)	23.4 (14.51)

Actual ground motion measurements from charges of 200 lb to 200 kt shows that the equation is valid; this covers a range of seven orders of magnitude.

It is within reason to expect the same relationship to apply for one more order of magnitude.

Peak earth motions alone are not sufficient to adequately describe damage effects from blast vibrations, but it is necessary to define the limits of possible damage.

SEISMIC ENERGY

The derivation of the energy of seismic waves at a detector does not present a problem. Extrapolating this energy back to the source to arrive at a total seismic energy relative to the total energy release is much more complex, due in part to the heterogeneity of the earth.

Romney (1959) related the equivalent earthquake magnitude to the yield of a nuclear detonation as:

$$M = 3.64 + \log Y$$

where

M is the magnitude from the Wood-Anderson standard seismograph

Y is the explosion yield in kilotons.

He has emphasized that comparisons of energy release from earthquakes and explosions are not valid. The energy in ergs of a local earthquake M_L as registered on the Wood-Anderson seismograph has been defined as:

$$\log E = 9.9 + 1.9 M_L - 0.024 M_L^2.$$

With the qualifications as stipulated above for validity, a combination of the two equations gives the following percentages of total source energy

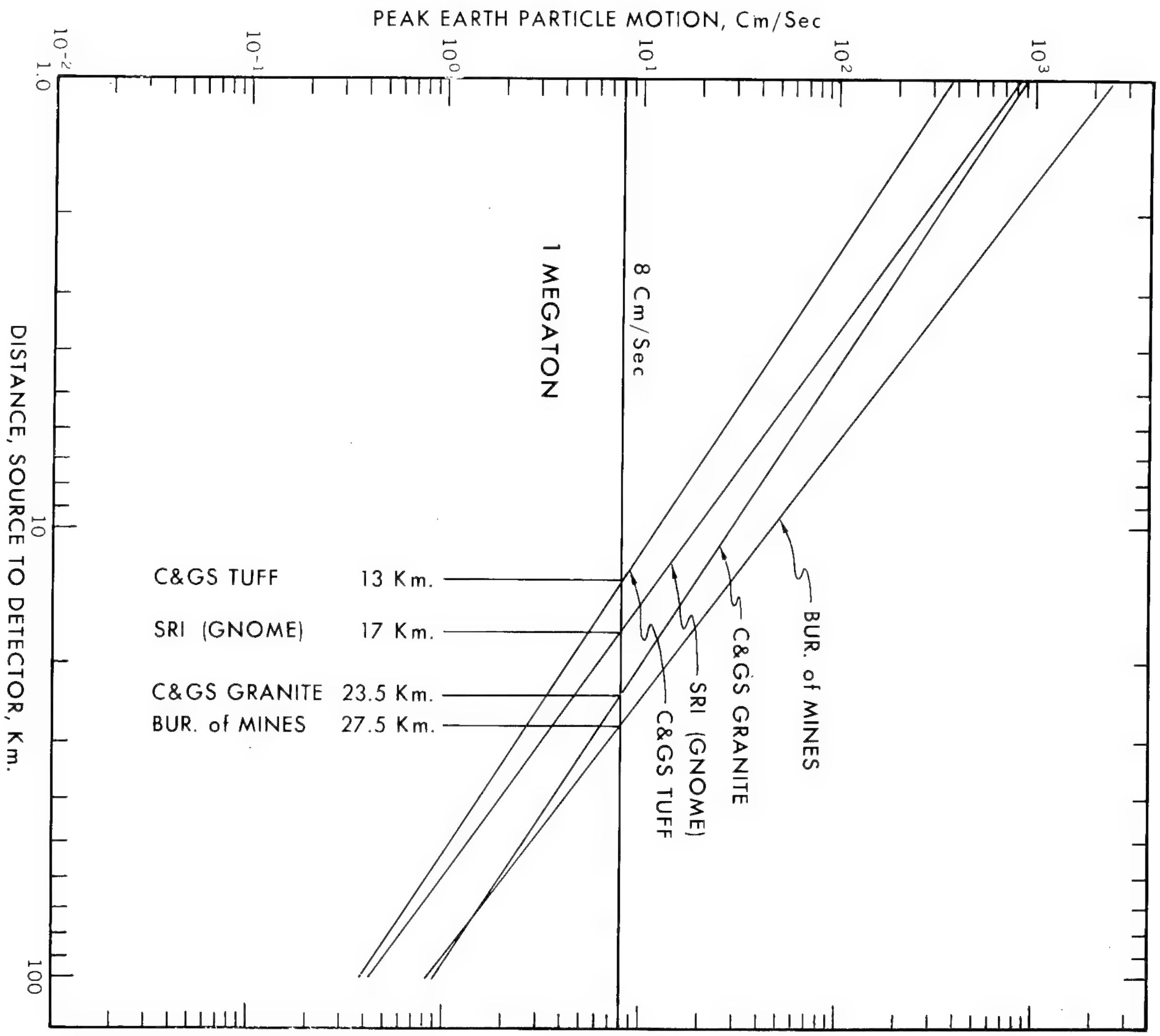

Fig. 6. Prediction equations for particle velocities from four sources based on a 1-megaton yield. Distance range for 8 cm/sec particle velocity is shown.

converted into seismic:

10 kt—0.34%
100 kt—1.67%
1000 kt—6.67%.

This compares to the 0.1% for a 20-kt nuclear detonation at a depth of 300 meters in tuff as reported by Griggs and Press (1960).

Frantti (1963) made seismic energy calculations from quarry blasts and reported the following:

It will be noted from the table that many of the detonations were in multiple holes with millisecond delays of 0 to 17. Devine and Duvall (1963) stated that for multiple detonations with delay intervals of 9 milliseconds or larger, the amplitudes were related to the individual detonations rather than the total charge.

Berg and Cook (1961) reported that 2.7% of the total energy of three large H. E. explosions was converted to seismic energy at zero distance from the blast.

		Description			
	Explosion (lb)	No. of holes	M. S. delay	Total seismic energy (ergs x 10^{13})	Fraction of available energy (%)
1	19828	47	9	1.1	0.015
2	11500	12	17	0.13	0.003
3	10033	28	0	0.49	0.015
4	3000	15	17	5.2	0.44
5	1400	7	17	0.75	0.13
6	1400	7	0	3.5	0.64
7	200	1	--	1.6	1.9
8	200	1	--	1.6	2.0

Listed at right are the percentages of total source energy converted to seismic energy for 20 large-scale detonations from calculation techniques presented in the Sedan report (Mickey, 1963).

Event	Total source energy converted to seismic energy
Antler	0.20
Mad	0.34
Stoat	0.29
Agouti	0.09
Stillwater	0.28
Armadillo	0.10
Hardhat	0.20
Chinchilla I	0.17
Cimarron	0.14
Danny Boy	0.24
Brazos	0.06
Hoosic	0.16
Dormouse II	0.17
Platte	0.018

Aardvark	0.31
Haymaker	0.07
Sedan	0.08
Bilby	0.25
Shoal	0.60
Scooter	0.80

SUMMARY

Review of several reports of thresholds of perception of humans to vibration suggest that the thresholds vary for a narrow range of frequencies from jerk to displacement. For lack of a more definitive threshold for earth-transmitted vibrations, it seems that the 0.001-g zone is as good as any.

Damage criteria data from at least four sources indicate that damage is proportional to particle velocity. Particle velocities of 5.08 cm/sec are suggested to be the dividing line between safe and a damage zone for typical residential structures; however, the minor damage zone is in need of further investigation.

Prediction equations developed for particular situations are appropriate when used within the observed ranges of distances and yields. Extrapolation of low-yield data to that derived from high yields for particle velocities is very good.

The percentage of available source energy converted to seismic energy varied from 0.015 to about 2% with the variance attributed to source conditions. Coast Survey calculations for yields of 0.43 to 200 kt vary from 0.018 to 0.8% with the large value observed from an H.E. rather than a nuclear source. The 100-kt cratering experiment, Sedan, coupled about one-fourth the energy as Aardvark, 40 kt, yet the available data seem to indicate that Haymaker, 56 kt, yielded less relative seismic energy than Sedan.

For the problems confronting the Plowshare experiments, earth-transmitted vibrations certainly are not in the major category, since the earth motions may be predicted with a degree of accuracy.

REFERENCES

1. Berg, J. W., Jr. and K. L. Cook, "Energies, Magnitudes, and Amplitudes of Seismic Waves from Quarry Blasts at Promontory and Lakeside, Utah," Bulletin of the Seismology Society of America, 51, No. 3, July 1961.
2. Crandell, F. J., "Ground Vibrations Due to Blasting and Its Effect upon Structures," Journal of the Boston Society of Civil Engineers, 36, No. 2, April 1949.
3. Devine, J. F. and W. I. Duvall, "Effect of Charge Weight on Vibration Levels for Millisecond Delayed Quarry Blasts," Earthquake Notes, XXXIV, No. 2, June 1963.
4. Duvall, W. I. and D. E. Fogelson, "Review of Criteria for Estimating Damage to Residences from Blasting Vibrations," Bureau of Mines Report of Investigations 5968, 1962.
5. Duvall, W. I., L. F. Johnson, A. V. C. Meyer and J. F. Devine, "Vibrations from Instantaneous and Millisecond Delayed Quarry Blasts," Bureau of Mines Report of Investigations 6151, 1963.
6. Edwards, A. T. and T. D. Northwood, "Experimental Studies of the Effects of Blasting on Structures," The Engineer, 210, September 30, 1960.
7. Frantti, G. E., "Seismic Energy from Ripple-Fired Explosions," Earthquake Notes, XXXIV, No. 2, June 1963.
8. Goldman, D. E. and H. E. von Gierke, "Effects of Shock and Vibration on Man," in "Shock and Vibration Handbook" edited by C. M. Harris and C. E. Crede, 3, pp. 44-1 to 51, McGraw-Hill Book Company, Inc., New York, 1961.
9. Griggs, D. R., and F. Press, "Probing the Earth with Nuclear Explosions," AEC Nuclear Explosion—Peaceful Applications, Lawrence Radiation Laboratory, Livermore, Rept. UCRL-6013, July 7, 1960.
10. Langefors, U., B. Kihlstrom and H. Westerberg, "Ground Vibration in Blasting," Water Power, February 1958.

11. Mickey, W. V., "Operation Plowshare, Project Sedan, Seismic Effects from a High-Yield Nuclear Cratering Experiment in Desert Alluvium," AEC PNE-213F, February 1963.
12. Neumann, F., "A Lateral-Force Formula Based on Seismological Concepts," The Trend in Engineering, 12, No. 3, July 1960.
13. Richter, C. F., "Elementary Seismology," W. H. Freeman and Company, San Francisco, 1958.
14. Romney, C., "Seismic Measurements," Proceedings of the Second Plowshare Symposium, May 13-15, 1959, San Francisco, California, Lawrence Radiation Laboratory, Livermore, Rept. UCRL-5675, Part 1.
15. Swift, L. M., "Project Gnome, Intermediate Range Earth Motion Measurements," AEC Nuclear Explosions—Peaceful Applications, PNE-111F, March 21, 1963.
16. Thoenen, J. R. and S. L. Windes, "Seismic Effect of Quarry Blasting," Bureau of Mines Bulletin 442, 1942.
17. Willis, D. E. and J. T. Wilson, "Maximum Vertical Ground Displacement of Seismic Waves Generated by Explosive Blasts," Bulletin of the Seismological Society of America, 50, No. 3, July 1960.

BIOGRAPHICAL SKETCH OF AUTHOR

Wendell V. Mickey attended Wayland Baptist College and Texas Technological College. Extension studies were pursued at Tulane and the University of Texas. Following a period from 1944 to 1946 in the U.S. Navy, he joined Western Geophysical Company and participated in oil exploration work. Since 1959 he has been a geophysicist with the Coast and Geodetic Survey where he is presently Chief of the Special Projects Branch. He has been active in investigating seismic effects from earthquakes, detonations, large-scale missile launches, industrial vibrations and acoustic-seismic coupling problems.

SEISMIC AMPLITUDES AT AN INTERMEDIATE RANGE FROM EXPLOSIONS

Dorris M. Hankins

Sandia Laboratory
Albuquerque, New Mexico

ABSTRACT

Short-period seismic waves from the Nevada Test Site shots have been recorded by Sandia Laboratory's four-station seismic net during the past ?-1/2 years. Epicentral distances vary from 130 to ?40 kilometers.

Raw maximum wave amplitudes usually vary as the yield to the 0.8 to 1 power. The medium in which the detonation takes place influences the magnitude of the seismic signals. Shots in dry alluvium produce the smallest seismic signals, while those in granite give the largest signals observed. Both the P-phase amplitude and its ratio to the S-and-surface-phase amplitude vary notably with travel path.

Plowshare projects will create ground motions which will travel some distance from the project location. Thus, ground motion must go on the list of safety criteria which must be satisfied. Whether or not a project can be pronounced safe from the standpoint of ground motion will depend on the amplitude, period, and duration of ground displacement at the range of nearest structures or installations of concern. Consequently, the variation of these elements of ground motion with yield, travel path, source medium, depth of burst, distance, and type of energy source needs. to be known. The purpose of this paper is to present some observations regarding ground motions and their variation with the stated parameters. These observations are chiefly those made from seismograms obtained by Sandia Laboratory from the current explosives test series in Nevada.

Since resumption of testing in September 1961, Sandia Laboratory has operated a net of four sesimic stations around the Nevada Test Site at an intermediate range. Two of the four original stations have been relocated since the project started. Figure 1 shows station locations in relation to test site areas.

Nevada Test Site Areas 3 and 9 are in Yucca Valley. Most of the shots in Area 3 have been in alluvium; the media for those in Area 9 have varied from alluvium through a range of types of tuff. Area 15 is the location of the Hardhat shot in granite. The Area 12 mesa has been the site of tuff shots. The Danny Boy cratering shot in basalt was located in Area 18.

The original stations (Darwin, Tonopah, Boulder City, and Pioche) were at a nominal distance of 170 kilometers from the test site and spaced about 90 degrees apart. The St. George location was chosen to replace the overly wet tunnel at Pioche, since its range assures a first arrival from the same seismic phase regardless of the NTS area. The Boulder City station was replaced by one at Nelson to obtain a lower noise level and to make all stations compatible insofar as being situated on hard rock bases in nonoperating mine tunnels. All stations are equipped with three components of Benioff short-period seismometers in addition to at least one Lehner-Griffith instrument used without filters to extend the low-frequency range observable. Radial and tangential instruments are oriented with respect to the center point shown in Fig. 1. This minimizes the orientation variation for the various test areas.

The study of explosion-generated seismic waves is still primarily an empirical science which is incapable of providing definitive answers to questions arising in Plowshare projects. We are able to give "ballpark" answers and have observed trends of variation with several parameters.

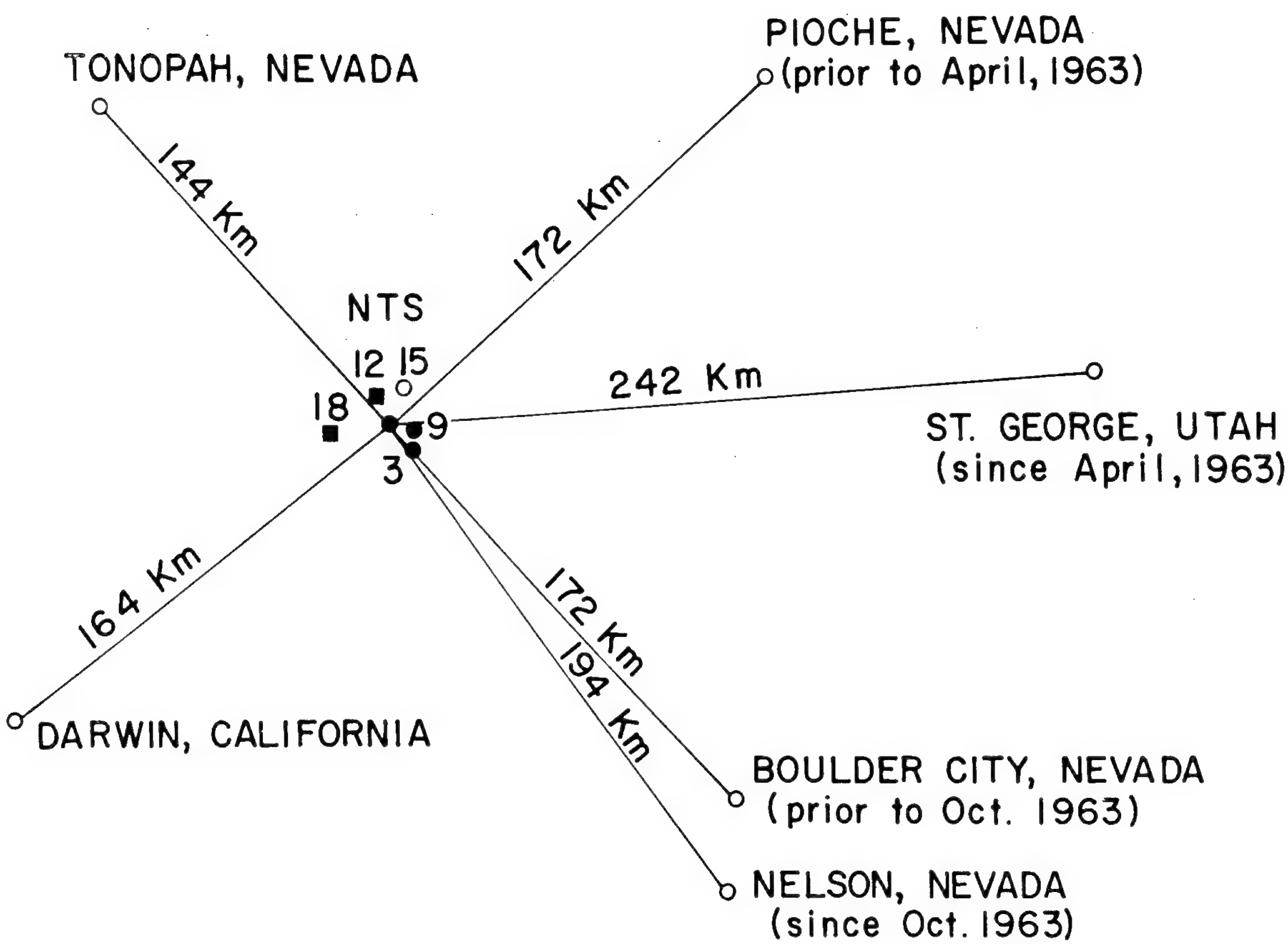

Fig. 1. Locations of stations in relation to Nevada Test Site areas.

Yield is the first parameter which will be discussed. From our data, the most consistent seismic amplitude-yield relationship is obtained from the maximum P (or compressional) wave from Area 3 shots recorded by the vertical component at the Darwin, California, station. There are logical reasons for this. First, the maximum deflection on the seismogram before the S, shear wave, arrival is repeatable - that is, it arrives with the same travel time, indicating that it has followed the same attenuation path. Furthermore, the maximum wave has the same shape and varies only slightly from a period of 0.7 second over a wide range of yields. Second, this seismometer system performance has been fairly constant for 2-1/2 years. A third reason for partiality toward Darwin seismograms is that for the majority of the tests these seismometers were underdamped and thus provided less than the nominal variation in frequency response over the range normally seen from Nevada tests. The maximum variation in displacement magnification over the frequency range from 1.1 to 4 cps is only 17.5 percent. In order to eliminate all parameters other than yield, only contained nuclear shots in alluvium with a maximum variation in location of 1.5 miles will be considered. Errors introduced by lack of precise yields and inaccuracies in reduction of seismic data still remain. Each of these for this situation is believed to be in the range of 5 to 10 percent. The best least-squares fit to a power law relationship was found for thirty maximum Darwin P-wave amplitudes from yields distributed between 0.01 and 15 kilotons. The seismic wave amplitude was found to vary as the yield to the 0.9 ± 0.03 power. Standard deviation of amplitudes from the 0.9 pow-

er fit curve was found to be 16 percent. A similar type, but less restrictive and not as careful, analysis was done with repeatable waves from other components and other stations. The amplitudes were found to vary as yield to the 0.8 to 1 power.

Variation of period with yield at the distance range where Sandia's observations are being made is not as great as predicted for the close-in range. The period of maximum deflections observed on the seismograms, which of course are unavoidably biased by the frequency response, varied by only about a factor of 2 from yields of 0.5 to 200 kilotons.

The time rate of signal decay also seems to be independent of yield. About 30 seconds after the arrival of the maximum signal in the Lg phase, the signal recorded by short-period seismometers has decayed to about one-fifth of the maximum amplitude, whether the yield is 1 or 100 kilotons.

The parameter considered is the travel path, since the remainder of the parameters cannot be isolated from this one. A more regular structure of the earth's crust would decrease the problems in seismological studies and probably allow more precise answers to the remaining ones. Each time a seismic wave traveling through the earth encounters a discontinuity it undergoes changes. A compressional wave impinging on the discontinuity will both reflect and refract energy in compressional waves and in shear waves. The same is true for shear waves. Energy partition is dependent on the angle of incidence and impedances of the media at the interface. The wave front emerging from an underground explosion is spherical at its inception, but waves at different angles will follow different paths. This spreads the energy over a wide range of travel paths, each with its own travel time. Thus, at a distance, energy from a sharp pulse arrives as a train of waves covering a time span which increases with distance. With practically the same source and receiver locations there is a good degree of consistency in seismograms, but much change in either changes the pattern of discontinuities and thus the resulting seismograms. Figure 2 illustrates this travel path effect. The top two traces are the seismic waves recorded by the tangential and radial components at Pioche during the Hardhat shot. Note the strong motion on the tangential component at time of arrival for the compressional wave. Since the shear wave cannot travel the total path distance by this time, there must be conversion from compressional to shear energy near the station. Amplitude of motions on the radial component at the time of S and Lg arrivals is significantly lower than during the P phase. For simplicity, the second prominent wave group will be referred to as S, even though Lg and some modes of surface waves are included. The bottom two traces were recorded by the same two seismometers from the Danny Boy shot in Area 18. Here a reversal of S to P ratios can be noted. Very small deflections on a tangential component and large deflections on the radial component would be expected during a P phase, since a compressional wave has only radial and vertical components. The variations of P to S ratios seen at other stations are different, which rules out the possibility of source characteristics as the cause of the difference. At Darwin, for instance, the radial component recorded about the same deflection for S and P, and the tangential component recorded four and three times as great an amplitude during S as during P.

Strength of signals, as well as P to S ratios, vary with azimuth. Maximum ground motions recorded at Tonopah, regardless of component or phase, have exceeded those at Darwin by a factor of 3 (the factor is 8 for uncorrected vertical P waves). This is not just a station correction factor, since a distant earthquake signal arriving from the southeast was larger at Darwin than at Tonopah.

The range in epicentral distance of our stations is not sufficient to evaluate the effect of distance. Wendell Mickey has reported that signals vary as $R^{-1.2}$ in our range. Using this value, the distance correction for the various test areas would always be less than 20 percent. Even though this parameter cannot be evaluated, it may be eliminated for all practical considerations.

The next parameter considered is the source medium which, for the most part, cannot be isolated from other parameters.

The amplitude-yield curve established for contained alluvium shots is given in Figure 3 which shows data from other media. Data are for the maximum P wave recorded by the vertical component at Darwin. The Area 3 points at 40, 56, and 200 kilotons are from Aardvark, Haymaker, and Bilby, respectively. Haymaker was in alluvium which was nearer saturation than is the alluvium at lesser depths where the lower yield range shots were detonated. Aardvark and Bilby were

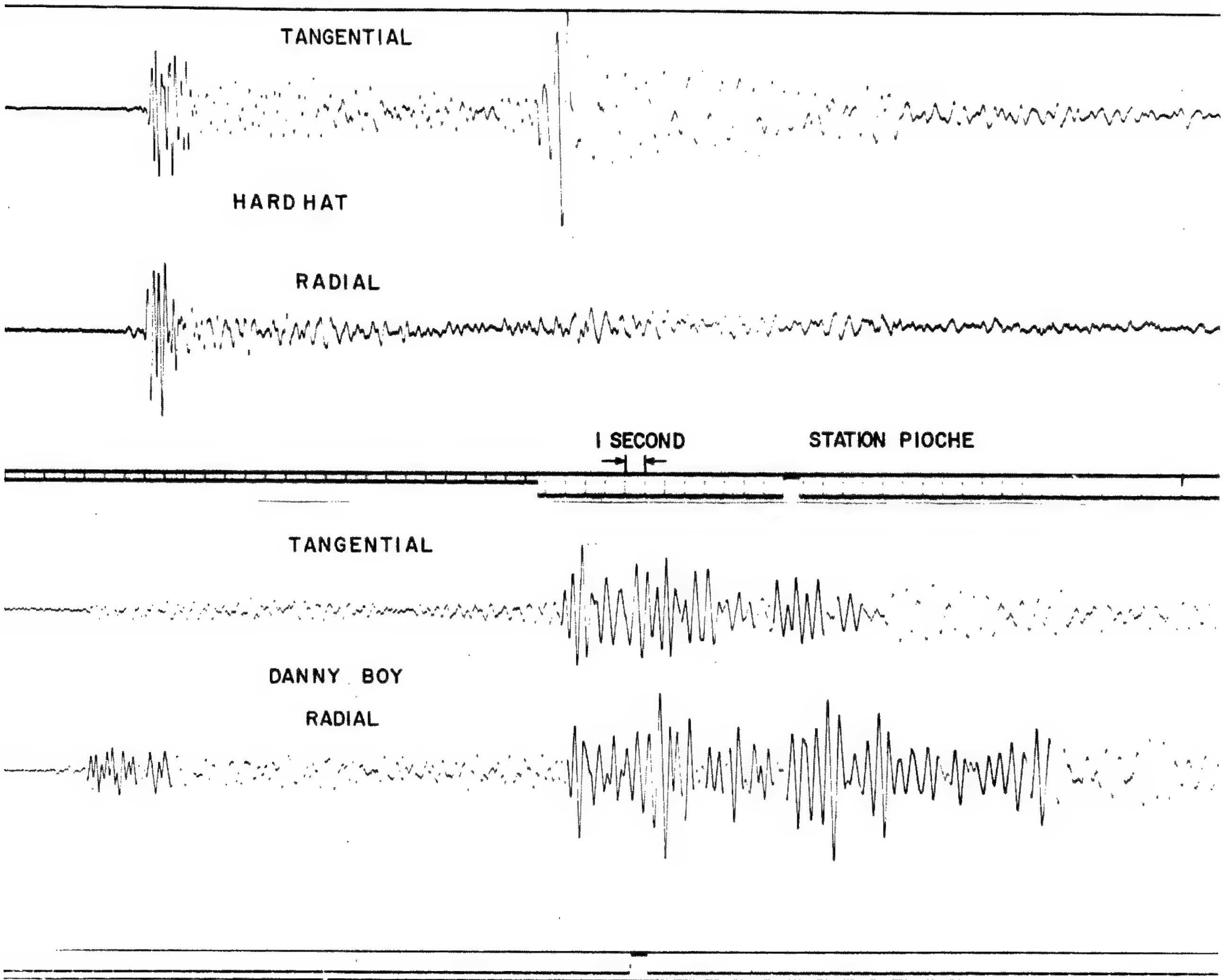

Fig. 2 Comparison of seismograms recorded at the same stations from two test areas.

in near-saturated and saturated tuff, respectively, which underlies the alluvium. These two produced seismic signals of about twice the amplitude predicted by the extrapolated alluvium curve. Haymaker falls between the curve and the tuff shots. Analysis of the tuff underlying the Yucca Valley alluvial fill compared to the fill shows the two media to behave essentially the same hydrodynamically except for the water content. Area 9 data taken from shots in media varying in degrees from alluvium to competent tuff fall along the alluvium curve fairly well, with no distinction among media being evident. Thus it may well be that for the Yucca Valley shots the medium effect is that of water content. Other tuff data have been received from the Area 12 mesa, which changes the travel path to our stations. Also, these shots have varied in location in the mesa and the medium has varied from weakly consolidated to competent tuff having a high water content. The two data points shown (Platte at 1.6 kt and Antler at 2.4 kt) represent this diversity. Since the area considered is not the same, it is not sufficient to examine only P wave ratios to alluvium. Comparison of maxima seen on any com-

ponent for any phase idicates that amplitudes of signals from Area 12 were from two to six times those from Area 3 alluvium.

Granite was the detonation medium for Hardhat and Shoal. The vertical P wave at Darwin from Hardhat was a factor of 4 about the alluvium curve. However, considering the maxima seen in any phase by any component and from Shoal data at Tonopah, a factor of 10 fits more of the data. The Tonopah station, which was about the same distance in the opposite direction from Shoal as from Hardhat, was the only comparable station.

Basalt is the other medium in which a nuclear device, Danny Boy, has been detonated. Since no contained bursts have been in basalt, the medium effect cannot be separated from either the depth of burst or travel path parameters. Sedan, plotted at 100 kilotons, was a nuclear cratering shot in alluvium. Danny Boy, 0.43 kiloton, gave significantly larger signals than contained alluvium shots, even though Sedan, an alluvium cratering shot with a similar scaled depth of burst, gave only one-fourth the amplitude which would have been expected for a contained shot. Basalt may appear to be similar to granite, but data are insufficient for any conclusion.

The periods of recorded maxima tend to be shorter for more competent source media; thus

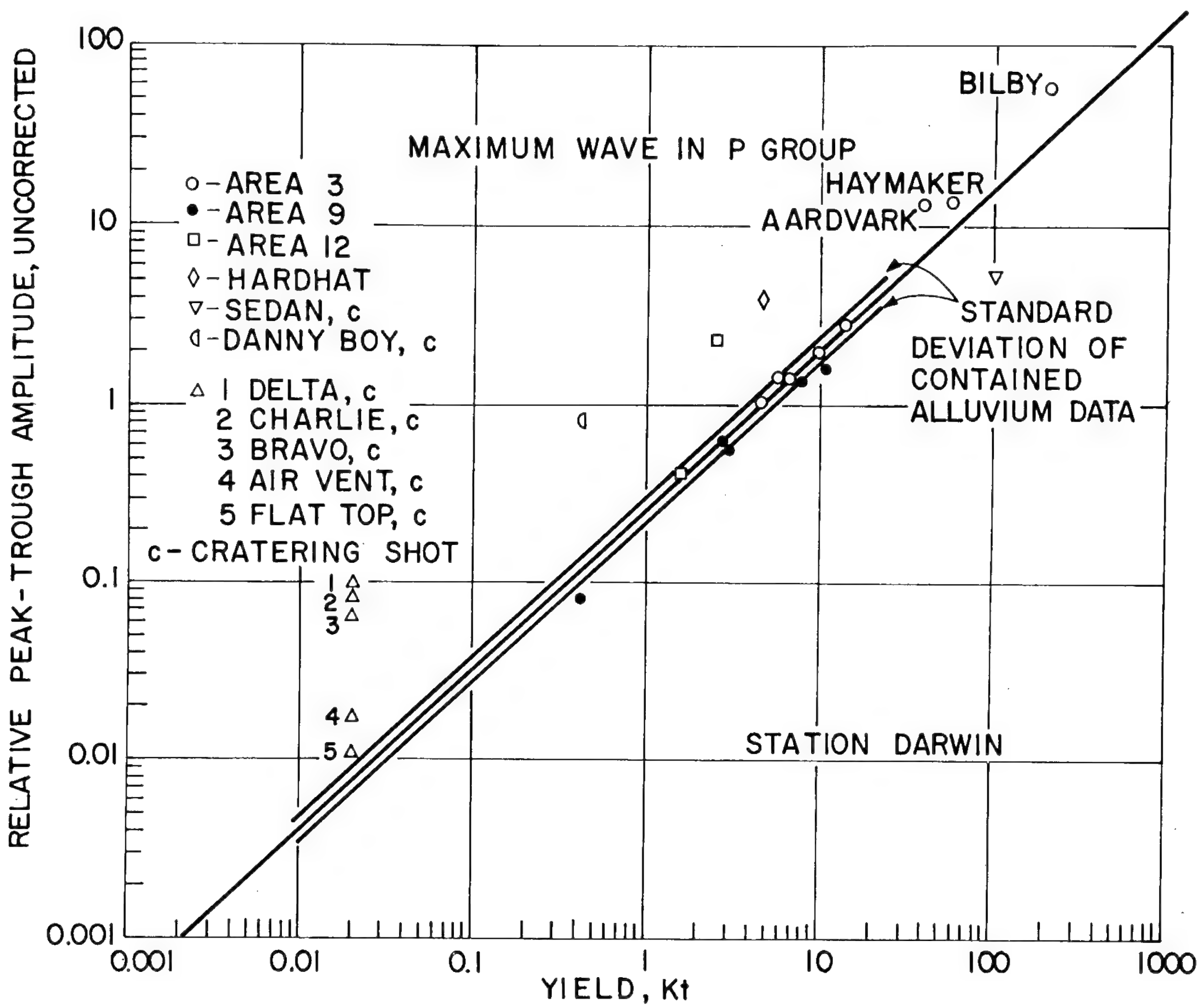

Fig. 3. Maximum phase amplitudes versus yield at Darwin. Selected data are compared to established curve for contained shots in Area 3 dry alluvium.

granite produces the highest frequencies and dry alluvium the lowest. The frequency change is not great and really does not change the range of frequencies to be considered for safety criteria.

Data from the NTS test series have been insufficient to allow adequate evaluation of the depth-of-burst effects. Data used by other researchers have shown that the strength of the seismic signal increases with depth of burial to containment depth, then slowly decreases. It has been noted that the Sedan shot at 1.1 gave only about one-fourth the signal expected from a contained shot. There have been some 20-ton high-explosive cratering shots. From Figure 3, Air Vent at a scaled depth of 0.5 produced about 1.75 the signal received from Flat Top, a surface burst in the same playa medium. Other data tend to reduce this ratio. Data for three shots in basalt, Delta, Bravo, and Charlie, at scaled depths of about 1.25, 1.5, and 2, do not provide a conclusive trend.

These data bring up another parameter, that of source mechanism. It has been noted that Air Vent and Flat Top, high-explosive shots, produced more signal compared to the curve, than did Sedan, a nuclear shot, at greater depth. Yet the Bravo, Delta, and Charlie shots in basalt are compatible with Danny Boy which was nuclear. Parameters cannot be separated sufficiently to explain this difference, but it may possibly indicate that the nuclear-to-high-explosive equivalence varies with medium. Or, it is possible that changing more than two parameters at a time precludes predictions within an order of magnitude.

Another source worth consideration is that of the cavity collapse subsequent to formation by a contained detonation. Here two sources at exactly the same epicenter may be examined. Short-period seismometers record signals from the collapse at roughly one-tenth the amplitude of the short signal. The collapse signals are of lower frequency than for the shot; this frequency change is more prominent than those observed for the yield and medium parameters previously mentioned.

Variation of seismic signals with various parameters have been examined. The following discussion presents some actual magnitudes of displacements and frequencies.

Data from the vertical P wave at Tonopah are most appropriate for prediction of actual ground displacements for two reasons. This station records higher amplitudes than some others, and the maximum seen on any component in any phase has never been greater than twice the verticle P-wave amplitude, which is very close for seismic signals. Figure 4 shows the 0.9 power curve fit to the maxima peak-to-trough ground deflection as determined from the vertical P wave recorded by short-period instruments for a number of alluvium shots. The band width of 1.5 would be expected to fit most alluvium shots. Data for other media are too scant to establish whether or not their curves parallel the alluvium curve. Therefore, curves have not been drawn, but a few data points are included for use with the previously quoted ratios. Such prediction curves should be used with caution. Azimuth variations can vary the amplitudes, and a change from rock to alluvium receiver can amplify the signal several times, as have been observed by other investigators.

Up to this point only body and Lg waves have been discussed. Seismograms from our longer period system have shown a fairly long duration train of waves with periods of about 2 seconds. Figure 5 shows the relative response of the long-period and short-period systems. The Darwin underdamped system curve has been added to illustrate its flatter response. The better response of the long-period system at 0.5 cps compared to 1 cps is obvious. Figure 6 compares the vertical seismograms obtained by the two instruments from an alluvium shot of about 10 kilotons. The actual ground motion measured for peaks arriving between about 2 minutes, 10 seconds and 2 minutes, 50 seconds is about the same magnitude as the short-period P waves (shown in Fig. 4). Periods in this wave train tend to increase with yield. For a yield of about 3 kilotons, the period was about 1.5 seconds; for the yield of about 10 kilotons shown in the illustration it is about 2 seconds, while for Bilby at about 200 kilotons it had increased to about 3 seconds. Decay rate of these waves is slower than that seen for the body waves. It takes about 2 minutes for a decay to one-fifth the amplitude if a maximum peak at about 1.5 minutes is chosen as the first time. The prominence of this wave train from the Bilby shot serves to focus attention on it. Further information obtained both with receivers on deep alluvial fill and at shorter distances than present net stations would prove of value here.

Frequency content of seismic signals can best be obtained from spectra which have been corrected for frequency response. Seismograms can

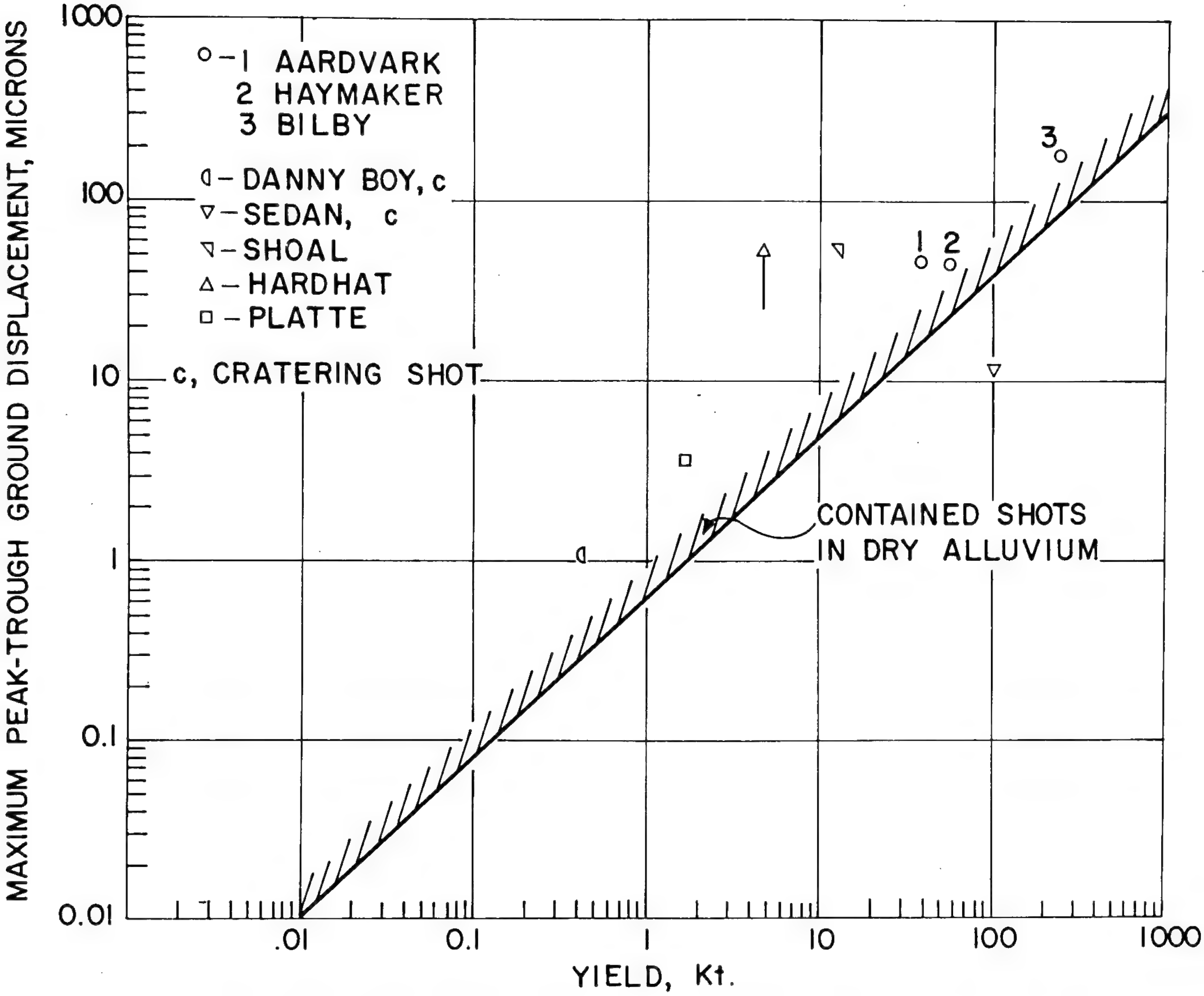

Fig. 4. Maximum peak-trough ground displacement versus yield for dry alluvium and other selected data at a nominal distance of 150 kilometers.

be misleading in that frequencies with greatest magnification rather than greatest ground displacement are often most prominent. Figure 7 shows the amplitude spectra of the radial seismogram from two stations. The records were for a contained alluvium shot of about 10 kilotons. The spectral magnitudes between 5 and 10 cps (obtained but not plotted) are below those shown for 5 cps. Ordinates are the integrals over the full seismogram separated into frequency components, then corrected for response. Figure 8 gives the velocity spectra of the tangential and radial components at Tonopah. These latter spectra were obtained by multiplying the amplitude values by the frequency. Fourier analysis, which does not smooth the points, were used to obtain these spectra. Figure 9 illustrates the difference in frequency content between seismograms from shots and the subsequent collapse, which has frequently occurred. Again an alluvium shot of about 10 kilotons and its collapse were the energy sources. The Tukey spectral analysis, which smooths the spectrum, was used here. Ratios of spectral estimates of shot to collapse were taken at each 0.2-cps frequency interval. No corrections were necessary for response or frequency. Values plotted are ratios of shot to collapse which are equally applicable to the integrated square of amplitude or velocity.

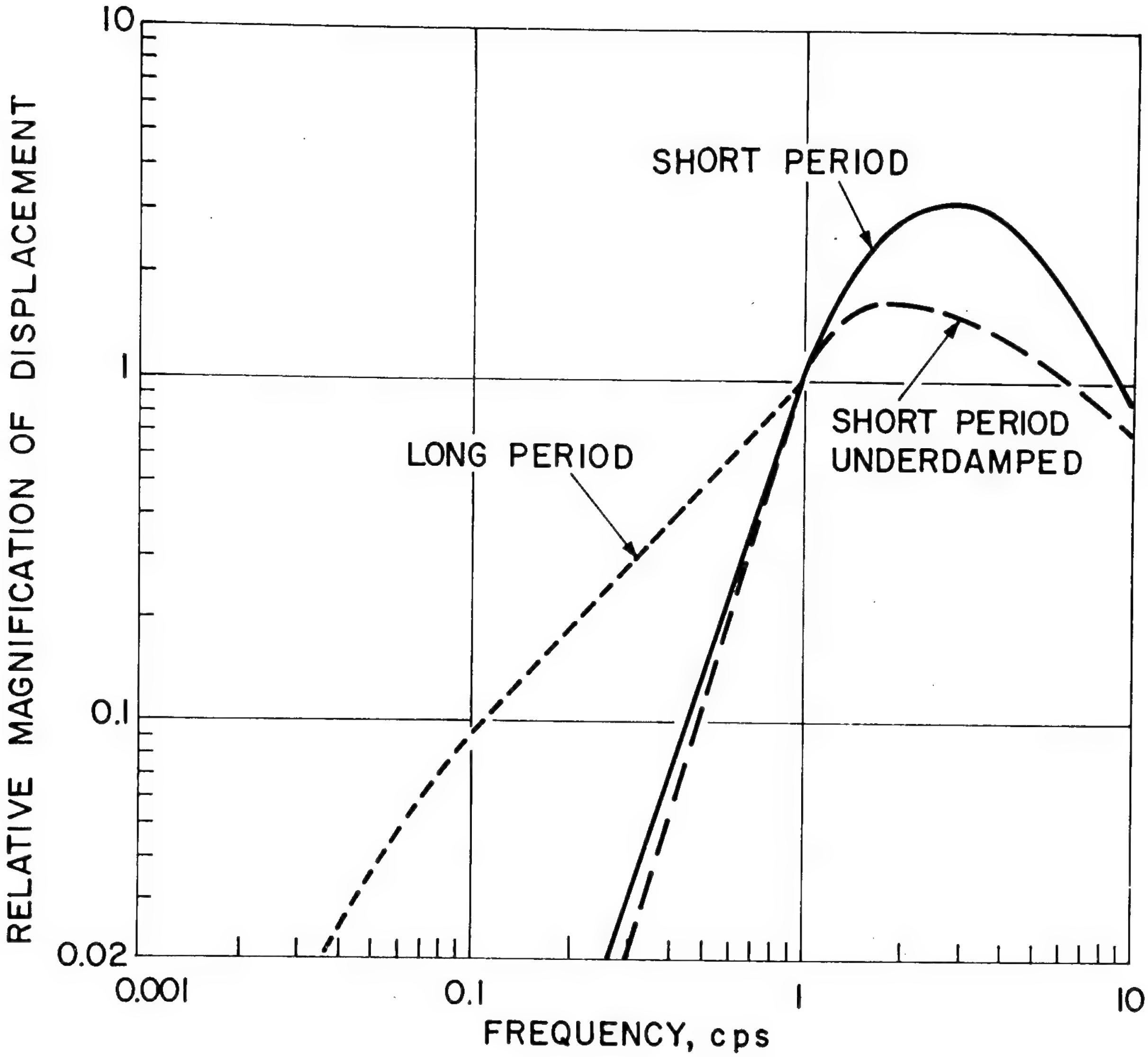

Fig. 5. Frequency response of seismometer systems.

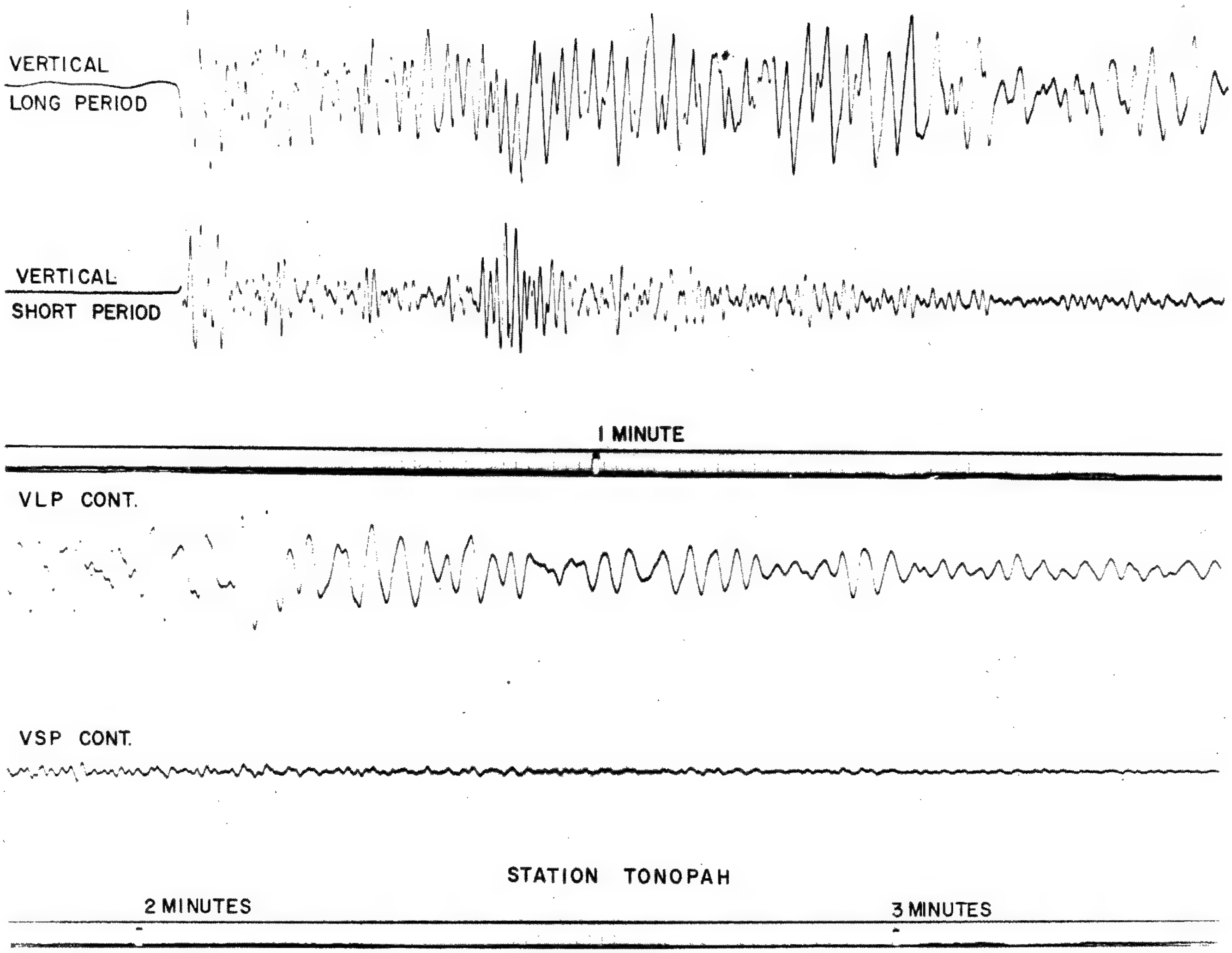

Fig. 6. Comparison of seismograms from two systems illustrating magnitude and duration of longer period waves.

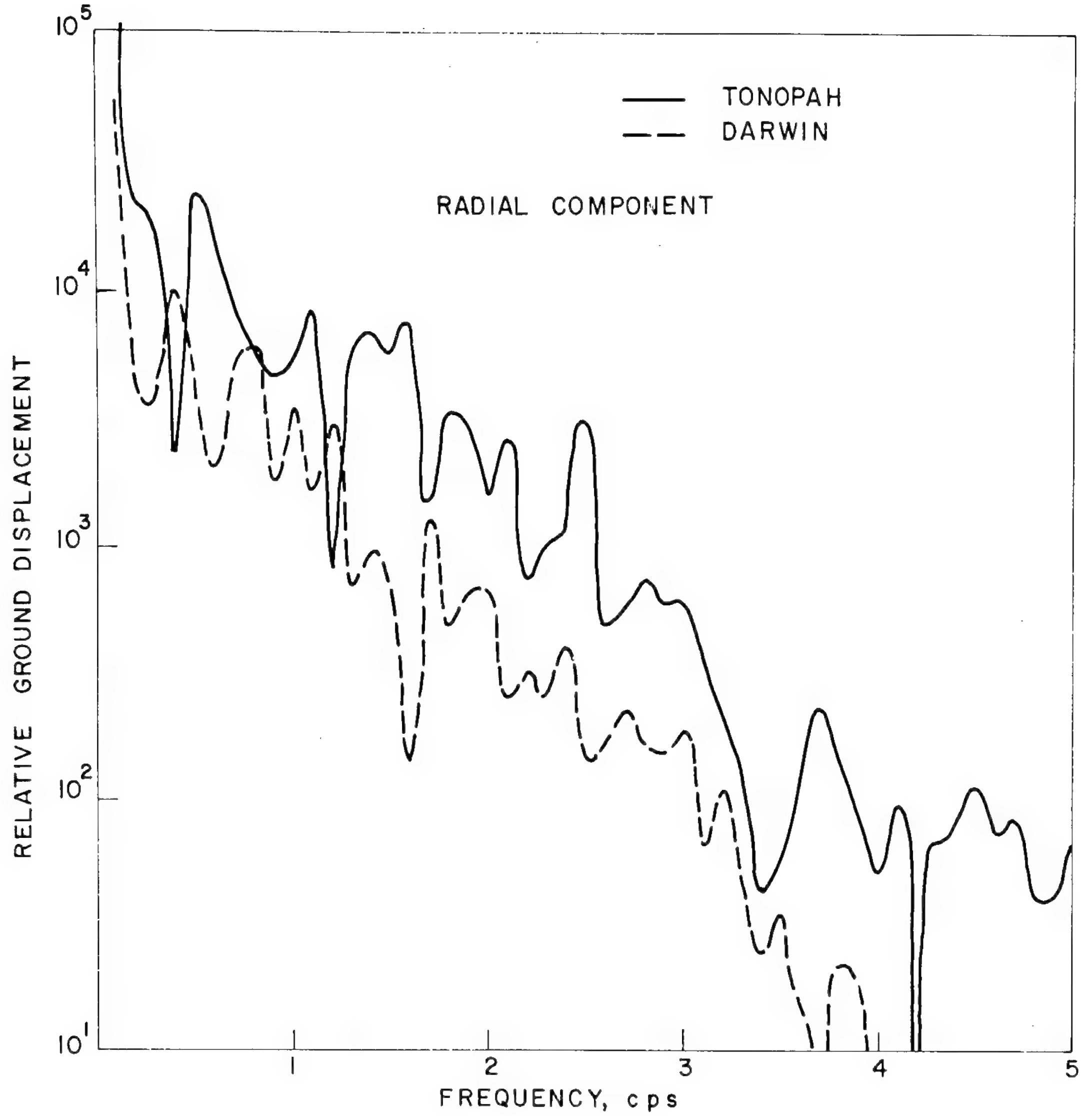

Fig. 7. Spectra of integrated ground displacement versus frequency.

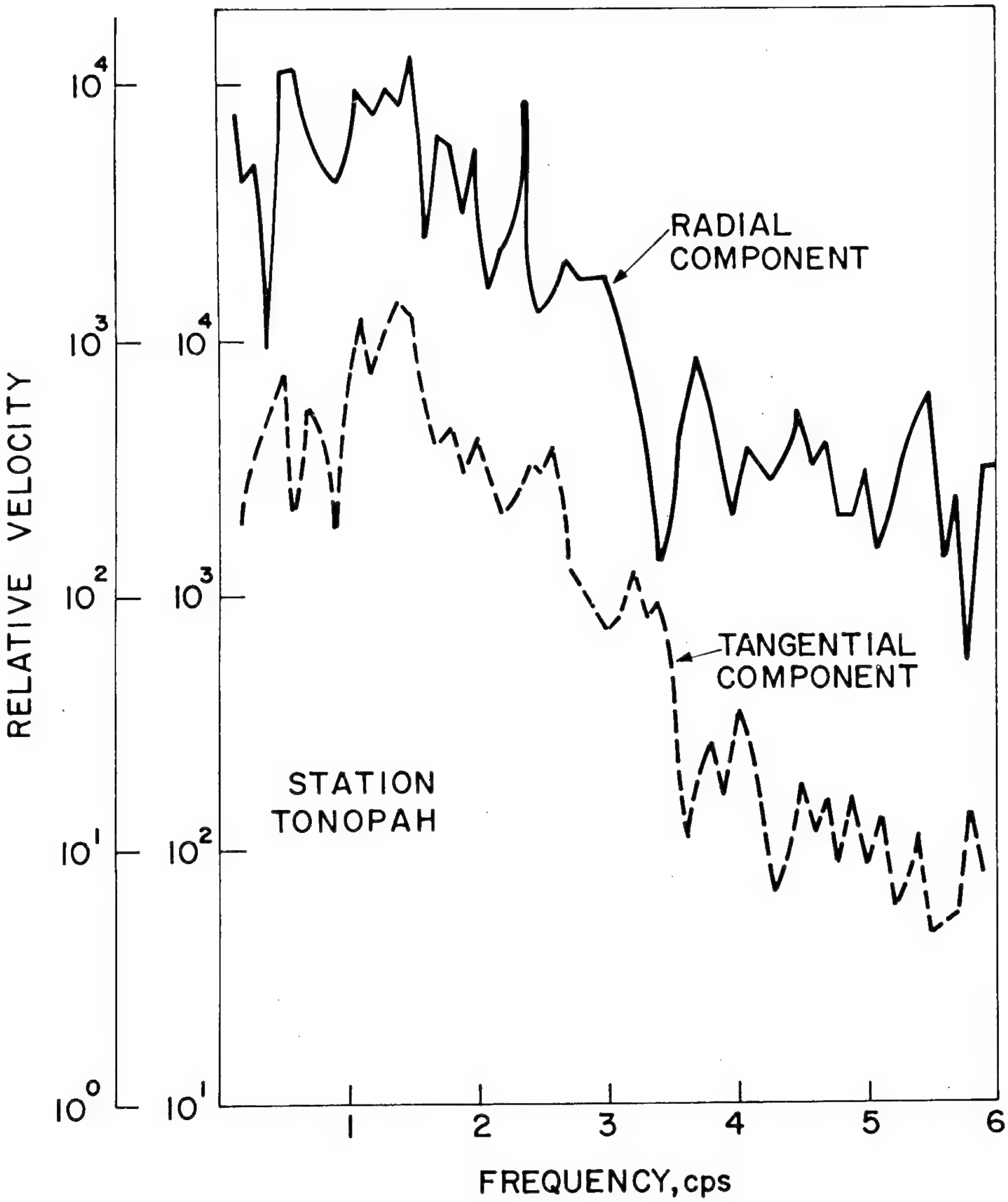

Fig 8. Spectra of integrated particle velocity versus frequency.

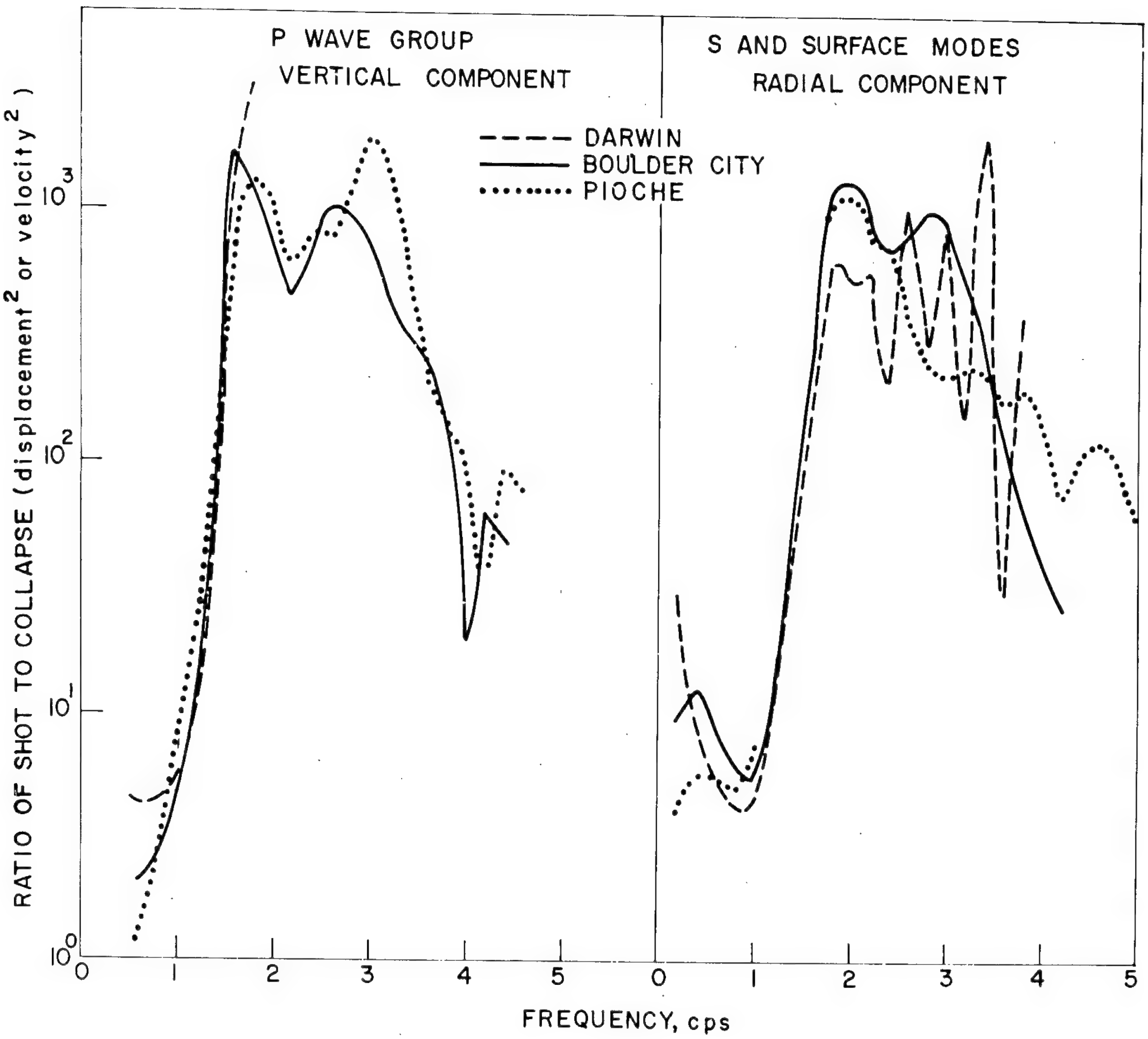

Fig. 9. Ratio of integrated amplitude^2 of shot to collapse versus frequency.

BIOGRAPHICAL SKETCH OF AUTHOR

Mrs. Dorris M. Hankins, nee Ehret, was born and educated in Iowa. She received a B.A. in mathematics from Central College in 1946 and M.S. in physics from Iowa State University, Ames, Iowa, in 1949. She was employed by NACA at Moffett Field as an aeronautical research scientist for 3-1/2 years. From there she went to the Southern California Cooperative Wind Tunnel, operated by CIT, where she worked on wind tunnel design. She joined the research staff at Sandia Corporation in 1952. At Sandia she has worked on problems in radiation protection, drag of block forms, crater scaling, and Plowshare projects. Since the fall of 1959 she has worked in the field of seismology. At present she is the Project Scientist for the Sandia NTS Seismic Net.

THE EFFECTS OF SEISMIC WAVES ON STRUCTURES AND OTHER FACILITIES

Lewis J. Cauthen, Jr., Captain, U. S. Army Corps of Engineers

Lawrence Radiation Laboratory, University of California
Livermore, California

ABSTRACT

The effects of explosion-induced ground motion must be evaluated in planning and executing any nuclear excavation project. For some projects ground motion intensity may dictate the use of less-than-optimum yields to minimize damaging effects. In remote areas, weighing the alternatives of outright purchase of some property or use of smaller yields may be required. The cost of indemnifying owners against damage must be considered in any case.

Discussions of the effects of ground motion on three broad types of facilities – engineered structures, residential buildings, and equipment required for the support of nuclear excavation operations – are presented. A method of predicting the response of single-and multistoried buildings, the response spectrum technique, is discussed, with emphasis on the application of explosion-induced spectra.

Conclusions drawn from several tests of damage to residential-type buildings are presented. Included are data from four investigations of damage caused by commercial and industrial blasting and the results of several studies made in conjunction with underground nuclear detonations.

Finally, a survey of damage to the equipment required to carry out excavation projects is summarized.

INTRODUCTION

It has been pointed out that the detonation of large yield devices underground produces seismic signals – ground motion – at considerable distances from the explosion. It is important that the significance of such motion in terms of damage potential be thoroughly evaluated in planning any Plowshare application.

While economics is not the only consideration in assessing the possible damage, it is probably the principal one. Very early in the study of a project yields would be selected which produce the optimum crater or chimney size, for example. The damage to cultural features which might be expected from the ground motion caused by the selected yield must be evaluated. If such damage were limited to isolated cases of minor cracking of plaster in old homes, agreements could probably be reached with the owners involved with a minimum of difficulty. If, on the other hand, more extensive damage could be reasonably expected, several alternatives would have to be considered. The yields tentatively selected as most efficient might be reduced to a "safe" level. However, the dimensions of the project may be such that this reduction would require yields which would not be sufficient to do the job, or to make nuclear excavation not competitive with conventional procedures. In some cases it might be obvious that damage would be so great that the property involved would have to be purchased outright, while in other situations the best solution would be to employ optimum yields fully expecting damage which could be indemnified at a more attractive cost than would be incurred by using such small devices that no damage or only negligible damage would occur.

In any event, means of evaluating the damage potential of the various alternatives would be necessary. In this paper the present state of the art of these evaluations is discussed, as related to broad types of facilities: buildings in which stresses and deformations can be analyzed using established engineering principles, i.e., "engineered structures;" "nonengineered structures" such as residential buildings; and some of the facilities used for construction and support in a nuclear excavation or mining project.

RESPONSE OF ENGINEERED STRUCTURES TO GROUND MOTION

It appears that the effect of explosion-induced ground motion on engineered structures can best be discussed by making use of an approach universally employed in the earthquake engineering field, the response spectrum technique. Its most straightforward application assumes for a building linear elastic behavior; viscous, or velocity, damping; rigid floor girders; and concentration of all the mass of each story at ceiling level. The use of these assumptions permits engineered structures to be treated as lumped mass-spring-dashpot vibrating systems.

In Figure 1 is shown a single degree of freedom (SDF) system with the equations which describe the free vibration of the mass.

To visualize the response of a single degree of freedom system to a time-dependent nonperiodic force, we should begin by examining the impulse response of the mass. An impulse acting on the mass will cause a change in velocity, from which it is possible to determine the motion of the mass as shown in Figure 2.

If the time-varying driving force can be expressed as a series of impulses, the motion of the mass can be defined by summing the response due to the individual impulses as in Figure 3 if the system is linear.

The previous discussion applied to motion

NOMENCLATURE

Symbols listed in order first used in test or figures, unless defined where first used.

k	stiffness
m	mass
x	displacement of mass
$\ddot{x}$	acceleration
W	weight (in section on Engineered Structures)
N	normal force
ΣF_h	summation of horizontal forces
p	natural frequency, radians/sec
t	time
x_0	initial displacement
v_0	initial velocity
$\dot{x}$	velocity
$\ddot{y}$	ground acceleration
e	base of natural logarithm
β	percent critical damping
τ	time at which imputse acts; same as t_n
$\dot{u}$	relative velocity
p_d	damped natural frequency
c	$2\beta pm$
S_d	$\left[-e^{-\beta pt}\int e^{-\beta p\tau}\,\ddot{y}(\tau)\sin p_d(t-\tau)\,d\tau\right]_{max}$
T	period, sec
kip	1000 lb
W	yield in kt (in section on Support Facilities)

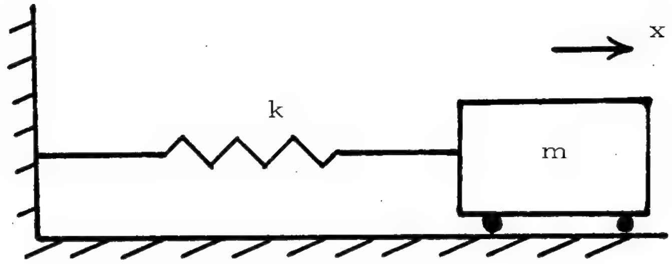

(a) Undamped single-degree-of-freedom system.

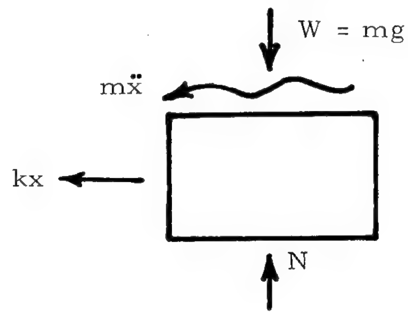

(b) Free-body diagram of mass displaced distance x.

$$\sum F_h = 0$$

$$m\ddot{x} + kx = 0$$

$$\ddot{x} + \frac{k}{m} x = 0$$

Letting $\frac{k}{m} = p^2$

Solution: $x = A \cos pt + B \sin pt$

From initial conditions: $A = x_0$; $B = v_0/p$

$$x = x_0 \cos pt + v_0/p \sin pt$$

(c) Equation of free vibration of mass.

Fig. 1. Free vibration of SDF system.

resulting from a force acting on the mass directly. A slight modification yields a procedure which can be used in cases where the excitation is at the base of the spring. If the displacement of the mass is x, and of the base, y, then

$$m\ddot{x} + k(x - y) = 0.$$

Subtracting $m\ddot{y}$ and letting u be the relative displacement of the mass with respect to the base:

$$m\ddot{u} + ku = -m\ddot{y}.$$

This is analagous to a system driven by a force $-m\ddot{y}$ applied to the mass, the displacement being relative.

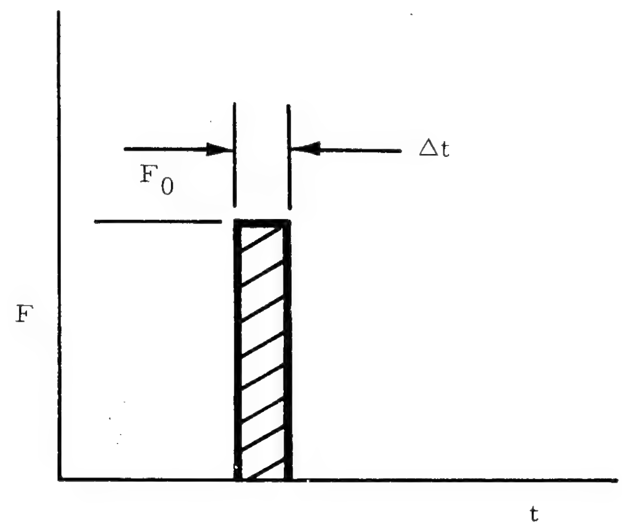

$$\text{Impulse} = F_0 \, \Delta t$$

$$\text{Impulse} = \text{change in momentum}$$

$$F_0 \, \Delta t = m\Delta\dot{x}$$

If system is initially at rest, $v_0 = 0$, $x_0 = 0$

$$F_0 \, \Delta t = m\dot{x}$$

$$\dot{x} = \frac{F_0 \, \Delta t}{m}$$

$$x = x_0 \cos pt + \frac{v_0}{p} \sin pt$$

$$x = 0 + \frac{F_0 \, \Delta t}{pm} \sin pt$$

Fig. 2. Impulse response of SDF system.

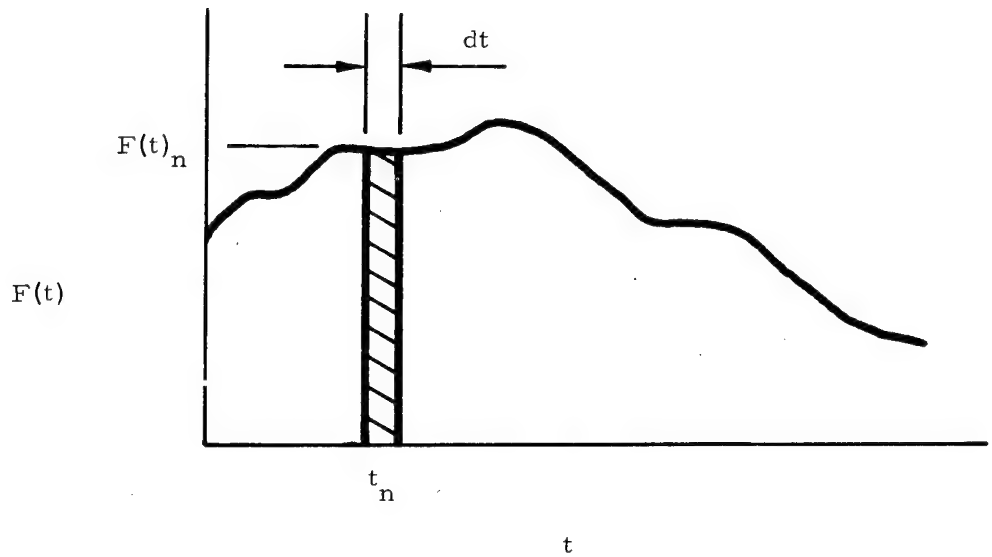

Impulse response: $x = \frac{F_0 \, dt}{mp} \sin pt$

Displacement at time t due to impulse $F(t)_n$:

$$x = \frac{F(t)_n \, dt}{mp} \sin p(t - t_n)$$

Displacement at time t due to series of impulses F(t)

$$x = \int_0^t \frac{F(t)}{mp} \sin p(t - t_n)$$

Fig. 3. Response of SDF system to driving force F(t).

Considering a system with viscous damping slightly changes the equation used thus far. The impulse response of such a system is given by:

$$u = e^{-\beta p(t-\tau)} \frac{\dot{u}}{p_d} \sin p_d(t - \tau)$$

or

$$u = e^{-\beta pt} \frac{F_0 d\tau}{mp_d} e^{-\beta p\tau} \sin p_d(t - \tau).$$

The response to a series of impulses is then:

$$u = e^{-\beta pt} \int \frac{F_0(\tau)}{mp_d} e^{-\beta p\tau} \sin p_d(t - \tau)\, d\ .$$

Making use of the analogy mentioned earlier:

$$u = \frac{e^{-\beta pt}}{p_d} \int - \ddot{y}(\tau)\, e^{-\beta p\tau} \sin p_d(t - \tau)\, d\tau.$$

A plot of the maximum values of this equation against various damped frequencies (p_d) is known as a response spectrum. The equation yields a spectrum for each value of damping, β.

As stated earlier, engineered structures can be considered as vibrating systems for analysis of their response to ground motion. In this case a one-story building would be treated as a single-degree-of-freedom system. The dynamic parameters, k, m, c (or β), p_d, are readily determined to the required accuracy. Because structures are invariably designed with excess gravity load capacity, the horizontal motion of the responding structure is of primary importance.

An idealized structure is shown in Figure 4. For this structure the velocity spectrum obtained from any ground motion, $\ddot{y}$, might be as shown in Figure 5, which is characteristic of both the structure and the ground motion. A more interesting case is the general one of the effect on various structures of some time-varying ground motion. The principal structural characteristics involved are β and p_d. Five spectra associated with the surface motion recorded near an underground nuclear blast are shown in Figure 6. Two features are obvious. First that structures having certain periods (or frequencies) respond more violently to the given ground motion; and second, that the amount of damping greatly influences the response, with even a small amount of damping markedly reducing peak spectral values.

Since the integral must be evaluated for the entire ground motion, the amount of computational work is tremendous, requiring some type of computer.

The use of response spectra to determine the effect of a given motion is surprisingly simple once the spectrum is obtained. For estimating

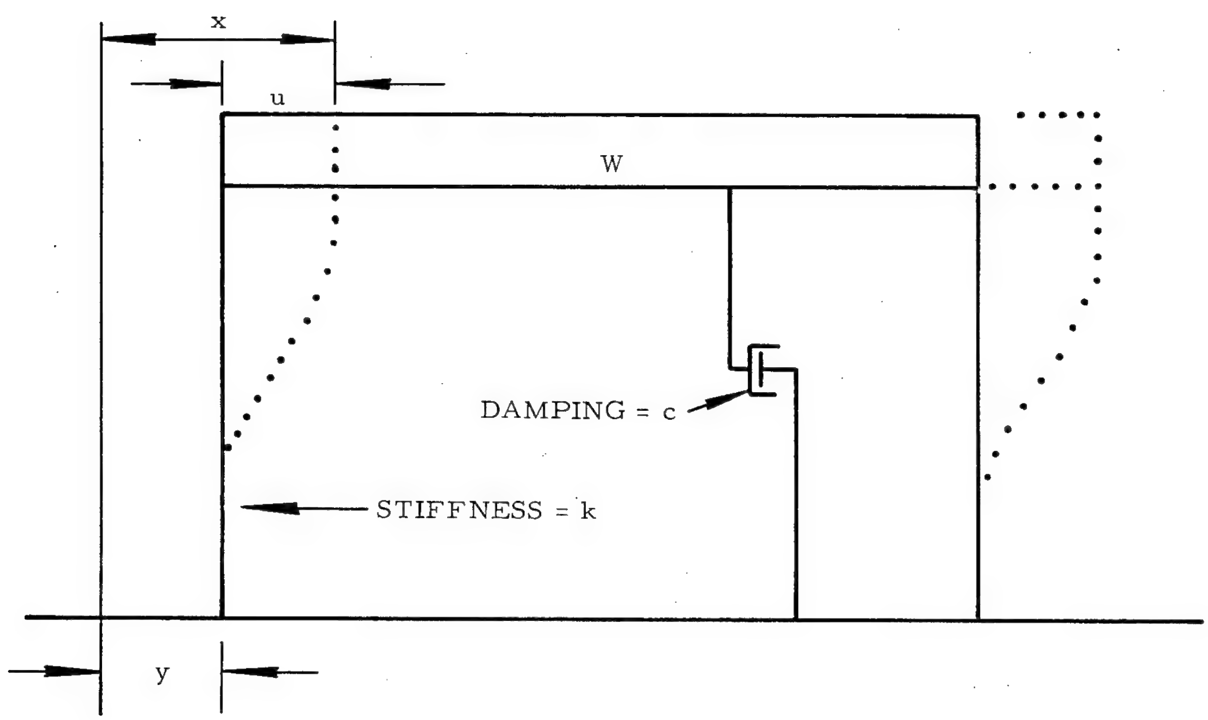

For unit deflection restoring force $= \dfrac{12\ EI}{L^3} = k$

Fig. 4. Idealized SDF structure.

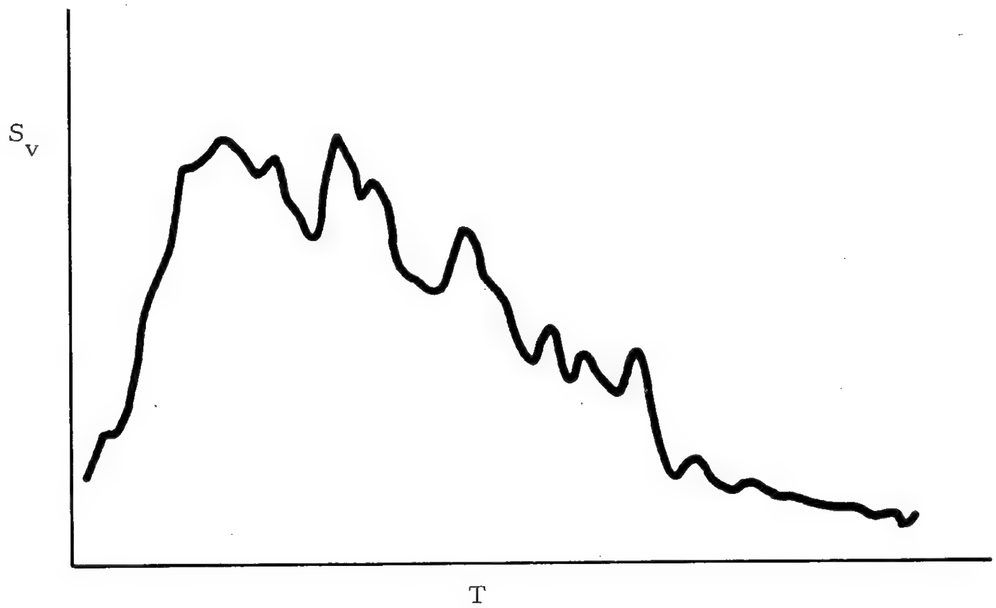

Fig. 5. Displacement spectrum for structures having a particular β. A single structure having a unique period, T, would be represented by a single point.

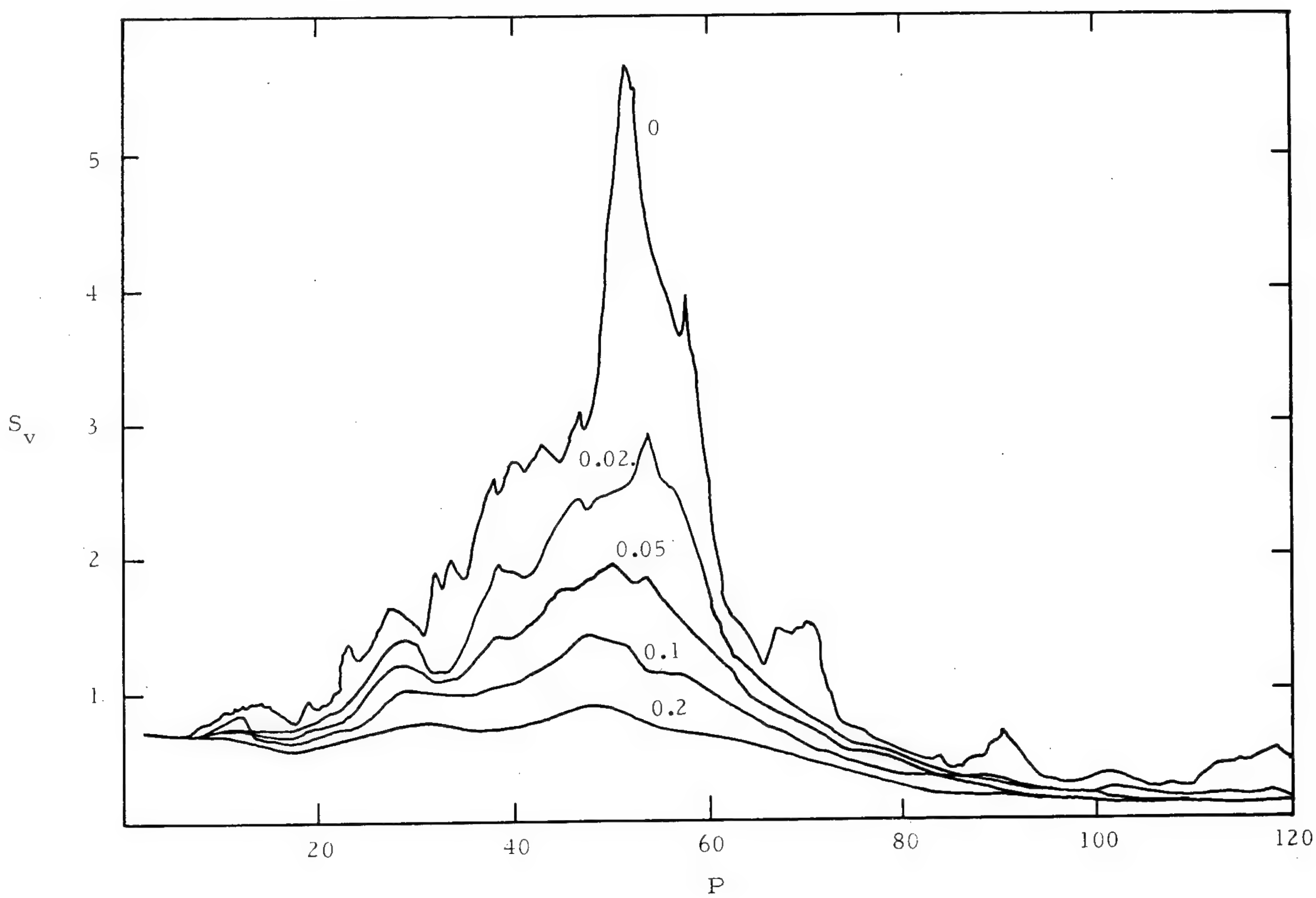

Fig. 6. Relative velocity spectrum for one GNOME accelerogram. Damping – 0, 2, 5, 10, 20% critical. S_V in units of 10 cm/sec. Frequency P in rad/sec.

the effect on a particular building, the procedure outlined in Figure 7 might be used.

This value could be compared with the lateral force for which the building was designed and a determination made of the likelihood of damage. It should be emphasized that each spectrum is uniquely related to the earth-motion history employed in obtaining the spectrum. For evaluating the response of a particular building to some planned detonation, some standard spectra would be highly desirable. Computer programs are in existence for preparing spectra from accelerograms of earlier shots, and it is anticipated that standard spectra for a broad range of situations will be available in the future.

Though this discussion has been limited to one-story buildings (single-degree-of-freedom systems) the same procedures can be use for multistory buildings.

A multistory building may vibrate in as many mode shapes as it has degrees of freedom. In structures having low damping, each mode is independent of all others, so that the maximum response of the building can be obtained by simply adding together the response in the individual modes.

While the dynamic parameters of single-degree-of-freedom structures have in many cases been reduced to tables, some calculation is required to determine these for multistory buildings. These procedures, which are extensively documented in the structural dynamics literature, generally involve assuming certain parameters—mode shapes, for example—and calculating other parameters, checking for consistency between the assumed parameters and their values derived from the calculations. Of course, for existing buildings, it may be possible to actually measure the period and modal deflections.

The response calculated by superposition of modes represents an upper limit because the maximum response in the various modes need not occur simultaneously. A study of the response of one building to an earthquake has shown that the calculated response exceeded the recorded by about 30%. A more realistic estimate of response might be obtained by adding some fraction, say one-half, of the higher mode response to the fundamental mode.

Other factors which might cause actual response to be less than that which would be calculated include inelastic behavior and participation by nonstructural members. Slight yielding of the many joints in a large building or minute cracking of concrete could absorb a tremendous amount of the input energy. Features such as walls and stairwells cause a significant departure from the assumed configuration.

While these procedures produce quite satisfactory results when applied to "older" buildings, there is a need for much additional work on the response of the modern buildings with their long, uninterrupted clear spans, a situation where the rigid girders assumption is clearly not justified.

Obviously, the likelihood of damage to engineered structures, which usually represent a large investment, would be studied by experts during the planning of any Plowshare project.

Structural engineers who have studied the problems are confident that present knowledge would permit such projects to be executed without risking damage to large buildings.

DAMAGE TO RESIDENTIAL-TYPE STRUCTURES

As a first step in resolving the question of what constitutes damaging ground motion to residential-type buildings, a search was made of available literature on the effect of industrial high-explosive detonations on residential-type construction since it is expected that damage to this type building represents one of the limiting problems in carrying out Plowshare projects. The four reports covered by this paper appear to be the most complete of those available.

Investigations studied all involved the assumption of simple harmonic ground motion so that maximum acceleration, velocity, and displacement are uniquely related for a given frequency (f). Therefore, if

$$\begin{aligned} X &= A \sin 2\pi ft \\ x &= A \\ v &= 2\pi fA \\ a &= 2\pi fv = 4\pi^2 f^2 A \end{aligned}$$

where X = displacement at time t, x = maximum displacement, v = maximum velocity, and a = maximum acceleration. All the investigators plotted their results on log-log graphs with "displacement" ordinates and "frequency" abscissas. Therefore, a -1 slope represents velocity (A and f to the first power) while a slope of -2 represents acceleration (A to the first power; f to the second).

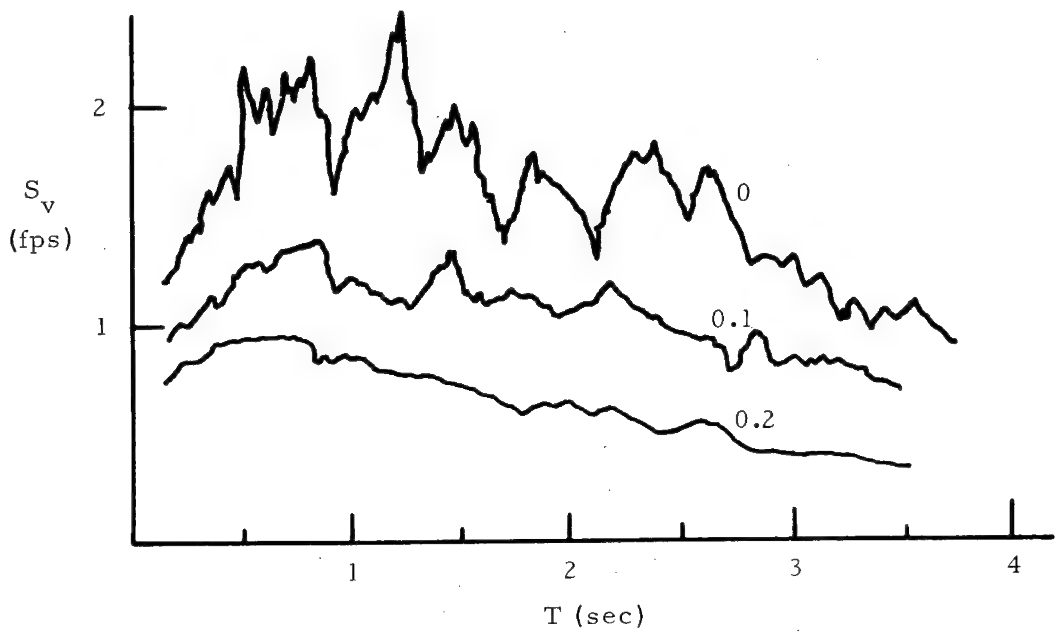

Maximum shear (v_{max}) in columns = kx_{max}

$$x_{max} = \left[\int e^{-\beta pt} \frac{-\ddot{y}}{P_d} e^{-\beta p\tau} \sin P_d(t - \tau)\, d\tau \right]_{max} \equiv \frac{S_v}{p_d}$$

$$v_{max} = \frac{KS_v}{p_d}$$

$$k = mp^2$$

$$v_{max} = mp_d^2 S_v / p_d = mp_d S_v$$

If the structure of interest has a period of 0.5 sec ($p_d = 2\pi/0.5$) and damping is 20% critical, from the spectrum S_v is 0.9 fps. If the weight of the structure is 20 kips, the base shear would be:

$$\frac{20 \text{ kips} \times 12.56 \text{ r/sec} \times 0.9 \text{ fps}}{32.2 \text{ ft/sec/sec}} = 7 \text{ kips}$$

Fig. 7. Calculation of column shear using velocity spectrum (S_v); $S_v = p_d S_d$.

Because of the great variety of structure types studied and the uncertainty of design and construction details, both of the buildings covered by these reports and those which will be the subject of future concern, empirical relationships based on a number of explosions which resulted in damage seem preferable to detailed theoretical analyses.

Experience has shown that the frequencies associated with underground nuclear blasts are in the range below 10 cps. Predominant frequency decreases as yield and range increase; and higher frequencies occur in hard rock than in low-velocity rock and soil. Unfortunately, there appears to be little data published covering the very low frequency range.

Throughout this section, damage refers to cracking of plaster, the weakest structural element in most houses, and therefore the first to show distress. The extent of damage is as indicated in the section on each investigation and in the conclusions.

Investigations

U.S. Bureau of Mines

One of the earliest investigations undertaken to study the effect of blasting operations on residential structures was reported by the U. S. Bureau of Mines in USBM Bulletin 442 (1942). Beginning in 1935, the Bureau instrumented a number of residential-type structures adjacent to operating quarries. The blasts associated with normal operations caused no detectable damage.

Vibrating machines were then developed which produced wave forms said to be sufficiently similar to those of high-explosive detonations for correlation. These machines, consisting of counter-rotating unbalanced rotors, were installed in several buildings in an attempt to excite each building as a unit to the point where some cracking of plaster occurred, but the machines were not able to produce large enough amplitudes to cause damage.

Tests were begun to study the effect of vibration of individual floor and ceiling panels using the shaking machines, which the investigators felt duplicated the effect of a quarry blast acting on the entire building. In each test a machine was fixed to the center of a panel, and seismometers were located at several points on the panel. The test consisted of adjusting the amplitude and frequency of panel motion until damage resulted or to some preselected level, recording the motion on the seismometers, and noting the extent of damage.

Approximately 160 tests were conducted in buildings of frame, brick, and masonry construction in the frequency range of 2 to 40 cps with most damage-producing tests at frequencies of 8 to 20 cps. Results of these tests are shown in Figure 8. It was concluded that the damage region could best be delineated by the bold solid line. This line, having a slope of -2 represents a constant acceleration of 32 ft/sec^2 (1.0 g). The lighter solid line represents an acceleration of 3.2 ft/sec^2 (1.0 g). It was considered that an acceleration of 1 g is the best damage index and that an acceleration of 0.1 g defines the threshold of damage.

The validity of these results as an indication of potential damage due to actual blasting is doubtful. The machine-induced vibrations are steady state sinusoids rather than complex transients (as would be the case with the blast) and also of somewhat longer duration than that of explosion-induced motion. The basis for correlating the machine and the blast-wave forms is not clear.

F. J. Crandell

In 1949 Crandell published a paper in which he proposed an "Energy Ratio," defined as (acceleration/frequency)^2, as an indicator of structural damage. As a result of a number of excavation shots in areas built up with homes, schools, and churches (more than 1000 buildings were involved). Crandell found that for average structures there was no damage in cases where E. R. < 3. Accelerations were recorded on the surface adjacent to buildings using an accelerograph which Crandell had developed. His report does not indicate his method for determining frequency. Whereas E. R. < 3 indicated a safe condition, an E. R. of 6 normally resulted in damage to residential-type buildings which had not been prestressed by settlement or shrinkage. An interpretation of these data is complicated by the omission in the paper of a definition of damage.

This work involved charges ranging from 1 to 100 pounds, and structures were all located less than 250 feet from the detonation. It appears that frequencies considered are in the 2- to 80-cps range.

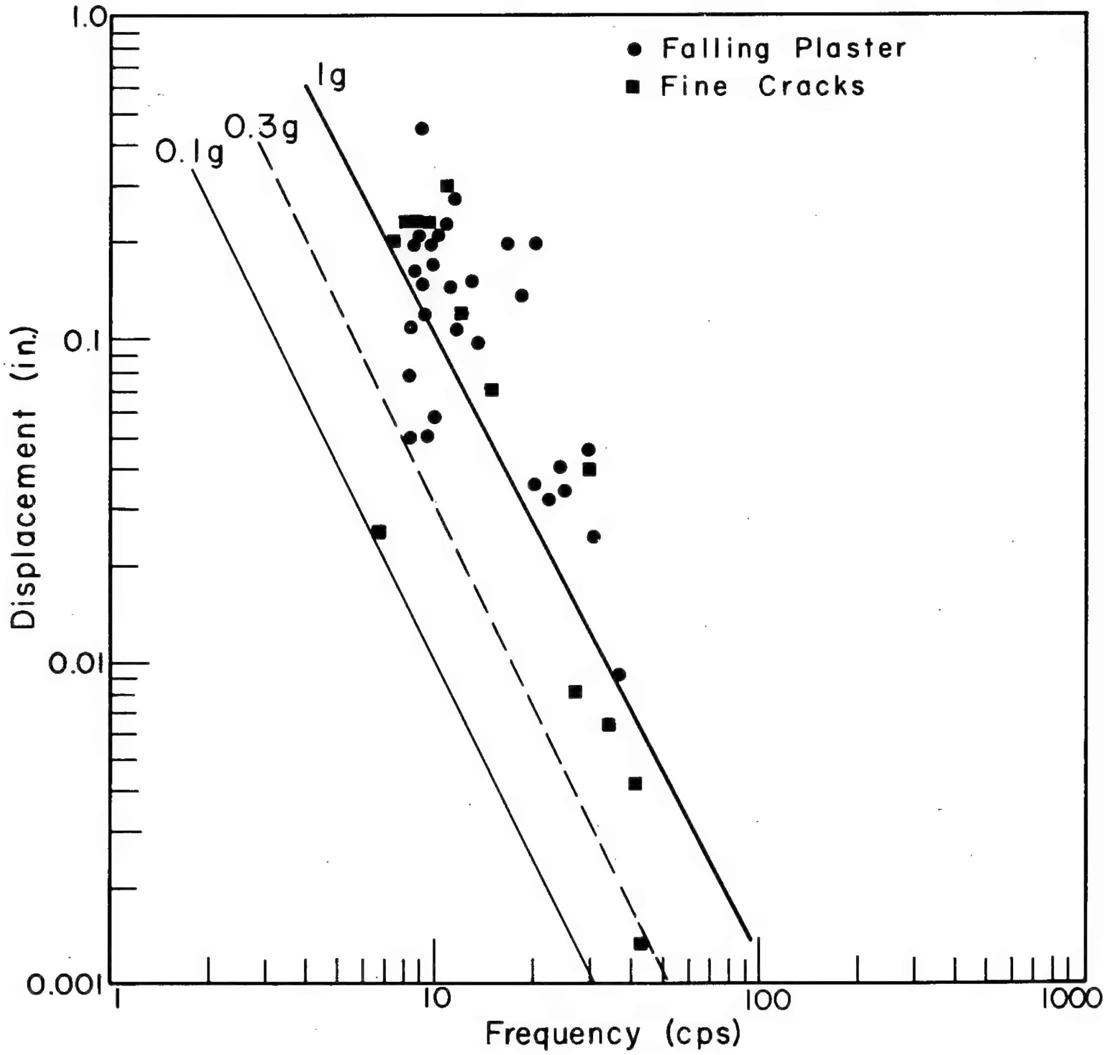

Fig. 8. Displacement vs frequency (USBM) "No Damage" not indicated.

Although Crandell recommends use of the Energy Ratio, manipulation of his equation and insertion of his limits results in the following restatement of his concept:

$$\text{E.R.} = \frac{a^2}{f^2} (\text{a in ft/sec}^2\text{, f in cps})$$

$$a = 2\pi f v$$

$$\text{E.R.} = 4\pi^2 v^2$$

$$v = \frac{\sqrt{\text{E.R.}}}{2\pi} \text{ (v in ft/sec).}$$

Damage to normal residential-type buildings is likely to occur when the velocity of the surface adjacent to the structure exceeds 4.7 in./sec. No damage would be expected in cases where maximum surface velocity is less than 3.4 in./sec.

Langefors, Kihlstrom, Westerberg

In the course of a major project in Stockholm in the 1950's a study was made of the effect of small charges (up to 220 pounds) detonated in hard rock close to a number of buildings. The buildings appear to be mainly of masonry construction. In planning this project it had been decided that from an economic standpoint it would be advantageous in some cases to use such large charges

that damage was inevitable. It was felt that greater savings would be realized by repairing this damage than by limiting charges to those which would cause no damage. As a result of this decision considerable damage information was collected.

Because of the small charges, hard-rock medium, and the proximity of measurement, high frequencies (50 to 500 cps) were recorded in this investigation.

In each test a Cambridge vibrograph was set up adjacent to a building. After a detonation the extent of damage experienced was plotted on a graph of amplitude vs frequency (see Figure 9). It was found that separation of the graph into regions of similar damage levels could best be done by lines having slopes of -1. On log-log plots this slope implies velocity, and the investigators calculated the velocities represented by each line as shown in Table I.

Table I.

Extent of damage	Velocity mm/sec	Velocity in./sec
Fine cracks	110	4-1/3
Cracks	160	6-1/3
Serious cracks	230	9

While the frequencies involved in this study are far above those experienced in underground nuclear blasts, one of the investigators had previously reported that for frequencies less than 10 cps, velocity is the parameter which can best be correlated to a given damage level. However, his values for limiting velocities are not presently available.

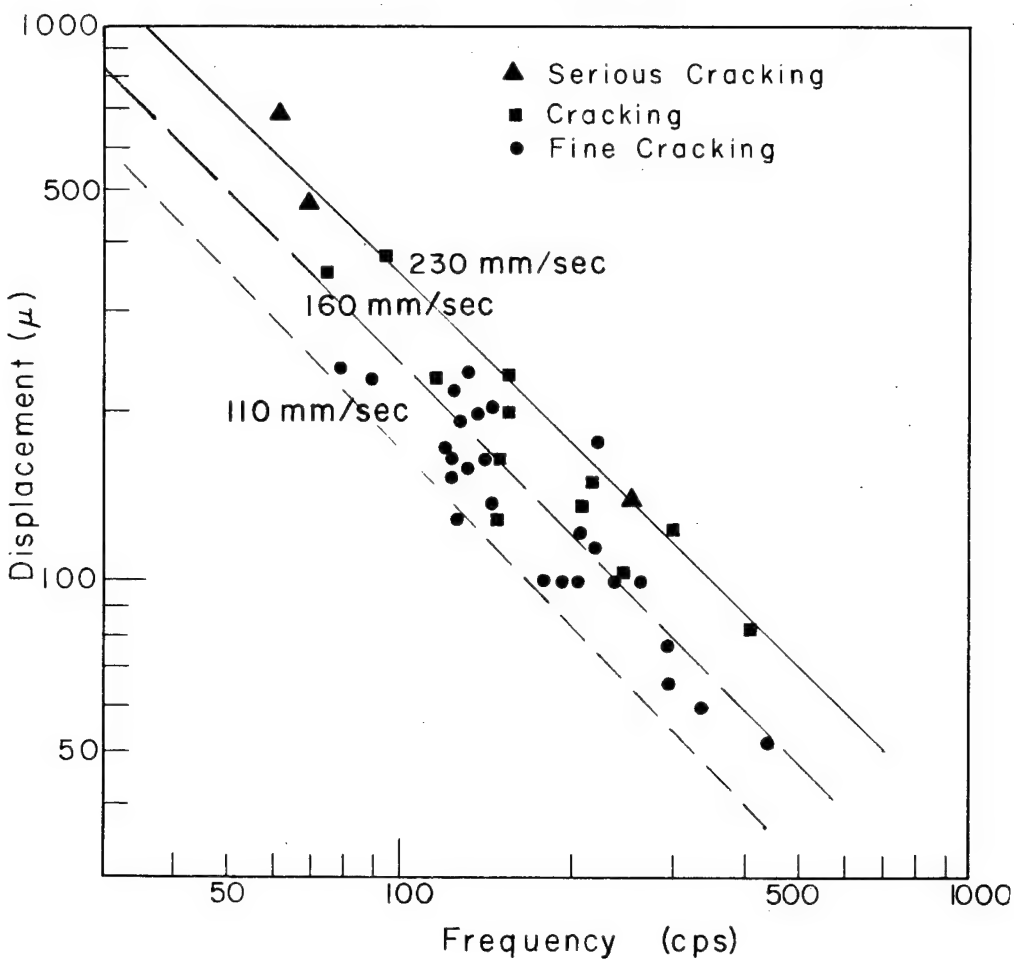

Fig. 10. Displacement vs frequency (Edwards & Northwood) "No Damage" not indicated.

Edwards and Northwood

During construction of the St. Lawrence Seaway, six buildings, three on till and three on wet sand-clay, slated for destruction were used to study earth-motion-damage relationships. The ground surface adjacent to each building was instrumented with accelerometers, velocity gauges, and displacement seismographs. Before each test a building was examined, paper tabs were pasted over cracks, plumb-bobs were installed, and a level survey made. Tests consisted of detonating charges of increasing size at decreasing ranges until damage occurred. The 26 charges varied from 42 to 750 pounds with 5 being less than 120 pounds, and 3 more than 550 pounds. Distances from shot to building were 25 to 200 feet with half the tests being conducted at distances of 95 to 160 feet. The ground motion and movement of the building were recorded for each shot, and the building carefully examined for visible damage, as indicated by torn paper tabs and new cracks, changes in elevation, and vertical nonalignment.

Of the three types of instruments used, only the accelerometers were used as had been planned. Velocity gauges showed evidence of moving parts striking stops so that useable velocity records were not obtained during the tests. The available displacement meters were too sensitive to record at damage levels. This was overcome by firing small calibration shots and measuring displacement at a building and at a remote location. For the actual test shot, only the remote meter was used, and the displacement at the building inferred.

Damage levels were defined as follows:

- Threshold: Opening of old cracks and formation of new plaster cracks, dislodging of loose bricks.
- Minor: Superficial, broken windows, falling plaster, cracks in masonry.
- Major: Serious weakening of structure; large cracks, settlement, lateral movement.

The investigators generally related damage to the type soil on which a building was founded. In the buildings on the sand-clay soil, vertical cracks which were associated with large settlements predominated. The buildings on till usually showed horizontal cracks or shattering of basement walls. On both soils chimneys often showed the first signs of damage. Test results are shown in Figure 10. Although there is considerable scatter, as would certainly be expected from the diverse nature of the buildings tested, the trend of points plotted for major, minor, and threshold damage suggests a best fit having a slope of approximately -1, which indicates each level of damage is associated with a constant velocity. The authors concluded that their results support the criteria of Langefors et al., and that a peak velocity of approximately 4.5 in./sec appears to represent a damage threshold for a variety of foundation materials.

Conclusions

Even though the data from any one of the reports studied show considerable scatter, when all data are compiled on one graph, such as Figure 11, covering the frequency range from 2 to 400 cps, a clearer indication of surface-motion-damage relationships emerges. Damage levels from the individual studies are regrouped as shown in Table II.

Clearly, the wave forms involved in surface motion are not pure sinusoids; however, successive differentiations generally result in displacement, velocity, and acceleration values which are not unreasonable. Thus, it would seem valid to designate the first derivative of displacement, which plots as a line with -1 slope on log-log paper,

Table II. Damage levels regrouped for plotting Fig. 11.

Fig. 4	USBM	Langefors, et al.	Edwards & Northwood
Threshold	Fine cracks	Fine cracking	Threshold
Minor	Falling plaster	Cracking	Minor

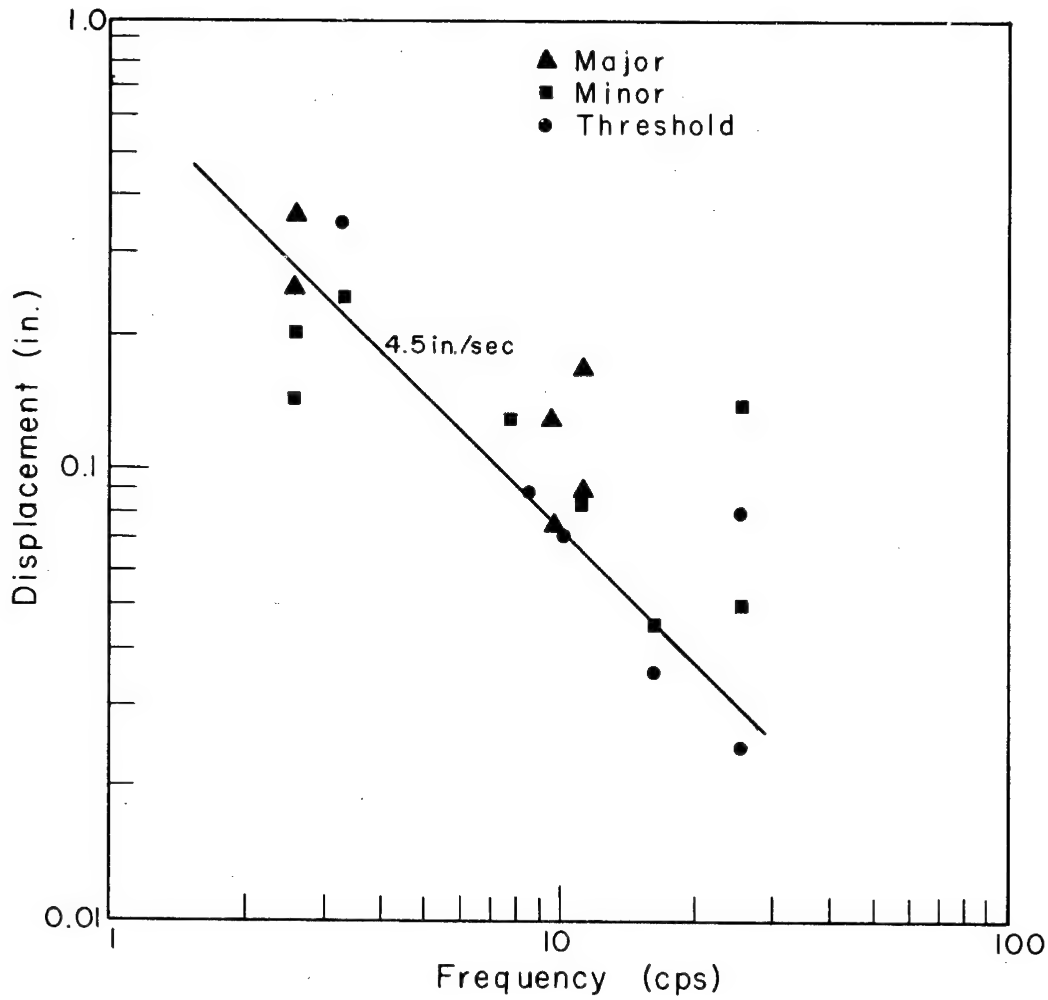

Fig. 10. Displacement vs frequency (Edwards & Northwood) "No Damage" not indicated.

as velocity. If this is done, then it appears that some velocity can be related to the threshold of damage for the type buildings studied.

Because of the dissimilarity in structural characteristics between "identical" small buildings, it is not surprising that there is considerable scatter in plotting test results. Perhaps grouping buildings by construction type would result in sets of data which are in good agreement. The fact that each group of tests was interpreted by different people doubtless introduces some inconsistency. Finally, the entirely different input motion and the fact that panel, rather than ground surface, measurements were made in the USBM work might explain the great departure of these data from the values taken from the other investigations.

Combining the data of the four test series clearly supports the criterion that a velocity of approximately 4.5 in./sec represents a limit below which average residential-type buildings should suffer little or no damage, and that velocities of less than 3-1/3 in./sec (E.R. = 3) are associated with negligible damage. Further, in the frequency range predominating at intermediate distances from underground nuclear detonations, displacements of less than 2-1/2 mm (0.1 in.) would appear to represent a conservative, safe surface-motion limit.

As a matter of interest, selected data collected by USC & GS in connection with three recent underground nuclear detonations are shown in Figure 11. Information pertaining to these events is summarized in Table III.

Table III.

Event and Type	Approximate yield (kt)	Shot medium
Danny Boy (cratering)	0.43	basalt
Gnome (contained)	3.1	salt
Sedan (cratering)	100	alluvium

Tests on Nuclear Experiments

In order to examine the applicability of the high-explosive damage criteria to nuclear-explosion-induced motion and to better define damage more serious than cracked plaster, a series of tests has been undertaken. The tests involve the erection of 16-foot square one-room model houses of various types of construction at distances from underground nuclear detonations at which selected velocities are predicted. Analysis of test data includes correlation of observed damage with the measured ground motion intensity.

Preliminary results of early tests of two concrete block and two frame houses suggest that no damage is experienced when peak velocities are 20 cm/sec. On one experiment where peak velocity is estimated at approximately 80 cm/sec, the entire plywood-sheathed house was shifted about 2 inches on its foundation, there was some cracking of plaster, and binding of the door indicated some relative movement in the building. The condition of the house was impaired only in an aesthetic sense; and except for homes, where appearance is of prime importance, such damage would be considered minor.

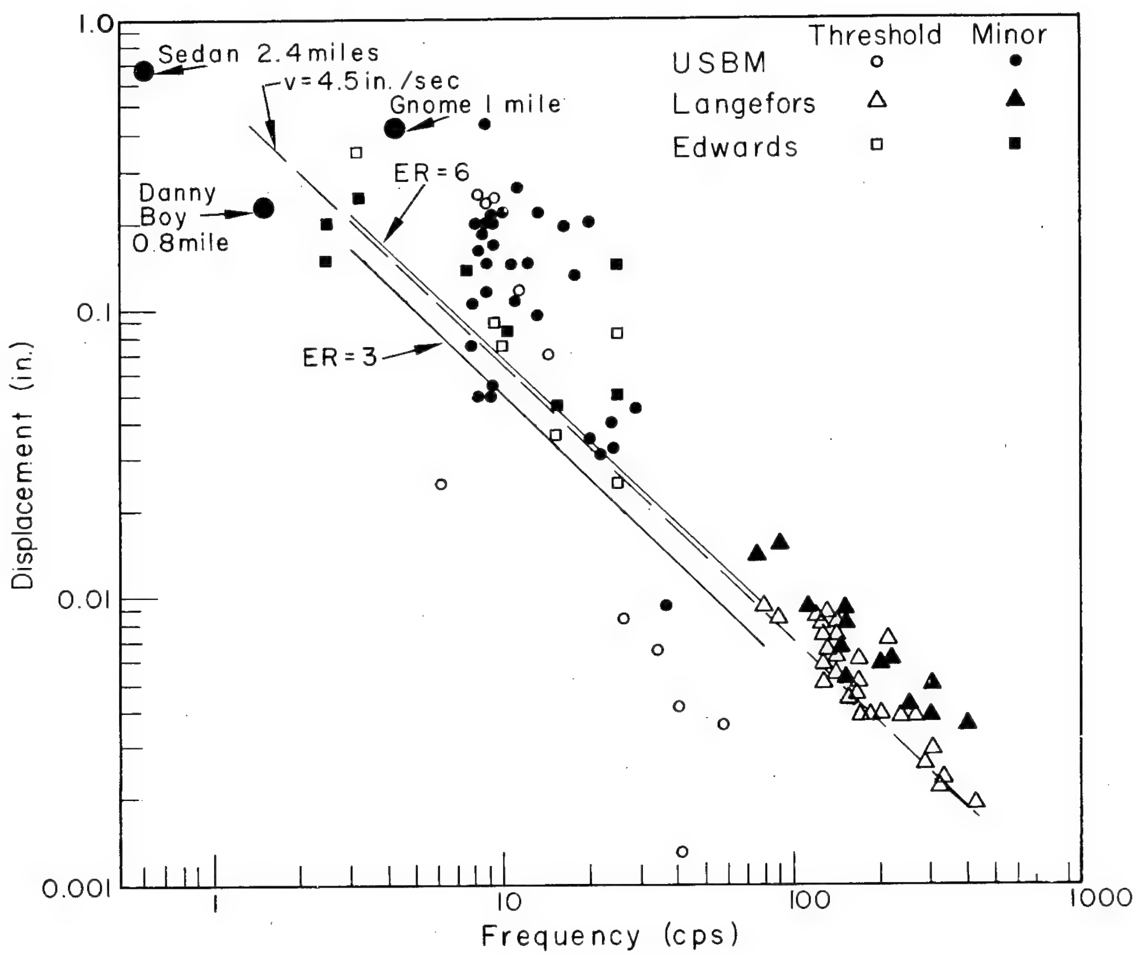

Fig. 11. Results of four test series.

It should be emphasized that these test houses are not necessarily directly representative of average buildings as they are newly-built in accordance with a rigid building code, and their size and shape are not typical.

On one experiment the lateral stability of residences on unbonded concrete-block pillars was studied. A pair of structures, different only in that timber cribs were placed adjacent to the pillars under one, was subjected to peak ground motion of 1.3-g acceleration, 20 cm/sec velocity, and 1.5-cm displacement. A second pair was located where the peak motion was 0.75 g, 10 cm/sec, and 1 cm. The postshot survey of the structures showed that the relative displacement had been so small, approximately 0.5 inch, that the 8-inch-wide block pillars had not approached overturning. Damage was limited to minor distortion of the wooden frame, which was not sheathed, cracking of some of the blocks, and slight displacement of a few of the blocks making up the foundations.

Although no dwellings have been subjected to motions in what would appear to be the damaging range, four houses were within 4 miles of the 3-kt Gnome shot. The complete absence of damage indicates that for nuclear-explosion-induced motion 2 cm/sec is clearly "non-damaging;" that being the peak velocity in the area of the houses.

DAMAGE TO CONSTRUCTION SUPPORT FACILITIES

A survey of construction support facilities damage suffered as a result of underground nuclear detonations has been made to provide information for planning and executing future detonations. Facilities which have been subjected to intense ground motion, and are therefore included in the survey, are: buildings; equipment such as generators, air compressors, and pumps; trailers; and storage tanks.

Prefabricated Metal Buildings

A few commercially available prefabricated metal buildings of various sizes have been subjected to severe ground motions on underground shots, and in no cases have the buildings been damaged. These standard structures are made of rigid gable steel bents with anchor bolts cast in individual column foundations or continuous footings. Longitudinal stiffness is provided by steel tie rods, and the structural frame is sheathed in corrugated metal panels.

A building of this type was not damaged in any way when subjected to 0.4 g, 10 cm/sec, 4 cm ground motion.

On the Gnome event four of the buildings were erected without special reinforcement approximately 1200 feet from surface zero, and none suffered structural damage, although three did show minor effects of the ground motion, which at that location is estimated to have been 5 g, 150 cm/sec, 10 cm. One building showed a slight (3/8 inch) differential set; and the concrete slab, which was monolithic with the deeper hoist foundation, was slightly cracked. Another house was not itself affected, but a ceramic toilet inside the building was shattered. The only evidence of motion at the third building was the jarring loose of one window screen. The fourth small metal building showed no effects whatever.

Postshot examination of all these buildings showed neither permanent displacement, except for the tilting of the one house, nor yielding of anchor bolts or tie rods.

As a result of this experience it appears that the prefabricated buildings can withstand the effects of ground motion at scaled ranges as small as 1000 $W^{1/3}$ without suffering any structural damage.

Plywood "Field Office" Type Buildings

While the extreme variation in quality of these buildings complicates a discussion of potential damage, it is clear that small plywood buildings can be of sufficiently rugged construction to survive very severe ground motions.

The vent house and two smaller (10 ft x 10 ft) plywood buildings at the Gnome shaft showed no shock damage although they were not reinforced. These buildings were of 1/2-inch plywood over 2 x 4 studs on 16-inch centers.

Even when these buildings break away from the ground, damage is limited. One small building 1500 feet from ground zero of a 200-kt detonation suffered some crushing of its skids and the building was slightly racked, but none of the seams were opened. In a skid-mounted office the nails in the floor had to be redriven following a shot, but there was no other damage even though the

ground motion is estimated at 0.75 g, 80 cm/sec, 10 cm.

Plywood buildings 10 ft x 10 ft x 10 ft with 2 x 4 studs on 16-inch centers are situated at ground zero on all deep shots, and the extent of damage suffered ranges from "none" to "demolished;" however, ground motion estimates are not available for correlation with damage.

Minor distortion would not generally be considered a problem because these buildings are most frequently intended only for protection from the elements.

The inherent rigidity of plywood panels makes possible the construction of strong, tight, small buildings if the individual panels are firmly connected. Diagonal bracing or lamination of panels should provide a small building with sufficient strength to survive motion at ranges of 200 $W^{1/3}$ feet if a shelter is required at this short range.

Damage to Mechanical Equipment

Observed damage to machinery such as motors, generators, pumps, and air compressors falls into two categories: failure of suspension systems, which leads to misalignment of parts or possibly more serious damage due to the forcing together of parts or dropping of assemblies; and cracking of brittle, cast-metal components.

On Gnome there was no damage to mechanical equipment although several pieces were in regions of severe ground motion. Fifteen hundred feet from ground zero four generators—two 500 kw on concrete machine foundations and two 600 kw skid mounted—were apparently unaffected by the detonation. Acceleration is estimated to have been 4 g; velocity, 100 cm/sec; displacement, 10 cm.

While the hoist at the Gnome shaft was not itself damaged by the explosion, axle bearings subsequently burned out as a result of differential settlement of the foundation on which the machinery rested.

A small electric pump located in the Gnome drift had been mounted on shock absorbers and suffered no shock damage.

On the one event, Bilby, for which damage has been reported, equipment was concentrated at four locations. Damage suffered includes bending and shearing of suspensions, misalignment, effects of impact of machinery components coming together or dropping on the ground, and cracking of brittle, cast housing and engine blocks.

Failure of Suspension Systems

The majority of the equipment surveyed had longitudinal steel skids resting on the ground with a transverse steel channel, on which the front of the engine rested, welded to the skids. At the rear of the engine a bracket was welded or bolted to the skids and to the engine block or clutch housing. The most frequently observed damage involved failure of the front and/or rear mounts, which, while sufficiently strong to support the load under normal conditions, are susceptible to failure under impulsive loading due to the inertia of the heavy supported machinery.

Of a total of approximately 30 pieces of skid-mounted equipment at the four locations where damage occurred, 10 were actually affected to the extent that they required repair, which generally consisted of realignment and rewelding of bent beams and twisted or broken brackets and welds. However, in two cases more serious damage occurred. One pump engine broke loose from its supports and moved into the radiator, bending the fan blades and radiator fins. On an air compressor the oil pan and block were broken when the engine dropped as a result of failure of the rear mounting brackets.

In addition to such damage associated with suspension failures, two cases of misalignment of parts have been reported, both involving drill rigs, which were at points where the estimated ground motion was 0.5 to 0.7 g, about 80 cm/sec, 5 to 7 cm. Both were blocked up with masts chained to stands. The rig nearer ground zero was oriented with the mast radial with respect to the shot, while the second rig, which was further away by about 2000 feet had the mast positioned transversely and was situated about 500 feet from the Yucca Fault. On both rigs the chain securing the mast broke, permitting twisting of the draw works motors, located on the rig platform, out of line. Repairs to the nearer rig required 2 days, while the other rig was out of operation for 5 days.

Before Bilby, however, a rig similar to the two discussed above suffered no damage even though it was only 400 feet from ground zero of a low-yield shot.

On Gnome two drill rigs were parked about 1 mile from the shot (1 g, 15 cm/sec, 2 cm). No special precautions were taken to protect these rigs beyond normal transporting procedures. The rubber tires and springs of the trucks on which

the rigs were mounted may have prevented damage, but damage on Bilby should probably be attributed to failure of the securing chains.

Damage to generators, compressors, pumps, steel tanks, and drill rigs is summarized in Table IV.

Table IV

Acc. (g)	Vel. (cm/sec)	Disp. (cm)	Equipment	Damage
1	150	15	9 air compressors	Cylinders on one 1000 cfm compressor broke off. Front support beams on 3 bent.
			3 mud pumps	Oil pan and block on one pump broke when engine dropped due to failure of mounting brackets. One cracked exhaust manifold.
			1 light plant 1 fuel tank	Collapsed due to excessive negative camber of wheels. Neither tank nor generator damaged.
			Two 500-bbl tanks	Both bent at saddles.
0.5	50	5	Drill rig w/3 engines on platform	Alignment of engines destroyed and 2 radiators cracked when chains securing mast broke.
			Light plant	Axles on trailer bent slightly.
0.75	80	7	Drill rig w/3 engines on platform	Engines required complete re-alignment. One water jacket cracked.
			10 compressors	One block cracked; 4 to 5 supporting beams bent or rear brackets failed.
			Two 500-bbl tanks	One split at joint between end and sidewall; other bent at saddles.
			2 mud pumps	None
0.75	80	7	Two 500-bbl tanks	One split at joint between end and sidewall; other bent at saddles.
			3 mud pumps	Radiator fins and fan on one slightly bent when engine moved after separating from mounts. Clutch housings on other two cracked.

Cracking of Cast Metal

As with suspension failures, cracks in engine blocks and other cast-metal components have been limited to machinery mounted on rigid skids. A total of ten cases of this type damage were found. The most common location of cracks was at points where mounting brackets were attached. Two large pumps were subjected to 0.75 g, 80 cm/sec, and 7 cm, and as a result the clutch housing on both cracked at the bracket. On an adjacent pump the welds on the brackets broke, but there were no cracks.

Two pumps and an air compressor located at one station (1.5 g, 150 cm/sec, 15 cm) were damaged to varying degrees. On one pump only the exhaust manifold was cracked. On a second both the oil pan and block cracked when the rear mounts failed. The compressor, a 1000 cfm Y-type, had the heavy cylinders broken off at the neck, and the drive pulley was cracked.

Two pieces of equipment at a second station (0.75 g, 80 cm/sec, 7 cm) suffered cracks. The bottom tank on the radiator of one drill-rig engine was split and had to be replaced, and the block on an air compressor was cracked.

The only other damage to castings was the cracking of the block on a compressor (0.5 g, 50 cm/sec, 5 cm) which required replacement of the entire block, and the cracking of two water jackets on drill rig engines.

Because of the small sample available for consideration and the use of interpolated ground motion, a rigorous interpretation of the effect of ground motion on engines would have little meaning. However, certain conclusions can be drawn. Cracking of cast blocks and housings might be expected on 25 to 33% of the skid-mounted engines exposed to ground motions of 0.5 to 1 g, 50 to 100 cm/sec, 5 to 10 cm, if the equipment is not anchored to the ground or provided with some form of shock mounting. About as frequently, varying degrees of failure of mounting systems might be experienced.

Comparison of the effects of Gnome and Bilby suggest that damage might be restricted by preventing equipment from achieving free fall and smashing against the ground. On Gnome the 150-kw generators similar to the equipment damaged on Bilby were subjected to ground-motion intensities estimated at about 4 times those experienced by the damaged engines on Bilby, but the Gnome generators were anchored to a concrete foundation so that the ground, foundation, and generators moved as a unit. In this situation the generators would not have been subjected to the sharp rebound motions characteristic of free fall which can be several times the initial peak values, on which the Bilby estimates have been based.

In view of this it appears that Bilby damage would have been much less serious had the equipment been firmly tied to the ground. Damage could have been further reduced by placing equipment on some type of shock-absorbing mount, such as frangible pads (used under trailers on Gnome and Bilby), conventional trailer systems, tire casings, or heavy coil springs.

Damage to Trailers

It appears that trailers, being sufficiently strong to withstand highway shocks, can generally survive explosion-induced motion with minimum precautions.

Three electronics trailer vans were located at the Gnome shaft. These trailers were supported on transverse steel outriggers which rested on 1-foot-thick styrofoam pads. The trailers suffered no damage, but were tilted due to differential crushing of the styrofoam. The slender posts on platforms adjacent to the trailers were twisted, but this difficulty was easily corrected.

Two other vans were located about 2600 feet from Gnome surface zero. One of these was placed on a large air-filled bag, but no special steps were taken to protect the second. Neither of these trailers was damaged.

On Bilby a trailer complex was located where acceleration is estimated to have been approximately 3 g; velocity 300 cm/sec; and displacement 40 cm. Most trailers were supported on timber cribbing under the trailer body with the wheels resting on thin (4-inch) frangible pads. Guys were strung between the trailer tops and buried anchors in order to have the trailers and ground move together. No damage was done to the trailers. However, the front struts were driven into the ground, and the cribbing was disarrayed and no longer bore any of the trailers' weight. While the trailers themselves were undamaged, some damage was done to the contained electronics equipment. The slack in the guys and the postshot scattering of the cribbing suggest that the trailers were separated from the ground.

Several trailer-mounted cooling units at the Gnome shaft were overbalanced by the surface motion, but none seem to have been damaged.

The only significant damage to trailers was observed on Bilby. At points where acceleration was estimated at 3 g; velocity 300 cm/sec; and displacement 40 cm; the light tubular axles of small, loaded two-wheel trailers were bent, causing a slight negative camber of the wheels. Three four-wheel trailers on which were mounted fuel tanks and lighting sets have experienced accelerations, velocities, and displacements estimated at about 1 g; 80 cm/sec, and 20 cm, resulting in complete collapse of the wheels as a result of severe negative camber; however, neither the tanks nor lighting set suffered any damage.

Damage to Steel Storage Tanks

As would be expected, the quality of materials and workmanship greatly affect the vulnerability of metal storage tanks. On Gnome a 126,000-gallon 14-gauge bolted tank and a 6000-gallon welded-steel tank were at surface zero (70 g, 560) cm/sec, 170 cm). The 6000-gallon tank, which was of 1/4-inch steel and was buried, suffered no noticeable damage. While the top of the larger tank was slightly buckled, it was not otherwise affected. At the Gnome shaft two small (about 1000 gallon) tanks—one empty, the other filled with water—appeared unaffected. A full 8000-gallon fuel tank mounted in a concrete cradle 1500 feet from Gnome suffered no damage.

Within 5 miles of the Gnome site were some ten small, privately owned water and fuel tanks, all of which appear to be standard catalog-ordered farm tanks. These were of a variety of types—steel plate and corrugated steel with welded, bolted, and riveted joints. None showed any evidence of leaking or other damage after the detonation.

At NTS two 500-barrel steel water tanks were demolished and four others slightly damaged as a result of one shot. These tanks of 3/16-inch steel reportedly contained about 1 foot of water. None had baffles to reduce sloshing. Although at different locations, both destroyed tanks were subjected to ground motion of about 0.75 g, 80 cm/sec, and 7 cm. Examination of the tanks showed that the steel was torn in a pattern which crossed the weld connecting the end and side wall of intervals of about 2 feet. At the opposite end of the tanks, the paint was flaked in the same pattern. At both stations where tanks were destroyed, as well as at a third, there were identical tanks which suffered only severe bending at the four supporting saddles. It appears that the ground motion was about 50% greater at the station where both tanks were slightly damaged than at the two stations where a tank was split open.

The difference in the level of damage to the identical tanks and the anomalous survival of tanks subjected to more severe ground motion than two tanks which were demolished emphasize the effect of the variation in quality of construction. No decision on locating steel tanks to assure survival in regions of strong ground motion should be made without a rigorous structural analysis of the tanks. However, the Gnome experience emphasized that, if necessary, steel tanks can be designed and fabricated to withstand the effect of severe motion.

Miscellaneous Effects

At one NTS location are a Butler building machine shop, a number of trailers connected by wooden platforms, and miscellaneous small buildings. While no structural damage has been reported as a result of nuclear shots, acceleration of 0.3 g, velocity of 30 cm/sec, and displacement of 2 cm are estimated to have been caused by Bilby at this area. The only damage reported was the destruction of approximately 160 feet of fluorescent fixtures caused by the opening of links in the light chain on which the fixtures were suspended. In the area, slight shifting of some of the office trailers on their wood-crib foundations required some realignment. Several office machines were thrown from, or slid off of, desks, and desks and tables moved as much as a foot.

Following Bilby, cracks in the asphalt paving on a bunker slope (0.75 g, 70 cm/sec, 7 cm) were found to have opened up and the majority of the asphalt moved down the 45°slope 1 to 2 feet. Numerous small cracks were known to exist earlier in the 3-inch-thick paving.

A switching station 1200 feet from Bilby survived with no damage to electric equipment, the only damage being a slight (2-inch) twist in the angles on which the heavy equipment was mounted.

Around Gnome ground zero, a large number of 25-foot wooden utility poles were erected in 5-foot concrete bases. These poles were not damaged by the shot. Approximately 1000 feet from Bilby were two 50-foot guyed steel towers. Although the surface in the area was severely cracked, particularly at the wide-flange section anchors, and the steel guys were loose, these old 8-inch-diameter towers seem unaffected by the detonation. A light, 150-foot, guyed communication tower was located about 2000 feet from Gnome and was not affected by the detonation.

A massive concrete bunker (0.75 g, 80 cm/sec, 7 cm) settled 4 inches as a result of Bilby. The principal result of this was a power outage in the bunker, the incoming power lines having been sheared off at the outer face of the wall where they entered the bunker. A 15-second power outage occurred some distance from the shot at Bilby zero time. A postshot survey of electrical facilities disclosed no cause for this, and it was concluded that a short had occurred when power lines in the area swayed together due to motion of the poles.

SUMMARY

The effect of nuclear-explosion-induced ground motion on various types of facilities has been summarized.

Evaluation of the potential damage to engineered structures can be made by using response spectrum techniques. The fundamentals of response spectra and one application have been presented.

Damage to residential-type buildings is most likely to occur as cracks in walls. It appears that peak surface velocities of about 10 cm/sec represent the threshold of damage in older homes having plastered interiors, while 20 cm/sec peak velocities appear to be non-damaging for well-built new homes with plastered walls or stuccoed exteriors.

Buildings and equipment of the types found at most large construction projects can survive very severe ground motions. Damage to mechanical equipment is summarized in Table IV.

This work was performed under the auspices of the U. S. Atomic Energy Commission.

REFERENCES

1. Crandell, F. J., "Ground Vibration Due to Construction Blasting and Its Effect Upon Structures," Journal Boston Society of Civil Engineers, pp. 222-245, April 1949.
2. Edwards, A. T. and Northwood, T. D., "Experimental Studies of the Effects of Blasting on Structures," The Engineer, pp. 538-546, September 30, 1960.
3. Langefors, U., Kihlstrom, B., and Westerberg, H., "Ground Vibrations in Blasting," reprint from Water Power, published by Nitroglycerin Aktiebolaget, Gyttorp, Sweden, 1958.
4. Leet, L. D., "Vibrations from Construction Blasting," reprint from The Explosives Engineer, published by Hercules Powder Co., Wilmington, Del., 1960.
5. Thoenen, J. R. and Windes, S. L., "Seismic Effects of Quarry Blasting," U. S. Bureau of Mines Bulletin 442, 1942.
6. "Project Shoal Test of Dribble Type Structures," Holmes and Narver, Inc., Atomic Test Support Organization, Las Vegas Division, 1964.
7. Clough, R. W., "Dynamic Effects of Earthquakes," Proceedings ASCE, p. 49, ST 4, April 1960.

BIOGRAPHICAL SKETCH OF AUTHOR

Lewis J. Cauthen, Jr. is a Captain in the U.S. Army Corps of Engineers, currently assigned to Lawrence Radiation Laboratory as a research associate. He graduated from The Citadel in 1954 with a B.S. in Civil Engineering and received his M.S. in Structural Dynamics from the University of Illinois in 1962. His military service includes assignments at Fort Bragg and Fort Devens with a combat engineer battalion, and a 3-year tour at the Engineer Intelligence Center, Heidelberg, Germany, where he served as an Intelligence Officer and as commander of a mapping unit. His work at Lawrence Radiation Laboratory has been primarily in the field of shot-induced ground motion and its effect on surface facilities.

PROGRESS AND PROMISE IN THE STUDY OF THE EARTH USING NUCLEAR EXPLOSIVES

Carl Romney
Wayne Helterbran

VELA Seismological Center
U. S. Air Force Technical Applications Center
Washington, D. C.

ABSTRACT

A review of measurements of seismic waves from nuclear explosions has shown a number of results which have implications of interest for basic studies of the earth. Among these are observations which show regional differences in travel times and amplitudes which have been interpreted in terms of structural differences, and variations in travel times and amplitudes at teleseismic ranges which suggest inhomogeneities in the mantle. Comparisons between explosion-and earthquake-generated waves have given new information on the nature of earthquake sources. A number of suggestions are made on methods for further study of fundamental problems by means of large explosions.

INTRODUCTION

The application of explosions to the study of the deep interior of the earth is, of course, not a recent development. Even before nuclear explosives were available, large chemical explosions, in some cases accidentally detonated, had produced seismic waves which gave useful information to seismologists. Notable examples were those at Oppau, Helgoland, and Port Chicago. Although seismic observations were often unplanned, and therefore not obtained at optimum locations nor with optimum instruments, they were very useful in checking and establishing tables of the travel times of various seismic waves through the earth --- the basic tool of the seismologist in the study of the earth structure.

More recently, the numbers of explosions which could provide useful seismological data have increased as a result of the nuclear development programs of the United States, the Soviet Union, the United Kingdom, and France.

Bullen (1958), in his Presidential address to the International Association of Seismology and the Physics of the Interior of the Earth, presented compelling arguments in favor of an earlier recommendation by a committee of that organization (Bullen, 1955) for nuclear explosions designed specifically for seismological research. In the same address, he reported significant results already derived from nuclear explosions in Australia. Because of the low natural seismicity of Australia, recordings of explosions had given the best data available on the structure of the earth's crust in central Australia.

Byerly (1959), at the Second Plowshare Symposium, also outlined areas where nuclear explosions could assist seismology. He mentioned, among other possibilities, the removal of ambiguity between determination of focal depth and crustal thickness as deduced from earthquake sources, determination of accurate amplitude-distance and travel time relationships, and attack on the long standing problems of the cause of anomalies in travel time and amplitude observed at 10°, 20°, 104°, and 142°. The first two anomalies are associated with the transition from waves which travel along the crust-mantle boundary to those which penetrate to some depth into the higher velocity upper mantle as shown in Figure 1. The other anomalies are associated with waves which penetrate to the boundaries of the core and inner core, respectively, as shown in Figure 2.

Griggs and Press (1961) reviewed progress in seismology resulting from study of recordings obtained from nuclear explosions. As of that time, a number of significant results had been achieved. Along these were:

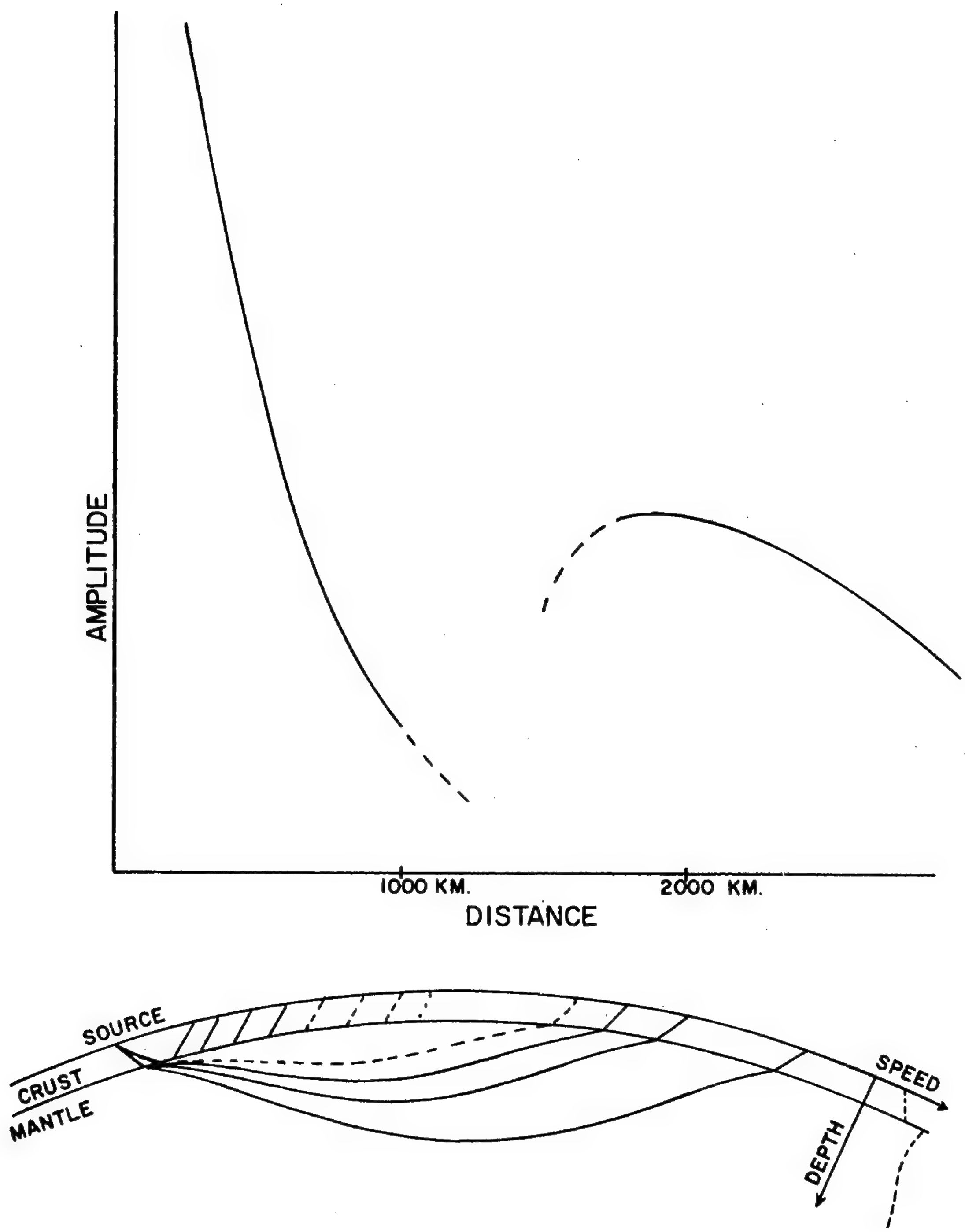

Fig. 1. Amplitude and ray paths of P at intermediate distances. Waves guided along the base of the crust are first arrivals between about 150 and 1000 kilometers. Amplitude falls off rapidly with distance. Beginning at about 1500 kilometers, energetic rays which penetrate the upper mantle emerge as first arrivals.

a. A study by Burke-Gaffney and Bullen (1958) of PKP and PKIKP which added the "final link in the chain of evidence for the existence of the earth's inner core". Travel paths for these waves are shown in Figure 2.

b. Observations by Gutenberg and Richter (1946) of seismic waves from the Bikini Baker underwater explosion gave P waves equivalent in amplitude to magnitude 5.5 earthquakes. The energy release was known, and coupling to the earth could be estimated, thus enabling the authors to calibrate the previously used earthquake magnitude-energy relationship against a source of known strength. This was a prime stimulus causing Gutenberg and Richter to revise that relationship downward by a factor of several hundred. The result was a major revision in estimates of the total energy released around the earth in the form of earthquakes.

c. A study by Oliver and Ewing (1958) which resulted in identification of higher mode surface waves which had not previously been found to propagate over oceanic paths. The results were useful in interpretation of the dispersion of earthquake surface waves and hence in determining properties of the crust and of the mantle of the earth.

d. A study conducted by Romney (1959) of the HARDTACK explosions produced P-wave travel time and amplitude data of greater precision than had previously been obtainable. The results gave much more conclusive evidence for the existence of the P-wave shadow zone in the vicinity of 10°, thought to be due to the existence of a low velocity layer in the upper mantle, than had previously been available from earthquake studies.

Griggs and Press also proposed an ambitious international program of explosions as large as 1

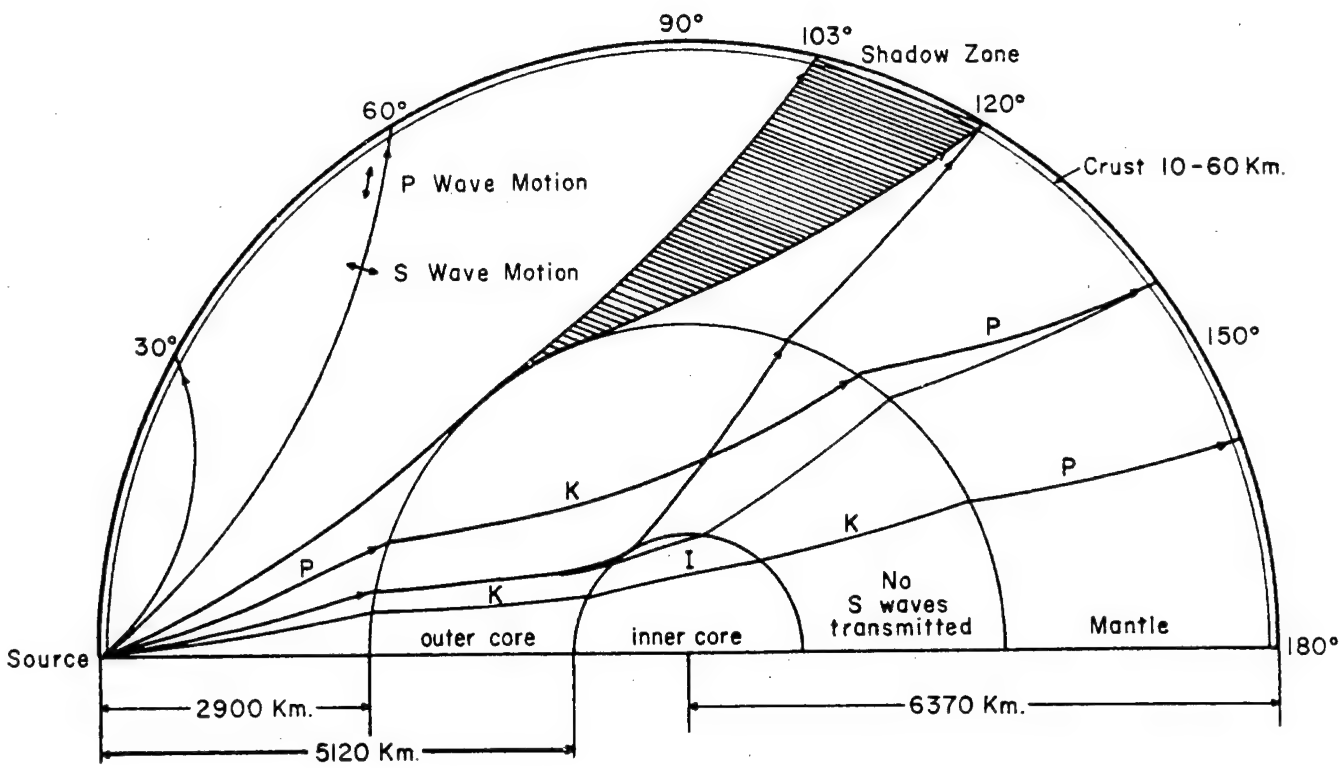

Fig. 2. Schematic diagram of the earth showing major divisions and representative travel paths of seismic waves. Weak waves diffracted around the earth's core are recorded in the "shadow zone" commending at 103°. Inner core causes sharp refraction of rays which emerge at 120°.

megaton for seismological research and proposed novel, deep oceanic seismometer lines for recording much of the data. Their objectives included investigation of such major geophysical questions as:

a. "Is the inner core liquid or solid?

b. "What is the nature of the outer boundary of the core?

c. "What is the difference in the mantle under continents and oceans?

d. "Are there variations from place to place in the mantle under the oceans, as would be required for convection currents in the mantle?

e. "What is the nature of the '20° discontinuity' in these oceanic regions?"

Since the time of the proposals and recommendations of Bullen, Byerly, and Griggs and Press, one nuclear explosion has been detonated for purely seismological research purposes and a very large amount of seismological research has been conducted on this and other explosions, stimulated chiefly by the Advanced Research Project Agency's VELA-UNIFORM Program. This paper will present some of the results of this recent research which have fundamental significance in the study of the earth, using data from nuclear explosions. It will also include some suggestions for further work, borrowing heavily from ideas contained in the three earlier papers mentioned above.

RECENT RESULTS FROM NUCLEAR EXPLOSIONS

Analysis of the 1958 HARDTACK underground explosions (Romney, 1959) showed that the amplitudes of Pn decreased more rapidly than could be explained by the theory for head waves transmitted along the interface between two homogeneous half spaces -- perhaps a crude model of the crust and mantle. Similar observations of earthquakes and of the RAINIER explosion in 1957 (Bailey and Romney, 1958) had previously led to the suggestion that this discrepancy was either caused by absorption or by a negative velocity gradient immediately below the curst. The HARDTACK data, of considerably higher quality than previous data, were used by Pasechnick, et al. (1960) to show that an additional term due to absorption at the rate of $e^{-0.0025/km}$ (or $Q \simeq 300$) was sufficient to explain the data between 200 and 1000 km. A similar conclusion was later reached by Wright, et al. (1962). This result does not explain regional differences in propagation which have been found, nor preclude the possibility that the velocity gradient below the crust is the more significant factor. More study is clearly indicated.

Regional travel times from HARDTACK explosions Logan and Blanca were studied by Lehman (1962). She found the results consistent with an upper mantle structure having a discontinuity surface at a depth of 215 km. Below this depth the velocity and velocity gradient increased abruptly, while the velocity appeared to be nearly constant above. No low velocity layer was found.

The Gnome explosion at Carlsbad, New Mexico was studied by Romney, et al. (1962). Mobile seismographic stations had been arranged principally to record waves travelling westward into the basin and range province, and eastward into the south central states and southern Appalachian region (see Figure 3). The advantage of planned nuclear explosions in the study of the earth is illustrated by the fact that over 90 temporary recording stations, in addition to standard observatories, were able to obtain useful data from this one event. Many of the stations were prospecting units, capable of recording data only over an interval of several seconds. Striking differences in P-wave travel times and amplitudes were found. Generally speaking, high velocities and large amplitudes were recorded to the east, correlating with low average elevation of the land and a relatively thin crust as inferred from gravity data. To the west, velocities and amplitudes were low, correlating with high average land elevation and a thick crust. The most striking feature of the observations is shown in Figure 4, where it may be seen that there are two separate sets of arrivals differing by 10 or more seconds. Such observations from earthquakes would be very difficult to separate because the process of determining the epicenters averages out real differences in travel time.

Herrin and Taggart (1962) correlated the low velocities and amplitudes with high heat flow and the inferred high thermal gradients in the upper mantle under western United States. They postulated differences in mantle composition as well, since the anomalies seemed too large to explain by temperature alone.

In a further study, Lehman (1964) analyzed P-wave travel times from Gnome and 14 explosions at the Nevada Test Site. Her previous con-

UNITED STATES

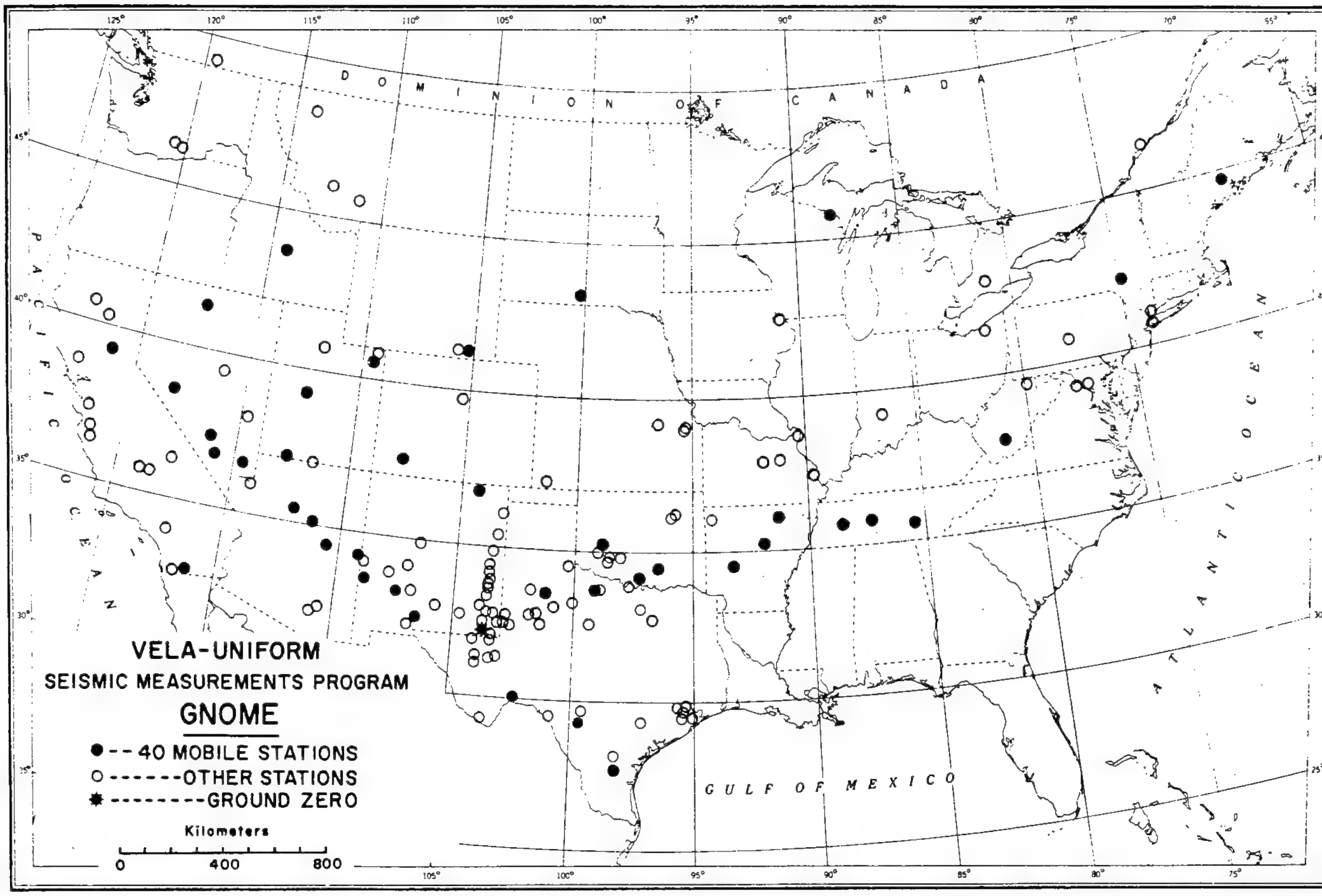

Fig. 3. Map of seismographic stations receiving signals from GNOME.

clusion on the existence of shallow low velocity layers was modified to the extent that she now finds evidence for such layers in the mountainous regions of the western United States. These same layers may also cause reduced velocities of S waves.

Pakiser (1963) and his associates at the US Geological Survey have carried out extensive studies of crustal structure, chiefly in the western states, using data primarily from chemical explosions, but also from nuclear explosions at the Nevada Test Site. One of his very significant conclusions, based on further observations that the velocity of Pn is high where the crust is thick, and laboratory evidence that upper mantle density is probably high where velocity is high, was that a large part of isostatic compensation is achieved by variations in the density of upper mantle rocks.

These studies just described constitute significant steps in understanding the structure and composition of the crust and upper mantle. Tentative correlation with postulated convection currents in the upper mantle should follow soon.

Teleseismic studies have also made use of explosion data. The highly important contribution of explosions in establishing the nature of the inner core was previously mentioned. Negative travel time residuals from explosions on Pacific islands were noted as early as 1946 from the Bikini Baker explosion (Gutenberg and Richter, 1946). These were assumed to be caused by the thinness of the crust in the Pacific, which meant that the P waves would propagate for a greater part of their paths in the high velocity mantle, and would thus arrive earlier than waves from a source on a thick continental crust. Jeffreys (1962) re-

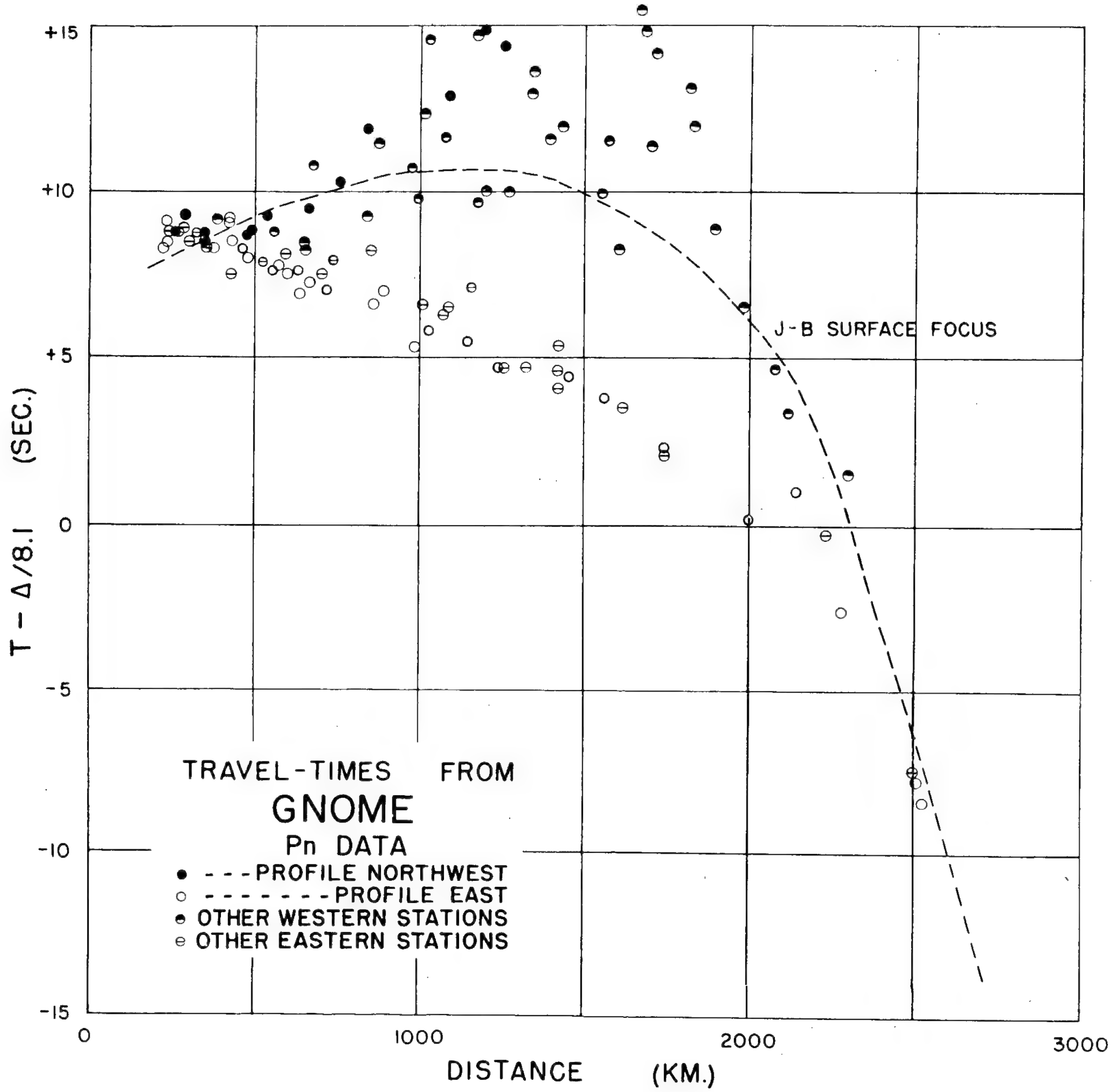

Fig. 4. Reduced travel times for P-waves from GNOME by profiles.

evaluated the travel times from Pacific sources, including the extensive data from the studies of Carder and Bailey (1958) and Kogan (1960). Early P-wave arrivals were noted at continental stations, confirming Gutenberg and Richter's results. If the effect were due to the postulated thin crust under the Pacific, then P waves from Pacific sources recorded on Pacific islands should be earlier yet. There was no sign of this effect, which should be of the order of 2. 5 seconds, contrary to what was expected. About the same time, Romney, et al. (1962) noted that P waves from Gnome, a continental source, recorded at stations in Europe, were early by about the same amount the Pacific sources were early. This suggests that the thin Pacific crust is not the cause of the anomaly.

Many more readings are now available from SHOAL, detonated near Fallon, Nevada, and from

several explosions at the Nevada Test Site. At distances greater than 3,000 km, these almost invariably give negative residuals from the Jeffreys-Bullen tables, apparently independent of distance, and of the same order observed from Pacific shots -- about 2 seconds. The thin Pacific crust cannot be the cause of these anomalies. Apparently the slower speeds through the thick continental crust are compensated by faster speeds through the subcontinental mantle. Further studies are obviously needed to determine structural or compositional changes which could cause this effect.

After making adjustments to the travel time curves for systematic effects revealed by the explosion data, Jeffreys found a scatter from the mean travel time curve of about ±1.0 second. He speculated that this scatter might reduce to individual station corrections, which in turn are caused by crustal variations under the stations in question. Flinn (1964) has looked for station corrections from explosion data, using only high quality station data, but has been unable to find conclusive evidence for them. The indications are that if the ccrrections exist, they are likely to be smaller in general than the residuals found by Jeffreys. This would lead to the inference that the main cause of the travel time scatter is variation of velocity distributed over the mantle portion of the P-wave path. The situation is thus quite different for teleseismic travel times, where anomalies seldom exceed 2 or 3 seconds, than for regional travel times where crustal and upper mantle differences cause travel time variations of 10 seconds or more.

Supporting evidence for mantle inhomogeneities is to be found from observations of amplitudes of P waves from explosions at teleseismic ranges. After correcting for variations of amplitude with distance by means of the earthquake magnitude scale, we have found that the amplitude scatter has a standard deviation of 0.3 magnitude units or greater at teleseismic ranges. The Gnome and HARDHAT explosions showed scatter almost twice this great. As is the case for the travel time scatter, by and large the amplitude variations are not explainable as station corrections. A station recording anomalously large waves from one explosion may record anomalously small waves from an explosion at another site, as compared to other stations at the same range. Systematic station corrections do appear to exist, however, explaining a portion of the observed scatter. This work needs to be extended to determine how amplitude and travel time scatter varies with wavelength. Such a study may give important information on the dimensions of mantle inhomogeneities.

Smith (1963) studied the generation of shear waves from nuclear explosions. By employing both the direct blast waves and the waves generated by the subsequent collapse of earth into chambers created by underground explosions, he was able to eliminate the effect of the path of propagation entirely. Spectral analysis of the recorded waves showed remarkable similarities in the shear waves from both sources, in spite of differences in the time scale and directions of the source functions. From this evidence, he was able to infer, among other things, that the shear waves originated primarily from conversion of P waves within several wavelengths of the source, rather than from structural induced asymmetry at the source or from mode conversion all along the path of propagation. This removed doubts about the meaning of interpretations of earth structure based on shear-wave data.

A study which can be viewed as pioneering in the quantitative use of amplitude data to investigate earth structure was made by Werth, Herbst, and Springer (1962). This work was made possible by having available measured displacements very near to underground explosions. From these measurements, displacements were calculated after propagating through various reasonable earth models. When corrected for attenuation and seismograph response, the waveforms and amplitudes were in excellent agreement with observations at several hundred km from the source. Amplitudes can thus provide an additional valuable constraint on our interpretation of structure when the source function is known, removing ambiguities from analysis based on travel times alone.

Numerous other examples of the use of explosion data could be cited. We believe those mentioned are fairly representative, and indicative of several courses for future work. The international nature of interest in results from nuclear explosions is apparent from the references cited, which included seismologists from Australia, Denmark, England, the Soviet Union and the United States.

ADDITIONAL EXPLOSIONS

From the nature of the work described, it is apparent that a feature of prime importance for additional large explosions is that they be detonated in new areas. Studies of mantle variations, and attempts to correlate these variations with mantle convection currents, will require data over hitherto unexplored propagation paths. The explosions must be large, preferably larger than 100 KT if detonated underground, if they are to penetrate deeply enough and be recorded at sufficient range for studies of the earth's mantle. This would appear to require nuclear sources. The diverse locations and yields now proposed for possible PLOWSHARE programs meet these requirements well, and could undoubtedly make substantial contributions to seismology, as was the case for GNOME.

Crustal studies, while they benefit by data from large sources, can proceed adequately with rather moderate chemical explosions, of the order of tons.

Little has been said about studies of the core of the earth, except the earlier study of Burke-Gaffney and Bullen. This reflects the fact that few underground explosions in the last few years have produced sufficiently energetic seismic waves to penetrate the deep interior. Explosions of very high yields, detonated under excellent coupling conditions, will be required to carry out the ambitious program recommended by Griggs and Press. We believe we can add little to their recommendations.

REFERENCES

1. Bailey, L. C., and C. F. Romney, "Seismic Waves from the Nevada Underground Explosion of September 19, 1957," (abstract), Bull. Geol. Soc. Am., 69, p. 1692, 1958.
2. Bullen, K. E., "Proposal on Detonation of Atomic Bombs for Seismological Purposes," Bull. d'information de I'U. G. G. I., 12, pp. 550-552, 1955.
   'Seismology in Our Atomic Age," Compt. Rend. Assoc. Seism. et Phys. Int. Terre, Strasbourg, 19-35, 1958.
3. Burke-Gaffney, T. N., and K. E. Bullen, "On the Seismological Aspects of the 1954 Hydrogen Bomb Explosions," Australian Jour. Phys., 11, pp. 318-321, 1958.
4. Byerly, P., "Seismological Problems Which Nuclear Explosions May Solve," Proceedings of the Second Plowshare Symposium, Part V, UCRL-5679, p. 49, 1959.
5. Carder, D. S., and L. F. Bailey, "Seismic Wave Travel Times from Nuclear Explosions," Bull. Seism. Soc. Am., 48, pp. 377-398, 1958.
6. Flinn, E. A., "Confidence Regions and Error Determinations for Seismic Event Location, "United ElectroDynamics, Inc., Seismic Data Laboratory Report No. 103, 1964.
7. Griggs, D. T., and F. Press, "Probing the Earth with Nuclear Explosions," Jour. Geophys. Res., 66, pp. 237-258, 1961.
8. Gutenberg, B., and C. F. Richter, "Seismic Waves from Atom Bomb Tests, "Trans. Am. Geophys. Union, 27, p. 776, 1946.
9. Herrin, E., and J. Taggart, "Regional Variations in Pn Velocity and Their Effect on the Location of Epicenters," Bull. Seism. Soc. Am., 52, pp. 1037, 1962.
10. Jeffreys, H., "Travel Times for Pacific Explosions," Geophys. Jour. of the Roy. Astron. Soc., 7, pp. 212, 1962.
11. Kogan, S. D., "Travel Times of Longitudinal and Transverse Waves, Calculated from Data on Nuclear Explosions Made in the Region of the Marshal Islands," Isvestia Akad. Nauk USSR No. 3, pp. 246 (English edition), 1960.
12. Lehman, I., "The Travel Times of the Longitudinal Waves of the Logan and Blanca Atomic Explosions and Their Velocities in the Upper Mantle," Bull. Seism. Soc. Am., 52, pp. 519, 1962.
    "On the Travel Times of P as Determined from Nuclear Explosions," Bull. Seism. Soc. Am., 54, p. 123, 1964.
13. Oliver, J. and M. Ewing, "Short Period Oceanic Surface Waves of the Rayleigh and First Shear Modes," Trans. Am. Geophys. Union, 39, p. 482, 1958.

14. Pakiser, L. C., "Structure of the Crust and Upper Mantle in the Western United States, "Jour. Geophys. Res., 68, p. 5747, 1963.
15. Pasechnick, I. P., S. D. Kogan, D. D. Sultanov, and V. I. Tsilbul'skiy, "The Results of Seismic Observations Made During Underground Nuclear and TNT Blasts, "Seismic Effect of Underground Explosions, Trans. Inst. of Physics of the Earth, Moscow, No. 15, p. 182, 1960.
16. Romney, C., "Amplitudes of Seismic Body Waves from Underground Nuclear Explosions," Jour. Geophys. Res., 64, p. 1489, 1959.
17. Romney, C., B. G. Brooks, R. H. Mansfield, D. S. Carder, J. N. Jordon, and D. W. Gordon, "Travel Times and Amplitudes of Principal Body Phases Recorded from Gnome," Bull. Seism. Soc. Am., 52, p. 1057, 1962.
18. Smith, S. W., "Generation of Seismic Waves by Underground Explosions and the Collapse of Cavities," Jour. Geophys. Res., 68, p. 1477, 1963.
19. Werth, G. C., R. F. Herbst, and D. L. Springer, "Amplitudes of Seismic Arrivals from the M Discontinuity," Jour. Geophys. Res., 67, p. 1587, 1962.
20. Wright, J. K., E. W. Carpenter, and R. A. Savill, "Some Studies of the P Waves from Underground Nuclear Explosions," Jour. Geophys. Res., 67, p. 1155, 1962.

BIOGRAPHICAL SKETCHES OF AUTHORS

Dr. Carl Romney is the Assistant Technical Director at the Air Force Technical Applications Center in Washington, and currently serves as the Director at the Vela Seismology Center. He graduated from the California Institute of Technology in 1945 and did graduate work at the University of California, 1946-49 and 1954-55, where he was awarded the Ph.D. in Geophysics. He was employed by the consulting firm of Beers and Heroy from 1949-55 as a seismologist and later Chief Seismologist, working on several seismological research contracts with the U.S. Government. He has been with the Air Force Technical Applications Center since 1955. He has done research and directed research and development projects on both basic seismological problems and problems associated with the detection of large explosions by seismological methods.

Wayne Helterbran is employed by the Air Force Technical Applications Center and currently serves as Chief of the Field Programs Branch of the Vela Seismology Center. He graduated from the University of Wyoming in 1954, receiving a B.S. in Mathematics. He was employed by the consulting firm of Beers and Heroy (later the Geotechnical Corporation) from 1952-59, working on several seismological research contracts with the U.S. Government. He has been with the Air Force Technical Applications Center since 1959. His work has primarily been concerned with analysis and evaluation of seismological data and more recently, planning and coordinating the field measurement program of collection of seismological data under the Vela-Uniform Program.

LARGE-DIAMETER DRILLING FOR EMPLACING NUCLEAR EXPLOSIVES

Paul R. Fisher

U.S. Army Corps of Engineers
Fort Worth, Texas

ABSTRACT

Techniques and costs have been studied for drilling large-diameter emplacement holes for nuclear explosives designed to produce craters: Limits of 66-in. i.d. (cased) and 2500-ft depth were chosen for the study. Of the three drilling methods studied—core, churn, and rotary—rotary drilling using a circulating fluid or gas was found to be the most widespread and to hold the greatest potential. Large-diameter rotary drilling required modifications in design of both drill bit and strings, in fluid circulation methods, and in casing design. Present costs will probably be greatly reduced as techniques and requirements become standardized.

INTRODUCTION

Engineering with nuclear explosives will require underground device emplacement which may be from about 100 to many thousands of feet below ground surface. The work to provide access to the depth required and emplace the device is expensive and, for the depths required by larger yields, may equal or exceed the charge for the device.

The Nuclear Cratering Group has engaged the Fort Worth District, Corps of Engineers, to make a study of private industry capability to perform emplacement construction. The study effort explores various emplacement techniques and attempts to develop a realistic idea of their costs.

Access, to some point underground can be accomplished vertically, horizontally, or at some inclination between the two. Vertical access can be made by mining or drilling. Horizontal access can be made by mining. This paper reports on the portion of the study concerned with drilling.

Rather than limit the drilling portion of the study to specific device diameters, a fairly broad range of emplacement hole dimensions was studied. These dimensions are shown in Table I.

There are four general drilling methods capable of boring holes of sufficient size to be used for device emplacement purposes: (1) churn drilling, (2) auger drilling, (3) core drilling, and (4) rotary drilling. Rotary drilling (that is full face rotary boring using a circulating fluid or gas to remove cuttings) is the most adaptable large diameter drilling technique of the four methods studied. Under production type conditions, without difficult circumstances, 36" to 66" finished diameter rotary drilled borings should cost from about $100 to $550 per foot of finished hole, depending on the harness of the materials being drilled.

DRILLING EQUIPMENT AND TECHNIQUES

Churn Drilling

Churn or cable tool percussion drilling has been used in the United States for mine ventilation

Table I. Nuclear device emplacement hole dimensions.

Cased Hole Diameter	Depth Range
12" ϕ I.D.	100'
24" ϕ I.D.	
36" ϕ I.D.	
48" ϕ I.D.	
60" ϕ I.D.	
66" ϕ I.D.	2,500'

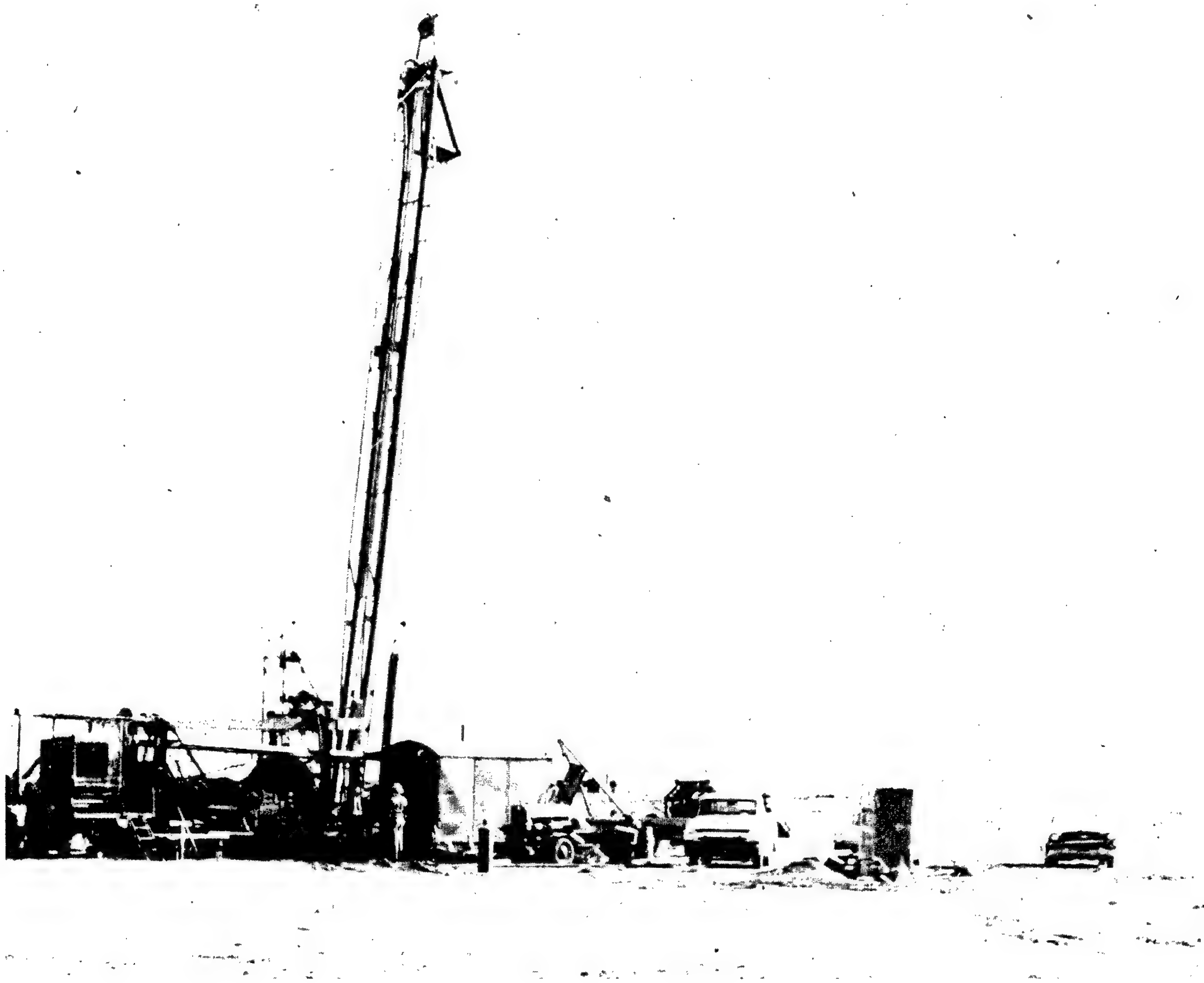

Fig. 1. View of a churn drill rig over a 42" hole. Photo-Layne Texas Co.

or escapeways in boring diameters of 4 feet or less to depths of 600 to 900 feet.[1] Borings up to 30 inches in diameter can be churn drilled in a single pass in moderately hard materials. Borings larger than 30 inches require multiple passes. Churn drilling penetration rates are relatively slow, ranging, for a 28"-diameter hole, from 12 feet per hour in soft materials to less than 6 inches per hour in hard materials.

Churn drilling does not appear to have a usable application in device emplacement work. The technique might be used in relatively shallow moderate sized borings where drilling time is not critical. Its best potential would be in moderate sized holes where the subsurface conditions provided problems for rotary drillings; for example, pronounced lost circulation conditions. See Figures 1 and 2.

Auger Drilling

Structural foundation techniques such as cast-in-place concrete pile and belled caissons have led to the development of highly mobile foundation boring drill rigs. These drills are usually in the form of flight or bucket augers. The maximum diameter for foundation drilling has been 10 feet. Specialized auger machines for missile silo

excavation have drilled 15'-diameter holes to depths of 65'.[2]

The auger drill rig is generally truck mounted, although those auger rigs specifically designed for 10-foot or larger diameters have been crawler mounted. Rotary power is provided to the bucket or auger flight by a square telescoping steel pipe, commonly known as the Kelly. See Figure 3.

There are auger rigs designed specifically for the flight auger and rigs designed specifically for the bucket auger. Both types of rigs can interchange tools, however, the flight auger rig can handle a bucket auger with greater facility than vice-versa. The normal operating depth limit for flight and bucket augers is 100 to 130 feet. This is controlled by the length of the telescoping kelly. There are bucket augers which are reputed to operate to depths of 300 feet. Operating to these depths involves the addition of drill pipe below the kelly with some time loss.

Augers are efficient in natural materials ranging from soft to moderately hard. They function best in materials which will allow the hole to stand open during drilling. However, caving or sloughing conditions can be handled by the addition of noncirculated drilling mud[3] or by the use of temporary casing with consequent reduction in hole size. Within its depth and hardness limits, the auger is easily the fastest and most economical method of drilling available at this

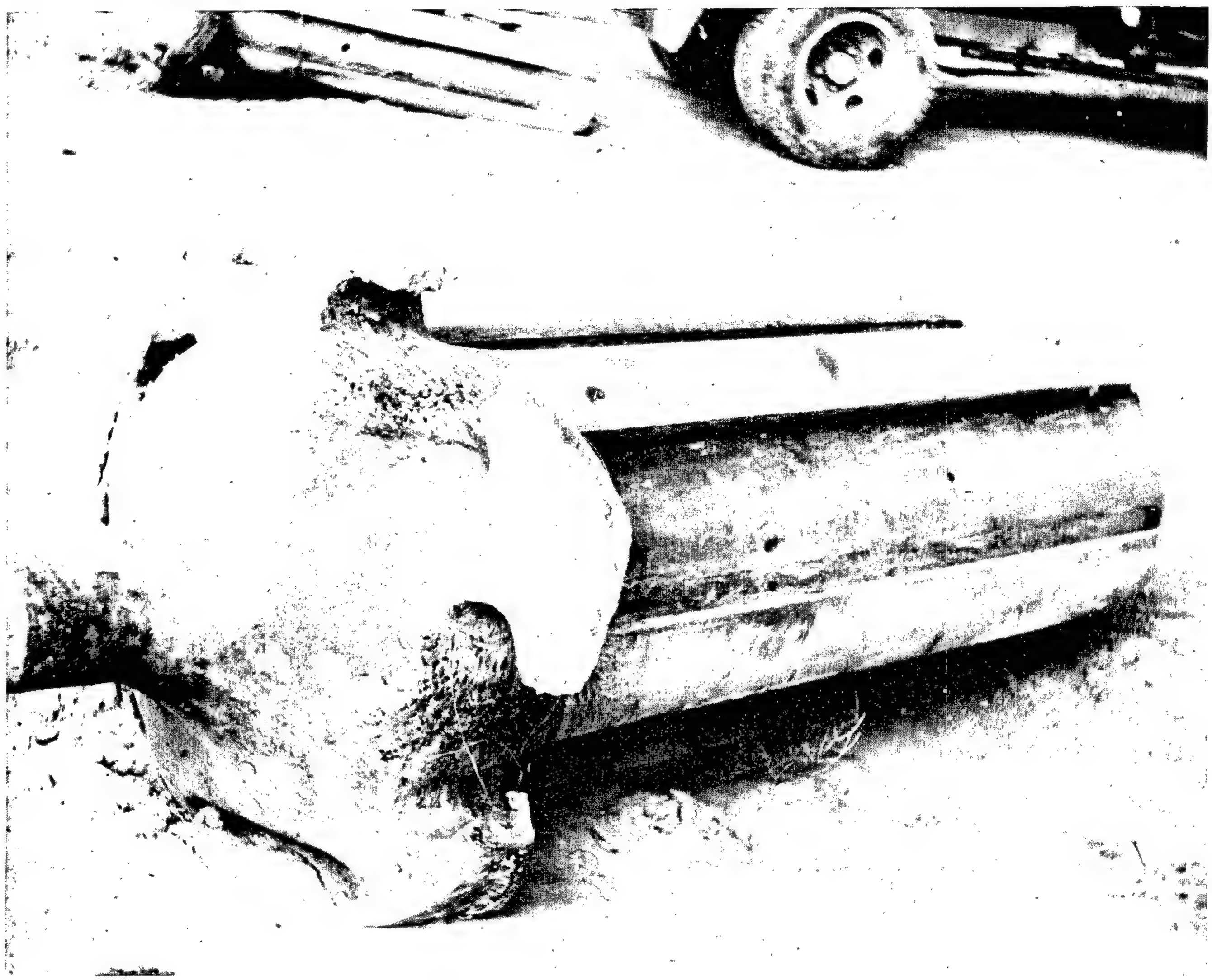

Fig. 2. View of a 32" to 42" churn drill hole opener bit. Photo-Layne Texas Co.

Fig. 3. View of flight auger drill rigs. Photo-USCE.

time. A flight auger can locate over a hole site, drill a 100-foot deep 36"-diameter hole in the hardest material that it is capable of digging efficiently, and move off in a 24-hour period[4] in many cases in an 8-hour shift. The flight or bucket auger would be a fast, low cost emplacement tool for low yield devices in subsurface materials as outlined above.

Core Drilling

Large diameter core drilling, popularly known as calyx drilling, with steel shot has been used extensively in this country since the turn of the century. The shot drilling method uses chilled steel shot as the core cutting material. The core barrel is no more than a steel cylinder with short slots cut at intervals in its lower edge. See Figure 4. The shot is fed into the kerf, is crushed below the edge of the core barrel, and then the angular shot fragments cut the rock. In some cases fluid circulation is maintained, with the chilled shot being introduced with fluid through the drill pipe. In other cases the fluid is not circulated, and the fluid level is maintained just above the core barrel. In materials which are not particularly hard (such as an argillaceous limestone) tungsten carbide tooth inserts have been substituted for the chilled steel shots. A relatively recent successful innovation has been the substitution of rolling cutter segments for steel shot.[5][6] Boring up to 8 feet in diameter have been core drilled.

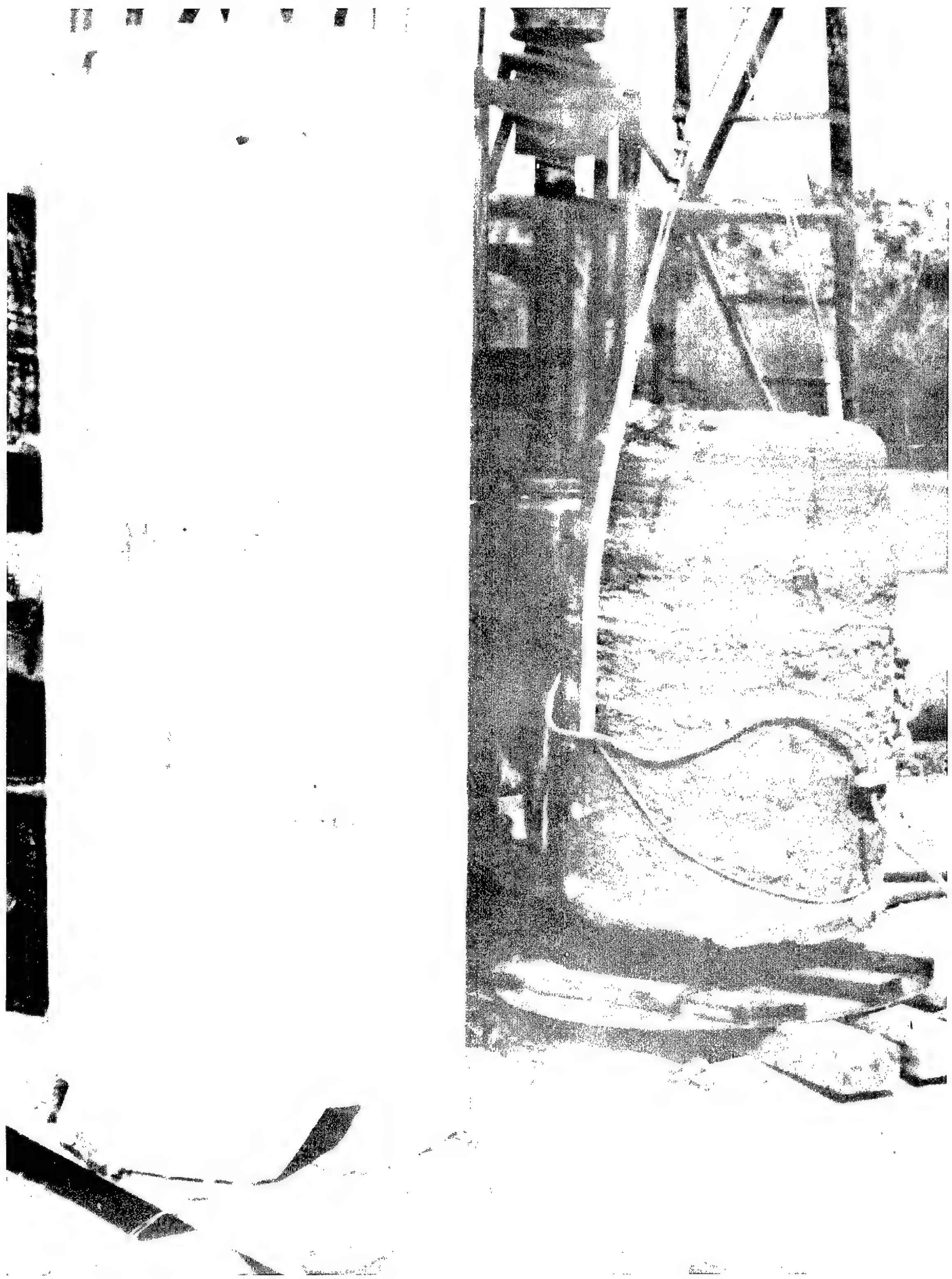

Fig. 4. View of a 36" diameter calyx core barrel with 36" core handing from the drill rig in the background. Photo-USCE.

Large diameter core barrels do not generally feature a core catcher assembly. As a consequence the core must be broken loose from the bottom of the hole and removed, essentially, by hand. If the rock is unbroken, it can be extracted as a single piece of core. If it is broken, hand mucking of individual fragments is required.

The torque, hoisting and circulation requirements for large-diameter core drilling are relatively low. As a consequence, fairly small drill rigs can be used. For example, truck mounted exploratory drills have efficiently drilled 200 feet deep 36"-diameter core holes in limestone.

Large diameter deep holes are often drilled with a "down the hole" machine that functions in the borings. Two examples of this are the Newsom type coring device and the Zeni-McKinney-Williams coring machine. (5) Both of these units consist of two units; an upper drive unit which is anchored to the side of the boring and drives a lower core barrel. The Zeni-McKinney-Williams concept has been modified to cut full face. These machines cut 5-1/2 to 6-foot-diameter holes.

The large diameter core drilling method requires that the subsurface materials be relatively impermeable and of sufficient competence to allow the boring to stand open without support. Heavy water inflows or caving conditions cannot be tolerated due to the fact that personnel must enter the hole to extract the core. Due to these rather rigid subsurface condition requirements, the application of core drilling to device emplacement is limited. The technique would be usable in the boring of moderately sized holes (say 36" to 48") in sound rock which is impervious or where the water table is below the total depth of the boring. The beginning point of application for the core drill would be the point of refusal for the auger drill. Due to the cyclic nature of the operation, net large diameter coring penetration rates are slow. However, in moderately sized holes in very hard rock coring penetration rates can compare with full face rotary drilling. Thirty-six inch core borings have been drilled in basalt at the Nevada Test Site for nuclear and high explosive emplacement, ranging to 126 feet in depth.

Rotary Drilling

In recent years the rotary drilling technique has become the most widely accepted method of boring deep large-diameter holes. Big hole rotary drilling has evolved from oil and gas drilling and from water well drilling. Areas which have provided impetus for the development of these techniques have been the use of natural or man-made underground openings for storage purposes; the increasing need by mining interests for relatively rapid access and/or ventilation for existing workings or new ore reserves; the U. S. Government protective construction programs; and the U. S. Atomic Energy Commission underground nuclear testing programs. The largest diameter rotary drilled hole in the U. S. to date is an access shaft in Louisiana, drilled in 1962. (7) This hole was drilled 130 inches in diameter to a depth of 570' and 90" in diameter from 570' to 1400'. Two shafts, 25' in diameter and 1700' in depth were drilled in Holland, however the drilling assembly was a portion of the shaft head-works as compared with a modified oilfield drill rig for the 130" hole in Louisiana.

Rotary Drilling Equipment

The rotary drilling equipment complex consists basically of the drill rig (surface component), the drill string (in hole components), and the circulating equipment.

Drill rig. The big hole drill rig is, in most cases, only slightly modified from the equipment used to drill an oil or gas well or a large water well. The substructure, draw-works, prime-movers, mast, block and tackle, and rotary table are generally stock items. Rotary tables designed to pass large diameter drilling tools and a mast designed to boom forward to pick up the heavy tools have been fabricated and are in operation. See Figures 5 and 6.

Table II illustrates, by draw-works input horsepower, the recommended rig size for various finished hole diameters and depths. (8)

Drill string. The drill string or in-hole components, consists of the bit, drill collars, drill pipe, and swivel. Significant advances have been and are being made in bit design. The rolling cutter bit appears to be the preferred tool for nearly all subsurface materials. Three-cone roller bits are made in diameters from 3-3/4" to 26". When a hole with a diameter greater than 26" is desired it can be achieved by the use of

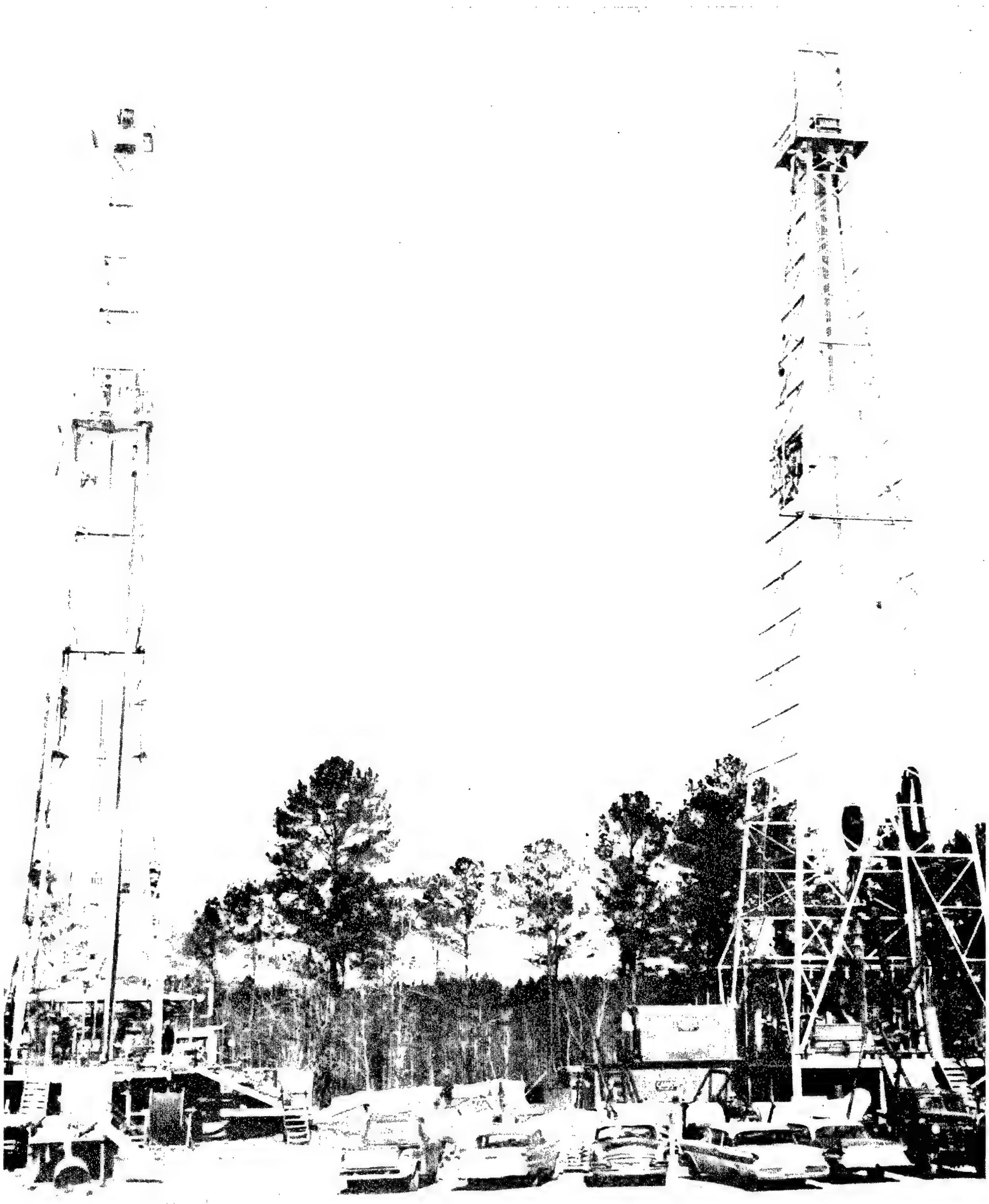

Fig. 5. View of two drill rigs over 57" and 88" diameter holes. Photo-Drilling Magazine.

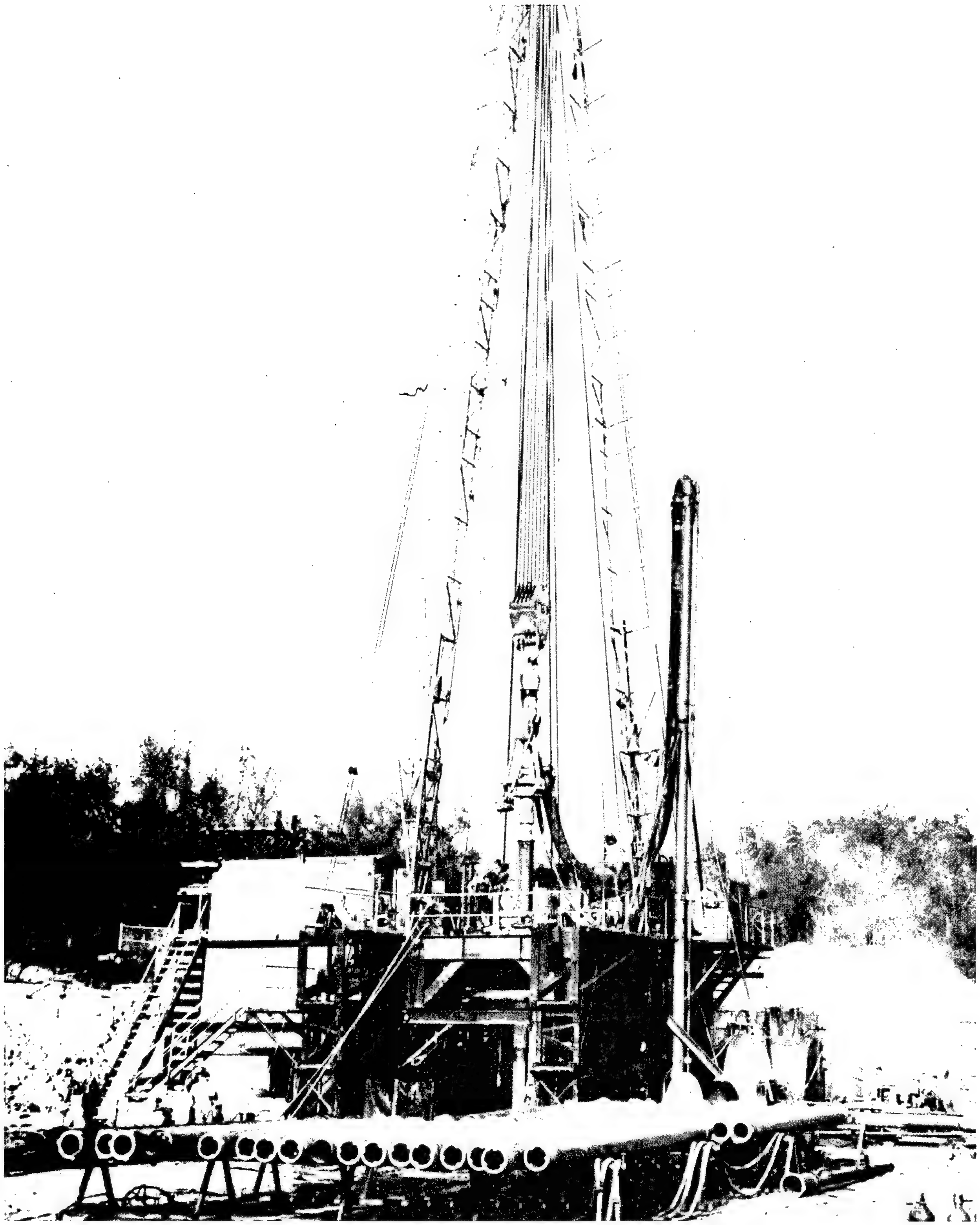

Fig. 6. View of a drill rig over a 130" diameter hole. Note the bipod mast which is designed to boom forward to pick-up heavy drilling tools or casing. Photo-Drilling Magazine.

Table II. Recommended drill rig capacities (by draw-works input horsepower) for various finished hole sizes and depths.

Finished Hole Size (Casing ID)	Depth Range	Rig Type	Input Horsepower
12"-66"	0'-100'	Auger-Truck Mtd	-- to 225
12"-24"	100'-500'	Truck-Trailer Mtd	125 to 225
24"-48"	"	Trailer Mtd	125 to 500
48"-66"	"	Trailer Mtd-Stationary	225 to 700
12"-24"	500'-1000	Trailer Mtd	225 to 500
24"-48"	"	Trailer Mtd-Stationary	225 to 700
48"-66"	"	Stationary	700 to 1000
12"-24"	1000'-1500'	Trailer Mtd-Stationary	225 to 700
24"-48"	"	Stationary	700 to 1000
48"-66"	"	"	1000 to 1375
12"-24"	1500'-2000'	Stationary	700 to 1000
24"-48"	"	"	1000 to 1375
48"-66"	"	"	1375 to 1625
12"-24"	2000'-2500'	Stationary	1000
24"-48"	"	"	1375 to 1625
48"-66"	"	"	1625

three, four, or six point hole openers or by the use of a flat or stage type bit. The use of hole openers usually requires multiple passes, enlarging the diameter of the hole from 6 to 12 inches per pass. The use of a flat or stage type bit allows the hole to be drilled in a single pass. It is possible to stack a series of hole openers, one above the other, and to drill a hole in a single pass. This method has been used successfully at the Nevada Test Site. These various big hole bits differ from the smaller three-cone roller bits in that they feature demountable rolling cutters. Two basic types of demountable cutters are available. One type bolts as an entire unit to the bit body. The other type mounts the rolling cutter cone in a yoke or straddle mounting assembly, which in turn is welded or bolted to the bit body. See Figures 7, 8, and 9.

There are various sizes of drill pipe available to the drilling industry. The most popular sizes being used in large diameter drilling are 6-5/8" and 13-3/8" in diameter with both sizes being made from seamless oilwell casing. The 6-5/8" pipe has been used to drill holes as large as 64" in diameter and 2500' in depth. The 13-3/8" pipe has been used to drill the largest holes produced in this country (130") and the same sized pipe was used to drill the 25'-diameter shafts in Holland. Aside from greater strength, the 13-3/8" drill pipe has the advantage of a larger fluid passageway with resultant lower fluid friction losses. See Figures 10, 11, and 12. In conventional rotary drilling the weight on the bit is provided by drill collars which are thick walled sections of pipe. The approach for large diameter drilling is to use the available larger diameter to

Fig. 7. View of a flat type large diameter drill bit. Photo-Smith Tool Company.

concentrate the weight near the bit. Various types of drill collar assemblies are made for the 13-3/8" drill pipe. The earliest assembly consisted of 40" by 8'10" lead-filled steel cylinders weighing 42,000 pounds apiece. These individual weights proved awkward to handle and a later assembly features a number of lighter weights. This assembly includes a 40'-long 16"-outside-diameter stem with a weight supporting flange at its base. The weighting elements are twenty 40"-diameter iron doughnuts weighing 5600 pounds each, which slip over the stem. See Figures 13 and 14.

Circulating equipment. The composition of the circulating media and the method of circulation control is the type of circulating equipment used. The standard oilwell drilling pump evolved to serve two purposes. One is to provide sufficient fluid volume to remove cuttings from the hole. The second is to provide sufficient pressure at the bit face so that cuttings can be cleared from the rolling cutters by fluid jets. This evolution culminated in large positive displacement pumps requiring high amounts of input horsepower. This high horsepower is needed to circulate the relatively large fluid volumes, overcome the high drill pipe head losses, and still have sufficient pressure reserve to clean the bit and push the cutting-laden fluid from the hole at an acceptable

velocity. The largest of these pumps requires about 1000 input horsepower and will discharge from 400 to 900 gpm at pressures of from 3500 to 1500 psi.

For large diameter holes, say 36" or larger, these oilwell pumps do not develop sufficient volume to effectively carry cuttings out of the boring. As a consequence, big hole drilling contractors have been using centrifugal pumps for circulating equipment. While the volumetric efficiency is low, these pumps will deliver large fluid volumes at relatively low heads. See Figure 15.

The use of air as a circulating media evolved as an adjunct to air-actuated rotary precussion drilling and has proved to be extremely efficient in dry conditions. Several types of equipment have been used in big hole work. For conventional air circulation, that is down the drill pipe and up the hole, banks of positive displacement compressors have been used. As many as 12 600 CFM compressors, operating in parallel were used at the Nevada Test Site on a 60" hole. See Figure 16. Reverse air circulation has also been used both at the Nevada Test Site and in private industry applications. Two methods have been used: (1) drawing a vacuum on the drill string; and (2) pressuring the hole annulus. In some cases both these methods have been used in combination. The drawing of a vacuum on the drill string has been performed, by use of a jet air educator. This system will draw about 6400 CFM at 80" of water. The pressuring of a big hole annulus has

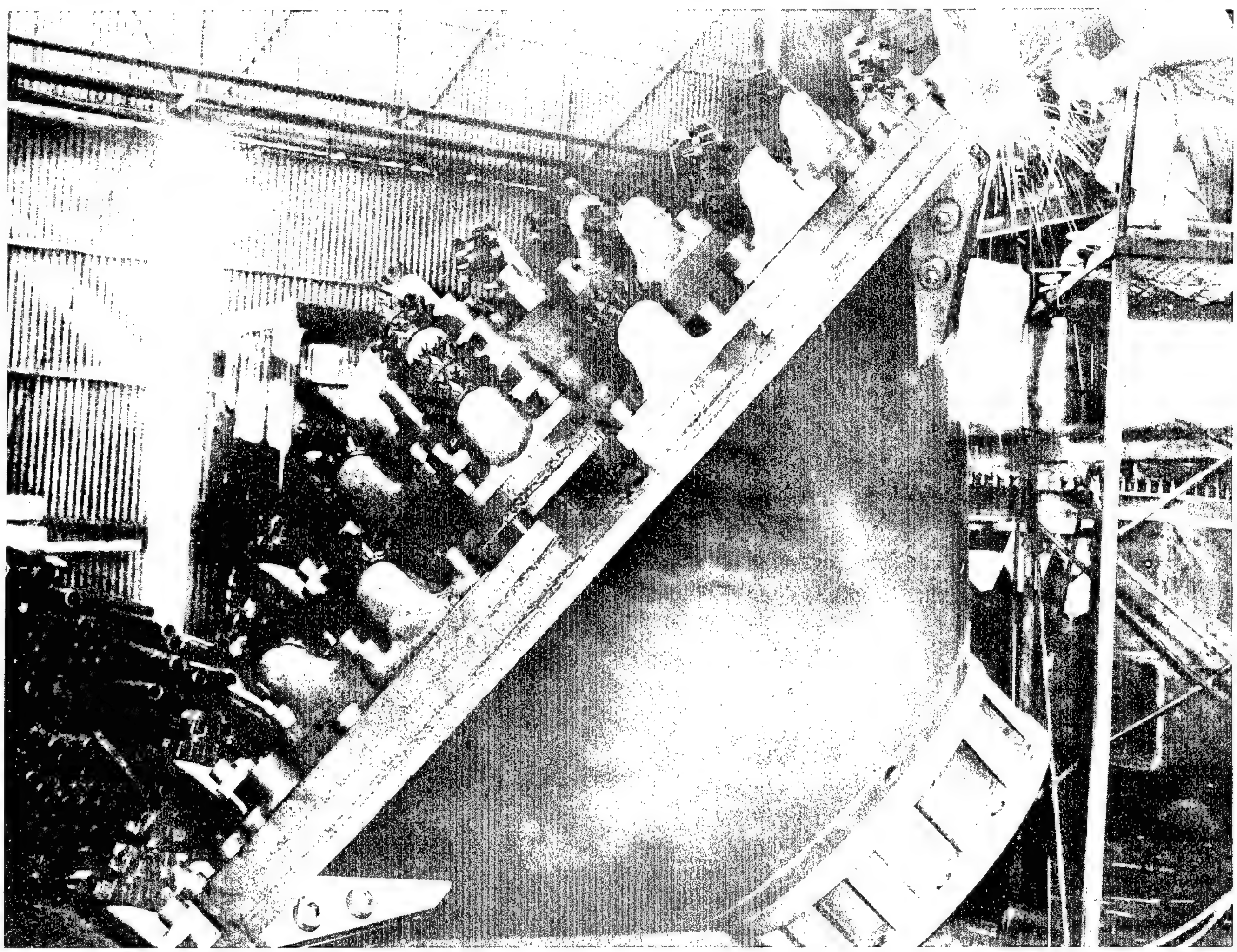

Fig. 8. View of a plate type large diameter drill bit. Photo-Hughes Tool Company.

Fig. 9. View of a hole opener type large diameter drill bit mounting carbide insert cutters. Photo-USAEC.

been used in conjunction with drawing a vacuum on the drill string and also as the prime circulating technique. The equipment consists of an air supply and a rotating pressure head to seal off the hole at the collar. To date, about 10 psi has been the maximum working pressure for rotating pressure heads. It is understood that pressure heads which will operate at 30 psi have been designed. The low pressure air supply for this method can be either in the form of industrial Rootes type blowers or as low pressure bleed-air from gas turbines.

Rotary drilling procedures. The selection of the overall drill bit configuration, whether in terms of multiple passes with hole openers, or a single pass with a flat or stage type bit or stacked hole openers, is largely a matter of personal opinion. The trend in the last 2 or 3 years has appeared to favor the single pass.

Excluding the effectiveness of cuttings removal, the drilling penetration rate is a function of the weight on the bit and the rotary speed. Recommended bit weights for small oilfield boring range from 1000 to 8000 pounds per inch of bit

diameter.[9] From this it can be seen that, ideally from 72,000 to 576,000 pounds would be required to drill a 72" hole. The higher weights are beyond the range of rig capacities at this time. The current practicable limit is about 200,000 pounds.

In conventional sized oilwell borings, drill string rotary speeds in excess of 200 rpm are common. Rotary speeds such as this would produce high peripheral velocities on large diameter bits (i.e. about 60mph on the outer row of cutters on an 8 foot bit) which would cause rapid tooth wear and bearing failure. These high speeds would also require prohibitively high torque. A rule of thumb for rotary speed in the drilling of large diameter holes is 120/D = RPM where D = the hole diameter in feet.[10]

The best circulating media, in terms of drilling penetration rates, is air or gas. The use of air has had limited use in large diameter drilling; it has been used primarily where it was undesirable to use a fluid. With conventional air circulation in small holes the return air velocity is normally high, sometimes exceeding 10,000

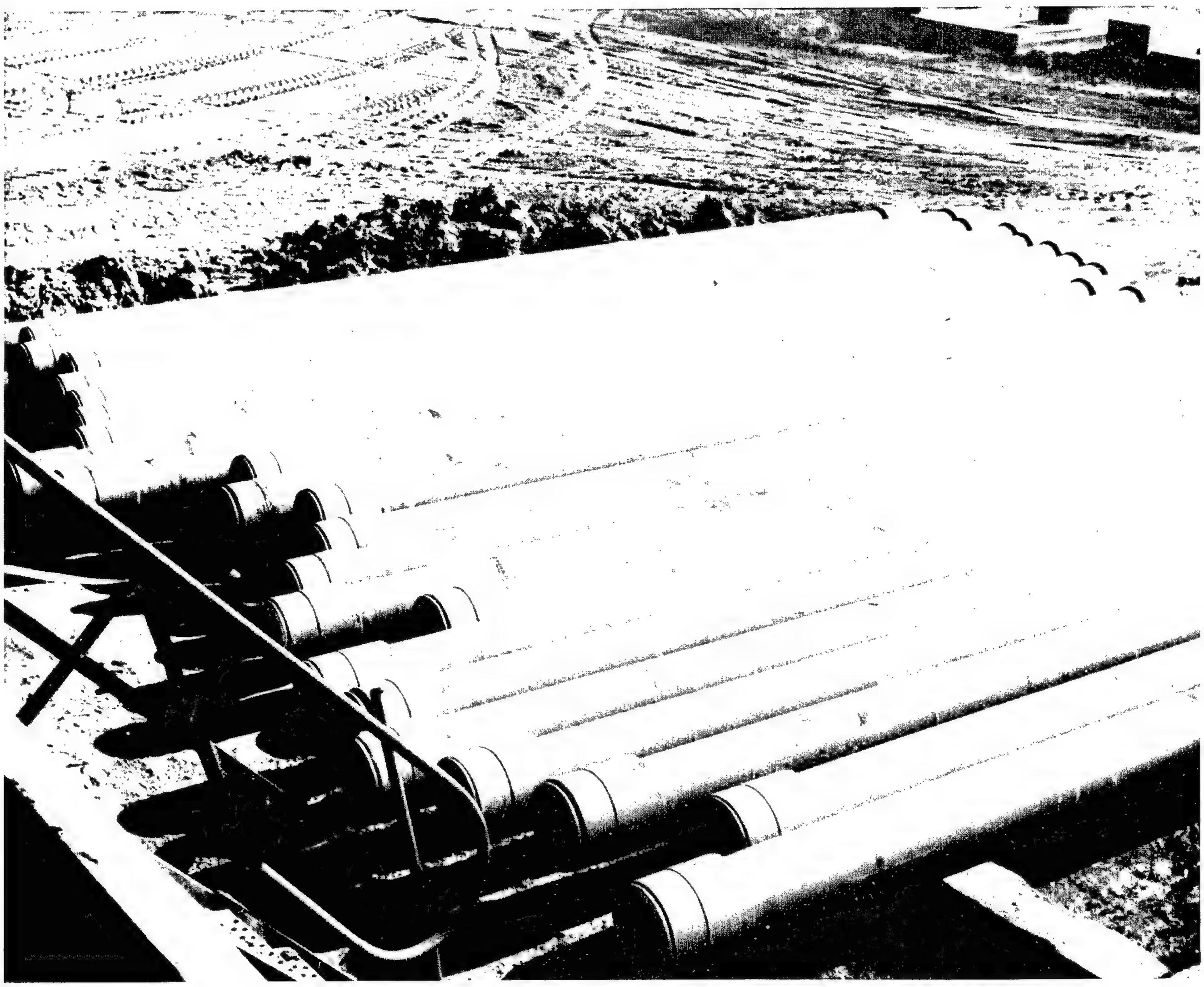

Fig. 10. View of 13-3/8" OD drill pipe designed for large diameter drilling. Photo-Drilling Magazine.

Fig. 11. View of a drilling swivel with a 12: fluid passageway designed for large diameter drilling. Photo-Hughes Tool Co.

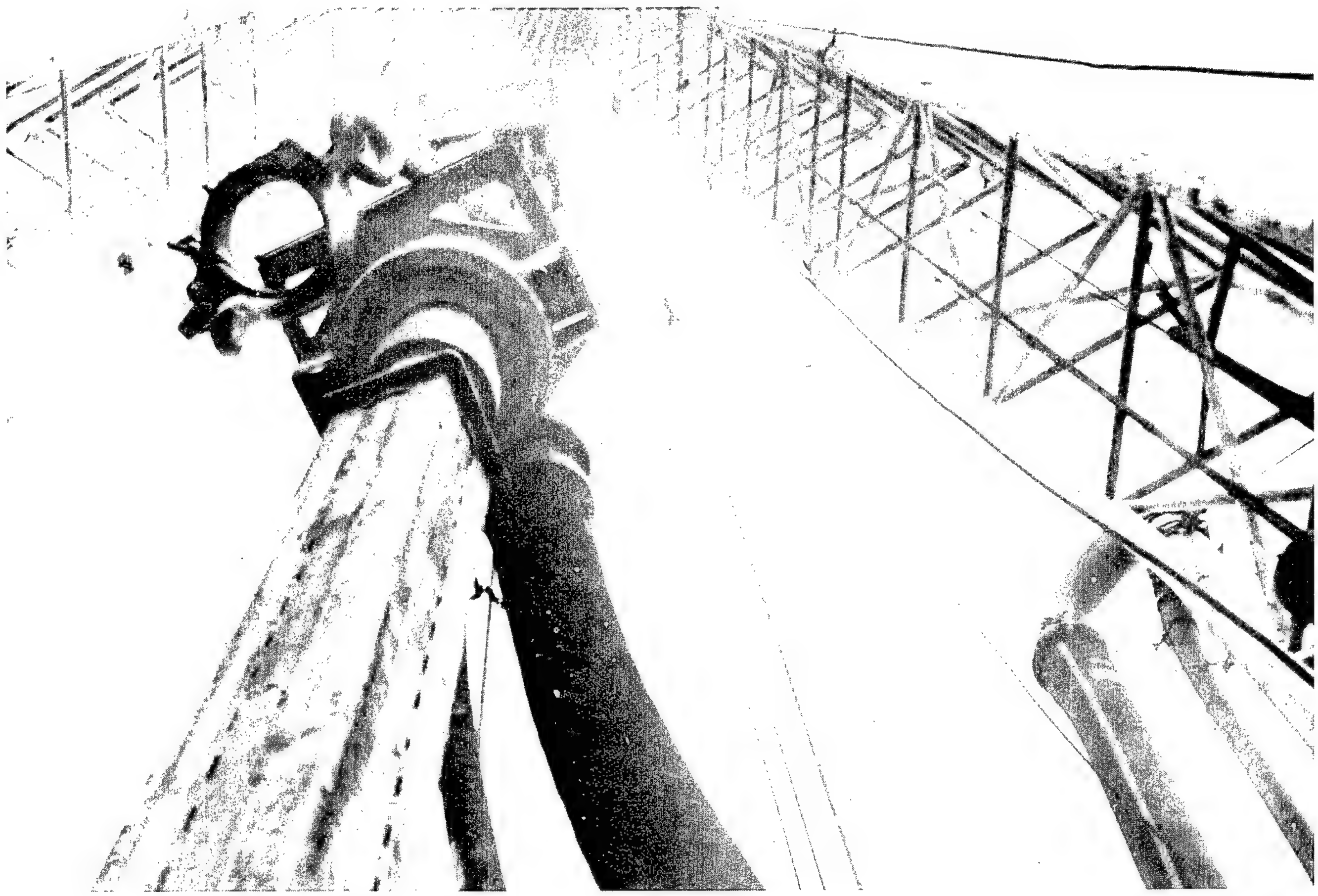

Fig. 12. View of a large diameter drill swivel, kelly, and rotary hose. Photo-Drilling Magazine.

fpm. In large diameter rotary drilling, return air velocities are considerably lower. The annular velocities experienced at the Nevada Test Site have been on the order of 700 fpm. These low velocities have been made workable by the injection of water and detergent into the air stream. This air-mist accomplishes two purposes: it increases the moisture content of the boring wall material, thereby reducing friction and inhibiting sloughing; and increases the carrying capacity of the air by producing foam. The reverse air circulation system, using the jet eductor system and/or the pressuring of the hole annulus can develop rising air velocities in the drill string which approach some of those obtained in conventional air circulation in smaller holes. Air drilling in big holes is limited to conditions where: water inflow is small, and the formations encountered are sufficiently competent to maintain an open hole without support.

Liquid circulation media can be divided into three categories: (1) plain water, (2) water-based drilling mud, and (3) water-oil emulsion or oil-based drilling mud. In terms of the rate of drilling penetration, and cost plain water is the best drilling liquid and is also the least costly. Many subsurface materials can be drilled satisfactorily with plain water. These materials are generally

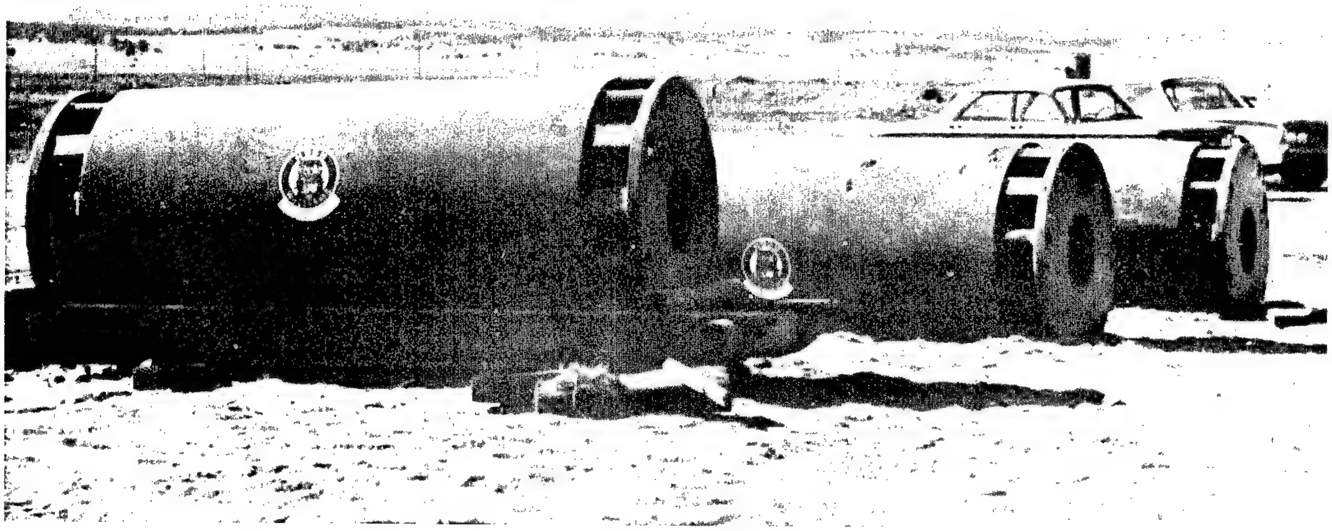

Fig. 13. View of 42,000 pounds, each, lead filled drill collars. Photo-Hughes Tool Co.

the moderately hard or harder sedimentary rocks, most igneous rocks, and most metamorphic rocks. If the drill water supply is abundant and close to the hole site, the return water can be wasted. An abundant supply of water near a drill site is a relatively rare occurrence. Consequently the drill water has to be reused continually after the cuttings have been removed by settling or shaker screens, etc. The only anticipated additive for the drilling of moderately hard to hard competent materials which produce nonplastic fines would be lost circulation control materials.

The most likely fluid system, when drilling soft to moderately soft compacted or cohesive materials such as clays or shales or soft noncohesive silts, sands, or gravels, would consist of a water-fine-solids mixture. In many cases the solids portion would consist of native drilled fines with processed clays or dispersants added as needed. The additives for a fresh water system would be a sodium bentonite and an inorganic dispersant. The function of the bentonite is to develop a sufficient percentage of colloidal particles to control the suspension of noncolloidal solids and to provide the optimum wall cake characteristics to control water loss to the materials being drilled. Some clays and clay shales will slake or swell when exposed to water. This

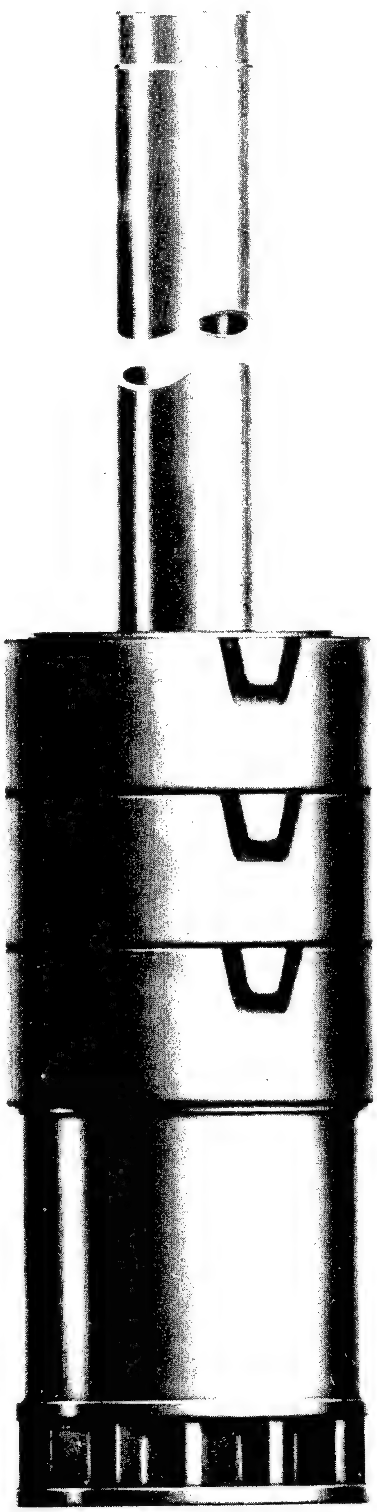

Fig. 14. View of a stacked "do-nut" drill collar assembly. Photo-Hughes Tool Co.

occurrence can have a marked deleterious effect on a boring regardless of its size. Under circumstances such as these, the denial of drill water to the formation materials would be of prime importance. The dispersant will break down the aggregate of natural drilled solids and render the fluid more workable. If salt occurs as the natural material being drilled or if the drill water becomes saline for any other reason, the sodium bentonites lose their ability to form a colloidal suspension and the inorganic dispersants do not function. In this case, the processed clay additives are either a calcium bentonite or an attapulgite. The dispersant would be organic.

Water-oil emulsion-based or oil-based muds are expensive. They are used, however, where extreme formation-water reactions occur.

The optimum annular rising velocity for a drilling fluid is the range of 100 to 125 feet per minute providing turbulent flow is maintained.[11] A rule of thumb for big hole drilling fluid flow rates is 50D = gpm.[10] (Where D = diameter in inches). Another big hole criteria presented is that a minimum rising velocity of 20 fpm should be maintained.[8] Table III compares flow rates for the optimum using velocity, the 20 fpm rising velocity and the "rule of the thumb." Excluding friction losses, current circulating equipment can maintain the pumping rate at 50D = GPM and/or a minimum rising velocity of 20 fpm for the boring diameter shown. The optimum rising velocity of 100 fpm cannot be maintained in boring larger than 48". This problem in rising velocity can be overcome by using reverse circulation, pumping the drilling fluid up through the relatively small diameter drill string. Air lifting has proved to be a simple but highly effective reverse circulation technique. This is done by discharging fairly high volumes of air through a small pipe which extends downward below the swivel inside the drill pipe. An imbalance is created in the fluid system by the aerated column of drilling fluid and reverse flow occurs. Fluid volumes of 5000 gpm have been circulated in 13-3/8"-drill pipe in this manner.

LARGE DIAMETER CASING

Regardless of the drilling method used to produce an emplacement boring, a casing or liner may be required to maintain the integrity of the boring until stemming of the nuclear device. The

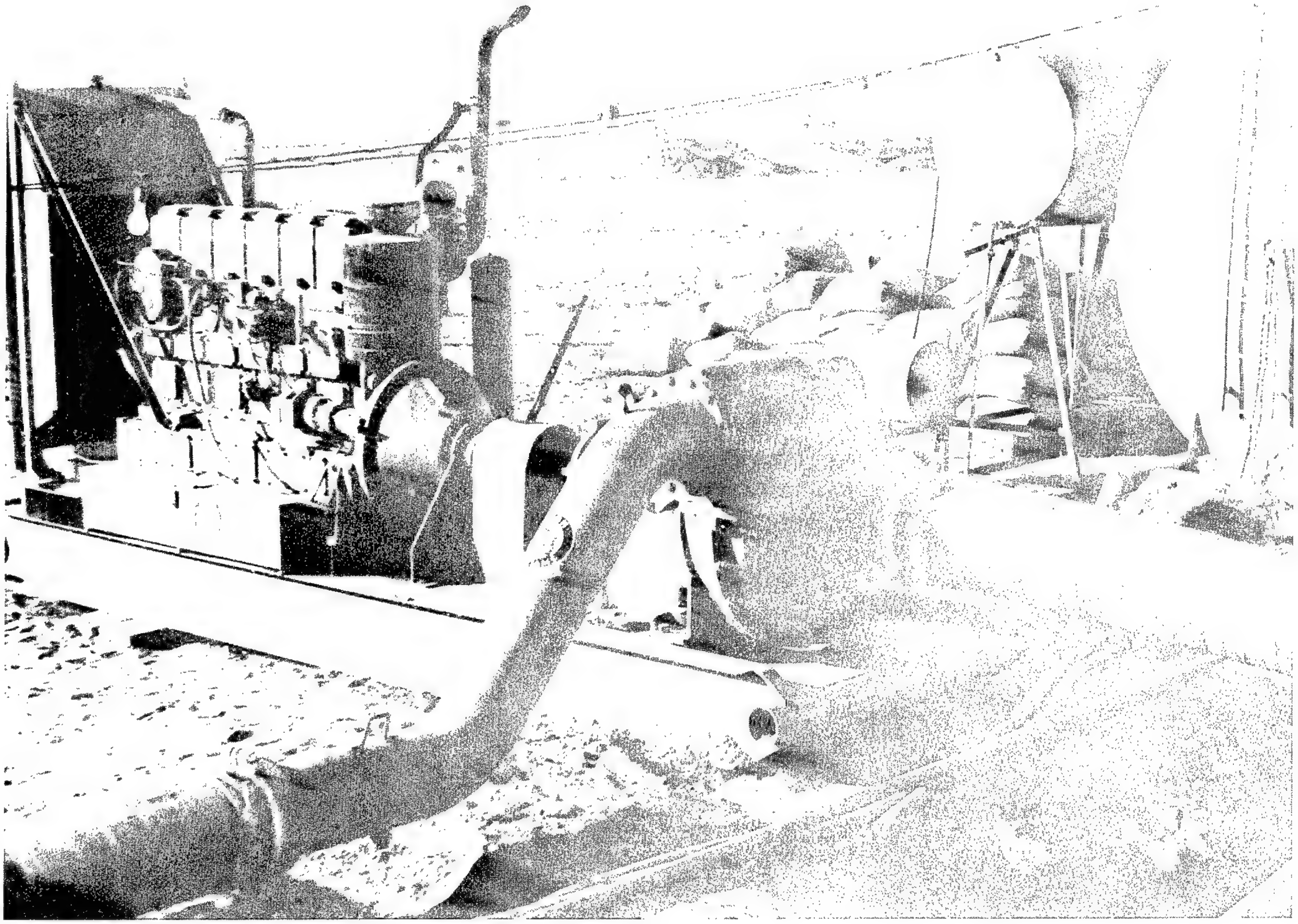

Fig. 15. View of a large centrifugal pump used for circulating large volumes of drilling fluid in large diameter drilling. Photo-Drilling Magazine.

current device implacement philosophy requires that the boring be dry. This condition demands that the liner structure have a collapse resistance at least equal to the anticipated ground water head.

It is generally accepted that the casing should be designed with a safety factor of 1. 3 to 2 times the anticipated hydrostatic head. It is thought that this range of strengths would also handle any lithostatic pressures that would occur. Because of the rapidly decreasing collapse resistance with increasing diameter, casings with diameters larger than 36 inches are usually designed with rib supports for stiffening purposes. The purpose of these rib supports is to bring the casing collapse point close to the yield point of the steel. A commonly accepted design is to combine moderate wall thicknesses with 2-1/2 or 3" ship channel stiffener rings at 2' to 4' intervals. See Figure 17.

There have been high strength relatively thin walled casings designed which, if put into practice, could result in a considerable weight and cost savings. [12]

Big hole casing is generally placed in the hole by casing elevator and the drill rig hoisting system so long as the weight of the casing string does not exceed the rig capacity. Deep, large diameter casing strings, which can weigh in excess of a million pounds, are generally placed with hydraulic

Table III. Drilling fluid flow rate comparisons.

Hole Diameter	50 D = GPM Velocity fpm	Total GPM	GPM at Optimum Velocity of 100 fpm	GPM at Velocity of 20 fpm
36"	39	1800	4600	920
48"	28	2400	8714	1742
60"	21	3000	14002	2800
72"	18	3600	20457	4119
84"	15	4200	28094	5618
96"	13	4800	36913	7382

Fig. 16. View of a bank of air compressors being used as the air supply for direct air circulation on a 64" diameter hole. Photo-USAEC.

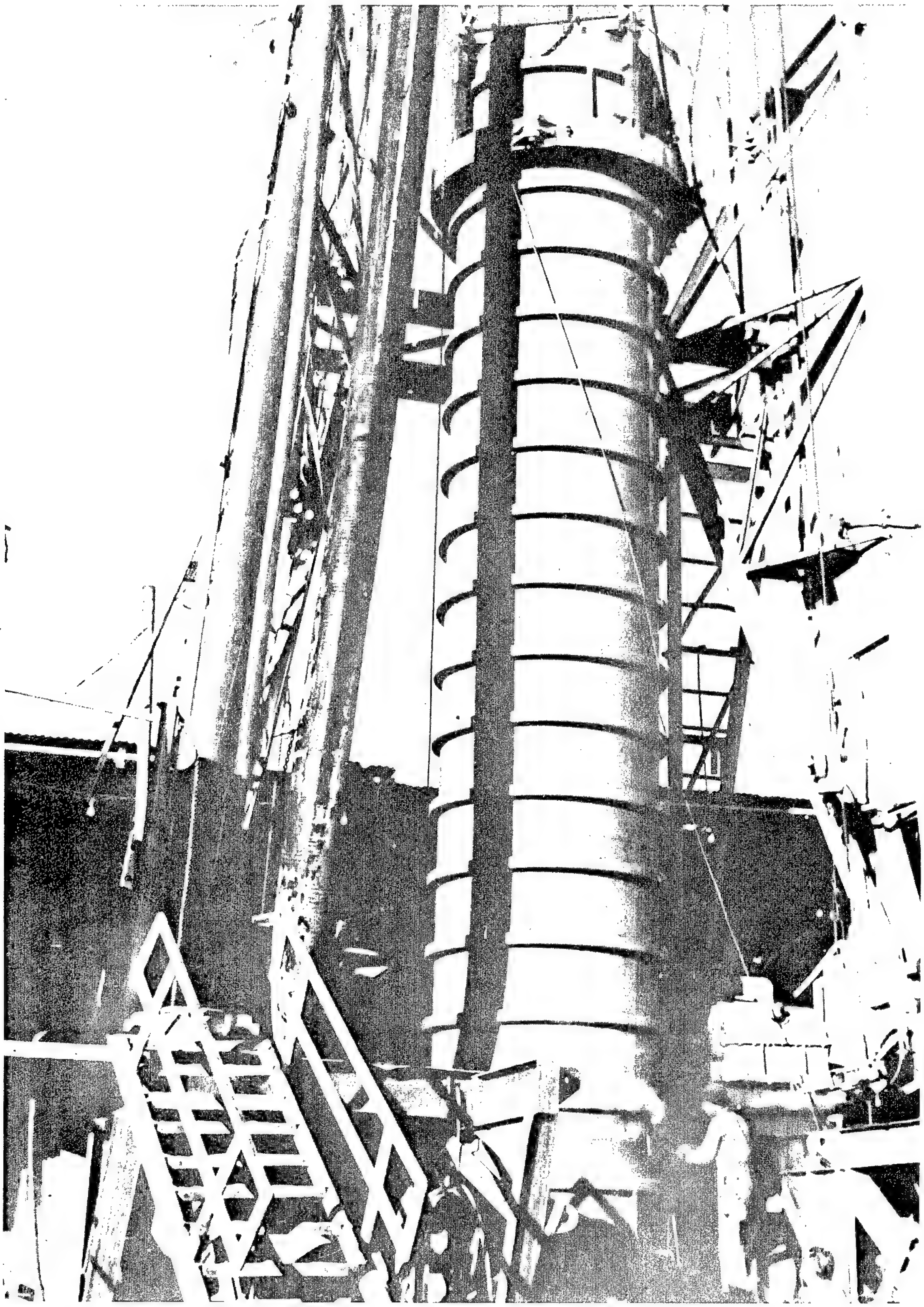

Fig. 17. View of rib reinforced large diameter casing being run into a drill hole with the drill rig hoisting equipment. Photo-Drilling Magazine.

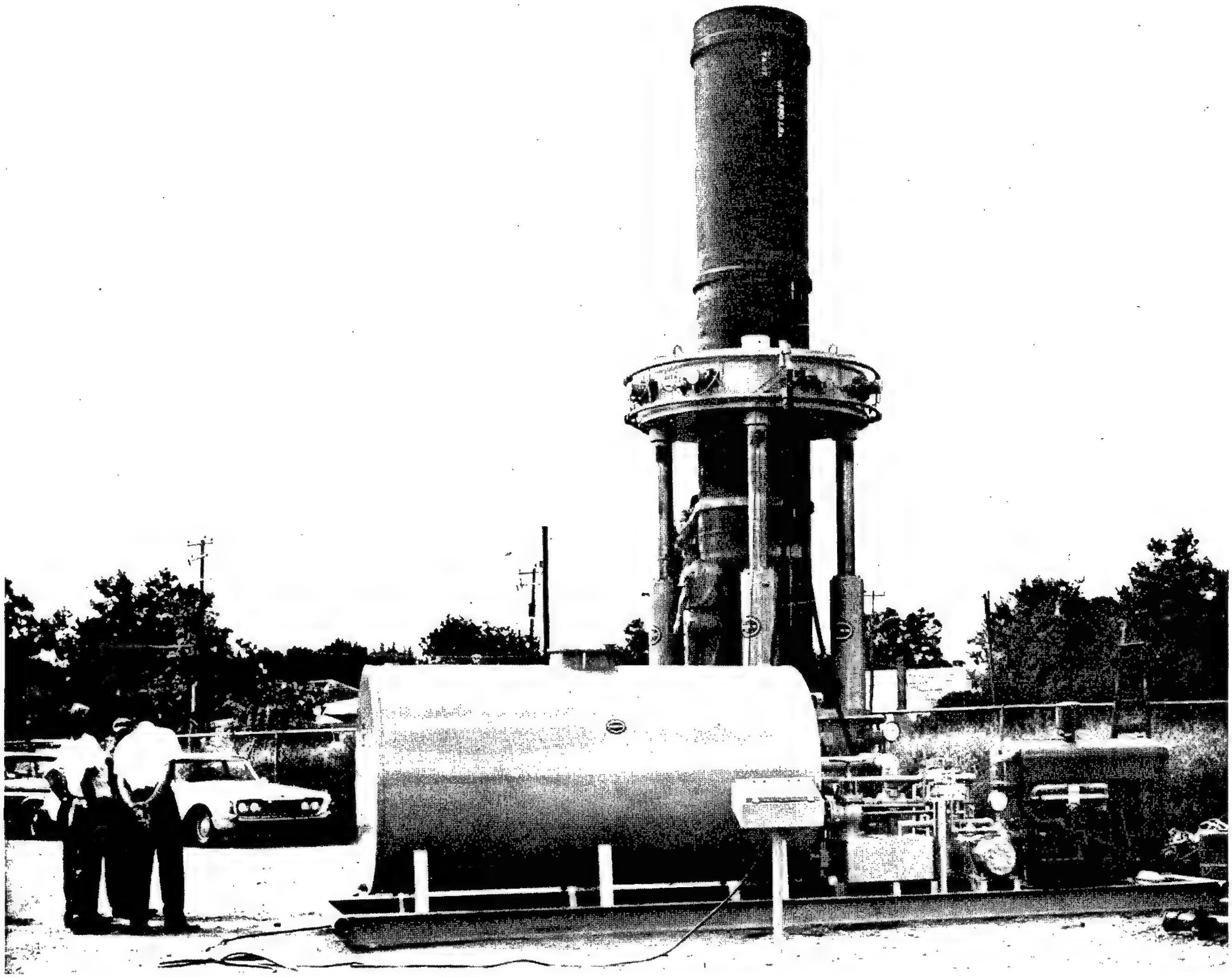

Fig. 18. View of hydraulic casing jacks. Photo-USAEC.

casing jacks. Casing jacks in use at the Nevada Test Site will handle casing outside diameters from 30 to 72 inches and weights up to 2 million pounds. See Figure 18.

After the casing has been placed it is normally cemented into the hole. The purpose of the cementing (in emplacement drilling) is to make the boring wall and the steel casing a structural unit. Large diameter casing cementing is being performed by standard oilwell cementing equipment. The cement placing techniques are: (1) where a casing shoe has been provided, cementing through drill pipe lowered inside the casing and fixed to a port in the casing shoe, and (2) cementing through grout lines located in the annulus between the casing and the boring wall. Cementing through the casing shoe requires continuous injection. In large diameter holes it can be difficult to inject cement at a rate which produces the optimum turbulent or plug flow. Also, if the casing is not filled with fluid, too rapid a rise of the cement in the annulus may cause collapse. When cementing with grout strings in the annulus, the injection operation can be stopped at any time. Thus the injection rate can be easily controlled.

A considerable savings in emplacement costs could be realized by design of a nuclear device cannister which is water tight to the hydrostatic

heads anticipated for excavation purposes. This development, coupled with the possibility of using drilling fluid for the stemming agent would allow a considerably lighter casing. The casing would be perforated and would not be designed to resist hydrostatic pressure. The function of the casing would be to prevent the sloughing of blocks of material from the boring wall. Corrugated metal pipe could serve admirably for this purpose. Twelve gauge (0.1040") to eight guage (0.1644") one by three inch corrugated steel pipe, in inside-diameters of 36 to 66 inches, will provide protection against a load of a minimum of 5,000 pounds per square foot (providing the pipe is restrained all the way around its circumference). The standard strap coupling used to fasten lengths of CMP together would not handle the tensile loads imposed in deeper holes. This deficiency could be remedied by the addition of longitudinal steel straps to the outside of the CMP at 90 degree points. There would be no need for cementing this type of casing into the boring, in fact, cementing would defeat its purpose.

EMPLACEMENT DRILLING AND CASING COSTS

The discussion of emplacement drilling and casing costs will deal primarily with rotary drilling. A brief summary of the range of costs will be shown for churn, auger, and core drilling.

Churn Drilling

There is a wide variation of costs for churn drilling. As stated earlier holes less than 30" in diameter can be drilled in one pass and holes larger than 30" require two passes (with 42" as the maximum size considered). Exclusive of drill rig mobilization costs, the domestic cost per foot of advance for a 42" hole would be from about $20 in soft materials to $40 in moderately hard materials.

Auger Drilling

In its efficient depth range (0 to about 120 feet) the flight or bucket provides rapid low cost drilling. It is limited in the hardness of materials which it can effectively penetrate. Assuming no adverse conditions (such as a caving hole or the rapid infiltration of water) the domestic drilling cost per foot of hole can be expected to range from as low as less than $1 per foot for a 36" hole in soft materials to about $20 for a 72" hole in moderately hard materials. As with churn drilling these costs do not include drill rig mobilization.

Core Drilling

Core drilling has a limited but definite application for device emplacement in hard materials. Cost information is limited to a 36" diameter hole. Exclusive of mobilization, a 36" core hole can be expected to cost from about $12 per foot in moderately soft materials to $150 per foot in very hard materials.

Rotary Drilling

The major factors which control the rotary drilling cost for a hole of a specific diameter and depth are the operating costs for the appropriate drill rig complex, and the cost of the materials expended such as the drill bit cutters and the drilling fluid. In developing these cost factors certain assumptions must be made concerning the optimum rig capacity for a given finished hole size and depth and the overall drilling penetration rates for various diameter holes in materials of various hardnesses. Further similar assumptions must be made concerning average drilling bit cutter costs and an average cost per unit volume for drilling fluid.

Table II has shown the recommended drill rig capacities for various finished hole sizes and depths. Table IV illustrates an average relationship of drilled hole diameter to casing ID for increasing increments of depth.

Table V shows current domestic average operating costs for the family of drill rigs believed capable of performing the work. These costs are based on a 24 hour working day. Table VI presents average gross and net rotary drilling penetration rates. The gross penetration rate (gross fph) shown in Table VI is in terms of on-bottom rotating time and the net penetration rate (net fph) assumes that the drill bit is rotating 60% of the time.

Table VII shows approximate drilling bit cutter costs for various material hardnesses. There has been some experience conformation in the ranges of soft to moderately hard, but none

Table IV. Average boring diameter for casing ID's from 36 to 66 inches at depths from 100 to 2500 feet.

Casing ID	Depth Range/Boring Diameter				
	100' to 500'	500' to 1000'	1000' to 1500'	1500' to 2000'	2000' to 2500'
36"	44"	48"	50"	52"	54"
48"	60"	62"	64"	66"	70"
60"	72"	74"	78"	80"	84"
66"	78"	80"	84"	88"	90"

Table V. Average domestic operating costs for various capacities of rotary drill rigs.

Input Horsepower	Type	Average Domestic Operating Cost	
		Per Day	Per Hour
225 to 500	Truck to Trailer Mtd.	$ 750	$ 31
700	Trailer Mtd to Stationary	1,200	50
1,000	Stationary	1,800	75
1,375	Stationary	2,000	83
1,625	Stationary	2,600	108

Table VI. Average penetration rates for hole diameters from 44 to 90 inches.

Hole Diameter	Average Penetration Rate Gross fph - Net fph				
	Soft	Mod. Soft	Mod. Hard	Hard	Very Hard
44"	12 - 7	9 - 5-1/2	7 - 4	4 - 2-1/2	3 - 2
48"	10 - 6	7 - 4	6 - 3-1/2	3 - 2	2 - 1
54"	9 - 5-1/2	6 - 3-1/2	5 - 3	3 - 2	2 - 1
66"	8 - 5	5 - 3	4 - 2-1/2	3 - 2	2 - 1
72"	7 - 4	4-1/2 - 3	3 - 2	2 - 1	1-1/2 - 3/4
90"	6 - 3-1/2	4- 2-1/2	3 - 2	2 - 1	1-1/2 - 3/4

Table VII. Approximate drilling bit cutter costs.

Material Hardness	Cutter Cost per ft^3 of Material Removed
Soft	$ 0.30
Mod Soft	0.70
Mod Hard	1.30
Hard	3.00
Very Hard	4.50

accessible to the writer for the ranges of hard to very hard.

Drilling fluid costs are based on the cost of the materials which comprise the fluid and are reported in terms of cost per barrel of the final fluid. This cost can vary widely (roughly from $0.50 to $6.00 per barrel) dependent on the conditions encountered in the individual boring.(13) For preliminary estimating purposes fluid costs are assumed at $2.00 per barrel for a drilling project composed of 1-4 holes and $1.00 per barrel for a drilling project of more than four holes.

If air circulation is used, rather than a drilling fluid, the cost is based on the required quantity of equipment, such as air compressors, and the costs of additive materials.

A significant cost factor, not yet discussed is the cost of mobilizing the drill rig complex to the boring location. The hauling of a drill rig is usually done by a heavy drayage company, and the cost is controlled by inter- and intra-state tariffs. Table VIII shows approximate costs per mile for the various sizes of drill rigs, which could be used for estimating purposes. An additional mobilization cost would be a time cost for the drill rig while in transit which would be based on about 70% of the rig's operating day rate.

Casing

The domestic cost for casings which are designed to resist external hydrostatic heads in an evacuated emplacement hole can be expected to range from $0.17 to $0.25 per pound of casing, dependent on the casing design utilized. Examples of these casings are shown in Table IX.

Cementing costs for the heavy casings would include the cost of cementing materials used and

Table VIII. Approximate transportation costs for various capacity drill rigs.

Input Horsepower	Transportation Cost per Road Mile
225 to 500	$ 5
700	10
1,000	15
1,375	17
1,625	22

the cost per unit time for the pumping equipment used. Cement costs vary with the type of cement used, but a rough first estimate could be made on the basis of $1.50 per cubic foot (1 sack at 94 lbs). Oilwell cementing service companies generally provide cementing placing services on a lump sum basis. These services vary from area to area, but a reasonable average would be $400 for a cementing unit and appurtenant equipment for the first 8 hours and $35 to $45 per hour after 8 hours.(17)

The approximate costs of light screen casings, constructed from corrugated metal pipe are shown in Table X.

Table IX. Examples of casing weights. Note that the 36" ID casing is smooth walled and the 66" casing has ship channel rib supports spaced from 2 to 2-1/2' apart, vertically.

Casings ID	Wall Thickness	Weight Lbs per foot
36"	1/2"	202
36"	5/8"	252
36"	3/4"	302
36"	7/8"	353
66"	5/8"	555
66"	3/4"	642
66"	7/8"	758
66"	1"	849

Table X. Approximate costs for a light screen casing made from perforated CMP.

CMP	Wall Gauge	Weight Per Foot	Cost Per Foot
36"	12	59	$10.50
42"	12	68	12.00
48"	12	78	13.50
54"	8	147	27.00
66"	8	166	29.00

In addition to the costs of the casings and cement, if required, there are the rig costs involved in the time to install and cement the casing. Another cost in the running of the heavy, hydrostatic-head-resistant casings is the cost for welding of casing joints. A reasonable casing welding cost can be approximated as the basis of $1.00 per diameter inch[8] per joint. Extremely fast casing running would be about one joint every 1-1/2 hours. For cost estimating purposes, 2 hours per joint of welded casing and 1 hour per joint of welded casing and 1 hour per joint of perforated CMP could be used.

SUMMARY OF DRILLING AND CASING COSTS

The description of costs for churn, auger and core drilling were presented in summary form. No further discussion will be made of these three techniques.

The discussion of rotary drilling and casing costs illustrated the major cost factors. No attempt was made to outline costs for drilling problems such as difficult access to the drill site, special site preparation requirements, purchase of special tools, excessive hole deviation, lost circulation, etc., and administrative costs such as bond and overhead.

Using the major cost factors shown, two examples of cost and time requirements are presented for rotary drilling and casing.

One hole is 750 feet deep with a finished diameter of 36 inches, the other is 1500 feet deep with a finished diameter of 66 inches. Both holes will be drilled in a moderately hard sandstone with moderately frequent clay shale interbeds. The water table is near ground surface and fluid circulation will be used. The drill rigs for the two holes will be mobilized 1000 miles.

Example No. 1—36" hole, 750' deep. The actual boring will be 48" in diameter and will be drilled by a drill rig with 700 input horsepower. The drill rig cost will be $1200 per day operating and $800 per day non-operating. Procedures and costs are as follows:

1. Rig Mobilization		
a. Hauling - 1000 @ $10		$10,000
b. Rig cost - 250 miles/day, 4 days @ $800		3,200
	TOTAL	$13,200
2. Site Preparation		
32 dozer hours @ $15		420
3. Rig-up		
a. Rig time 3-1/2 days @ $1200		4,200
b. Hauler support		1,200
	TOTAL	$ 5,400
4. Surface Hole - 50' deep		
a. Drilling 54" hole		
(1) Rig time - 15 hours @ $50		$ 750
(2) Cuttercosts - 50' @ $21		1,050
(3) Fluid cost - Water plus Drilled material		---
b. Surface Pipe		
(1) Pipe - 6696 lbs @ 20¢		$ 1,339

(2) Cement - 115 ft^3 @ $1.50		172
(3) Rig time - 2 days @ $1200		2,400
	TOTAL	$ 5,711

5. Drill 48" hole 50' - 75'

a. Rig time - 200 hours @ $50		$10,000
b. Cutter costs - 7000' @ $16		11,200
c. Fluid costs - 2500 Bbls @ $2.00		5,000
	TOTAL	$26,200

6A. Condition hole and run heavy casing. (Hole will be evacuated of fluid on completion)

a. Casing cost - 750' of 3/4" wall 226,500 lbs @ $0.20		$45,000
b. Casing welding cost - $36/joint for 19 joints (each joint 40' long)		684
c. Cement cost - 3700 ft^3 @ $1.50		5,050
d. Cement pumping		400
e. Rig time - run casing, cement, wait on cement, pump hole dry - 8 days @ $1200		9,600
	TOTAL	$60,834

6B. Run light perforated casing. (Hole will remain filled with fluid on completion)

a. Casing cost 750' @ $10.50		$ 7,875
b. Rig time 2 days @ $1200		2,400
	TOTAL	$10,275

7. Tear-down

a. Rig time, 3 days @ $1200		$ 3,600
b. Hauler support		1,000
	TOTAL	$ 4,600

8. Rig demobilization

Same as mobilization	$13,200

9. Totals

a. Cost to drill and case with heavy cemented casing.	
1. Total	$129,565
2. Per foot	172
b. Cost to drill and case with light perforated casing.	
1. Total	$ 79,006
2. Per foot	105

Example No. 2—66" Hole, 1500' deep. The actual boring will be 84" in diameter and will be drilled by a rig with 1375 input horsepower. The drill rig cost will be $2000 per day operating and $1500 per day non-operating. Procedures and costs are as follows:

1. Rig Mobilization

a. Hauling 1000 miles @ 17		$17,000
b. Rig cost - At 250 miles/day, 4 days @ $1500		6,000
	TOTAL	$23,000

2. Site Preparation

a. 64 dozer hours @ $15		$ 900
b. Concrete pad		1,500
	TOTAL	$ 2,400

3. Rig-up

a. Rig time, 5 days @ $2000		$10,000
b. Hauler support		4,000
	TOTAL	$14,000

4.	Surface Hole - 50' deep		
	a. Drilling 92" Hole		
	(1) Rig time, 25 hours @ $83		$ 2,075
	(2) Cutter Costs, 50' @ $50.02		3,000
	(3) Fluid Cost - Water plus drilled material		---
	b. Surface Pipe		
	(1) Pipe - 1726 lbs @ 20¢		3,454
	(2) Cement - 290 ft^3 @ $1.50		435
	(3) Rig time, 3 days @ $2000		6,000
		TOTAL	$14,964
5.	Drill 84" hole 50' - 1500'		
	a. Rig time - 825 hours @ $83		$68,478
	b. Cutter costs - 1450' @ $50.02		72,529
	c. Fluid costs - 13000 Bbls @ $2.00		26,000
		TOTAL	$187,007
6A.	Condition hole and run heavy casing. (Hole will be evacuated of fluid on completion)		
	a. Casing cost		
	0 to 500' - 500' @ 460 lbs = 230,000 lbs		
	500 to 1000' - 500' @ 642 lbs = 231,000 lbs		
	1000 to 1500' - 500' @ 849 lbs = 424,500 lbs		
	Total weight, 975,500 lbs @ $0.20		$195,100
	b. Casing Welding, $66/joint for 38 joints (each joint 40' long)		2,508
	c. Cement cost, 22,000 ft^3 @ $1.50		33,000
	d. Cement pumping		1,200
	e. Rig time - run casing, cement, wait on cement, pump hole dry -- 11 days @ $2000		22,000
		TOTAL	$253,808
6B.	Run light perforated casing. (Hole will remain filled with fluid on completion)		
	a. Casing cost - 1500' @ $29		$43,500
	b. Rig time - 3 days @ $2000		4,000
		TOTAL	$47,500
7.	Tear - down		
	a. Rig time, 4 days @ $2000		$ 8,000
	b. Hauler support		4,000
		TOTAL	$12,000
8.	Rig demobilization		
	Same as mobilization		$23,000
9.	Totals		
	a. Cost to drill and case with heavy cemented casing		
	1. Total		$522,297
	2. Per foot		350
	b. Cost to drill and case with light perforated casing		
	1. Total		$323,871
	2. Per foot		216

These two cost and time examples have outlined the major anticipated cost factors in drilling large diameter holes. Any unusual or unanticipated circumstances can appreciably increase any or all of the cost factors. The same 66" finished diameter hole in very hard materials would cost \$530 per foot with heavy casing and \$390 per foot with the light perforated casing.

SUMMARY

In review, churn drilling is a low cost method of making a moderate sized hole, but its application to nuclear device emplacement is severely limited. Auger and core drilling are low and moderate cost methods of making moderate sized borings and have a restricted but definite application in device emplacement. This application is limited in terms of depth and subsurface conditions.

Rotary drilling has shown itself to be the most adaptable method for device emplacement. It is moderately expensive but has very little limitation in terms of depth or subsurface material conditions. Rotary drilling appears to have the greatest potential for improvement in technique and equipment. Several drilling and supply organizations have done some design work on the concept of a drill rig specifically designed for large-diameter drilling. Dual concentric drill strings, designed to provide the advantages of both direct and reverse circulation have been designed. One such drill string (fabricated from off-the-shelf equipment) has been put to work at the Nevada Test Site.[14] Consideration has been given to large-diameter rotary-percussion drilling where a cluster of high speed pneumatic drills would provide equal or greater vertical force than the tremendously high optimum static weights presently required.[15] The rotary-percussion technique has worked very effectively in conventional sized oilwell drilling. Currently, the technique requires direct air circulation. Some consideration has been given to developing the rotary force in the boring at the bit by the use of hydraulic motors. This idea approaches the down-hole drill conception.

This paper has discussed rotary drilling to depths of 2500 feet and in finished diameters up to 66 inches. The rotary drilling principles do not change as these dimensions are exceeded. Large-diameter borings are currently being drilled to depths of 4000 feet at the Nevada Test Site using techniques and equipment discussed above. The possibility of a large-diameter hole, say with a drilled diameter of 72 inches and a cased diameter of 36 inches to a depth of 10,000 feet is considered entirely feasible.[16] The largest technical problem in this range would be in circulating the drilling fluid. The annulus between the boring wall and 13-3/8 inch drill pipe would be about 27 ft^2. Maintenance of even a 20-fpm rising velocity in the annulus would be about 4000 gpm at possibly 500 psi. These volumes and pressures could be provided by five or six large positive displacement oilwell pumps in parallel. Another solution might be to use a dual concentric drill string which would provide a small cross section area for the drilling fluid in both directions.

REFERENCES

1. Warren L. Bayse, Layne Texas Company, Dallas, Texas (verbal communication), October 1963.
2. "Giant Augers Sink 15-ft-Dia Missile Shafts," Construction Methods, May, 1963.
3. Jack R. McKinney and Dr. G. R. Gray, "The Use of Drilling Mud in Large-Diameter Construction Borings," (not published).
4. "Drilling Logs," Investigations Section, U. S. Army Engineer District, Fort Worth.
5. James H. Allen, "A Report on the Possible Utilization of Specially Designed Rotary Drilling Equipment for Missile Silo Construction," U. S. Army Research and Development Laboratories, Fort Belvoir, Va., August 1959.
6. Management Improvement Program, U. S. Army Engineer District, Portland, Oregon; Project No. NPP 63-18, November 23, 1962.
7. J. W. Bawcom, North American Drilling Company, Mt. Pleasant, Mich. (verbal communication), July 1963.
8. James H. Allen, Smith Tool Company, Dallas, Texas (verbal communication), August 1963.
9. Hughes Tool Company, Rotary Drilling Bits, 1960.
10. Morlan, E. A., "Boring Large Hole Mine Openings," Paper 61 AU27 (pre-print), Society of Mining Engineers of AIME, March 1961.
11. C. E. Williams, Jr., and G. H. Bruce, "Carrying Capacities of Drilling Muds," Petroleum Transactions, AIME, T. P. 3026, 1951.
12. R. L. Brockenbrough, U. S. Steel Applied Research Laboratories, Monroeville, Pa. (verbal communication), October 1963.
13. Bariod Davision, National Lead Co., Houston, Texas (verbal discussions).
14. Walter H. Johnson, Lawrence Radiation Laboratory, NTS, Mercury, Nevada, April 1964.
15. Robert E. Bates, Jr., Mission Manufacturing Co., Houston, Texas (verbal communication), July 1963.
16. William W. Liddell, Jr., Kerr-McGee Oil Industries, Inc., Oklahoma City, Oklahoma (letter), December 1963.
17. William White, Halliburton Co., Rio Vista, California (verbal communication), April 1964.

BIOGRAPHICAL SKETCH OF AUTHOR

Paul R. Fisher received his B.A. in Geological Sciences from the University of California, Berkeley, in 1954. He served in the U.S. Army from 1954 to 1956. He is Chief, Earth Sciences Section, U.S.A. Engineer Nuclear Cratering Group, of the U.S. Army Corps of Engineers, stationed at Lawrence Radiation Laboratory, Livermore, Calif.

He has been with the Corps of Engineers since 1956, participating in the following projects: Sacramento District, California, 1956-1962, Resident Geologist, Success Dam Project, 1958-1961; Resident Geologist, New Hogan Dam Project, 1961-1962; Fort Worth District, Texas, 1962-1964, Project Geologist, several dam and reservoir projects in design and construction phases, 1962; coordinated geologic effort on the investigation of failure and reanalysis of design for Waco Dam, 1962-1963; conducted the initial phase (drilling) of a study on "Construction Techniques for Underground Emplacement of Nuclear Explosives," which were delegated to the Fort Worth District by the Nuclear Cratering Group, 1963-1964.

APPLICATIONS OF NUCLEAR EXPLOSIVES TO INCREASE EFFECTIVE WELL DIAMETERS

Henry F. Coffer
Bruce G. Bray
Carroll F. Knutson

Continental Oil Company
Ponca City, Oklahoma

ABSTRACT

Large, currently uneconomical, hydrocarbon reservoirs are known to exist in this country. The stimulation of such reservoirs by contained nuclear explosions is discussed in this paper.

The effect of such an explosion is to increase the apparent well-bore diameter by creating a cavity, a chimney, and an associated annular fractured zone. This geometry results in a complex flow regime yielding increased productivity of the fluids present in the reservoir. A discussion of this flow regime and the economics of utilizing nuclear stimulation for a low productivity gas-bearing reservoir are considered.

Under certain conditions, it is shown that such nuclear stimulation results in favorable economics for reservoir development. However, it is believed that current uncertainties in technology and the "economic risk factor" require testing of a nuclear device in a hydrocarbon-bearing, or at least more typical, reservoir formation.

INTRODUCTION

Late in 1957, the Atomic Energy Commission announced that Rainier, a small 1.7-kiloton nuclear device, had been exploded and completely contained in an underground formation at the Nevada test site. At that time Continental Oil Company began a research program concerned with the feasibility of conducting an underground nuclear explosion in a nonproductive, hydrocarbon-bearing formation. The aim of the program was the technical and economic "stimulation" of such a formation to release the hydrocarbon resources present for commercial production.

Since its beginning, the petroleum industry has experimented with, and used on a practical scale, various methods for applying energy in the form of pressure and heat to petroleum reservoirs for stimulation. Application of hydraulic pressure for fracturing hydrocarbon-bearing formations was being used commercially a decade before Rainier. The "shooting" of oil wells with small chemical high-explosive charges to increase well productivity has been practiced almost since the inception of oil well drilling. Thus, it was apparent from the first announcement of the Rainier event that a compact source of tremendous energy would be available to the industry in their continuing efforts to recover more efficiently the nation's petroleum resources.

Since the Rainier event, there have been a number of other completely contained nuclear explosions of varying size in different rock formations. These have provided more data on the environments created by the energy release. For one of the more recent, the Project Plowshare Gnome Event in the Salado Salt Formation near Carlsbad, New Mexico, a large number of reservoir rock and crude oil samples were placed near the nuclear device by the Bureau of Mines and various oil companies. Recovery and analysis of these samples led to the conclusion that the shock energy from the nuclear device could be used to upgrade or change the properties of reservoir rock. Examination of the salt surrounding the shot point showed the cavity with chimney and fractured zone, typical of contained nuclear explosions.

When a nuclear explosion occurs in a hydrocarbon reservoir, there should result a cavity with chimney, surrounded by a fractured area of increased permeability. In contact with this

fractured zone would be the undisturbed original reservoir rock. Formation of this broken and fractured zone around the wellbore changes the flow pattern of the original hydrocarbon towards the wellbore. Now there is established a flow regime in which oil or gas from the original tight reservoir rock flows through a mass of highly permeable rock and into the new wellbore. This broken rock serves as a supply reservoir from which the hydrocarbon is recovered, the rate of flow being controlled by the low-permeability rock of the original reservoir at the boundary of the broken zone. In this paper, we will discuss how this broken zone should increase the productivity or flow capacity from the reservoir.

APPLICATION OF NUCLEAR EXPLOSIONS IN PETROLEUM RESERVOIRS

Effects on Reservoir Rock

Studies of a number of contained underground nuclear explosions have yielded a rather consistent picture of the geometric features produced.[1,2] The major features of cavity, chimney, and fractured zone are illustrated by a schematic drawing of the Gnome postshot environment, Figure 1. The scaling formulas for calculating the size of the various features as a function of yield, depth of burial, and media are:[1,3]

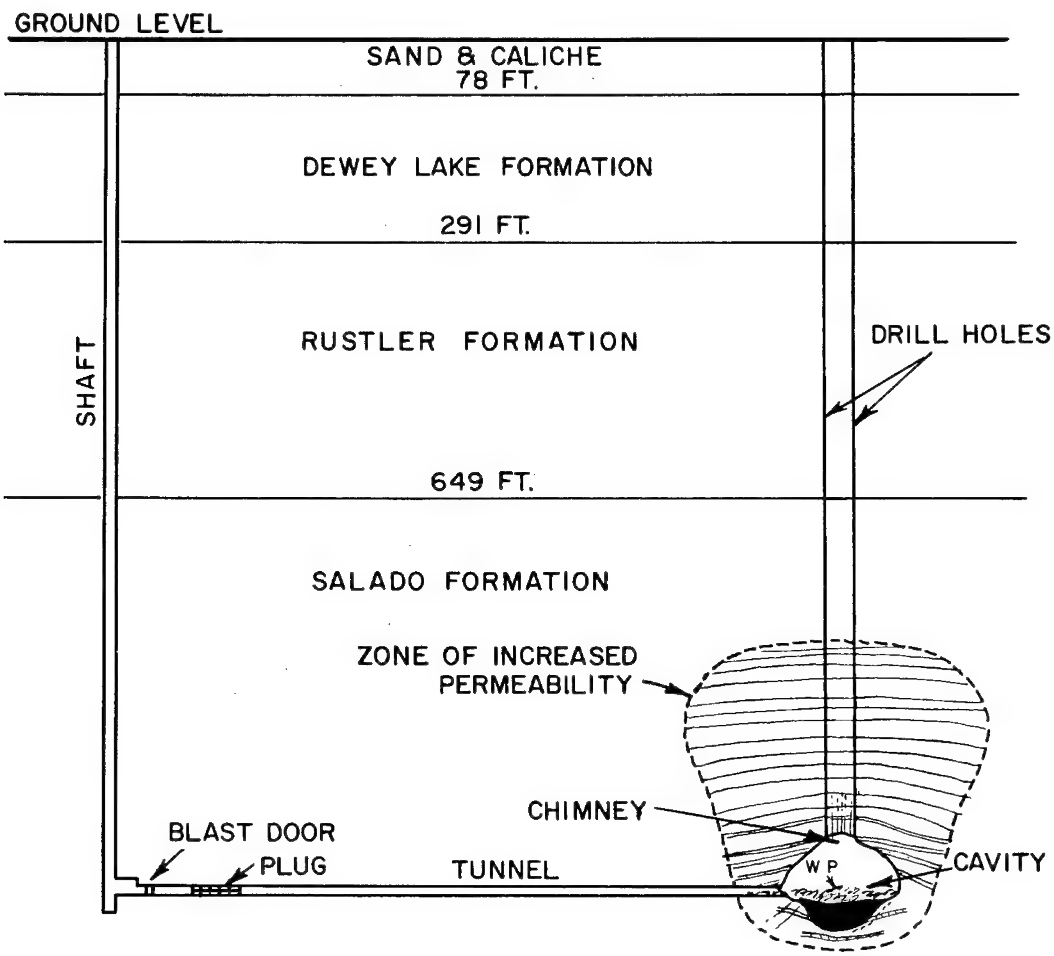

Fig. 1. Cross section through the Gnome event.

Cavity radius:

$$R = \frac{C\,W^{1/3}}{(\rho h)^{1/4}} \qquad (1)$$

where R = cavity radius in feet
C = a constant depending upon rock and fluid content (ranges from 261 to 343)
W = yield in kilotons
ρ = overburden density in grams per cc
h = depth of burial in feet.

Chimney height:

$$H = \frac{4}{3} LR \qquad (2)$$

where H = chimney height in feet
L = inverse of porosity increase in rubble
R = cavity radius in feet.

Radius of permeable zone:

$$R_p = C_R R \qquad (3)$$

where R_p = radius of permeable zone in feet
C_R = a constant (ranges from 2.41 to 3.47)
R = cavity radius in feet.

Height of permeable zone:

$$Hp = C_H R_p \qquad (4)$$

where H_p = height of permeable zone in feet
C_H = a constant (approximately 2.34)
R_p = radius of permeable zone in feet.

Scaled depth of burial:

$$SDB = \frac{h}{W^{1/3}} \qquad (5)$$

where SDB = scaled depth of burial
h = depth of burial in feet
W = yield in kilotons.

The small-scale effects upon the reservoir rock have also been investigated.[3] Knowledge of this behavior is useful in predicting the chimney height (used to obtain L in Eq. (2)), as well as in providing an insight into the fluid transmission characteristics (permeability) of the rubble and fractured zone matrix.

The effect of a shock wave from the Gnome nuclear explosion on the reservoir rock samples could be correlated with rock type. Limestones and dolomites were extensively fractured and showed large increases in permeability and porosity. Sandstones were reduced in permeability, while their porosity was unchanged. These results indicate that limestone reservoirs are probably the most suitable candidates for stimulation through atomic explosions. Other good possibilities are reservoirs which are composed of rock which deform by brittle fracturing.

The porosity and permeability behavior of the reservoir rock samples included in the Gnome event are illustrated in Figures 2 and 3.

Deliverability Calculations - Fluid Flow in Porous Media

An aspect of the environment created by the explosion which is important to the petroleum industry, is the increased productivity of wells tapping the postshot cavity-chimney-fractured zone. A brief review of fluid flow in porous media will be presented as background for the discussion.

The petroleum reservoir is an interconnected pore system within the rock. The hydrocarbon flows from this pore system into the wellbore by virtue of an energy gradient. The simplest steady state form of gradient equation for fluid flow is:

$$Q = \frac{kA}{\mu} \frac{\partial P}{\partial X} \qquad (6)$$

where Q = flow rate
k = rock permeability
A = cross-sectional area
μ = fluid viscosity
P = fluid pressure
X = distance.

This assumes the steady state laminar flow of an incompressible fluid through a homogeneous isotropic media. The wellbore can be visualized as draining a radial flow system, see Figure 4. Integrating Eq. (6) using the boundary conditions of horizontal radial flow of an incompressible fluid yields:[4]

$$Q = \frac{ckh' (P_e - P_w)}{\mu \ln(r_e/r_w)} \qquad (7)$$

where Q = flow rate
c = constant depending upon units used
k = permeability of reservoir rock
h' = thickness of reservoir
P_e = pressure at drainage radius
P_w = pressure at wellbore
μ = fluid viscosity
r_e = radius of drainage area
r_w = wellbore radius.

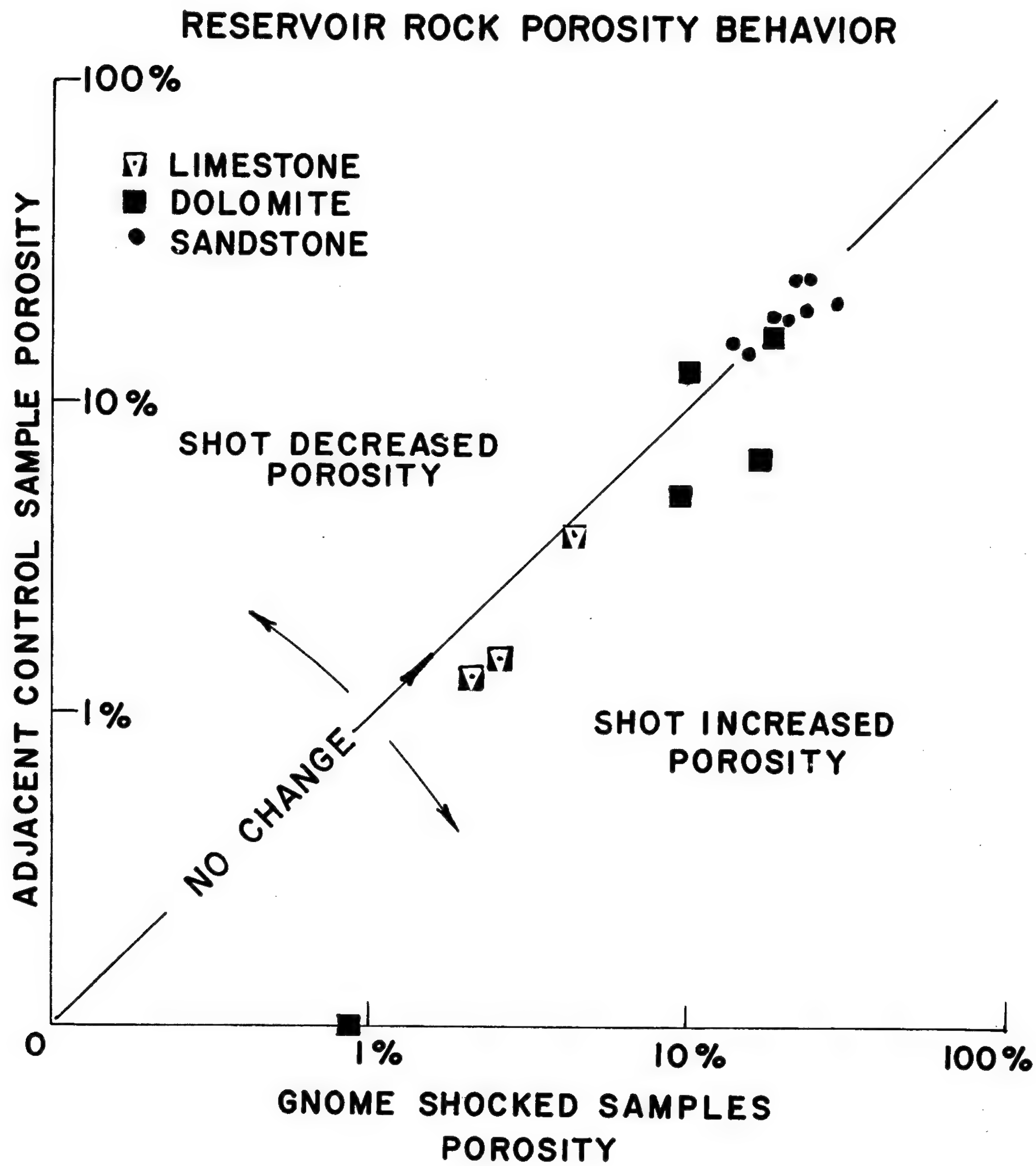

Fig. 2. Postshot reservoir rock porosity behavior.

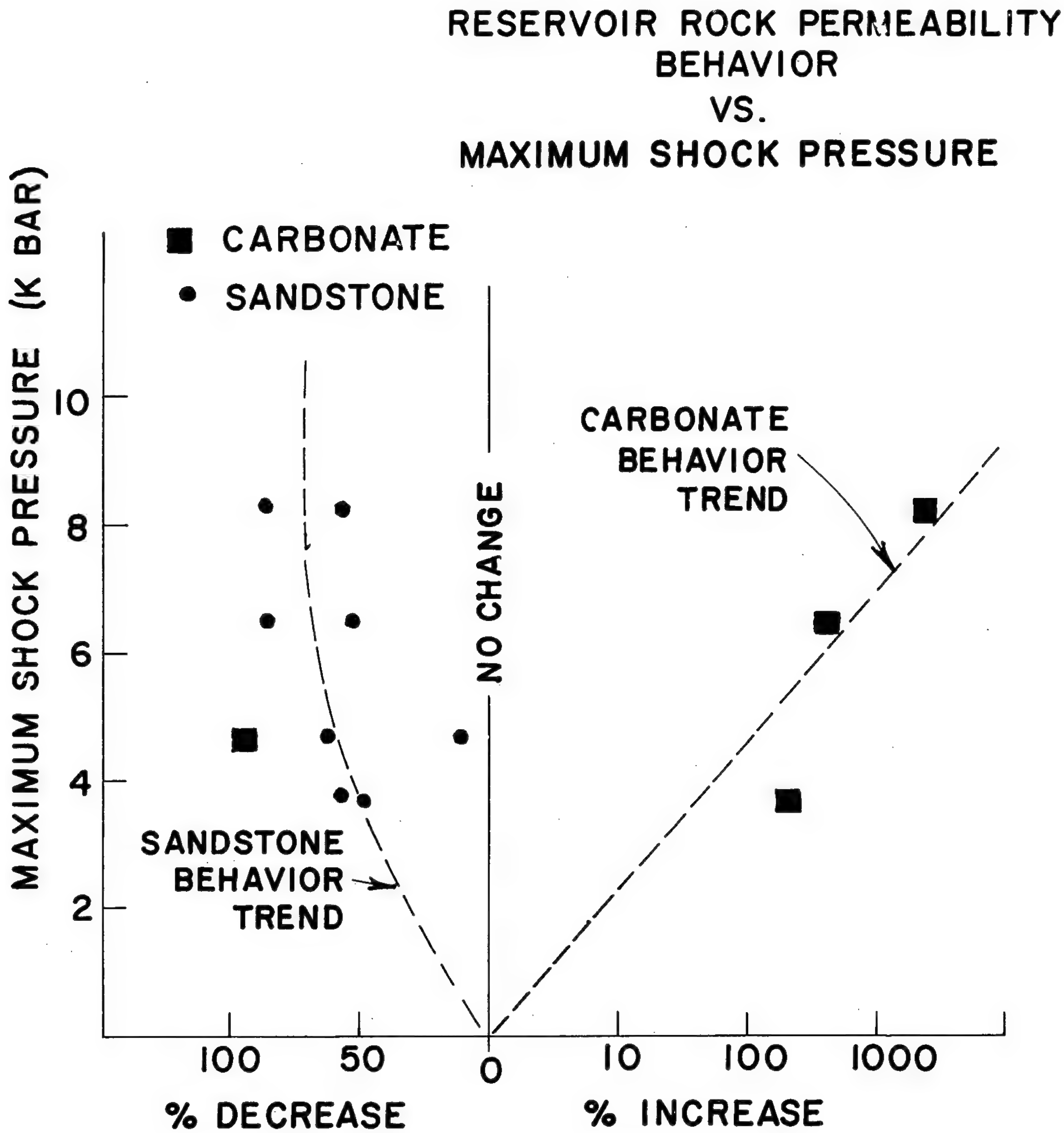

Fig. 3. Postshot reservoir rock permeability behavior.

It is apparent that the rate is inversely proportional to the log of the radius ratio, hence rate is not very sensitive to moderate changes in this radius ratio.

Integrating the radial flow equation for compressible fluid flow (gas) yields:[5]

$$Q_s = \frac{c'kh\left(P_e^{\,2} - P_w^{\,2}\right)}{\mu P_s \ln(r_e/r_w)} \tag{8}$$

where the subscript s indicates the base pressure at which the gas volume is calculated.

When more than one fluid phase is flowing, Eq. (6) is still applicable if the relative permeability concept is applied. Simply stated, the rate of one flowing phase can be predicted if the permeability term is scaled down. Figure 5 shows a typical relative-permeability-versus-saturation plot. The plot shows that the oil rate can be predicted for this reservoir rock at an average oil

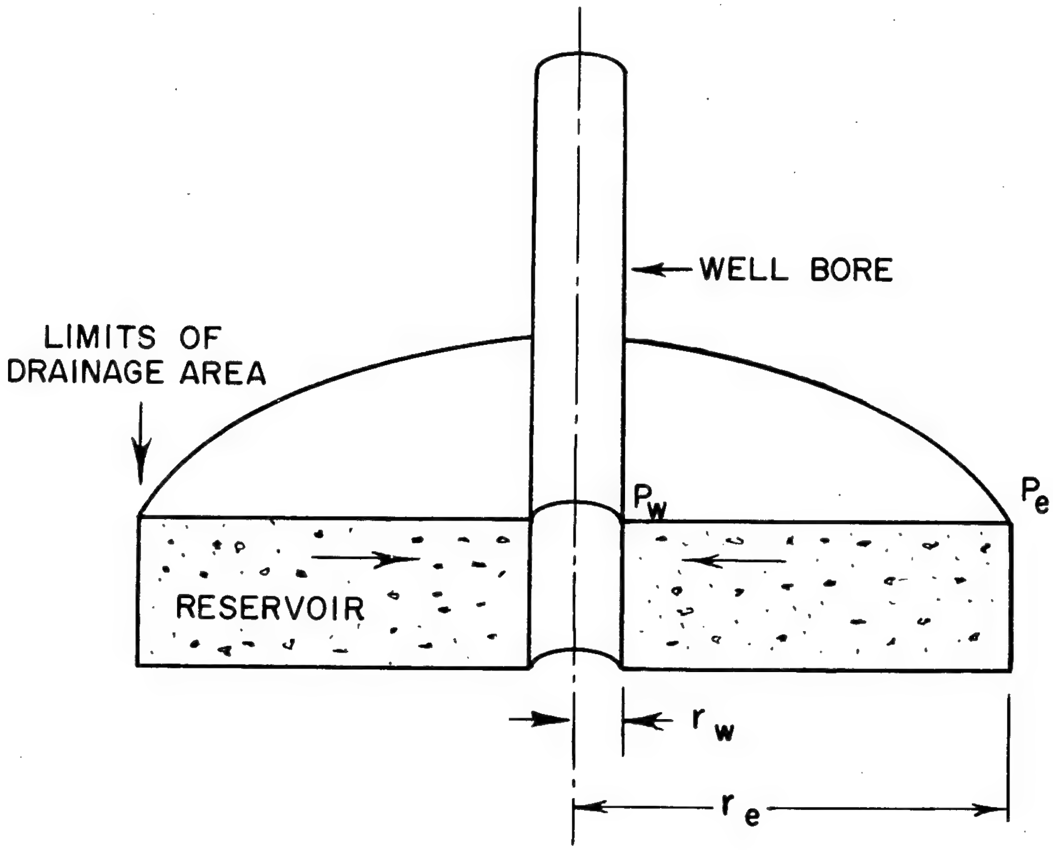

Fig. 4. Simplified radial flow model.

saturation of 50% if the permeability is scaled down to 15% of its original value.

The geometry of the postshot nuclear environment can be used in the simple steady state radial flow equation by assigning concentric annular configurations to the chimney cavity and the fractured zone. The equivalent permeability of the complex radial system is:[5]

$$\bar{k} = \frac{\log r_e/r_w}{\sum_{i=1}^{i=n} \frac{\log r_i/r_{(i-1)}}{k_i}} \qquad (9)$$

where $\bar{k}$ = equivalent permeability of complex flow system

r_e = radius of well drainage area

r_w = radius of wellbore

r_i = radius of the ith annular zone

k_i = permeability of the ith annular zone.

Probably one of the simplest ways to illustrate the effect of the postshot environment on the productivity, or producing rate, is to assume it acts like an enlarged wellbore. Figure 6 is a plot of rate versus "wellbore radius" for a gas well drilled on a 640-acre spacing. It is apparent from this figure that after a radius of several hundred feet is obtained, only relatively small increases in rate are obtained with further relatively large radius increases.

These elementary concepts should give the reader some appreciation of the flow of fluids through porous media. The actual equation used in the analysis of the deliverability of low productivity wells with and without nuclear stimulation is somewhat more sophisticated. Unsteady state gas flow in a single-well, symmetric, radial system of varying radial permeability can be described by the equation:[6,7]

$$2\phi\mu \frac{\partial P}{\partial t} = \frac{1}{r} \frac{\partial}{\partial r} k_r r \frac{\partial P^2}{\partial r} \qquad (10)$$

where ϕ = the effective porosity

μ = the viscosity

P = pressure

t = time

r = radius

k_r = permeability as a function of radius.

In essence, the equation represents the basic principles of conservation of mass (continuity equation) and of momentum (Darcy's law in the radial case) applied to flow in porous media. It assumes an ideal gas at constant temperature with viscosity independent of pressure and neglects gravitational effects. Because of the nonlinear properties of the equation, analytic solutions are only available for certain special cases. However, numerical solutions may be effected by the use of high-speed computers employing finite difference techniques.[6-9] As such then, solution of the equation with appropriate boundary conditions gives a detailed accounting of flow for any drainage geometry from the vicinity of the wellbore to the drainage radius of the well. The radial extent of a fracture system created by an explosion in a gas-bearing formation and the radial permeability distribution of the system can be studied. In addition, the flow capacity including the effect of "wellbore storage unloading" of the postshot fracture system can be compared with preshot formation deliverability.

Effects upon Hydrocarbons

The problem of radioactive contamination of hydrocarbons has at least two facets. One is the possibility of induced radioactivity in the hydrocarbon, another is the possibility of producing radioactive products of the nuclear reaction with the hydrocarbon. One of the petroleum industry

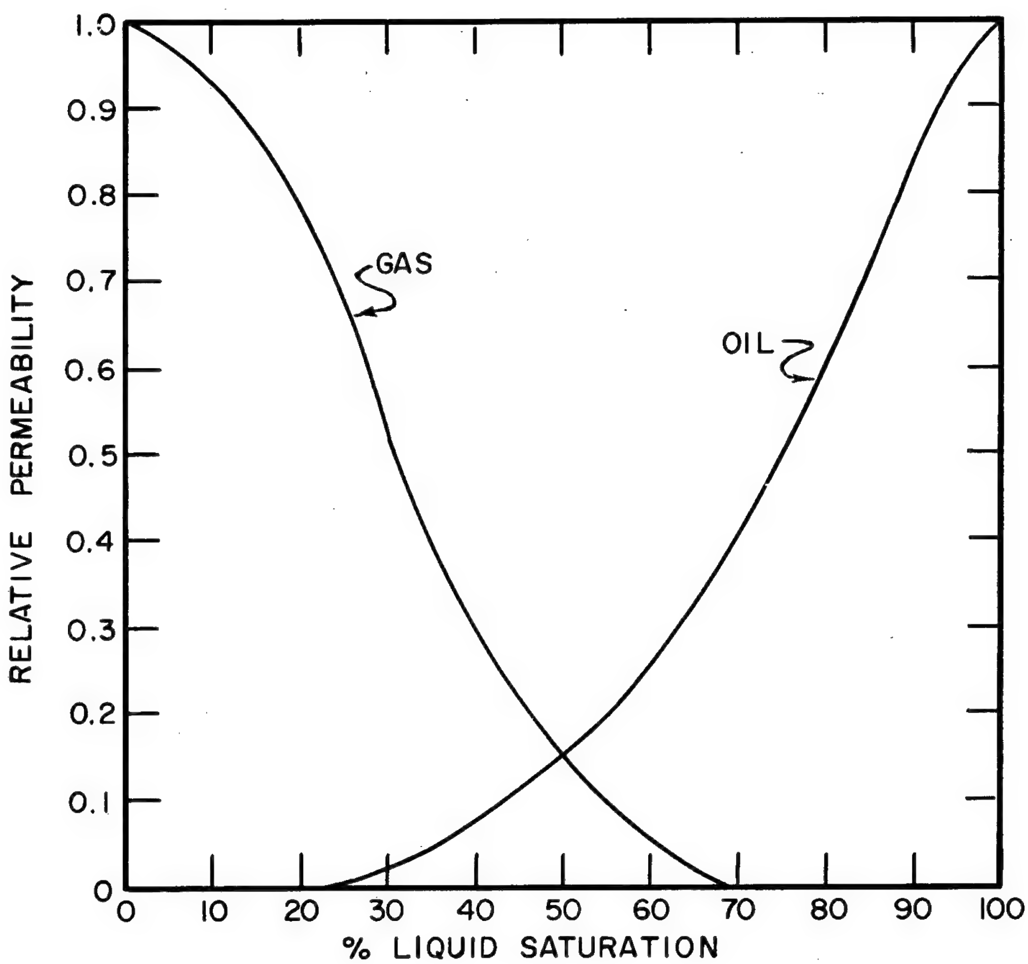

Fig. 5. Relative permeability curves.

objectives in the Gnome sample program was to investigate the effects of heavy gamma and neutron bombardment upon the properties of natural hydrocarbon mixtures and "refined" hydrocarbon products. The results of analyses of some of the Gnome hydrocarbon samples can be summarized as follows:[3] The radiation of as much as 7 x 10^5R and shock levels as high as 10 kilobars had only minor effects on the hydrocarbon samples. In no case was more than 10% of the sample affected. The effects were mixed polymerization and cracking. No residual induced radioactivity was detected.

The second facet of the problem is more complex. The amounts of gaseous and oil-soluble radioactive products of the nuclear event are predictable from the physical consideration of a fusion, fission, or combination event.[1, 10-14] $Krypton^{85}$ and tritium will probably be the problem nuclides in the gas and oil.

Other particulate material could be dissolved or physically entrained in the produced fluid. Water produced with the hydrocarbons could leach additional radioactive material from the meld. These problems can be dealt with through the choice of producing techniques and the selection of reservoir to be stimulated with nuclear explosions. Additional work is indicated on the occurrence and concentrations of the problem nuclides in the hydrocarbons in the reservoirs and upon the upper limits of radioactive material in saleable gas and oil.

EXAMPLE RESERVOIR STIMULATION

Probably the easiest way to visualize an explosion-stimulated, dynamic fluid-flow model in porous media is by examining an actual reservoir example. A gas-bearing formation has been selected because it is believed that possible radiation contamination of the produced fluid will be minimal in the gas phase. In addition, a single fluid phase allows more accurate evaluation of the stimulation mechanism upon deliverability. As pointed out earlier, however, mathematical

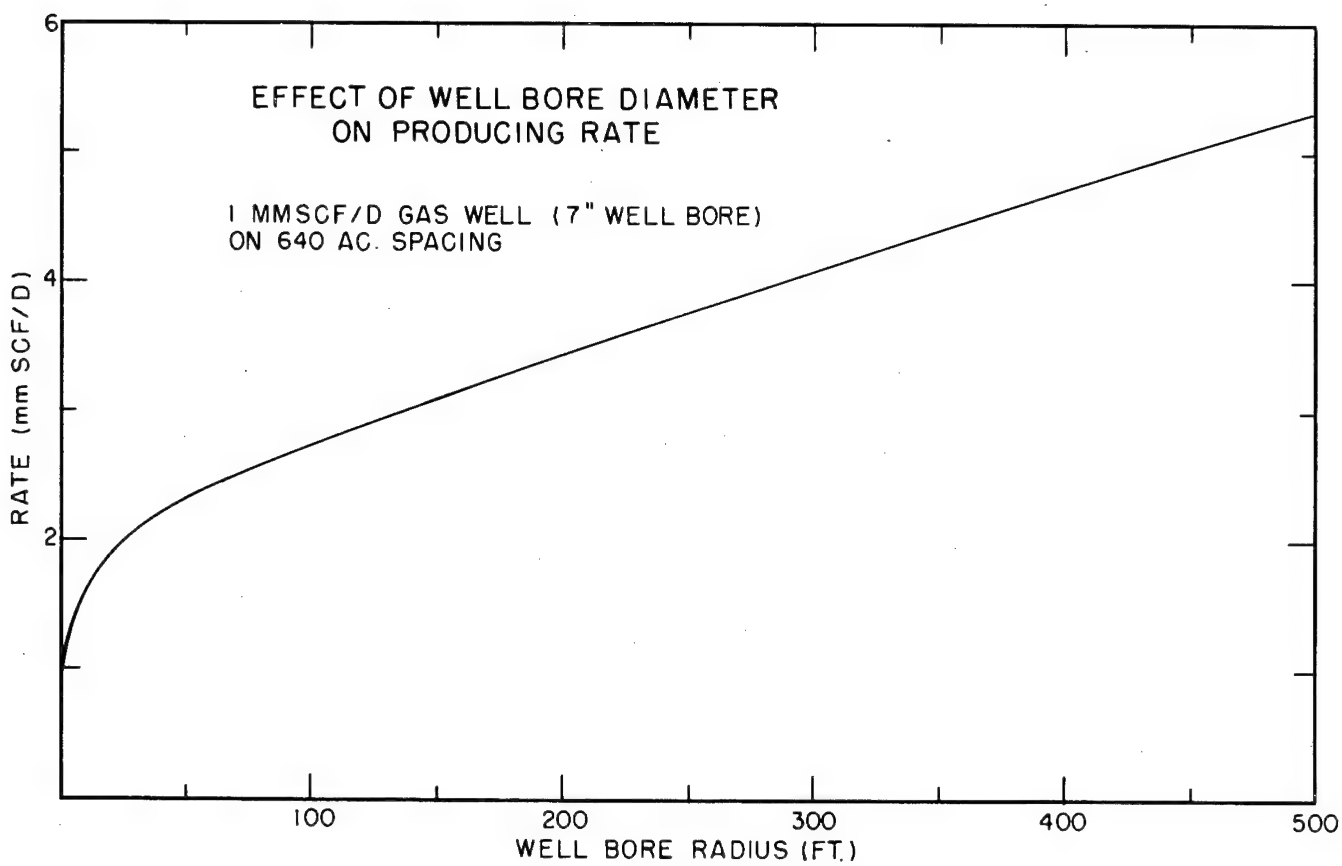

Fig. 6. Effect of wellbore diameter on producing rate.

models for two-phase flow are available and similar calculations can be made for the case of oil reservoir stimulation.

The actual reservoir properties used for this example calculation are from an existing low deliverability gas-bearing formation. It is interesting to note that a number of such formations are available and are believed susceptible to blast stimulation.

Formation Characteristics

As with a number of such low productivity formations, examination indicates a highly laminated sandstone, siltstone, shale sequence as shown in Figure 7. The individual sandstone lenses and lamellae are usually less than an inch thick and frequently terminate in the space of a 3-1/2-inch core. The sands are fine to medium grained, poorly sorted with a clayey matrix. The salinity of the formation water is approximately 85,000 ppm and the formation is fresh-water sensitive due to the clay content. A summary of the sandstone lense properties from core analyses of the formation are given in Table I.

In addition to the properties given in the table, a number of practical geologic, geographic, and political assumptions must be made concerning

Table I. Reservoir properties for nuclear stimulation calculations.

Reservoir characteristics:	
Top hydrocarbon-bearing formation	2300 feet
Gross thickness	400 feet
Net effective pay thickness (37.5%)	150 feet
Pressure	450 psia
Temperature	95° F
Gas specific gravity (air = 1.00)	0.647
Gas deviation (compressibility) factor	0.94
Pressure base	15.025 psia
Formation properties:	
Porosity	12.7%
Permeability	5.7 md
Median permeability	1.3 md
Residual oil saturation	5%
Residual water saturation	37%
Irreducible water saturation (based on median permeability)	37%
Grain density	2.68 g/cc
Bulk density	2.38 g/cc
Calculated reserves:	
Hydrocarbon pore volume	$33.4 \times 10^7 \dfrac{\text{cubic feet}}{\text{640 acres}}$
Initial gas in place	$9.96 \times 10^9 \dfrac{\text{std cuft gas}}{\text{640 acres}}$
	or 9.96 billion standard cubic feet per section

Fig. 7. Photograph of porosity-permeability plugs of a low deliverability gas reservoir showing laminations.

the reservoir. Among the more important of these are:

1. That the hydrology of the area is known.
2. That the producing formation is located sufficiently below any water-bearing zone so that not only is the explosion contained, but no contamination of the water-bearing zones occurs.
3. That it is located in a rather isolated area.

Predicted Stimulation Environment

In order to take maximum advantage of the uplift-rebound effect of the explosion on the lenticular formation, the device should be located at or somewhat below the base of the formation. For these calculations, a true depth of burial was assumed to be just at the base of the gas-bearing formation at 2700 feet.

The scaled depth of burial for various device sizes at an assumed true depth of burial, h, of 2700 feet were calculated from Eq. (5). The results of the calculations are given in Figure 8a. Scaled depths of burial for previous contained underground explosions in salt, granite, and tuff are also shown on the figure.[1, 2, 10-12]

The predicted cavity radius created by an underground explosion was calculated from Eq. (1). A constant of 290 was selected for the calculations because of the low total water content and low probability of gas evolution through matrix decomposition. Cavity radius is shown on Figure 8b.

The chimney height can be calculated based on the chimney formation and collapse concept.[1,10] The height of a cylindrical chimney has been calculated from Eq. (2) and is plotted in Figure 8c.

Two permeable zone radii, corresponding to the most probable and maximum values observed at the Gnome event, can be calculated. At Gnome, the permeable zone radius was 150 feet and the cavity radius was 62 feet.[3,15] Therefore, the constant, C_R, for extrapolation of the "probable" radius of permeability increase is 62/150 = 0.413; and the probable permeable zone radius is:

$$R_{p\ prob} = \frac{R}{0.413}\,.$$

The maximum permeable zone radius from the Gnome event data is based on damaged salt observations at 215 feet and water seep data observed in the new drift at 212 feet from the shot point.[1, 3, 15] Therefore, the constant for the maximum radius of increased permeability is 62/215 = 0.288; and the maximum permeable zone radius is:

$$R_{p\ max} = \frac{R}{0.288}\,.$$

Both $R_{p\,prob}$ and $R_{p\,max}$ are plotted in Figure 8b.

Similarly, the height of the permeable zone can be calculated from the Gnome data and Eq. (4). The extrapolations based on the Gnome data result from the surface drill-hole definitions of the zone of increased permeability during postshot drilling into the cavity and also from the core holes from the postshot drift.[3,15] The zone was observed approximately 350 feet above the working point. The extrapolation constant, C_H, for height of the permeable zone is 350/150 = 2.34. Therefore, the scaled heights of the permeable zone increase from the Gnome data are:

$$H_{p\ prob} = 2.34\,R_{p\ prob}\,.$$

This value is plotted in Figure 8c.

Volumes of (1) the spherical cavity, (2) a chimney having a bulk porosity of 25%, (3) the probable permeable zone, and (4) the maximum permeable zone were calculated and are plotted in Figure 9.

Although the deliverability could be calculated for a number of explosion yields, it is sufficient for this example to show the calculations for a single reasonably sized device. Since published information on device cost[16] is invariant for the range of devices which might be applicable for stimulation of the reservoir, the cost factor has no bearing on the decision. And, since scaling was determined primarily from the Gnome event data, the environment from a 40-kiloton explosion was chosen to illustrate the flow and economic calculations. The scaled depth of burial for a 40-kiloton explosion at this depth is 790 feet, or approximately the same as the Gnome and Tamalpais events.

A 40-kiloton underground nuclear explosion 2700 feet below the surface will produce the following calculated environment in the producing formation:

1. A cavity radius of 110 feet.
2. A probable permeable zone radius of 270 feet. (The maximum radius is 385 feet.)
3. A probable permeable zone height of 630 feet. (The maximum height is 900 feet.)
4. A cavity and/or chimney void volume of 5.7 million cubic feet.
5. A probable permeable zone volume of 140-million cubic feet or 3220 acre-feet. (The maximum permeable zone volume could be 420-million cubic feet or 9650 acre-feet.)
6. A total cavity and chimney volume of 23-million cubic feet or 528 acre-feet.

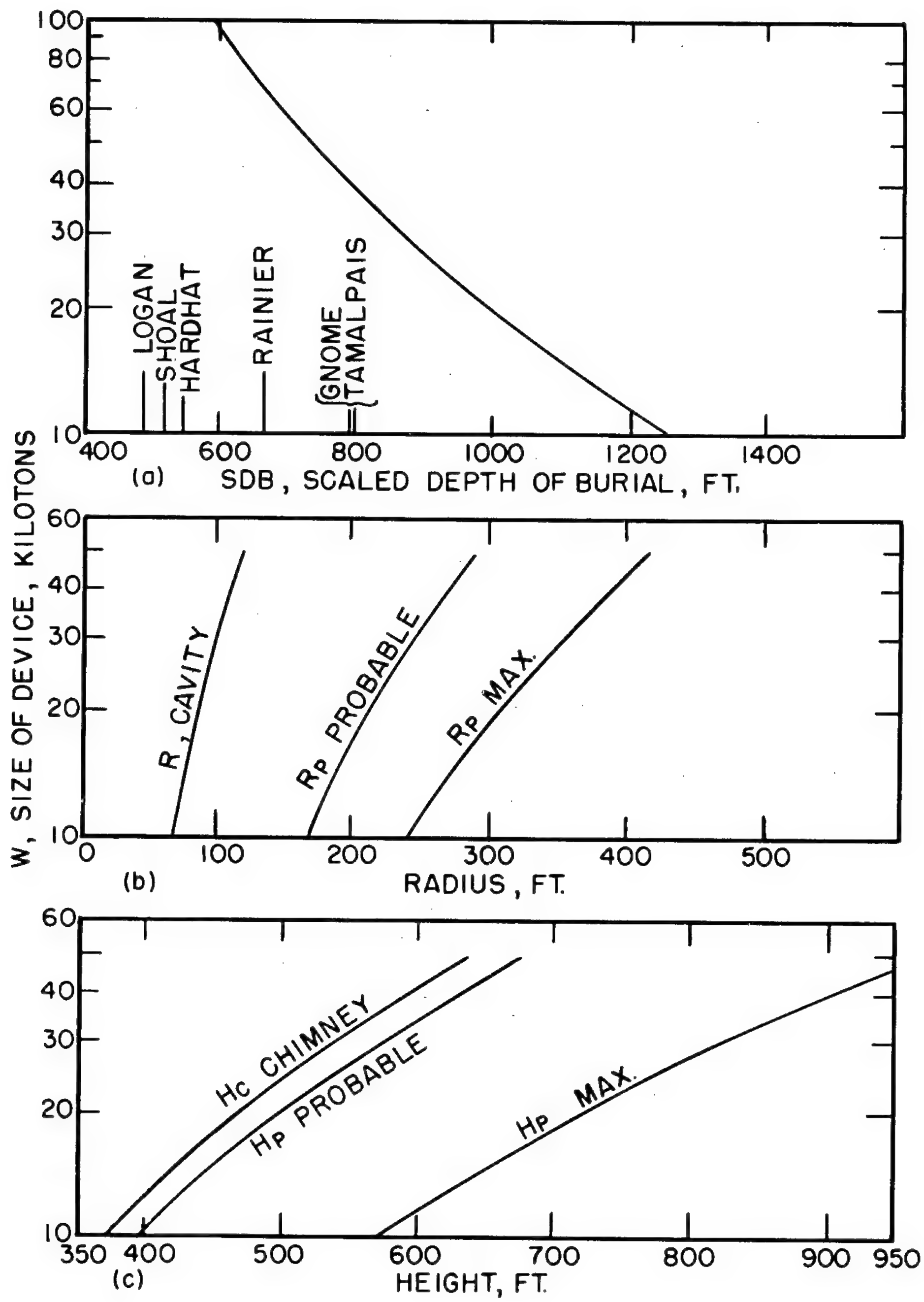

Fig. 8. Calculated data for nuclear explosion environment at 2700-ft depth of burial.

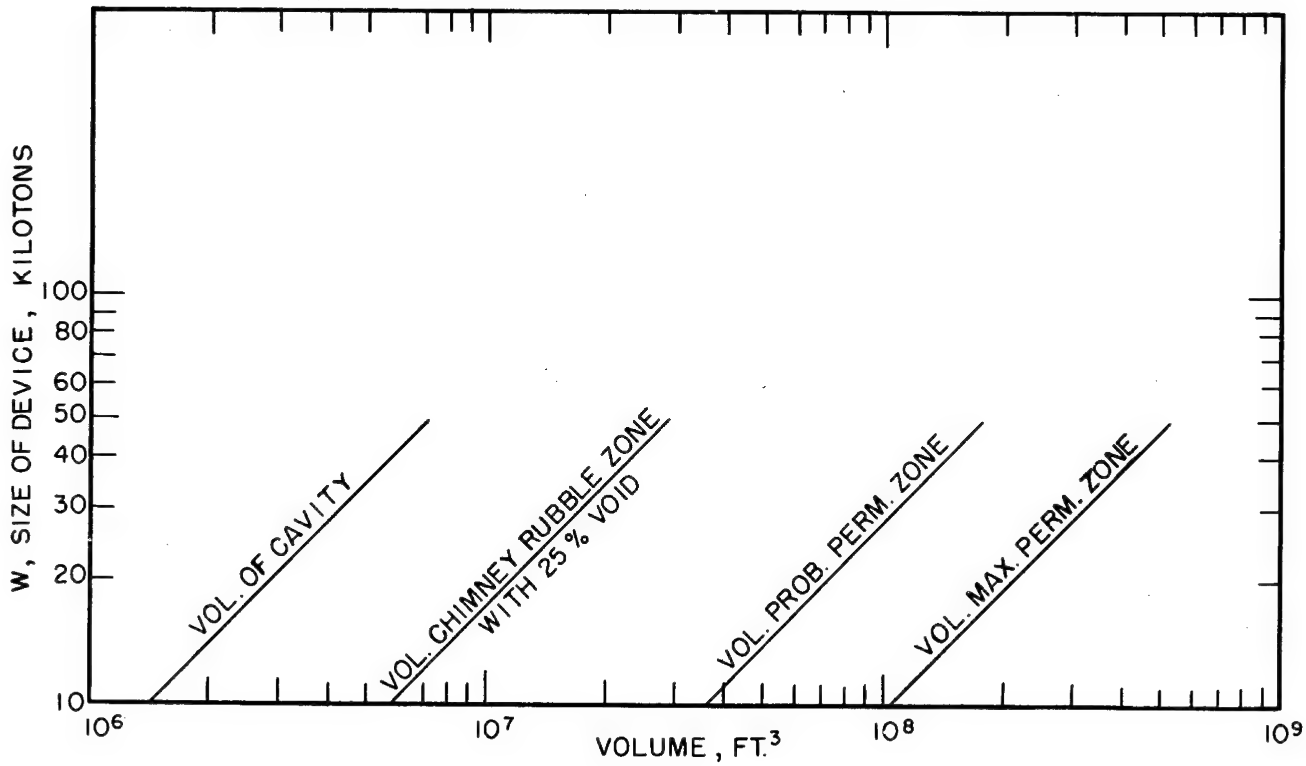

Fig. 9. Total volumes created by a nuclear explosion at 2700-ft depth of burial.

Calculated Well Deliverability

A complete description of the finite difference approximations for the solution of Eq. (10) for the transient isothermal flow of gas in porous media have been reported previously[9-12] and need only to be summarized here. The solution involved breaking the total wellbore drainage area into a number of cells (here 40 or 50 concentric, annular, cylindrical shells) of specified permeability and calculating the well production-pressure-time history for a large number of time increments. Flow capacity of the existing reservoir matrix was determined from a computer fit of well test data from existing wells in the formation. This value was also used in the unaffected area in the explosion-stimulated calculations. Permeability (or capacity) in the cavity-chimney area near the wellbore in the explosion-stimulated cases was arbitrarily assumed to be more than 100 times greater than that of the unaffected formation. This ratio was arbitrarily decreased to unity at the radius of the shot-affected zone. In effect, this variation implies that a large wellbore was created, but it allows material balance accounting of the gas present in the blocks of rubble and in the matrix rock between fractures. An example of the permeability function characteristic for an explosion-stimulated well is given in Figure 10. In addition, the production schedule was started by picking an initial production rate consistent with an estimated saleable quantity of gas from a well in the area. It was also specified that after pressure in the wellbore reached approximately 100 psia, no further reduction should occur. This was a practical specification to provide satisfactory delivery pressure of gas to the gathering system.

The computer model was used to predict the production-pressure-time history for five cases; two unstimulated and three bomb stimulated. Specifically, these cases correspond to:

1. One conventional well per 640-acre section; a 4-3/4-inch open hole completion through the entire producing section.
2. Four conventional wells per 640-acre section; each well draining 160 acres.
3. One "probable" nuclear-stimulated well per section. The fractured, permeable zone radius was 270 feet.

4. One "minimum" nuclear-stimulated well per section. It was assumed that no fracturing occurred beyond the initial cavity and chimney formed by the shot, and that the permeable zone radius was 110 feet.
5. One "possible" nuclear-stimulated well per section. The fractured permeable zone radius was assumed to be 385 feet.

The resultant numerical data for each of the cases includes the pressures in each incremental cell for each time period. Two such pressure-radius relationships are shown in Figure 10. The gas deliverability for each of the five cases is shown in Figure 11. A summary of pertinent production data and events is given in Table II.

ECONOMICS

The economic incentive for nuclear stimulation can be shown by combining the example reservoir and the productivity calculations with typical cost and revenue data:

The following fixed economic data have been used:

Company net interest	0.81933
Federal and State income tax	54%
Gas contract	145/MSCF with 1-cent escalation each 5 years

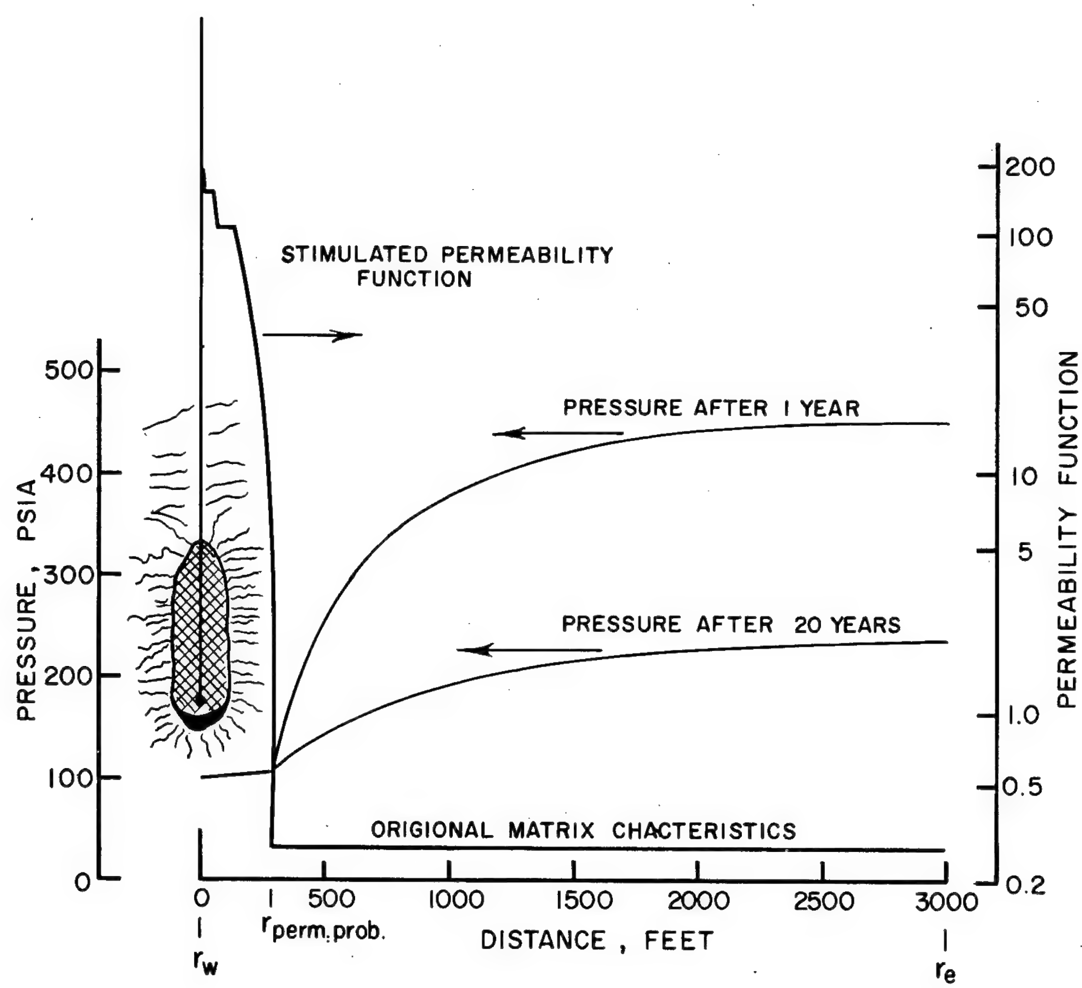

Fig. 10. Plot of permeability and pressure characteristics for a nuclear-stimulated well.

Gas production tax	\$3.00/MMSCF
Cost of producing well	\$25,000/well
Operating costs (excluding production tax)	\$900/well year
Calculation period	20 years.

Costs for large-diameter cased emplacement holes from several sources—drilling contractors, company records, and the literature—were obtained. These cost data are displayed in Figure 12. The solid curve represents the most realistic hole costs with the limits of "bids" shown as dashed curves. The costs increased exponentially with hole diameter. Thus, the smallest hole which can accommodate the device should be used for emplacement.

Four different investment costs of \$650,000 (includes published device costs of \$500,000)[16], \$400,000, \$275,000, and \$165,000 were evaluated for the most probable postshot environment. In addition, the economics were calculated for the "minimum" and "maximum" postshot permeable-zone geometry at the intermediate \$400,000 investment cost. The economic summaries given in Table III also contain evaluation for conventional well development in the area. Examination of Table III reveals that conventional wells are the most economic method of developing the location. The lower device-plus-emplacement costs make the nuclear stimulation attractive as a development technique. However, this emphasizes the

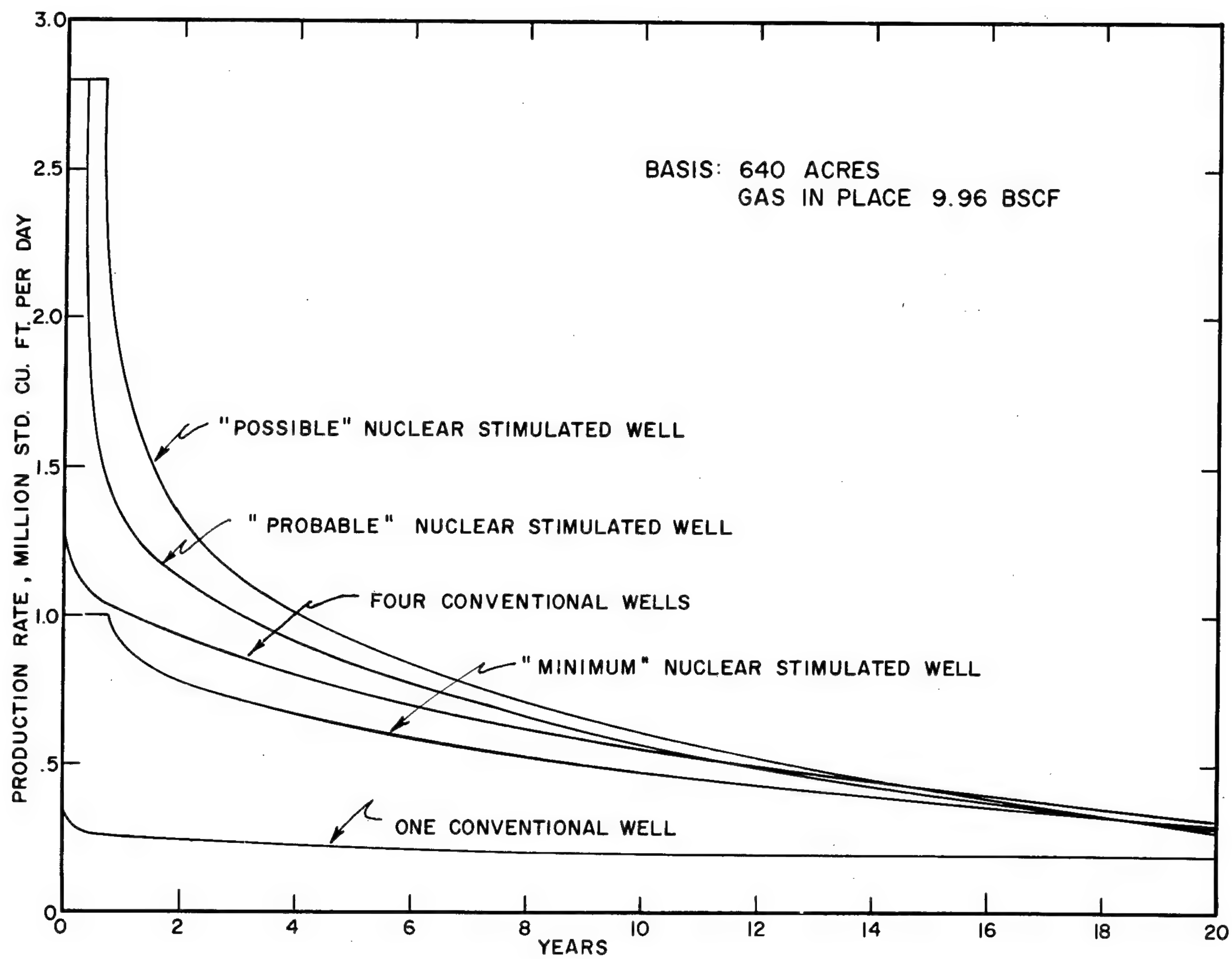

Fig. 11. Gas deliverability from original and nuclear-stimulated formation.

Table II. Calculated reservoir production characteristics.

Based on 640 acres, and 20 years total production time
9.96-billion std cu ft initial gas in place

	Initial rate (MSCFPD)	Time on initial rate (days)	Pressure at the drainage radius after 20 years (psia)	Prod. rate at end of 20 years (MSCFPD)	Total production in 20 yrs (BSCF)	Total recovery %
Unstimulated cases:						
One conventional well	350	4	383	176	1.54	15.4
Four conventional wells	1400	4	257	311	4.31	43.2
Stimulated cases:						
"Probable" well	2800	130	237	284	4.99	50.1
"Minimum" well	1000	275	286	299	3.81	38.2
"Possible" well	2800	245	217	290	5.53	55.5

Table III. Economic calculation summary.

	Total investment (dollars)	Gas produced (BSCF)	Recovery (%)	Payout (years)	Company net after FIT ($)	Rate of return (%)
Unstimulated cases:						
One conventional well	25,000	1.54	15.4	2.7	102,425	33.8
Four conventional wells	100,000	4.31	43.2	2.8	255,871	29.4
Stimulated cases:						
"Probable" well	650,000	4.99	50.1	13.0	85,500	2.9
"Probable" well	400,000	4.99	50.1	6.6	193,689	9.4
"Probable" well	275,000	4.99	50.1	4.2	252,652	16.2
"Probable" well	165,000	4.99	50.1	2.4	295,418	28.6
"Minimum" well	400,000	3.81	38.2	10.5	112,775	5.2
"Possible" well	400,000	5.53	55.5	5.3	229,629	11.7

importance of knowing what the actual costs of nuclear devices and emplacement will be, since this will govern their economic feasibility for reservoir stimulation.

One of the favorable factors to which a monetary value was not placed is the large "wellbore" storage capacity. If a nuclear-stimulated gas field were located on a gas transmission line, this large storage capacity could serve as a balance and provide high productivity emergency capacity for the line in times of maximum demand.

Deliverability and economic evaluations can also be made for marginal oil reservoirs, using similar techniques. Here again, we find that given favorable (1) reservoir configurations, (2) device-plus-emplacement costs, and (3) operating costs,

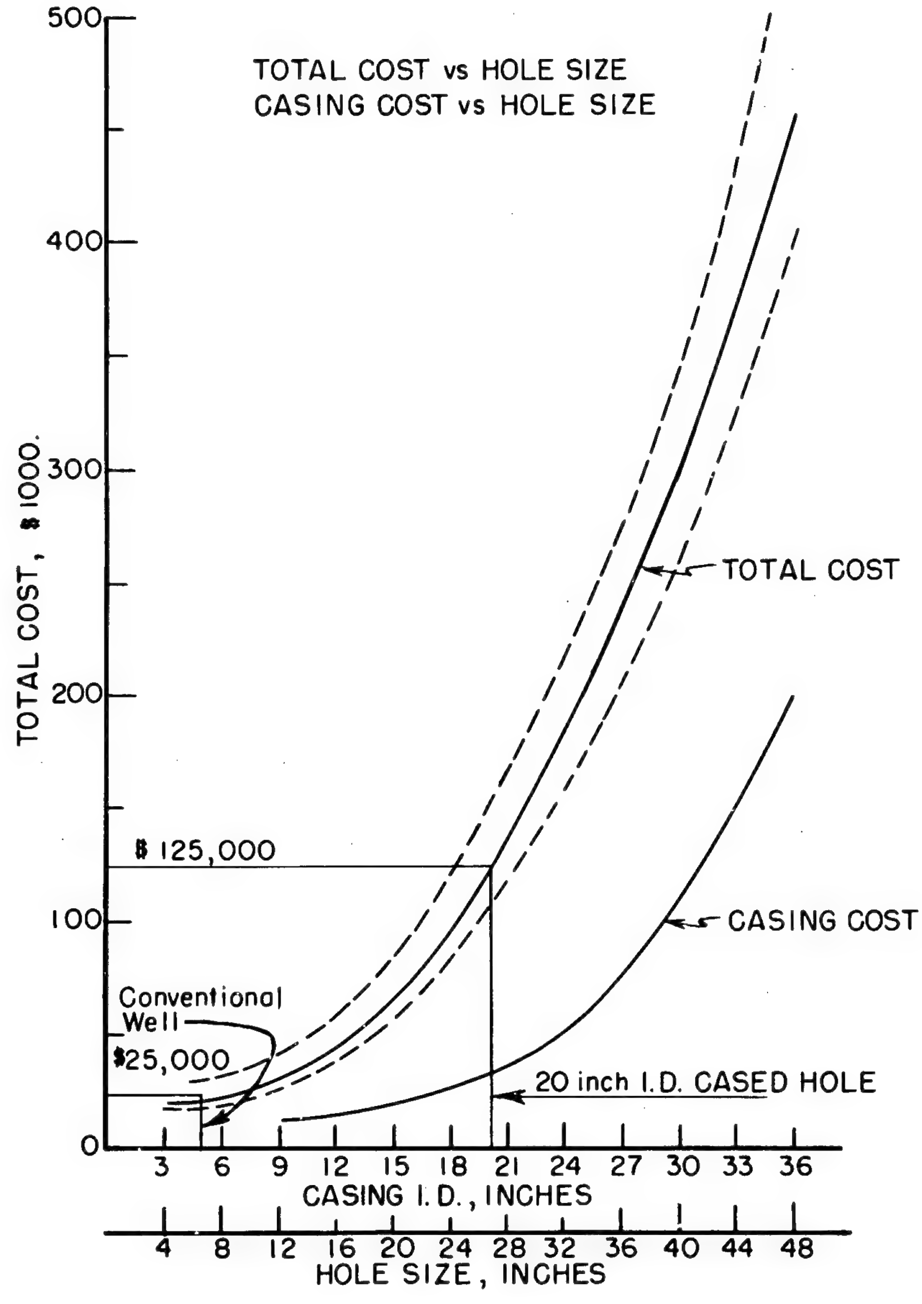

Fig. 12. Effect of hole size on well costs for 2700-ft well.

nuclear stimulation appears to be an attractive proposition.

CONCLUSIONS AND RECOMMENDATIONS

Use of nuclear explosives to stimulate low productivity gas or oil reservoirs is feasible. The shock wave from such an explosion in a reservoir would create a cavity, chimney, and broken or fractured zone which would yield much higher deliverabilities of gas or oil to the wellbore. The actual rate of production would be controlled by the size of the broken rock zone and the permeability of the matrix since the flow restriction will be at the junction of the broken rock and unchanged zones.

Reservoirs suitable for economic application of nuclear explosives must be:

1. Sufficiently deep to completely confine the explosion through weight of the overburden.
2. Thick enough to confine the fractured zone to the hydrocarbon-bearing formation or, at least, to a hydrocarbon formation and non-water-bearing formations immediately above and below the hydrocarbon zone. Thus, not only would the explosion be contained, but there would be no contamination of any water-bearing zone with hydrocarbons or radioactivity released by the explosion.
3. Relatively nonproductive by existing production methods. Thus, resources released by the technique would provide hydrocarbon energy reserves not available at present-day standards.

The first test of nuclear stimulation should be in a low productivity gas zone. Here the possible contamination by leaching of particulate matter from the fused zone would be eliminated and the only contaminant would be radioactive gases. Verification of the calculations in such a gas reservoir should lead to applications in light oil reservoirs if the leaching problems can be solved. Of course, an obvious answer to the leaching problem would be development of cleaner devices.

In the final analysis, economics will govern the application of this new method of oil or gas recovery. At present there are no device or emplacement cost figures that would provide economic incentive for use of this stimulation technique in the petroleum industry. The published data[16] of \$500,000 for a small device and \$1,000,000 for a large one completely eliminates any widespread economic use of this energy source. Reduction of the cost figures and removal of the large hole-size requirement would do much to speed up actual development of nuclear stimulation as an economic method.

Nuclear stimulation looks attractive enough so that a field test in reservoir rock should be carried out. A gas reservoir such as the one used in the calculations appears ideal as a test site. Successful utilization of nuclear explosions would release otherwise unavailable hydrocarbons which can be used to produce many times the energy contained in the device.

ACKNOWLEDGMENTS

We would like to thank the management of Continental Oil Company for encouragement and permission to publish this work. In addition, we thank Gerald Kiel for his assistance with the deliverability calculations. The interest and technical advice of Don Rawson and Gary Higgins and other Lawrence Radiation Laboratory personnel is gratefully acknowledged. Discussions with personnel from the U. S. Bureau of Mines and the A. E. C. San Francisco Operations office have also been beneficial to the authors.

REFERENCES

1. Boardman, C. R., D. D. Rabb, R. D. McArthur, "Characteristic Effects of Contained Nuclear Explosions for Evaluation of Mining Applications," Lawrence Radiation Laboratory, Livermore, Rept. UCRL-7350, May 1963.
2. Korver, J. A., C. R. Boardman, D. E. Rawson "The SHOAL Postshot Environment," UOPKA 64-7, February 4, 1964.
3. Coffer, H. F., B. G. Bray, C. F. Knutson, D. E. Rawson, "Some Effects of Nuclear Explosions on Oil Reservoir Stimulation," AIME-SPE Paper 600 presented at Rocky Mountain Joint Regional Meeting of the SPE, May 27-28, 1963; see also Lawrence Radiation Laboratory, Livermore, Rept. UCRL-7293, March 21, 1963.
4. Muskat, Morris, "The Flow of Homogeneous Fluids Through Porous Media," McGraw-Hill Book Company, Inc., New York 1937. Also J. W. Edwards, Inc., Ann Arbor, Michigan, 1946.
5. Amyx, J. W., D. M. Bass, R. L. Whiting, "Petroleum Reservoir Engineering," McGraw-Hill Book Company, Inc., New York, 1960.
6. Swift, G. W., O. G. Kiel, "The Prediction of Gas-Well Performance Including the Effect of Non-Darcy Flow," Trans AIME, 225, pp. I-791-798, 1962: also Journal Pet. Tech. 14, No. 7, pp. 791-798, July 1962.
7. Kiel, O. G., J. M. Campbell, "Analysis of Gas-Well Behavior Using a Two-Dimensional Unsteady-State Model, AIME-SPE Paper No. 562 presented at Oklahoma University-SPE Production Research Symposium, Norman, Oklahoma, April 29-30, 1963.
8. Kiel, O. G. PhD Dissertation, University of Oklahoma, Norman, Oklahoma, 1963.
9. Bruce, G. H., D. W. Peaceman, H. H. Rockford, Jr. and J. D. Rice, "Calculations of Unsteady State Gas Flow in Porous Media," Trans AIME, 198, p. 79, 1953.
10. Johnson, G. W., C. E. Violet, "Phenomenology of Contained Nuclear Explosions," Lawrence Radiation Laboratory, Livermore, Rept. UCRL-5124 Rev. I, December 1958.
11. Bennett, W. P., A. L. Anderson, B. L. Smith, "Cavity Definition, Radiation and Temperature Distributions from the Logan Event," Lawrence Radiation Laboratory, Livermore, Rept. UCRL-6240, December 1960.
12. Peterson, J. D., W. P. Bennett, "Radiation and Temperature Measurements of the Neptune Event," Lawrence Radiation Laboratory, Livermore, Rept. UCRL-6251, January 1961.
13. Batzel, R. E., "Radiactivity Associated with Underground Nuclear Explosions," Lawrence Radiation Laboratory, Livermore, Rept. UCRL-5623, June 1959.
14. Batzel, R. E., "Distribution of Radioactivity from a Nuclear Excavation," Lawrence Radiation Laboratory, Livermore, Rept. UCRL-6249-T, October 1960.
15. Rawson, D. E., "Review and Summary of Some Project Gnome Results," Lawrence Radiation Laboratory, Livermore, Rept. UCRL-7166, December 1962.
16. "Proceedings of the Second Plowshare Symposium Part II Excavation," pp. 2-3, Lawrence Radiation Laboratory, Livermore, Rept. UCRL-5676, May 14, 1949.

BIOGRAPHICAL SKETCHES OF AUTHORS

H. F. Coffer received his B.S. in Chemistry in 1947 from the University of Arizona. Earlier, between his second and third year of education, he spent four years in the Army Air Force. Returning to the University of Arizona, he received his M.S. in Organic Chemistry in 1948. At the University of Southern California in 1951 he received his Ph. D. in Colloid Chemistry. He joined the Production Research Division of Continental Oil Company in the summer of 1951. In the Well Engineering Section his research work was principally development of new drilling methods and fracturing techniques. He was promoted to assistant research director in 1957 and became research director in 1959.

Bruce G. Bray is a Research Group supervisor in the Production Research Division, Research and Development Department, Continental Oil Company in Ponca City, Oklahoma. He is supervisor of the Reservoir Fluids Laboratory and is primarily concerned with research and applications of phase and thermodynamic behavior and fluid properties of hydrocarbon systems to petroleum production and field processing problems. He received his B.S. (1953), M.S. (1954) and Ph. D. (1957) in Chemical Engineering from the University of Michigan. From 1953 to 1957 he was a Research Associate with the Engineering Research Institute in Ann Arbor, Michigan. He joined Continental Oil Company in 1957.

C. F. Knutson was employed by Continental Oil Company in 1951 after receiving his M.S. degree in Geology from Stanford University. He subsequently received his Ph. D. in Geology from U.C.L.A. in 1959. In the period from 1951 to date, he has served as a subsurface geological specialist, reservoir engineer, and production engineer with Continental's Production Department. He is currently Group Supervisor of the Coring and Reservoir Geology Group in Continental's Production Research Division, Ponca City, Oklahoma.

DEPOSITION OF THERMAL ENERGY BY NUCLEAR EXPLOSIVES*

R. A. Heckman

Lawrence Radiation Laboratory, University of California
Livermore, California

ABSTRACT

A fraction of the energy released by the underground detonation of nuclear explosives is locally deposited as residual thermal energy. An accurate prediction of this usable fraction of the energy released is necessary to evaluate the feasibility of several of the proposed projects in the Plowshare Program.

Analysis of dynamic temperature distribution data derived from experimental measurements in three different geological media – tuff, granodiorite, and salt – indicates that the distribution of residual thermal energy several months after detonation may be deduced from currently available computer-code predictions of the energy distribution at very early times.

However, the actual fraction of energy remaining is strongly dependent on the degree of containment achieved during the nuclear detonation.

In addition, the thermodynamic quality of the residual heat energy is directly a function of the total water content of the medium in which the detonation takes place.

INTRODUCTION

The Plowshare Program was established in 1957 by the Atomic Energy Commission to investigate and develop industrial and scientific uses of nuclear explosives. Several large-scale chemical engineering proposals have been made to utilize the energy deposited by nuclear explosives. Grebe et al.[1] have suggested the concept of an underground "retort" where the high temperatures and pressures associated with a nuclear detonation could carry out a variety of chemical syntheses. Indeed, one of the objectives of Project Gnome[2] was to investigate the problems of recovery of heat from the post-detonation environment in a salt medium. The use of nuclear explosives to assist in recovery of petroleum products from tar sands has been studied in great detail.[3] Similar studies on oil shales are available.[4] Teller[5] has suggested the possible use of nuclear explosives to aid lunar expeditions in developing a lunar water supply. Higgins et al.[6] have studied the general problem of induced chemical reactions with nuclear explosives.

Evaluation of these proposals requires a detailed analysis of the energy deposition from an underground nuclear detonation. Electronic computer codes[7,8] have been developed which provide the required energy deposition analysis at early times. Because of the complexity of the partial differential equations used in the codes and experimental uncertainties in the input data relating to transitions between gaseous, liquid, plastic, fractured and elastic states, experimental verification of the mathematical predictions would be reassuring.

This paper will present a summary of the available data on residual thermal energy from nuclear detonations in three different geological media: tuff, halite, and granodiorite.

ENERGY DEPOSITION MECHANISMS

The fraction of energy deposited by an underground nuclear detonation is dependent on the degree of containment achieved. In order to better define containment, we look at a plot of the cavity radius and shock front position as a function of time. (See Figure 1.)

Above the shot the shock front travels vertically until it reaches the surface where it is re-

*Work performed under the auspices of the U. S. Atomic Energy Commission

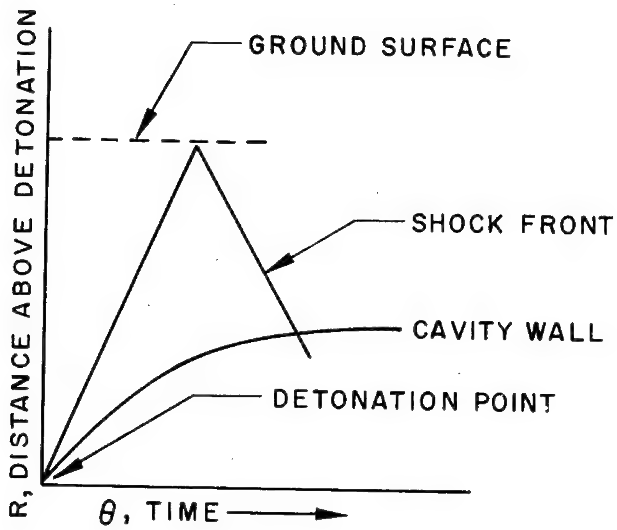

Fig. 1. Cavity radius and shock front position as a function of time.

fracted downward again. Containment is achieved if the internal cavity pressure is equal to or less than overburden or lithostatic pressure at the time this reflected wave reaches the cavity wall.

This containment concept is based on the model that energy released by the nuclear detonation vaporizes the nuclear explosive materials, forming a rapidly enlarging fireball.[7]

As the shockwave passes radially from the point of detonation, its strength decreases rapidly. Thus, the energy density falls rapidly so that the temperature to which the surrounding medium is heated decreases. This is shown in Figure 2; the percentage of the total nuclear energy available as residual heat is shown as a function of the minimum temperature rise produced.

This temperature distribution is calculated for very early times. The time required for the cavity to grow, referred to as the hydrodynamic

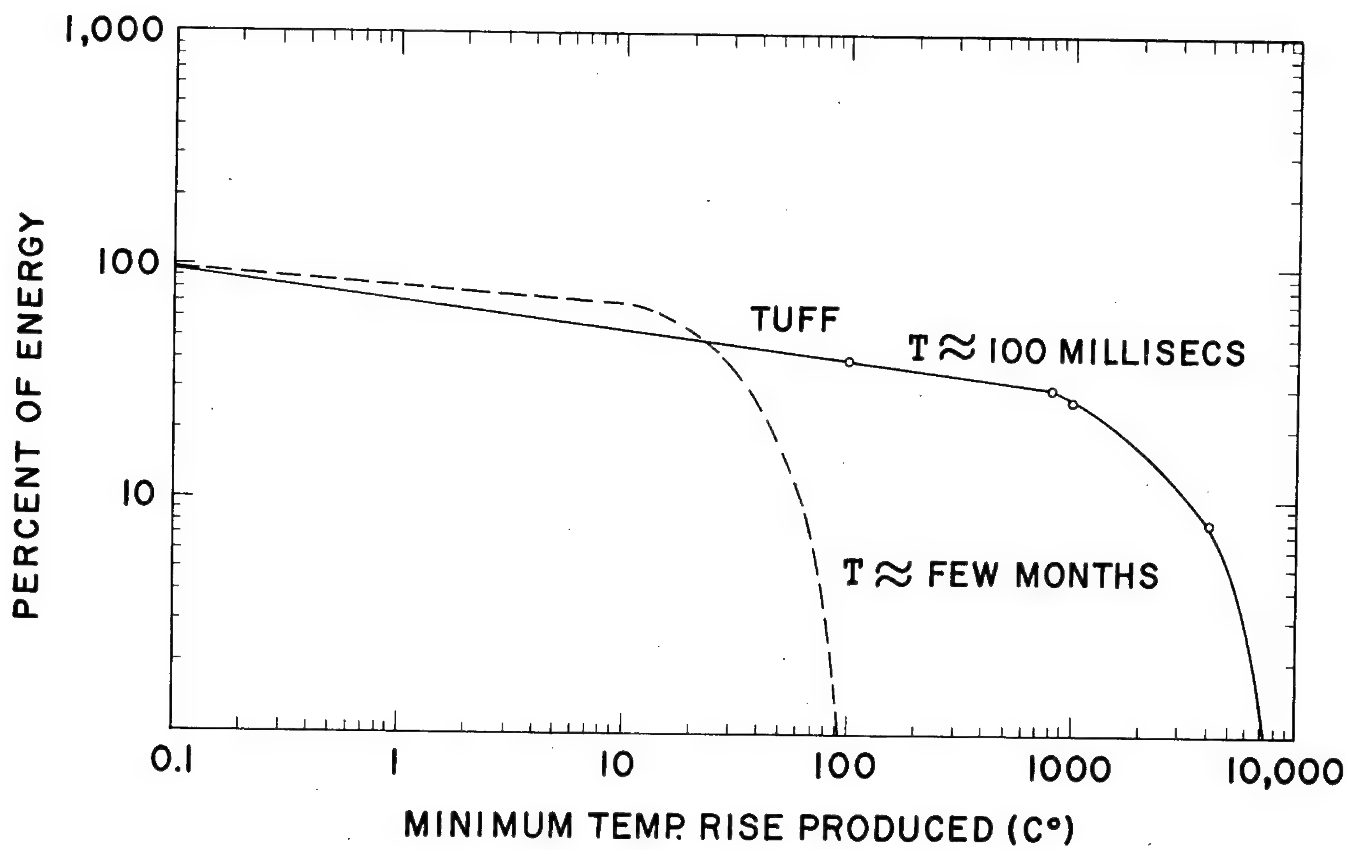

Fig. 2. Calculated minimum temperature rise produced (tuff).

phase, is of the order of 100 milliseconds. The distribution shown in Figure 2 was calculated at the end of the hydrodynamic phase.[6] As the cavity region cools, the distribution of energy shifts such that the fraction originally at higher temperature flows into lower temperature regions, producing a distribution similar to the dashed curve, Figure 2.

Energy Loss Mechanisms

At the end of the hydrodynamic phase, the molten rock flows to the cavity bottom, and thermal stress and decrepitation spall wall material into the cavity. Within usually a few seconds to minutes, the massive chimney collapse occurs.

The principal heat loss mechanisms that occur at late times are: (1) conduction through the fractured zone surrounding the bottom half of the cavity; (2) conduction into the shattered chimney material; and (3) gas phase convective loss into the chimney material. A refluxing zone is set up within the chimney region proper with water acting as the refluxing agent. At very late times (several months), liquid water will exist in the lower chimney regions so that liquid phase convection will play a minor role.

Because of the complexities involved in the heat transfer calculations, no precise techniques exist for analytical solution of the problem. No three-dimensional unsteady state heat transfer computer codes exist at the present time. Since the energy distribution calculated by the existing computer codes[7,8] is given only at the end of the hydrodynamic phase of cavity growth, and no analytical methods exist for predicting the dynamic character of the energy loss mechanisms for the time period from a few minutes to a few months, an experimental approach must be used. Therefore an attempt is made in this paper to analyze the existing data relating to the general problem of residual thermal energy from underground nuclear explosions.

Residual Energy Calculations

Because of the great expense involved in drilling suitable holes through postdetonation environments, temperature data have been obtained only from holes that were drilled primarily to obtain radiochemical samples. Thus, in a number of the events studied, the amount of temperature data available is sparse and its location within the postdetonation environment is not optimum. For example, a very complete system of holes was drilled through the lower hemisphere of the Rainier event[7,10] but no data are available on temperature distributions within the chimney region where an appreciable fraction of the device energy remains. In the case of the Shoal event,[11] only a single vertical hole was drilled. No horizontal holes are planned to be drilled in the lower hemisphere within the time that high temperatures in this region would still exist.

Table I summarizes pertinent data on the events used in this paper.

Temperature profiles deduced for the various events in this report are shown in Figures 3 through 8.[10, 13, 16]

The volume of material included within the given isotherm was estimated by graphical integration techniques using the theorem of Pappus.[14] Physical properties are listed in Table II.[15]

Specific heat data were obtained from Birch.[9]

The energy content contained within each isotherm is given by:

$$Q = 28317\ (\rho V)\ (C_p \cdot 10^7)\ \Delta T$$

where

V = volume, ft^3

ρ = media density, g/cc

C_p = joules/g, °C

ΔT = average temperature rise above ambient, °C

Q = energy content in ergs.

The energy released by 1 kiloton of nuclear yield is equivalent to 4.185×10^{19} ergs or 10^{12} calories.

Figure 9 summarizes the energy distribution data for the detonations that were conducted in tuff media. Only the data for Rainier, Logan, and Blanca are plotted since but one drill hole each was completed for the Neptune and Tamalpais events. A meaningful temperature profile could not be constructed due to the location of the single drill hole. The Rainier event (Figure 10) is known to have contained completely. Postshot exploration of the Logan site indicated penetration of the preshot drift by the expanding cavity. The asymmetries in the deduced Logan temperature profile clearly indicated that such penetration did indeed occur. The Blanca event cratered to the surface (see Figure 11). The asymmetry in the Blanca

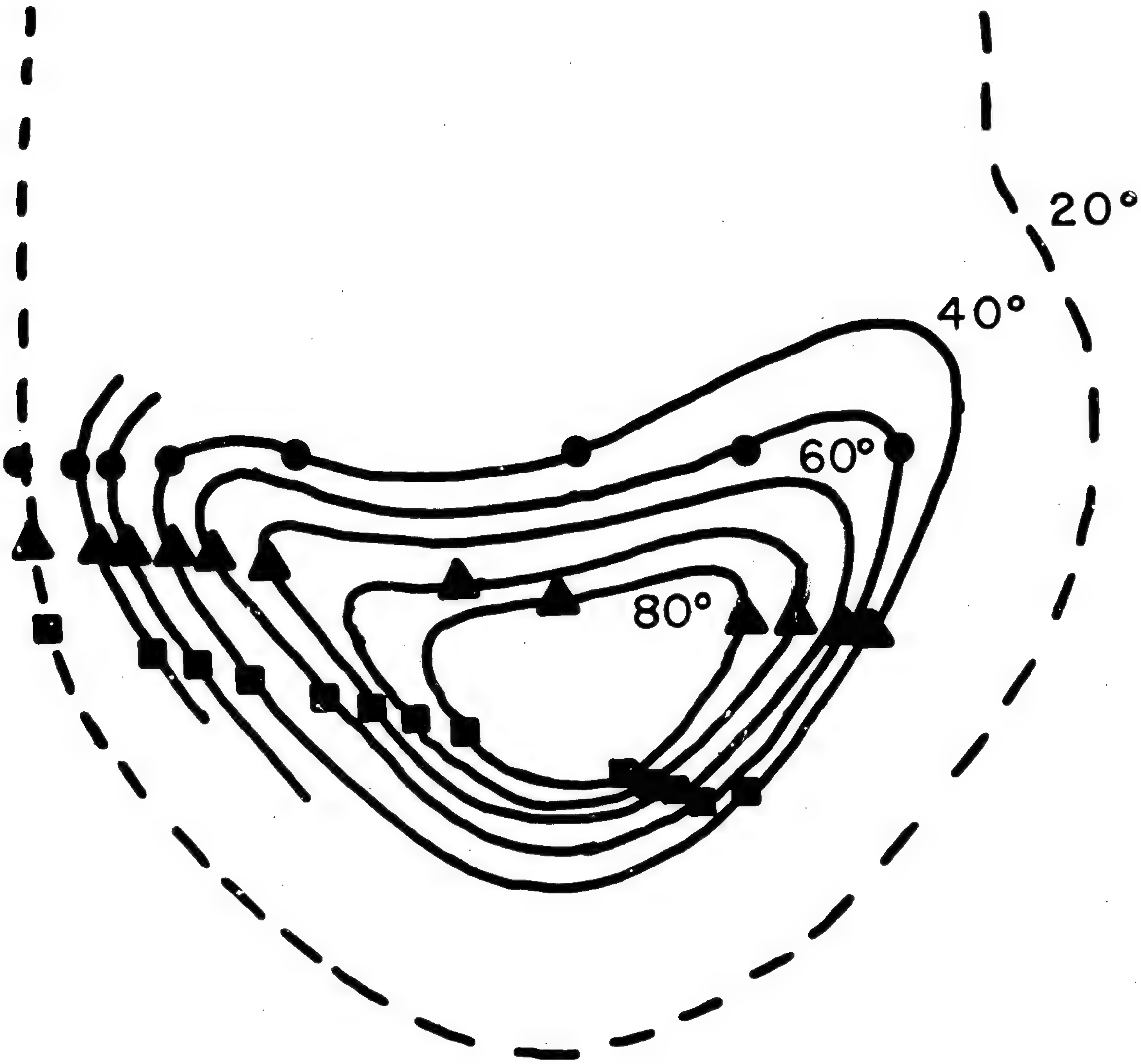

Fig. 3. Rainier temperature profile.

temperature profile is probably due to the chimney collapse mechanism, since the chimney broke through a steep slope rather than a level plane as is the case in alluvial shots. Comparison of the curves which show percent of energy vs minimum temperature rise produced clearly indicate the effect of containment on the percent of residual energy. In the case of Blanca, where effectively little containment was achieved, the fraction of residual energy remaining is very low. The maximum temperature observed is consistent with

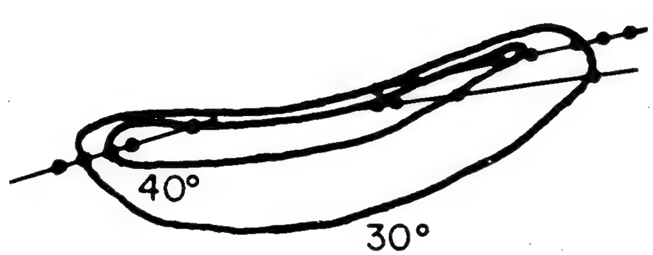

Fig. 4. Blanca temperature profile.

Table I. Data Summary.

Event	Detonation date	Yield(W) (kt)	Medium	Vertical burial depth (D) (feet)	Calculated fraction of thermal energy residual	Max temp observed (°C)	Elapsed time before temp measurements (months)
Neptune	10/14/58	0.115	tuff	99	--	20.5	6
Blanca	10/30/58	19	tuff	835	0.0692	50	4
Logan	10/16/58	5.0	tuff	830	0.228	85	6
Rainier	9/19/57	1.7	tuff	790	0.2295	90	5
Tamalpais	10/ 8/58	0.072	tuff	330	--	53	3
Gnome	12/10/61	3.0	salt	1184	0.95	83	6.5
Hardhat	2/15/62	4.5	granodiorite	939	0.410	88	11
Shoal	10/26/63	12.5	granodiorite	1205	1.0685	599	2.5

these data. The Logan event, where partial containment was obtained, shows that an appreciable fraction of energy remains at a relatively lower temperature. Figure 12 shows the comparison between the calculated and observed energy deposition in a salt medium.

Venting was observed from the Gnome event (Figure 13) within 7 minutes after detonation.[12] The gray smoke and steam emanating from a shaft may have carried away as much as 10 percent of the energy released. This figure is estimated from the total energy remaining at late times.

In the comparison of the salt and tuff data, it is significant that both media contain relatively high water concentrations. Therefore, these media rapidly approached the boiling point of water as the maximum temperature that can be expected to exist.

In Figure 14 are shown the results of two shots in granodiorite, Shoal[11] and Hardhat.[16] We note that in the case of Hardhat, where appreciable quantities of water were artificially introduced during postshot drilling into a normally dry en-

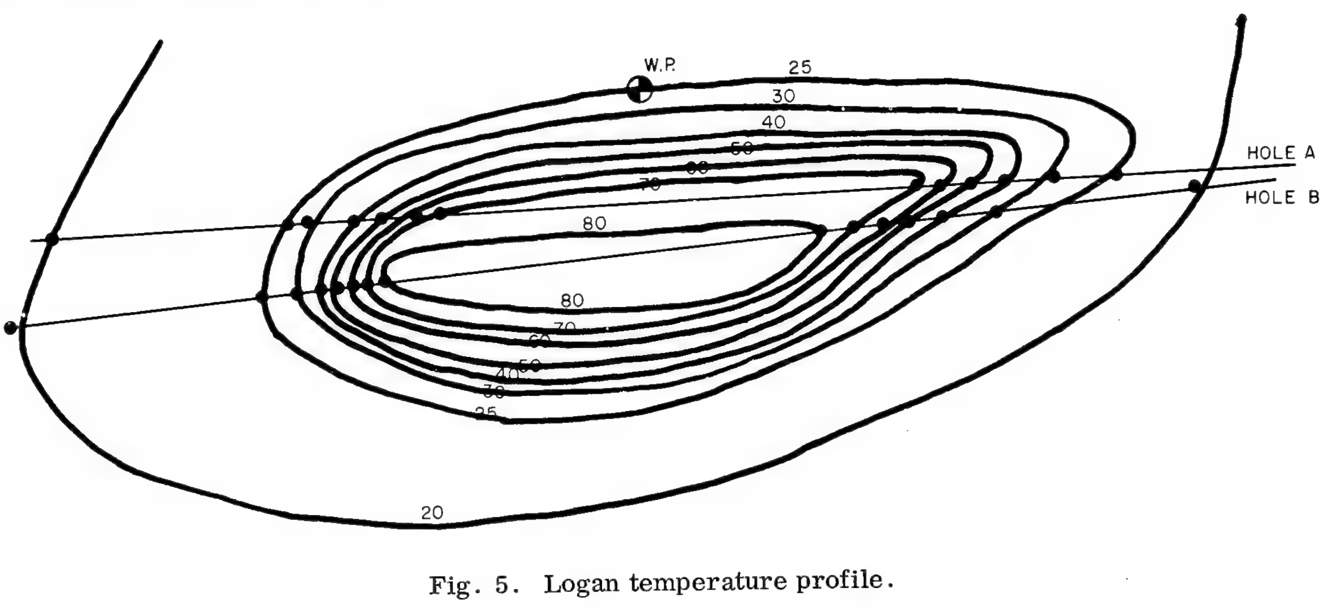

Fig. 5. Logan temperature profile.

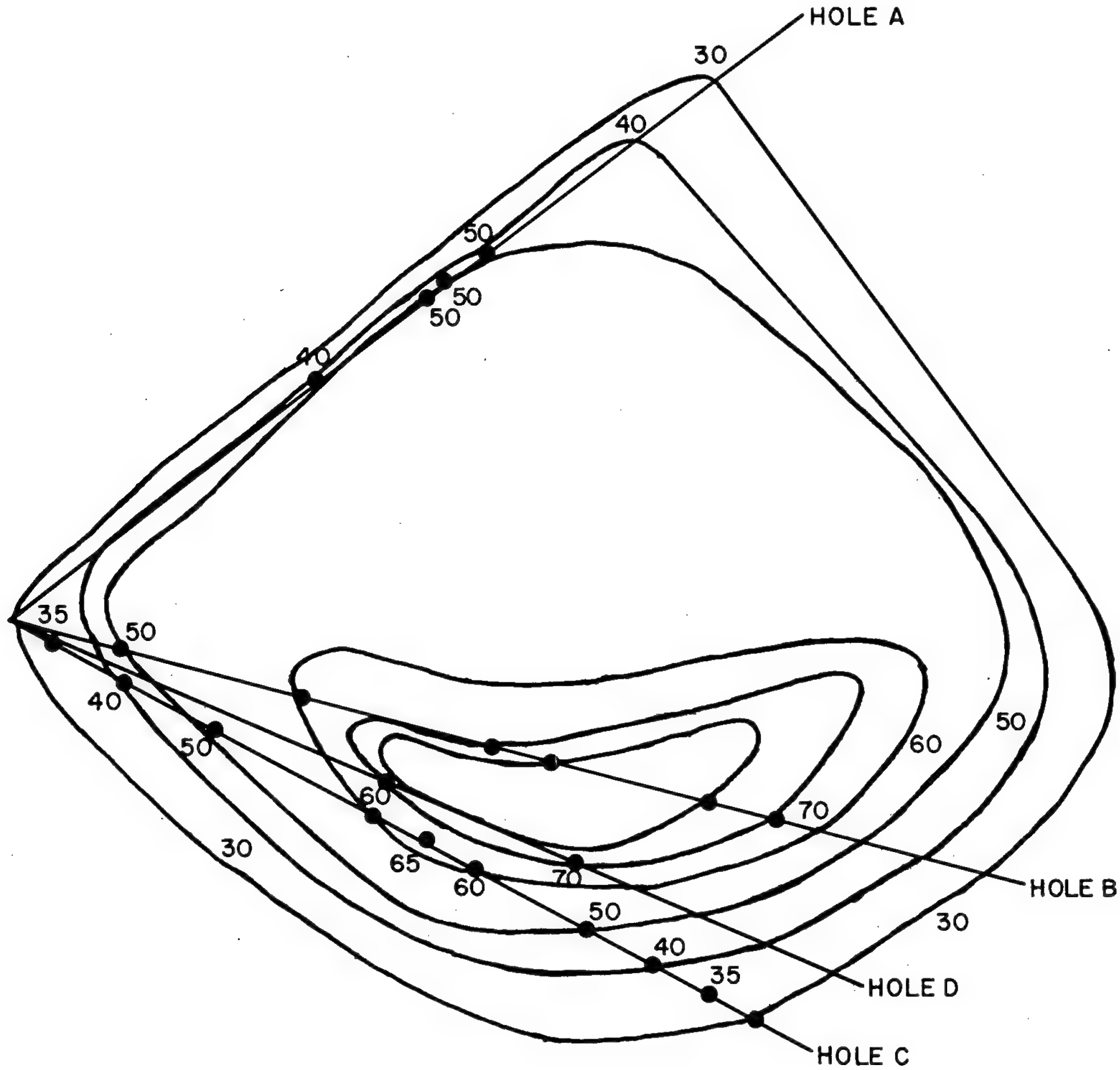

Fig. 6. Gnome temperature profile.

Table II. Some typical properties of four rock types

Physical Properties	Granodiorite	Salt	Tuff
Bulk density (natural state)	2.67[a]	2.2[b]	1.85[c]
Bulk density (dry)	2.67[a]	2.18[b]	1.6[c]
Grain density	2.69[a]	2.25[b]	2.35[c]
Porosity	0.9%	3%	32%
Total water content (by wt)	0.9%	1%	20%

[a]Skrove, J. W., Lawrence Radiation Laboratory, Livermore, private communication.
[b]U. S. G. S., 1962.
[c]Diment et al., 1959

vironment, the maximum temperatures achieved are limited because of the boiling point of water.

An apparent error in the integration of the residual energy in the Rainier event, as reported by Olsen et al.,[7,10] has led to the erroneous conclusion that a maximum of only one-half the energy released by an underground nuclear detonation remains as residual thermal energy. The results of the work reported in this paper show that 90 to 95 percent of the nuclear energy release remains as residual thermal energy if complete containment is achieved. These results are in essential agreement with the values predicted for very early times by the computer codes.

Correlation of the energy deposition with radial distance from the shot point is difficult because of the asymmetries in the temperature profiles. Table III summarizes the radial data derived from the temperature profiles shown in Figures 3 to 8.

In general, it appears that at late times ambient temperatures exist at distances equivalent to a cavity diameter below the original shot point.

From the temperature profiles and the energy distribution curves presented earlier, it is important to note that an appreciable fraction of the residual thermal energy exists in a large volume of material at very low temperature increases

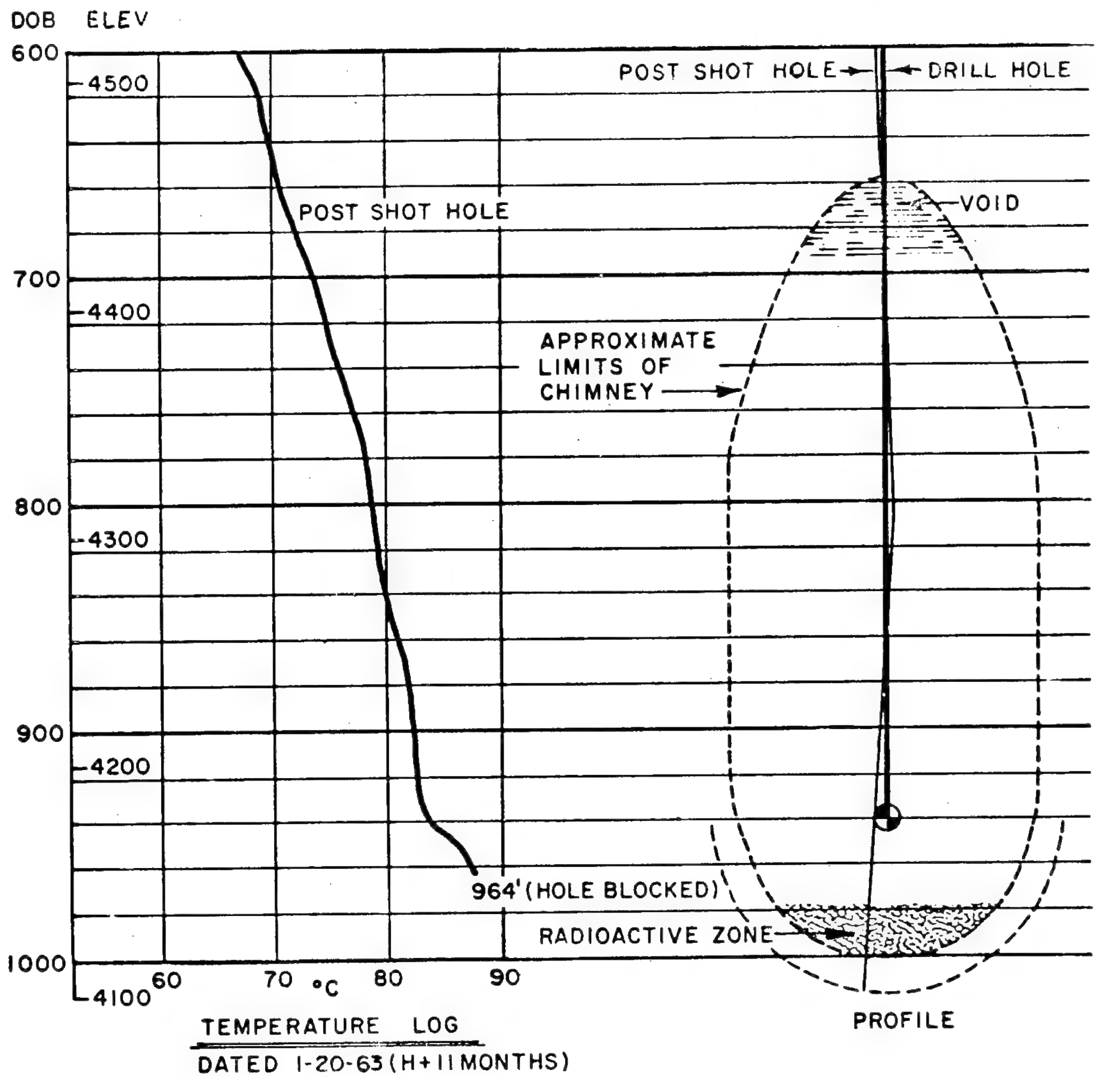

Fig. 7. Hardhat temperature profile.

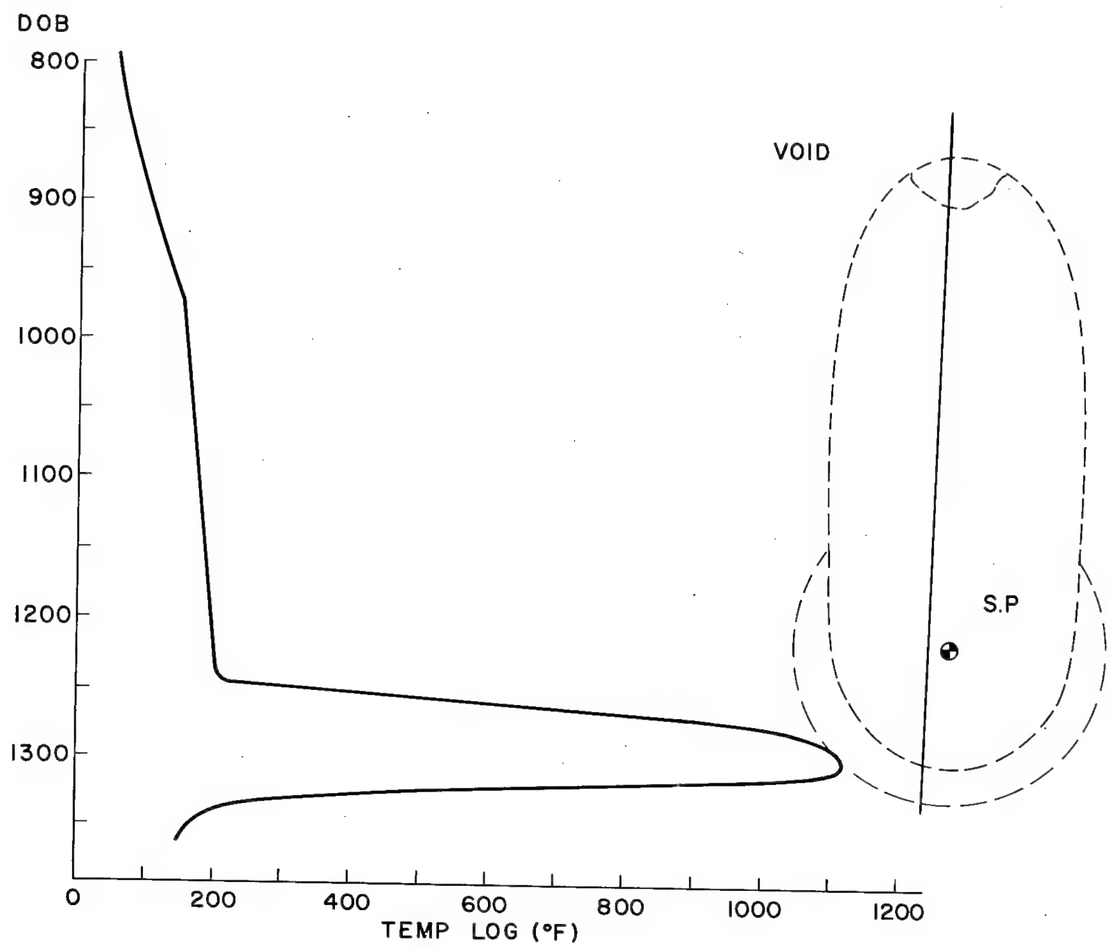

Fig. 8. Shoal temperature profile.

Table III. Radial energy distribution at late times.

Event	Media	Radial distance to ambient media temp. Fractional cavity radius
Gnome	salt	2.68
Rainier	tuff	1.69
Logan	tuff	1.41 - 1.96
Blanca	tuff	1.21 - 1.93
Shoal	granodiorite	1.72

above ambient. In the case of Rainier, 50 percent of the energy release is contained in material within a 4° C rise above ambient.

CONCLUSIONS

In summary, the work presented in this paper shows that the analysis of the distribution of residual thermal energy at late times, i.e., a few months after detonation, is consistent with the energy distribution predicted by current computer codes for very early times, i.e., fractions of a second after detonation.

The actual fraction of residual energy that might be expected within a given isotherm in any detonation medium is most strongly influenced by the degree of containment of the nuclear explosion that is achieved. As would be expected from first principals, the thermodynamic quality of the residual heat energy is directly proportional to the amount of water present in the postshot environment. In experience to date, the water has come from one of three sources: artificially induced, e. g., by postshot drilling; the natural water table; or chemical water found in the minerals of the medium.

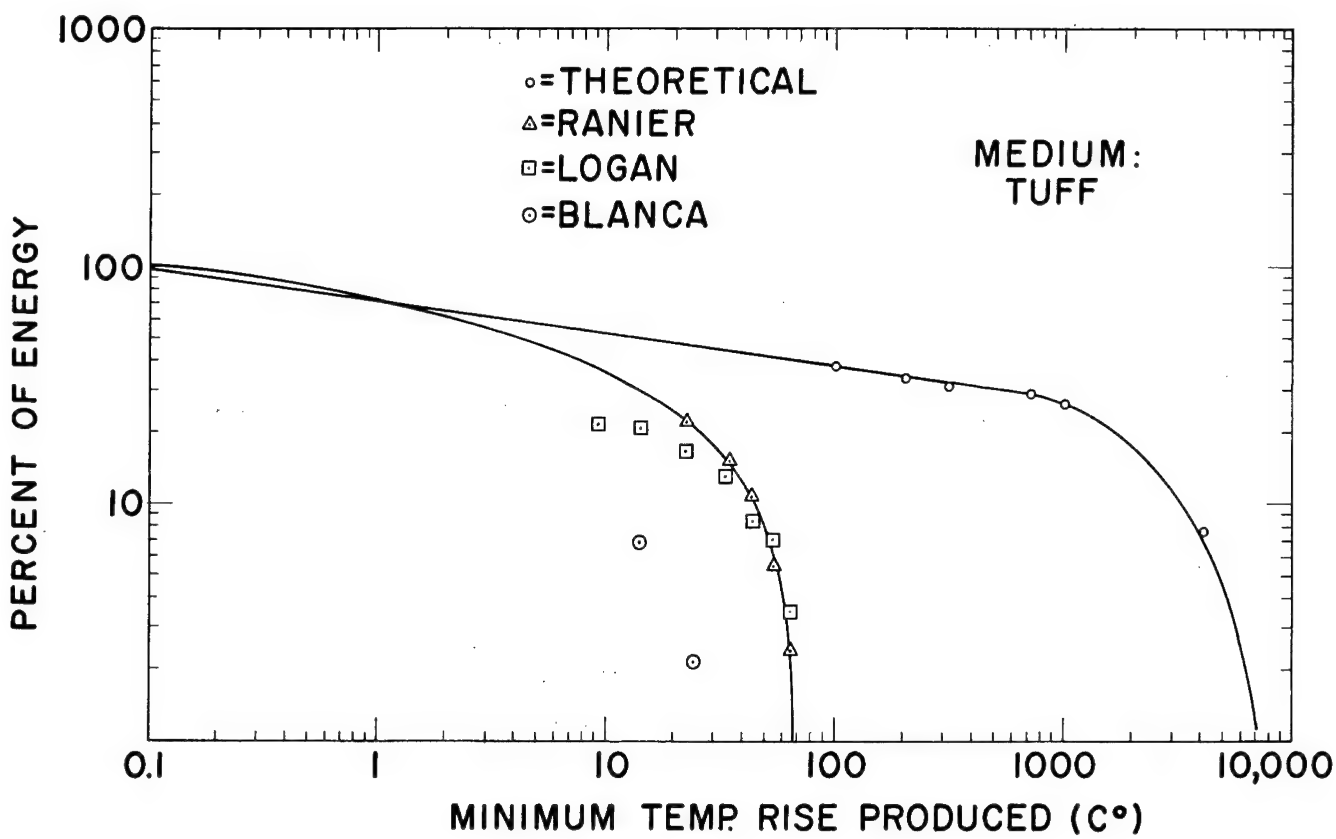

Fig. 9. Observed minimum temperature rise produced (tuff).

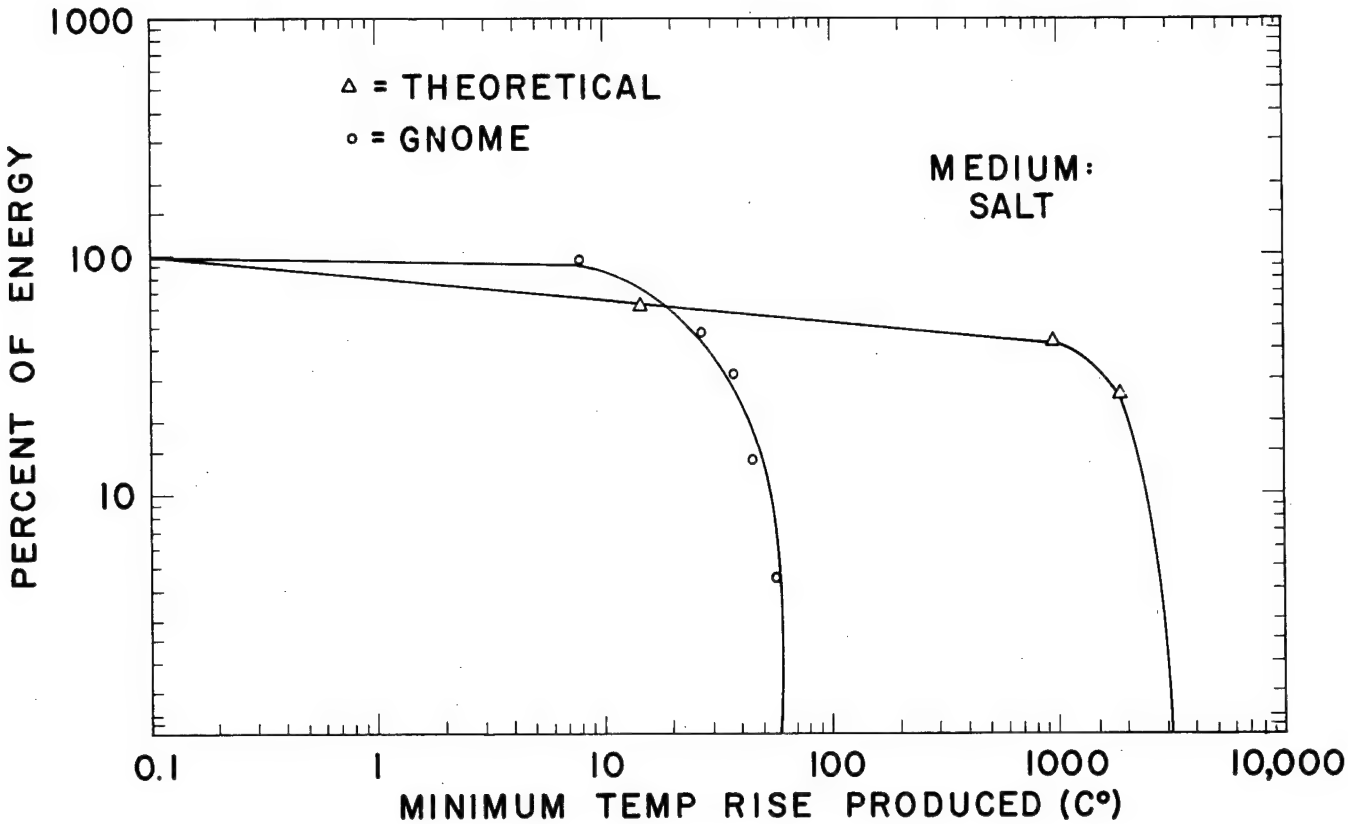

Fig. 10. Observed minimum temperature rise produced (salt).

BIBLIOGRAPHY

1. Proceedings of the Second Plowshare Symposium, Part IV, "Water Resources, Mining, Chemicals, Petroleum," Lawrence Radiation Laboratory, Livermore, Rept. UCRL-5678, May 15, 1959.
2. Lombard, D. B., "Plowshare," Physics Today, 14, No. 10, pp. 24-34, October 1961.
3. Natland, M. L., "Project Oilsand," presented to the Joint Technical Feasibility Committee, Ottawa, Ontario, Canada, Richfield Oil Co., July 1959.
4. UCRL-5678, ibid.
5. Teller, E., "Project Plowshare," Nuclear News, 6, No. 3, March 1963.
6. Higgins, G., Rawson, D., Wade, W., "Chemical Reactions Induced by Underground Nuclear Explosions," Lawrence Radiation Laboratory, Livermore, Rept. UCRL-5882 Rev., June 30, 1961.
7. Proceedings of the 2nd Plowshare Symposium, Part I, "Phenomenology of Underground Nuclear Explosions," Lawrence Radiation Laboratory, Livermore, Rept. UCRL-5675, May 15, 1959.
8. Butkovitch, T. R., Third Plowshare Symposium, "Calculation of the Shock Wave from an Underground Nuclear Explosion," Lawrence Radiation Laboratory, Livermore, Rept. UCRL-7762, April 21, 1964.
9. Birch, F., Handbook of Physical Constants, Geological Soc. of America, 1942.
10. Olsen, et al., "Temperatures and Radiation Distributions from Underground Nuclear Detonations," Internal memorandum, June 25, 1959.
11. Krover, Boardman, and Rawson, "The Shoal Postshot Environment," Internal memorandum, February 4, 1964.
12. Rawson, D. E., "Review and Summary of Some Project Gnome Results," UCRL-7166, December 12, 1962.

13. Roberts, D. W., "Project Gnome Post-Shot Radiation and Temperature Measurements," Internal memorandum, June 29, 1962.
14. Perry, J., "Chemical Engineers Handbook," 4th Ed., 1963.
15. Boardman, Rabb, and McArthur, "Characteristic Effects of Contained Nuclear Explosions for Evaluation of Mining Applications," Lawrence Radiation Laboratory, Livermore, Rept. UCRL-7350 Rev. 1, September 12, 1963.
16. Rabb, D., "A Mining Experiment in Granite," Lawrence Radiation Laboratory, Livermore, Rept. UCRL-7608, December 2, 1963.

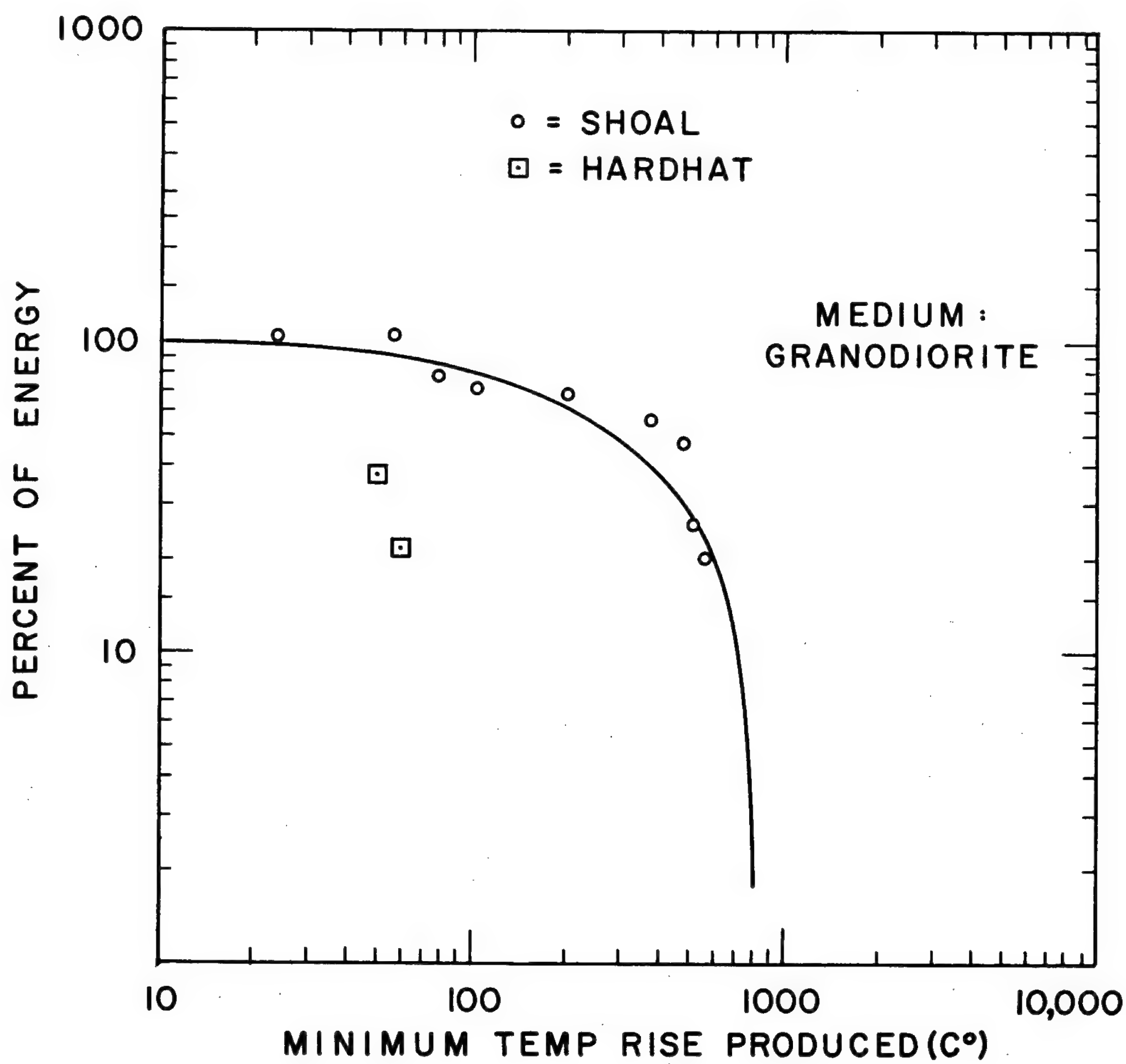

Fig. 11. Observed minimum temperature rise produced (granodiorite).

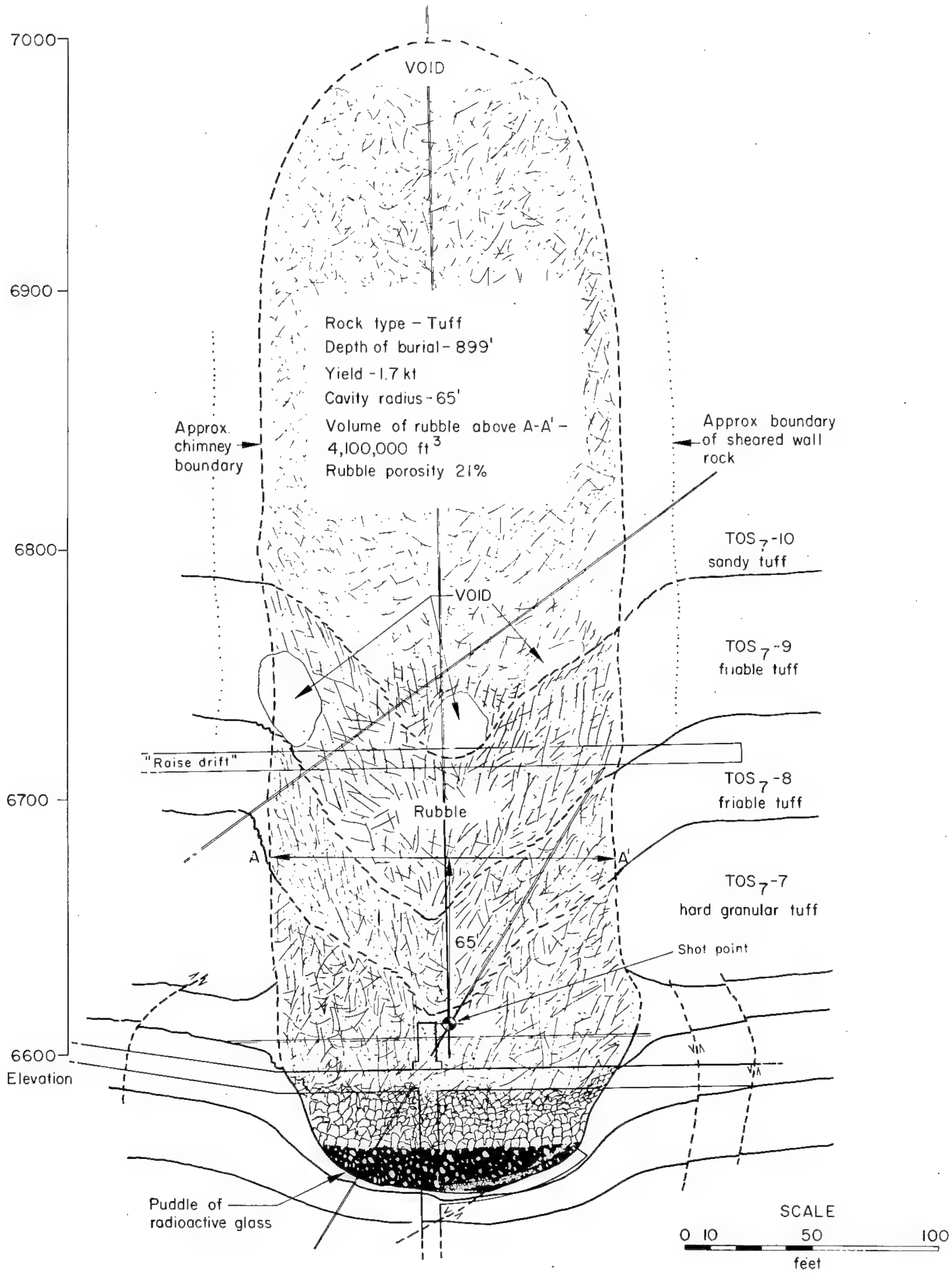

Fig. 12. Rainier schematic cross section.

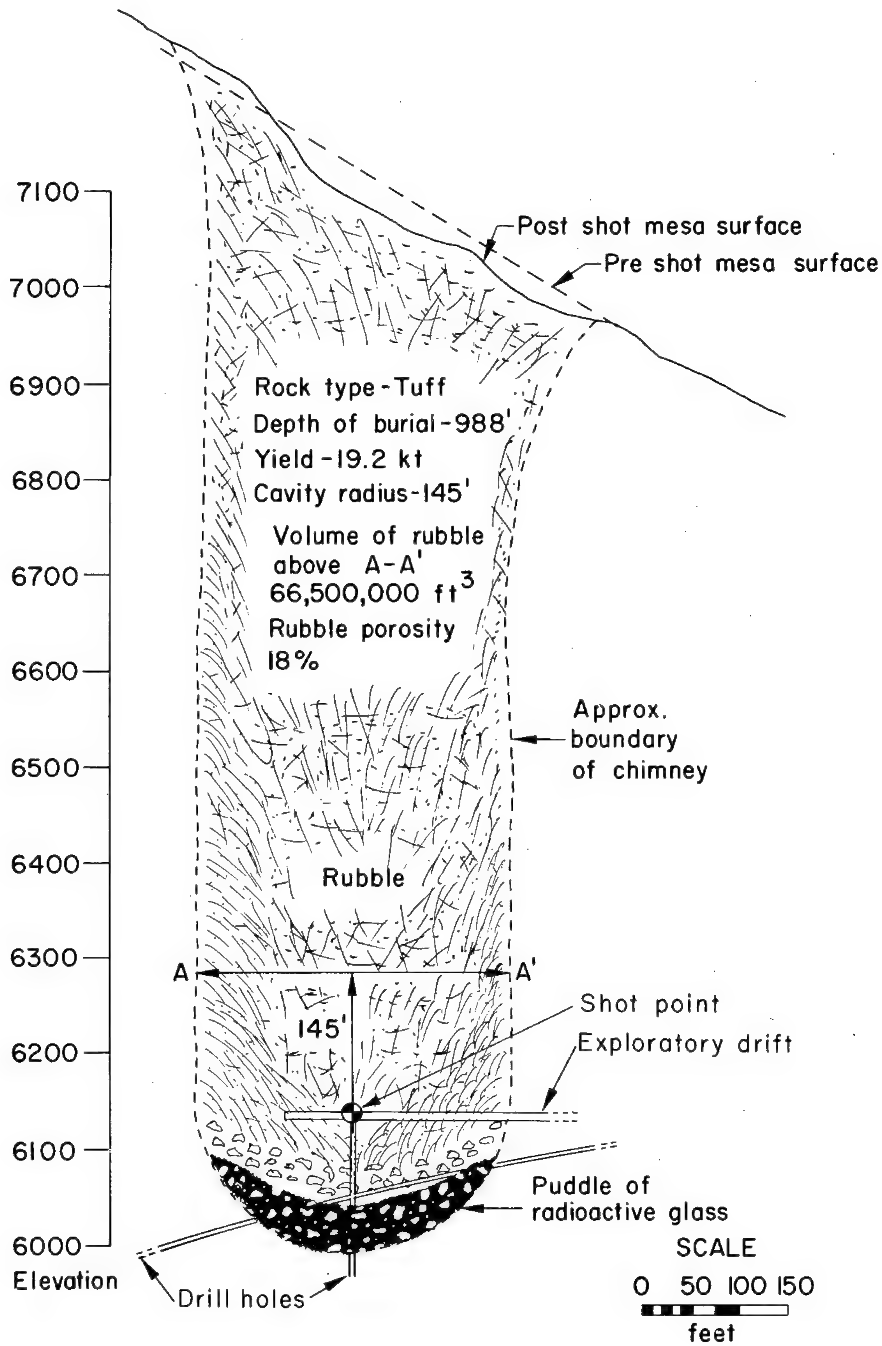

Fig. 13. Blanca schematic cross section.

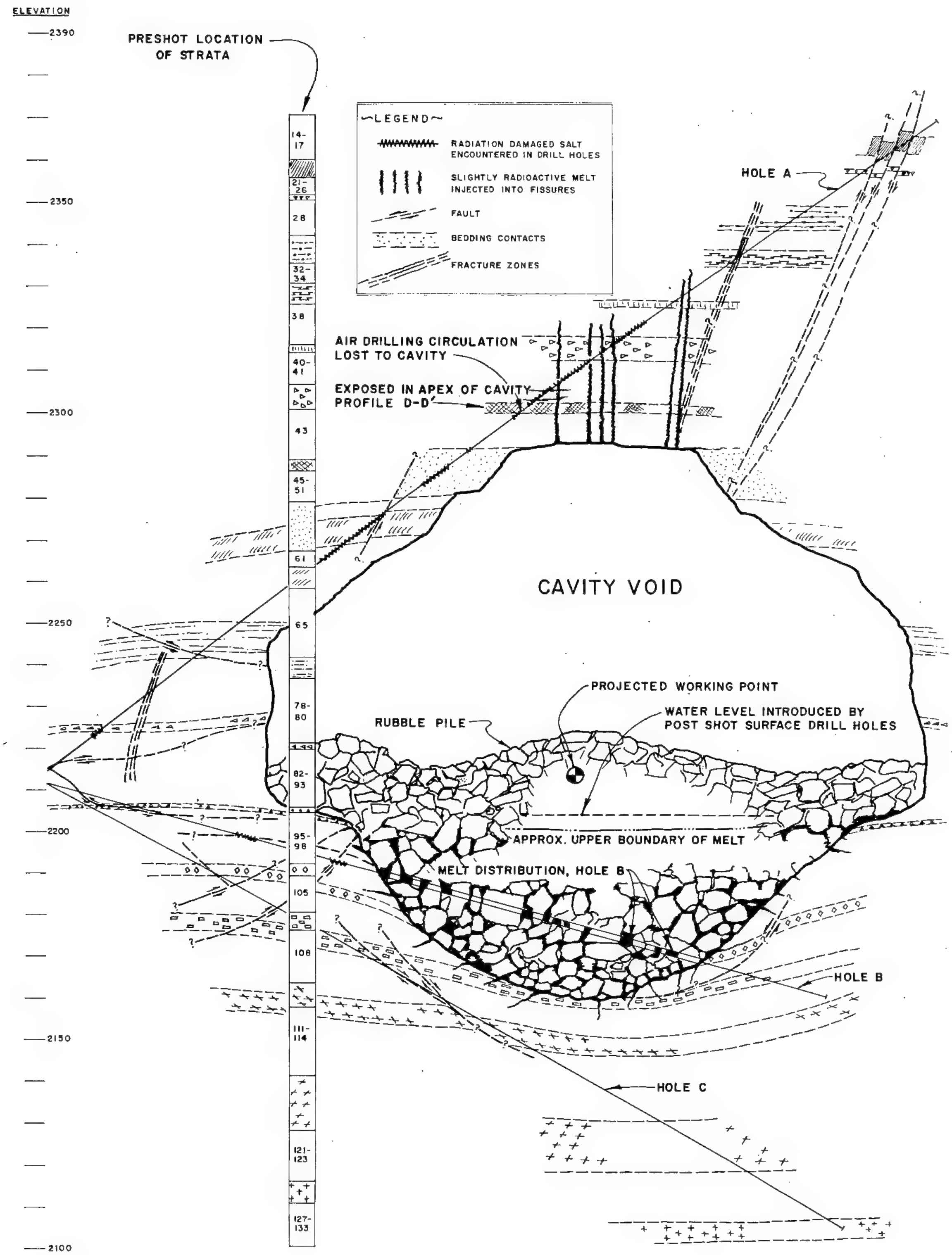

Fig. 14. Gnome cavity profile.

BIOGRAPHICAL SKETCH OF AUTHOR

Richard A. Heckman, is Section Leader of the Chemical Engineering Section at Lawrence Radiation Laboratory. He has done extensive research work in process development and evaluation studies on several of the projects within the Plowshare project, e.g., Project Gnome, Project Coach, Project Oilsand, and Project Moses. Development of sampling techniques to provide radiochemical data from both atmospheric and underground detonations led to participation in several test series: Operation Teapot, Operation Plumbbob, Operation Hardtack, and Operation Nougat. Before this, he had worked on materials development for nuclear devices and nuclear rocket core materials.

He holds a B.S. in Chemical Engineering from the University of California.

A PROPOSAL FOR A NUCLEAR POWER PROGRAM

George C. Kennedy, Professor of Geochemistry

University of California
Los Angeles, California

ABSTRACT

Substantial areas of the world are underlain by rocks of abnormally high temperature. In many places heat flow in these regions is as much as ten times that of the normal crust. Deeply buried nuclear explosives can be detonated and will produce rubble cones. The quantity of heat available in these rubble cones, made up of hot fragmented rock, is sufficiently large to appear economically interesting. A proposal is outlined for the mining of earth heat. Approximately five times as much energy is available from a cone of hot rubble as is released by the nuclear device which produces the rubble cone.

The mean heat flow from the interior of the earth to the surface of the earth in continental North America averages approximately 1.2×10^{-6} calorie per centimeter per second.

Zones or areas with much higher heat flow are known. A zone approximately 50 to 100 miles wide and several thousand miles long extends from Easter Island in the Pacific into the Gulf of California and on into the southern part of the United States where the heat flow is 5 to 8 times normal.

The average heat flow indicates a temperature gradient in a geological region of average rock type of approximately 1° C per 100 feet of depth. In areas of abnormally high heat flow, the temperature gradient may be as much as 10°C per 100 feet of depth or more. In areas of hot spring activity or recent volcanic activity, substantially higher temperature gradients may be found over extensive areas.

In many cases, deeply circulating ground water of meteoric origin is heated by a cooling magmatic body, at depths which may be as much as 10,000 or more feet. The upward-rising heated water carries magmatic heat to shallow depths and heats large volumes of rock. Enormous quantities of energy are stored in these volumes of heated rock which in many cases are larger than tens of cubic miles. Certainly, several scores of areas of this type exist in the continental United States. Steaming regions of the earth and hot springs are the guide posts to these regions of abnormally high temperature gradient. In many of these regions, temperatures of as much as 500° C may be found at depths of 10,000 feet or shallower. The amount of energy stored in such a volume of hot rock is large. It seems feasible to mine this heat via an underground nuclear blast.

Very large shots at very substantial depths are required before the economic potential of mining underground heat can be fully realized. Let us consider, for instance, the general phenomenology of a 5-megaton shot detonated at a depth of 10,000 feet in rock where the temperature at 10,000 feet is approximately 500° C. We can anticipate, by extrapolation of data from past underground shots, that a cavity of approximately 500 feet radius will be formed. This cavity will have a volume of approximately 5×10^8 cubic feet. This cavity will collapse a few seconds after its formation and a rubble cone extending upward toward the surface of the earth will form by successive caving actions. Assuming the porosity of the rubble to be approximately 12%, a volume of rubble in the cone equal to approximately eight times the volume of the cavity will be formed. This rubble cone will extend upward to approximately 2000 feet from the surface of the earth. There will be approximately 4×10^9 cubic feet of rubble in the cone and the mean temperature of this rubble will be at approximately 350° C. Water

introduced into the top of the rubble cone should flash immediately over to steam and this steam can be produced at a rate controlled by the introduction of water into the cone. If we assume that the specific gravity of this rock is 2.5 and its specific heat is 0.25, we can readily compute the available calories at temperatures above 100° C. Approximately 4.5×10^6 calories are available from each cubic foot of rock. Thus, there are 1.8×10^{16} calories of available energy in our rubble cone. This contrasts with the heat liberated by the explosive, which is approximately 5×10^{15} calories. In summary, the amount of heat available is approximately five times the energy of the explosive and this heat can be produced at a controlled rate, i.e., simply by the injection of water into the top of the rubble cone and the recovery of the steam via a separate conduit. Something like 10^{11} pounds of superheated steam can be produced from the energy of this rubble cone.

Fortunately, we can set a value on this steam. The Pacific Gas and Electric Co., is now buying steam from some steam wells at The Geysers in Sonoma County, Calif. They have completed construction of one 12,500-kilowatt generator and are now building a second 12,500-kilowatt electric generator for use of this steam. They are paying approximately $1 per 9000 pounds for the very low-pressure, low-grade steam coming from these wells. This amounts to a payment of 2-1/2 mils per kilowatt-hour of power generated. The cost of generation and transmission of the power is 3 mils per kilowatt-hour. The net cost of 5-1/2 mils makes the Sonoma County steam generating plant one of the cheapest in California.

There is enough available energy in the described rubble cone of hot rock to generate 10^{11} pounds of steam. This steam would be of higher grade, i.e., higher pressure and temperature than the Sonoma geysers steam, but if we evaluated it at the same rate the steam would be worth approximately $10,000,000. Its actual value, because of higher temperature and pressure, would be substantially more than this.

It is possible to make some rough estimates of the cost, life, and possible returns from such a venture.

The cost of drilling a 30-inch-diamter hole to 10,000 feet is estimated to be not in excess of $4,000,000 (personal communication, Hugh Gallagher). The service charge of the device to be detonated will be approximately $1,000,000. Thus, it appears that this project may be economic by a factor of 2.

Another approach may be taken to the project. With drilling costs and shooting service charges set at $5,000,000, the costs of generating electricity will be about 1 mil for the steam and 3 mils for generating and transmission costs. Thus, at 4 mils per kilowatt-hour, such a power plant would be substantially the cheapest steam plant in California. This is certainly much cheaper than any costs projected for conventional nuclear power plants even in the distant future.

Wide options are available as to the rate at which the energy is extracted from such a rubble cone. Inasmuch as we are extracting earth heat, and not the heat stored in the ground by the explosive, it is not incumbent upon us to mine this heat in a hurry lest it diffuse into the surrounding rock. Slightly more energy is available in fact, if the heat is extracted over a long period of time.

Approximate calculations show that a rubble cavity of the type described will supply energy to a 50,000-kilowatt steam plant on a steady basis for approximately 10 years. This calculation is based on the assumption that the 2000-foot cap over the rubble cone has little mechanical integrity and that high-pressure, high-temperature steam cannot be produced. If the converse is true, the higher efficiency of higher temperature steam will yield substantially more power.

Once the energy from a single rubble cone is exhausted, a second shot would be made slightly more than one cavity radius away from the first cavity. The two rubble cones would presumably coalesce, and rubble production from the second shot should be substantially greater than from the first shot. Further, water introduced into the first cone could extract some of the residual degraded heat before entering the hotter rocks of the second rubble cone.

The problem of ground motion, associated with large underground shots, is one of the most serious considerations associated with such a sequence of shots. Obviously, multiple shots around a common center could not be made if the later shots destroyed all surface installations. It seems likely that even with earthquake-proof "sprung" construction, the electricity generating plant would need to be located some miles from the epicenter of the underground nuclear shots of

the size envisioned. This does not present any particular problem. The steam can be carried substantial distances in appropriately insulated pipes with little transmission loss.

Some aspects of a deep nuclear shot in hot rock may be anticipated. Deep circulating waters may enter the rubble column and flash into steam. These will carry with them some of the heat from the surrounding regions and to this extent will increase the potential heat yield from a shot. However, in a porous, well-fractured region, this influx of ground water might be at a rate greater than that desired for steady steam production. Thus, some aspect of care must be used in the selection of drilling site and shot location.

Some question might be raised about the behavior of rubble in a rubble cone at this depth and temperature. Pressure at a depth of 10,000 feet amounts to approximately 600 atmospheres. If the shot were made in salt, limestone, or shales, we might expect very substantial compaction of the rubble after its formation and some loss of permeability through the rubble cone with time. However, if the shot were made in basalts, metamorphic rocks, or granite - common rock types in regions of high heat flow - one could expect the rubble cone to stay open and permeable for almost indefinite periods. The pressures and depths involved in this proposed shot are about the same as are currently being encountered under mining conditions in the Rand gold mines in Africa. Here, stopes filled with crushed ore stay open and permeable almost indefinitely.

There is abundant experience from block-caving mining operations which suggest that the rubble produced from a collapsing cavity ranges in size from inches up to a few feet. Only under rare circumstances do larger blocks fall in a caving operation. If we presume that the heat from these rubble cones is produced over a 10-year period, even blocks up to 20 feet in diameter will give up most of their heat before this time period is up. Only a fraction of the total heat, if any at all, will be unavailable because of the poor thermal conductivity of rocks and large-size rubble formation.

BIOGRAPHICAL SKETCH OF AUTHOR

George C. Kennedy was born in Dillon, Montana. He attended Harvard University, receiving his B.S. in Geology in 1940, his M.A. in 1941, and his Ph.D. in 1947. His professional experience is as follows: 1942-1945 U.S. Geological Survey Geologist. 1945-1949 Society of Fellows, Harvard University Junior Fellow. 1949-1953 Harvard University Assistant Professor. 1953 Harvard University Associate Professor. 1953-Institute of Geophysics University of California at Los Angeles Professor of Geochemistry.

APPLICATION OF NUCLEAR EXPLOSIVES FOR A MOUNTAIN PASS HIGHWAY AND RAILROAD

H. C. Prentice

California State Division of Highways

ABSTRACT

A study has been made of the feasibility of using nuclear explosives in the excavation of an unusually large rock cut through the Bristol Mountains near Amboy, California, for the joint use of a transcontinental railroad and an interstate highway.

The study (named Project Carryall) was made by the Santa Fe Railroad Company and the California State Division of Highways with the technical assistance of the Atomic Energy Commission and the Plowshare Division of the University of California Lawrence Radiation Laboratory.

The Santa Fe has investigated a possible realignment about 10 miles northerly of Amboy and about 1 mile southerly of a proposed highway realignment. In the Bristol Mountain area, however, this projection required either a severe southerly detour around the mountains or a 2-mile tunnel. Neither alternate was economically feasible using conventional methods.

The study group developed mutually satisfactory alternate alignments converging through the proposed nuclear cut area, and located slightly to the north of the Santa Fe's "tunnel" route. This cut would be about 2 miles long with a maximum depth of about 340 ft and a maximum top width of about 1300 ft. A total roadway bottom width of about 330 ft would be provided with the railroad located along the toe of the southerly slope, the eastbound highway through the center, and the westbound at the toe of the northerly slope. This design provides adequate width for a double-track railroad and an ultimate 8-lane divided freeway.

The tentative design provides for detonation of a row of 22 nuclear devices ranging in yields from 20 to 200 kilotons with a total yield of 1730 kilotons, to remove a volume of 68-million cubic yards.

Prior to the detonations, extensive on-site studies would be necessary. These are related primarily to safety considerations and include core drilling, seismic surveys, hydrological investigations, and population and weather surveys. This study would better define the safety problems and verify the assumptions used in the feasibility study.

Operations activities would also include the emplacement and firing of the nuclear charges, shot-time safety and control, and postshot safety measures.

Based on present knowledge of the Carryall area, safety hazards such as radioactivity, fallout, air blast, and ground shock have been evaluated and it has been concluded there would be no hazard of such magnitude as to cause significant structural damage or endanger local inhabitants.

The present Plowshare experimental program will provide additional data for the conduct and design of the project. The time schedule is compatible with the interstate highway completion schedule, the interests of the railroad company and the present experimental schedule of the Plowshare Program.

Following the detonation, detailed mapping, evaluation, and design would be accomplished in order to derive the most economical use of the excavation.

The fallback material on which the roadways would be built would be rock fragments and relatively well compacted due to the large drop height and containment by the walls of the true crater. Settlement is not expected to be a problem. Side slopes of the channel should be relatively stable, but rock-fall zones would be provided. Postshot roadway construction would be accomplished by conventional methods.

An additional 100-kiloton crater is proposed to intercept runoff from a large drainage area in lieu of diverting the flow by channel and passing it under the roadbeds through bridges.

The total cost of the most economical conventional solution is about 22-million dollars. The nuclear solution, exclusive of the cost of the devices, is estimated at about one-third less. If the 68-million cubic yards of proposed nuclear excavation were removed by conventional methods, the cost would probably exceed 50-million dollars.

The study group has concluded that Project Carryall is technically and economically feasible. The use of the resultant pass-type cut for railroad and highway purposes would effectively demonstrate the use of nuclear explosives for practical engineering applications.

INTRODUCTION

Project Carryall is the code name for the feasibility studies and possible nuclear excavation of a large rock cut or channel through the summit of the Bristol Mountains in the Mojave Desert for the joint use of a double-track railroad and a divided freeway

HISTORY

Between Barstow and Needles the present alignment of both the Santa Fe Railway and the State Highway diverge to the south of a straight line rather severely - especially through the central portion (Figure 1). Both lines also lose more than 1000 ft of elevation in descending to the Amboy-Cadiz area, and in turn must regain it at the expense of operating time and economy.

This two-lane highway is to be reconstructed to freeway standards as a portion of the Interstate Highway program. A new and 10-mile shorter alignment has been projected between Ludlow and Mountain Springs, passing about 13 miles to the north of the existing alignment at Amboy. This line will permit construction to Interstate standards, with a design speed of 70 miles per hour. Separate roadway prisms with a wide median are to be provided with a maximum grade of 3% and a minimum curve radius of 5000 ft.

Concurrently, the Santa Fe has examined the possibilities of a similar realignment between Goffs and Ash Hill as another phase of their continuing program of providing faster schedules and greater operating efficiencies. Their preliminary investigations favored a line through the Bristol Mountain area southerly of the proposed highway realignment. This line is about 15 miles shorter than their existing one, avoids the loss of elevation, and would be about 50 minutes faster in travel time. It also permits the use of present-day railroad location criteria; grades of not more than 1%, one-degree curves (5,730 ft radii), and a minimum of undulation (Figure 2). In the Bristol Mountain area, however, it would be necessary either to construct a 2-mile tunnel or excavate through a large mountain mass with solid rock cuts up to 500 feet deep, or to detour about 2-1/2 miles to the south on a line requiring heavy cuts and fills. Neither of these alternates is economically sound using conventional methods of construction through the Bristols.

In an effort to find a more economical solution, the Santa Fe approached the Atomic Energy Commission concerning the possibility of utilizing nuclear explosives to make the cut.

The State Division of Highways was in turn contacted concerning the possibility of a joint relocation and alignment through the Bristol Mountains so that it too could utilize the proposed nuclear channel.

A study group was formed early in the summer of 1963, and the first-phase feasibility study was completed in November. The group included representatives of the State Division of Highways, the Santa Fe Railway Company, the Atomic Energy Commission, and the University of California Lawrence Radiation Laboratory.

NUCLEAR EXCAVATION ALIGNMENT

It was determined that the proposed highway alignment could be shifted to the south and the railroad line slightly to the north of the tunnel route to join through the area of possible excavation. The highway line shift is about 18 miles in length, some 400 ft ± longer, but would permit the same standards. The railroad line change was about 4 miles long. The joint alignment was located to the north of the railroad tunnel alignment to reduce the maximum depth of cut and the amount of side hill excavation. Here also the same design standards may apply to the nuclear alignment as to the conventional.

NUCLEAR EXCAVATION DESIGN

A row of explosions properly spaced and detonated simultaneously, will produce a series of interconnected craters to form a channel. This channel will be roughly parabolic in cross section, with dimensions and smoothness that depend on the spacing, the depth of burial, and the size of the charges.

In Project Carryall the problem is to design the emplacement conditions and yields of the nuclear explosions so that the channel or cut produced will meet the excavation requirements of the Santa Fe and the State.

Since the railroad grade cannot exceed 1%, while the highway grade can be as great as 3%, the railroad grade was used as the datum plane for the cut.

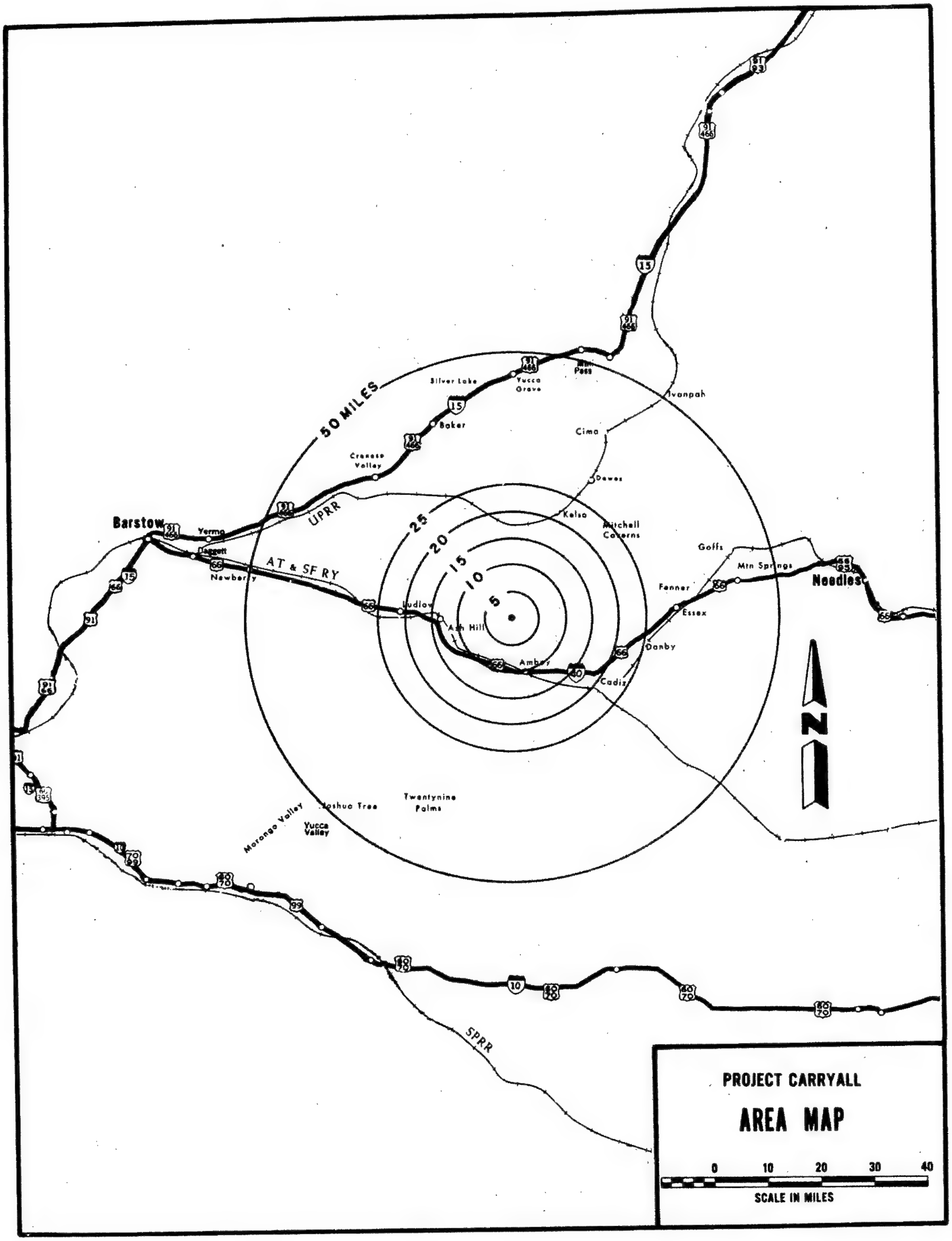
PROJECT CARRYALL
AREA MAP
0 10 20 30 40
SCALE IN MILES
50 MILES
25
20
15
10
5
Barstow
Yermo
Daggett
Newberry
UPRR
AT & SF RY
Ludlow
Ash Hill
Amboy
Cadiz
Danby
Essex
Fenner
Goffs
Mtn Springs
Needles
Kelso
Mitchell Caverns
Dawes
Cima
Ivanpah
Baker
Silver Lake
Yucca Grove
Mtn Pass
Cronese Valley
Twentynine Palms
Joshua Tree
Yucca Valley
Morongo Valley
SPRR
N

Fig. 1

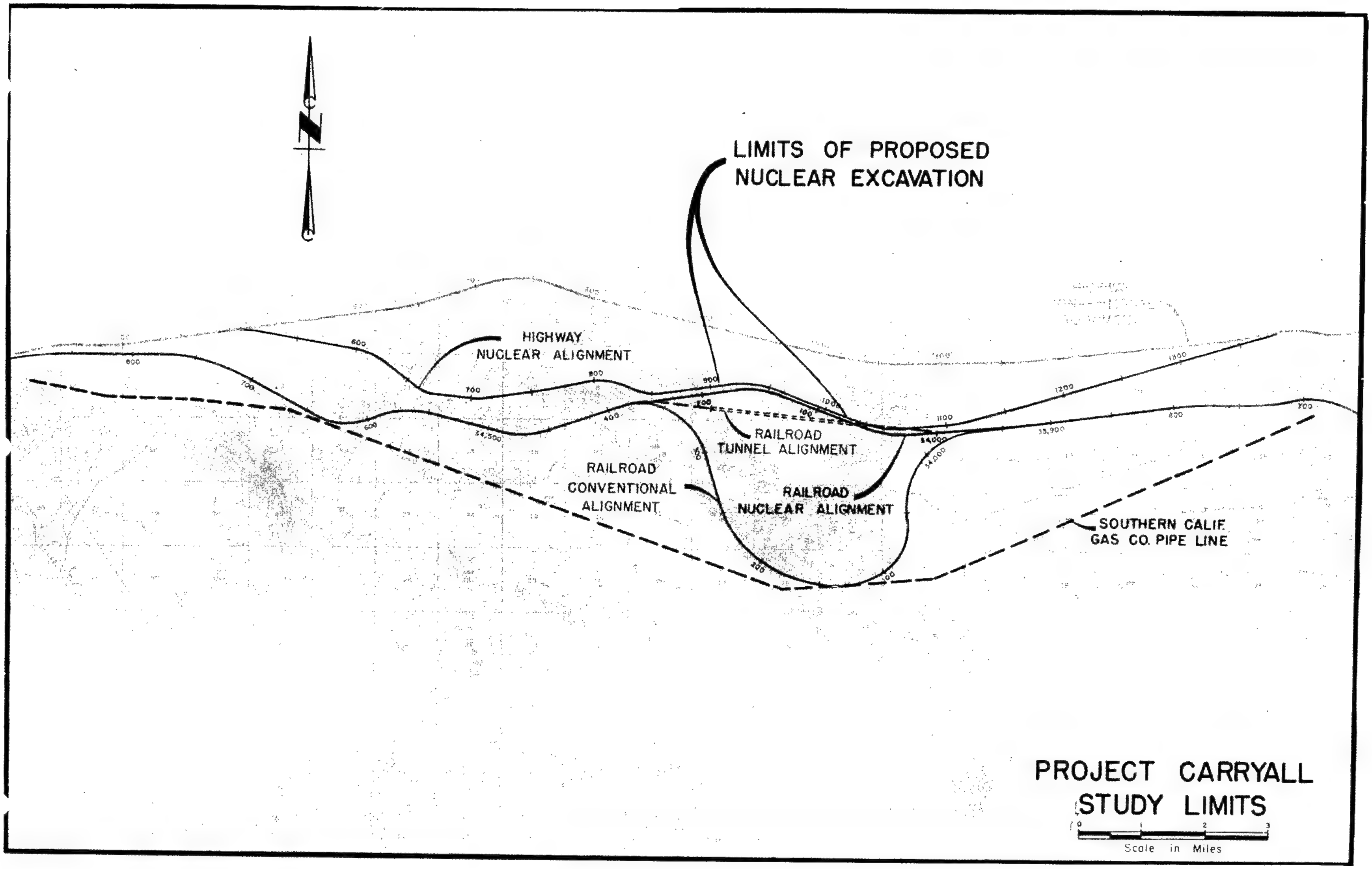

Fig. 2. Study limits of Project Carryall, showing conventional and nuclear alignments.

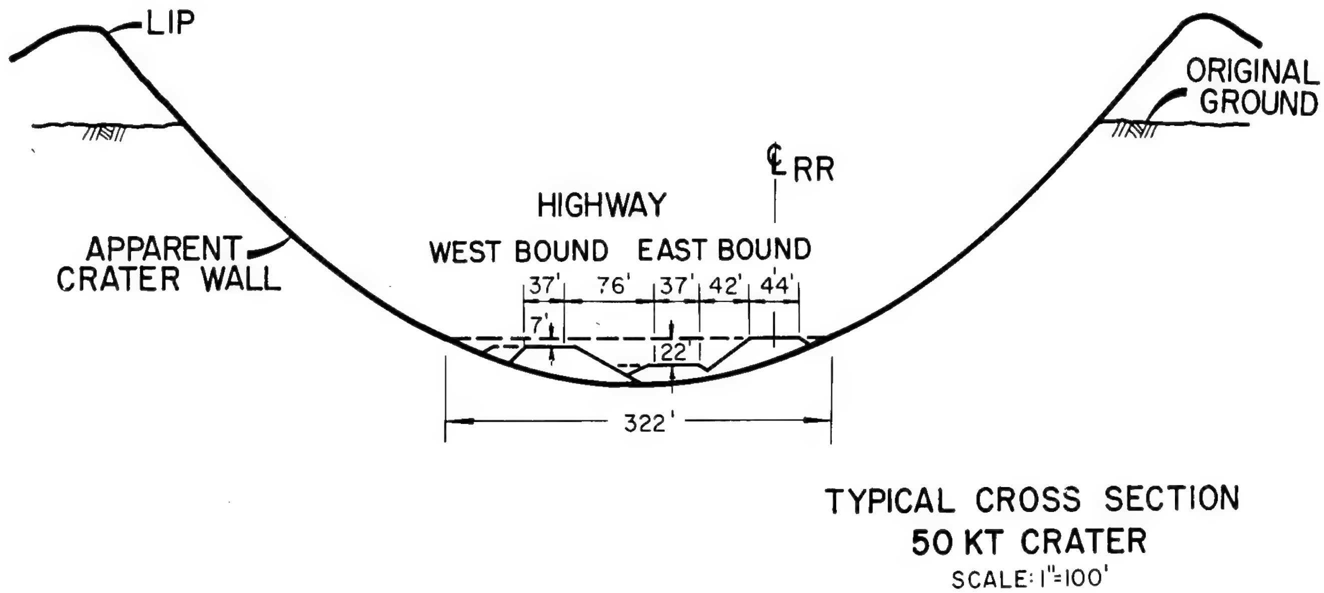

Fig. 3. Typical cross section of the roadway in the nuclear excavation proposed for Project Carryall.

One roadway of the divided freeway would be located along the bottom of the nuclear channel, with the other roadway slightly higher on the northerly slope, and with the railroad correspondingly higher along the southerly slope (Figure 3). Initial freeway construction would provide for four traffic lanes (two in each direction), with room for ultimate expansion to a total of eight lanes, with a standard-width median.

The proposed cut would be about 11,000 ft long with a maximum depth of about 360 ft, and a top width ranging from about 600 to 1300 ft. A total roadway width of about 330 ft was determined to be sufficient to accommodate both the railroad and the highway. The roadway design was based on consideration of width, grade, headlight glare, channel shape, and future highway lane requirements. It was assumed that cuts having depths of less than 100 ft would be excavated by conventional methods for technological and economic reasons. Present geological knowledge of the area indicates that the medium consists of soft volcanic rock underlain by meta-granite bedrock.

Nuclear excavation technology developed by Plowshare was applied to this problem and a tentative design developed. This design contemplates excavation by means of detonation of a row of 22 nuclear devices ranging in yield from 20 to 200 kt with a total yield of 1730 kt (Figure 4). The size, location, and depth of burial of each explosive was designed to contribute toward the result of a relatively uniform channel or cut with a bottom grade approximating the desired highway and railroad grades. The row would probably be fired in two detonations, each comprising about half of the nuclear explosives. A total volume of about 68,000,000 cubic yards would be excavated.

NUCLEAR EXCAVATION SOLUTION OF A DRAINAGE PROBLEM

There is one unusual drainage problem associated with the project. Orange Blossom Wash crosses the easterly end of the proposed nuclear alignment. Here, the proposed roadbed grades within the channel are at elevations about 100 ft below the present flow line of the wash. The conventional solution would be to divert this flow easterly to a point where roadbed elevations would permit passing it under railroad and highway bridges.

In lieu of such, it is proposed to trap this flow in a separate nuclear crater upstream from the proposed channel (Figure 5). Cuts would be made through the crater lip to train the runoff from the wash and a smaller drainage area to the west into the crater.

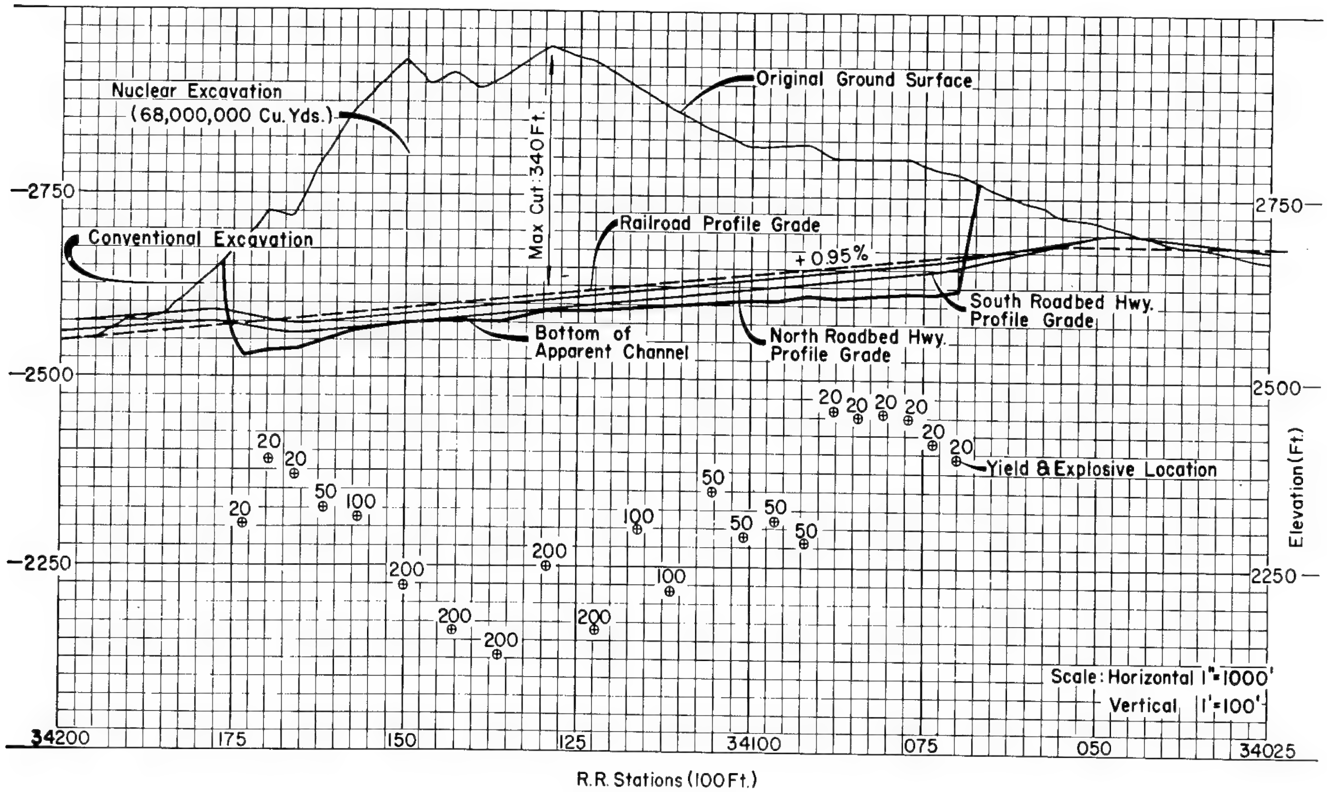

Fig. 4. Profile and nuclear explosive location for Project Carryall.

The maximum estimated storm would deliver 3,450 cfs to the proposed crater for 3 hours with a total runoff volume of 850 acre-feet. The tentative design for this crater utilizes a 100-kt explosive buried at a depth of 690 ft, which will produce an apparent crater with a diameter of 870 ft and a depth of 240 ft. This would provide a storage volume of about 1,600 acre-feet, not including the voids in the 450 ft of fallback material. (For comparison, this is almost double the capacity of the Baldwin Hills Reservoir.) Water trapped by this crater would either flow into underground storage or evaporate. If subsequent studies indicate the possibility of water seepage into the channel excavation, the location as well as the size of the crater may be modified.

PRELIMINARY SITE INVESTIGATIONS

The second phase of Project Carryall would consist of preliminary site investigations to verify the assumptions used in the first phase or preliminary feasibility study. These investigations would include geological surface mapping plus about four exploratory core-drill holes. A survey of the exact number and locations of all inhabitants and structures in the entire area would be made, and weather data and groundwater characteristics would be investigated.

Information gathered during these investigations would permit conclusive evaluation of the tentative assumptions, and, if the feasibility was confirmed, the project could proceed.

PRESHOT CONVENTIONAL CONSTRUCTION

The third phase of the project would include early additional exploratory drilling with a 3-inch core-drill at each planned location for the 23 explosive emplacement holes. This would further define the environment for each shot location.

About 20 miles of graded access roads would be constructed as well as leveled work areas at each charge location.

A 36-inch-diameter placement hole would in turn be drilled at each charge location. These

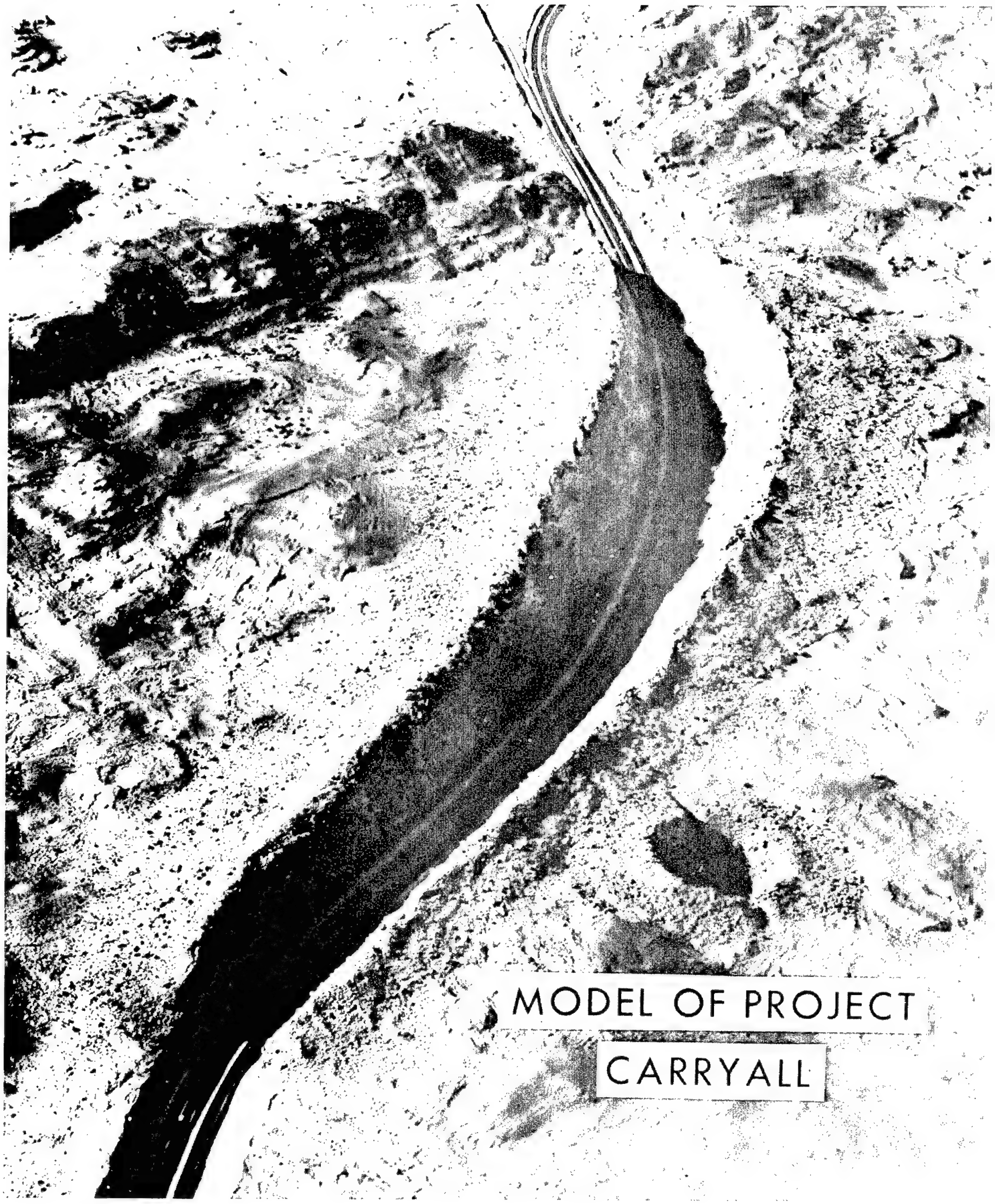

Fig. 5. Model of Project Carryall showing roadway excavation and drainage crater.

holes would range in depth from 340 to 780 ft, with a total depth of about 12,000 ft. They would be lined with 30-inch inner-diameter casings to prevent jamming of the device as it is lowered and to prevent loose rock from falling on it after installation. Substantial savings in time and cost would be possible if it is later determined that the devices may be accommodated by smaller diameter holes. There are few rigs available that can drill holes of this size in rock. Nine months time has been provided in the time schedule, and 1-1/2 million dollars in the cost estimate, for this drilling and casing.

OPERATIONAL PERIOD

The operational phase would follow the completion of roads and emplacement holes, and would include preshot safety studies, emplacement and firing of the devices, shot-time safety and control, and postshot safety measures. It is assumed the excavation would be accomplished by two detonations, each consisting of simultaneous firing of about 11 of the devices. All holes would be drilled and cased in advance of the first detonation, and holes required for the second detonation, which would be endangered by the first, would be filled with heavy mud at the time of the initial firing.

Three device teams would be used to achieve and emplacement time of 7 days. Equipment for each team would include a trailer-mounted, 15-ton, speed-controlled hoist with a drum machined to receive flat wire rope, and a 15-ton capacity head-frame with a clear height of 20 feet.

After emplacement, each hole would be stemmed with dry sand or pea gravel.

A shot-time operational control area to accommodate 8 to 10 trailers, and a device assembly area would be required. The assembly area facilities would include six 10 ft x 10 ft earth-covered igloos for storage of components and an assembly building with a 15-ton overhead crane.

A device signal system would be required. This might be either radio operated, or hard-wire circuitry.

Communications systems would include three separate radio nets as well as a telephone system.

SHOT-TIME SAFETY AND CONTROL

The Atomic Energy Commission would be responsible for public safety during detonation. Involved in this is the exercise of all on-site control and in particular radiological safety control during emplacement and detonation, and as long as necessary following detonation. When the excavated area was deemed radiologically safe for mechanical earthwork operations, the AEC would open the area for construction purposes.

Nuclear excavation poses some special safety problems not inherent in conventional construction. Should the project be undertaken, detailed studies of ground water, meteorology, geology, etc., would be required to evaluate each safety factor prior to the nuclear detonations.

Radiological Safety

The cloud resulting from each of the two row shots would be cylindrical in shape, about 2 miles high, and 7 miles in diameter. The density of dust in this cloud might be such as to obscure vision during its passage within the first 100 miles. While radioactivity levels in the cloud would not present a hazard, it might be necessary from a traffic hazard viewpoint to close any highways in the path of the cloud during passage within the first 100 miles.

Based on the Sedan experience, it is estimated that access to the channel for limited periods of time for inspection purposes would be possible within about 24 hours. Entry for an 8-hour work day or 40-hour work week without unusual safeguards should be possible within about 4 days.

Close-In Air Blast

The major problem associated with close-in air blast is related to the town of Amboy. The estimate of such predicts overpressures ranging from 0.9 to 4.3 millibars, which would not be expected to cause damage.

Long-Range Air Blast

Long-range air blast predictions are from 0.65 to 2.8 millibars. Overpressures in this range would be expected at the caustic range of between 100 and 150 miles, and are below the threshold of damage.

Ground Shock

The ground shock at Amboy would be expected to range from 6 to 10 cm/sec. Since the damage

threshold is 8 cm/sec it is possible that minor damage, such as cracked plaster, might occur; however, no large-scale damage would be anticipated.

A separate ground shock problem is related to a 30-inch, 900-psi pressure gas line located about 2-1/2 miles south of the proposed cut. It is buried except for 16 unsupported spans of between 30 and 70 feet. Such pipes are extremely invulnerable to shock and damage when buried. However the possibility of damage to the long spans is of greater concern. Plans are being made to include experiments with both buried and suspended pipe on future excavation experiments to permit precautionary measures to be developed to adequately protect this installation.

Dust, Rocks, and Ejecta

The hazard from dust, rock, and ejecta would be limited principally to areas in the immediate vicinity of the site. The area covered by the base surge, which would be approximately 7 miles wide extending for the length of the cut, would be covered with a coating of fine dust. Occasional rock missiles would be experienced at distances as great as 4,000 ft from the centerline of the cut. The principal mass of the ejecta, however, would be confined to an area extending from the lip of the crater out to a distance approximately equal to the width of the cut. Beyond that area, only dust coverage and isolated missiles would be expected.

POSTSHOT CONSTRUCTION

Following the nuclear detonations, and as soon as radioactivity had decayed sufficiently for work crews to enter (probably in about 4 days), conventional postshot engineering activity would begin. Access roads would be constructed to permit surveys, evaluation, and exploration, and revised mapping would be developed and final design completed.

The cut should approximate a parabola in cross section and be relatively smooth longitudinally. The depth is expected to be within about 5% of the design depth. The final alignments and grades of the roadbeds would be adjusted to most economically fit the slopes.

The subsequent highway and railroad construction would be performed with conventional construction equipment. The maximum rock size in such a crater generally approximates the fracture pattern of the medium. In this excavation, it is contemplated that the fallback material would include rock sizes up to about 2 feet.

No particularly difficult settlement problems are anticipated. The fallback material would be fractured rock particles in a point-bearing condition and should be similar to a rock fill or a talus slide positively confined by the walls of the true crater. The lower portions would be consolidated by the force and vibration applied by the upper layers falling several hundred feet. The use of conventional earth-moving and compaction equipment in constructing embankments on the top of this material would result in additional consolidation in the upper layers. However, settlement measuring devices would be placed at the bottom of embankments within the channel, to measure possible settlement. If indicated, corrective measures such as surcharging or additional mechanical compaction effort would be employed.

The embankments for the roadbeds would be constructed of material obtained from the conventional excavation at each end of the nuclear cut and would be topped with a blanket of alluvium readily available to the east.

No significant rockfall or slide hazard from the sides of the channel is expected. Scaling of loose rock and potential slide material would be performed during construction of the roadbeds, and adequate rockfall zones would be provided along each side of the channel.

COST ESTIMATES

Conventional Solution

Concerning estimates of costs, the Santa Fe's most economical conventional construction (although not economically feasible) would be the "Tunnel Route." The cost for the 4-1/3 miles of railroad used for comparison, including 12,800 feet of double-track tunnel, is estimated at about 14-1/2-million dollars. Almost 10 million of this would be for tunnel construction.

To provide a base for comparison of highway costs, the 18 miles from divergence to convergence of the highway conventional and nuclear routes was used. The estimate for construction on the conventional route is about 7.2 million.

Nuclear Solution

The nuclear solution would first involve a cost of about 330-thousand dollars for the second-phase studies and site investigations. About two-thirds of this would be for exploratory core-drilling.

The construction of access roads and leveled work areas, and the drilling of exploration and emplacement holes at each device location would cost about 2.3-million dollars.

The nuclear operations costs are estimated at about 1.9-million dollars. These include the additional preshot safety studies, emplacement and firing, shot-time safety and control, construction of facilities necessary for emplacement and detonation, and postshot safety measures. They do not include charges for the nuclear explosives.

The postshot construction costs for the railroad are estimated at about 2.9 million. A great portion of this is for grading into and out of the channel.

The postshot highway construction costs for the 18 miles used for purposes of comparison are about 6.3-million dollars.

Comparison of Solutions

In comparison, the total cost to the two agencies each on their own conventional alignment and using conventional construction methods would be about 21.8-million dollars, while the total estimated cost of the nuclear solution is 13.8 million, an apparent reduction in cost of about 8 million (again, not including the charges for the nuclear explosives).

It is interesting to note that if the 68-million cubic yards of proposed nuclear excavation were removed by conventional methods, the cost would probably exceed 50-million dollars. In comparison, the Carryall estimates indicate a cost of less than 5 million for this portion of the work (plus charges for the devices).

SCIENTIFIC BENEFITS

The execution of Project Carryall would provide much data of vital significance to the development of nuclear excavation technology. Its value as a demonstration of the safety, practicality, and usefulness of nuclear excavation and the interest it would generate in similar projects would, of course, be of major significance. But there would be many other scientific and engineering benefits of a much more real and lasting nature. These would include:

1. Confirmation on the accuracy of prediction techniques for row craters in a new medium through irregular terrain at yields significantly larger than any previous row experience.
2. Data on the immediate and long-range slope and foundation stability of crater slopes.
3. Data on the suitability of crater fallback debris for heavy construction purposes and the accommodation of surface drainage.
4. If fired in two or more detonations, the information on interaction between an existing crater and an intersecting crater.
5. Additional data on the nature of the safety questions associated with rows of nuclear charges.

Such information is essential to the orderly development of nuclear excavation as an engineering tool and its ultimate usage as a construction technique, and it would be of significant worth to the Plowshare Program.

CONCLUSIONS

The study group has concluded that this project is technically feasible. It can be done, and it can be done safely.

The projected time schedule for development of appropriately designed nuclear explosives, the conduct of the prerequisite experiments and the completion of the project are compatible with the Interstate Highway completion schedules and the desires of the Santa Fe.

Academically, the project is economically feasible, in that it is about 8-million dollars cheaper than the conventional alternate, not including the cost of the explosives, and it is reasonable to assume that the charges the government would make for fabrication and delivery of the devices would be less than that figure.

This comparison is academic because it compares the nuclear solution to a combination of an economically feasible highway alternate, but an infeasible railroad alternate.

The practical economic feasibility is contingent upon determination of the amounts the Santa Fe and the State could economically and equitably expend on this solution, the charges the Government would make for the explosives, and the degree of participation by Plowshare.

Continuation with the project to its ultimate conclusion is now under consideration by management of the three agencies.

If it is decided to proceed, the second-phase site investigations should be completed this summer.

Third-phase scheduling provides for completion of the preshot conventional construction and for transport and assembly of the nuclear devices by the end of 1965.

The two detonations would be scheduled for early 1966. Postshot railroad and highway engineering and final design would immediately follow, with construction under way in 1968, and with the facility under traffic by mid-1969.

BIOGRAPHICAL SKETCH OF AUTHOR

Mr. Prentice's early career was with the San Bernardino County, California Department of Public Health. In late 1942 and 1943 he was employed by the U.S.E.D. on the Honduras portion of the Inter-American Highway Project. This was followed by Army service including more than a year in the China-India Theater of Operations.

His career with the California State Division of highways began with assignments as construction inspector and progressed in turn through Resident Engineer, District Construction Engineer and District Maintenance Engineer of District VIII. Currently he is Assistant District Engineer of that District, with general supervision over all Design Departments.

NUCLEAR EXCAVATION OF A SEA-LEVEL, ISTHMIAN CANAL

E. Graves, Lt. Col.

U. S. Army Corps of Engineers
Nuclear Cratering Group

ABSTRACT

The feasibility of digging a sea-level, Isthmian canal by nuclear explosions depends on several major factors. One is the availability of suitable alternative sites. Another is the ability to make stable excavations of adequate size by means of large explosions. A third is the ability to control the potential safety hazards. Still another is the time, effort, equipment and materials required for the nuclear excavation and major conventional construction necessary to complete an operating inter-oceanic waterway. Integration of these factors into an overall plan leads to an assessment of feasibility in terms of safety, time schedule, and estimated total costs.

INTRODUCTION

Is it feasible to dig a sea-level, Isthmian canal with nuclear explosions? Answers range from an emphatic "yes" to expressions of serious doubt. This paper examines some of the important aspects of the problem on which the ultimate answer will depend.

The range of opinion results in part from different definitions of "feasible." The dictionary synonym is "possible." However, there is no longer much doubt about the physical possibility of blasting a row of holes big enough for an inter-oceanic canal. The evidence of the great natural craters, such as Meteor Crater in Arizona and the Chubb Crater in northern Quebec, is convincing.[1-3] Man has already produced nuclear explosions which would have made craters large enough for the canal had they taken place at the proper depth underground. The Sedan crater, from a 100-kiloton nuclear explosion in alluvium, showed that the general concept is scientifically sound.[4,5]

The real questions about feasibility concern cost and safety--and politics. Can the project be done at a cost which compares favorable with the economic benefits or can be justified in terms of enhancement of our defense or improvement in our international political position? Can it be done with sufficient guarantees of safety to be politically acceptable? Can mutually satisfactory diplomatic arrangements be worked out between the host country and all the countries who may be involved in the building and use of such a canal?

Scientists and engineers cannot answer the economic, defense and political questions. They can and should determine sound estimates of the cost and safety, on which the ultimate political decision will depend. Major factors affecting this determination are the alternative sites, the excavation scheme, the safety hazards and control measures, and the overall effort which the project would entail.

ALTERNATIVE SITES

A sea-level canal across the American Isthmus has been considered for over four hundred years, since the time of Balboa.[6] A French company went bankrupt trying to build one in the late 1800's. At the turn of the century the United States considered it, then decided to build a lock canal. The United States has studied a sea-level, Isthmian canal extensively since World War II. A major study in 1947 considered thirty different routes, from the Isthmus of Tehuantepec in Mexico on the north to the Atrato and San Juan Rivers in Columbia on the south.[7,8] The 1947 study concluded that conversion of the present Panama Canal to sea-level was the least costly conventional solution by a substantial margin. In 1959 and 1960 the 1947 data were reviewed, and five of the routes were studied for excavation by nuclear explosions. These five routes are shown on the map in Figure 1. The numbers and names correspond to the

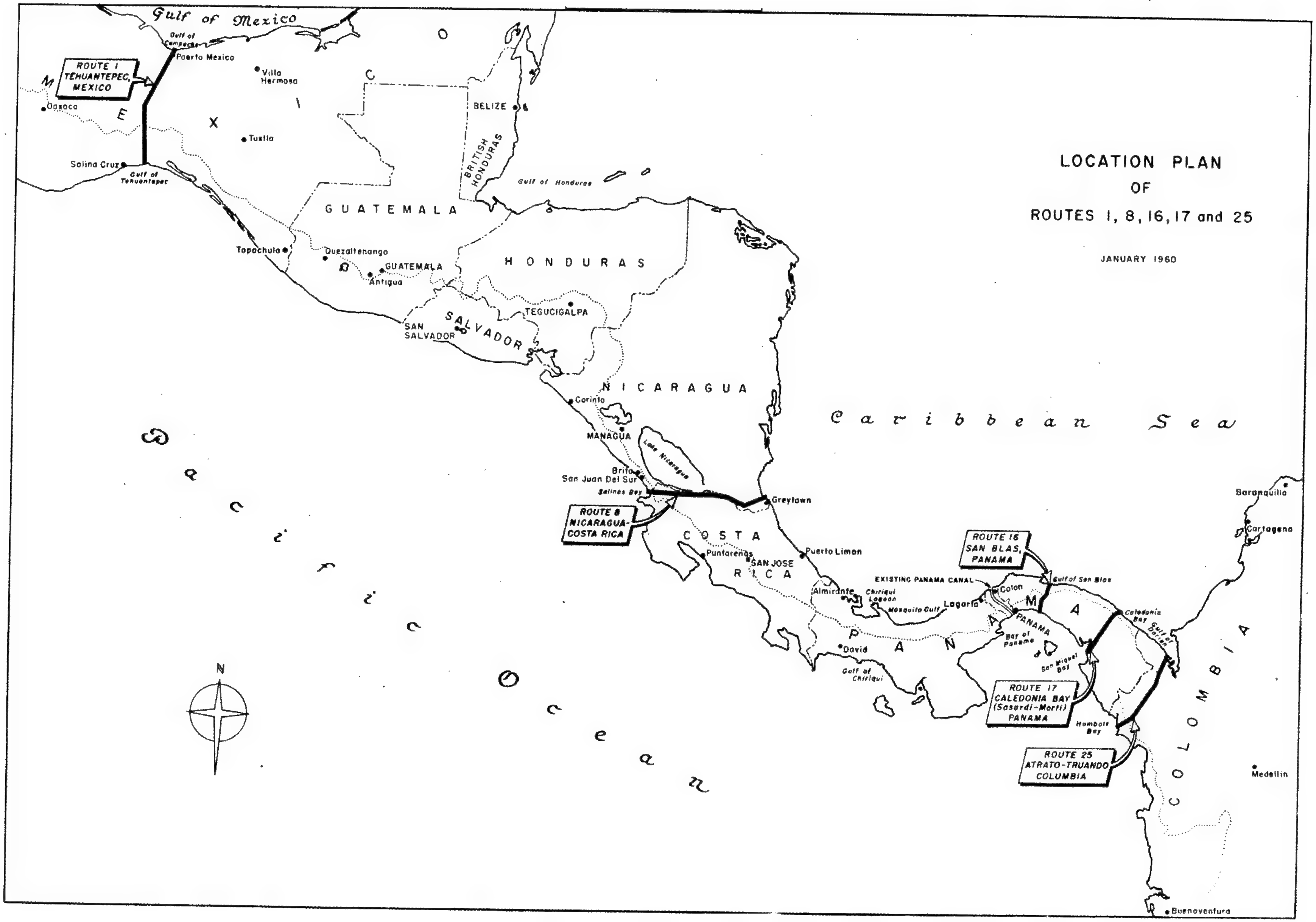

Fig. 1. Sea-level canal routes.

Table I. Sea-level canal routes

Country	Route Number	Route Name	Excavation Method	Cost Estimate From Isthmian Canal Plans - 1960
Mexico	1	Tehuantepec	Nuclear	$2,270,000,000
Nicaragua/ Costa Rica	8	Greytown-Salinas Bay	Nuclear	$1,850,000,000
Panama	14	Panama Canal Sea-Level Conversion	Conventional	$2,286,900,000
	16	San Blas	Nuclear	$ 620,000,000
	17	Sasardi-Morti	Nuclear	$ 770,000,000
Colombia	25	Atrato-Truando	Nuclear	$1,210,000,000

designation of the routes in the 1947 study. Table I summarizes the results published in Isthmian Canal Plans - 1960.[9]

Since 1960 studies have concentrated on the conventional conversion of the present Panama Canal to sea level and on the routes for nuclear excavation which combine the greatest economy with remoteness from concentrations of population. Two areas appear most favorable from these standpoints: the vicinity of Route 17, the Sasardi-Morti Route, in the Darien region of Panama and the vicinity of Route 25, the Atrato-Truando Route, in northwest Colombia.

Very little is known about these remote, primitive jungle areas. There are no good maps. Routes 17 and 25 were picked by survey parties working their way up rivers and streams. The survey profiles and the geology mapped from surface exposures are the only data available for conceptual studies. When good maps become available, a variety of alignments in these areas can be evaluated in light of the advantages and limitations of nuclear excavation. Alignments better suited to nuclear methods than Routes 17 and 25 will almost certainly result. In the meantime these two routes serve as valuable tools for generalized feasibility studies.

EXCAVATION SCHEME

The design of nuclear cuts, particularly the cut for a sea-level, Isthmian canal, has been discussed in a number of excellent papers over the last few years.[10-13] Here is a summary of the approach and results of some of the latest calculations.

The concept is to blast the sea-level channel with a row of buried nuclear explosive charges. The explosions would be designed to blow enough rubble out of the channel to leave it wide and deep enough for navigation without any excavation by machinery. The cost saving comes from the low unit cost of nuclear energy compared to the chemical energy, machinery and labor used in conventional excavation.

Table II summarizes the excavation data for the two sea-level canal routes where nuclear methods appear most promising. The cratering calculations were based on the dimensions of the Danny Boy crater from a 420-ton nuclear explosion in basalt.[14] These dimensions were scaled up by the 3.4 root of the explosive energy to determine the yields required to make the canal cut.[15] With this scaling crater size just about doubles for each tenfold increase in yield. Charges in a row were spaced a crater radius apart to assure a relatively smooth cut.[16]

The nuclear cut for the Panamanian route would require 300 nuclear charges ranging in individual yield from 100 kilotons to 10 megatons, with a total yield for all charges of 170 megatons. To emplace the charges would require drilling 300 holes with cased diameters of 36 inches for the smaller yields and 54 inches for the larger

Table II. Excavation data - sea-level, Isthmian Canal

		Route 17 (Sasardi-Morti) Panama	Route 25 (Atrato-Truando) Colombia
Land length of route		46 miles	100 miles
Divide elevation above mean sea level		1,100 feet	950 feet
<u>Nuclear Excavation</u>			
Length of cut		46 miles	43 miles
Channel dimensions:	Width	1,000 feet	1,000 feet
	Minimum depth	60 feet	60 feet
	Center depth	200 to 380 feet	200 to 380 feet
Nuclear explosives:	Number of devices	300	260
	Smallest device	100 kilotons	100 kilotons
	Largest device	10 megatons	10 megatons
	Total yield	170 megatons	270 megatons
Emplacement holes:	Diameters	36 and 54 inches	36 and 54 inches
	Smallest depth	550 feet	550 feet
	Largest depth	2,130 feet	2,130 feet
	Total depth	250,000 feet	250,000 feet
Detonations:	Number	14	21
	Average yield	10 megatons	10 megatons
	Largest yield	35 megatons	35 megatons
	Devices per detonation	4 to 50	4 to 50
	Canal length per detonation	1 to 6 miles	1 to 6 miles
<u>Conventional Excavation</u>			
Channel dimensions:	Width	1,000 feet	600 feet
	Depth	60 feet	60 feet
Quantity:	Hydraulic dredging	16,000,000 cubic yards	1,100,000,000 cubic yards
	Other conventional methods	30,000,000 cubic yards	44,000,000 cubic yards

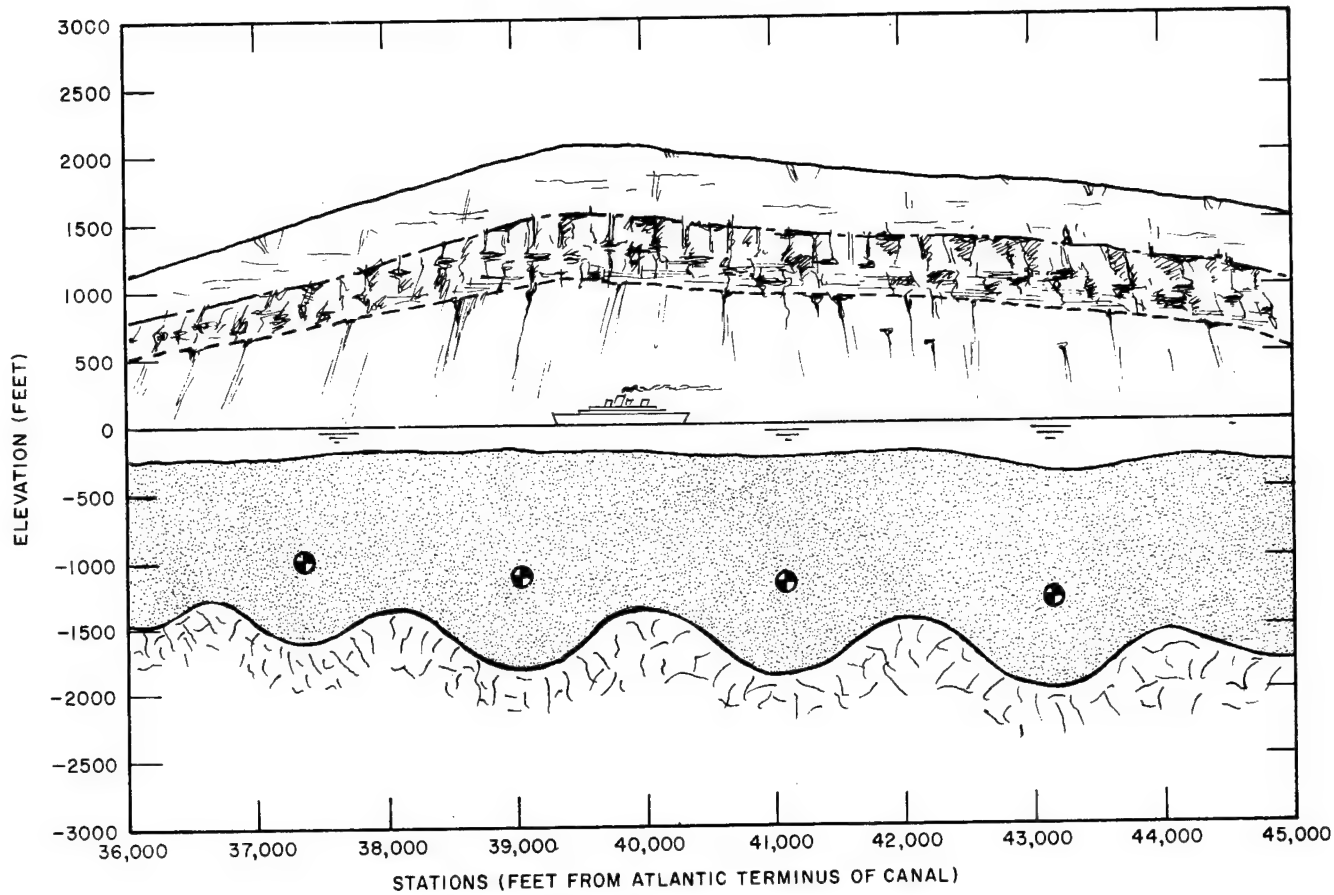

Fig. 2. Profile through Divide cut, Route 17.

yields and depths ranging from 550 feet to 2,130 feet. There would be 14 detonations. In each detonation a row of nuclear charges would be fired simultaneously to blast a section of the canal. These sections would be from 1 to 6 miles in length, depending on the depth of cut, and require from 4 to 50 nuclear charges in a row. The average yield per detonation would be 10 megatons, but a 35-megaton explosion would be required to blast the deep cut through the Continental Divide.

Nuclear excavation would be used for somewhat less than half the length of the Colombian route. Hydraulic dredging would be used for 57 miles from the Atlantic terminus to the Salaqui River. This stretch is all below 50 feet in elevation and is characterized by deep alluvial deposits of saturated clay-silts, known as Atlantic muck. There is a serious question whether nuclear craters would be stable in such material, and, in any event, the estimates for hydraulic dredging of a channel 600 feet wide and 60 feet deep are less than for nuclear excavation with 100 or 200-kiloton explosives. The nuclear cut through the the higher elevations of the Colombian route is quite similar to the cut for the Panamanian route. The main differences are a higher total yield, due to more of the Colombian route being above 700 feet in elevation, and more detonations, in order to keep the average yield about 10 megatons, for air blast and ground shock safety reasons.

More should be said about the large explosion required for the section of the canal through the Continental Divide. Our very meager information on the Sasardi-Morti area of Panama shows the Divide to be about 1,100 feet above sea level. A cut this deep by any means would be an engineering achievement of the first magnitude. To do it in less than a minute with a single explosion staggers the imagination. Nevertheless, the scientists and engineers who have studied the problem have faith it can be done. In its day the construction of the present canal was no less staggering an engineering feat.

Figure 2 is a section through the Continental Divide along the Route 17 alignment showing a conceptual view of the completed nuclear cut. The

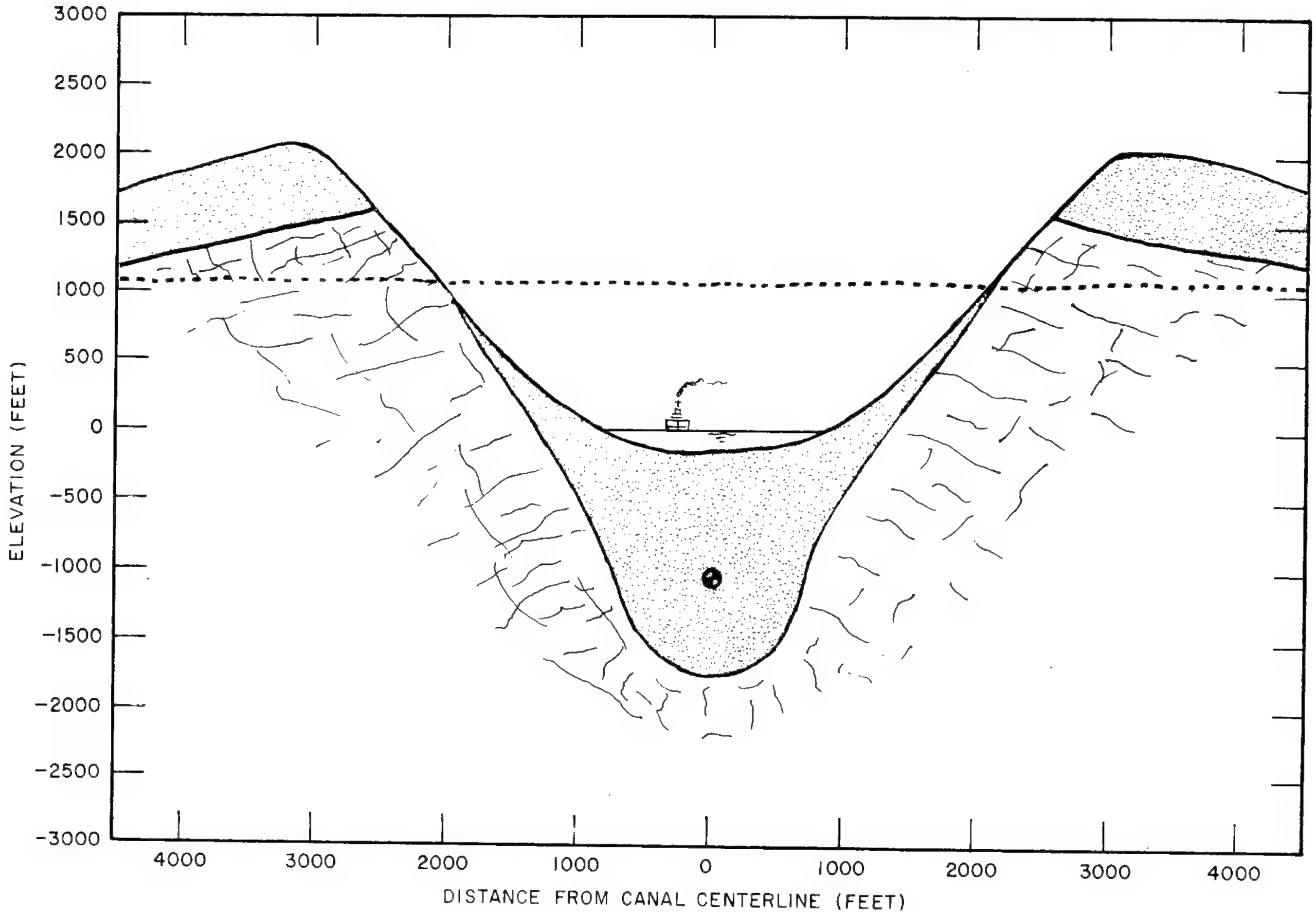

Fig. 3. Divide cut cross section at station 39034, Route 17.

present concept is to dig this section with three 10-megaton nuclear charges and one 5-megaton charge fired simultaneously. The bottom of the apparent crater would average about 200 feet below sea level. The rubble zone in the true crater would extend down 1,500 to 2,000 feet. The slopes, including the upthrust true lip and the apparent lip from throwout, would rise 1,500 to 2,000 feet above sea level, compared to the original crest elevation of 1,100 feet. The ship shown in the cut is the size of the Queen Mary.

Figure 3 shows a cross section of the cut at the position of one of the 10-megaton devices. The width of the cut at the original ground elevation would be about 4,000 feet.

The scientists and engineers do recognize that the feasibility of this cut is one of the main points which must be demonstrated by nuclear excavation development. Three questions must be answered favorably. First, it must be shown that the present scaling laws, by which we predict the size of craters from large explosions, apply well up into the megaton range, so that we can be sure a 35-megaton explosion will produce a deep enough cut. Second, it must be established that a cut this deep produced by a nuclear explosion will be stable, and the sides will not fail and slide down blocking the channel. Third, it must be determined that an explosion this large can be fired safely from the standpoint of long-range air blast and ground shock.

If the answers to these questions are not entirely favorable, then the problem may be eased by several alternatives. When the present military mapping program is completed this summer, there is reason to believe that a stretch of the Divide may prove to be less than 1,100 feet high. If so, realignment to this lower stretch would reduce the required yield of the explosion. The yield could be reduced to less than 10 megatons by leaving the

bottom half of the cut to be made by machinery. The rock in this region would be broken up by the explosion. It has been estimated that it could be removed by machinery for between $200,000,000 and $400,000,000. Making a shallower cut by the explosion and completing it by machinery would afford more control over the factors affecting the slope stability. This could allow a greater factor of safety against slide failures. Another way to reduce the yield would be to use two successive explosions, excavating part way down with the first and cutting to final depth with the second. These alternatives reinforce the judgement that the problem of the Divide cut can be solved at an acceptable cost.

SAFETY

Except for the Divide cut, the question of technical feasibility is essentially the question of safety. Can we control the main potential hazards: radioactivity, air blast and ground shock? We have estimated the extent of these hazards and compared it with our experience in nuclear testing. On this basis, at least, we are convinced the hazards can be controlled. Here is a summary of the extent of the hazards and the control measures conceived for the nuclear excavation of a sea-level canal.

Radioactivity

Radioactivity would be limited in the first instance by using thermonuclear explosives developed with the primary objective of minimizing the initial production of radioactivity. The Atomic Energy Commission has already announced substantial progress in such development.[17] Deep burial of the explosives would trap a large percentage of the radioactivity underground.[18] The prevailing winds from the north and northeast are essentially across the Isthmus and along the canal axis, so that the land area subject to fallout would be minimized. The projected levels of radioactivity in the fallout are quite low, so that dilution and decay both on land and in the ocean can be expected to reduce concentrations to harmless levels in a short time.

Figure 4 shows projected fallout patterns for the Panamanian and Colombian routes. These patterns were prepared assuming explosives projected to be available by the time the canal might be built and wind conditions averaged from prevailing winds at Albrook Field in the Canal Zone. The outside contour represents a maximum yearly gamma ray exposure of 0.5 roentgen, corresponding to the internationally accepted radiation protection guide for segments of the public. People would have to be evacuated from the area inside this contour, at least at the time of the detonations.

The current concept is to conduct the nuclear detonations over a period of two to three years, at a rate of about one per month when a series is in progress. In this dense jungle area, it would not be practical to evacuate the settlers and local Indians temporarily for each detonation. Therefore, the plan would be to work through the local government and tribal headmen, before any detonations begin, to resettle all the people from the land area where radioactive fallout would be likely to occur. The evacuation areas are shown in Fig. 4. They would be 30 to 50 miles wide at the northeast end, upwind, and about 100 miles wide at the Pacific end, downwind.

The evacuation plan would mean resettlement in adjacent frontier areas of approximately 30,000 people from the vicinity of either Route 17 or Route 25. The resettlement would be similar to programs which have been required in conjunction with some large reservoir projects except that return to most of the canal area would be permissible within a year after completion of the nuclear excavation. Current cost estimates for the sea-level canal include amounts for resettlement and new village construction.

Air Blast

The deeply buried nuclear explosions for the sea-level canal project would cause much less air blast than the same yields on the surface.[19] Nevertheless, for the large yields required, one must be concerned about both close-in damage from the direct blast wave and minor, longer-range damage from focusing of refracted waves, possibly as far away as 300 miles. Focusing can occur if there is a layer up to 200,000 feet in altitude where wind or temperature causes a higher sound velocity than at the surface.

Air blast results from the Danny Boy 420-ton nuclear explosion in basalt and the Sedan 100-kiloton explosion in alluvium were quite different. Different interpretations of these data lead to a rather wide range of predictions for the air blast effects from the canal project explosions. On the basis of Danny Boy the direct blast waves would fall to insignificant levels well within the evacuated

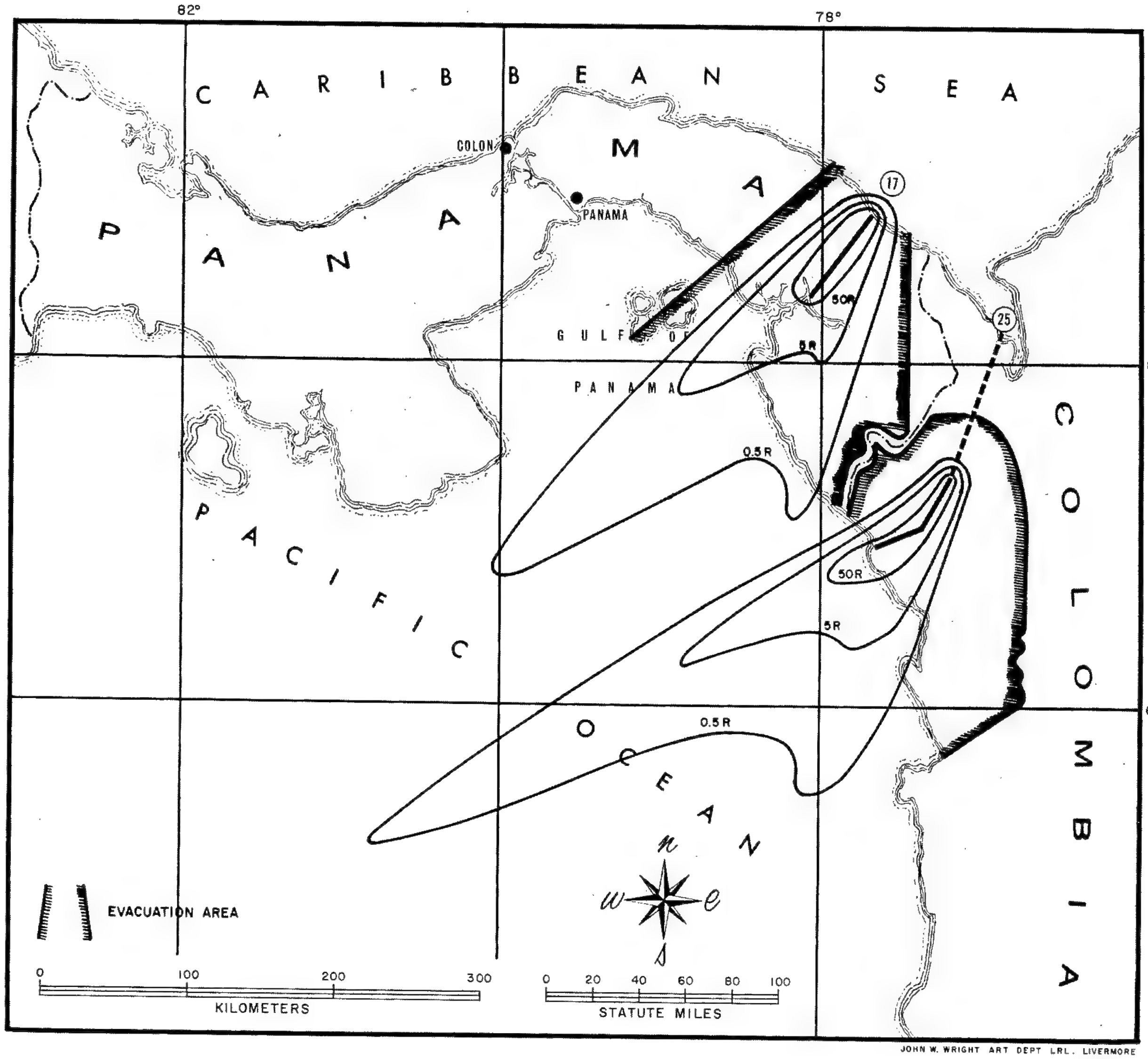

Fig. 4. Projected fallout patterns and evacuation areas, Routes 17 and 25.

area. On the basis of Sedan some direct blast damage could be expected beyound this area.

At longer ranges weather becomes the determining factor. Focusing from refraction in the troposphere below 50,000 feet should not be a problem because jet stream winds, the main cause, rarely occur in tropical latitudes. Focusing from refraction in the ozonosphere, between 100,000 and 200,000 feet in altitude, would depend on regional high-altitude wind patterns, as yet not measured. To avoid window damage in more heavily populated areas, such as Panama City, it may be necessary to restrict firing to certain seasons of the year or to limit the maximum yield. High-altitude weather measurements in the Isthmian region are essential to determine these limitations. Final determination will depend also on further studies of air blast in conjunction with large-scale nuclear cratering experiments, in order to resolve questions of the kind raised by the differences between Danny Boy and Sedan.

Ground Shock

The range of possible ground shock hazard from an underground nuclear explosion depends on a number of factors:[20,21]

size of the explosion;

coupling of explosive energy into the earth;
propagation characteristics of the regional geology;
local geology beneath structures at the range of concern;
structural response.

Information on most of these factors for the Isthmian region is limited or lacking entirely. However, experience with underground testing in Nevada gives us an idea of what to expect. Significant damage should be confined to the evacuated area, except possibly in the case of the 35-megaton shot for the Divide cut. Some minor damage might occur beyond the evacuated area. However, the surrounding jungle region is sparsely settled, and the minimal frontier construction could be fully indemnified at reasonable cost. Levels as far away as Panama City would be well below the threshold of damage. These rough preliminary estimates need to be checked by investigating the significant factors in the region of the canal routes.

The foregoing safety evaluations for radioactivity, air blast and ground shock lead to some tentative conclusions. There is a close-in region where the hazards are severe and must be handled by evacuation. There may be isolated problem areas further out. These are in the range of uncertainty where more information is needed before control measures can be worked out. The possible problems look manageable, granted the necessary development of nuclear excavation technology and surveys of site conditions.

SCHEDULE

The schedule, shown in Table III, divides the sea-level canal project into three phases. The first phase, feasibility and site selection surveys, would begin after Congress had authorized the surveys, executive agreements had been concluded with Panama and Colombia, and Congress had appropriated funds. These surveys would provide the site data needed for a thorough evaluation and comparison of the two routes from the standpoint of both cost and safety, leading to a final determination of feasibility and the most favorable route for the canal.

The second phase, engineering surveys and design, would begin after Congress had authorized construction, a treaty with the host country had been negotiated and ratified, and Congress had appropriated funds, or other financing had been arranged. The engineering surveys would provide the data for the detailed design of the canal along the selected route. During this phase contracts would be let for the initial construction for access of the main work force to the canal site, and mobilization would begin.

The third phase, construction, would begin with the movement of the first major construction forces to the Isthmus. The first work would be construction of over 200 miles of all-weather access roads through the virgin jungle and camps for 4,000 construction workers, including sanitation and medical facilities. For Route 25 hydraulic dredging at the Atlantic end would begin at once. As the first increments of roads and camps were completed, forces would move in to drill emplacement holes for the nuclear explosives. Alternate sections along the canal alignment would be prepared for the first of two series of nuclear detonations. When drilling had progressed sufficiently, the first series of detonations would begin, starting at the downwind end and progressing across the Isthmus in the upwind direction at the rate of about one detonation per month. Within a month of completing the first series, emplacement drilling would resume in the alternate sections skipped in the first pass. The second series of shots would begin again at the downwind end, blasting out the sections between the excavations made in the first series. Figure 5 is a photograph of a model of Route 17 showing the excavations made by Detonations 1-9. General construction would resume around the completed nuclear cut within a month after the last detonation of the second series. Major tasks required to complete an operating interoceanic canal would be dredging of approach channels, construction for stream diversion and other flood control works, installation of navigation aids and provision of terminal facilities for an operating force of about 600 people--compared to 14,000 for the present lock canal.

The first phase of surveys covering both routes would require 3 years; the second phase on the selected route, one year. The construction phase would be 6 years for Route 17 (Sasardi-Morti) in Panama or 9 years for Route 25 (Atrato-Truando) in Colombia. Thus the total time for surveys and construction would be 10 years for the Panamanian route or 13 years for the Colombian route. This schedule gives the time required from the technical standpoint of engineering and

Table III. Project schedule - sea-level, Isthmian Canal

	Route 17 (Sasardi-Morti) Panama	Route 25 (Atrato-Truando) Colombia
Phase I - Feasibility & Site Selection Surveys		
Field surveys in Panama & Colombia	1st Year 2nd Year	1st Year 2nd Year
Survey data analysis & report	3rd Year	3rd Year
Phase II - Engineering Surveys & Design		
Field surveys in host country; design; initial contracting & mobilization	4th Year	4th Year
Phase III - Construction		
Construction for site access	5th Year	5th Year* 6th Year*
Emplacement drilling	6th Year	7th Year*
1st detonation series Emplacement drilling 2nd detonation series	7th Year 8th Year	8th Year* 9th Year* 10th Year*
Permanent construction	9th Year	11th Year* 12th Year*
Canal completed & open for traffic	10th Year	13th Year*

*Hydraulic dredging in progess

construction, without allowance for additional time between phases which might be required for the diplomatic negotiations and political deliberations mentioned above.

Estimated Cost

Table IV summarizes the estimates of cost for construction of a sea-level canal along Route 17 (Sasardi-Morti) in Panama or Route 25 (Atrato-Truando) in Colombia, using nuclear explosions to do the main dry excavation. Nuclear excavation, including emplacement drilling, area evacuation, safety programs and explosives and firing services would be about half the cost for the Panamanian route and about a third of the cost for the Colombian route. The total cost for Route 17 is estimated to be $650,000,000; for Route 25, $1,260,000,000.

The estimated nuclear construction cost for a sea-level canal in Panama is about one-third the 1960 estimate of $2,286,900,000 for the conventional alternative of converting the present Panama Canal to sea level. The estimate for the nuclear alternative in Colombia is about two-thirds the conventional alternative. Studies in 1960 indicated that, with no change in toll rates, revenue from canal traffic projected in 1980 could carry the charges for a sea-level canal if it could be built for $1,250,000,000 or less.[22] On this basis a nuclear-built canal could pay for itself, but the conventional alternative could not.

Fig. 5. Model of Route 17 showing nuclear excavations from Detonations 1-9.

Table IV. Estimated cost of construction - sea-level, Isthmian Canal

	Route 17 (Sasardi-Morti) Panama	Route 25 (Atrato-Truando) Colombia
Phase I - Feasibility & Site Selection Surveys	$17,000,000	$17,000,000
Phase II - Engineering Surveys & Design	13,000,000	18,000,000
Phase III - Construction		
General construction:		
Construction for site access	90,000,000	130,000,000
Conventional excavation & embankments	70,000,000	470,000,000
Permanent facilities	60,000,000	80,000,000
Nuclear excavation:		
Emplacement drilling	60,000,000	70,000,000
Area evacuation	30,000,000	30,000,000
Safety program	50,000,000	60,000,000
Explosives & firing services*	150,000,000	150,000,000
Engineering	30,000,000	75,000,000
Total	$570,000,000	$1,100,000,000
Contingency (15% of Phase III)	80,000,000	160,000,000
Total Estimated Cost of Construction	$650,000,000	$1,260,000,000

*Estimate for engineering and production of a stockpile of a few hundred nuclear explosives for excavation, including services associated with firing them, given in public hearings before the Joint Committee on Atomic Energy, February 25, 1964, by Dr. Gerald W. Johnson, and further mentioned in public hearings before the Senate Committee on Commerce, March 4, 1964, by Dr. Glenn T. Seaborg and Mr. John S. Kelly. This estimate is consistent with the new charges announced by the Atomic Energy Commission.

CONCLUSION

In conclustion, current cost and safety estimates are promising for digging a sea-level canal with nuclear explosions. Clearly, there are uncertainties, but none appear prohibitive. In view of the great potential benefit of this project, what is needed is to push ahead with nuclear excavation development and on-site surveys, so that any decision can be based on sound estimates of cost and safety, thoroughly supported by field experience and site data.

BIBLIOGRAPHY

1. Shoemaker, E. M., "Impact Mechanics at Meteor Crater, Arizona, "The Solar System (Vol. 4, Planets and Comets, Part 2), Kuiper, G. P., Editor, University of Chicago Press, Chicago, 1963; also U. S. Geological Survey open file report, December 28, 1959.
2. Meen, V. B., "Chubb Crater, Ungava, Quebec," Journal of the Royal Astronomical Society of Canada, 44, p. 169, 1961.
3. Meen, V. B., "Chubb Crater, A Meteor Crater," Journal of the Royal Astronomical Society of Canada, 51, p. 137, 1961.
4. Annual Report Congress for 1962 of the U. S. Atomic Energy Commission, pp. 247-249.
5. Carlson, R. H., and Roberts, W. A., "Project Sedan, Mass Distribution and Throwout Studies," The Boeing Company, Seattle, Washington, PNE-217F, August 6, 1963.
6. Mark, G., The Land Divided, Alfred A. Knopf, New York, 1944.
7. Isthmian Canal Studies, 1947 (Report of the Governor of the Panama Canal Under Public Law 280, 79th Congress, 1st Session, November 21, 1947).
8. Special Report of the Governor of the Panama Canal on the Atrato-Truando Canal Route, 1949.
9. Isthmian Canal Plans—1960, Panama Canal Company, Balboa Heights, Canal Zone, February 11, 1960.
10. Vortman, L. J., "Earth Moving with Nuclear Explosives," Industrial Uses of Nuclear Explosives, Plowshare Series Report No. 1, Lawrence Radiation Laboratory, Livermore, Rept. UCRL-5253, September 8, 1958.
11. Vortman, L. J., "Excavation of a Sea-Level Ship Canal," Proceedings of the Second Plowshare Symposium, Plowshare Series Report No. 2, Lawrence Radiation Laboratory, Livermore, Rept. UCRL-5676, May 14, 1959.
12. Vortman, L. J., "Construction of a Sea-Level, Transisthmian Canal Using Nuclear Explosives," Sandia Corporation, Albuquerque, New Mexico, SC-4929 (RR), February 1964.
13. Fry, J. G.; Stone, R. A., and Crutchfield, W. H., "Preliminary Design Studies in a Nuclear Excavation—Project Carryall," presented at 43rd Annual Meeting of the Highway Research Board, Washington, D. C., January 13-17, 1964.
14. Nordyke, M. D., and Wray, W. R., "Cratering and Radioactivity Results from a Nuclear Cratering Detonation in Basalt," Lawrence Radiation Laboratory, Livermore, Rept. UCRL-6999 Rev. II, October 10, 1963.
15. Nordyke, M. D., "On Cratering. A Brief History, Analysis and Theory of Cratering," Lawrence Radiation Laboratory, Livermore, Rept. UCRL-6578, August 22, 1961.
16. Nordyke, M. D., "Cratering Experience with Chemical and Nuclear Explosives," presented at Third Plowshare Symposium on Engineering With Nuclear Explosives, University of California, Davis, April 21-23, 1964.
17. Annual Report to Congress for 1963 of the U. S. Atomic Energy Commission, pp. 223 and 224.
18. Williamson, M. D., "Fallout Calculations and Measurement," presented at Third Plowshare Symposium on Engineering With Nuclear Explosives, University of California, Davis, April 21-23, 1964.
19. Reed, J. W., "Air Blast from Cratering Explosions," presented at Third Plowshare Symposium on Engineering With Nuclear Explosives, University of California, Davis, April 21-23, 1964.
20. Mickey, W. V., "Seismic Wave Propagation," presented at Third Plowshare Symposium on Engineering With Nuclear Explosives, University of California, Davis, April 21-23, 1964.
21. Cauthen, L. J., "The Effects of Seismic Waves on Structures and Other Facilities," presented at Third Plowshare Symposium on Engineering With Nuclear Explosives, University of California, Davis, April 21-23, 1964.
22. Report on a Long-Range Program for Isthmian Canal Transits, House Committee on Merchant Marine and Fisheries, 86th Congress, 1st Session, June 23, 1960.

BIOGRAPHICAL SKETCH OF AUTHOR

Lt. Colonel Ernest Graves, Jr., graduated from West Point in 1944 and received his Ph. D. in physics from MIT in 1951. His military assignments have included duty with an engineer combat battalion in Europe and the Philippines at the end of World War II, staff duty in Eighth Army Headquarters and SHAPE and command of an engineer construction battalion in Korea.

His first nuclear energy assignment was with the Manhattan Project at Sandia Base in Albuquerque. He was on duty with the Los Alamos Scientific Laboratory and participated in the Sandstone nuclear test series at Eniwetok in 1948. He was in charge of organizing and training the crew for the Army's first nuclear power plant at Fort Belvoir from 1955-1957. His initial work on nuclear excavation was as a research associate in the Lawrence Rcdiation Laboratory from 1959-1961. He was assigned as the first director of the U.S. Army Engineer Nuclear Cratering Group in 1962.

EXPLOSIVELY CREATED HARBORS

John D. Isaacs

School of Oceanography, University of California
La Jolla, California

ABSTRACT

The characteristics of natural explosively or volcanically created harbors are compared with the common estaurine harbors. It is held that such harbors are immune to many of the ills afflicting estuarine harbors. Some unique harbors of other origins are also discussed. Harbor-imposed limitations on ocean-going vessels are considered, and the implications of deeper harbors to transportation is discussed. Need for new harbors is related to fishing, export, and haven. The rationale and plans for a resurvey of the Bikini Crater and environs are presented.

"This is the way to dredge a harbor, and the plough ... will have in front of it spikes shaped like ploughshares ... "

Leonardo Da Vinci (CA 1500 AD)

So far in this symposium we have dwelt upon what might be done in the engineering uses of nuclear explosives. Without departing from this theme, I wish, however, to approach the matter from a somewhat different perspective, for it is my purpose in this presentation to outline and to discuss some observations in the natural world that elucidate the opportunities for explosively generated marine harbors created under the control of man. That is, I wish to explore what nature has done; in what ways we should copy her; and which of her experiments we should avoid.

I will discuss types of natural harbors and their attendant ills; consider PLOWSHARE'S opportunities to avoid these ills; present some glimpses into unique harbors that suggest unusual opportunities for explosive harbor construction; and consider the world's needs for merchant terminals and small craft havens.

Also briefly mentioned, are plans for a resurvey of the Bikini craters and an outline of the insight into PLOWSHARE factors that I believe we can glean from such an inquiry. Most of the matters discussed are covered very briefly. For a thorough coverage of specific aspects I have some references.

In general, harbors found on emergent coasts differ from those on submergent coasts, but since the most recent world-wide geological event has been the glacial retreat and the consequent considerable rise in sea level, most coasts have been submergent in the time scale of 10,000 to 25,000 years. Thus, the origin of most of the world's present harbors is traced to the progressive inundations of river and glacial valleys, and other land features. Glacial rebound and other earth movements alter this trend in some localities, but the great majority of the harbors of the world are drowned topographic lows and one origin or another, and as topographic lows, they are almost universally subject to fresh water run-off and sedimentation. Without question sedimentation is the single most important factor in the configuration, limitation of draft of ships, and cost of harbor development and maintenance. Only harbors formed in great glacial valleys, faulted regions and coral atolls enjoy any partial immunity to sedimentation problems and here the relative immunity

is only a temporary condition resulting from the magnitude of the basins. That is, in these cases, sedimentation merely has not yet entirely caught up.

Even those harbors that we are wont to regard as ideal, such as Puget Sound, San Francisco, and Tokyo, are not immune. Despite the ostensibly deep portal of the Golden Gate, the offshore bar of the harbor of San Francisco is a profound limitation, a significant danger, and an expense to maintain at useful depths.

Leonardo Da Vinci well understood the role of sedimentation and the influence of man's activities upon it, as shown in the following two quotes from his notebooks:

"I perceive that the surface of the earth was from of old entirely filled up and covered over in its level plains by the salt waters, and that the mountains, the bones of the earth, with their wide bases, penetrated and towered up amid the air, covered over and clad with much high-lying soil. Subsequently the incessant rains have caused the rivers to increase, and by repeated washing have stripped bare part of the lofty summits of these mountains, leaving the sight of the earth, so that the rock finds itself exposed to the air, and the earth has departed from these places. And the earth from off the slopes and the lofty summits of the mountains has already descended to their bases, and has raised the floors of the seas which encircle these bases, and caused the plain to be uncovered, and in some parts has driven away the seas from there over a great distance.

"The rivers make greater deposits of soil when near to populated districts than they do where there are no inhabitants, because in such places the mountains and hills are being worked upon, and the rains wash away the soil that has been turned up more easily than the hard ground which is covered with weeds."

Sedimentation is by no means exclusively a characteristic of humid rainy coasts. Quite the contrary, the maximum sedimentation is found on semi-arid coasts where erosion is greatest. Such coasts may now be virtually harborless. A millenium or two ago the coastal valleys of Southern California were deep, long oceanic inlets where Indians harvested fish and molluscs. In the brief time of increasing aridity of the area, however, sediment completely filled these valleys. In a small valley where I live, which was a harbor 1000 years ago, the rate of sedimentation was of the order of one-million cubic yards of material per year over several thousand years. This total of about one-quarter of a cubic mile of sediment in 2000 years, is, of course, carried to sea by the Mississippi in only about two years, but illustrates the dimensions of the problem even in small harbors.

I wish to pursue this matter of sedimentation of harbors to some degree, for not only is sedimentation the most important factor in most present harbors, but also PLOWSHARE provides a potential emancipation from this ill because of the freedom it grants in the selection of sites!

As I already have said, most natural harbors of this world, whether drowned river or glacial valleys or faulted blocks, intercept fresh water drainage. This drainage carries with it a suspended load of silt and coarser material. A bed load of coarse material also is carried, especially in time of freshet. Silt and other fine material may settle in any quiet waters of the harbor and especially in regions where ionic floculation results from the mixing of fresh and salt water. The fine material also is precipitated at sea at such depths and width of the river, as tidal and wave currents permit. In the morphogenesis of a harbor this is the beginning or outpost of a baymouth bar or spit, which eventually will receive coarser material from littoral drift along the coast, or from the development of the more highly channelized flow within the bay that is capable of carrying the coarser material to the bay-mouth.

On sediment-rich coasts, both of these processes are important. Longshore transport of sand often dominates, and this has been responsible for some of the fiascos of harbor construction. The Santa Barbara Breakwater and the Ceara Harbor in Brazil are important classical cases of serious sedimentation, and there are many others.

The effect of longshore transport is exemplified by Figure 1, that shows the entrance to Nestucca River on the Oregon Coast crowded against Cape Kiwanda by the implacable southward transport of sand. The accumulation of littoral drift against the north jetty of the Columbia River (Figure 2) forms the hazardous Peacock spit. In Figure 3 is shown the Columbia's own special contribution to navigational hazard: Desdemona Sands, and Jetty Sands - baymouth bars on which the swell of the North Pacific break almost constantly. (My own particular argument with the Columbia in which I lost both craft and crew and spent some

hours swimming, began over Jetty Sands in rough weather.)

Figure 4 displays the classical case of the Santa Barbara breakwater where longshore transport, engendered by the perpetually oblique waves, has (through a series of steps) finally necessitated the dredging of some 100,000 cu. yards of material for the forseeable future. Prior to this dredging, the construction also set up an erosional wave that over a number of years slowly passed many miles down the coast and destroyed much property.

A priori, it is by no means clear why the equilibria between estuarine harbors, the sea, and sediment should be such that entrance and channel depths, both natural and maintained, should be limited to about 3 to 8 fathom, as they are. Estuaries and river mouths vary by at least a factor of 100 more in width than in depth! It is clear that two limits undoubtedly dominate: the depth of significant wave motion off the harbor mouth, and, in the channels, the depth at which turbulence is sufficient to reach the bottom inter-

Fig. 1. The entrance to the Nestucca River on the Oregon coast illustrates the condition sketched in Figure I-1-4. An excess of fine debris has filled in the bay and built the spit; seacliff at the right is protected by a sandy beach and the coast fairly straight.

Fig. 2. Peacock Spit North of the Columbia River Entrance. This is a treacherous area and has been responsible for the loss of a considerable number of ships in recent years. Depths inside the Columbia River Entrance are adequate for any vessel.

Lat. 46° 16'

face; that is, a depth is approached that is sufficiently shallow so that the currents develop no significant laminar layer against the bottom. Some lesser depth than this latter is required to bring sediment transport into partial equilibrium with supply.

This curious limiting depth and the sediment transport inflict two unhappy requirements on ocean traffic about the oceans of this planet. First, ships cannot be operated that have greater draft than about 35, or at the very greatest, 47 feet. This generally restricts the feasible tonnage of ships, as will be discussed later. Secondly, with the exception of the rare harbors still in the erosion stage and "with which sedimentation has not yet caught up", a large, expensive, and often

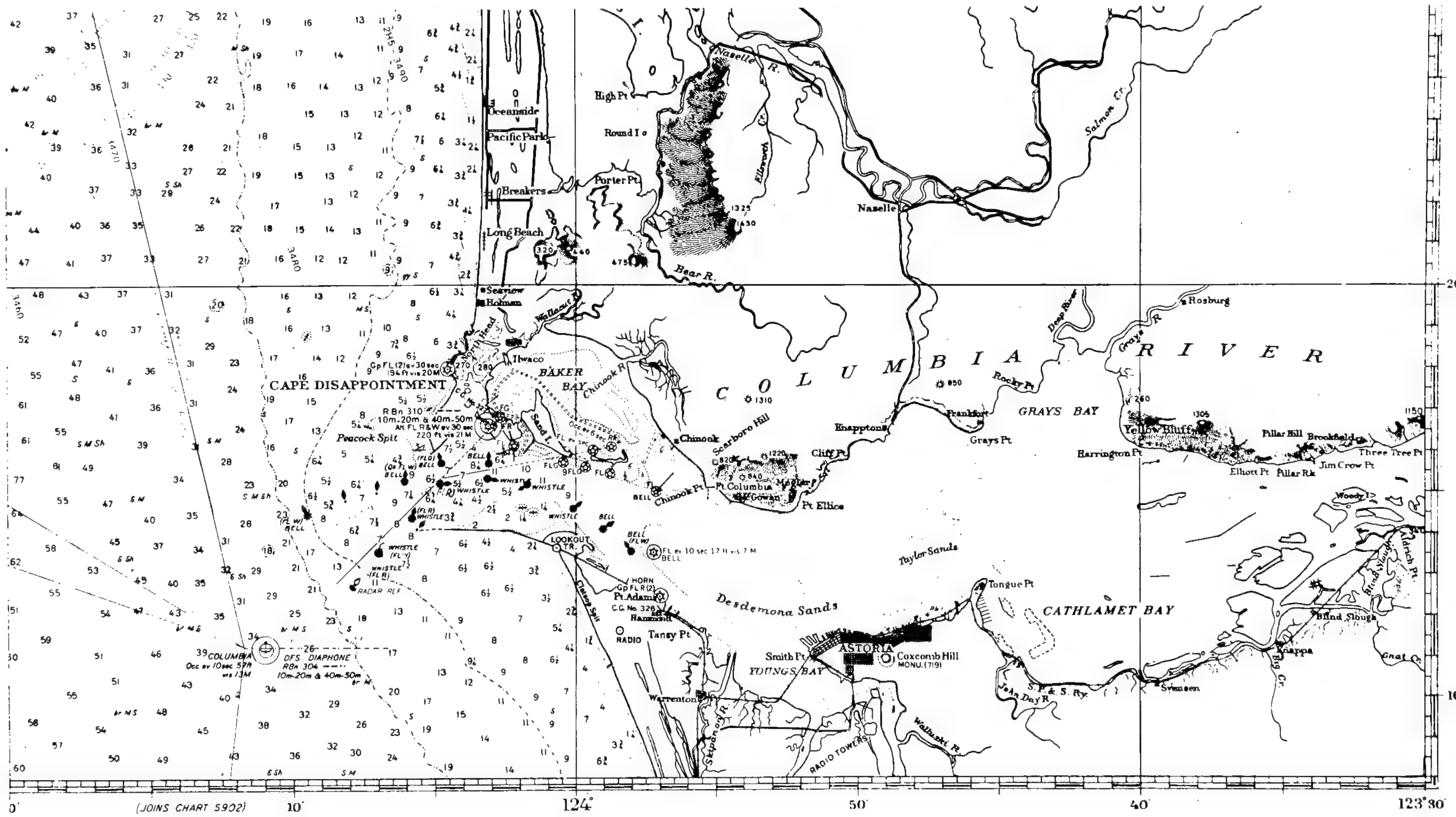

Fig. 3. Map showing Desdemona Sands.

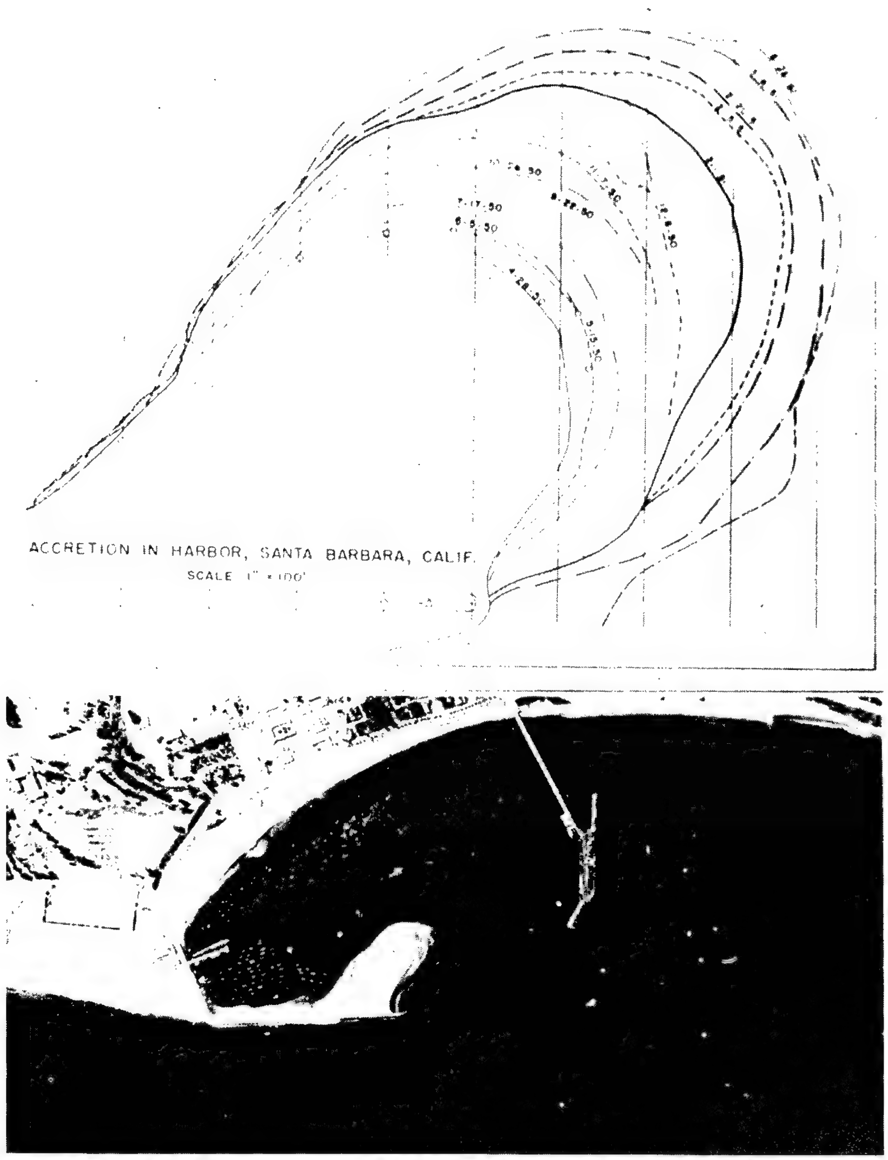

Fig. 4. Santa Barbara, California, has a serious sand and beach problem created by the construction of a breakwater. Sand which moves eastward along the coast (left to right) under the influence of the prevailing westerly waves is unable to pass the breakwater and deposits in its quiet lee. Besides blocking the harbor, this starves the beaches at the right of the picture, which retreat rapidly. The upper diagram shows successive stages in the growth of the sand spit. The sewage, lower right, shows that currents exist even on this calm day.

unsatisfactory dredging program must be maintained. The magnitude of this problem is apparent in that the annual cost of harbor projects in the United States is between one-half and one-third of the annual income to all shippers, foreign and domestic, for all cargo carried through U. S. ports.

The other ills of conventional harbors are sometimes also extremely serious defects. The entrances of many harbors are often impassible because of the breaking of swell in the outer harbor. Figure 5 is a photograph of the Coquille Harbor on the Oregon Coast closed by winter swell. On our own Pacific Coast of the United States, all harbors between San Francisco and the Straits of Juan da Fuca are often closed by swell to all shipping except for the small-boat harbor of Depoe Bay, a curious harbor that I will inspect later.

Ice and log flotsam, nipa rafts, floods, tidal bores, surging and seiching are other troublesome, dangerous, or crippling conditions of conventional harbors. Ice forms more readily on fresh or brackish water than on sea water because of the stabilities and temperatures involved and hence is common in river estuaries. Logs and nipa rafts also are dangerous obstacles in river estuaries. Floods carry ships out of control and rapidly alter channels. Tidal bores, as occur on the Hooghy, Severn, Yangsi and Colorado, are dangerous waves that ascend the rivers during spring tides. They are almost unknown outside of fluviatile estuaries, except in such extreme cases as the Bay of Fundy and some Norwegian fjords. Surging is a resonant oscillation that is especially troublesome in small harbors.

An inspection of the harbors of the world reveals some few that are probably virtually permanently immune to many of the chronic illnesses of conventional harbors.

One of these, Pago Pago, presents us with a picture of an explosively generated harbor. Pago Pago in western Samoa is a breached volcanic caldera. Perhaps some subsequent faulting has contributed to the formation. As can be seen in Figure 6, the entrance to Pago Pago is very deep, 30 to 40 fathom, and the inner harbor is more than 16 fathom in depth. Such breached volcanic craters are rare in the coasts of this planet. The Greek Island of Thira, is of this ilk, but most of the protecting crater wall has been blown or eroded away and the harbor is poorly protected. The coral atoll of Taongi may be built on a basement of an eviscerated volcano, for the depths between the north and south cornu of this island exceed 1600 fathom. Haunauma Bay on Koko Head probably was breached by erosion of one crater wall, coral has subsequently grown on the debris and it is shallow, but most deep calderas or eviscerated volcanos have either occurred well removed from the sea, as Crater Lake, or have completely obliterated any significant remnants of the crater wall, such as in the case of Krakatoa.

Thus the production of useful harbors by cratering has been a rare event, and we should take a few minutes to examine the reasons for this, for vulcanism is common, especially along the rim of the Pacific.

For a useful harbor to be formed, not only must the process have taken place near sea level, of course, but the breach must have been or now be well below sea level. Most of the crater rim must have been preserved, but lava flows and ejecta cannot obstruct the entrance. Yet the ejecta and material of the crater must be dense and resistant. Various volcanos of the Aleutians, the famous Falcon Reef and others, are rapidly planed to sea level because of the light cinder of which they are composed. Figure 7 shows a diver on the submerged summit of Falcon Reef, which only a few decades ago was some hundreds of feet above water. In fact, sea level volcanos only rarely are of a dense lava and it is believed that this is because of the access of an abundance of deep ground water to the lava pipe, which then produces much pumice and cinder. Harbors of meteorite origin do not appear to exist. Indeed the total rarity of craters of meteorite origin would almost preclude their occurrence along a shoreline.

Thus, for natural explosively generated harbors we must be content with a very few examples of which the excellent harbor of Pago Pago is perhaps the best. From the single example of Pago Pago, however, it is clear that explosively generated harbors in resistant material, with adequate but not excessive communication to the sea, and not associated with rivers or other sources of sediment, can be remarkably superior to the common estuarine harbor.

The fact that PLOWSHARE harbors can be located so that they are free of the serious effects of run-off drainage does not preclude their rapid deterioration from the longshore transport of sediment. This can be avoided only by a further consideration in the choice of location.

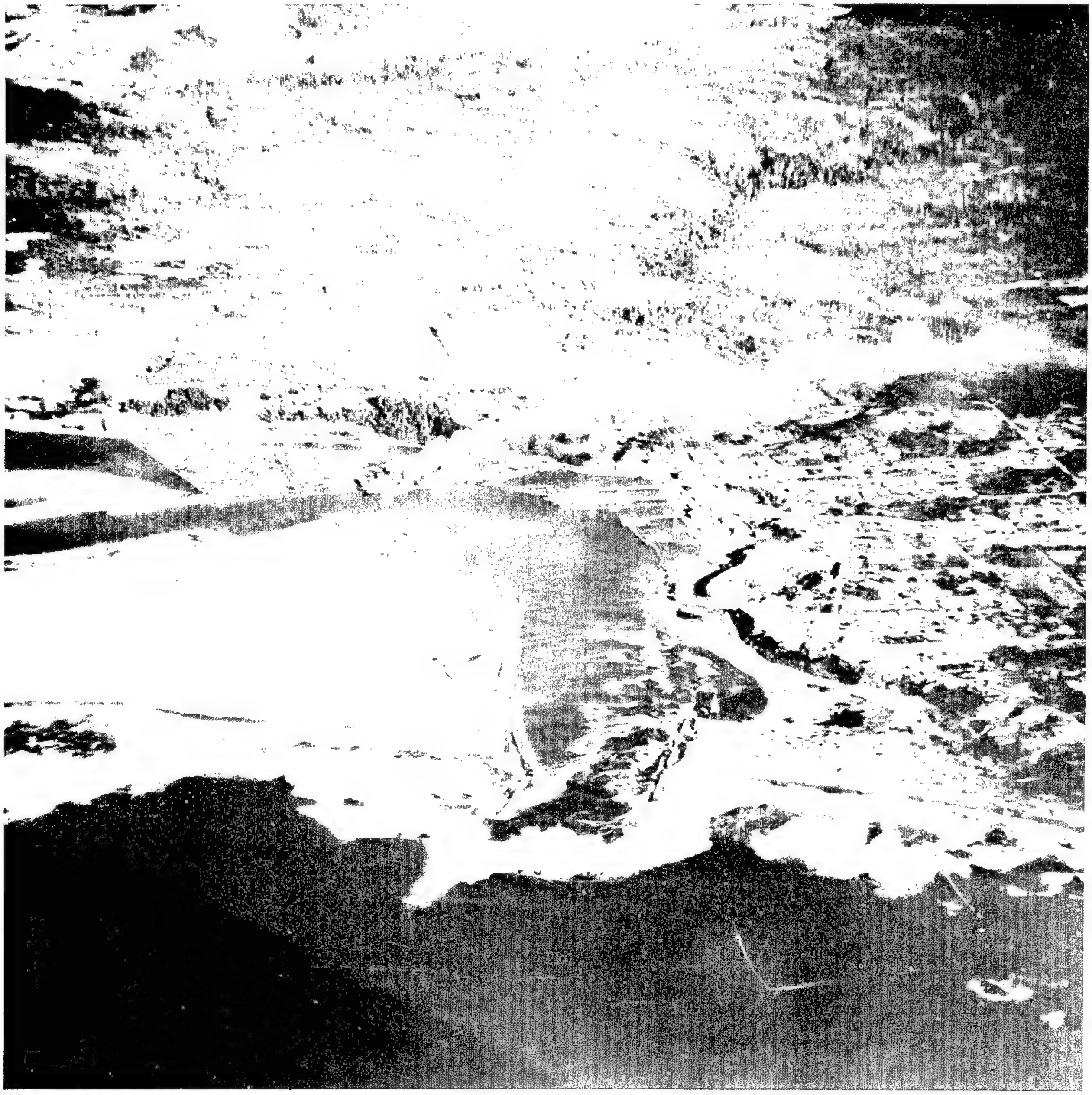

Fig. 5. Coquille River entrance. This entrance is improved by two jetties, the northern one being a monolithic concrete structure. Depths on the entrance are sufficient for coastal lumber schooners of light draft. The surf existing at the time this photograph was taken would preclude use of this entrance by any craft. In the summer and prior to winter freshets, bars are apt to shoal.

Lat. 43° 07'

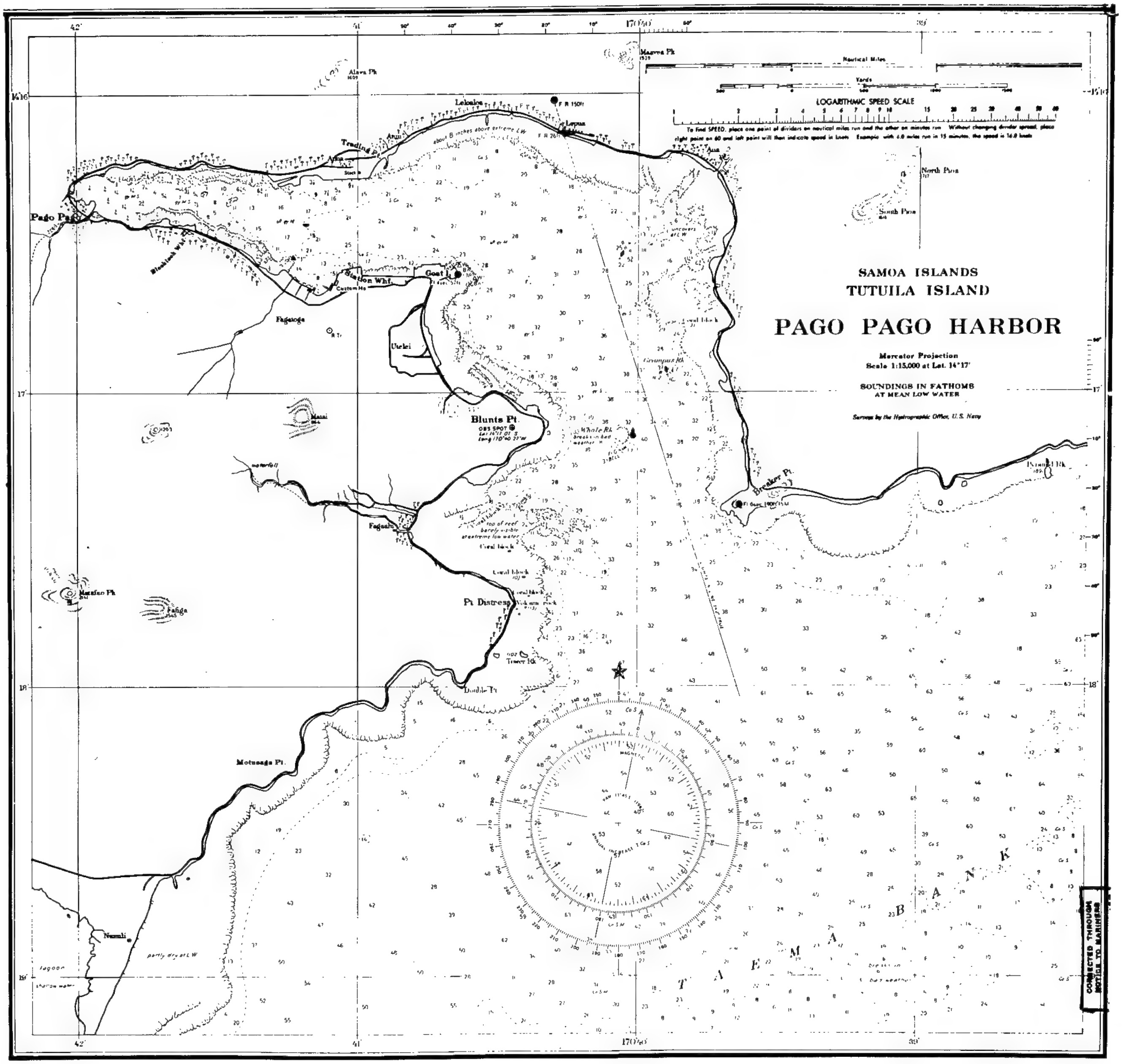

Fig. 6. Map showing entrance to Pago Pago Harbor.

Two possibilities exist. The first includes the case of Pago Pago that is located on a reach of prominent rocky coast. Such regions are not influenced to any consequential degree by longshore sediment transport and, hence, are excellent sites for the construction of explosive harbors. Great stretches of these emaciated coasts are harborless, but some other portions contain excellent small harbors and refuges.

One harbor on such a coast particularly possesses a set of unique characteristics that is worthy of close attention by PLOWSHARE planners. This harbor is Depoe Bay on the central Oregon Coast, to which I previously referred as often being the only available harbor along almost 1000 miles of coast during heavy weather. (Figure 8) This harbor is on a hard basaltic portion of the coast where there is little sediment. Although it is use-

Fig. 7. Summit of Falcon Reef.

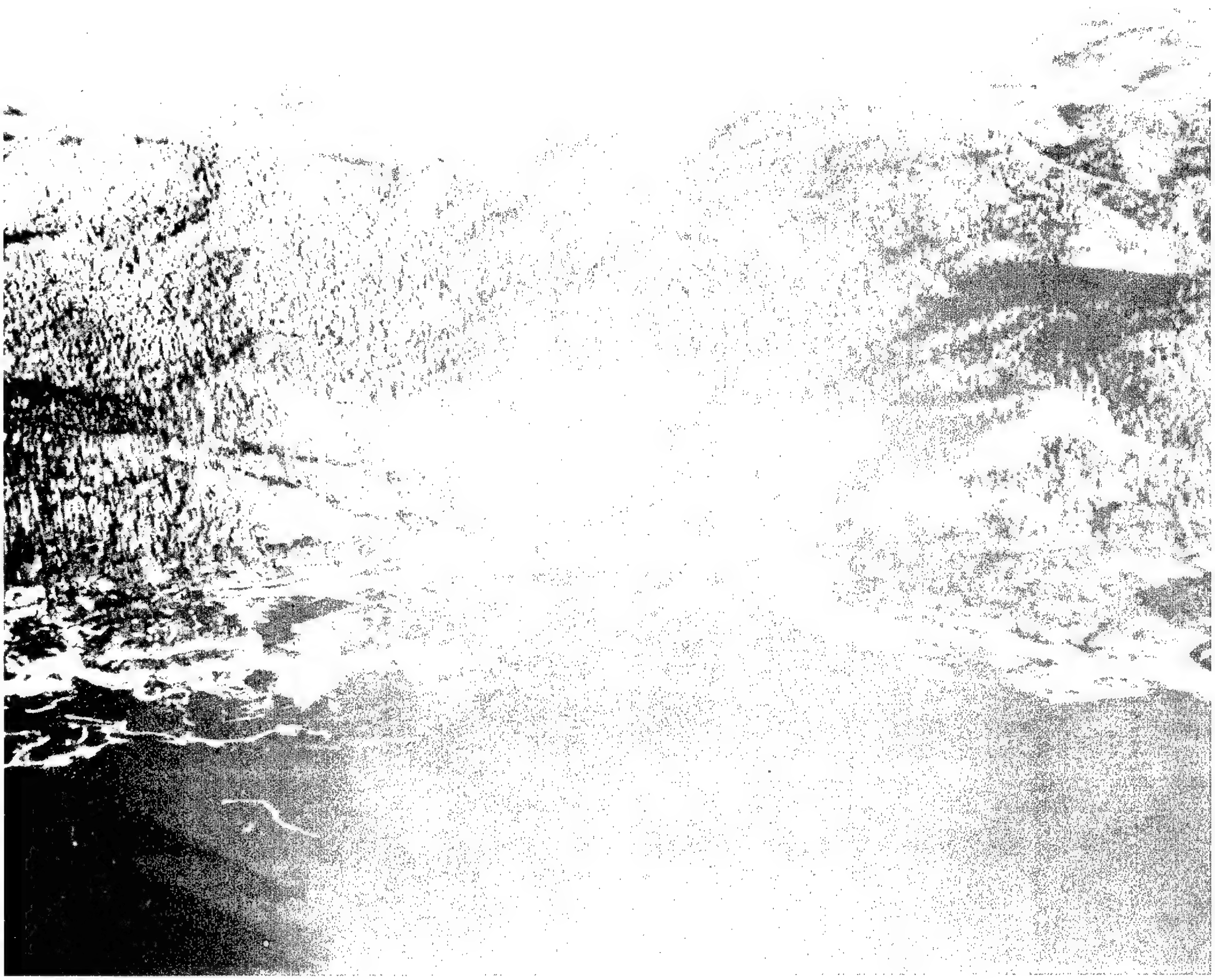

Fig. 8. Depoe Bay, Cape Foulweather. This is a unique entrance which is considered passable by fishermen having local knowledge under any conditions of weather. The extremely narrow entrance to the bay proper is a cleft through the rocks immediately seaward of the bridge. Restricted anchorage is available in the harbor. The entrance is protected from the direct effect of sea by flanking reefs and refraction conditions.

Lat. 44° 46'

ful only to small craft, this harbor is enterable when the far greater Humbolt Bay, Coos Bay, Columbia and Grey's Harbor entrances are impassable from the immense seas breaking across them. The configuration that gives rise to this almost miraculous characteristic of Depoe Bay can be qualitatively understood by an inspection of Figure 9. The entrance to the outer harbor is flanked by two pincher-like shoals, and the outer harbor itself is relatively deep. The entrance to the inner harbor is almost ridiculously narrow and steep sided, a sort of a fifty-foot wide steep sided slot in the wall of the hard basalt of which this entire area is composed.

Such configuration as Depoe Bay is not entirely unlike the plan of a number of man-made harbors, but it is much more successful. In the usual constructed harbor, flanking man-made steep-sided jetties reflect the sea and swell, and set up a serious wave interference with tossing billows that threaten any entering small craft with capsizal in heavy weather. In addition, the aperature between the jetties admits considerable swell, which then defracts into the inner harbor. At Depoe Bay these flanking reefs are rather flat in profile and result in an almost complete refraction of the swell onto them so that it largely dissipates itself on these reefs in immense complex breakers of an unusual character. Apparently there is more to the process than this, however, and refraction alone cannot satisfactorily explain the unusual protection that the reefs of Depoe Bay afford. The ridiculous inner passage also possesses an almost inexplicable character. Any sensible planner would insist on a wider entrance, but it is said that no matter how poorly a small craft is handled in entering, it is impossible for it to come to grief in this curious little entrance, and the record appears to support this contention. Even when quite sizeable seas are affecting this inner channel, a boat is prevented from being carried against and striking the walls of the inner entrance by a sort of "Mach stem" reflection from the walls that is generated as the wave propagates up the channel. This prevents breaching of the craft. I have studied this analogue of the Mach stem in breaking waves and find it responsible for many of the anomalies of near-shore processes. Its salutary effect on small boats in this channel is astonishing.

I cannot at this time discuss this one harbor at great length, but my point in discussing Depoe Bay at all is, of course, that here nature has inadvertently presented us with a small-harbor configuration that is of considerable importance to the PLOWSHARE objectives, and which is hardly derivable from any existing design criteria! We should study this harbor and attempt to understand the action of the basic law that bequeaths its remarkable qualities. We should consider whether or not a similar configuration is attainable by explosives. The flanking reefs and outer harbor resemble a crater and crater lip much more than they do a harbor with a conventional rubble mound breakwater. Figure 10 shows a fishboat entering a very similar harbor of conventional design.

You may well ask however, what do we do on sediment sated coasts where, without a perpetual program of dredging, longshore transport of sediments can rapidly render a small harbor useless? In the general case, nature does not appear to provide an answer. However, in the case of coasts without an extensive continental shelf, such as our own California coast, she does give us a hint of the means by which a stable harbor might be achieved. Two dangers stem from the artificial interruption of the longshore flow of sediment by jetties or other structures: the deposition of sediment on the upcurrent side, and the wave of erosion that moves down current. Where interruption has long ago occurred naturally, however, the erosional problem is eliminated, or, at least, ameliorated. In nature, the longshore transport of sediment is terminated or interrupted in two ways. In extensive deep coastal bights or against large headlands, this wave-induced transport may encounter a contrary littoral current. In these traps are produced the great sand dunes as at Point Sal or Oso Flaco on our coast, parts of the West Coast of South Africa, and elsewhere. Where the flow is terminated by contrary currents near a headland, the area is tantamount to a sand starved coast, but in a few cases (La Jolla, Hueneme, Moss Landing, Alviso, and Cape San Lucas), the sediment flow is terminated and much or all of the sediment is disposed of by a much more curious mechanism -- great turbidity currents that intermittantly flow down submarine canyons into the oceanic abyss. In some cases, Monterey, for example, the submarine canyon is

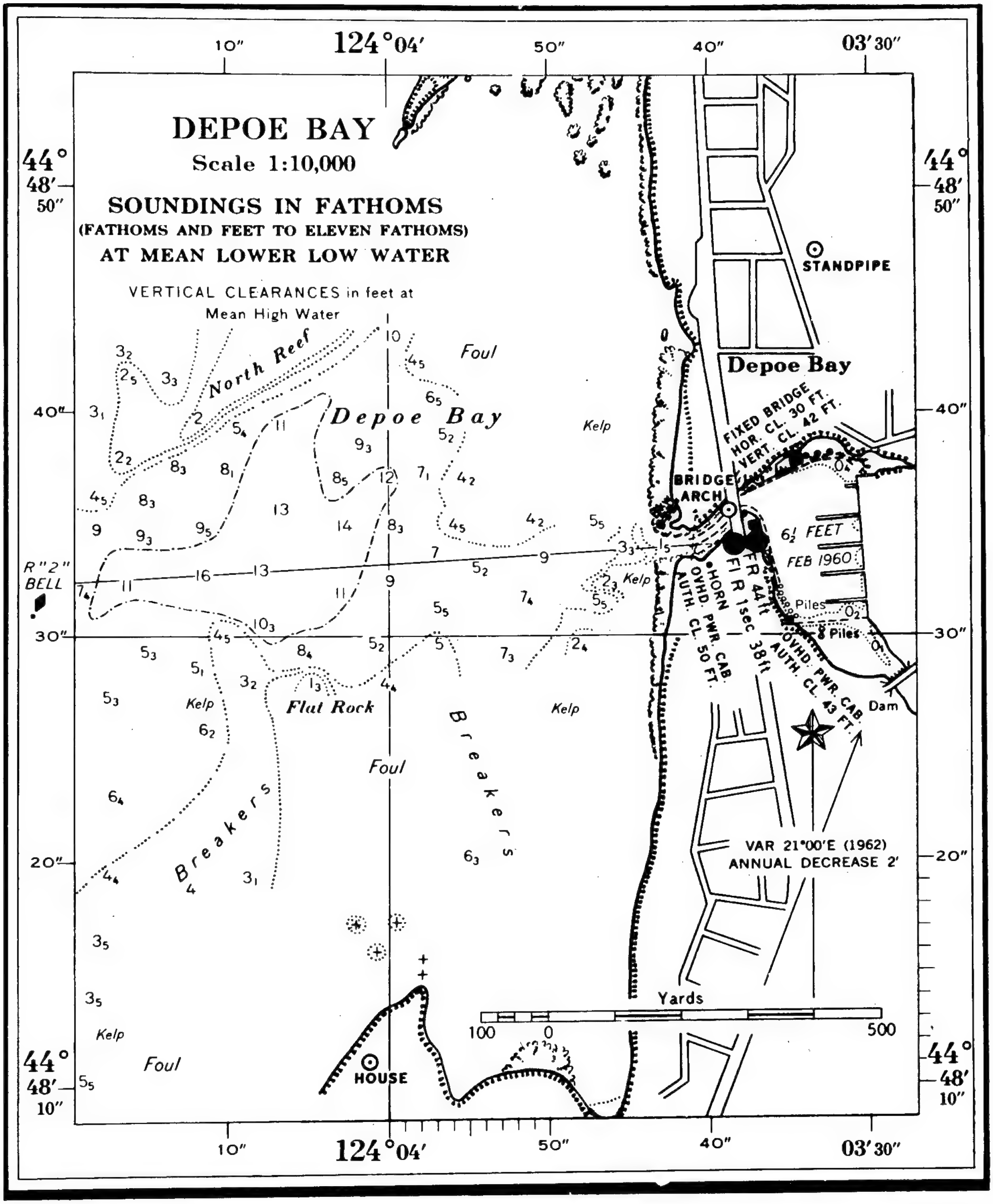

Fig. 9. Outer and inner harbors of Depoe Bay.

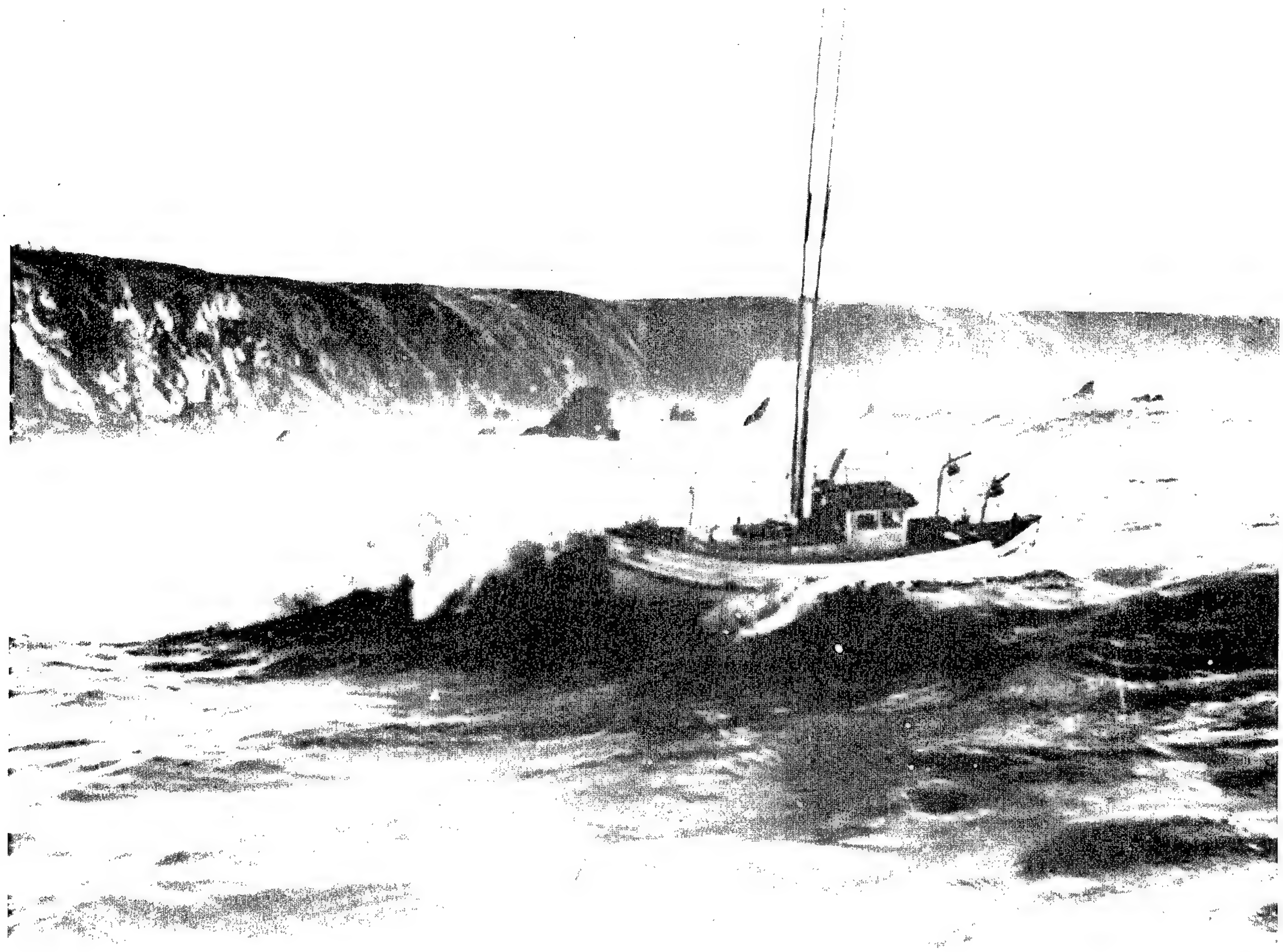

Fig. 10. Fishing boat entering harbor of conventional design.

almost the dimension of the Grand Canyon of the Colorado, but much smaller canyons apparently are also effective. Whether the canyons were preexisting features or eroded by the turbidity currents is uncertain, but that they constitute a major sink for sediments is unquestionable. These sediments are spread as turbidities far and wide over the near-continental ocean floor, attesting to the frequency and importance of the event.

A harbor developed at the head of such a submarine canyon would enjoy the most advantageous divergent wave refraction. It also presumably would be partly immune to the accumulation of sediment and would not require a great dredging program to prevent a wave of sand erosion destroying down-current beaches and installations. The possibilities of producing effective submarine canyons at positions of choice by forming an initial small channel with underwater explosions should also be investigated, where the erosion would not be damaging.

To my knowledge the only harbor whose entrance jetties embrace a submarine canyon is Port Hueneme. The construction of the Hueneme jetties have caused beach erosion, but the beach already was in equilibrium with a loss of 2/3 of the longshore transport down the canyon. Hence the Hueneme erosion was brought to equilibrium with less than 1/3 of the sand transfer by dredging that probably would have been required in a similar location without a canyon. In addition, the harbor enjoys the several other advantages of the location at the head of a submarine canyon. Similarly,

Moss Landing is located at the head of the great Monterey Canyon and the seas are consequently very low at its entrance.

So far in this discourse I have attempted to point out that: 1) explosively generated harbors can be far superior to harbors of other origins, and 2) that nature gives us some insight into the possibility of constructing harbors with unique qualities, not considered in conventional design.

I now wish to discuss the implications of the depth of explosively generated harbors. I believe that the unusual depth of such harbors is the particular factor of these excavations that holds a great potential for a revolution in oceanic shipping. In this discussion of depth, I will skip over such possibly important matters as military sea mines (it might be very difficult to mine a deep PLOWSHARE harbor with contact or influence mines). The important factor is that a series of these harbors could emancipate ships of the future from the important consequences of the limitation of draft from which they now suffer.

The economy of marine transport is clearly tied to the size of the transport vessel. In the past, the advanced maritime nations were able to maintain their lead by continuously building larger and larger ships ("Leaving them sweating and swearing a dozen years behind" as Kipling has said) - despite the greater labor costs that the advanced social regimes in these nations necessitated. In the last thirty years, however, the U.S. maritime position has seriously degraded, and no order of magnitude increase in the size of vessels has been possible. This penultimate limit in the size of vessels has been the restriction of draft because of harbor limitation and the effect of this limitation on the structure. Of the stresses to which a ship is subjected, the longitudinal bending stress from waves is the most demanding. Since this stress must be resisted by the vertical beam strength of the ship (beam in the structural sense), the limitation of beam thickness by harbor depth is particularly serious and constitutes an important obstacle to increasing vessel size.

A bit of simple dimensional analysis will roughly quantify these factors. First let us consider propulsion power requirements in a series of geometrically similar ships by Raleigh scaling (wave resistance accounts for less than 25% of a merchant ship's power requirements, and hence Froude scaling can be disregarded in this analysis).

If L represents the linear dimension in a series of geometrically similar ships then Mass

$$W \sim L^3 \tag{1}$$

and resistance

$$R \sim L^2 V^2, \text{ where V is the velocity,} \tag{2}$$

the power

$$P \sim L^2 V^3, \tag{3}$$

and the power per unit mass,

$$\frac{P}{W} \sim \frac{P}{L^3} \sim \frac{V^3}{L} \tag{4}$$

Thus the power required to haul a ton of material at a fixed velocity decreases linearly with the length of a ship.

Inversely, for a <u>fixed power/mass ratio,</u>

$$V \sim L^{1/3}, \tag{5}$$

thus the velocity can be increased as the cuberoot of L without an increase in unit power cost.

Ship maintenance increases only as L^2, and hence decreases on a unit basis. Likewise manning costs increase only slightly with increasing size.

If we now examine the dimensional relationships of stress, the picture is somewhat different.

The moment imposed on a ship by a seaway, (where the length of the ship is less than two wave lengths of the longest significant wave) is

$$M_e \sim W \times L \sim L^4 \tag{6}$$

The strength or internal resisting moment for <u>a constant stress</u> in the ship

$$M_i \sim L^3 \tag{7}$$

Thus even when no depth restriction exists, a ship scaled in a series of dimensionally similar shapes rapidly becomes less conservatively designed with increasing length. Under the condition where one dimension (i.e. the draft) must remain constant, equation 7 becomes even worse.

$$M_i \sim L^2 \tag{7a}$$

and the marine architectural problem is very badly compromised. To double the length of a ship the product of proportionally increased metal cross-section and increased strength of the metal must be four!

Were it possible to design a ship over twice as long as the longest oceanic swell, however, the imposed moment would no longer increase with the fourth power of the length but rather with the third power only (i.e.

$$M_e{}' \sim L^3) \tag{6a}$$

and from then on to greater lengths, a simple, approximately proportional scaling of a ship is feasible!

Ocean-going vessels have never been designed to this critical length (ca. 1/2 mile), although Great Lakes ore carriers have exceeded their related limit for Great Lakes waves.

With an increased available depth of operating harbors to say 150 feet, a ship could be constructed that would reach this threshhold! This 3000 foot, three million ton vessel would operate between such ports at perhaps 1/3 of the ton/mile cost of the present-day largest freighters. Greater ships could then be constructed with no further immediate limits! Tankers or ore carriers (the latter possibly receiving ore from the crater wall or lip) seem the most immediately feasible vessels in this size range because of the in-port cargo handling problems of general freighters.

The U.S. is now carrying only 15% of her exports and only 5% of her imports in her own bottoms. Our merchant marine is rapidly becoming depleted, despite government subsidies. Great Britain also is in difficulty and much shipping carried out by these two countries is unprofitable, but with explosively created harbors a new dimension is feasible for the economic distribution of man's resources and goods among the world's peoples!

The need for small boat harbors for fishing, recreation and haven should not be overlooked.

The peoples of the world are hungry but they do not suffer so greatly from lack of common agricultural crops as they do for protein and particularly for animal protein. The world is and will continue to be a protein hungry planet. Ocean fisheries potentially can supply this entire requirement for 10 billion or perhaps 30 billion people.

Today the great pelagic fisheries of the world are conducted by Japan and the Soviets. The U.S. tuna fishery also is far reaching. Figure 11 is a chart indicating one month's coverage by the vast Japanese pelagic tuna fleet. These fishing fleets are composed of deep-sea vessels and mother ships and utilize large commercial harbors. Equally important, however, are those fisheries that can be conducted only from small craft. In technologically developed countries this includes certain types of fresh-fish fisheries and the sport fishery. (The sport fishery is a vital use of the resource in a region such as California, where wholesome recreational outlet is essential to the members of a highly mechanized society.) The nature of the creatures that these local fisheries seek is such that only small craft are economically feasible. Even in Southern California these fisheries are then restricted to the ocean area within a few tens of miles from ports. Thus along the Central California, Oregon, and Washington coasts, large reaches are virtually unavailable to any local fishery.

In some other parts of the world a forty mile stretch or even a twenty mile stretch of harborless coast denies to the local inhabitants this marine source of vital nutrition. Figure 12 shows the coastal types of the world. The sea cliff coasts (purple) are virtually harborless, and except for the glaciated coasts (green) all others possess many stretches of forty to one hundred miles without harbor or haven. Across these harborless stretches the primitive peoples of the world drag log rafts and dugout canoes in an effort to supply themselves with the foods that the sea can so abundantly provide. A hole in the wall, such as Depoe, could make this abundance available to them.

This rambling discussion would be grossly incomplete were I not to mention the craters at Bikini Atolls. The deep blue man-made harbors now cowering under the censorious eyes of the world seem to me to be harbingers of the potentialities of the new muscular power that man now possesses to better the world in which he lives. As a part of understanding this potentiality I have proposed to study the stability of the seafilled craters of Bikini Atoll, and to gain some insight into the new equilibria that are being approached by the crater slopes and the surrounding terrain.

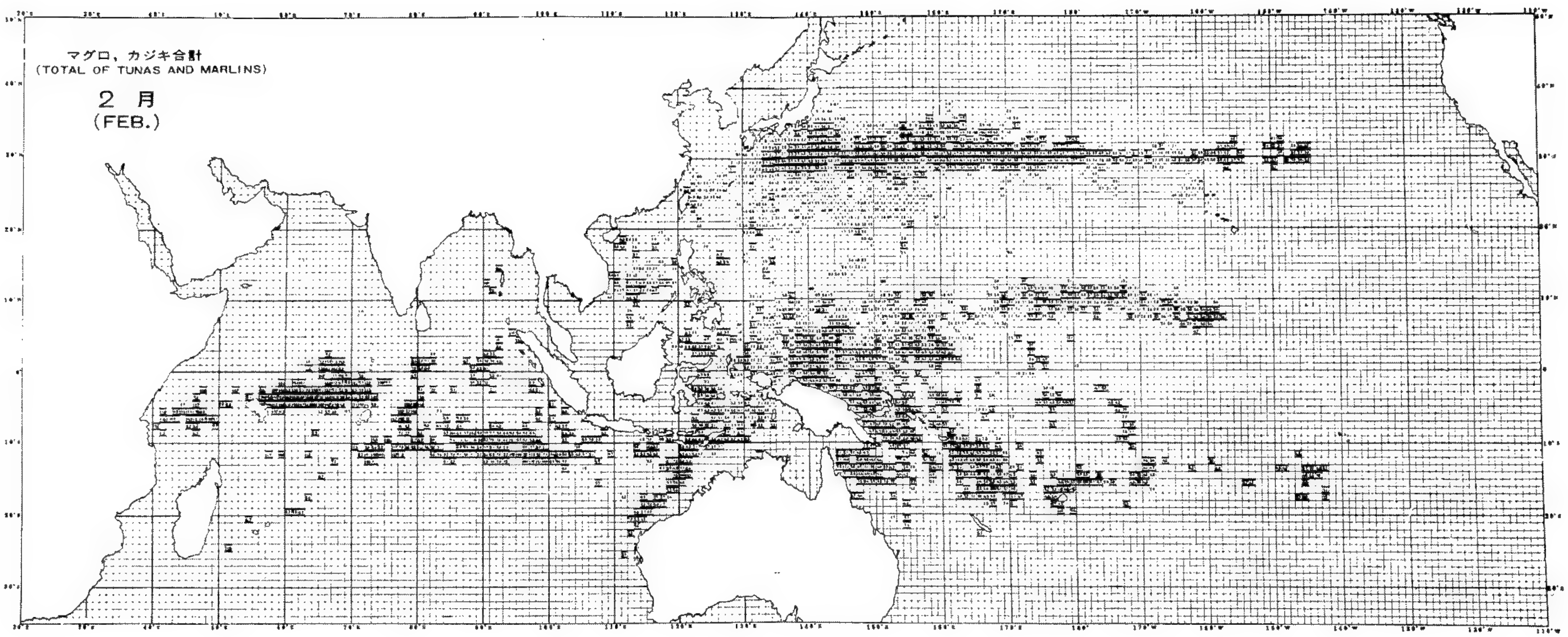

Fig. 11. Chart indicating one month coverage of Japanese tuna fleet.

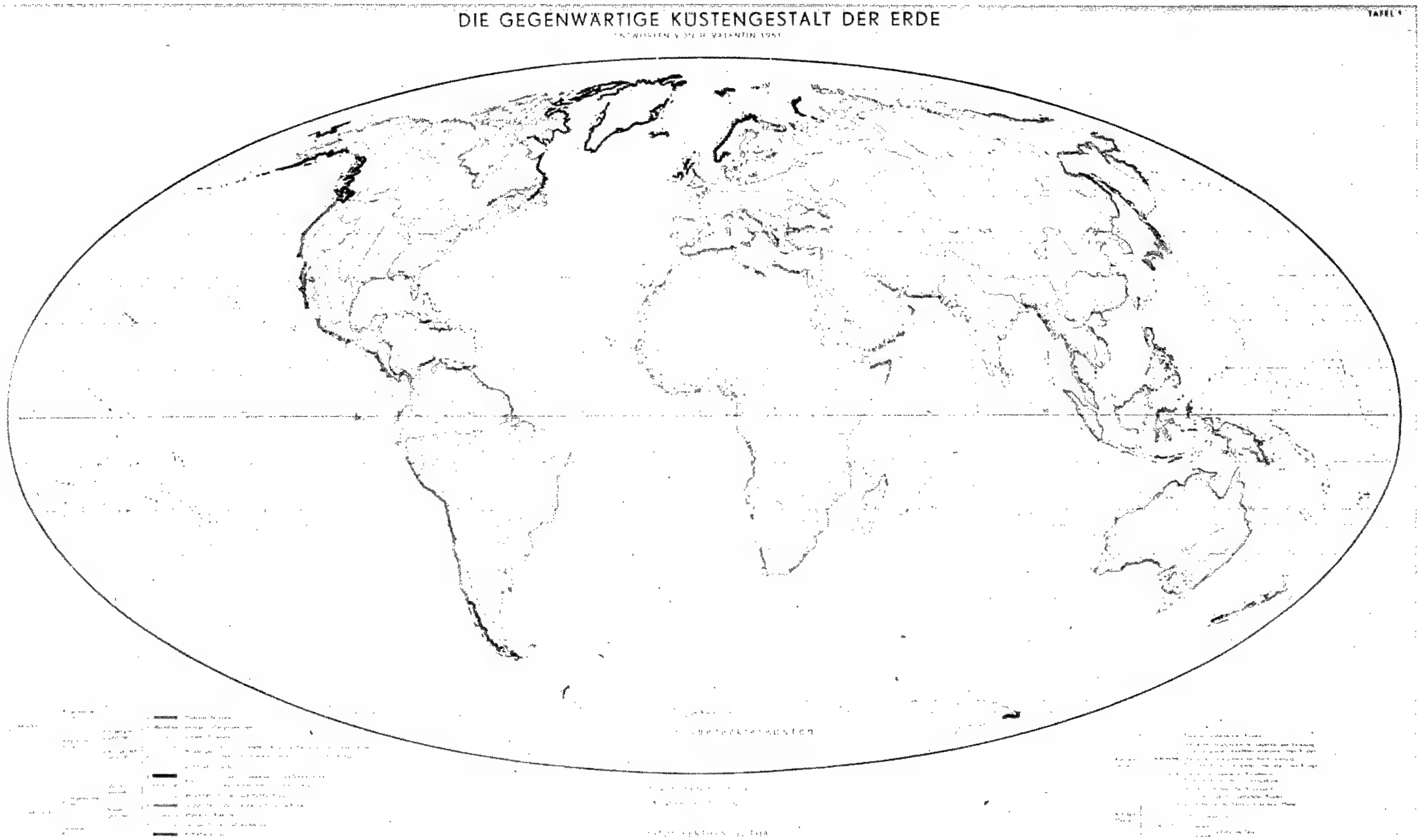

Fig. 12 Coastal types of the world.

The regrowth of coral on the crater slopes is, of course, a part of this stability as is erosion and soil formation on the surrounding land areas. At the same time, I propose to carry out measurements of penetration of radioactivity in the deep sea sediments under the Bravo fallout and gather organisms from these depths for measurements of uptake. These inquiries will be integrated with those of the University of Washington and are planned for the summer of 1965.

In summary, I wish to reiterate that it is my belief that project PLOWSHARE presents us with some unusual opportunities to create greatly improved conditions for the world's peoples; that one vital part of this is the creation of harbors by nuclear explosives; that these explosively generated harbors, thoughtfully carried out with insight into the hints nature has provided can be vastly superior to the harbors from which man now conducts his marine intercourse; and that the freedom of design that the depth of these harbors permit, can untrammel oceanic shipping and permit a new dimension of distribution of the world's resources to the world's peoples.

BIBLIOGRAPHY

Isaacs and Schmitt, "Resources from the Sea," International Science and Technology, June 1963.

King, C. A.M., "Beaches and Coasts," Arnold, 1959.

Putnam, W. C. et al., "Natural Coastal Environments of the World," ONR and UCLA, 1960.

Steers, J. A., "The Sea Coast," Collins, 1953.

Valentin, H., "Die Kuesten der Erde," Gotha, 1952.

U. S. Bureau of the Census, "Statistical Abstract of the United States," 1962.

BIOGRAPHICAL SKETCH OF AUTHOR

John Dove Isaacs, III, is Professor of Oceanography, Director, Marine Life Research at the University of California's Scripps Institution of Oceanography. His chief field of study are marine resources, interrelationship between organisms and circulation, waves, organisms, radioactivity in the sea, and the implementation required for such study. He received his B.S. degree from the University of California in 1944.

He has held the following positions: Project engineer, seaplane base construction, Austin Company, 1941-43 Waves investigations, University of California, 1944-48. Associate Oceanographer and Assistant to the Director, Scripps Institution of Oceanography, 1948-55. Associate Professor of Oceanography and Assistant to the Director, Scripps Institution of Oceanography, 1955-58. Associate Professor of Oceanography and Director, Marine Life Research, Scripps Institution of Oceanography, 1958-61. Professor of Oceanography, Director, Marine Life Research, Scripps Institution of Oceanography, Acting Director, Institute of Marine Resources, 1961-62. Professor of Oceanography, Director, Marine Life Research, Scripps Institution of Oceanography, 1961-present.

ISOTOPE RECOVERY FROM A NUCLEAR DETONATION IN SALT

D. G. Karraker

Savannah River Laboratory, E. I. du Pont de Nemours and Co.
Aiken, South Carolina

ABSTRACT

The production of isotopes by the detonation of a nuclear device involves recovery of the debris from a contained explosion, and separation of the products from the shot debris by chemical processing. The choice of a salt formation for explosion of the device is extremely favorable for chemical processing, since the solubility of salt in water affords a natural beginning for recovery in an aqueous system. The major problem of chemical processing is the separation of a few ppb of product isotopes from the mass of salt and other minerals present in the shot debris. A simple model of the nuclear production process and data from the debris of the Gnome experiment indicates that the product isotopes are associated in the debris with minerals of roughly the same volatility; thus a "carrier" mineral retains most product isotopes and permits the removal of the salt by water leaching without significant loss of most products. The product isotopes are concentrated and recovered by chemical processing of the carrier. Processing methods that can be applied to the recovery of isotopes of the alkali, alkaline earth, rare earth, actinide, and transition metals will be outlined.

INTRODUCTION

Reactor irradiation of a target isotope is the normal method for production of heavier isotopes —depending on the neutron capture cross section and the extent of irradiation, an increase in mass number of one to three units is not too difficult to achieve. The detonation of a nuclear device is accompanied by an intense neutron flux, and this novel source of neutrons can add 15 or more neutrons to a target nucleus within an instant,[1] producing isotopes that would require decades to produce in a nuclear reactor, if they could be produced at all. The recovery of the products from a nuclear detonation, however, is a formidable task—the explosion must be contained to prevent loss of the products to the atmosphere, and the shot debris must be recovered and the products separated from the extraneous material of the debris. The most practical method of containment is to explode the nuclear device underground in a stratum that does not decompose at high temperatures, as do limestone and dolomite, and which contains the minimum amount of volatiles, such as water, oil, etc. The nuclear explosion will normally produce 500 to 1000 tons of debris per kiloton of energy released, and the recovery of kilogram quantities of products from the debris requires a separation factor of about 10^6; the recovery of gram quantities requires separation factors of the order of 10^9. The recovery of the products will require the processing of large quantities of material, and the choice of the rock strata for the detonation is of primary importance.

Considering the possible strata for a nuclear detonation, salt formations are easily the most favorable for isotope recovery. The solubility of salt in water allows an easy beginning for aqueous processing, and the relatively low melting point of salt is favorable for molten salt processing. Salt beds or salt domes are fairly widespread in the USA, and allow a wide choice of sites. There is a wide variation in the impurities associated with salt. The salt domes of the Gulf area are

*The information contained in this article was developed during the course of work under contract AT(07-2)-1 with the U. S. Atomic Energy Commission.

pure dry salt—99.9% NaCl, but salt beds of the Southwest may contain as high as 30% of other minerals. These beds are quite extensive, and are the most favorable location for a nuclear explosion. The most common mineral impurities in salt are anhydrite ($CaSO_4 \cdot H_2O$), olivine (Mg_2SiO_4), polyhalite ($NaCl \cdot KCl$), clay (potassium aluminum silicates), and iron silicates, but small amounts of many other elements are also present. The analyses of two samples of an impure salt are shown in Table I.

Table I. Composition of Gnome salt debris samples.

Component	Sample 1[a] (wt %)	Sample 2[b] (wt %)
NaCl	90	86
Mg	0.2	0.9
Ca	1.7	2.2
SO_4	4.3	6.8
Al	0.3	--
SiO_2	2.2	1.7
Fe	0.1	0.3
Cu	--	0.2
Minor Cations:	(0.1-1%) Al, B, Cr, Mn, Ni, K	
Trace Cations:	(0.1%) Ag, Pu, Sn, Sr, Ti	

[a] W. D. Bond, quoted in ORNL 3452.
[b] W. C. Perkins, SRL, unpublished data (1962)

The presence of impurities in salt strata imposes two restrictions on its use for isotope production—production of elements that are present in the impure salt will result in an isotopically diluted product, and neutron activation of an impurity can handicap recovery operations. However, the impurities can act to collect the product from the mass of salt. In chemical processing this is a distinct advantage; and in considering production in a very pure salt formation, addition of a few tons of a "carrier" to collect the product might be advantageous.

ISOTOPE PRODUCTION

A simple model of the processes involved in the production of the isotopes by a nuclear device is useful to the planning of isotope recovery. At the detonation, all matter in the immediate vicinity of the device is volatilized by the energy of the nuclear reactions, forming a sphere of very-high-temperature gases, or fireball. The fireball immediately begins to transfer energy to the surroundings—more matter is volatilized, but the temperature of the fireball decreases.[2] As the temperature drops, elements recombine into compounds, and after a sufficient decrease in temperature, the less volatile compounds condense. Heat is still being transferred to the surroundings—the salt surrounding the fireball melts, and expands the cavity. As the cavity expands, the roof is weakened—blocks of salt fall from the roof of the cavity and melt into liquid salt debris. Finally, the heat loss lowers the cavity temperature to the point that the molten salt freezes. The system will normally be oxygen-rich, even in salt strata, and the species condensing will be oxides for most elements, although the species in the vapor phase may not necessarily be oxides. The vaporization temperatures for some compounds of interest are shown in Table II.

The detonation irradiates the target isotope with an intense burst of neutrons, producing heavy, unstable isotopes that decay toward the final products. These elements are volatilized with the fireball, but as the temperature within the cavity drops, the product elements condense. These isotopes will be present in low concentration, so their condensation will result chiefly in particulate matter, rather than solid particles. The particulates will be carried out of the vapor phase by the condensation of macro species with a lower volatilization temperature, for example, a rare earth oxide would be predicted to condense to particulate solids at about 4000°K, but would remain suspended until the condensation of a macro component, such as MgO, removed it from the gas phase. This model indicates that products of low volatility would be found associated in the debris with compounds of nearly the same volatility. This prediction must be modified because of the addition of salt from the roof of the cavity to the molten debris. The unvolatilized salt adds minerals to the molten salt that might otherwise not be present, such as sulfates which are decomposed at temperatures above 1200°K. Elements that are volatile at the melting point of salt will be volatilized from the debris.

The solid debris from an impure salt will contain silicates and sulfates as separate phases in the solid matrix of salt. The isotopes produced in the explosion will be distributed between the separate mineral phases. The association of the

ammonium nitrate solution, and the silicates were decomposed by boiling in concentrated nitric acid, dissolving the cations present and leaving hydrated silica as a solid residue. The behavior of trace elements and fission products in this treatment allows an inference as to the solid phase that contained each species. These results are shown in Table III.

Table III. Elements in solid phases of Gnome debris.[a]

Salt Ca, Rb, K	$CaSO_4$	Silicates Zr
Mg (20%)		Mg (80%)
Sr (60%)	Sr (40%)	Al
		Cr
		Mn
		Ti
		Rare earths
		Actinides
		Pb
		Fe
		Ru
	Cu (80%)	Cu (20%)
		Ag
		Ni
		Sn

[a]Based upon unpublished data of W. C. Perkins SRL (1963).

The results in Table III demonstrate a general agreement with a model for the formation process. Some elements, such as alkali metals, rare earths, and actinides are found essentially within one solid phase of the debris; in these cases, the volatility of the elements is roughly the same as the mineral that forms the phase. Some elements, such as Sr, Mg, and Cu, are removed with the components of two different phases, indicating that these elements probably dissolve to some extent in salt and are thus distributed between the solid phases.

Other data provide evidence for the hypothesis that the actinides were removed from a vapor phase by condensation of the silicates. Dissolution of the water-insoluble debris in acid or base dissolves the plutonium to about the same extent as the mass of debris (Table IV), indicating that plutonium is a homogeneous component of the silicates, and is not absorbed on the surface of silicate particles.

CHEMICAL PROCESSES FOR ISOTOPE RECOVERY

For the production of isotopes in a strata similar to that used for the Gnome shot, chemical recovery methods can be outlined for the recovery of general groups of elements—the alkali metals, alkaline earths, rare earths and actinides, and some of the transition metals.

Recovery of the alkali metals is reduced to the recovery of Rb and Cs because potassium is a major impurity in the salt. These elements will be associated mainly with the salt phase, which allows a major simplification in their recovery. Instead of mining operations to recover the entire debris, water could be pumped into the shot debris to dissolve the salt, the brine pumped to the surface and processed to recover cesium and rubidium.

Chemically, cesium could be recovered most easily by the ion exchange of cesium for potassium in solid potassium-cobalt-ferrocyanide. The exchange of cesium is complete even from a 21% salt solution; tracer experiments at SRL[3] show that half of the potassium in solid potassium-cobalt-ferrocyanide can be replaced by cesium. In one test, over 40,000 bed volumes of 21% salt solution containing Cs^{137} tracer were fed through a bed of potassium-cobalt-ferrocyanide over a period of 1 year with a loss of less than 1% of the Cs^{137}. Recovery of rubidium by this same method may be practical, but no experimental data are available. Solvent extraction with substituted phenols[4] has been demonstrated to give excellent separation of cesium and rubidium from each other, and from other alkali metals. This process could be used to purify the crude product obtained by ion exchange.

Because of Ca and Mg minerals in the salt, only recovery of strontium, barium, and radium of the alkaline earths will be discussed. It is assumed that barium and radium dissolve with strontium from the salt debris; Sr is associated (Table III) in about equal amounts with the salt and $CaSO_4$. A significant amount of $CaSO_4$ dissolves in brine, and an estimated 70 to 80% of the Sr, Ba, and Ra

Table II. Vaporization temperatures.

Compound	Vaporization temp (°K) 10^{-3} atm	1 atm
NaCl	1123	1738
KCl	1079	1680
RbCl	1050	1654
CsCl	1003	1573
CaO	2650	3800
MgO	2450	3350
SiO_2	2250[a]	--
Al_2O_3	2740[a]	3800[a]
K_2O	1150[a]	1750[a]
Na_2O	1330[a]	2040[a]
FeO	2300[a]	3400[a]
Y_2O_3	--	4570
La_2O_3	--	4470
ThO_2	--	4670
Ti_2O_3	--	3300
UO_2	2000°K (~10^{-8} atm)	
Am_2O_3		4200-4700 (estimated)
PuO	1850° (10^{-6} atm)	

[a]Vaporization by decomposition

Sources: Oxides: L. Brewer, Chem. Rev. 52 1 (1953).
Chlorides: L. Brewer, "The Fusion and Vaporization Data of the Halides." Paper 7 in Quill, L., NNES IV-19B, Chemistry and Metallurgy of Miscellaneous Materials: Thermodynamics, McGraw-Hill Book Co., New York (1950).

products with compounds of nearly the same volatility is changed, for some elements, by their dissolution in molten salt and absorption on the solid minerals present in the melt.

SOLUBILITY TESTS ON GNOME DEBRIS

The Gnome experiment in 1961 took place in impure salt strata, and data for the dissolution of fission products and trace elements from the debris are of interest in the planning of chemical processes for isotope recovery. The major solid minerals in Gnome debris are salt, calcium sulfate, and silicates of iron, magnesium, and aluminum. In solubility tests on samples of Gnome debris, the salt was dissolved in water saturated with $CaSO_4$, leaving the other minerals largely intact. The calcium sulfate was dissolved with

can be recovered with the salt by a water dissolution of the debris from the shot cavity.

The precipitation of a carrying agent can remove Sr and Ba from the brine solution in a relatively concentrated form. To avoid isotopic dilution, precipitation of a calcium or magnesium compound is desirable; calcium oxalate or calcium carbonate will remove 90 to 95% of the alkaline earths from the brine, and the separation of the precipitate from the brine by settling is a relatively routine operation. Fission-product strontium is recovered routinely by solvent extraction with di(2-ethylhexyl) phosphoric acid at Hanford[5,6] and this solvent extraction process can probably be adapted to the separation and recovery of Sr, Ba, and Ra from a precipitate of calcium carbonate. Recovery of radium by absorption of radium on a solid, such as the minerals barytes[5] and clinoptilolite,[6] is an effective method for decontamination of waste streams, and could also be applied to radium recovery.

The recovery of elements that are associated with the silicate phase of the debris presents some additional problems. Dissolution of the debris from the shot cavity with water is not practical; therefore, after a time delay to allow the short-lived fission products to decay, the debris would be removed from the ground by mining before chemical processing. Removal of salt by dissolution in water and removal of calcium sulfate by dissolution in ammonium nitrate solution reduces the bulk of material to be processed by a factor of about 20, leaving a residue consisting mainly of magnesium and iron silicates. This silicate residue contains rare earths, actinides, transition metals, zirconium and its homologues, and niobium and its homologues.

Of these elements, the major interest is in the recovery of actinides, since production of new isotopes of the actinides, or a new element might be achieved[9,10] by the irradiation of a heavy isotope with neutrons from a nuclear device. In many cases, such isotopes would be too short-lived to survive until large-scale processing of the debris is carried out, but heavy isotopes of unusual nuclear stability may exist long enough to permit their recovery.[1]

Several methods have been suggested for recovery of actinides from the silicate residues, including precipitation, solvent extraction, and anion exchange. These processes all require as an initial step the destruction of the silicates and dissolution of the cations by treatment of the silicate residue with strong acid. This treatment produces a gelatinous precipitate of silica that is difficult to separate from the solution, unless the silica is coagulated either by refluxing with strong acid or by precipitation with gelatin. The clarified solution contains 80 to 90% of the actinides, rare earths, and transition metals; roughly 50% of the

Table IV. Dissolution of water-insoluble residue.[a]

Sample	Dissolving solution	w/o residue dissolved	% Pu dissolved
B	1.7M K_2CO_3	9.4	6.5
E	1.7M K_2CO_3	6.8	11
F	1.7M K_2CO_3	6.7	13
B	8M HNO_3	67	92
E	8M HNO_3	72	89
F	8M HNO_3	71	96
B	1.3M HNO_3	78	74
B	8.4M HNO_3	71	85

[a]W. C. Perkins, SRL unpublished data (1962).

zirconium and niobium and their homologues will be held on the silica by surface adsorption.

From the nitric acid solution, actinides and rare earths may be concentrated by precipitation and separated from other cations by solvent extraction,[4] or separated by solvent extraction and concentrated by evaporation of the dilute product stream.[11] Either method is chemically practical, and a choice between the two would probably be based upon economics. Several extracting agents can be used; in general, these are all organic phosphorus compounds, such as tributyl phosphate, dioctyl pyrophosphoric acid, and ditetramethylbutyl phenyl phosphonate. Solvent extraction under controlled conditions would discard iron and other transition metals, and could recover 99% of the actinides and rare earths.

The solution resulting from solvent extraction is concentrated by a factor of 10^4 from the original acid solution of the silicates, and further processing to separate the actinides of rare earths from other elements is reduced to a small-scale operation. The radioactivity of these elements requires that final processing be carried out behind heavy shielding for the protection of personnel; although processes for the final purification are well-demonstrated, the requirement of remote operation demands considerable skill on the part of operating personnel. Rare earths and actinides can be separated either by extraction with a tertiary amine from lithium chloride solution,[12,13] or by several ion exchange processes—cation exchange from 13M HCl,[14] anion exchange from 10M LiCl,[15] anion exchange from alcoholic HCl,[16] and anion exchange from ammonium thiocyanate solution.[17] Because of the scale of operations, solvent extraction would be preferred to minimize operating problems. The solvent extraction process includes one cycle to remove nitrates and convert to a chloride solution, and a second cycle for tertiary amine extraction of actinides from the rare earths. Both the rare earth and actinide fractions can be separated into individual elemental fractions by chromatographic elution from cation exchange resin. A schematic diagram of these processing operations is shown in Figure 1.

Transition metals can be recovered from the aqueous waste solution remaining from the recovery of the actinides by solvent extraction; in general, most transition elements are amenable to recovery by amine extraction[4] or by anion exchange from hydrochloric acid solution. Unfortunately, the presence of trace amounts of transition metals in salt strata will cause severe isotopic dilution of these metals; their recovery would probably not be worthwhile from an impure salt formation.

In summary, the recovery of isotopes produced by a nuclear explosion in impure salt strata is a formidable and challenging undertaking. However, chemical processes are available that will recover most of the isotopes produced, and a further study may reveal more economical and efficient processes. This paper has not aimed for completeness; many elements are not discussed, but chemical processes that would recover these elements could be devised after appropriate study and investigation. The recovery of isotopes produced by a nuclear device in salt is a unique and interesting chemical recovery operation.

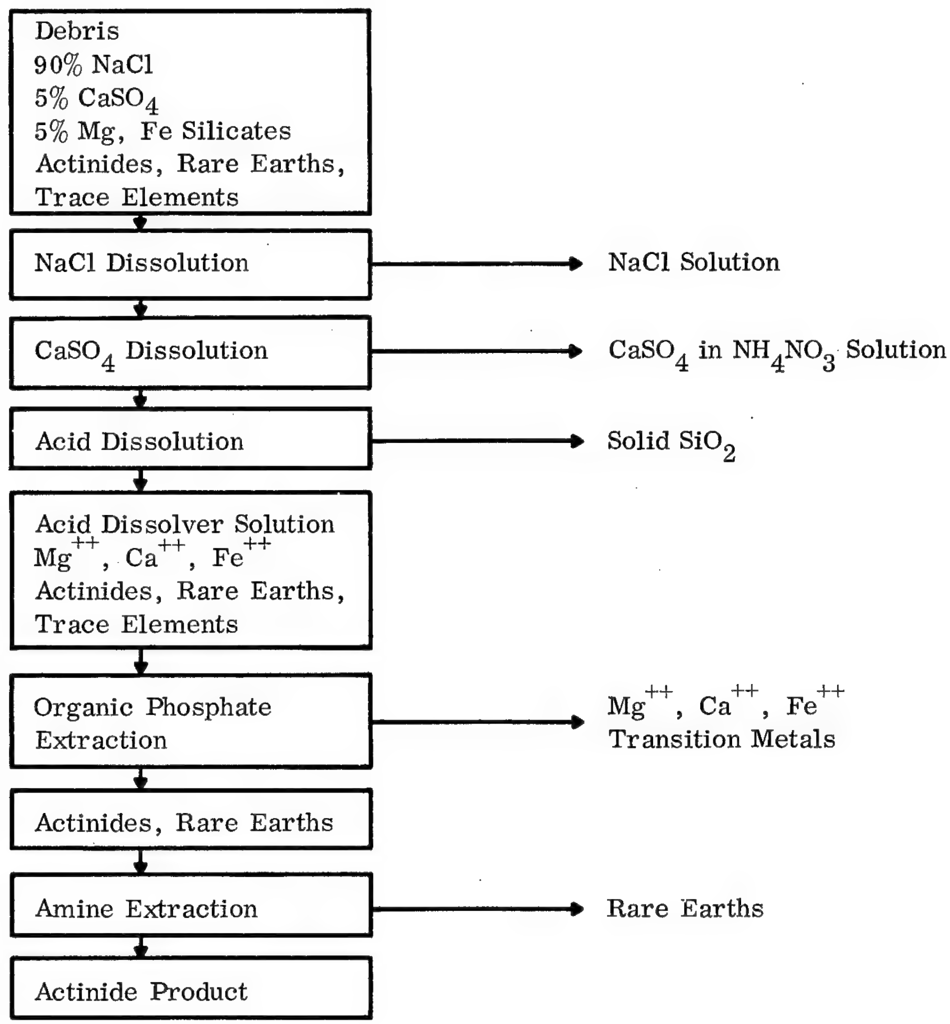

Fig. 1. Actinide recovery from salt debris.

REFERENCES

1. Cowan, G. A., "Scientific Applications of Nuclear Explosions," Science 133, pp. 1739-44, 1961.
2. Cornell, H. G. and A. D. Suttle, Jr., Proceedings of the Second Plowshare Symposium, May 13-15, 1959, San Francisco, California. Part III. The Recovery of power and Isotopes from Contained Underground Nuclear Explosions, Lawrence Radiation Laboratory, Livermore and San Francisco Operations Office, AEC, UCRL-5677, 1959.
3. Prout, W. E., E. R. Russell, and H. J. Groh, "Ion Exchange Absorption of Cesium," presented at Symposium on Radionuclidic Exchange on Soils, Minerals, and Resins, 147th ACE Meeting, April 5-10, 1964.
4. Chemical Technology Division Annual Progress Report for Period Ending May 31, 1963, Oak Ridge National Lab., Oak Ridge, Tenn., ORNL-3452, 1963.
5. Research and Development Activities Fixation of Radioactive Residues, Quarterly Progress Report, October—December 1961, E. R. Irish, Ed. General Electric Co., Hanford Atomic Products Operation, Richland, Wash., HW-72324, 1962.
6. McDowell, W. J. and C. F. Coleman, "Reagent Dependence in Sodium and Strontium Extraction by di(2-ethylhexyl) phosphoric Acid," J. Inorg, Nucl. Chem. 25, p. 234, 1963.
7. Feldman, M. H., Isotopic Analysis of Thorium in Mill Effluents and Natural Waters, Summary Report, January 1959—September 1961, National Lead Co., Inc. Winchester Lab., Winchester, Mass., WIN-125, 1961.
8. Chemical Technology Division Annual Progress Report for Period Ending June 30, 1962, Oak Ridge National Lab., Oak Ridge, Tenn., ORNL-3314, 1962.
9. Seaborg, G. T., J. Franklin Institute 276, p. 459, 1963.
10. Seaborg, G. T., "The Transuranium Elements," presented at the 146th ACS Meeting, January 19-24, 1964.
11. Karraker, D. G. and W. C. Perkins, SRL unpublished data, 1963.
12. Moore, F. L., Anal. Chem. 33, p. 748, 1961.
13. Baybarz, R. D. and B. Weaver, Separation of Transplutoniums from Lanthanides by Tertiary Amine Extractions, Oak Ridge National Lab., Oak Ridge, Tenn., ORNL-3185, 1961.
14. Street, K., Jr. and G. T. Seaborg, "The Separation of Americium and Curium from the Rare Earth Elements," J. Am. Chem. Soc. 72, p. 2790, 1950
15. Street, K., Jr. and P. Gray, U. S. Patent Application File No. 724-487.
16. Thompson, S. G., et al., "Chemical Properties of Elements 99 and 100," J. Am. Chem. Soc. 76, pp. 6229-36, 1954.
17. Surls, J. P., Jr. and G. R. Choppin, "Ion-Exchange Study of Thiocyanate Complexes of the Actinides and Lanthanides," J. Inorg. Nucl. Chem. 4, pp. 62-73, 1957.

BIOGRAPHICAL SKETCH OF AUTHOR

David G. Karraker graduated with High Honors from Southern Illinois University in 1947 and received the Ph.D. degree in nuclear chemistry in 1950 from the University of California at Berkeley. In 1951 he joined the Atomic Energy Division of the DuPont Company and worked at Argonne and Oak Ridge National Laboratories for two years prior to his assignment at the Savannah River Laboratory. He was promoted to research supervisor in 1955 and has directed research in solvent extraction processing of nuclear fuel, radiation chemistry, and inorganic chemistry. In addition to a personal research program on metal-organic compounds of the actinide elements, Dr. Karraker directs the Plowshare research program at the Savannah River Laboratory.

EXCAVATION FOR WATER CONVEYANCE WITH NUCLEAR EXPLOSIVES

J. W. Keysor
M. B. Andrews

State of California Department of Water Resources

ABSTRACT

The California Department of Water Resources is charged with a continuous study program for the future development of water resources throughout the State. The Atomic Energy Commission, through its Plowshare Program, is responsible for investigating and developing industrial uses for nuclear explosives. The West Side Conveyance System is a possible feature of future work for conveyance of water from the North Coastal area to areas of efficiency. Joint reconnaissance studies of this possible feature indicates substantial savings in cost may be possible if nuclear explosives can be used for excavation. Further studies are proposed for evaluation of hazards and engineering feasibility.

INTRODUCTION

The California Department of Water Resources, in its continuous study program for the future development of water resources throughout the State, attempts to keep abreast of all new ideas which indicate possible useful application. The Atomic Energy Commission, through its Plowshare Program is responsible for investigating and developing peaceful uses for nuclear explosives. A potentially significant use for such explosives, appropriate to the water development field, is in the excavation of channels of great depth and length for the conveyance of water. In 1961 representatives of the Lawrence Radiation Laboratory and ten California Department of Water Resources initiated a study of the application of nuclear explosives to the West Side Conveyance System, a possible feature of one of the alternative plans for development of water in Northern California. This is in conformance with the objective of developing needed water supplies at minimum cost to the people of the State of California. A joint study group was established to make such a survey.

It is axiomatic that both the State and the AEC are interested not only in minimum cost but in positive assurance of safety to the general public. Considerations of hazards which may be involved are therefore of the utmost concern. Because of the nature of nuclear explosives, their use must necessarily be limited to areas having sparse population and a minimum of structures which might be subject to damage. The West Side Conveyance System meets these qualifications.

The use of nuclear explosives must be fully explored and tested prior to any firm proposal for such a method of construction. The Plowshare Program is making substantial progress in this direction, with its experimental testing at the Nevada Test Site, and its continuing studies both of the potential hazards and of their reduction to a tolerable level. Thus a possible project such as the West Side Conveyance System, the construction of which lies many years in the future, is logical for consideration. Before it could be recommended for construction, the various potential hazards will have to be well defined and fully evaluated.

This paper is a brief discussion of the results

to date of rough reconnaissance studies currently underway.

PLANS FOR WATER DEVELOPMENT

The State Water Project is now under construction. The initial features, including Oroville Dam and the California Aqueduct, are scheduled for completion in 1972. Together with other projects under construction or proposed by federal and local agencies, the project is expected to provide enough water for use within the State until about 1975 or 1980. Additional water supplies are required as depletions occur, however, to meet the state's contractual commitments to its water users for 4, 000, 000 acre-feet annually from the Sacramento-San Joaquin Delta.

To meet those commitments, the Director of the Department of Water Resources has recently authorized additional facilities to be located in the Upper Eel River Basin. Construction is expected to be undertaken within a few years following the completion of Oroville Dam in 1968. These additional facilities were authorized in accordance with legislation that established the State Water Project. Funds for construction are provided for in the California Water Resources Development Bond Act, approved by the voters in 1960.

However, even this additional water supply will not keep pace with the State's growing demands. It is presently contemplated that the next major diversions will be from the Trinity River. The West Side Conveyance System is a potential alternative feature in these later developments. This system, along with others, is under study.

THE WEST SIDE CONVEYANCE SYSTEM

The West Side Conveyance System comprises a series of interconnected reservoirs extending about 40 miles along the foothills on the west side of the Sacramento Valley, roughly at elevation 1, 000 feet, from the Middle Fork of Cottonwood Creek to Thomes Creek, principally in western Tehama County. See Figures 1 and 2. This system would convey Trinity River water, discharging from the Cottonwood Creek tunnel, into the Glenn Reservoir complex, a possible very large reservoir on Thomes and Stony Creeks.

The conveyance system is one of several alternatives being considered in the overall development of the Trinity diversion project.

In addition to conveying Trinity River diversions, the West Side Conveyance System would have other purposes. Significantly, it could provide: (1) a high order of flood control of the streams it crosses; (2) flows for fisheries enhancement; and (3) substantial recreational benefits. The flood control aspect may be particularly significant if it is ultimately decided not to build the Iron Canyon Reservoir on the Sacramento River near Red Bluff. By using the series of reservoirs interconnected by large cuts rather than by tunnels, essentially the total surplus runoff of the west side streams can be diverted and conveyed to Glenn Reservoir.

TOPOGRAPHY AND GEOLOGY

The West Side Conveyance System would be located in an area of moderate topographic relief in the foothills of the Coast Range. The highest ridges and peaks in the immediate area lie at an elevation of 1, 500 feet, and major stream channels have an elevation just under 1, 000 feet. The streams all run nearly due east from sources in the Coast Range toward the Sacramento River.

The region is underlain by two major geologic units, the bedrock series adjacent to the mountains and the Tehama formation on the valley side. Areas underlain by bedrock units consist of parallel northwest trending rolling ridges and saddles, while the younger flat-lying Tehama units have developed an intricate feather-like drainage pattern.

The bedrock series includes the Cretaceous marine sediments of the Sacramento Valley section as well as the Knoxville formation of Jura-Cretaceous age, both of which are commonly referred to simply as Cretaceous. This bedrock series has relatively uniform northwest strike and dips steeply to the east. Rock types include mudstone-shale, sandstone, and conglomerate, with mudstone-shale accounting for roughly 70 percent of the entire Cretaceous series. The sandstones and conglomerates are generally hard competent rocks. The mudstone-shale is a relatively hard and well consolidated rock having an unconfined compressive strength on the order of 1, 000 psi. For a shale, it is unusually resistant to weathering. All three rock types are essentially impervious, and contain no ground water in the usual sense.

DESIGN AND CONSTRUCTION-CONVENTIONAL METHODS

The conveyance system would be designed to carry a normal flow of 10,000 cubic feet per second, and would simultaneously be capable of controlling flood flows occurring on watersheds intercepted along the route. The open cut channel dimensions and slopes would be varied throughout the route dependent largely upon the topography and the flood flow requirements. Side slopes would be variable dependent upon rock conditions encountered, particularly upon the dip of the formation. Generally, since the channels roughly parallel the strike, they would be located in the mudstone-shale, both because that unit has in most cases eroded to a lower elevation than the adjacent sandstone and conglomerate, and for greater ease of excavation.

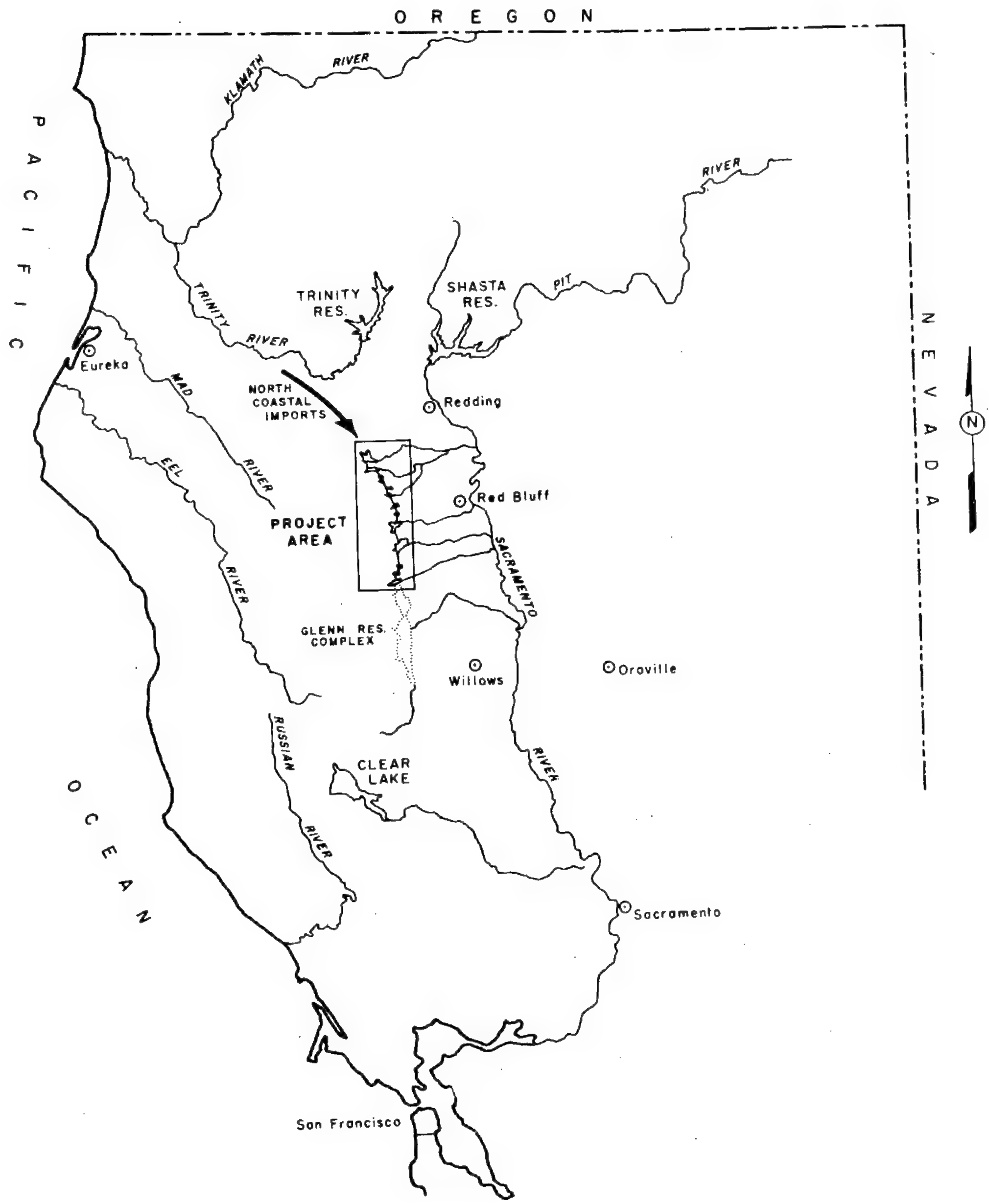

Fig. 1. Location map of West Side conveyance system.

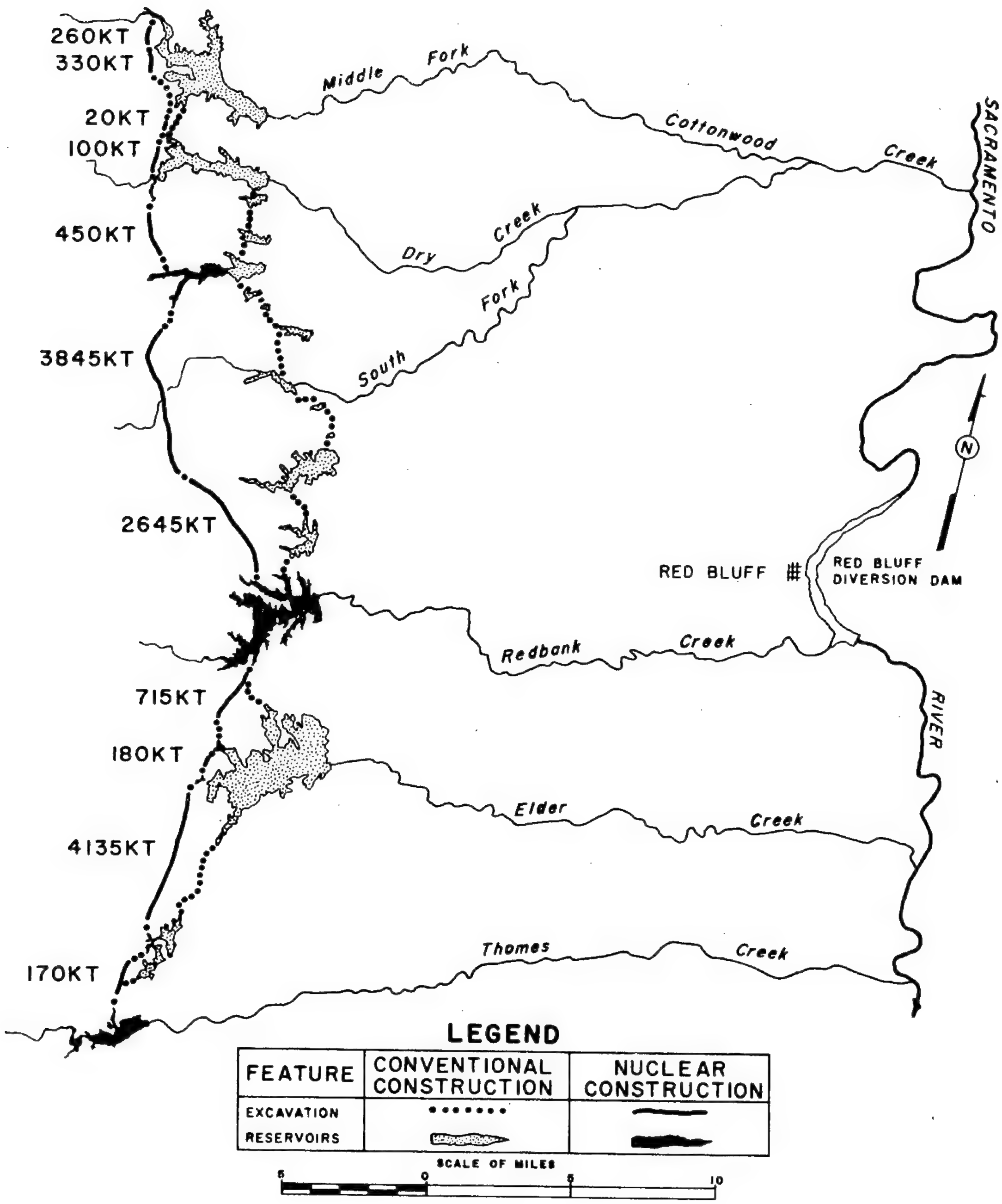

Fig. 2. Alternative alignments - West Side conveyance system.

The maximum section would have a bottom width of about 80 feet, a depth on the order of 300 feet, and average side slopes of about 1-1/2:1. The side slopes would not necessarily be identical on each side; because of the easterly dip of the formations it is expected that the east slope may be somewhat steeper and the west side slope somewhat flatter than 1-1/2:1.

A head loss of about 50 feet would be required to convey the water approximately 40 miles from Fiddlers Reservoir on the Middle Fork of Cottonwood Creek to the Glenn Reservoir at Thomes Creek.

The dams forming the reservoirs would all be earthfill and would have outlet works for downstream releases as necessary. Although the sys-

tem would be designed to control and divert floods of the magnitude of the standard project flood, the major reservoirs would have spillways with capacity as necessary to pass greater floods including the probable maximum flood. The dams would be of conventional design, generally utilizing materials from the nearby Tehama formation. Since the mudstone-shale has unknown characteristics for earthfill construction, its use in fill is not presently being considered.

Construction of the connecting channels would be a routine (albeit very large) earth moving job consisting of excavation and transportation of material to disposal areas. Engineering geologists have estimated that the mudstone-shale could be excavated by means of heavy rippers and push-loaded rubber-tired scrapers to a depth of about 80 feet below the surface. At greater depths it is expected that drilling and blasting would be required with the excavation to be performed by power shovel, loading into dump trucks. In the sandstone and conglomerate, the shovel and truck operation would be used exclusively.

Total volume of excavation for interconnecting channels, in the most economical conventional plan, would be about 124, 000, 000 cubic yards, and is estimated to cost about $67, 000, 000. Total volume of embankment in dams would be about 34, 000, 000 cubic yards, with total reservoir costs of about $63, 000, 000. Total cost of the system, utilizing conventional techniques, would be about $130, 000, 000, based on 1961 unit prices.

DESIGN AND CONSTRUCTION NUCLEAR METHODS

Feasibility and cost of construction of the project by nuclear excavation methods along the alignment of the conventional route was investigated as an alternative to conventional methods. Personnel of the Lawrence Radiation Laboratory studied the excavation requirements and determined that all cuts of over one million cubic yards in volume and in excess of 120 feet in depth could probably be excavated more economically by nuclear than by conventional means. Some saving in cost of excavation was indicated, but the cost of the reservoirs, aggregating about half the total cost of the conventional route, remained unchanged so there was no significant gain.

This finding led to the decision to investigate new routes more favorable to nuclear techniques, requiring fewer dams but without a correspondingly greater excavation cost. Toward this end another alignment was plotted as shown on Figure 2. This route is about 42 miles long of which 30 miles consist of channel, 7 miles of the channel to be constructed by conventional means and 23 miles by nuclear methods. Figure 2 shows the approximate total yield required to excavate each portion of the channel. The maximum single yield is estimated to be 500 kilotons.

Total volume of excavation along the nuclear route is about 600, 000, 000 cubic yards or more than 4 times that of the conventional route.

COMPARISION OF COSTS

The nuclear route would permit the elimination of several intermediate reservoirs, thus reducing the volume of earthfill in dams from about 34, 000, 000 cubic yards in the conventional solution to about 7, 000, 000 cubic yards in the nuclear solution. This results in a saving of about $50, 000, 000 in the cost of the dams.

Based on 1958 device charges, which have been released by the Atomic Energy Commission, the nuclear excavation costs would exceed the conventional excavation costs on the conventional route, significantly reducing the savings effected by reduction in dam costs. However, the Atomic Energy Commission has stated "If a number of assemblies were fired in the same location, or a large number of assemblies were required, the service charge per unit would be substantially reduced."* which could effect major savings by virtue of the large number of devices required for this project. Furthermore, at the time contemplated for possible construction of this project, it is anticipated that developments will have occurred to permit significant reductions in the Atomic Energy Commission's charges.

SAFETY CONSIDERATIONS

As mentioned earlier, a factor of paramount importance in evaluating the feasibility of the use of nuclear explosives is safety. In addition to the hazards associated with conventional chemical explosives such as ground shock and the throwout of material, other hazards peculiar to nuclear explosives, namely, radioactivity and air blast, must be taken into account.

*UCRL-5676, page 2

The project consists of eleven separate excavations of varying sizes along the 42 mile route (Figure 2), and each must be considered individually in assessing safety problems. Special emphasis would be placed on the combination of factors that would present the most critical safety hazard at each location. A maximum yield of 500 kilotons for a single device was selected as a reasonable size for this project. Seven of the separate excavations could be made by the use of smaller devices (see Figure 2). However, the efficiency of excavation is improved by simultaneous firing of a line of charges. Therefore, the total maximum allowable yield for each detonation at the other four remaining larger excavations would be made as high as permitted by safety requirements. These yields would have to be determined by detailes site investigations.

The hazards of nuclear cratering explosion are the following:

1. Radioactivity
   a. The amount released to the atmosphere
   b. The effect on surface water
   c. The effect on ground water
2. Seismic Effects
3. Air Blast
   a. Direct air blast
   b. Intermediate and long-range air blast

RADIOACTIVITY

Radioactivity produced by a nuclear explosion is derived from fission products and the interaction of neutrons with surrounding materials (induced activity). Also, in a thermonuclear reaction, tritium is formed. Most of the fission product radioactivity would be contained in the fused material near the shot point or in the crater rubble. It is estimated that the proposed depth of emplacement of the nuclear explosives, no more than 3 percent of the radioactivity would escape to the atmosphere. The vented radionuclides become attached to dust particles, some of which travel radially outward in the base surge; some fall back into and around the edge of the crater; the rest rise in the cloud, to be dissipated by the wind.

It has been assumed that relatively "clean" devices may be available at the time currently envisioned for this project, and that average meteorological conditions for the area would prevail at the time of firing.

Based on these assumptions, in the downwind direction the lifetime radiation dose from a 500-kiloton detonation would not exceed 0. 5 roentgens at a distance of about 10 miles. This means that during the lifetime of a person residing continuously at this distance he would receive this dose. If residents were evacuated for 24 hours following the shot, these exposures would be reduced by a factor of two. For comparison with the above indicated lifetime does, the Federal Radiation Council recommends, for continuous exposure, that a does not be permitted to exceed 0. 5 roentgens per year.

Of significant importance is the lapse of time following the shot when entry into the channel would be permissible. It is estimated that access for limited periods would be permissible within a few days; access for a 40-hour work week would be possible after a few weeks.

A consideration of perhaps even more importance that airborne radioactivity is that of the contamination of water, both the existing ground and surface water in the shot area and water which would later be conveyed in the excavated channel.

The problem of ground water contamination has been carefully examined. First, there is no aquifer in the Cretaceous formation in which the route would be located. Second, even if leaching of radioactive ions to a hypothetical ground water basin did occur, the concentration of the ions in the percolating water would be far less than tolerance due to the assumed high distribution coefficients characteristic of the soils along the route.

It is assumed that most of the radioactivity would be incorporated into fused glass material and would not be readily available for surface water contamination or transport. Of the radionuclides available for transport, strontium (Sr-90) is by far the most critical. The long-lived isotope cesium (Cs-137) has a tolerable limit 100 times greater than Sr-90 with about equal production. Thus, the hazard from Sr-90 predominates. If all the Sr-90 activity per unit area fell into a stream 1 cm deep and were immediately soluble, the concentration would be 10 times the tolerable level. However, since only about 10 percent of the Sr-90 would be immediately soluble, the concentration would be at or less than tolerance. Since the water depth in the channel, or in any nearby stream, will obviously be greatly in excess of a depth of 1 cm, the Sr-90 concentration would be diluted to far less than a tolerable level. The disposition of

fission products that remain insoluble is determined by the characteristics of the stream flow and the ecology of the region. The self-cleansing characteristics of streams is well documented in the literature.

An excellent study has been performed by the United States Geological Survey* which evaluates the potential contamination effects of "Project Chariot" on local water supplies. Fission product activities which would have resulted from the then available nuclear devices, in streams in the immediate vicinity of the Chariot site, would have a concentration about 20 times greater than tolerance. Since a significant decrease in radioactivity is expected from the devices assumed in the reconnaissance studies of the West Side Conveyance System, concentrations would be much less than the level of tolerance, if such devices actually are developed.

SEISMIC EFFECTS

Seismic effects of the nuclear shots require careful evaluation. The intensity of the ground shock is a function of the yield of the detonation, the geology of the area, and distance. Rock types are particularly important since the efficiency of energy transmission to the surrounding material varies widely with the medium; it is much greater in hard rock than in alluvium. On the other hand, higher accelerations and ground displacements are observed in alluvial materials than in rock. Tests with small scale chemical explosives in the rock along the West Side Conveyance System would permit reasonably accurate predictions of the magnitude and propagation of the shock wave.

Equations developed by the United States Coast and Geodetic Survey for relating peak surface acceleration and velocity to yield and range for cratering shots in hard rock were used to evaluate hazards due to ground motion. Criteria of 0.1g acceleration and 3 inches per second velocity were used as the threshold of damage for residential-type structures. Velocity appears to be the more reliable criterion because it has been derived from actual blasting tests.

Uniform geologic conditions were assumed for the seismic evaluation. Using the velocity criterion, a 500-kiloton nuclear explosive could be safely detonated along the nuclear route without seismic damage to towns along Highway 99. Detailed geologic investigations are necessary to define this problem and to determine the maximum allowable yield in each of the four cuts requiring greater than 500 kilotons. Small communities and isolated structures in the immediate area would have to be individually investigated to evaluate the amount of damage which might be incurred.

AIR BLAST

Air blast from an underground explosion, as expected, would be much less than that from a surface explosion. If we accept 2 milibars overpressure as the threshold of damage to large windows, then the area controlled for purposes of direct air blast damage would be about 4 to 5 miles in radius for the 500-kiloton shot. The intensity and propagation of the intermediate air blast out to 100 miles is dependent upon wind and temperature distribution in the troposphere. A preshot calculation would be made, based upon local weather conditions, to determine pressures which would occur at inhabited locations. Another possible hazard from air blast exists - that due to refraction of sound waves from the ozonosphere which may strike the ground between 80 and 150 miles downwind from the shot. It is expected that the resulting pressures from this effect would not be sufficient to break windows or create structural damage.

CONCLUSIONS

The reconnaissance studies made to date have indicated the following tentative conclusions with regard to construction of the West Side Conveyance System, by utilization of nuclear explosives for deep excavation:

1. It is technically and structurally feasible to construct water conveyance channels, in the Cretaceous formation of western Tehama County, by nuclear means.

2. Based upon current knowledge and a reasonable projection of knowledge expected to be developed prior to the contemplated time of possible construction (perhaps about 1985 or 1990), it would be possible to detonate the nuclear devices with safety.

*Piper, Arthur M. - Potential Effects of Project Chariot on Local Water Supplies. USGS. TEI-810, 1961

3. Radioactive contamination of water flowing through the excavated channels, or in ground water, would be far less than the level of tolerance.

4. It may be possible to make significant savings in overall cost of the System.

The joint study group expects to complete this rough reconnaissance study and prepare a report for the use of both agencies. Although we cannot say today that nuclear excavation would ever be used for a project such as the West Side Conveyance System, it is sufficiently promising to support a recommendation for further studies, and to encourage further development of the techniques in this field.

BIOGRAPHICAL SKETCHES OF AUTHORS

J. W. Keysor is a graduate in civil engineering from Colorado State University. He has been employed in the California Department of Water Resources for the past 12 years, of which nearly 5 were in project planning investigations for future water developments. At present he is Chief of the Staff Engineering Branch in the Division of Design and Construction. His earlier experience has included six years with the City of San Diego and four years with the U.S. Bureau of Indian Affairs in connection with the design and construction of dams, water conveyance systems, and appurtenant works.

M. B. Andrew is a graduate in Mechanical engineering from the University of Washington. He has been employed in the California Department of Water Resources for the past 6 years, being in charge of the nuclear energy and sea water conversion program for most of the period. At present he is in charge of the department's activities in atomic energy and isotopes applications. Prior to his employment with the State he worked for Westinghouse on the design of the Shippingport Atomic Power Station. This was preceded by two years with the Atomic Energy Commission on the design of the Savannah River Plant. His earlier experience consisted of about 20 years with the Corps of Engineers in mechanical and electrical design of dams.

COMPLETELY CONTAINED NUCLEAR EXPLOSIVES FOR MINING BY CAVING

S. M. Hansen
D. B. Lombard

Lawrence Radiation Laboratory, University of California
Livermore, California

ABSTRACT

Rock breaking technology utilizing contained nuclear explosions is reviewed, and applicable nuclear experiments are briefly summarized. A new design for an underground bulk mining method known as "nuclear caving" is described, and design and applicability comparisons are drawn with conventional block caving. Special safety aspects of the nuclear case are discussed, and a comprehensive economic evaluation of the two methods is made, based partly on applications of the design to existing orebodies. It is concluded that nuclear caving with the new design is more economical than with previously proposed nuclear designs, and that the new nuclear caving design has a substantial economic potential, compared to conventional block caving, in orebodies of several million tons and larger.

INTRODUCTION

Underground mining with nuclear explosives has long been considered to be among those Plowshare applications with maximum potential. The firing and exploration of underground nuclear tests, two of which were in granitic rock, has provided the effects data needed to advance the study of nuclear explosives as underground mining tools.

PERTINENT EXPLOSION EFFECTS

Successful applications will depend on the development of new mining methods which take advantage of the unique rock-breaking characteristics of these explosives. Our study suggests a mine design similar to block caving in many respects, but distinct from it in others. The effects and characteristics of nuclear explosives which are of primary importance in underground mine design are considered briefly in the following paragraphs.

Chimney of Fragmented Rock

A cylinder-shaped zone or chimney of rubble with sharp, regular boundaries is produced above and around the explosion center. (See Figure 1.)* The chimney is formed by gravity collapse of the shock-weakened rock overlying the nuclear explosion cavity void. Collapse continues upward until the broken rock has swelled to fill the void space almost completely, and will support the upward arch.

Zone of Fracturing

A zone of fracturing, within which rock strength is reduced, surrounds the chimney and extends laterally two cavity radii or more from the chimney boundary. Fractures result from a combination of direct shock-wave effect, and post-shock gravity subsidence and adjustment. As shown diagrammatically in Figure 1, the zone of fracture weakening is not symmetrically developed around the chimney. Experience at Shoal and Hardhat, the two experiments in granitic rock, indicates that the rock will support mine openings

*Figure 1 is a diagrammatic representation of Hardhat, a 5-kt nuclear explosion in granodiorite at the Nevada Test Site, February 15, 1962. Hardhat, buried 939 ft, made a cavity 63 ft in radius and a rubble chimney extending 281 ft above the short point.

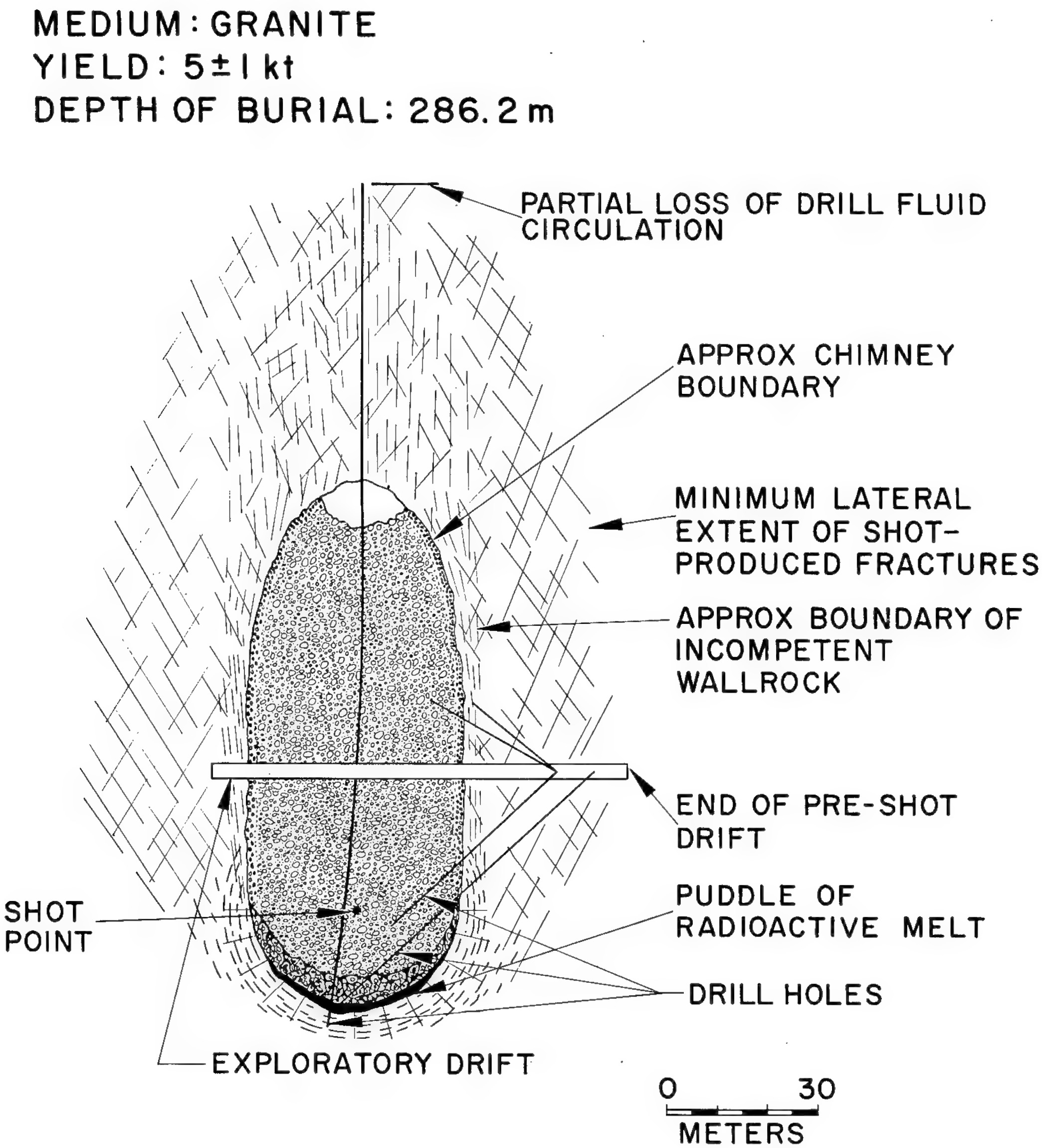

Fig. 1. Hardhat chimney.

without significantly increased ground support problems, at distances of a few tens of feet beneath the bottom of the cavity, depending on the energy yield of the explosion. In the case of Shoal,* the intensely shocked and compacted zone extended downward for only about 25 feet. Drilling evidence indicates that the rock beneath this 25-foot zone is essentially unchanged from its preshot condition, with regard to its ability to support mine openings.

*Shoal: A 12.5-kt experimental nuclear explosion conducted in granite near Fallon, Nevada on October 26, 1963. The explosion was buried at 1205 ft; it produced a cavity of 84-ft radius, and a chimney with a height of 356 ft above the shot point.

Package Sizes of Nuclear Explosives

The Atomic Energy Commission has recently announced the availability of 10- and 100-kiloton nuclear explosives which can be emplaced in drill holes of about 13 and 19 inches inside diameter, respectively. Other (larger) package sizes and explosive yields are also available. Both drift

and drill-hole emplacement are technically feasible for virtually all nuclear explosive applications.

Chimney Parameter Predictive Capability

Available experimental data permits the prediction of cavity size, chimney height, and tonnage of broken rock for underground nuclear explosions with considerable confidence. For a specified rock type, predictive accuracy is within 10%. Criteria for establishing minimum depths of burial to prevent dynamic venting have also been established. For explosions in hard rock, such dynamic venting can be prevented by a depth of burial equal to the anticipated chimney height plus a 300- to 500-foot-thick "buffer" of overlying hard-rock cover. Figures 2, 3, 4, and 5 show chimney parameters plotted against depth of burial for various yields. These curves are terminated at the depths where the chimneys are calculated to intersect the ground surface. At such depths some dynamic venting would be expected to occur. The depths of burial giving 300- and 500-foot buffer thicknesses are also indicated on the curves. These figures are based on preliminary data and are subject to future modification, as more information becomes available.

MULTIPLE NUCLEAR EXPLOSIONS

The irregular shape of most ore bodies precludes their complete breakage by a single nuclear explosion. It thus becomes necessary to consider the use of a number of explosions to break a mass of rock of large tonnage and irregular dimensions. A multiple explosive approach will offer greater flexibility in cases where the boundary of the broken rock must be adjusted to the

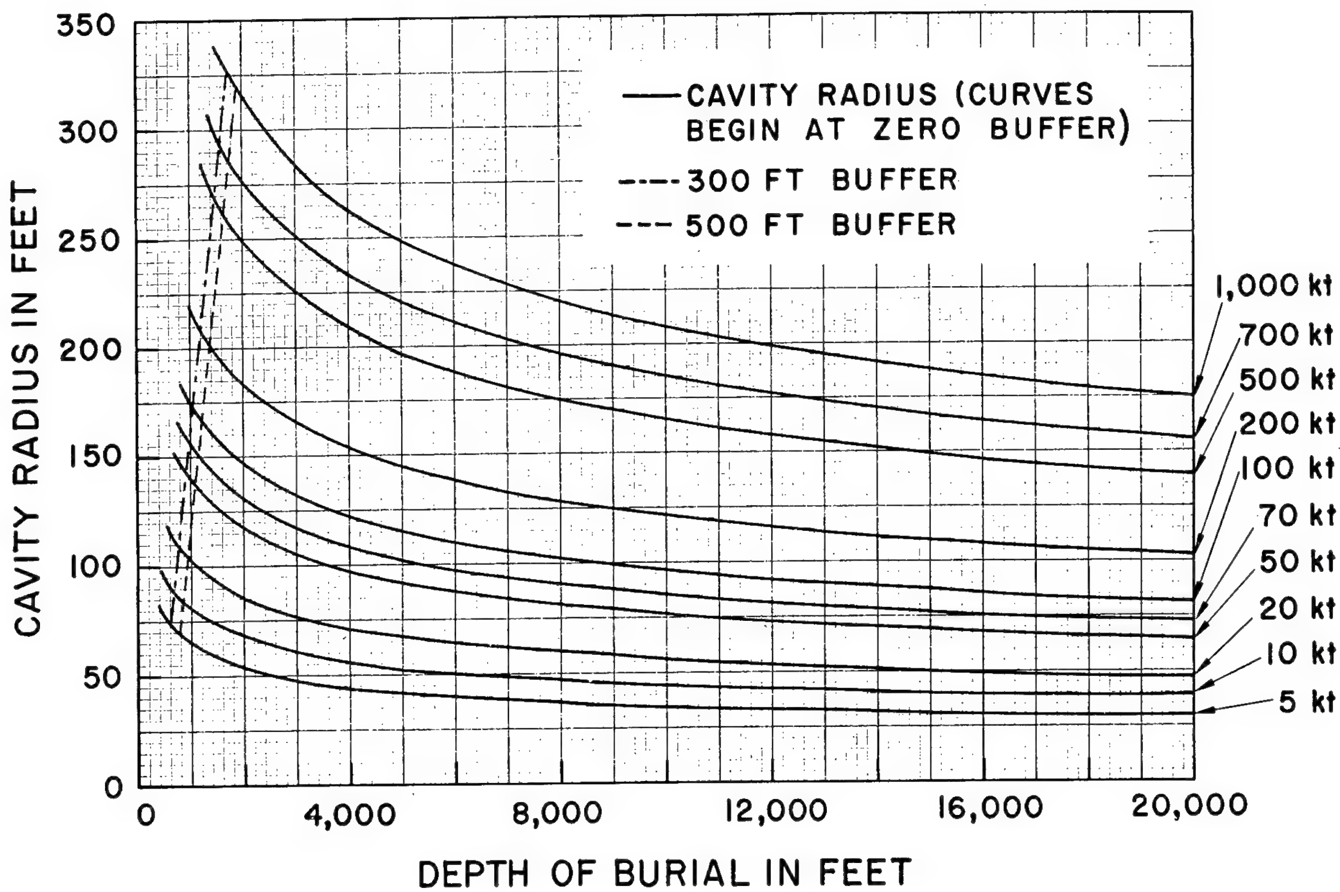

Fig. 2. Cavity radius for underground nuclear explosions in granitic rock.

boundary of the ore zone. Three approaches are possible:

1. A series of single explosives, emplaced and detonated alternately;

2. A horizontal array of nuclear explosives, detonated simultaneously or with millisecond delays; and

3. A combination of 1 and 2, wherein several simultaneous explosive arrays are emplaced and detonated separately, each array being emplaced after the detonation of the previous array.

A series of single explosions has, in some cases, the advantage of minimal seismic and shock-wave damage. The simultaneous detonation approach, where feasible, has the advantage of enhancement of rock breakage caused by the interaction of shock waves from adjacent explosions, and the practical use of a single underground drift system for emplacing the entire array. It is likely in most applications, however, the maximum benefit can be realized by the combination approach, allowing the use of multiple detonations up to the maximum seismic yield limitation at a given site.

NUCLEAR CAVING

Underground mining by block caving has established a technology for handling large tonnages of broken rock. Many design characteristics from block caving are adaptable to mining rock broken by underground nuclear explosions. For purposes of comparison, Figures 6 and 7, generalized drawings of conventional block-cave designs are included. One of the first successful block caving designs utilized a grizzly level for ore sizing and gravity transfer to the haulage level; an example is shown in Figure 6. The slusher gravity design, shown in Figure 7, utilizes a scraper on a slusher level to transport ore from the ore passes to a single grizzly. This is the most widely used block-cave design at present, largely because of its advantage of better production control. In both these block-caving designs, the ore is broken by

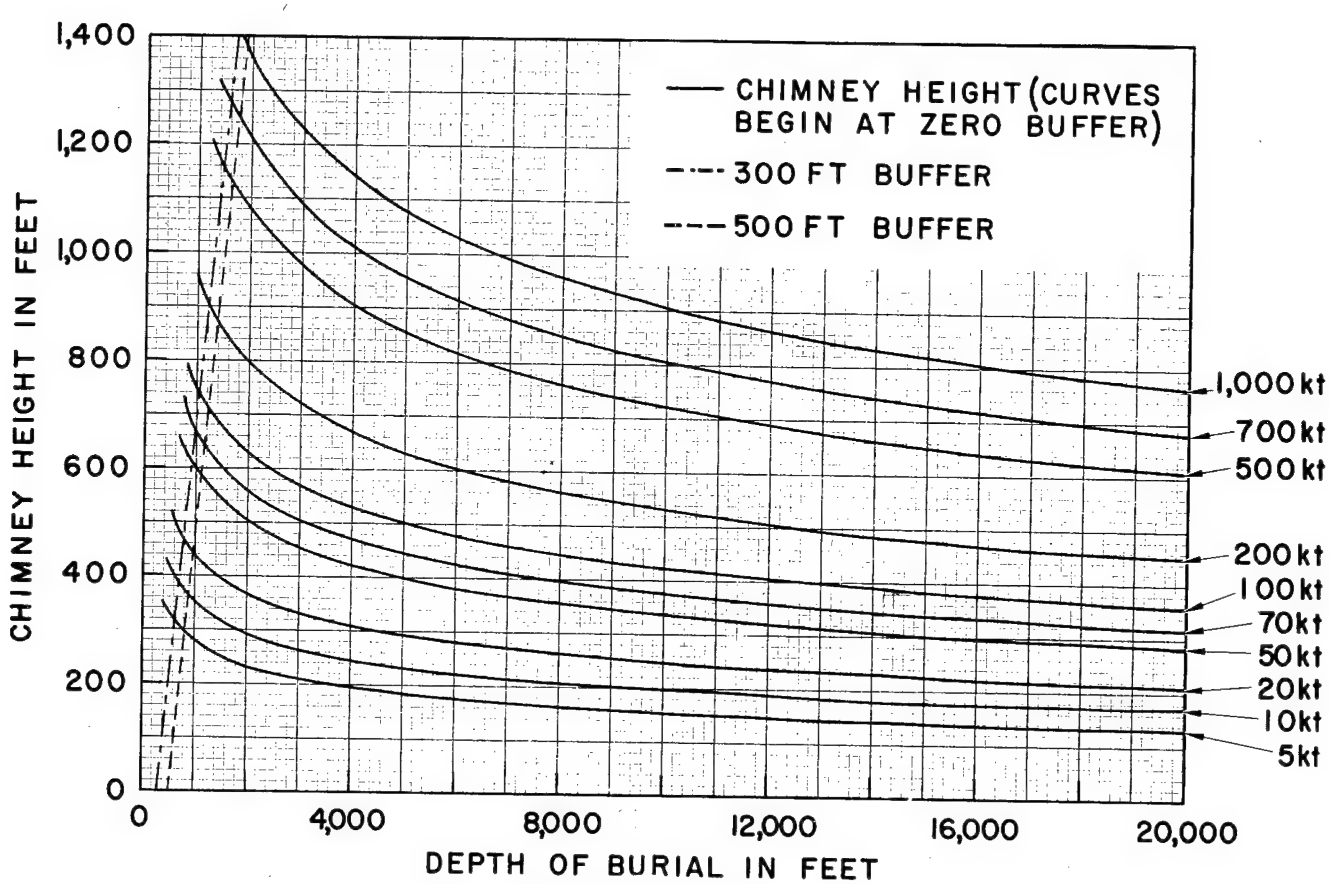

Fig. 3. Chimney height for underground nuclear explosions in granitic rock.

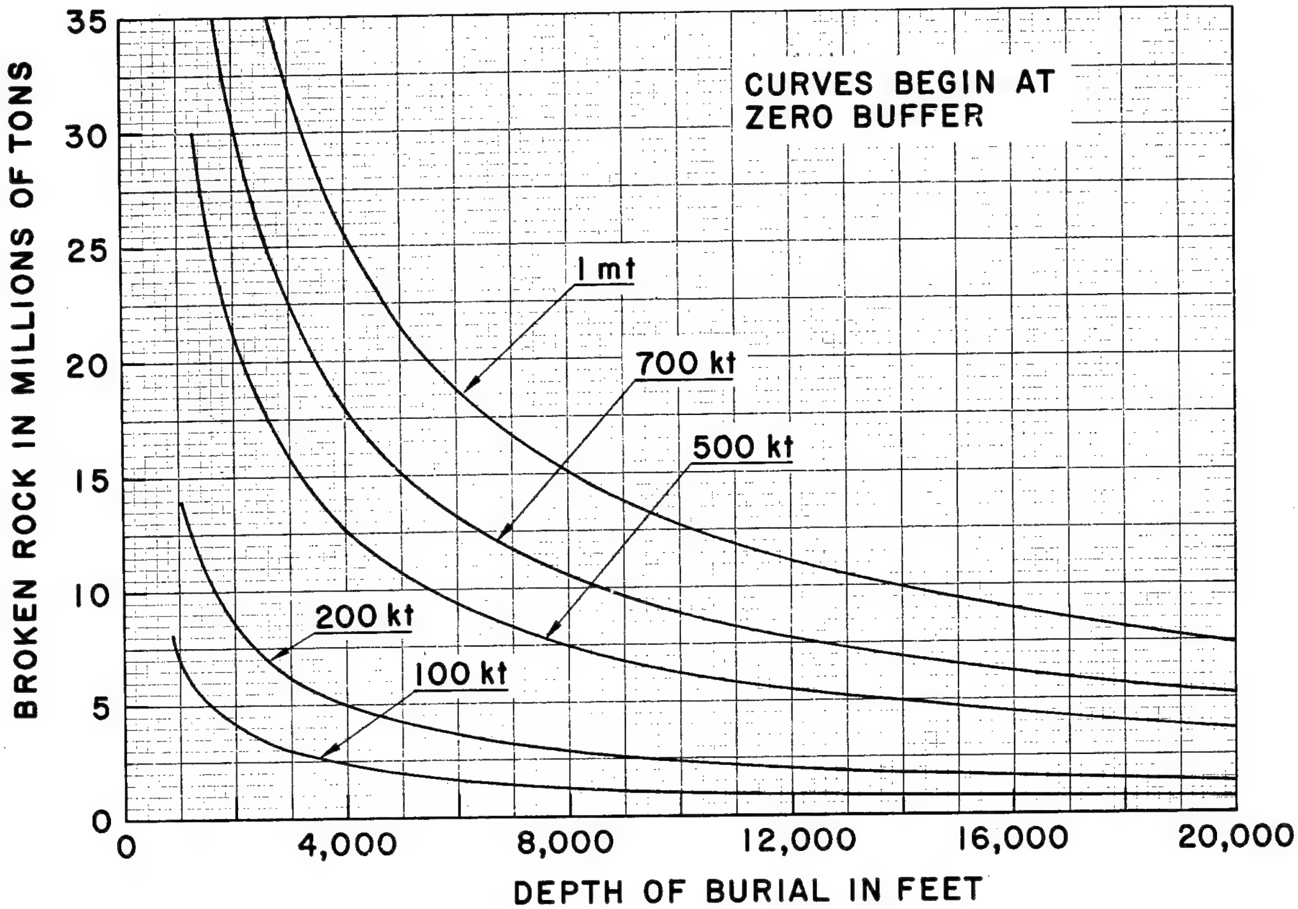

Fig. 4. Tonnages of granitic rock broken by underground nuclear explosions (50 kt).

gravitational stresses resulting from the weight of the rock overlying an undercut. Among the most important limitations of the method are its sensitivity to rock strength, and difficulties in maintaining control of the draw. The latter include: dilution of the ore by waste from beyond the boundaries of the ore; upward termination of caving by arching; and "piping," caused by a narrow angle of draw, which results in poor ore recovery and dilution by rock from above the ore zone.

Figure 8 is a generalized nuclear caving mine layout designed to recover ore broken by a horizontal array of nuclear explosives fired simultaneously. This nuclear caving design utilizes a slusher-gravity method of ore handling similar to the block-caving design shown in Figure 7. Similarities to block caving design include:

1. Similar layouts for slusher and haulage drifts;

2. Ore sizing by grizzly on the slusher levels; and

3. Gravity ore transfer to the haulage levels.

The most significant differences between this nuclear caving design and block caving designs are:

1. The lack of an undercut level for caving, since the ore body will have been completely broken by nuclear explosions prior to mining;

2. The grander scale of mining and the increased size of the mine development units. The horizontal dimensions of an individual conventional development block seldom exceed 200 or 300 feet, while a maximum lateral extent of several thousand feet is possible in nuclear caving. The average height for block caving from a single level varies from about 250 to 400 feet. The thickness or ore recovered from a single level in nuclear caving may be 1000 feet or more, as a result of the upward development of the rubble chimney.

Figure 9 is a detailed plan of the nuclear caving slusher level with a draw-point spacing of 50 to 65 feet. The corresponding spacing between the ore passes is 12 to 30 feet in conventional block caving. Proper draw-point spacing depends on the angle of draw, i. e., the angle of the cone of fragmented rock which draws to a given point. Broader draw angles permit wider draw-point spacing, which reduces mine development costs. Draw angle has been shown in a qualitative way to be related to: competency and degree of fragmentation; fragment size distribution; the nearness and number of boundaries producing lateral confinement; and the thickness of fragmented rock above the draw points. These factors all correspond to differences between nuclear caving and block caving in such a way that one would expect broader draw angles in the nuclear case. Optimum draw-point spacing for a nuclear caving mine will depend on the draw angles which develop under the conditions present, and will need to be determined on an individual basis.

An additional area of concern in the use of nuclear explosives underground will be the post-shot rock temperatures, since a substantial portion of the nuclear explosive energy is deposited as heat in the rock. Residual heat problems have been overcome satisfactorily at the Nevada Test Site and have not interfered seriously with mining operations there. The maximum rock temperatures in the re-entry workings in the Hardhat chimney 13 months after detonation were 160° F before ventilation. After 2 to 3 weeks of good ventilation, working temperatures had dropped to within the 80 to 100° F range. No refrigeration was employed.

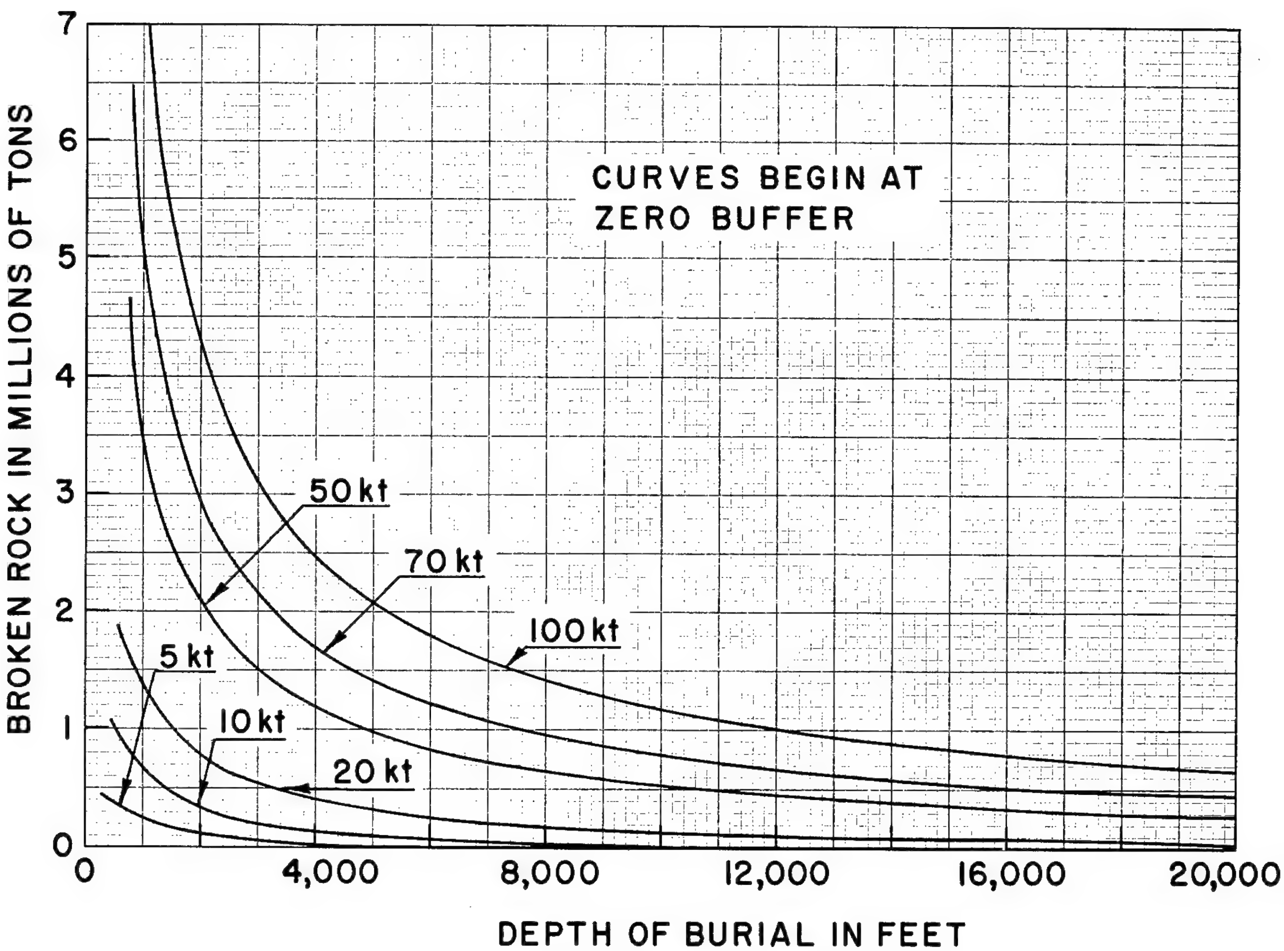

Fig. 5. Tonnages of granitic rock broken by underground nuclear explosions (1 Mt).

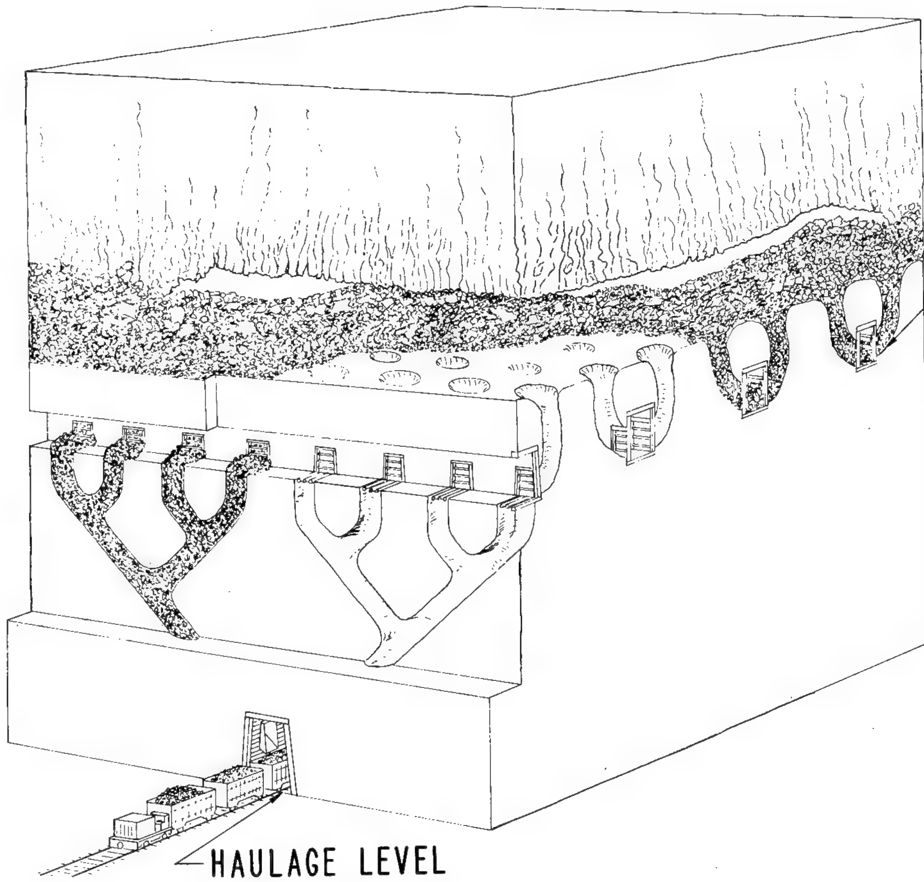

Fig. 6. Conventional grizzly control gravity transfer.

SAFETY

Possible hazards to personnel and property in the use of nuclear explosions for underground mining can be separated into those from seismic and shock waves, and those from radioactivity. Radioactive fallout and airblast, major considerations for nuclear explosions at shallow depths of burial or in the atmosphere, present no serious difficulties for deeply buried explosions.

Shock And Seismic Damage

Shock Damage to Underground Mine Workings

Experience has shown that the shock wave may cause severe damage to mine openings. Three stages of damage are defined in Figure 10, in which shock damage underground is plotted as a function of explosive yield and range. The categories are gradational. These curves should be useful for planning but are based on preliminary data. Complete closure: mine workings are solidly filled with fragmented rock from the top. sides, and bottom, and are completely inaccessible. Spalling: damage is substantially the result of fall of rock from the top of the drift. Closure is only partial, and re-entry and repair are relatively simple. Heavy drift damage may occur at ranges significantly greater than those shown here, for short distances where drifts intersect zones of rock weakness. Minor damage and offset: limited spalling and minot offsets of shafts, shaft guides and track result from minor differential rock movements. Also, some damage to permanently mounted mine equipment, such as hoists and generating plants may occur.

Seismic Damage to Surface Structures

Damage to surface structures may occur at distances up to tens of thousands of feet from the explosion, depending on the energy yield, the type of structure, the local geology, and the sensitivity of the structures. A comprehensive discussion of seismic damage is beyond the scope of this paper.

Radioactive Hazards

Radioactive Rock Melt

Mining operations several months after detonation will encounter solidified radioactive rock melt at the bottoms of the explosion cavities. Here, special mining techniques will be needed to avoid the over-exposure of workers to radiation during brief periods while these areas are being mined.

Radioactive Gases and Dust

After mine workings have penetrated the explosion cavities, noncondensible radioactive gases and radioactive dust from the chimneys could, if ignored, result in hazards to personnel. This dust problem has been solved successfully at the Nevada Test Site by equipping mine personnel with respirators. Problems from radioactive gases and particles not filtered by respirators have been solved at the Nevada Test Site by increasing mine ventilation, which dilutes and disperses such radioactive material to below tolerance levels. Tritium will be present in water, water vapor, and possibly in elemental gaseous form, where thermonuclear explosions are detonated, and could result in personnel hazards. Here also, effective mine ventilation can be used to lower the concentration of tritium in gaseous froms to nondangerous levels. Another method of controlling an antic-

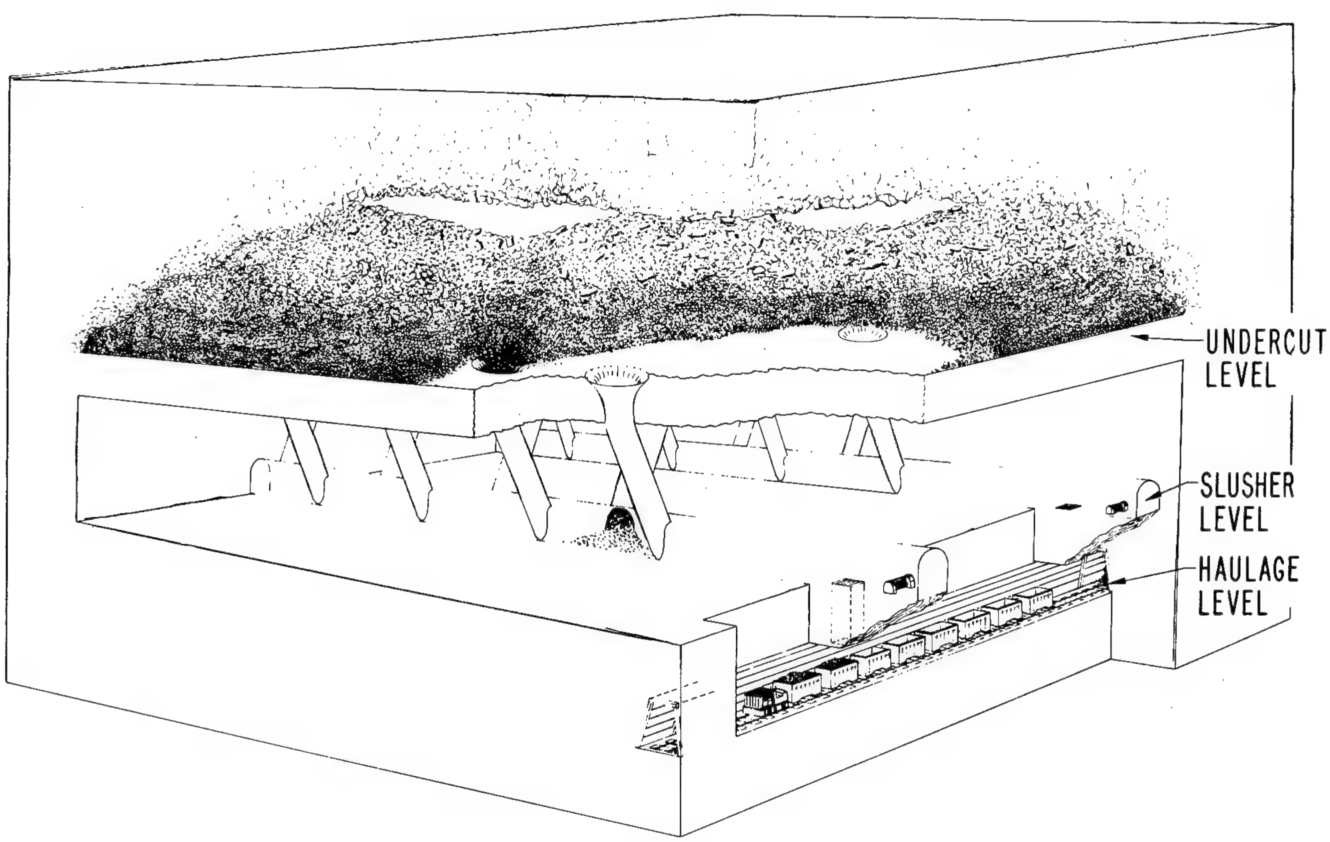

Fig. 7. Conventional grizzly control slusher block.

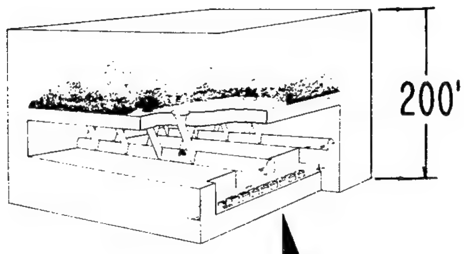

CONVENTIONAL SLUSHER BLOCK SHOWN TO SAME SCALE

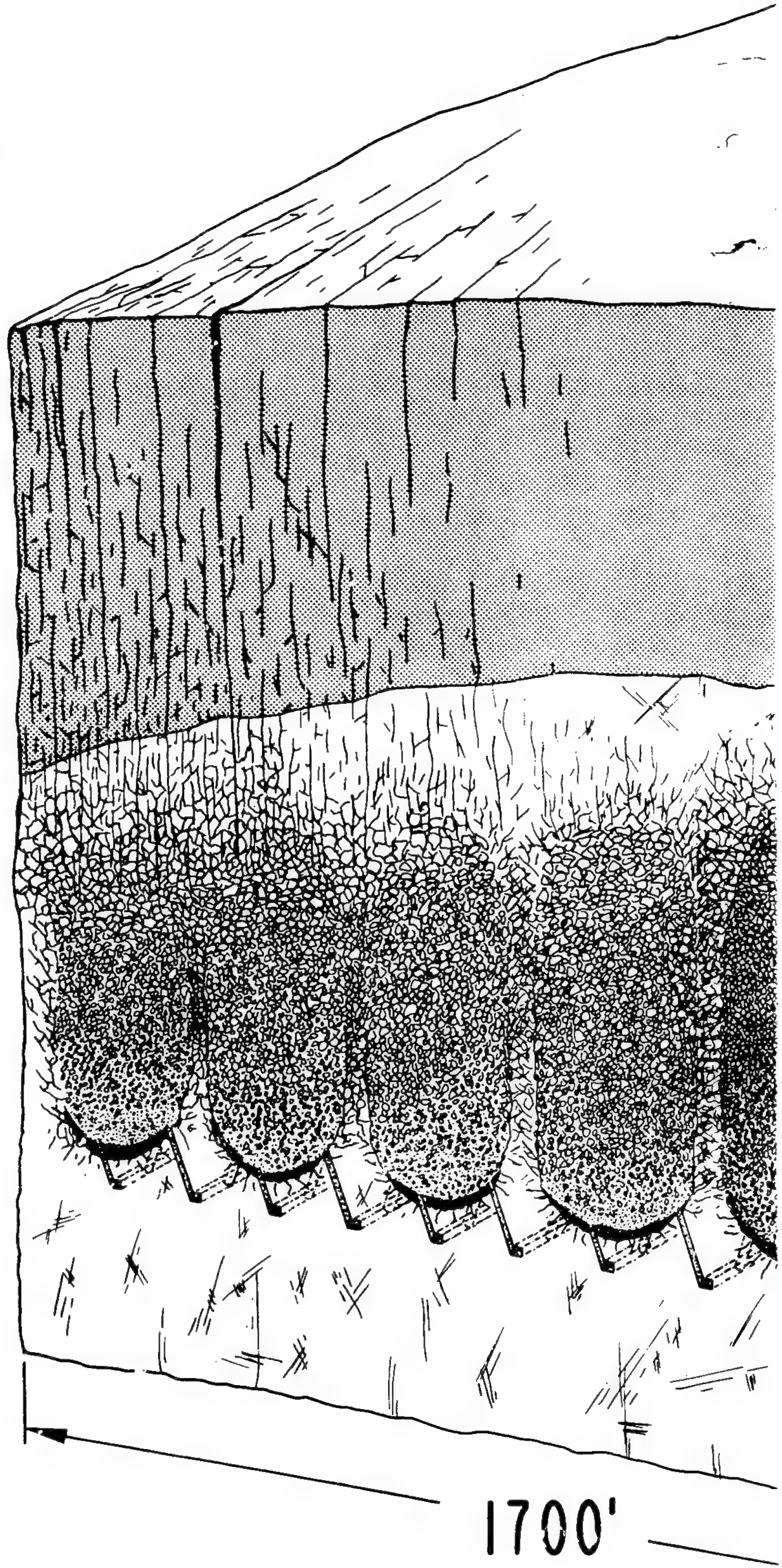

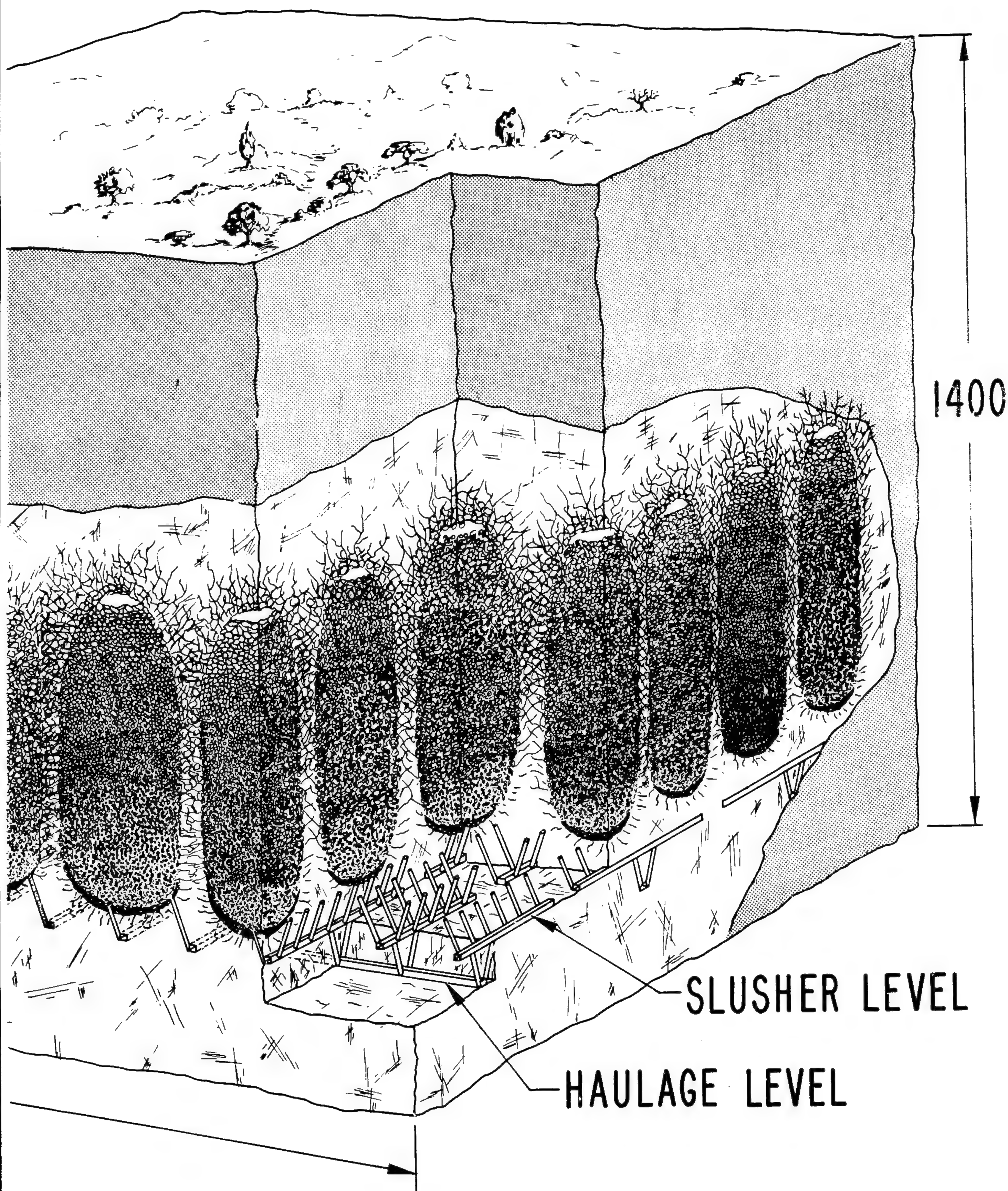

Fig. 8. Nuclear caving mine.

2

ipated tritium hazard would be to avoid its production by employing nuclear explosives which derive more of their energy from fission.

Contamination of the Ore

Possible contamination of the ore by radioactivity is an additional consideration. The principal radioisotopes which can be expected on the surfaces of the rubble particles are of strontium, cesium, and ruthenium. The levels of such radioactivity on rocks in the Rainier and Hardhat chimneys were very low, since only a small fraction of the total fission-product radioactivity was distributed throughout the chimney. The most serious potential problem of ore contamination is that one or more of the radioactive species might tend to become concentrated at some point in the processing of the ore. Pilot studies would be useful in evaluating this possibility, as well as potential contamination of the final product.

ECONOMICS

On the basis of substantial experimental evidence, we conclude that the use of nuclear explosives for breaking rock for underground mining is technically feasible, as is the mining of rock thus broken. The question that must next be considered is a vital one - can nuclear explosives in underground mining offer a substantial economic advantage? If not, there will be no reason to use nuclear explosives, technically feasible or not.

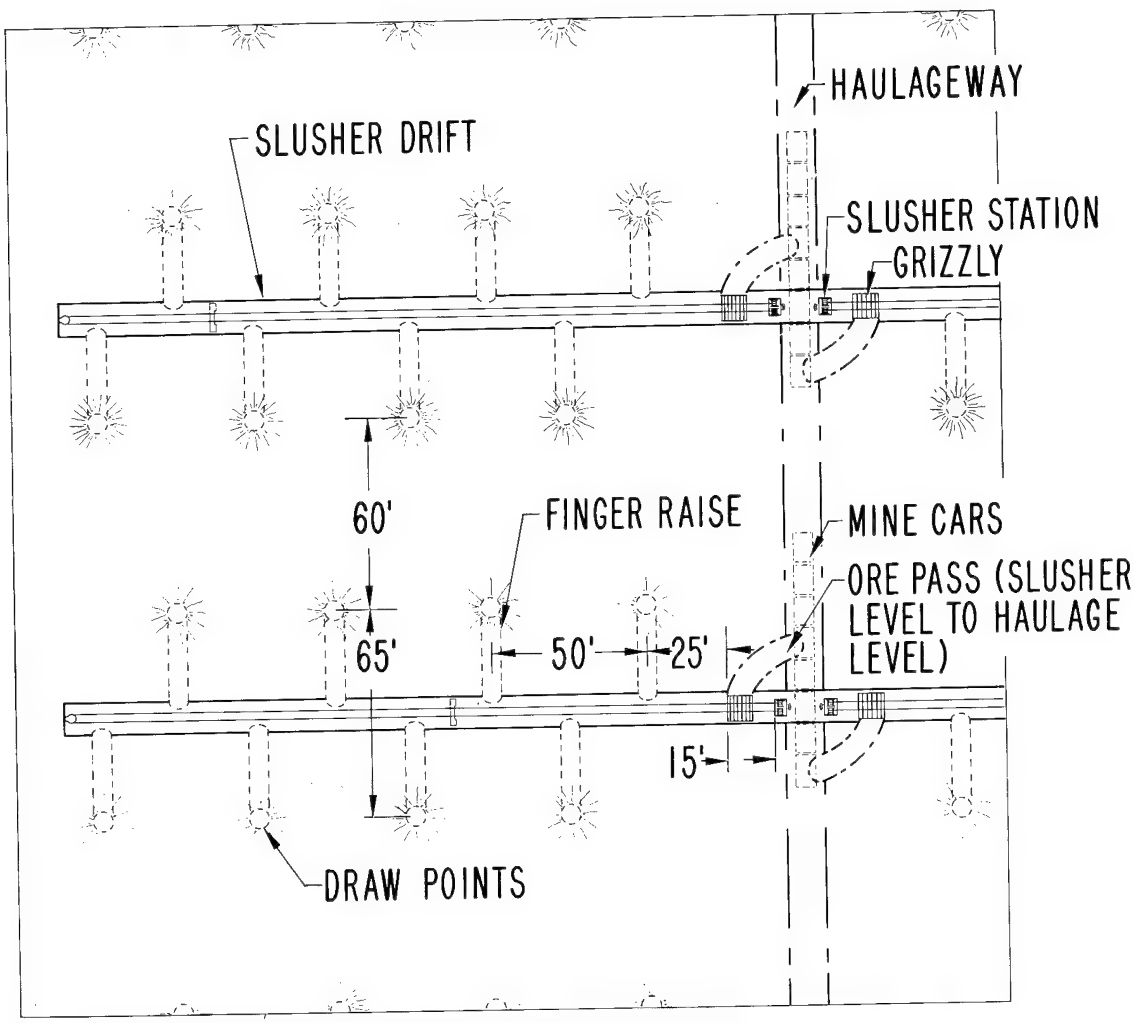

Fig. 9. Nuclear caving slusher drift layout.

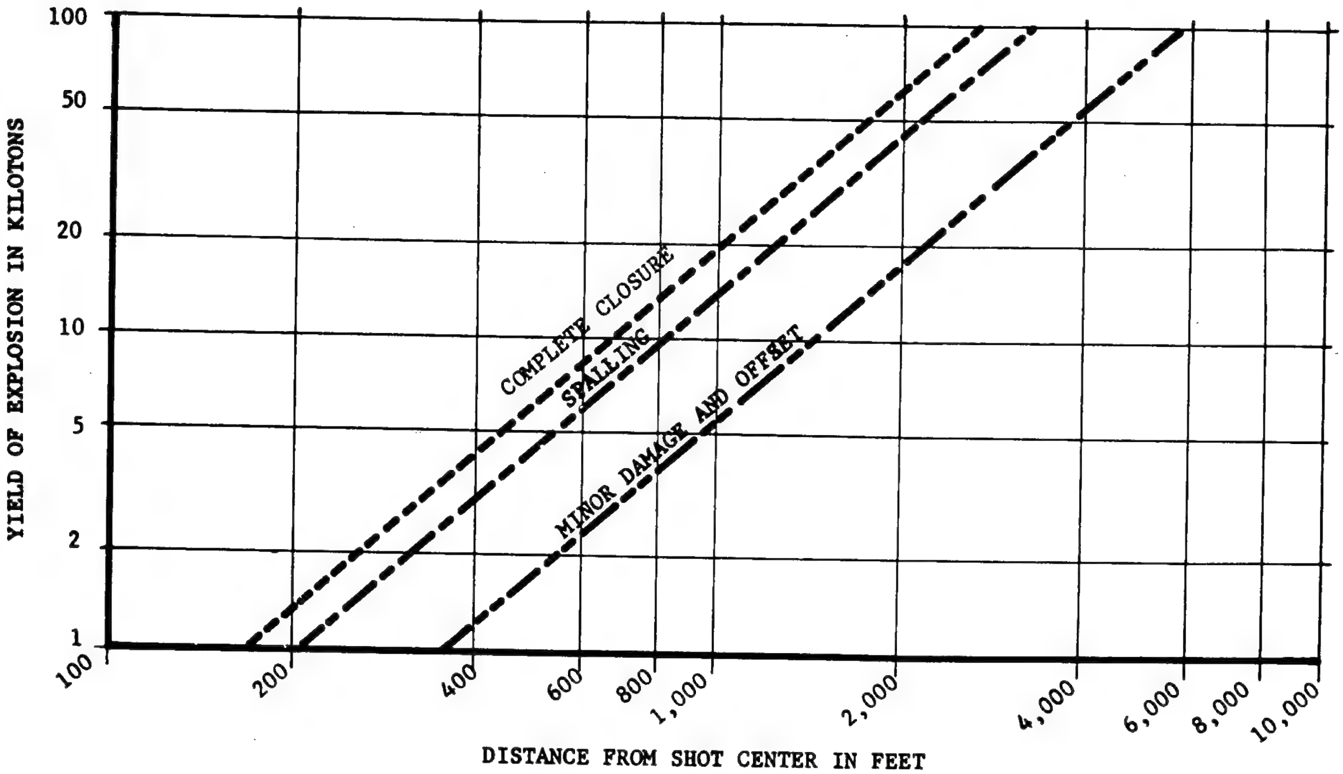

Fig. 10. Damage to mine workings from nuclear explosions in granitic rock.

Economic Advantages of Nuclear Caving

The areas of possible economic advantage with nuclear caving are:

1. Nuclear caving may permit the exploitation of ore bodies which cannot be mined by other methods. For example, those too deeply buried for open-pit mining, those with rock strength characteristics not suitable for block caving, and those with insufficient grade or with mineral distribution unsuited for stoping.

2. A number of factors may tend to reduce the costs of nuclear caving relative to conventional underground bulk mining:

   a. Improvements in mine efficiency by the scaling up of mine elements to permit increased mechanization and greater efficiency or ore drawing and handling.

   b. Reduction of the number of development levels by caving greater thicknesses of ore from each level.

   c. Elimination of the need for an undercut level, which is necessary in block caving.

   d. Separation of ore from wall rock, and reduction of contamination and overdraw, by planning chimney edges to coincide with ore body boundaries.

   e. Increased ore fragmentation from both shock fracturing and the greater distance of movement during withdrawal.

Economic Disadvantages of Nuclear Caving

There are, of course, a number of economic disadvantages of nuclear caving. These include:

1. Expenses from shock wave and seismic damage to:

   a. Underground mine workings and mine equipment;

   b. Surface mine and mill installations and other company property; and

   c. Property owned by others (public liability damage).

2. Expense from radioactivity, including:

   a. Underground mine safety, such as radioactive monitoring, the use of respirators, and increased ventilation;

b. Construction of mine workings through zones of radioactive rock;

c. Handling and disposal of small quantities of radioactive rock;

d. Ore dressing and mill treatment problems arising from radioactive containments.

3. Expense from the construction, support, and maintenance of mine workings beneath the caved zone under the rock stress conditions which will exist there.

SUMMARY AND CONCLUSIONS

The potential applicability of nuclear explosives to underground mining is greatest in the case of large, massive, regularly shaped ore bodies too deeply buried for open-pit mining. Nuclear caving may also find application in the mining of ore bodies too competent for mining by block caving, or of too low a grade for mining by stoping. The minimum size ore body to which nuclear caving can be economically applied, although dependent on individual characteristics, will probably be at least several million tons.

There remain technical questions to be answered. These include: the effects of nuclear explosions in carbonate rocks; the quantitative effects of arrays of nuclear explosives fired simultaneously; and the effects of an explosion fired near a rubble chimney. Research designed to answer these questions is currently underway. However, technology has advanced to the point where nuclear caving can, at the present time, be applied in many situations.

It is the conclusion of the authors that nuclear caving will offer real technical and economic advantages in some instances, and will permit the mining or ore bodies with suitable characteristics at lower cost. Nevertheless, it is clear that nuclear caving is not universally applicable. As in all Plowshare applications, the judgement of applicability must be made first on the basis of individual technical feasibility, and second, on whether or not an economic advantage is to be gained.

BIOGRAPHICAL SKETCHES OF AUTHORS

Spenst M. Hansen was born in Logan, Utah. He received his B.S. in Geological Engineering from the University of Utah in 1957. In 1962 he was awarded the Ph.D. by the University of Mississippi School of Mines and Metallurgy. He is engaged in experimental research in the Earth Sciences Group of the Lawrence Radiation Laboratory Plowshare Division.

Dr. Hansen's professional background is as follows: Jr. Geological Engineer, Bear Creek Mining Company, 1956-57; Geological Engineer, Roberts Mining Company, 1958; Graduate Teaching Assistant, Mississippi School of Mines, 1958-60; El Dorado Consolidated Mining Company, Summer 1959; Assistant Instructor in Geology, Mississippi School of Mines 1960-61; Consolidated Mining Company of Canada, 1961; Assistant Professor, Geological Engineering, school years 1962-63; Lawrence Radiation Laboratory, 1963 to present.

David B. Lombard was born in Lexington, Massachusetts. He received his B.S. in Physics from Northeastern University in Boston in 1953. From 1953 to 1959 he was a graduate student at the Pennsylvania State University. Penn State awarded him the M.S. in Physics in 1955 and the Ph.D. in Physics in 1959.

Dr. Lombard is employed at Lawrence Radiation Laboratory in Livermore. He is engaged in experimental research on strong shocks in solid materials under the auspices of the AEC Plowshare Program.

ATTENDEES

Ackerman, Frank	L.R.L.
Ackerman, Hyman	Andrews AFB
Adelman, Frank	Instit. for Defense Analysis
Agresta, Joseph	Union Carbide Corp.
Alcedo, Lt.Jg. J. J.	U. S. Naval Schools Command
Allaire, W. W.	A.E.C.
Allen, D. C.	L.R.L.
Allen, Phillip	U.S.Dept. of Commerce
Anderson, D. C.	I.I.T. Research Instit.
Andrew, M. B.	Calif. Dept. of Water Resources
Anthony, Michael	Boeing Co.
Arnold, Maj. H. L.	U.S. Army
Aronson, H. H.	Reynolds Elect. & Eng.
Ash, Richard	Univ. of Missouri
Atkinson, Charles	U.S. Bureau of Mines
Auld, Capt. Harry	Kirtland AFB
Axford, Roy	Northwestern Univ.

Babuel-Peyrissac	A L'Energie Atomique
Bainer, Roy	Dean of Engineering
Balbiani, Andrew S.	Tippatts-Abbett-McCarthy-Stratton
Ball, Russell	U.S.A.E.C.
Ballou, Dr. N. E.	U.S. Naval Rad. Def. Lab.
Bankhardt, Philip	Aerospace Corp.
Barona, Alfred	U.S. Army Eng. Dist.
Barr, Frank	Esso Research & Eng.
Barsdale, Ray	U.S. Army Eng. Div.
Bartholomew, John	A. C. Spark Plug
Bartlett, John	Univ. of Rochester
Bator, George	Colo. School of Mines
Bauer, Frank L.	L.R.L.
Beeman, William	Tracer Lab.
Beetem, W. A.	U.S. Geol. Survey
Bell, Mayhue	U.S.A.E.C.
Bender, J. H.	Sci. Corp
Bennett, George	Sandia Corp
Bett, Frank	Australian Embassy
Beyor, G. H.	Univ. of Missouri
Bird, John	U.S. Army Corps of Eng.
Bishop, H. W.	Kennecott Copper
Black, L. F.	U.S. Steel Corp
Blackwell, Percy	U.S. Dept. of Commerce
Blanc, Gene	Office of Atomic Eng. Dev. & Rad. Protection

Bletcacker, Richard	Ohio State Univ.
Boardman, A. G.	Operating Engineers
Boardman, Charles	L.R.L.
Bond, Walter	Oak Ridge Nat'l Lab.
Bonell, John	Univ. of Nevada
Book, H. E.	U.S.A.E.C.
Boresi, Arthur	Univ. of Illinois
Botz, Maxwell	Hazleton Nuclear Sci. Corp.
Bouton, Edwin	U.S.Army Nuc. Def. Lab.
Boynton, Wm.	Boynton Assoc.
Bradley, Dick	Geo. M. Philpott Co.
Bradley, Philip R.	Consulting Mining Eng.
Bray, B. G.	Continental Oil Co.
Brewer, John	L.R.L.
Brier, Roger L.	L.R.L.
Brinkley, Thomas	Sunray DX Oil Co.
Browne, Harry	Hazleton-Nuc. Sci. Corp.
Brown, F. R.	U.S. Army Eng. Waterways
Brownlee, Robert	Los Alamos Science Lab.
Brownscombe, E. R.	Atlantic Refining Co.
Bruce, Robert	Tulane University
Brummer, Joseph	U.S.A. Corps of Eng.
Burke, Eugene	L.R.L.
Burkovich, Theodore	L.R.L.
Burson, Zolin G.	Edgerton, Germeshausen & Grier, Inc.
Busquet	A L'Energie Atomique
Camozzi, R. D.	Reynolds Elect. & Eng. Co.
Campbell, Ernest	U.S.A.E.C.
Campbell, Henry	Univ. of Rhode Island
Carbon, Max	Univ. of Wisconsin
Carder, B.	Edgerton, Germeshausen & Grier, Inc.
Carlson, R. H.	Boeing Co.
Carpenter, Lewis	Kaiser Engineers
Carson, John	L.R.L.
Carter, Melvin	Dept. of Health, Ed. & Wel.
Carter, Ralf	Eng. - Science Inst.
Chabai, A. J.	Sandia Corp.
Chan, Clarence K.	Univ. of Calif.
Circeo, Louis	L.R.L.
Claflin, Alan B.	U.S. Army Nuc. Def. Lab.
Clark, Fred, Jr.	U.S.A.E.C.
Clark, George	Univ. of Missouri
Clark, Kenneth	College Park High School
Clark, L. L.	Bureau of Public Roads
Closmann, P. J.	Shell Dev. Co.
Coffer, H. F.	Continental Oil
Cohen, P.	C.E.A., Neuilly/Seine, France
Cohron, Gerald	Wilson, Nuttall, Raimond
Coler, Myron	Markite Corp.
Colp, John	Sandia Corp.

Compton, Joseph	U.S. Army Eng. Waterways
Conrad, A. G.	Univ. of Calif., S.B.
Cook, T. B.	Sandia Lab.
Corner, Dr. J.	British Embassy
Cowan, George A.	L.A.S.L.
Cowles, John	L.R.L.
Cowser, K. E.	Oak Ridge Nat'l Lab.
Crandall, Dr.	Northrup Ventura
Crawford, Ray	San Fernando Valley St. Col.
Crockett, J. R.	Reynolds Elect. & Eng.
Curtis, Harold	U.S.A.E.C.
Dagostino, Tom	U.S.A.E.C. - N.V.O.O.
Davenport, Monty	Texas Tech. College
Davies, Lee E.	Sandia Corp.
Davis, G. James	A.V.C.O.
Davis, James W.	Bureau of Mines
Davis, Jared	U.S.A.E.C.
Davis, R. E.	U.S. Geol. Survey
Davis, Robert	U.S. Geol. Survey
Davis, S. N.	Carroll Bradberry & Assoc.
Day, Walter	Nuclear Cratering Group
Della Rosa, R. J.	Univ. of Calif.
Dettmer, Harry	U.S. Army Eng. Dis.
Diven, B. C.	Los Alamos Sci. Lab.
Dickinson, Wade	Bechtel Corp.
Dirks, Charles H.	Gardner-Denver Co.
Doan, R. L.	A.E.C. & Phillips Pet.
Dorn, D. W.	L.R.L.
Duncan, Mike	Univ. of Calif.
Dunlap, H. F.	Atlantic Refining Co.
Du Temple, Octave	Am. Nuclear Soc.
Dybczak, Z. W.	Tuskegee Instit.
Eckel, Edwin	U.S. Geol. Survey
Eckhart, J. C.	Sandia, Corp.
Edgerton, A. T.	N.A.A.
Ehrlich, Melvin P.	N.R.A. Incorp.
Eichholz, G. G.	Georgia Inst. of Tech.
Eisler, Joseph	
Elson, R.	L.R.L.
Erdle, John	Morrison-Knudsen Co., Inc.
Farin, S. E.	Bureau of Public Roads
Faulkner, Rafford	U.S.A.E.C.
Felegy, E. W.	U.S. Bureau of Mines
Fidler, Harold	L.R.L.
Field, H. C.	U.S.A.E.C.
Fields, Paul	Argonne Nat'l Lab.

Fishburne, W. N.	Aetron
Fisher, Paul R.	L.R.L.
Fisher, Robert	I.I.T. Research Instit.
Fistedis, Stanley	Argonne Nat'l Lab.
Flangs, William	Reynolds Elect. Eng. Co.
Fleisher, C. W., Jr.	Pitman-Dunn Inst.
Ford, A. D., Jr.	Sandia Corp.
Ford, Warren	El Camino College
Forrest, R. M.	Columbia Gas System
Fox, Raymond	George Washington Univ.
Fox, Robert	Calif. Dept. of Water Resources
Frandsen, Alton	U.S.A. Corps of Eng.
Fraser, Richard	Corps of Eng. N.C.G.
Freiling, E. C.	U.S. Naval Rad. Def. Lab.
Friend, Walter F.	Ebasco Services Inc.
Gailledreau, M.	A L'Energie Atomique
Galva'n, Lizardo	Stanford Univ.
Gamertsfelder, Carl	Gen. Electric Co.
Garg, Prahlad Saran	U.C.D.
Garland, Clyne	Univ. of Calif.
Gaylord, John	Calif. Research Corp.
Geesaman, Lynn	L.R.L.
George, T. A.	Office of Sec. of Defense
Gerber, Carl	U.S.A.E.C.
Geringer, K. R.	Hazleton Nuclear Science
Gilat, Jacob	L.R.L.
Ginsburg, Dr. Theo	Swiss Embassy
Glass, Eugene	Cities Service Research & Dev.
Go, Mateo L.P.	A.S.E.E. Univ. of Hawaii
Gofman, John	L.R.L.
Goldberg, John	Purdue Univ.
Goldman, Marvin	Univ. of Calif.
Gram, Andrew	Caltech
Graves, Ernest, Jr.	L.R.L.
Grebe, Dr. John	Dow Chem. Co.
Gregoire, W. E.	Bureau of Public Roads
Grubbs, David	Univ. of Alabama
Guthrie, Patrick	U.S. Army Corps of Eng.
Hagedorn, Zach	Def. Atomic Support Agency
Hale, W. E.	U.S. Geol. Survey
Hall, Lt. Col. William	U.S.A.E.C.
Hamburger, Richard	U.S.A.E.C.
Hamelin, Dr. Raymond	Embassy of France
Hammon, R. L.	Edgerton, Germeshausen & Grier
Hankins, Doris	Sandia Corp.
Hansche, G. E.	Sandia Corp.
Hansen, Peter	Univ. of Missouri
Hansen, Spenst	L.R.L.

Hardin, Luther	U.S. Army Nuc. Def. Lab.
Hardwick, William	U.S. Bureau of Mines
Harrison, M. A.	L.R.L.
Harroun, Dale	Univ. of Penna.
Hartman, Howard	Penn. State Univ.
Harten, Philip	Tracer Lab.
Hawkins, Myron	United Research
Hawthorn, David	Petroleum Consultants
Heckman, Richard	L.R.L.
Heierli, Werner	Swiss Fed. Office of Civil Defense
Helterbran, Wayne	HG USAF/AFTAC
Henderson, Krieger	Rolland Biers
Herlihy, W. J.	L.R.L.
Hesselbacher, Cd. Geo.	Hq. Def. Atomic Sup. Ag.
Higgins, Dr. Gary H.	L.R.L.
Hollingsworth, L. E.	Sandia Corp.
Hollis, W. T.	El Paso Natural Gas Products
Holmes, R. S.	U.S. Army Eng. Nuclear Cratering Grp.
Holzer, Alfred	L.R.L.
Houser, F. N.	U.S. Geol. Survey
Howard, Ephraim	Aerojet
Howard, Robert	Univ. of Wichita
Hudson, Cecil, Jr.	L.R.L.
Huffaker, R. C.	Univ. of Calif.
Hughes, Bernard	L.R.L.
Hull, Arthur	U.S. Army Corps of Eng.
Hungate, F. P.	Gen. Electric Co.
Hurd, John	L.R.L.
Hurdlow, William	L.R.L.
Huttl, John	Eng. and Min. Journal
Hyne, Allan	L.R.L.
Isaacs, John D.	Univ. of Calif.
Italia, Santo	Aerospace Corp.
Jacobson, Roger J.	Caterpillar Tractor Co.
Jaffe, Harold	Aerojet-Gen. Nuc.
James, Allan	Kennecott Copper Corp.
Jaske, Robert	Gen. Electric Co.
Jean, Ouvry	French Atomic Energy
Jensen, J. A.	L.R.L.
Jones, Allan	Gen. Dynamics Corp.
Jones, W. E.	Climax Molybdenum Co.
Joy, K. N.	A.E.C.
Judd, Deane	L.R.L.
Just, Evan	Stanford Univ.
Kaplan, Kenneth	United Research
Karraker, David	E.I. Du Pont De Nemours & Co.

Karrakon, D.	Savannah River Lab.
Kase, Kenneth	L.R.L.
Kathren, Ronald	L.R.L.
Keim, Paul	Univ. of Calif.
Keim, S. R.	Univ. of Calif.
Keith, J. M.	John Blume & Assoc. Research
Keizur, John	Sandia Corp
Keller, Harry	L.R.L.
Kelley, Donna	San Francisco State Coll.
Kellogg, F. H.	Univ. of Mississippi
Kelly, John	U.S.A.E.C.
Kemper, John	Univ. of Calif.
Killgore, Charles	La. Polytechnic Inst.
Kinnaman, Ross	U.S.A.E.C.
Kleiman, William	State Div. of Highways
Klement, Alfred, Jr.	U.S.A.E.C.
Klickmand, Alton	Dev. Assoc., Inc., Atomic Power
Knott, Dr. R. F.	Canadian Industries, Limited
Knutson, C. F.	Continental Oil Co.
Knittel, Robert	A.T. & S.F. Ry. - L.A.
Kochanosky, Prof.	Penn. State Univ.
Kochendorfer, D. B.	U.S. Naval Rad. Def. Lab.
Kondner, Dr. Robert	Northwestern Univ.
Korver, John	L.R.L.
Krieger, H. A.	Sandia Corp.
Kriegsman, Wm. E.	U.S.A.E.C.
Krouse, Otto	L.R.L.
Krueger, R. E.	Union Oil Co. of Calif.
Kruger, Paul	Stanford Univ.
Kubitza, Wilhelm	Kansas State Univ.
de Laborderie	A L'Energie Atomique
Landry, John	Oak Ridge Nat'l Lab.
Lauson, Herrick S.	Los Alamos Sci. Lab.
Leach, LCDR E. N.	U.S. Naval Schools Command
Lee, K. L.	Univ. of Calif.
Legate, Gail	U.S. Air Force Ac.
Lekqs, Mitchell	U.S.A.E.C.
Leonard, Anthony	Rand Corp.
Leventhal, Mr.	Tracer Lab.
Levy, Allan	San Francisco State Col.
Lombard, David	L.R.L.
Love, Colin	Calif. Div. of Hwys.
Loving, Frank	E.I. Du Pont De Nemours & Co., Inc.
Lowen, Walter	Union College
Lundberg, A. W.	L.R.L.
Lynch, Charles	Conover-Mass Publ. Co.
Lynch, E. J.	Carroll Bradberry & Assoc.

MacCaulty, Thomas	U.S.A.E.C.
MacGuish, Earl	Space Tech. Lab.
McBride, Robert	Dept. of the Army
McCauley, Marvin	Calif. Div. of Hwys.
McConeghy, James	Dept. of H, Ed, & Wel.
McGregor, D. R.	Reynolds Elect. & Eng.
McKeown, F. A.	U.S. Geol. Survey
McNichols, H. B.	Columbia Gas Sys. Ser. Corp.
Maccabee, Howard	Univ. of Calif.
Major, William	Tracer Lab.
Maggard, Samuel P.	New. Mex. State Univ.
Maizitis, Laindota	L.R.L.
Mann, John	Hazleton-Nuclear Sci. Corp.
Mann, Marvin	U.S.A.E.C.
Marcus, Henri	U.S. Naval Research Lab.
Marks, Robert	L.R.L.
Martin, William	Univ. of Calif.
Mason, H. G.	United Research
Mawardi, O. K.	Case Instit. of Tech.
Max, Andrew	Sandia Corp.
Mears, David	Univ. of Calif.
Melching, F. W.	Aerospace Corp.
Mellor, Elmer	U.S. Army Corps of Eng.
Merkel, George	Construction Op. Branch
Meyer, Lew	Lawrence Rad. Test Site
Michaud	A L'Energie Atomique
Mickey, Wendell V.	U.S. Coast & Geodetic Survey
Middleton, W.	Thermal Power Co.
Miller, R. E.	A. E. C.
Milsted, M. G.	Student UCD
Misiaszek, Edw'd	Clarkson College of Tech
Miskel, John	L.R.L.
Mitchell, James	Univ. of Calif.
Mooser, Mrs. Clare	Mexico, D. F.
Mooser, Federico	C.F.E., Mexico, D.F.
Morrell, Warren	Sacramento Union
Morris, Phillip	U.S. Army Eng. Res. & Dev.
Mullikin, Dr. Harwood	Montana State College
Murphy, Glenn	Iowa State Univ.
Murrin, F. E.	A C Spark Plug
Myers, Bruce	L.R.L.
Naar, Dr. Jacques	Stanford Research Inst.
Nance, Olen	Rand Corp.
Narver, David	Holmes & Narver Inc.
Nathans, M. W.	L.R.L.
Natland, J.	No. American Aviation
Natland, M. L.	Richfield Oil Corp.

Neef, Melvin E.	U.S.A.E.C.
Ne'eman, Yuval	Calif. Instit. of Tech.
Nel, Barend M.	So. African Atomic Energy Bd.
Nelson, Curtis	U.S.A.E.C.
Nickel, George H.	Dept. of App. Sci., U.C.D.
Nims, John	Atomic Power Dev. Assoc., Inc.
Nish, Glen	L.R.L.
Nordyke, Milo D.	L.R.L.
O'Brien, Capt. Thomas	Kirtland AFB
O'Gwin, James	U. S. A. E. C.
Oldberg, Sidney	L. R. L.
Olson, R. L.	Lockheed
Onerry, J. T.	L. R. L.
Oshier, Edwin H.	ASEE Group
Otter, J. V.	Morrison-Knudsen Co. , Inc.
Overton, Harold L.	University of Houston
Pack, P. D.	Holmes & Narver
Palmer, Darwin G.	Sandia Corp.
Palmiter, C. C.	Fed. Rad. Council
Palumbo, Ralph	Univ. of Wash.
Parker, H. W.	Stanford Univ.
Parker, Henry	Stanford Univ.
Parra, Raul de la	Comision Federal de Electricidad, Mexico, D. F.
Pederson, Ole E.	Int'l Atomic Energy Agency, Vienna, Austria
Peiry, Gideon	Consulate Gen. of Israel
Perkins, Walter W.	Naval Rad. Defense Lab.
Peters, Chester	Intern'tl Eng. Co., Inc.
Petersen, Robert	San Francisco State Col.
Perry, O. W.	State Div. of Hwys.
Phelps, Paul	L.R.L.
Philip, John	U.S.A.E.C.
Pierce, Richard	U.S. Army Eng. Nuc. Cratering
Pinkel, Benjamin	Rand Corp.
Piper, Arthur	U.S. Geological Survey
Pitney, Richard J.	Stanford University
Plows, William H.	L.R.L.
Pon, Wing	San Francisco State Col.
Porzel, Francis B.	Instit. for Def. Analysis
Possony, Mrs. Regina	Stanford Univ.
Possony, Dr. Stefan	Stanford Univ.
Post, Edward	Div. of Highways
Power, Dean	L.R.L.
Powers, P. N.	Purdue Univ.
Prentice, H. C.	State Div. of Hwys.
Preston, Roger	L.R.L.
Price, Robert	L.R.L.
Price, Sterling	Maryland Casualty Co.
Quarterman, Mrs. E. A.	12th Naval Dist. Pub. Works
Quarterman, E. A.	12th Naval Dist. Pub. Works

Rambicur, Robert	Eng. School, Fort Belvoir, Vir.
Ransohoff, J. A.	Nuclear Utility Services, Inc.
Rawson, Don	L.R.L.
Reed, Jack W.	Sandia Corp.
Remboldt, Adam L.	L.R.L.
Reynolds, W. B.	Univ. of Calif.
Rhoades, Robert C.	L.R.L.
Rhoads, Williams	Univ. of Calif.
Rice, Robert J.	Kaiser Engs. International
Richards, Gordon V.	P.G.& E.
Roach, T. M.	Bureau of Public Roads
Roberts, George D.	Dames & Moore
Roberts, Gilbert	U.S. Army District of Eng.
Roberts, Wayne A.	Boeing Co.
Rogers, Leo	L.R.L.
Rosenbaum, Dr. Marcus	G.E. Tempo
Rowell, Monte	U.S. Naval Rad. Def. Lab.
Russell, Paul	U.S. Dept. of Interior
Ruvkun, Sam	Kaiser Engineers Int'l.
Sables, Dr. Bruno	Isotopes, Inc.
Salmen, C. R.	Bureau of Public Roads
Samuelson, Wallace	U.S. Army Corps of Eng.
Sauer, Fred	Stanford Research Inst.
Saxe, Harry C.	Univ. of Notre Dame
Scheffey, Charles F.	U.S. Bur. of Public Roads
Schiffman, T. H.	I.I.T. Research Instit.
Schimming, Bruce	Univ. of Notre Dame
Schmid, Dr. Paul	Swiss Embassy
Schmidt, Richard M.	L.R.L.
Scisson, S. E.	Fenix & Scisson, Inc.
Scott, S. A.	Intern'l Material & Chem.
Seyler, J. W.	Univ. of Ill.
Seymour, Alan	Univ. of Wash.
Shaffer, L. W.	Univ. of Calif.
Shanahan, William J.	L.R.L.
Sheridan, Emmett	Dept. of Commerce
Sherman, W. C.	U.S. Army Eng. Waterways
Shon, Frederick	U.S.A.E.C.
Short, Nicholas M.	L.R.L.
Sisemore, Clyde	L.R.L.
Skolil, Lester	San Diego State
Slykhouse, Tom	Dow Chemical Co.
Smith, Joseph	Res. Eng. Jet Propulsion Lab.
Smith, Robert	Sandia Corp.
Smith, Samuel	El Paso Natural Gas Products
Smyth, Sam	Kennecott Copper Corp.
Sollenberger, Norman J.	Princeton Univ.
Somerton, Wilbur	Min. Tech., Univ. of Calif.
Spencer, Ned	C of E
Spottswood, A. D.	Intern'l Bank for Reconst'n & Dev.

Spruill, Joseph L.	L.R.L.
Stafford, G. V.	Calif. Div. of Hwys.
Stahl, R. H.	General Atomic
Stane, R. A.	A.T. & S.F. Ry. -L.A.
Stanley, Walter E.	L.R.L.
Stapleton, Thomas	Op. Eng. Local Union
Stead, Frank W.	U.S. Dept. of Int.
Stephens, Douglas R.	L.R.L.
Stinnett, Landy	Univ. of Calif.
Strandberg, Odin	Stanford Univ.
Stripsika, Alex	L.R.L.
Struxness, Edward	Oak Ridge Nat'l Lab.
Sullivan, R. J.	Caterpillar Tractor Co.
Sutton, Alex	U.S. Army Eng. Waterways
Swift, Elijah, Jr.	U.S. Naval Ordnance Lab.
Szasz, S. E.	Sinclair Research
Talley, Wilson K.	Dept. of Applied Science, U.C.D.
Teagle, Charles	U.S. Army Engineer District
Tejaoa, X	Aetron Div. of Aerojet Gen.
Teller, Dr. Edward	L.R.L.
Ternault	A L'Energie Atomique
Thomas, R. J.	L.R.L.
Thompson, Andrew	Ballistic Research Lab.
Thompson, D.	Edgerton, Germeshausen & Grier
Thompson, Louis	Univ. of New Mex.
Thompson, Miss Cynthia	Albuquerque, N.M.
Thornburgh, Dick	Student
Tilles, Alse	L.R.L.
Toman, John	L.R.L.
Tomnovec, F. M.	U.S. Naval Rad. Def. Lab.
Toole, R. H.	U.S.A.E.C.
Tower, Mr.	Westinghouse
Tracy, James F.	L.R.L.
Tracy, Mrs. Margaret J.	L.R.L.
Trolan, R. C.	U.S. Naval Rad. Def. Lab.
Turberville, Dave	United Nuc. Corp.
Turner, Frederick	Univ. of Calif.
Twenhofel, W. S.	U.S. Geol. Survey
Urban, V. Doyle	U.S. Dept. of Commerce
Vaile, R. B.	Stanford Research Instit.
Van Zandt, R. P.	Caterpillar Tractor Co.
Vermillion, Henry	U.S.A.E.C.
Vesic, Aleksanaar	Georgia Instit. of Tech.
Videon, Fred F.	L.R.L.
Vieira, Gerald J.	L.R.L.
Viets, Warren	U.S. Army Eng. Div.
Vortman, Luke	Sandia Corp.

Wadlin, George K.	Univ. of Maine
Wagner, J. E.	U.S.A.E. N.C.G.
Wagner, Paul	Calif. Div. of Highways
Wagniere, C. F.	Ebasco Services
Wahls, H. E.	N.C. State
Waldorf, Harry	Citrus College
Wallstedt, Roland W.	L.R.L.
Warner, B. P.	Edgerton, Germeshausen & Grier
Watkins, J. Wade	Bureau of Mines
Weber, W. G.	Calif. Div. of Hwys.
Weidenbaum, B	
Werner, Louis	Hazleton-Nuclear Sci.
West, John B.	Oklahoma State Univ.
Westfall, Fredrick	U.S. Air Force Ac.
West, Larry	Bechtel Corp.
Wessman, Robert	Tracer Lab.
Whatley, A.	Edgerton, Germeshausen & Grier
White, Alfred	U.S.A.E.C.
White, Merritt	Univ. of Mass.
Whitehead, C. F.	Ebasco Services, Inc.
Whitman, Robert	M.I.T.
Wiese, John	Richfield Oil Corp.
Wilk, I. J.	Morse Lab.
Williams, Clarke	Brookhaven Mat Lab
Williamson, T. N.	Hughes Tool Co.
Wilmarth, Verl	U. S. Geological Survey
Wilson, C. M.	State Crime Lab.
Wolfe, Dr. John	U.S.A.E.C.
Wolfskill, L. A.	M.I.T.
Wood, Edward	Stanford Research Instit.
Wood, Wm. G.	Stanford Univ.
Woodward, Eliot	Stanford Research Instit.
Wygant, James	Am. Oil Co.
Yaffe, Dr.	San Jose State College
Yoshihara, Takeshi	Dept. of Navy
Young, George A.	Mich. Tech. Univ.
Zemanek, Joseph	Socony Mobil Oil Co.